AWARD NUMBER: DAMD17-99-1-9483

TITLE: NEUROTOX-98 NEUROPROTECTION BY PROGESTERONES THROUGH STIMULATION OF MITOCHONDRIAL GENE EXPRESSION

PRINCIPAL INVESTIGATOR: Gary M. Fiskum

ORGANIZATION: University of Maryland School of Medicine
Baltimore, MD 21201

REPORT DATE: June 2006

TYPE OF REPORT: Final

PREPARED FOR: U.S. Army Medical Research and Materiel Command
Fort Detrick, Maryland 21702-5012

REPORT DOCUMENTATION PAGE

Form Approved
OMB No. 0704-0188

1. REPORT DATE	**2. REPORT TYPE**	**3. DATES COVERED**
June 2006	Final	1 August 1999- 30 May 2006

4. TITLE AND SUBTITLE
NEUROTOX-98 NEUROPROTECTION BY PROGESTERONES THROUGH STIMULATION OF MITOCHONDRIAL GENE EXPRESSION

5a. CONTRACT NUMBER

5b. GRANT NUMBER
DAMD17-99-1-9483

5c. PROGRAM ELEMENT NUMBER

6. AUTHOR(S)
Gary M. Fiskum

5d. PROJECT NUMBER

5e. TASK NUMBER

5f. WORK UNIT NUMBER

7. PERFORMING ORGANIZATION NAME(S) AND ADDRESS(ES)
University of Maryland School of Medicine
Baltimore, MD 21201

8. PERFORMING ORGANIZATION REPORT NUMBER

9. SPONSORING / MONITORING AGENCY NAME(S) AND ADDRESS(ES)
U.S. Army Medical Research and Materiel Command
Fort Detrick, Maryland 21702-5012

10. SPONSOR/MONITOR'S ACRONYM(S)

11. SPONSOR/MONITOR'S REPORT NUMBER(S)

12. DISTRIBUTION / AVAILABILITY STATEMENT
Approved for Public Release; Distribution Unlimited

13. SUPPLEMENTARY NOTES

14. ABSTRACT

See next page

15. SUBJECT TERMS- none provided

16. SECURITY CLASSIFICATION OF:			**17. LIMITATION OF ABSTRACT**	**18. NUMBER OF PAGES**	**19a. NAME OF RESPONSIBLE PERSON**
a. REPORT	**b. ABSTRACT**	**c. THIS PAGE**			USAMRMC
U	U	U	UU	180	**19b. TELEPHONE NUMBER** *(include area code)*

Abstract

Neurotoxic agents or trauma can produce direct brain damage or seizures resulting in neuronal cell death. Recent evidence indicates that the gonadal steroid progesterone greatly attenuates the excitotoxicity that leads to neuronal cell loss. However, surprisingly little is known of the mechanism for this effect. The **working hypothesis** for the proposed studies is that the ovarian hormone, *progesterone, either alone or through its metabolites, can protect or intervene against brain injury* and that **one mechanism of neuroprotection involves upregulation of mitochondrial genes.** The **specific hypotheses** to be tested are: 1. Progesterone *per se* protects against neuronal death caused by **status epilepticus** *in vivo* and by **NMDA**-induced death of **cerebellar granule neurons** *in vitro.* 2. Excitotoxic levels of glutamate down-regulate the expression of mitochondrial genes *in vitro and in vivo* leading to greater vulnerability to injury. 3. Progesterone up-regulates mitochondrial **gene expression**, hence increasing the resistance of neurons to excitoxicity. **Methods** to be used include kainate-induced seizures in intact or ovariectomized rats, exposure of primary cultures of cerebellar neurons to NMDA, histological assessment of necrotic and apoptotic cell death, measurements of cytochrome oxidase gene expression, and *in vitro* measurements of mitochondrial electron transport, respiration, Ca^{2+} transport, and cytochrome-c release. *The **significance** of these studies is that they will provide further evidence that progesterone possesses neuroprotective properties relevant to military-related brain injury and that regulation of mitochondrial gene expression is one mechanism by which the vulnerability of neurons to excitotoxicity can be controlled.*

Table of Contents

1. **INTRODUCTION:** Narrative that briefly (one paragraph) describes the subject, purpose and scope of the research.

Neurotoxic agents or trauma can produce direct brain damage or seizures resulting in neuronal cell death. Recent evidence indicates that the gonadal steroid progesterone greatly attenuates the excitotoxicity that leads to neuronal cell loss. However, surprisingly little is known of the mechanism for this effect. The purpose of this project was to both explore the ability of progesterone to provide neuroprotection and to determine if mitochondria are a target of action by progesterone. Research was performed with rat models of acute brain injury caused by either status epilepticus or head trauma. Additional, more basic research was performed with isolated brain mitochondria.

2. **KEYWORDS:** Provide a brief list of keywords

   Steroid, hormones, neuron, apoptosis, mitochondria, excitoxicity, calcium, cytochrome c, traumatic brain injury, respiration, methoxychlor, apoptosis

3. **OVERALL PROJECT SUMMARY:**

1. Starkov, A.A., Polster, B.M., and Fiskum, G., Regulation of mitochondrial reactive oxygen species generation by calcium and Bax., J. Neurochem. 83, 220-228 (2002). (PMID:12358746)

Abnormal accumulation of Ca2+ and exposure to pro-apoptotic proteins, such as Bax, is believed to stimulate mitochondrial generation of reactive oxygen species (ROS) and contribute to neural cell death during acute ischemic and traumatic brain injury, and in neurodegenerative diseases, e.g. Parkinson's disease. The results obtained from this study indicate that in the presence of ATP and Mg2+, Ca2+ accumulation either inhibits or stimulates mitochondrial H2O2 production, depending on the respiratory substrate and the effect of Ca2+ on the mitochondrial membrane potential. Bax plus a BH3 domain peptide stimulate H2O2 production by brain mitochondria due to release of cytochrome c and this stimulation is insensitive to changes in membrane potential. These results relate to the mechanisms of neuroprotection by progesterone since we and others found that progesterone increases expression of Bcl2, which we have shown substantially reduces mitochondrial sensitivity to Ca2+-induced damage and to Bax-induced H2O2 production.

2. Starkov, A.A. and Fiskum, G., Regulation of brain mitochondrial H_2O_2 production by membrane potential and NAD(P)H redox state, J. Neurochem. 86: 1101-1107 (2003). (PMID:12911618)

Mitochondrial production of reactive oxygen species (ROS) at Complex I of the electron transport chain is implicated in the etiology of neural cell death in acute and chronic neurodegenerative disorders. However, little is known regarding the regulation of mitochondrial ROS production by NADH-linked respiratory substrates under physiologically realistic conditions in the absence of respiratory chain inhibitors. Our findings indicate that ROS production by mitochondria oxidizing physiological NADH-dependent substrates is regulated by membrane potential and by the NAD(P)H redox state over ranges consistent with those that exist

at different levels of cellular energy demand. The significance of these results is that they support the hypothesis that increased mental activity and associated oxidative cerebral energy metabolism reduce mitochondrial ROS formation and associated oxidative stress. This relationship may be the reason why people who are mentally very active as they grow old appear to have a lower incidence of Alzheimer's disease.

3. Hoffman, G.E., Moore, N., Fiskum, G., and Murphy, A.Z., Ovarian steroid modulation of seizure severity and hippocampal cell death after kainic acid treatment, Exp. Neurol. 182: 124-134 (2003). (PMID:12821382)

To determine whether maintained estrogen or progesterone levels affect kainic acid (KA) seizure patterns or the susceptibility of hippocampal neurons to death from seizures, ovariectomized Sprague–Dawley rats were implanted with estrogen pellets or progesterone capsules that generated different serum hormone levels. Seven days later, the rats were administered kainic acid and scored for seizure activity; 96 h later, the rats were killed and their brains processed for localization of neuron nuclear antigen (NeuN), a general neuronal marker. The results obtained from this study are consistent with the hypothesis that progesterone produces its neuroprotective effects by reducing seizures, whereas estrogen has little beneficial effect on seizure behavior but protects the hippocampus from the damage seizures produce. This is one of the two most important studies documenting neuroprotection by progesterone that was supported by this grant. In addition to blocking status epilepticus, progesterone may inhibit seizure activity associated with traumatic brain injury or exposure to nerve agents.

4. Fiskum, G., Starkov, A., Polster, B.M., and Chinopoulos, C., Mitochondrial mechanisms of neural cell death and neuroprotective interventions in Parkinson's disease, Ann. NY Acad. Sci. 991: 111-119 (2003). (PMID:12846980)

Mitochondrial dysfunction, due to either environmental or genetic factors, can result in excessive production of reactive oxygen species, triggering the apoptotic death of dopaminergic cells in Parkinson's disease. Mitochondrial free radical production is promoted by the inhibition of electron transport at any point distal to the sites of superoxide production. Neurotoxins that induce parkinsonian neuropathology, such as MPP(+) and rotenone, stimulate superoxide production at complex I of the electron transport chain and also stimulate free radical production at proximal redox sites including mitochondrial matrix dehydrogenases. The oxidative stress caused by elevated mitochondrial production of reactive oxygen species promotes the expression and (or) intracellular distribution of the proapoptotic protein Bax to the mitochondrial outer membrane. Interactions between Bax and BH3 death domain proteins such as tBid result in Bax membrane integration, oligomerization, and permeabilization of the outer membrane to intermembrane proteins such as cytochrome c. Once released into the cytosol, cytochrome c together with other proteins activates the caspase cascade of protease activities that mediate the biochemical and morphological alterations characteristic of apoptosis. In addition, loss of mitochondrial cytochrome c stimulates mitochondrial free radical production, further promoting cell death pathways. Excessive mitochondrial Ca(2+) accumulation can also release cytochrome c and promote superoxide production through a mechanism distinctly different from that of Bax. Ca(2+) activates a mitochondrial inner membrane permeability transition causing osmotic swelling, rupture of the outer membrane, and complete loss of mitochondrial structural and

functional integrity. While amphiphilic cations, such as dibucaine and propranolol, inhibit Bax-mediated cytochrome c release, transient receptor potential channel inhibitors inhibit mitochondrial swelling and cytochrome c release induced by the inner membrane permeability transition. These advances in the knowledge of mitochondrial cell death mechanisms and their inhibitors may lead to neuroprotective interventions applicable to Parkinsons's disease. This review article provides important new insights into mitochondrial mechanisms of Parkinson's disease and brain injury caused by neurotoxins.

5. Fiskum, G., Rosenthal, R.E., Vereczki, V., Martin, E., Hoffman, G.E., Chinopoulos, C., and Kowaltowski, A., Protection against ischemic brain injury by inhibition of mitochondrial oxidative stress, J. Bioenerg. Biomemb. 36: 347-352 (2004). (PMID: 15377870)

Mitochondria are both targets and sources of oxidative stress. This dual relationship is particularly evident in experimental paradigms modeling ischemic brain injury. One mitochondrial metabolic enzyme that is particularly sensitive to oxidative inactivation is pyruvate dehydrogenase. This reaction is extremely important in the adult CNS that relies very heavily on carbohydrate metabolism, as it represents the sole bridge between anaerobic and aerobic metabolism. Oxidative injury to this enzyme and to other metabolic enzymes proximal to the electron transport chain may be responsible for the oxidized shift in cellular redox state that is observed during approximately the first hour of cerebral reperfusion. In addition to impairing cerebral energy metabolism, oxidative stress is a potent activator of apoptosis. The mechanisms responsible for this activation are poorly understood but likely involve the expression of p53 and possibly direct effects of reactive oxygen species on mitochondrial membrane proteins and lipids. Mitochondria also normally generate reactive oxygen species and contribute significantly to the elevated net production of these destructive agents during reperfusion. Approaches to inhibiting pathologic mitochondrial generation of reactive oxygen species include mild uncoupling, pharmacologic inhibition of the membrane permeability transition, and simply lowering the concentration of inspired oxygen. Anti-death mitochondrial proteins of the Bcl-2 family also confer cellular resistance to oxidative stress, paradoxically through stimulation of mitochondrial free radical generation and secondary up-regulation of antioxidant gene expression. This review article focuses on oxidative damage and inactivation of the pyruvate dehydrogenase complex, which is strongly implicated in the pathophysiology of both acute brain injury and neurodegenerative diseases.

6. Starkov, A.A., Fiskum, G., Chinopoulos, C., Lorenzo, B.J., Browne, S.E., Patel, M.S., and Beal, M.F., Mitochondrial alpha-ketoglutarate dehydrogenase complex generates reactive oxygen species, J. Neurosci. 24: 7779-7788 (2004). (PMID:15356189)

Mitochondria-produced reactive oxygen species (ROS) are thought to contribute to cell death caused by a multitude of pathological conditions. The molecular sites of mitochondrial ROS production are not well established but are generally thought to be located in complex I and complex III of the electron transport chain. Isolated mitochondrial alpha-ketoglutarate dehydrogenase (KGDHC) and pyruvate dehydrogenase (PDHC) complexes produced superoxide and H2O2. NAD(+) inhibited ROS production by the isolated enzymes and by permeabilized mitochondria. We also measured H2O2 production by brain mitochondria isolated from heterozygous knock-out mice deficient in dihydrolipoyl dehydrogenase (Dld). Although this

enzyme is a part of both KGDHC and PDHC, there was greater impairment of KGDHC activity in Dld-deficient mitochondria. These mitochondria also produced significantly less H2O2 than mitochondria isolated from their littermate wild-type mice. The data strongly indicate that KGDHC is a primary site of ROS production in normally functioning mitochondria. This ground-breaking article provides evidence against the dogma that mitochondrial ROS formation occurs exclusively within the electron transport chain. This study is the first to provide strong evidence that the Kreb's cycle enzyme, alpha ketoglutarate dehydrogenase complex, is as or more important a source of ROS than the electron transport chain. This finding is very important to understanding the molecular pathophysiology of neurodegeneration.

7. Polster, B.M. and Fiskum, G., Mitochondrial mechanisms of neural cell apoptosis, J. Neurochem. 90: 1281-89 (2004). (PMID: 15341512)

The importance of calcium overload, mitochondrial dysfunction, and free radical generation to neuropathological processes has been recognized for many years. Only more recently has evidence accumulated that the programmed cell death process of apoptosis plays an integral role not only in the development of the nervous system, but in the loss of cells following acute neurological insults and chronic disease. In 1996 came the landmark discovery that cytochrome c, an evolutionary old and essential component of the respiratory chain, has a second and deadly function when it escapes the mitochondrion: triggering the cell death cascade. A flurry of activity has since ensued in an effort to understand the mechanistic events associated with mitochondrial permeabilization during apoptosis and regulation by an enigmatic family of proteins characterized by homology to the proto-oncogene Bcl-2. This review discusses the evidence for various release mechanisms of apoptotic proteins (e.g. cytochrome c) from neural cell mitochondria, focusing particularly on roles for calcium, Bax, p53, and oxidative stress. The need for new drugs that act at the level of the mitochondrion to prevent apoptosis is also highlighted. This review article provides an overview of mitochondrial mechanisms of apoptosis and targets for neuroprotective interventions.

8. Chinopoulos, C., Gerencser, A.A., Doczi, J., Fiskum, G., and Adam-Vizi. V., Inhibition of glutamate-induced delayed calcium deregulation by 2-APB and La^{3+} in cultured cortical neurons, J. Neurochem. 91: 471-483 (2004). (PMID:15447680)

Exposure of neurones in culture to excitotoxic levels of glutamate results in an initial transient spike in [Ca2+]i followed by a delayed, irreversible [Ca2+]i rise governed by rapid kinetics, with Ca2+ originating from the extracellular medium. The molecular mechanism responsible for the secondary Ca2+ rise is unknown. Our results indicate that 2-APB and La3+ influence non-store-operated Ca2+ influx in cortical neurones and that this route of Ca2+ entry is involved in glutamate-induced delayed Ca2+ deregulation. This study describes a new mechanism by which exposure of mitochondria to elevated Ca2+ causes bioenergetics failure. Since Ca2+-induced mitochondrial damage is central to neuronal cell death, these findings contribute to the understanding of neurodegeneration, providing direction toward neuroprotective drug development.

9. Kowaltowski, A.J., Fenton, R.G., and Fiskum, G., Bcl-2 family proteins regulate mitochondrial reactive oxygen production and protect against oxidative stress, Free Rad. Biol. Med. 37: 1845-1853 (2004). (PMID:15538043)

Bcl-2 family proteins protect against a variety of forms of cell death, including acute oxidative stress. Previous studies have shown that overexpression of the anti-apoptotic protein Bcl-2 increases cellular redox capacity. Here we report that cell lines transfected with Bcl-2 paradoxically exhibit increased rates of mitochondrial H2O2 generation. Our results indicate that chronic and mild elevations in H2O2 release from Bcl-2, Bcl-xL, and Mcl-1 overexpressing mitochondria lead to enhanced cellular antioxidant defense and protection against death caused by acute oxidative stress. This study provides the first explanation for the apparent "antioxidant" effect of Bcl-2 and other related anti-apoptotic proteins. Since progesterone increases Bcl-2 gene expression, our results may also help explain the neuroprotection observed with progesterone.

10. Ahn, E.S., Robertson, C.L., Vereczki, V., Hoffman, G.E., and Fiskum G., Synthes Award for Resident Research on Brain and Craniofacial Injury: Normoxic ventilatory resuscitation after controlled cortical impact reduces peroxynitrite-mediated protein nitration in the hippocampus. Clin Neurosurg. 52: 348-356 (2005). (PMID:16626092)

Ventilatory resuscitation with 100% O2 is routinely administered after severe TBI to prevent early hypoxemia. In addition, the use of normobaric hyperoxia after severe TBI has recently been supported for the main therapeutic goal of shifting from anaerobic metabolism to aerobic metabolism in the injured brain. Other investigators have called into question this metabolic benefit. Furthermore, the use of normobaric hyperoxia heightens the concern for oxygen toxicity and ROS-mediated damage to the brain. Our results show that rats administered 100% O2 for 1 hour after CCI had significantly increased levels of ROS-mediated damage to proteins in the CA1 and CA3 regions of the hippocampus when compared with rats administered room air. Levels of ROS-mediated protein nitration in the normoxic group were no different than those of non-injured rats. Additionally, there was no beneficial effect of hyperoxic resuscitation on neuronal survival or abnormal neuronal morphology 1 week after injury. These results warrant additional caution in the empiric use of hyperoxic resuscitation in the treatment of severe TBI. If future studies support this concern for increased ROS-mediated damage with hyperoxia, then efforts will need to be made toward early adjustments in the O2 concentration administered during resuscitation after severe TBI. This study addresses the controversy about the use of high inspired O2 following TBI, indicating that it can indeed exacerbate oxidative damage to the brain. These findings reinforce the need for therapeutic interventions that target oxidative stress, e.g., progesterone.

11. Mehrabian, Z., Liu, L.-I., Fiskum, G., Rapoport, S.I., Chandrasekaran, K., Regulation of mitochondrial gene expression by energy demand in neural cells, J. Neurochem. 93:850-860 (2005). (PMID:15857388)

MitochondrialDNA (mtDNA) encodes critical subunit proteins of the oxidative phosphorylation (OXPHOS) complex that generates ATP. This study tested the hypothesis that mitochondrial gene expression in neural cells is regulated by energy demand, as modified via stimulation of

cellular sodium transport. Exposure of primary cerebellar neuronal cultures to the excitatory amino acid glutamate caused a rapid and significant increase followed by a significant decrease in cell mt-mRNA levels. These results suggest a physiological transcriptional mechanism of regulation of mitochondrial gene expression by energy demand and a post-transcriptional regulation that is independent of energy status of the cell. Although not included in the publication, we tested for effects of progesterone on mitochondrial gene expression in these experiments and found that it had no detectable effects. These findings do not support the hypothesis that neuroprotection by progesterone is mediated by stimulation of mitochondrial gene expression.

12. Martin, E., Rosenthal, R.E., and Fiskum, G., Pyruvate dehydrogenase complex: Metabolic link to ischemic brain injury and target of oxidative stress, J. Neurosci. Res. 79:240-247 (2005). (PMID:15562436)

The mammalian pyruvate dehydrogenase complex (PDHC) is a mitochondrial matrix enzyme complex (greater than 7 million Daltons) that catalyzes the oxidative decarboxylation of pyruvate to form acetyl CoA, nicotinamide adenine dinucleotide (the reduced form, NADH), and CO2. This reaction constitutes the bridge between anaerobic and aerobic cerebral energy metabolism. PDHC enzyme activity and immunoreactivity are lost in selectively vulnerable neurons after cerebral ischemia and reperfusion. Evidence from experiments carried out in vitro suggests that reperfusion-dependent loss of activity is caused by oxidative protein modifications. Impaired enzyme activity may explain the reduced cerebral glucose and oxygen consumption that occurs after cerebral ischemia. This hypothesis is supported by the hyperoxidation of mitochondrial electron transport chain components and NAD(H) that occurs during reperfusion, indicating that NADH production, rather than utilization, is rate limiting. Additional support comes from the findings that immediate postischemic administration of acetyl-L-carnitine both reduces brain lactate/pyruvate ratios and improves neurologic outcome after cardiac arrest in animals. As acetyl-L-carnitine is converted to acetyl CoA, the product of the PDHC reaction, it follows that impaired production of NADH is due to reduced activity of either PDHC or one or more steps in glycolysis. Impaired cerebral energy metabolism and PDHC activity are associated also with neurodegenerative disorders including Alzheimer's disease and Wernicke-Korsakoff syndrome, suggesting that this enzyme is an important link in the pathophysiology of both acute brain injury and chronic neurodegeneration. This review stresses the use of "alternative biofuels", e.g., acetyl-L-carnitine, as neuroprotectants, based on their compensation for impaired brain pyruvate dehydrogenase activity during acute and chronic neurodegeneration.

13. Schuh, R.A., Kristian, T., Gupta, R.K., Flaws, J.A., and Fiskum, G., Methoxychlor inhibits brain mitochondrial respiration and increases hydrogen peroxide production and CREB phosphorylation, Toxicol. Sci., 88: 495-504 (2005). (PMID:16177237)

The organochlorine insecticide methoxychlor (mxc) is an established reproductive toxicant that affects other systems including the central nervous system (CNS), possibly by mechanisms involving oxidative stress. This study tested the hypothesis that mxc inhibits brain mitochondrial respiration, resulting in increased production of reactive oxygen species (ROS). Similarly, state 3 respiration was inhibited following in vivo mxc exposure using complex I substrates. H2O2 production was stimulated after in vitro mxc treatment in the presence of complex I substrates,

but not in mitochondria isolated from in vivo mxc-treated mice. Because previous studies demonstrated a relationship between oxidative stress and CREB phosphorylation, we also tested the hypothesis that mxc elevates phosphorylated CREB (pCREB) in mitochondria. Enzyme-linked immunosorbent assay (ELISA) measurements demonstrated that pCREB immunoreactivity was elevated by in vitro mxc exposure in the presence or absence of respiratory substrates, indicating that stimulation of H2O2 production is not necessary for this effect. These multiple effects of mxc on mitochondria may play an important role in its toxicity, particularly in the CNS. This study focuses on mitochondria as a target of neurotoxicity by methoxychlor, a common pesticide used widely around the world. The described effects of methoxychlor on mitochondrial respiration and ROS production are similar to those observed with rotenone and paraquat, two toxins that are strongly implicated in the cause of sporadic Parkinson's disease

14. Soane, L. and Fiskum, G., Inhibition of mitochondrial neural cell death pathways by protein transduction of Bcl-2 family proteins, J. Bioenerg. Biomemb. 95: 230-243 (2005). (PMID: 16167175)

Bcl-2 and other closely related members of the Bcl-2 family of proteins inhibit the death of neurons and many other cells in response to a wide variety of pathogenic stimuli. Bcl-2 inhibition of apoptosis is mediated by its binding to pro-apoptotic proteins, e.g., Bax and tBid, inhibition of their oligomerization, and thus inhibition of mitochondrial outer membrane pore formation, through which other pro-apoptotic proteins, e.g., cytochrome c, are released to the cytosol. Bcl-2 also exhibits an indirect antioxidant activity caused by a sub-toxic elevation of mitochondrial production of reactive oxygen species and a compensatory increase in expression of antioxidant gene products. While classic approaches to cytoprotection based on Bcl-2 family gene delivery have significant limitations, cellular protein transduction represents a new and exciting approach utilizing peptides and proteins as drugs with intracellular targets. The mechanism by which proteins with transduction domains are taken up by cells and delivered to their targets is controversial but usually involves endocytosis. The effectiveness of transduced proteins may therefore be limited by their release from endosomes into the cytosol. Considering the fact that progesterone and other agents exert their neuroprotection through stimulation of Bcl-2 gene expression, this review covers the possibilities of using protein transduction techniques to stimulate uptake of exogenous Bcl-2 directly into cells.

15. Chinopoulos, C., Starkov, A.A., Grigoriev, S., Dejean, L.M., Kinnally, K.W., Liu, X., Ambudkar, I.S., and Fiskum, G., Diacylglycerols activate mitochondrial cationic channel(s) and release sequestered Ca^{2+}, J. Bioenerg. Biomemb., 37: 237-247 (2005). (PMID:16167179)

Mitochondria contribute to cytosolic Ca2+ homeostasis through several uptake and release pathways. Here we report that 1,2-sn-diacylglycerols (DAGs) induce Ca2+ release from Ca2+-loaded mammalian mitochondria. Patch clamping brain mitoplasts reveal DAGs-induced slightly cation-selective channel activity that is insensitive to bongkrekic acid and abolished by La3+. The presence of a second messenger-sensitive Ca2+ release mechanism in mitochondria could have an important impact on intracellular Ca2+ homeostasis. This study describes a completely new trigger for release of mitochondria that is connected with phosphoinositide signal

transduction. Interestingly, a recent article indicates that high-physiologic levels of progesterone inhibit opening of ion channels regulated by this pathway.

16. Schuh, R., Kristian, T., and Fiskum, G., Calcium-dependent dephosphorylation of brain mitochondrial calcium/cAMP response element binding protein, J. Neurochem. 92:388-394 (2005). (PMID:15663486)

Calcium-mediated signaling regulates nuclear gene transcription by calcium/cAMP response element binding protein (CREB) via calcium-dependent kinases and phosphatases. This study tested the hypothesis that CREB is also present in mitochondria and subject to dynamic calcium-dependent modulation of its phosphorylation state. These results further suggest that mitochondrial CREB is located in the matrix or inner membrane and that a kinase and a calcium-dependent phosphatase regulate its phosphorylation state. A recent study indicates that progesterone receptors act together with at least nuclear CREB to stimulate expression of the anti-apoptotic gene bcl-x. It remains to be determined if progesterone receptors interact with mitochondrial CREB.

17. Robertson, C.L., Puskar, A., Hoffman, G.E., Murphy, A.Z., Saraswati, M., and Fiskum, G., Physiologic progesterone reduces mitochondrial dysfunction and hippocampal cell loss after traumatic brain injury in female rats, Exp. Neurol. 197: 235-243 (2006). (PMID:16259981)

Growing literature suggests important sex-based differences in outcome following traumatic brain injury (TBI) in animals and humans. Progesterone has emerged as a key hormone involved in many potential neuroprotective pathways after acute brain injury and may be responsible for some of these differences. Many studies have utilized supraphysiologic levels of post-traumatic progesterone to reverse pathologic processes
after TBI, but few studies have focused on the role of endogenous physiologic levels of progesterone in neuroprotection. We hypothesized that progesterone at physiologic serum levels would be neuroprotective in female rats after TBI and that progesterone would reverse early mitochondrial dysfunction seen in this model. Progesterone in the low physiologic range reversed the early postinjury alterations seen in mitochondrial respiration and reduced hippocampal neuronal loss in both the CA1 and CA3 subfields.
Progesterone in the high physiologic range had a more limited pattern of hippocampal neuronal preservation in the CA3 region only. Neither progesterone dose significantly reduced cortical tissue loss. These findings have implications in understanding the sex-based differences in outcome following acute brain injury. This is the second highly important study supported by the grant which demonstrates neuroprotection by progesterone (against traumatic brain injury) and protection against early, post-injury mitochondrial dysfunction. These findings and those of others from several other laboratories form the basis for the current clinical trial (PROTECT) testing for neuroprotection by progesterone with traumatic brain injury patients.

4. **KEY RESEARCH ACCOMPLISHMENTS:** Bulleted list of key research accomplishments emanating from this research. Project milestones, such as simply completing proposed experiments, are not acceptable as key research accomplishments. Key research accomplishments are those that have contributed to the major goals and objectives and that have potential impact on the research field.

1. Twelve peer-reviewed published research articles and five peer-reviewed review articles
2. Demonstration that physiologic levels of progesterone protect against kainite-induced seizure activity and therefore kainite-induced neuronal death in rats.
3. Demonstration that physiologic progesterone protects against early mitochondrial bioenergetics dysfunction and delayed neuronal death caused by traumatic brain injury.
4. Demonstration that hyperoxic resuscitation after moderate traumatic brain injury in rats exacerbates oxidative modification of brain proteins, reinforcing the need for effective antioxidant interventions.
5. Documentation that the pesticide methoxychlor causes oxidative damage to the brain. This damage appears due to inhibition of Complex 1 of the mitochondrial electron transport chain, which stimulates mitochondrial production of superoxide.
6. Discovery that the alpha-ketoglutarate dehydrogenase complex of the mitochondrial Kreb's cycle is a major producer of reactive oxygen species.
7. Demonstration that anti-death proteins, e.g., Bcl-2, Bcl-x_L and Mcl-1, increase resistance of cells to oxidative stress by slightly increasing mitochondrial free radical production, which in turn result in stimulation of anti-oxidant gene expression.
8. Elucidation of the mechanism by which glutamate excitotoxicity results in delayed intraneuronal Ca2+ deregulation, which is the event that causes irreversible damage to neurons.
9. Demonstration that diacylglycerol, a common second messenger, can regulate Ca2+ release from mitochondria.
10. Demonstration that cellular energy demand stimulates mitochondrial gene expression in neural cells

5. CONCLUSION: Summarize the importance and/or implications with respect to medical and /or military significance of the completed research including distinctive contributions, innovations, or changes in practice or behavior that has come about as a result of the project. A brief description of future plans to accomplish the goals and objectives shall also be included.

The most translationally significant aspect of our research is the demonstration that progesterone protects against brain injury associated with status epilepticus and traumatic brain injury. These published findings taken together with many others from several other laboratories have led to clinical trials testing for neuroprotection by progesterone for traumatic brain injury. The two Phase II trials were encouraging. Two or more Phase III trials will be completed by the end of the year. Positive results from these trials will likely lead to progesterone neuroprotection trials for other forms of acute CNS injury and for neurodegenerative diseases, e.g., Parkinson's disease.

The additional more basic scientific discoveries we made have supported the general hypothesis that injury or toxin-induced mitochondrial bioenergetic dysfunction results in oxidative stress, contributing to both necrotic and apoptotic death of neurons and other cell

types. These findings are being used by many laboratories as a guide toward development of neuroprotective drugs and other interventions.

6. PUBLICATIONS, ABSTRACTS, AND PRESENTATIONS:

a. List all manuscripts submitted for publication during the period covered by this report resulting from this project. Include those in the categories of lay press, peer-reviewed scientific journals, invited articles, and abstracts. Each entry shall include the author(s), article title, journal name, book title, editors(s), publisher, volume number, page number(s), date, DOI, PMID, and/or ISBN.

Peer-reviewed publications in scientific journals

1. Starkov, A.A., Polster, B.M., and Fiskum, G., Regulation of mitochondrial reactive oxygen species generation by calcium and Bax., J. Neurochem. 83, 220-228 (2002). (PMID:12358746)

2. Fiskum, G., Starkov, A., Polster, B.M., and Chinopoulos, C., Mitochondrial mechanisms of neural cell death and neuroprotective interventions in Parkinson's disease, Ann. NY Acad. Sci. 991: 111-119 (2003). (PMID:12846980)

3. Hoffman, G.E., Moore, N., Fiskum, G., and Murphy, A.Z., Ovarian steroid modulation of seizure severity and hippocampal cell death after kainic acid treatment, Exp. Neurol. 182: 124-134 (2003). (PMID:12821382)

4. Starkov, A.A. and Fiskum, G., Regulation of brain mitochondrial H2O2 production by membrane potential and NAD(P)H redox state, J. Neurochem. 86: 1101-1107 (2003). (PMID:12911618)

5. Kowaltowski, A.J., Fenton, R.G., and Fiskum, G., Bcl-2 family proteins regulate mitochondrial reactive oxygen production and protect against oxidative stress, Free Rad. Biol. Med. 37: 1845-1853 (2004). (PMID:15538043)

6. Chinopoulos, C., Gerencser, A.A., Doczi, J., Fiskum, G., and Adam-Vizi. V., Inhibition of glutamate-induced delayed calcium deregulation by 2-APB and La^{3+} in cultured cortical neurons, J. Neurochem. 91: 471-483 (2004). (PMID:15447680)

7. Polster, B.M. and Fiskum, G., Mitochondrial mechanisms of neural cell apoptosis, J. Neurochem. 90: 1281-89 (2004). (PMID: 15341512)

8. Starkov, A.A., Fiskum, G., Chinopoulos, C., Lorenzo, B.J., Browne, S.E., Patel, M.S., and Beal, M.F., Mitochondrial alpha-ketoglutarate dehydrogenase complex generates reactive oxygen species, J. Neurosci. 24: 7779-7788 (2004). (PMID:15356189)

9. Fiskum, G., Rosenthal, R.E., Vereczki, V., Martin, E., Hoffman, G.E., Chinopoulos, C., and Kowaltowski, A., Protection against ischemic brain injury by inhibition of mitochondrial oxidative stress, J. Bioenerg. Biomemb. 36: 347-352 (2004). (PMID: 15377870)

10. Schuh, R.A., Kristian, T., Gupta, R.K., Flaws, J.A., and Fiskum, G., Methoxychlor inhibits brain mitochondrial respiration and increases hydrogen peroxide production and CREB phosphorylation, Toxicol. Sci., 88: 495-504 (2005). (PMID:16177237)

11. Martin, E., Rosenthal, R.E., and Fiskum, G., Pyruvate dehydrogenase complex: Metabolic link to ischemic brain injury and target of oxidative stress, J. Neurosci. Res. 79:240-247 (2005). (PMID:15562436)

12. Mehrabian, Z., Liu, L.-I., Fiskum, G., Rapoport, S.I., Chandrasekaran, K., Regulation of mitochondrial gene expression by energy demand in neural cells, J. Neurochem. 93:850-860 (2005). (PMID:15857388)

13. Ahn, E.S., Robertson, C.L., Vereczki, V., Hoffman, G.E., and Fiskum G., Synthes Award for Resident Research on Brain and Craniofacial Injury: Normoxic ventilatory resuscitation after controlled cortical impact reduces peroxynitrite-mediated protein nitration in the hippocampus. Clin Neurosurg. 52: 348-356 (2005). (PMID:16626092)

14. Chinopoulos, C., Starkov, A.A., Grigoriev, S., Dejean, L.M., Kinnally, K.W., Liu, X., Ambudkar, I.S., and Fiskum, G., Diacylglycerols activate mitochondrial cationic channel(s) and release sequestered Ca^{2+}, J. Bioenerg. Biomemb., 37: 237-247 (2005). (PMID:16167179)

15. Soane, L. and Fiskum, G., Inhibition of mitochondrial neural cell death pathways by protein transduction of Bcl-2 family proteins, J. Bioenerg. Biomemb. 95: 230-243 (2005). (PMID: 16167175)

16. Schuh, R., Kristian, T., and Fiskum, G., Calcium-dependent dephosphorylation of brain mitochondrial calcium/cAMP response element binding protein, J. Neurochem. 92:388-394 (2005). (PMID:15663486)

17. Robertson, C.L., Puskar, A., Hoffman, G.E., Murphy, A.Z., Saraswati, M., and Fiskum, G., Physiologic progesterone reduces mitochondrial dysfunction and hippocampal cell loss after traumatic brain injury in female rats, Exp. Neurol. 197: 235-243 (2006). (PMID:16259981)

b. List presentations made during the last year (international, national, local societies, military meetings, etc.). Use an asterisk (*) if presentation produced a manuscript.

7. INVENTIONS, PATENTS AND LICENSES: List all inventions made and patents and licenses applied for and/or issued. Each entry shall include the inventor(s), invention title,

patent application number, filing date, patent number if issued, patent issued date, national, or international.

NONE

8. **REPORTABLE OUTCOMES:** Provide a list of reportable outcomes that have resulted from this research. Reportable outcomes are defined as a research result that is or relates to a product, scientific advance, or research tool that makes a meaningful contribution toward the understanding, prevention, diagnosis, prognosis, treatment and /or rehabilitation of a disease, injury or condition, or to improve the quality of life. This list may include development of prototypes, computer programs and/or software (such as databases and animal models, etc.) or similar products that may be commercialized.

   NONE

9. **OTHER ACHIEVEMENTS:** This list may include degrees obtained that are supported by this award, development of cell lines, tissue or serum repositories, funding applied for based on work supported by this award, and employment or research opportunities applied for and/or received based on experience/training supported by this award.

   For each section, 4 through 9, if there is no reportable outcome, state "Nothing to report."

   1. The PhD dissertation research of Dr. Rosemary Schuh was partially supported by this award. She is now Assistant Professor of Neurology at the University of Maryland School of Medicine.
   2. The Neurosurgical Residency research requirement of Dr. Edward Ahn was partially supported by this award. He is now Assistant Professor of Neurosurgery at the Johns Hopkins University School of Medicine.
   3. This award partially supported the research of Dr. Courtney Robertson, who then received an NIH K08 mentored research training award. She is now Associate Professor of Anesthesiology and Critical Care and of Pediatrics at the Johns Hopkins University School of Medicine.
   4. The postdoctoral research of Dr. Christos Chinopoulos was partially supported by this award. He is now Adjunct Professor of Medical Biochemistry at the Semmelweis University, Budapest, Hungary.
   5. The postdoctoral research of Dr. Alicia Kowaltowski was partially supported by this award. She is now Professor of Biochemistry at the Universidade de São Paulo, Brazil.
   6. The postdoctoral research of Dr. Anatoly Starkov was partially supported by this award. He is now Associate Professor of Neurology at the Weil Medical College, Cornell University.

10. **REFERENCES:** List all references pertinent to the report using a standard journal format (i.e., format used in *Science*, *Military Medicine*, etc.).

11. **APPENDICES:** Attach all appendices that contain information that supplements, clarifies or supports the text. Examples include original copies of journal articles, reprints of

manuscripts and abstracts, a curriculum vitae, patent applications, study questionnaires, and surveys, etc.

APPENDIX

PUBLISHED MANUSCRIPTS

Journal of Neurochemistry, 2002, **83**, 220–228

Regulation of hydrogen peroxide production by brain mitochondria by calcium and Bax

Anatoly A. Starkov, Brian M. Polster and Gary Fiskum

Department of Anesthesiology, University of Maryland School of Medicine, Baltimore, Maryland, USA

Abstract

Abnormal accumulation of Ca^{2+} and exposure to pro-apoptotic proteins, such as Bax, is believed to stimulate mitochondrial generation of reactive oxygen species (ROS) and contribute to neural cell death during acute ischemic and traumatic brain injury, and in neurodegenerative diseases, e.g. Parkinson's disease. However, the mechanism by which Ca^{2+} or apoptotic proteins stimulate mitochondrial ROS production is unclear. We used a sensitive fluorescent probe to compare the effects of Ca^{2+} on H_2O_2 emission by isolated rat brain mitochondria in the presence of physiological concentrations of ATP and Mg^{2+} and different respiratory substrates. In the absence of respiratory chain inhibitors, Ca^{2+} suppressed H_2O_2 generation and reduced the membrane potential of mitochondria oxidizing succinate, or glutamate plus malate. In the presence of the respiratory chain Complex I inhibitor rotenone, accumulation of Ca^{2+} stimulated H_2O_2 production by mitochondria oxidizing succinate, and this stimulation was associated with release of mitochondrial cytochrome *c*. In the presence of glutamate plus malate, or succinate, cytochrome *c* release and H_2O_2 formation were stimulated by human recombinant full-length Bax in the presence of a BH3 cell death domain peptide. These results indicate that in the presence of ATP and Mg^{2+}, Ca^{2+} accumulation either inhibits or stimulates mitochondrial H_2O_2 production, depending on the respiratory substrate and the effect of Ca^{2+} on the mitochondrial membrane potential. Bax plus a BH3 domain peptide stimulate H_2O_2 production by brain mitochondria due to release of cytochrome *c* and this stimulation is insensitive to changes in membrane potential.

Keywords: apoptosis, BH3 domain, cytochrome *c*, membrane potential, respiration, superoxide.

J. Neurochem. (2002) **83,** 220–228.

Mitochondrial production of reactive oxygen species (ROS) is thought to contribute significantly to neuronal cell death caused by excitotoxicity and various acute and chronic neurological disorders, e.g. cerebral ischemia/reperfusion and Parkinson's disease (Benzi *et al*. 1982; Sciamanna *et al*. 1992; Dykens 1994; Fiskum *et al*. 1999; Murphy *et al*. 1999; Fiskum 2000; Nicholls and Budd 2000). Among other factors, mitochondrial accumulation of Ca^{2+} that occurs in response to these conditions has been reported to promote the generation of ROS (Dykens 1994; Kowaltowski *et al*. 1995; Kowaltowski *et al*. 1996; Kowaltowski *et al*. 1998a; Kowaltowski *et al*. 1998b; Fiskum 2000; Nicholls and Budd 2000). However, massive mitochondrial Ca^{2+} accumulation also inhibits the electron transport chain, potentially reducing the flow of electrons necessary for reduction of O_2 to superoxide anion and its metabolites, including H_2O_2 (Villalobo and Lehninger 1980). Mitochondrial Ca^{2+} sequestration also reduces the mitochondrial membrane potential ($\Delta\Psi$), which is thermodynamically linked to the redox potential of sites in the electron transport chain responsible for production of ROS. Although several reports have demonstrated that Ca^{2+} loading enhances ROS generation in brain (Dykens 1994) and liver (Kowaltowski *et al*. 1995; Kowaltowski *et al*. 1996; Kowaltowski *et al*. 1998a; Kowaltowski *et al*. 1998b) mitochondria, the mechanism responsible for this stimulation remains elusive.

Mitochondrial functions may also be perturbed during acute neural cell injury by redistribution of pro-apoptotic proteins, such as Bax and Bid, to mitochondrial membranes where permeability changes occur that result in release to the cytosol of other pro-apoptotic proteins, e.g. cytochrome *c* (Fiskum 2000). Release of cytochrome *c* has been associated with increased cellular oxidative stress (Cai and Jones 1998),

Received June 13, 2002; revised manuscript received July 25, 2002; accepted July 25, 2002.

Address correspondence and reprint requests to Dr Gary Fiskum, Department of Anesthesiology, University of Maryland School of Medicine, 685 W. Baltimore Street, MSTF-5.34, Baltimore, MD 21201, USA. E-mail: gfisk001@umaryland.edu

Abbreviations used: BSA, bovine serum albumin; FCCP, *p*-trifluoromethoxycarbonylcyanide phenylhydrazone; TPP, tetraphenyl phosphonium; ROS, reactive oxygen species.

although a direct cause and effect relationship between release and stimulated mitochondrial ROS generation has not been demonstrated.

One purpose of this study was to clarify the effect of Ca^{2+} uptake on ROS production by isolated brain mitochondria. Experiments were designed to test the hypothesis that Ca^{2+} can either stimulate or inhibit mitochondrial ROS generation, depending on the source of electrons donated to the respiratory chain, and the effects of Ca^{2+} accumulation on the retention of mitochondrial cytochrome *c*. Another aim of the study was to test the hypothesis that mitochondrial ROS production is stimulated by cytochrome *c* release elicited by exposure to Bax and a peptide containing a BH3 cell death domain.

Materials and methods

Reagents

Oligomycin, antimycin A3 and rotenone (Sigma, St Louis, MO, USA) were dissolved in ethanol, and Amplex Red (N-acetyl-3,7-dihydroxyphenoxazine; Molecular Probes, Eugene OR, USA) was dissolved in dimethylsulfoxide. All other reagents were purchased from Sigma. All reagents and ethanol were tested and exhibited no interference with the H_2O_2 assay at the concentrations used in our experiments. The sources of full-length human recombinant Bax protein and of the synthetic Bax BH3 domain peptide have been described previously (Fiskum and Polster 2001; Polster *et al*. 2001).

Isolation of brain mitochondria

All animal experiments were conducted in accordance with guidelines established by the Institutional Animal Care and Use Committee of the University of Maryland, Baltimore.

Non-synaptosomal rat forebrain mitochondria were isolated by the Percoll gradient separation method as described in (Sims 1990). The quality of the mitochondrial preparation was estimated by measuring the acceptor control ratio defined as ADP-stimulated (State 3) respiration divided by resting (State 4) respiration. For these experiments, the incubation medium consisted of 125 mM KCl, 20 mM HEPES (pH 7.0), 2 mM KH_2PO_4, 1 mM $MgCl_2$, 5 mM glutamate, 5 mM malate, plus 0.8 mM ADP. Oxygen consumption was recorded at 37°C with a Clark-type oxygen electrode. State 3 respiration was initiated by the addition of 0.5 mg per ml rat brain mitochondria to the incubation medium. State 3 respiration was terminated and State 4 initiated by the addition of 1 μM carboxyatractylate, an inhibitor of the ADP/ATP transporter. Only mitochondrial preparations that exhibited an acceptor control ratio greater than 8 were used in this study.

Measurement of H_2O_2

Incubation medium contained 125 mM KCl, 20 mM HEPES (pH 7.0), 2 mM KH_2PO_4, 4 mM ATP, 5 mM $MgCl_2$, 1 μM Amplex Red, 5 U/mL horseradish peroxidase superoxide dismutase (HRP) and 40 U/mL Cu,Zn SOD, and was maintained at 37°C, unless stated otherwise. A change in the concentration of H_2O_2 in the medium was detected by fluorescence of the oxidized Amplex Red product using excitation and emission wavelengths of 550 and 585 nm, respectively (Zhou *et al*. 1997). The response of Amplex Red to H_2O_2 was calibrated either by sequential additions of known amounts of H_2O_2 or by continuous infusion of H_2O_2 at 100–1000 pmol/min. The concentration of commercial 30% H_2O_2 solution was calculated from light absorbance at 240 nM employing $E_{240} = 43.6\ M^{-1} \times cm^{-1}$ $13.6\ M^{-1} \times cm^{-1}$; the stock solution was diluted to 100 μM with water and used for calibration immediately.

Cytochrome *c* release from mitochondria

Aliquots of mitochondrial suspensions were taken either during or at the end of experiments in which H_2O_2 generation was monitored. Mitochondria were separated from the suspending medium by centrifugation at 14 000*g* for 5 min. The supernatant was carefully removed and both the supernatant and mitochondrial pellet fractions were immediately frozen and stored at −20°C. Cytochrome *c* concentration was measured in both fractions using an ELISA kit (R & D Systems, Minneapolis, MN, USA). Before measurement, the supernatant and pellet samples were diluted 1 : 40 and 1 : 60, respectively. The release of cytochrome *c* from mitochondria was expressed as the content of cytochrome *c* in the supernatant as a percentage of the total content of cytochrome *c* present in the supernatant plus pellet.

Measurements of ΔΨ and extramitochondrial $[Ca^{2+}]$

Qualitative changes in ΔΨ were followed using the fluorescence of safranine (5 μM) with excitation and emission wavelengths of 495 nm and 586 nm, respectively (Votyakova and Reynolds 2001). A semiquantitative measurement of ΔΨ was estimated from TPP^+ ion distribution between the medium and mitochondria using a custom-made TPP^+-selective electrode (Kamo *et al*. 1979). For these experiments, incubation medium was supplemented with 1.6 μM TPP^+Cl^-. Both the TPP^+-sensitive and reference electrodes were inserted directly into the fluorimeter cuvette, and data were collected using an amplifier and a two-channel data acquisition system, with one channel acquiring the amplified TPP^+-electrode signal while another was dedicated to the Amplex Red fluorescence signal. The electrode response was calibrated by sequential addition of TPP^+Cl^- in the concentration range 0.2–1.6 μM, and the mitochondrial ΔΨ was calculated as described by Rolfe *et al*. (1994). Alternatively, ΔΨ values were calculated by the procedure reported by Rottenberg (1984), assuming that the matrix volume for brain mitochondria is 1.2 μL per mg protein. Both procedures yielded similar results.

Changes in the extramitochondrial medium free Ca^{2+} were followed using the fluorescence of Calcium Green 5N, with excitation and emission wavelengths of 506 nm and 532 nm, respectively.

Results

To measure relatively low rates of H_2O_2 production by brain mitochondria, we used a fluorescent dye/horseradish peroxidase detecting system employing the new peroxidase substrate Amplex Red, based on its high sensitivity and very low background fluorescence in the absence of a biological peroxide-generating system (Fig. 1a, curve 1). We also utilized an incubation medium that contained physiologically relevant concentrations of K^+, P_i, ATP and Mg^{2+}, as

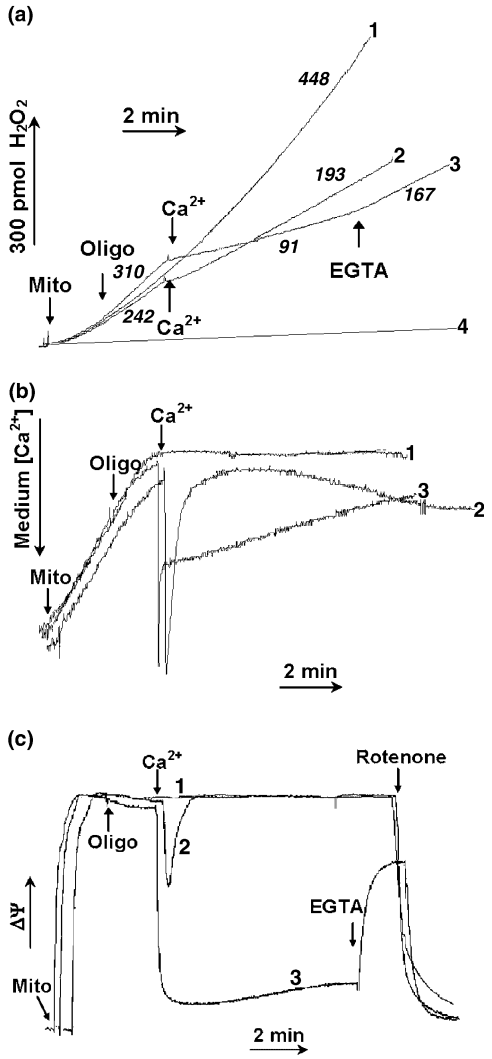

Fig. 1 Effects of Ca^{2+} uptake on ΔΨ and H_2O_2 production by brain mitochondria oxidizing glutamate and malate. Incubation medium maintained at 37°C was supplemented with 5 mM glutamate, 5 mM malate and either 1 μM Amplex Red (a), 100 nM Calcium Green 5N (b) or 5 μM safranin O (c) for measurements of H_2O_2, medium Ca^{2+} concentration or ΔΨ, respectively. Mitochondria (Mito) were added at 0.25 mg per mL mitochondria; Ca^{2+} at 0.2 mM; EGTA at 0.5 mM, oligomycin (Oligo) at 0.5 μg/mL, and rotenone at 0.5 μM. In tracings 1, no additions were made following the addition of mitochondria. In tracings 2, Ca^{2+} was added following the addition of mitochondria. In tracings 3, oligomycin was added before the addition of Ca^{2+}. In tracings 4, no mitochondria were added. The italicized numbers in (a) represent rates of H_2O_2 production in pmoles per minute per milligram mitochondrial protein.

these components exert dramatic effects on the response of respiring mitochondria to high levels of Ca^{2+} (Murphy *et al.* 1999). Under these conditions, brain mitochondria are resistant to catastrophic bioenergetic and morphological alterations caused by the Ca^{2+}-induced inner membrane permeability transition compared with, for example, liver mitochondria, but are still susceptible to Ca^{2+}-induced alterations in membrane potential and cytochrome *c* release across the outer membrane (Andreyev and Fiskum 1999).

Figure 1a curve 1 illustrates that isolated rat brain mitochondria respiring on the NAD-linked substrates glutamate and malate produce significant amounts of H_2O_2 in the absence of added Ca^{2+} or electron transport chain inhibitors. Under these conditions the medium contaminating free Ca^{2+} (approximately 5 μM or 20 nmol per mg protein), as measured by the fluorescent indicator Calcium Green 5 N, was accumulated by the added mitochondria and a steady-state medium [Ca^{2+}] was maintained for at least 10–15 min (Fig. 1b, curve 1). Parallel safranin O fluorescent measurements of ΔΨ indicated that ΔΨ stabilized within 2 min of the mitochondrial addition and remained constant for at least 15 min thereafter, but rapidly dissipated upon addition of the respiratory Complex I inhibitor rotenone (Fig. 1c, curve 1). When brain mitochondria were exposed to a single addition of Ca^{2+} (800 nmol per mg protein), H_2O_2 production was reduced by approximately 60% (193 vs. 448 pmol per mg protein) (Fig. 1a, curve 2). This amount of added Ca^{2+} was accumulated entirely by the rat brain mitochondria, followed by a slow and partial release back into the medium 5–10 min later (Fig. 1b, curve 2). The addition of Ca^{2+} resulted in a transient reduction in ΔΨ, as expected because mitochondrial Ca^{2+} uptake occurs via an electrophoretic uniporter that draws upon the ΔΨ for active Ca^{2+} sequestration. The reduction in ΔΨ (Fig. 1, curve 2) stimulates respiration-dependent H^+ efflux that, in turn, drives $H_2PO_4^-$ influx via the electroneutral $H_2PO_4^-/OH^-$ antiporter. Thus, electophoretic uptake of Ca^{2+} followed by electroneutral uptake of P_i results in a transient collapse of ΔΨ without an increase in pH. Approximately 1 min after the addition of Ca^{2+}, when most of it had been accumulated, ΔΨ recovered back to its initial level and remained stable for at least 10 min.

Mitochondrial Ca^{2+} uptake can be driven by electrogenic H^+ efflux mediated by the mitochondrial F_oF_1 ATPase in addition to H^+ extrusion mediated by the electron transport chain. Experiments were therefore performed in the presence of oligomycin, a specific inhibitor of the mitochondrial ATPase, to determine the influence of ATPase activity on mitochondrial Ca^{2+} uptake, ΔΨ and H_2O_2 production. In the presence of oligomycin, the rate of H_2O_2 production before Ca^{2+} addition was slightly higher than in its absence (310 vs. 242 pmol per mg protein). However, following the addition of Ca^{2+}, the rate of H_2O_2 production was approximately 50% of that in its absence (91 vs. 193 pmol per mg protein), and only 20% of that observed in the absence of added Ca^{2+} (91 vs. 448 pmol per mg protein) (Fig. 1a, curve 3). In the presence of oligomycin, mitochondrial Ca^{2+} uptake was initially as, or more, rapid than in its absence but converted to a relatively very slow, sustained rate of net uptake within a minute after the addition of Ca^{2+} (Fig. 1b, curve 3). The presence of oligomycin also resulted in a greater decline in

$\Delta\Psi$ upon addition of Ca^{2+} and a sustained reduction in $\Delta\Psi$ for at least 8 min (Fig. 1c, curve 3). The Ca^{2+}-dependent reduction in $\Delta\Psi$ was partially reversed by the subsequent addition of the Ca^{2+} chelator EGTA (Fig. 1c, curve 3), as was the Ca^{2+}-dependent reduction in H_2O_2 production (Fig. 1a, curve 3). Thus, ATPase-mediated electrogenic H^+ efflux contributes to the maintenance of $\Delta\Psi$ during and following mitochondrial uptake of large Ca^{2+} loads, but is incapable of completely sustaining $\Delta\Psi$ in the absence of respiration.

Mitochondrial ROS production was much faster with Complex II-linked substrate succinate compared with Complex I-dependent substrates. Within 2 min following the addition of rat brain mitochondria to the incubation medium containing 5 mM succinate, there was a dramatic increase in H_2O_2 production (Fig. 2a), at a rate that was seven to eight times faster than that observed in the presence of glutamate plus malate (1700–2000 vs. 250 pmol per mg mitochondrial protein). The delayed activation of succinate-supported H_2O_2 production corresponded to the time at which the $\Delta\Psi$ reached its maximum level following addition of mitochondria to the medium (Fig. 2b) (Korshunov *et al.* 1997). Subsequent addition of 0.2 mM Ca^{2+} resulted in an immediate and almost complete inhibition of H_2O_2 production (68 vs. 1760 pmol per mg protein) (Fig. 2a, curve 1). At this level of Ca^{2+}, $\Delta\Psi$ was transiently reduced then recovered, albeit to a level that was lower than that maintained in the absence of added Ca^{2+} (Fig. 2b, curve 1). Whereas EGTA significantly reversed the effect of Ca^{2+} on ROS production and $\Delta\Psi$ in the presence of Complex I-linked substrates, it was unable to reverse the effects of Ca^{2+} in the presence of the Complex II substrate succinate (Figs 2a and b, curves 1).

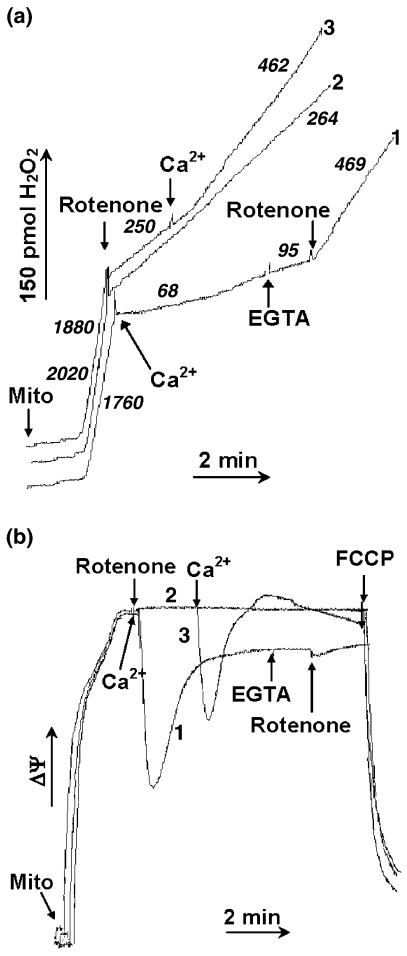

Fig. 2 Effects of Ca^{2+} uptake on $\Delta\Psi$ and H_2O_2 production by brain mitochondria oxidizing succinate. Incubation medium maintained at 37°C was supplemented with 5 mM succinate and either 1 μM Amplex Red (a) or 5 μM safranin O (b) for measurements of H_2O_2 or $\Delta\Psi$, respectively. Mitochondria (Mito) were added at 0.125 mg per mL mitochondria; Ca^{2+} at 0.2 mM; EGTA at 0.5 mM, rotenone at 0.5 μM and FCCP at 50 nM. The italicized numbers in panel (a) represent rates of H_2O_2 production in pmoles per minute per milligram mitochondrial protein.

The Complex I inhibitor rotenone was capable of stimulating mitochondrial H_2O_2 production in the presence of Ca^{2+} but had a negligible effect on the Ca^{2+}-induced reduction of $\Delta\Psi$ (Figs 2a and b, curves 1), as expected as rotenone inhibits NAD-linked but not succinate-supported respiration. The rate of H_2O_2 production observed following the addition of Ca^{2+} and then rotenone was still far lower than the initial rate observed in the absence of both agents (469 vs. 1760 pmol per mg protein). This finding verifies the contribution of rotenone-sensitive reversed electron flow through Complex I as a major site of ROS production supported by succinate (Hinkle *et al.* 1967; Hansford *et al.* 1997; Korshunov *et al.* 1997; Turrens 1997; Lass *et al.* 1998; Votyakova and Reynolds 2001; Liu *et al.* 2002). However, in the absence of added Ca^{2+}, the addition of rotenone resulted in a rate of H_2O_2 production that was substantially lower than that following the addition of Ca^{2+} (264 vs. 469 pmol per mg protein; Fig. 2a, curve 2). This stimulatory effect of Ca^{2+} on succinate-supported H_2O_2 production in the presence of rotenone was further verified by the addition of Ca^{2+} following rotenone, after which the rate of H_2O_2 production increased from 250 to 462 pmol per mg protein (Fig. 2a, curve 3). In contrast to the sustained reduction in $\Delta\Psi$ observed upon addition of Ca^{2+} in the absence of rotenone, mitochondrial Ca^{2+} uptake in the presence of rotenone resulted in the normal transient drop in $\Delta\Psi$ followed by a complete recovery and a subsequent steady but minor depolarization (Fig. 2b, curve 3). These results further demonstrate that when exposure of mitochondria to high levels of Ca^{2+} results in a reduction in $\Delta\Psi$, ROS production is inhibited. Under conditions in which ROS production is independent of $\Delta\Psi$, e.g. in the presence of rotenone, Ca^{2+} can actually stimulate ROS production.

Experiments were then performed to test the hypothesis that a reduction in $\Delta\Psi$ is a sufficient explanation for the inhibition of H_2O_2 production by Ca^{2+} with either succinate or the NAD-linked substrates glutamate and malate. It is

known that succinate-supported H_2O_2 production is inhibited by mitochondrial depolarization (Hansford *et al*. 1997; Korshunov *et al*. 1997). The dependence of succinate-supported ROS generation on $\Delta\Psi$ is due to the reverse electron transport from Complex II through coenzyme Q to Complex I. The potential energy of $\Delta\Psi$ is necessary to overcome the redox potential difference between Complex I and coenzyme Q that promotes Complex I oxidation and coenzyme Q reduction. Although the quantitative relationship between $\Delta\Psi$ and ROS production during succinate-dependent reversed electron transport is established (Korshunov *et al*. 1997), it has not been determined for ROS generation that occurs during electron transport driven by NAD-linked substrates. This relationship was explored by measuring mitochondrial H_2O_2 production in the presence of glutamate and malate and in the presence of several concentrations of FCCP, a protonophoric uncoupling agent. In order to demonstrate a quantitative relationship, the experimental system utilized the mitochondrial uptake of the lipophilic cation TPP^+ as a measure of $\Delta\Psi$. The system was also simplified by omitting ATP from the medium and adding the Ca^{2+} chelator EGTA to prevent possible interference from contaminating Ca^{2+} in the medium. The results shown in Fig. 3 indicated that H_2O_2 production supported by oxidation of NAD-linked substrates is indeed dependent on $\Delta\Psi$, being very sensitive to fluctuations in $\Delta\Psi$ between approximately 150 and 180 mV. These results however, also demonstrate that approximately 30% of the maximal H_2O_2 production is insensitive to $\Delta\Psi$.

The reduction in $\Delta\Psi$ caused by mitochondrial Ca^{2+} accumulation is a sufficient explanation for the inhibition by Ca^{2+} of H_2O_2 production both with succinate (in the absence of rotenone) or NAD-linked substrates. This effect cannot, however, explain the increase in succinate-supported H_2O_2 generation caused by Ca^{2+} in the presence of the Complex I inhibitor rotenone. We hypothesized that Ca^{2+}-induced cytochrome *c* release might be responsible for this phenomenon because cytochrome *c* release has been associated with increased oxidative stress in apoptotic cells (Cai and Jones 1998), and cytochrome *c* is released by brain mitochondria in response to Ca^{2+} uptake under conditions similar to those used in the current study (Andreyev *et al*. 1998; Andreyev and Fiskum 1999). A comparison between rates of H_2O_2 production and the distribution of cytochrome *c* between the mitochondria and the suspending medium at the end of the H_2O_2 measurements is provided in Figs 4 and 5 for succinate (in the presence of rotenone) and glutamate plus malate, respectively. The accumulation of Ca^{2+} resulted in a net 10% release of cytochrome *c* in the presence of succinate and 5% release in the presence of glutamate plus malate. This was accompanied by an approximately 60% increase in H_2O_2 formation with succinate and a greater than 60% reduction in H_2O_2 with glutamate and malate. Thus Ca^{2+} induces the release of mitochondrial cytochrome *c* in the presence of either malate plus glutamate or succinate but only stimulates H_2O_2 production when succinate is present as the electron donor and rotenone is present to inhibit reversed electron transport that is driven by $\Delta\Psi$.

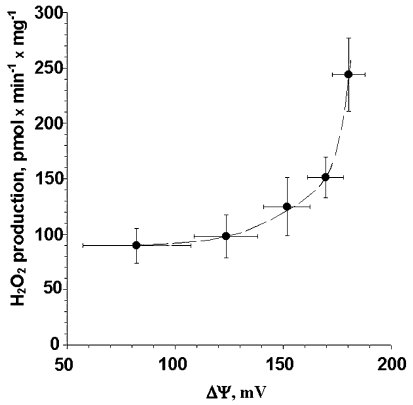

Fig. 3 Relationship between rate of H_2O_2 production and $\Delta\Psi$ for brain mitochondria oxidizing glutamate and malate. Mitochondria were added at a concentration of 0.25 mg/mL to the standard incubation medium except that ATP was omitted, $MgCl_2$ was present at 1 mM, and the medium was supplemented with 0.25 mM EGTA, 1.6 μM TPP^+Cl^-, 5 mM glutamate and 5 mM malate. A TPP^+ electrode was used to measure the medium TPP^+ concentration both in the absence of FCCP and in the presence of 22, 47, 76 and 110 pmol FCCP per mg mitochondrial protein to modulate the $\Delta\Psi$. Values for $\Delta\Psi$ were calculated as described in Materials and Methods. Values represent means ± SE of four independent experiments.

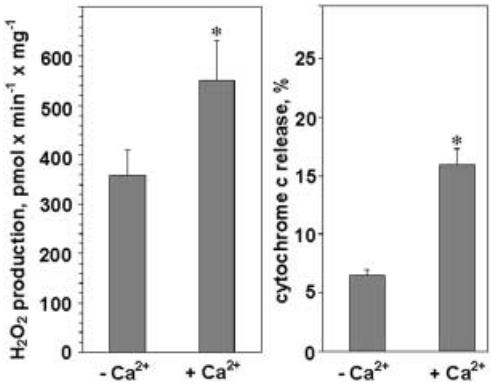

Fig. 4 Ca^{2+}-induced cytochrome *c* release and stimulation of H_2O_2 production by brain mitochondria oxidizing succinate. Mitochondria were added at a concentration of 0.25 mg/mL to the standard incubation medium maintained at 37°C and supplemented with 5 mM succinate. As in Fig. 2, approximately 3 min later, rotenone (0.2 μM) was added, followed 2 min later by either Ca^{2+} (0.2 mM) or vehicle control (H_2O). The rate of H_2O_2 production was determined by the rate of increase in Amplex Red fluorescence. At approximately 8 min following the addition of Ca^{2+}, the suspension was centrifuged and the pellet and supernatant fractions used for ELISA of cytochrome *c* content, as described in Materials and Methods. Values represent the mean ± SE of four independent experiments. *$p < 0.05$ versus without Ca^{2+} by Student's *t*-test.

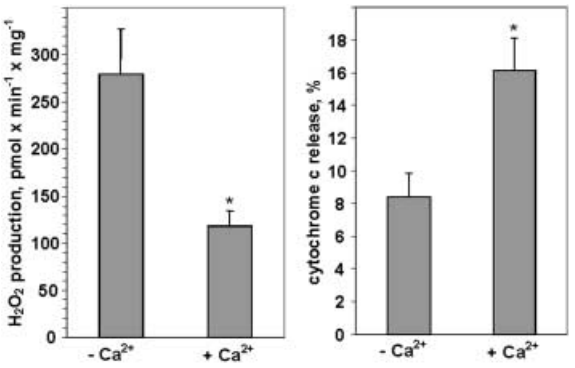

Fig. 5 Ca^{2+}-induced cytochrome *c* release and inhibition of H_2O_2 production by brain mitochondria oxidizing glutamate and malate. Mitochondria were added at a concentration of 0.25 mg/mL to the standard incubation medium maintained at 37°C and supplemented with 5 mM glutamate and 5 mM malate. As in Fig. 1, approximately 4 min later, Ca^{2+} (0.2 mM) or vehicle control (H_2O) were added and the rate of H_2O_2 production was determined by the rate of increase in Amplex Red fluorescence. At approximately 10 min following the addition of Ca^{2+}, the suspension was centrifuged and the pellet and supernatant fractions were used for ELISA of cytochrome *c* content, as described in Materials and Methods. Values represent the mean ± SE of four independent experiments. *$p < 0.05$ versus without Ca^{2+} by Student's *t*-test.

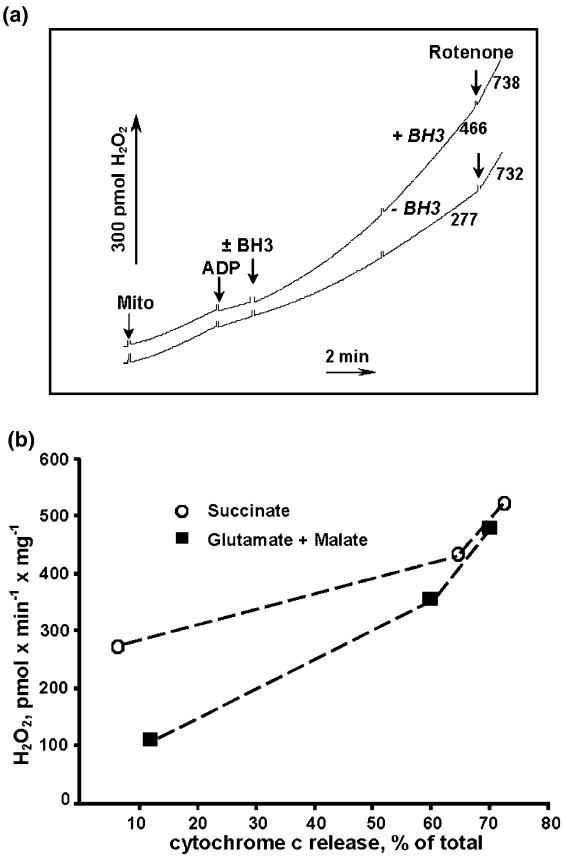

Fig. 6 Stimulation of cytochrome *c* release and H_2O_2 production by brain mitochondria by addition of Bax plus a BH3 domain peptide. Mitochondria were added at a concentration of 0.125 mg/mL to the standard incubation medium maintained at 37°C and supplemented with either 5 mM glutamate and 5 mM malate or 5 mM succinate. (a) Amplex Red measurements of H_2O_2 generation. At approximately 3 min following addition of brain mitochondria to media containing glutamate and malate and 100 nM Bax (see Materials and methods), 0.1 mM ADP was added to initiate State 3 respiration. Approximately 2 min later, 50 μM BH3 peptide or vehicle control (H_2O) was added. Rotenone (0.2 μM) was added 9 min later to elicit maximal H_2O_2 production. (b) Relationship between H_2O_2 production and release of cytochrome *c* caused by exposure of brain mitochondria to Bax plus a BH3 peptide. In experiments such as that shown in (a) aliquots of the mitochondrial suspension were removed before and two or three times after addition of the BH3 peptide or vehicle, centrifuged and used for ELISA of cytochrome *c* release from the mitochondria into the medium. The corresponding rate of H_2O_2 production refers to the rate obtained just before removal of the aliquot for cytochrome *c* measurement. Experiments were performed either in the presence of 5 mM succinate (○) or 5 mM glutamate and 5 mM malate (■).

Additional evidence for the direct role of cytochrome *c* release in stimulating mitochondrial ROS formation came from experiments in which release was mediated by exposure of brain mitochondria to the pro-apoptotic protein Bax together with a synthesized peptide that contains the BH3 death domain amino acid sequence. We previously demonstrated that this peptide triggers Bax-dependent release of cytochrome *c* by specifically increasing the permeability of the mitochondrial outer membrane without affecting inner membrane permeability or other components of the electron transport chain (Polster *et al.* 2001). Figure 6a provides representative fluorescent measurements of H_2O_2 generation by rat brain mitochondria respiring on glutamate and malate in the presence of 100 nM human recombinant full-length Bax and in the absence or presence of 50 μM BH3 peptide. In the absence of the peptide, H_2O_2 produced in the presence of Bax was identical to that in its absence (not shown). In these experiments, ADP was added to the suspension, inducing State 3 respiration. Under these conditions, the redox state of potential sites of ROS production is relatively oxidized and therefore inhibition of electron transport by release of cytochrome *c* should cause a maximal shift toward a reduced redox state. In the absence of BH3 peptide, H_2O_2 formation increased slowly over approximately 10 min and was stimulated by over 100% upon addition of the Complex I inhibitor rotenone (732 vs. 277 pmol per min per mg protein). The rate of H_2O_2 generation observed 10 min following the addition of the BH3 peptide was 70% greater than the timed control (466 vs. 277 pmol per min per mg protein) and was further stimulated by the addition of rotenone. In the absence of added Bax, BH3 peptide had no effect on ROS production by adult rat brain mitochondria (not shown), consistent with its inability to release cytochrome *c* from these mitochondria in the absence of exogenous Bax (Polster *et al.* 2001). Thus, in contrast to

the inhibition of H_2O_2 production by added Ca^{2+} when NAD-linked respiratory substrates were present (Fig. 1a), the presence of Bax plus a BH3 peptide substantially stimulates mitochondrial H_2O_2 formation. An approximately 70% stimulation of H_2O_2 formation by Bax plus the BH3 peptide was observed in the presence of succinate plus rotenone (not shown). Thus, cytochrome *c* release *per se* stimulates mitochondrial ROS generation in the presence of either Complex I or Complex II respiratory substrates.

As the rate of H_2O_2 production was non-linear during the course of these experiments and as Bax–BH3-mediated cytochrome *c* release takes several minutes to occur, we took aliquots of the mitochondrial suspension during the course of the H_2O_2 measurements for quantification of cytochrome *c* distribution to determine if a relationship exists between the extent of release and the rate of H_2O_2 formation. These aliquots were taken immediately before the addition of the BH3 peptide or vehicle and 5 and 8 min later. The extent of cytochrome *c* release and the corresponding rates of H_2O_2 generation measured just before sampling using glutamate and malate or succinate (in the presence of rotenone) are presented in Fig. 6b. The H_2O_2 production rate was greater for mitochondria respiring on succinate than on glutamate and malate in the absence of BH3 peptide with background release of 5–12% of the total cytochrome *c*. However, after 5 min exposure to the BH3 peptide, the extent of cytochrome *c* release was similar under these two conditions (60–65%), as were the rates of H_2O_2 formation (360–420 pmol per min per mg protein). An additional 3-min exposure to the BH3 peptide resulted in an additional approximately 10% release of cytochrome *c* and rates of H_2O_2 production that were very similar for the two sets of respiratory substrates (466–520 pmol per min per mg protein). These results indicate that the release of cytochrome *c* by Bax plus a BH3 peptide results in a dose-dependent stimulation of mitochondrial ROS formation under physiologically relevant *in vitro* conditions with either succinate or NAD-linked respiratory substrates.

Discussion

The main conclusion that can be drawn from this study is that when $\Delta\Psi$ is reduced with mitochondria respiring on either NAD-linked substrates or succinate in the absence of rotenone, ROS production is inhibited (Figs 1, 2, 3 and 5). Conversely, the release of cytochrome *c* by either mitochondrial Ca^{2+} accumulation or by exposure to Bax and a BH3 domain peptide can significantly stimulate mitochondrial ROS production apparently independently of $\Delta\Psi$ (Figs 2, 4 and 6). These observations were made *in vitro* in the absence of respiratory inhibitors and in the presence of physiologically relevant levels of ATP, Mg^{2+} and other ions that have a profound influence on mitochondrial energy coupling and on mitochondrial responses to raised levels of Ca^{2+}. We therefore believe that these observations may be highly relevant to the effects of both pathological levels of Ca^{2+} and the apoptotic redistribution of Bax and BH3 domain proteins that occurs in response to many forms of neuronal stress.

The modulation of mitochondrial ROS generation observed in the presence of NAD-linked oxidizable substrates is particularly important as these substrates constitute the primary source of fuel for oxidative cerebral energy metabolism. In the presence of ATP, the uptake of Ca^{2+} inhibited H_2O_2 generation (Figs 1 and 5). This inhibition appears to be due to more than one mechanism, as indicated by differences in Ca^{2+}-induced mitochondrial depolarization and inhibition of ROS production in the absence and presence of oligomycin (Fig. 1). When ATP turnover was blocked by oligomycin, Ca^{2+} caused a substantial collapse in $\Delta\Psi$ and $\sim 60\%$ inhibition of H_2O_2 generation. In the absence of oligomycin, Ca^{2+} accumulation resulted in no sustained reduction in $\Delta\Psi$ but ROS generation was still inhibited by $\sim 80\%$. As independent experiments performed in the absence of Ca^{2+} and in the presence of different concentrations of the protonophore uncoupler FCCP demonstrated that $> 50\%$ of NAD-linked ROS production is sensitive to $\Delta\Psi$ (Fig. 3), we conclude that mitochondrial depolarization is one of the mechanisms by which Ca^{2+} inhibits H_2O_2 formation. Votyakova and Reynolds (2001) reported previously that the presence of an uncoupler does not stimulate NAD-linked mitochondrial ROS production; however, the rates of H_2O_2 generation they observed using the scopoletin method of detection were too low to detect any inhibitory influence of membrane depolarization. The mechanism by which loss of $\Delta\Psi$ reduces mitochondrial H_2O_2 formation probalby involves the oxidation of redox centers, e.g. coenzyme Q or iron-sulfur proteins, which probably mediate the generation of superoxide and therefore H_2O_2.

Ca^{2+}-induced mitochondrial depolarization cannot explain the inhibition of NAD-linked H_2O_2 formation observed in the absence of oligomycin as $\Delta\Psi$ was fully preserved (Fig. 1). One possible explanation for this $\Delta\Psi$-independent inhibition is that Ca^{2+} may impair the flow of electrons within the electron transport chain at a site, most likely within Complex I, that is proximal to the site of ROS generation. Evidence for selective impairment of NAD-linked respiration by Ca^{2+} was originally reported for ascites tumor cell mitochondria (Villalobo and Lehninger 1980), and more recently for neural cell mitochondria (Murphy *et al.* 1996). Although such inhibition could be caused by release of mitochondrial NAD(H) mediated by the Ca^{2+}-activated permeability transition (Maciel *et al.* 2001), it is clear from the maintenance of $\Delta\Psi$ that the permeability transition did not occur under these conditions.

Mitochondrial Ca^{2+} uptake had an even greater inhibitory effect on succinate-driven H_2O_2 production than on

NAD-linked ROS generation (Fig. 2). The explanation for the greater inhibition with succinate is that Ca^{2+}-induced loss of $\Delta\Psi$ deprives mitochondria of the energy required for reverse transport of electrons from Complex II through coenzyme Q to Complex I where sites of succinate-based ROS formation are located (Korshunov *et al*. 1997; Turrens 1997; Lass *et al*. 1998; Liu *et al*. 2002). The most novel observation made with succinate as the respiratory substrate in the presence of rotenone was that Ca^{2+} actually stimulated H_2O_2 production. Under these conditions, Ca^{2+}-induced changes in $\Delta\Psi$ were not expected to affect H_2O_2 production as reverse electron transport is inhibited by the presence of rotenone. Therefore, Ca^{2+}-induced release of cytochrome *c* was pursued as a possible mechanism for its stimulation of H_2O_2 generation.

Quantitative analysis of the extent of cytochrome *c* released by the end of experiments such as those shown in Figs 1 and 2 indicated that a small but significant percentage of cytochrome *c* was released following the addition of Ca^{2+} when either glutamate and malate, or succinate were used as respiratory substrates (Figs 4 and 5). Although cytochrome *c* was released in response to the addition of Ca^{2+} under both conditions, Ca^{2+} only stimulated the production of H_2O_2 in the presence of succinate plus rotenone. The fact that cytochrome *c* release was observed under these conditions suggested, but did not prove, that it was responsible for the stimulation of H_2O_2 generation by Ca^{2+}. Further support for this hypothesis came from experiments performed in the absence of Ca^{2+} but in the presence of Bax and a BH3 death domain peptide.

Ca^{2+}-independent stimulation of H_2O_2 production was dependent on the presence of both the human recombinant full-length Bax and the BH3 peptide as neither component alone had any effect on either ROS generation or cytochrome *c* release (Fig. 6) (Fiskum and Polster 2001; Polster *et al*. 2001). Release of cytochrome *c* was accompanied by increased H_2O_2 production in the presence of glutamate plus malate, or succinate plus rotenone. As the release of cytochrome *c* interrupts the flow of electrons at a site distal to the sites of ROS generation, their redox states shift to a more reduced level. Under these conditions, these redox centers are unaffected by $\Delta\Psi$ because electron transport is severely inhibited by the loss of cytochrome *c*. Therefore, mitochondrial H_2O_2 production is insensitive to $\Delta\Psi$ when cytochrome *c* is released by conditions, e.g. the Bax/BH3 system, in which no other electron transport activities are altered.

Although the most plausible explanation for the stimulation of ROS production by the release of cytochrome *c* relates to the effect of respiratory inhibition on the redox state of superoxide-generating sites proximal to the site of inhibition, other mechanisms may also contribute. One mechanism is the reduction of superoxide scavenging by cytochrome *c* when it is lost from the mitochondrial intermembrane space to the cytosol (Korshunov *et al*. 1999). This mode of action is supported by the findings that a substantial fraction of mitochondrial superoxide formation occurs at the outer side of the inner membrane, where cytochrome *c* is normally present in equilibrium with the unbound protein in the intermembrane space at a concentration of 100–700 μM (Hackenbrock 1966; Hackenbrock 1968). Despite its possible exacerbation of mitochondrial ROS generation, the redistribution of cytochrome *c* into the cytosol has been proposed to help scavenge superoxide or other ROS in that compartment during glutamate excitotoxicity (Atlante *et al*. 2000).

Considerable attention has been focused on the role of raised intracellular Ca^{2+} in mitochondrial dysfunction and ROS production preceding neural cell death (Fiskum 2000). Recent investigations indicate that the interaction of Bax with BH3 death domain only proteins, e.g. Bid, at the mitochondrial level also contributes significantly to cell death in animal models of acute brain injury and neurodegenerative diseases (Plesnila *et al*. 2001; Vila *et al*. 2001). One study demonstrated a relationship between these two forms of stress with Ca^{2+}-induced mitochondrial permeability transition signaling the redistribution of cytosolic Bax to the mitochondrial membrane before cytochrome *c* release during apoptosis (De Giorgi *et al*. 2002). Our observations suggest that the stimulation of mitochondrial ROS generation by Bax-mediated cytochrome *c* release may be particularly important in the pathogenesis of neural cell death. This stimulation can occur in the presence of either Complex I or Complex II respiratory substrates, physiological concentrations of ATP and inorganic ions, and in the absence of respiratory poisons. Development of inhibitors of Bax-mediated cytochrome *c* release is extremely important as they should both block caspase-mediated apoptosis and obstruct the mitochondrial generation of ROS that can promote either apoptotic or necrotic cell death.

Acknowledgements

This work was supported by USAMRMC Neurotoxin Initiative (DAMD 17-99-1-9483), NIH NS34152 and ES11838.

References

Andreyev A. and Fiskum G. (1999) Calcium induced release of mitochondrial cytochrome *c* by different mechanisms selective for brain versus liver. *Cell Death Differ.* **6**, 825–832.

Andreyev A. Y., Fahy B. and Fiskum G. (1998) Cytochrome *c* release from brain mitochondria is independent of the mitochondrial permeability transition. *FEBS Lett.* **439**, 373–376.

Atlante A., Calissano P., Bobba A., Azzariti A., Marra E. and Passarella S. (2000) Cytochrome *c* is released from mitochondria in a reactive oxygen species (ROS)-dependent fashion and can operate as a ROS scavenger and as a respiratory substrate in cerebellar neurons undergoing excitotoxic death. *J. Biol. Chem.* **275**, 37159–37166.

Benzi G., Pastoris O. and Dossena M. (1982) Relationships between gamma-aminobutyrate and succinate cycles during and after cerebral ischemia. *J. Neurosci. Res.* **7**, 193–201.

Cai J. and Jones D. P. (1998) Superoxide in apoptosis. Mitochondrial generation triggered by cytochrome *c* loss. *J. Biol. Chem.* **273**, 11401–11404.

De Giorgi F., Lartigue L., Bauer M. K., Schubert A., Grimm S., Hanson G. T., Remington S. J., Youle R. J. and Ichas F. (2002) The permeability transition pore signals apoptosis by directing Bax translocation and multimerization. *FASEB J.* **16**, 607–609.

Dykens J. A. (1994) Isolated cerebral and cerebellar mitochondria produce free radicals when exposed to elevated Ca^{2+} and Na^{+}: implications for neurodegeneration. *J. Neurochem.* **63**, 584–591.

Fiskum G. (2000) Mitochondrial participation in ischemic and traumatic neural cell death. *J. Neurotrauma* **17**, 843–855.

Fiskum G. and Polster B. (2001) BH3 cell death domain peptide-induced release of cytochrome *C* from mitochondria within cerebellar granule neurons and neural cell lines. *J. Neurochem.* **77**(Suppl. 1), 30.

Fiskum G., Murphy A. N. and Beal M. F. (1999) Mitochondria in neurodegeneration: acute ischemia and chronic neurodegenerative diseases. *J. Cereb. Blood Flow Metab.* **19**, 351–369.

Hackenbrock C. R. (1966) Ultrastructural bases for metabolically linked mechanical activity in mitochondria. I. Reversible ultrastructural changes with change in metabolic steady state in isolated liver mitochondria. *J. Cell Biol.* **30**, 269–297.

Hackenbrock C. R. (1968) Chemical and physical fixation of isolated mitochondria in low-energy and high-energy states. *Proc. Natl Acad. Sci. USA* **61**, 598–605.

Hansford R. G., Hogue B. A. and Mildaziene V. (1997) Dependence of H_2O_2 formation by rat heart mitochondria on substrate availability and donor age. *J. Bioenerg. Biomembr.* **29**, 89–95.

Hinkle P. C., Butow R. A., Racker E. and Chance B. (1967) Partial resolution of the enzymes catalyzing oxidative phosphorylation. XV. Reverse electron transfer in the flavin-cytochrome beta region of the respiratory chain of beef heart submitochondrial particles. *J. Biol. Chem.* **242**, 5169–5173.

Kamo N., Muratsugu M., Hongoh R. and Kobatake Y. (1979) Membrane potential of mitochondria measured with an electrode sensitive to tetraphenyl phosphonium and relationship between proton electrochemical potential and phosphorylation potential in steady state. *J. Membr. Biol.* **49**, 105–121.

Korshunov S. S., Skulachev V. P. and Starkov A. A. (1997) High protonic potential actuates a mechanism of production of reactive oxygen species in mitochondria. *FEBS Lett.* **416**, 15–18.

Korshunov S. S., Krasnikov B. F., Pereverzev M. O. and Skulachev V. P. (1999) The antioxidant functions of cytochrome *c*. *FEBS Lett.* **462**, 192–198.

Kowaltowski A. J., Naia-da-Silva E. S., Castilho R. F. and Vercesi A. E. (1998a) Ca^{2+}-stimulated mitochondrial reactive oxygen species generation and permeability transition are inhibited by dibucaine or Mg^{2+}. *Arch. Biochem. Biophys.* **359**, 77–81.

Kowaltowski A. J., Netto L. E. and Vercesi A. E. (1998b) The thiol-specific antioxidant enzyme prevents mitochondrial permeability transition. Evidence for the participation of reactive oxygen species in this mechanism. *J. Biol. Chem.* **273**, 12766–12769.

Kowaltowski A. J., Castilho R. F. and Vercesi A. E. (1995) Ca(2+)-induced mitochondrial membrane permeabilization: role of coenzyme Q redox state. *Am. J. Physiol.* **269**, C141–C147.

Kowaltowski A. J., Castilho R. F. and Vercesi A. E. (1996) Opening of the mitochondrial permeability transition pore by uncoupling or inorganic phosphate in the presence of Ca^{2+} is dependent on mitochondrial-generated reactive oxygen species. *FEBS Lett.* **378**, 150–152.

Lass A., Sohal B. H., Weindruch R., Forster M. J. and Sohal R. S. (1998) Caloric restriction prevents age-associated accrual of oxidative damage to mouse skeletal muscle mitochondria. *Free Radic. Biol. Med.* **25**, 1089–1097.

Liu Y., Fiskum G. and Schubert D. (2002) Generation of reactive oxygen species by the mitochondrial electron transport chain. *J. Neurochem.* **80**, 780–787.

Maciel E. N., Vercesi A. E. and Castilho R. F. (2001) Oxidative stress in Ca(2+)-induced membrane permeability transition in brain mitochondria. *J. Neurochem.* **79**, 1237–1245.

Murphy A. N., Bredesen D. E., Cortopassi G., Wang E. and Fiskum G. (1996) Bcl-2 potentiates the maximal calcium uptake capacity of neural cell mitochondria. *Proc. Natl Acad. Sci. USA* **93**, 9893–9898.

Murphy A. N., Fiskum G. and Beal M. F. (1999) Mitochondria in neurodegeneration: bioenergetic function in cell life and death. *J. Cereb. Blood Flow Metab.* **19**, 231–245.

Nicholls D. G. and Budd S. L. (2000) Mitochondria and neuronal survival. *Physiol. Rev.* **80**, 315–360.

Plesnila N., Zinkel S., Le D. A., Amin-Hanjani S., Wu Y., Qiu J., Chiarugi A., Thomas S. S., Kohane D. S., Korsmeyer S. J. and Moskowitz M. A. (2001) BID mediates neuronal cell death after oxygen/glucose deprivation and focal cerebral ischemia. *Proc. Natl Acad. Sci. USA* **98**, 15318–15323.

Polster B. M., Kinnally K. W. and Fiskum G. (2001) BH3 death domain peptide induces cell type-selective mitochondrial outer membrane permeability. *J. Biol. Chem.* **276**, 37887–37894.

Rolfe D. F., Hulbert A. J. and Brand M. D. (1994) Characteristics of mitochondrial proton leak and control of oxidative phosphorylation in the major oxygen-consuming tissues of the rat. *Biochim. Biophys. Acta* **1188**, 405–416.

Rottenberg H. (1984) Membrane potential and surface potential in mitochondria: uptake and binding of lipophilic cations. *J. Membr. Biol.* **81**, 127–138.

Sciamanna M. A., Zinkel J., Fabi A. Y. and Lee C. P. (1992) Ischemic injury to rat forebrain mitochondria and cellular calcium homeostasis. *Biochim. Biophys. Acta* **1134**, 223–232.

Sims N. R. (1990) Rapid isolation of metabolically active mitochondria from rat brain and subregions using Percoll density gradient centrifugation. *J. Neurochem.* **55**, 698–707.

Turrens J. F. (1997) Superoxide production by the mitochondrial respiratory chain. *Biosci. Rep.* **17**, 3–8.

Vila M., Jackson-Lewis V., Vukosavic S., Djaldetti R., Liberatore G., Offen D., Korsmeyer S. J. and Przedborski S. (2001) Bax ablation prevents dopaminergic neurodegeneration in the 1-methyl-4-phenyl-1,2,3,6-tetrahydropyridine mouse model of Parkinson's disease. *Proc. Natl Acad. Sci. USA* **98**, 2837–2842.

Villalobo A. and Lehninger A. L. (1980) Inhibition of oxidative phosphorylation in ascites tumor mitochondria and cells by intramitochondrial Ca^{2+}. *J. Biol. Chem.* **255**, 2457–2464.

Votyakova T. V. and Reynolds I. J. (2001) DeltaPsi(m)-dependent and -independent production of reactive oxygen species by rat brain mitochondria. *J. Neurochem.* **79**, 266–277.

Zhou M., Diwu Z., Panchuk-Voloshina N. and Haugland R. P. (1997) A stable nonfluorescent derivative of resorufin for the fluorometric determination of trace hydrogen peroxide: applications in detecting the activity of phagocyte NADPH oxidase and other oxidases. *Anal. Biochem.* **253**, 162–168.

Mitochondrial Mechanisms of Neural Cell Death and Neuroprotective Interventions in Parkinson's Disease

GARY FISKUM,[a] ANATOLY STARKOV,[a,b] BRIAN M. POLSTER,[a,c] AND CHRISTOS CHINOPOULOS[a]

[a]*Department of Anesthesiology, University of Maryland School of Medicine, Baltimore, Maryland 21201, USA*

[c]*Department of Molecular Microbiology and Immunology, The Johns Hopkins University School of Public Health, SHPH 5132, 615 N. Wolfe Street, Baltimore, Maryland 21205-2179, USA*

ABSTRACT: Mitochondrial dysfunction, due to either environmental or genetic factors, can result in excessive production of reactive oxygen species, triggering the apoptotic death of dopaminergic cells in Parkinson's disease. Mitochondrial free radical production is promoted by the inhibition of electron transport at any point distal to the sites of superoxide production. Neurotoxins that induce parkinsonian neuropathology, such as MPP^+ and rotenone, stimulate superoxide production at complex I of the electron transport chain and also stimulate free radical production at proximal redox sites including mitochondrial matrix dehydrogenases. The oxidative stress caused by elevated mitochondrial production of reactive oxygen species promotes the expression and (or) intracellular distribution of the proapoptotic protein Bax to the mitochondrial outer membrane. Interactions between Bax and BH3 death domain proteins such as tBid result in Bax membrane integration, oligomerization, and permeabilization of the outer membrane to intermembrane proteins such as cytochrome c. Once released into the cytosol, cytochrome c together with other proteins activates the caspase cascade of protease activities that mediate the biochemical and morphological alterations characteristic of apoptosis. In addition, loss of mitochondrial cytochrome c stimulates mitochondrial free radical production, further promoting cell death pathways. Excessive mitochondrial Ca^{2+} accumulation can also release cytochrome c and promote superoxide production through a mechanism distinctly different from that of Bax. Ca^{2+} activates a mitochondrial inner membrane permeability transition causing osmotic swelling, rupture of the outer membrane, and complete loss of mitochondrial structural and functional integrity. While amphiphilic cations, such as dibucaine and propranolol, inhibit Bax-mediated cytochrome c release, transient receptor potential channel inhibitors inhibit mitochondrial swelling and cytochrome c release induced by the inner membrane permeability transi-

Address for correspondence: Dr. Gary Fiskum, Dept. of Anesthesiology, Univ. of Maryland School of Medicine, 685 W. Baltimore St., MSTF 5.34, Baltimore, MD 21201. Voice: 410-706-3418; fax: 410-706-2550;
Gfisk001@umaryland.edu

[b]Current address: Department of Neurology, Weil Medical College, Cornell University, 510 E. 70th St., New York, NY 10021.

Ann. N.Y. Acad. Sci. 991: 111–119 (2003).

tion. These advances in the knowledge of mitochondrial cell death mechanisms and their inhibitors may lead to neuroprotective interventions applicable to Parkinsons's disease.

KEYWORDS: apoptosis; cytochrome c; calcium; excitotoxicity; Bax

INTRODUCTION

Parkinson's disease (PD) is a progressive neurodegenerative disease characterized clinically by bradykinesia, rigidity, resting tremor, and ataxia. These symptoms are caused by decreased dopamine release in the striatum. Pathologically, PD is characterized primarily by the death of dopaminergic neurons in the substantia nigra pars compacta and the formation of ubiquitin- and α-synuclein–positive cytoplasmic inclusions (Lewy bodies). The molecular mechanisms responsible for these changes are not clearly understood. One theory is that mitochondrial dysfunction, due to either environmental or genetic factors, results in excessive oxidative stress that triggers apoptotic cell death.

EVIDENCE FOR A MITOCHONDRIAL ETIOLOGY OF PARKINSON'S DISEASE

Several lines of evidence support the hypothesis that mitochondrial dysfunction contributes to the etiology of Parkinson's disease. Electron transport chain complex I activity is reduced in PD substantia nigra autopsy specimens as well as in PD platelets.[1,2] A mitochondrial genomic etiology for defective complex I in PD is strongly suggested by the presence of altered complex I activity, abnormal mitochondrial morphology, and impaired mitochondrial energy-dependent activities in cybrid cell lines containing a normal nuclear genome but mitochondrial DNA from PD patients.[3–5] Parkinson's disease cybrids are also more sensitive to death induced by MPP^+, a dopaminergic neuron-selective toxin that induces Parkinson-like lesions and symptoms in both humans and animals.[4] Additional evidence for a mitochondrial etiology of PD is the finding that chronic systemic treatment of rats with rotenone, a highly specific complex I inhibitor, can induce Lewy body neuropathology in addition to nigrostriatal dopaminergic degeneration and neurologic features of PD.[6]

MITOCHONDRIAL INITIATION OF NECROTIC AND APOPTOTIC CELL DEATH

Mitochondria have long been considered as mediators of cell death in neurodegenerative disorders. The significance of mitochondrial injury was previously thought to be limited to the potential effects such injury has on maintaining sufficient cellular ATP to avoid necrotic cell death. However, we now understand that mitochondria are the primary mediators of cell death caused by abnormal levels of intracellular Ca^{2+} elicited during excitotoxicity[7] and that mitochondrial mechanisms of neural cell death include oxidative stress and apoptosis in addition to metabolic failure (FIG. 1). Relatively mild mitochondrial injury, where ATP levels are maintained

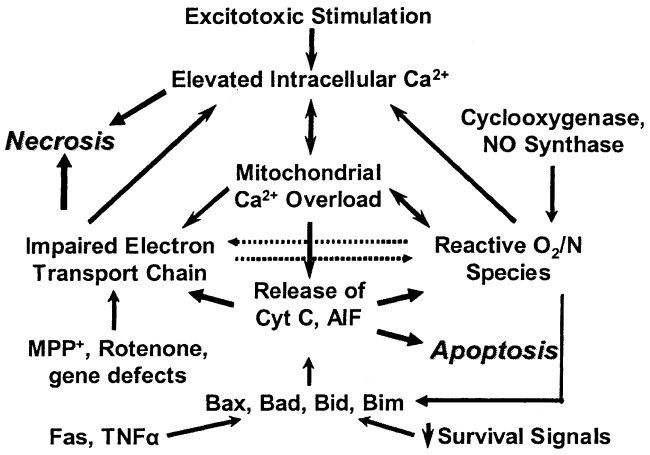

FIGURE 1. Mitochondrial mechanisms of neural cell death. Exitotoxic levels of intracellular Ca^{2+} accumulate within mitochondria, potentially causing metabolic failure, oxidative stress, and apoptosis via the release of cytochrome c and other proapoptotic mitochondrial proteins. Proteins, such as Bax, also mediate the release of mitochondrial cytochrome c, which, in addition to activating the caspase apoptotic cascade, can also stimulate mitochondrial free radical production. The levels and (or) subcellular distribution of these proteins is under the control of trophic factors and is also affected by oxidative stress. Mitochondrial free radical production is stimulated by the neurotoxins MPP^+ and rotenone and may be elevated by genomic or environmentally mediated alterations in electron transport chain activities.

near normal, results in mainly apoptotic cell death. More extensive injury that causes ATP depletion shifts the form of cell death toward necrosis. Excessive accumulation of Ca^{2+} that occurs during excitotoxic stimulation is likely not the only mediator of mitochondrial injury. Mitochondria are the targets of reactive oxygen species (ROS) generated by a number of different systems, including the mitochondrial electron transport chain (ETC), cyclooxygenases, Fe^{2+}-catalyzed hydroxyl radical ($OH^{\bullet}$) formation, and peroxynitrite formed from the reaction of nitric oxide ($NO^{\bullet}$) with superoxide (O_2^{-}). The levels and activities of mitochondrial antioxidant defense systems—for example, superoxide dismutase and glutathione peroxidase—and the redox state of mitochondrial NAD(P)H are therefore extremely important determinants of the extent of oxidative mitochondrial injury and neural cell survival.

THE INTRINSIC MITOCHONDRIAL PATHWAY OF APOPTOSIS

Discovery of the involvement of the release of mitochondrial cytochrome c in the activation of the cell death protease (caspase) cascade leading to apoptosis is one of the most important and certainly most unexpected events in the history of cell death research (FIG. 2). Release of several proapoptotic mitochondrial proteins, such as cytochrome c and apoptosis initiating factor (AIF), and their redistribution to the cytosol and nucleus during neural cell death *in vitro* and *in vivo* are well documented.[7] Sev-

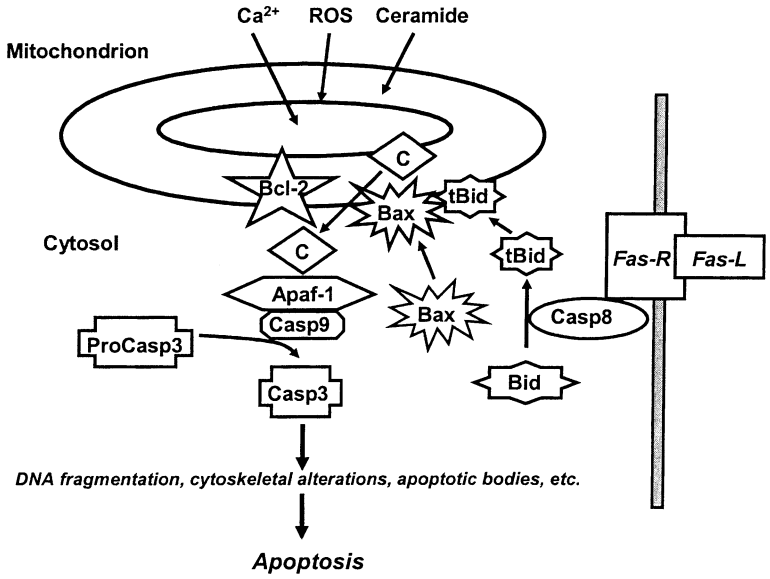

FIGURE 2. Mitochondrial participation in apoptosis. Agents, such as Ca^{2+}, ROS, and ceramide, as well as proapoptotic proteins, such as Bax, stimulate the release of other proapoptotic proteins—for example, cytochrome c (C in the figure)—from the mitochondrial intermembrane space into the cytosol. Cytochrome c and procaspase 9 together with apoptosis activating factor 1 (Apaf-1) form a multiprotein complex (apoptosome) that activates caspase 9, which then cleaves procaspase 3, forming active caspase 3. This caspase, together with other caspases it activates, proteolytically degrades a variety of proteins, causing the molecular and morphological alterations characteristic of apoptosis. Cell surface "death receptors," such as Fas, can activate caspase 3 directly through activation of caspase 8 (not shown) or participate in the mitochondrial pathway by processing Bid to form tBid, which greatly stimulates the release of cytochrome c by Bax. The antiapoptotic protein Bcl-2 is capable of inhibiting the release of cytochrome c mediated by either Ca^{2+} or Bax.

eral factors are capable of triggering the release of proapoptotic proteins from mitochondria, including elevated Ca^{2+}, ROS, ceramide, and other cell death proteins, such as Bax and tBid. Some apoptotic proteins, such as tBid, are activated by proteolytic cleavage and redistribute to the mitochondria in response to signals—for example, activation of the Fas and tumor necrosis factor (TNF)-α "cell death receptors." In addition to setting the mitochondrial pathway in motion, these receptors can trigger apoptosis via an "extrinsic pathway" by stimulating caspase 8–medated activation of caspase 3 through proteolytic cleavage. We obtained evidence for Fas receptor activation in the penumbra surrounding brain infarcts caused by closed head injury in humans.[8] The involvement of Fas and TNFα receptor activation in PD dopaminergic cell death is less clear. While the ligands for these receptors and other inflammatory cytokines are elevated in nigrostriatal dopaminergic regions and in the cerebrospinal fluid of PD patients,[9] these changes may reflect nonneuronal, proinflammatory cell activation.[10] Despite this controversy, abundant evidence obtained from patients and from animal models indicates that apoptosis plays a critical role in PD dopaminergic

cell death and that the mitochondrial pathway of apoptosis is integrally involved.[11] Therefore, the molecular mechanisms responsible for the release of proapoptotic proteins from mitochondria are potential targets for therapeutic intervention in PD.

There are two fundamentally different mechanisms of mitochondrial protein release under consideration. The first involves physical disruption of the mitochondrial outer membrane and simple diffusion of cytochrome c from its normal exclusive location in the space located between the outer and inner mitochondrial membranes. The second mechanism involves transport of cytochrome c through a pore located in the outer membrane.

A likely cause for the physical disruption of the outer membrane is the osmotic swelling of the compartment surrounded by the inner membrane (matrix) due to an increased permeability of the inner membrane to small osmotically active solutes. There is a large body of literature describing this swelling phenomenon known as the mitochondrial membrane permeability transition (MPT).[12] This activity is triggered by abnormal mitochondrial Ca^{2+} accumulation and is promoted by oxidative stress and reactive metabolites, such as peroxynitrite. The MPT is generally defined as a relatively nonspecific increase in inner membrane permeability that results in a substantial increase in matrix volume and a decrease in mitochondrial membrane potential that can be inhibited by the presence of the drug cyclosporin A (CsA) and by overexpression of the antiapoptotic gene Bcl-2,[13] both of which protect against MPP^+-induced dopaminergic cell death.[14,15] Although CsA is very effective at inhibiting the MPT for non neural cell mitochondria, Ca^{2+}-induced cytochrome c release from brain mitochondria is relatively resistant to inhibition by CsA in the presence of physiologically realistic concentrations of the cytosolic components Mg^{2+} and ATP.[16]

We recently found that 2-aminoethoxydiphenyl borate, an inhibitor of transient receptor potential (TRP) channels, is much more effective than CsA at protecting against Ca^{2+}-induced cytochrome c release from brain mitochondria.[17] This observation and others suggest that the MPT is associated with activation of Trp channels, a potential new class of targets for neuroprotection in PD and other brain disorders.

The MPT is an attractive mechanism of acute neural injury due to its activation by factors known to be associated with excitotoxicity and because of its sensitivity to inhibition by certain drugs and gene products known to be neuroprotective. However, increasing evidence indicates that the mechanism by which proapoptotic proteins such as Bax and tBid release cytochrome c and cause other forms of mitochondrial dysfunction is independent of the MPT and involves either pore formation or lipid alterations at the mitochondrial outer membrane.[18–20] The potential importance of Bax in PD is illustrated by the observation that Bax-knockout mice are resistant to nigrostriatal cell death induced by MPP^+.[21]

The Bax-mediated mechanism of cytochrome c release is not inhibited by CsA but is inhibited by specific amphiphilic cations, such as dibucaine and propranolol, known to affect membrane lipid–protein interactions.[22] In addition to activation of proapoptotic proteins like Bid by cell death receptors, expression of the genes coding for these proteins and mitochondrial–protein interactions are promoted by high Ca^{2+} and ROS through their stimulation of complex signal transduction cascades.[23] Therefore, Ca^{2+} together with oxidative stress can promote cytochrome c release and apoptosis by both the MPT- and Bax-mediated molecular mechanisms that exhibit different pharmacologic sensitivities.

Mechanisms of mitochondrial proapoptotic protein release in addition to the MPT- and Bax-dependent pathways should also be considered. As AIF release appears downstream of cytochrome c release and caspase activation,[24] it is possible that proteolytic cleavage of AIF or an anchoring protein might be necessary. Also, as cytochrome c release stimulates mitochondrial generation of reactive oxygen species,[25] the oxidative modification of mitochondrial membrane lipids or proteins could be another event responsible for or promoting release of proapoptotic mitochondrial proteins.

A possible key to the development of mitochondrial neuroprotective interventions is the understanding of the mechanisms by which the antiapoptotic, mitochondrial protein Bcl-2 inhibits cytochrome c release mediated by both MPT-dependent and -independent pathways. Bcl-2 and its close relative Bcl-X_L exert some form of antioxidant activity that confers cytoprotection against ROS that may also inhibit activation of the MPT.[13,26] In contrast, Bcl-2 inhibition of Bax appears to involve direct protein–protein interaction, impairment of Bax oligomerization, and consequently inhibition of pore formation.[27] Stimulation of Bcl-2 expression has been demonstrated in several ischemic preconditioning paradigms and may represent a primary mechanism of neuroprotection by estrogen.[28] Investigators have also utilized protein transduction domains to deliver exogenous Bcl-X_L to cells throughout the brain and have demonstrated neuroprotection when these fusion proteins were administered by intraperitoneal injection up to 1 hour following the occlusion of the middle cerebral artery of mice.[29] Delivery of neuroprotective proteins, such as Bcl-2 and glial cell line–derived neurotrophic factor (GDNF), as a therapeutic approach for neurodegenerative disorders like Parkinson's disease is therefore possible and may prove to be effective.

MITOCHONDRIAL MECHANISMS OF REACTIVE OXYGEN SPECIES GENERATION

As several lines of evidence suggest that elevated mitochondrial ROS production contributes to the etiology of Parkinson's disease and as oxidative stress is a potent activator of apoptosis, understanding the mechanisms of mitochondrial free radical production is critically important in elucidating the pathophysiology of Parkinson's and other neurodegenerative diseases. The two most commonly cited sites of mitochondrial ROS production are ubisemiquinone (during complex III reduction) and complex I, although others, such as complex II, may also contribute.[30] The site of mitochondrial ROS production implicated most strongly in Parkinson's disease is complex I of the electron transport chain. Some neurotoxins that induce PD neuropathology *in vivo*, such as MPP^+ and rotenone, are inhibitors of complex I and stimulate ROS generation *in vitro*.[31] Acting along with hydroxyl radical ($OH^{\bullet}$) and peroxynitrite ($HNOO^-$), these ROS species can cause oxidative damage and inhibition of mitochondrial enzyme activities, including those of complex I and alpha-ketoglutarate dehydrogenase complex (αKGDC) (FIG. 3).[32,33] This inhibition can lead to metabolic failure through impairment of electron transport–dependent generation of the proton-motive force that drives the synthesis of ATP. Complete detoxification of superoxide depends on the enzymes superoxide dismutase (SOD), glutathione peroxidase (GPX), and glutathione reductase (GR) together with glutathione and a

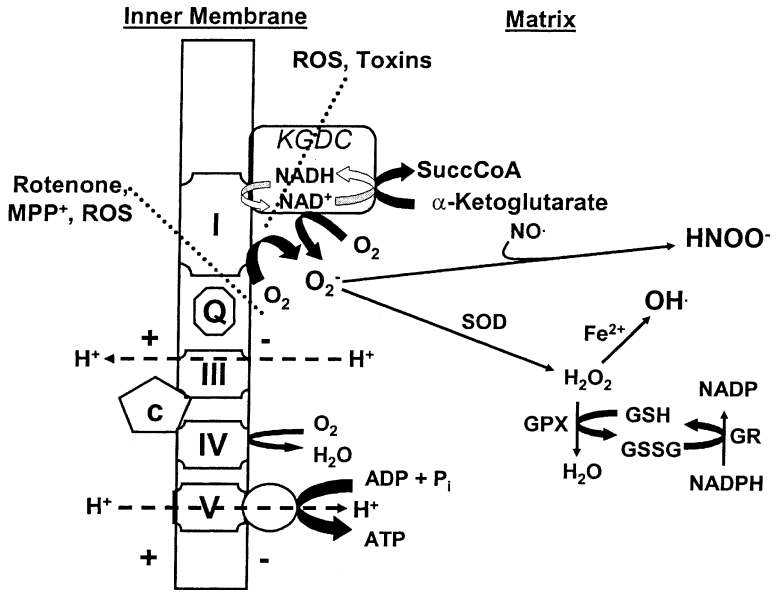

FIGURE 3. Mitochondrial generation and detoxification of reactive oxygen species. The site of mitochondrial reactive oxygen species (ROS) production most widely implicated in Parkinson's disease is complex I of the electron transport chain. Indirect evidence for involvement of complex I includes the observations that neurotoxins capable of inducing Parkinson's symptoms and neuropathology *in vivo*, such as MPP^+ and rotenone, are inhibitors of complex I and stimulate ROS generation *in vitro*. However, these same agents result in inhibition of the overall enzyme activity of α-ketoglutarate dehydrogenase complex (αKGDC), a multisubunit complex that can also catalyze superoxide (O_2^-) and consequently H_2O_2 production. The ROS metabolites most likely to mediate oxidative injury to mitochondria and other cellular constituents are hydroxyl radical ($OH^•$) and peroxynitrite ($HNOO^-$). These agents can cause oxidative damage and inhibition of mitochondrial enzyme activities, including those of complex I and αKGDC. This inhibition can lead to metabolic failure through impairment of electron transport–dependent generation of the protonmotive force that drives the synthesis of ATP at complex V (F_1F_0 ATP synthetase). Complete detoxification of superoxide depends on the enzymes superoxide dismutase (SOD), glutathione peroxidase (GPX), and glutathione reductase (GR) together with glutathione and a sufficiently reduced redox state of NAD(P)H to drive the reduction of glutathione and consequently the reduction of H_2O_2 to H_2O.

sufficiently reduced redox state of NAD(P)H to drive the reduction of glutathione and consequently the reduction of H_2O_2 to H_2O.

Our recent observations indicate that in addition to complex I, several tricarboxylic acid cycle dehydrogenases are potential sources of ROS, with αKGDH appearing the most active.[34] In particular, the rate of ROS production by isolated brain mitochondria measured under a state of rapid metabolism, as normally exists in neurons, was highest with α-ketoglutarate as respiratory substrate, even though several other substrates support higher rates of respiration. Zinc also promotes ROS production by the lipoamide dehydrogenase component of aKGDH, but it inhibits overall

enzyme activity.[35] Considering the findings that environmental exposure to zinc is a risk factor for Parkinson's disease and that αKGDH enzyme activity is reduced in PD and in Alzheimer's disease,[36] the relationships between this enzyme complex, ROS production, and dopaminergic cell death in cellular and animal models of PD require further investigation.

REFERENCES

1. PARKER, W.D.J., S.J. BOYSON & J.K. PARKS. 1989. Abnormalities of the electron transport chain in idiopathic Parkinson's disease. Ann. Neurol. **26:** 719–723.
2. SHULTS, C.W., R.H. HAAS, D. PASSOV & M.F. BEAL. 1997. Coenzyme Q10 levels correlate with the activities of complexes I and II/III in mitochondria from parkinsonian and nonparkinsonian subjects. Ann. Neurol. **42:** 261–264.
3. SWERDLOW, R.H., J.K. PARKS, S.W. MILLER, *et al*. 1996. Origin and functional consequences of the complex I defect in Parkinson's disease. Ann. Neurol. **40:** 663–671.
4. SHEEHAN, J.P., R.H. SWERDLOW, S.W. MILLER, *et al*. 1997. Calcium homeostasis and reactive oxygen species production in cells transformed by mitochondria from individuals with sporadic Alzheimer's disease. J. Neurosci. **17:** 4612–4622.
5. TRIMMER, P.A., R.H. SWERDLOW, J.K. PARKS, *et al*. 2000. Abnormal mitochondrial morphology in sporadic Parkinson's and Alzheimer's disease cybrid cell lines. Exp. Neurol. **162:** 37–50.
6. BETARBET, R., T.B. SHERER, G. MACKENZIE, *et al*. 2000. Chronic systemic pesticide exposure reproduces features of Parkinson's disease. Nat. Neurosci. **3:** 1301–1306.
7. FISKUM, G. 2000. Mitochondrial participation in ischemic and traumatic neural cell death. J. Neurotrauma **17:** 843–855.
8. QIU, J., M.J. WHALEN, P. LOWENSTEIN, *et al*. 2002. Upregulation of the Fas receptor death-inducing signaling complex after traumatic brain injury in mice and humans. J. Neurosci. **22:** 3504–3511.
9. NAGATSU, T., M. MOGI, H. ICHINOSE & A. TOGARI. 2000. Changes in cytokines and neurotrophins in Parkinson's disease. J. Neural Transm. Suppl. 277–290.
10. FERRER, I., R. BLANCO, B. CUTILLAS & S. AMBROSIO. 2000. Fas and Fas-L expression in Huntington's disease and Parkinson's disease. Neuropathol. Appl. Neurobiol. **26:** 424–433.
11. DAWSON, T.M. & V.L. DAWSON. 2002. Neuroprotective and neurorestorative strategies for Parkinson's disease. Nat. Neurosci. **5** Suppl.**:** 1058–1061.
12. FRIBERG, H. & T. WIELOCH. 2002. Mitochondrial permeability transition in acute neurodegeneration. Biochimie **84:** 241–250.
13. KOWALTOWSKI, A.J., A.E. VERCESI & G. FISKUM. 2000. Bcl-2 prevents mitochondrial permeability transition and cytochrome c release via maintenance of reduced pyridine nucleotides. Cell Death. Differ. **7:** 903–910.
14. SEATON, T.A., J.M. COOPER & A.H. SCHAPIRA. 1998. Cyclosporin inhibition of apoptosis induced by mitochondrial complex I toxins. Brain Res. **809:** 12–17.
15. YANG, L., R.T. MATTHEWS, J.B. SCHULZ, *et al*. 1998. 1-Methyl-4-phenyl-1,2,3,6-tetrahydropyride neurotoxicity is attenuated in mice overexpressing Bcl-2. J. Neurosci. **18:** 8145–8152.
16. ANDREYEV, A. & G. FISKUM. 1999. Calcium induced release of mitochondrial cytochrome c by different mechanisms selective for brain versus liver. Cell Death. Differ. **6:** 825–832.
17. CHINOPOULOS, C., A.A. STARKOV & G. FISKUM. 2003. Cyclosporin A-insensitive permeability transition in brain mitochondria: inhibition by 2-aminoethoxydiphenyl borate. J. Biol. Chem. In press.
18. KORSMEYER, S.J., M.C. WEI, M. SAITO, *et al*. 2000. Pro-apoptotic cascade activates BID, which oligomerizes BAK or BAX into pores that result in the release of cytochrome c. Cell Death Differ. **7:** 1166–1173.
19. KUWANA, T., M.R. MACKEY, G. PERKINS, *et al*. 2002. Bid, Bax, and lipids cooperate to form supramolecular openings in the outer mitochondrial membrane. Cell **111:** 331–342.

20. POLSTER, B.M., K.W. KINNALLY & G. FISKUM. 2001. Bh3 death domain peptide induces cell type-selective mitochondrial outer membrane permeability. J. Biol. Chem. **276:** 37887–37894.
21. VILA, M., V. JACKSON-LEWIS, S. VUKOSAVIC, *et al*. 2001. Bax ablation prevents dopaminergic neurodegeneration in the 1-methyl- 4-phenyl-1,2,3,6-tetrahydropyridine mouse model of Parkinson's disease. Proc. Natl. Acad. Sci. USA **98:** 2837–2842.
22. POLSTER, B.M. & G. FISKUM. 2003. Inhibition of Bax-induced cytochrome c release from neural cell and brain mitochondria by dibucaine and propranolol. J. Neurosci. **23:** 2735–2743.
23. MARTIN, L.J. 2001. Neuronal cell death in nervous system development, disease, and injury. Int. J. Mol. Med. **7:** 455–478.
24. ARNOULT, D., P. PARONE, J.C. MARTINOU, *et al*. 2002. Mitochondrial release of apoptosis-inducing factor occurs downstream of cytochrome c release in response to several proapoptotic stimuli. J. Cell Biol. **159:** 923–929.
25. STARKOV, A.A., B.M. POLSTER & G. FISKUM. 2002. Regulation of hydrogen peroxide production by brain mitochondria by calcium and Bax. J. Neurochem. **83:** 220–228.
26. OUYANG, Y., S. CARRIEDO & R. GIFFARD. 2002. Effect of Bcl-X(L) overexpression on reactive oxygen species, intracellular calcium, and mitochondrial membrane potential following injury in astrocytes. Free Radic. Biol. Med. **33:** 544.
27. CHENG, E.H., M.C. WEI, S. WEILER, *et al*. 2001. BCL-2, BCL-X(L) sequester BH3 domain-only molecules preventing BAX- and BAK-mediated mitochondrial apoptosis. Mol. Cell **8:** 705–711.
28. ALKAYED, N.J., S. GOTO, N. SUGO, *et al*. 2001. Estrogen and Bcl-2: gene induction and effect of transgene in experimental stroke. J. Neurosci. **21:** 7543–7550.
29. CAO, G., W. PEI, H. GE, *et al*. 2002. In vivo delivery of a Bcl-xL fusion protein containing the TAT protein transduction domain protects against ischemic brain injury and neuronal apoptosis. J. Neurosci. **22:** 5423–5431.
30. BOVERIS, A. 1977. Mitochondrial production of superoxide radical and hydrogen peroxide. Adv. Exp. Med. Biol. **78:** 67–82.
31. LENAZ, G., C. BOVINA, M. D'AURELIO, *et al*. 2002. Role of mitochondria in oxidative stress and aging. Ann. N.Y. Acad. Sci. **959:** 199–213.
32. HILLERED, L. & L. ERNSTER. 1983. Respiratory activity of isolated rat brain mitochondria following in vitro exposure to oxygen radicals. J. Cereb. Blood Flow Metab. **3:** 207–214.
33. NULTON-PERSSON, A.C. & L.I. SZWEDA. 2001. Modulation of mitochondrial function by hydrogen peroxide. J. Biol. Chem. **276:** 23357–23361.
34. STARKOV, A. & G. FISKUM. 2002. Generation of reactive oxygen species by brain mitochondria mediated by alpha-ketoglutarate dehydrogenase. Soc. Neurosci. 194.17.
35. GAZARYAN, I.G., B.F. KRASNIKOV, G.A. ASHBY, *et al*. 2002. Zinc is a potent inhibitor of thiol oxidoreductase activity and stimulates reactive oxygen species production by lipoamide dehydrogenase. J. Biol. Chem. **277:** 10064–10072.
36. GIBSON, G.E., L.C. PARK, K.F. SHEU, *et al*. 2000. The alpha-ketoglutarate dehydrogenase complex in neurodegeneration. Neurochem. Int. **36:** 97–112.

ACADEMIC PRESS

Available online at www.sciencedirect.com

SCIENCE DIRECT®

Experimental Neurology 182 (2003) 124–134

Experimental Neurology

www.elsevier.com/locate/yexnr

Ovarian steroid modulation of seizure severity and hippocampal cell death after kainic acid treatment

G.E. Hoffman,[a,*] N. Moore,[a] G. Fiskum,[b] and A.Z. Murphy[a]

[a] *Departments of Anatomy and Neurobiology, University of Maryland, School of Medicine, Baltimore, MD 21201, USA*
[b] *Anesthesiology, University of Maryland, School of Medicine, Baltimore, MD 21201, USA*

Received 24 October 2002; revised 10 January 2003; accepted 22 January 2003

Abstract

To determine whether maintained estrogen or progesterone levels affect kainic acid (KA) seizure patterns or the susceptibility of hippocampal neurons to death from seizures, ovariectomized Sprague–Dawley rats were implanted with estrogen pellets, 0.1 or 0.5 mg, that generated serum levels of 42.4 ± 6.6 (mean ± SEM) and 242.4 ± 32.6 pg/ml or one to six capsules of progesterone that generated serum levels of 11.00 ± .72 to 48.62 ± 9.4 ng/ml. Seven days later, the rats were administered KA (8.5mg/kg, ip) and scored for seizure activity; 96 h later, the rats were killed and their brains processed for localization of neuron nuclear antigen (NeuN), a general neuronal marker. The hippocampus was scored for spread (the number of separate regions showing cell loss), and the area within the CA fields occupied by NeuN immunoreactivity was measured (indicating surviving neurons). Administration of estrogen or progesterone (independent of dose) significantly reduced mortality from KA seizures. Progesterone reduced seizure severity in animals that received one to four implants; compared with controls, no difference in seizure severity was noted for animals with six progesterone implants. The reduced seizures in progesterone-treated animals were accompanied by a reduction in the spread of hippocampal damage ($r^2 = 0.87$; $P < 0.05$). Likewise, in progesterone-treated rats, neuron survival and reduction in seizure scores were correlated ($r^2 = 0.76$; $P < 0.0001$). Estrogen had no effect on seizure severity ($P > 0.05$), but reduced both the spread ($P < 0.05$) and degree of neuronal loss ($P < 0.05$). Indeed, in the estrogen-treated rats, neuronal death was significantly lower than that observed in progesterone-treated animals with equally severe seizures ($P < 0.05$). These data are consistent with the hypothesis that progesterone produces its effects by reducing seizures, whereas estrogen has little beneficial effect on seizure behavior but protects the hippocampus from the damage seizures produce.

Keywords: Estrogen; Progesterone; Neuroprotection; Excitoxicity; Limbic seizures; Epilepsy; Neuronal nuclear antigen

Introduction

Complex partial seizures involve the limbic system and comprise the most common form of epilepsy. In women, the pattern of complex partial seizures is influenced by the hormonal changes that occur across the menstrual cycle (Herkes et al., 1993; Herzog et al., 1997; Morrell, 1992, 1999; Murri and Galli, 1997; Schachter, 1988). Increased seizure incidence is observed in the menstrual phase, when both estrogen and progesterone levels are low, as well as in the follicular phase, when estrogen levels are on the rise. By contrast, decreased seizure incidence is noted during the luteal phase when progesterone levels are high relative to estrogen. In animals, estrogen administration decreases while progesterone increases seizure thresholds (Beyenburg et al., 2001; Buterbaugh, 1987, 1989; Buterbaugh and Hudson, 1991; Edwards et al., 1999; Hom and Buterbaugh, 1986); these differential steroid effects are used to explain the cycle-dependent changes in seizure patterns in women. Indeed, the effects observed with progesterone form the basis for progesterone treatment of women with catemenial epilepsy (Bauer, 2001; Bonuccelli et al., 1989; Herzog, 1995; Herzog et al., 1997; Holmes et al., 2001; Morrell, 1992, 1999; Murri and Galli, 1997).

Limbic system seizures, when persistent, increase the risk of permanent damage to the hippocampal formation

* Corresponding author. Fax: +1-410-706-2512.
E-mail address: gehoffma@umaryland.edu (G.E. Hoffman).

0014-4886/03/$ – see front matter © 2003 Elsevier Science (USA). All rights reserved.
doi:10.1016/S0014-4886(03)00104-3

(Kalviainen et al., 1998; Mathern et al., 1998; Moshe, 1998; Salmenpera et al., 2001; Tasch et al., 1999; Theodore et al., 1999). Thus, an understanding of the hormonal effects on limbic seizures and the damage they produce is critical to the design of rational treatments. In animals, the use of the toxin kainic acid, an excitatory amino acid analog, produces limbic seizures that damage neurons in the hippocampal formation and surrounding structures, particularly CA1, CA3, hilus, and entorhinal cortex, while sparing CA2 and the dentate gyrus (Ben-Ari et al., 1980; Gayoso et al., 1994; Jarrard, 1983; Lothman and Collins, 1981; Olney et al., 1979, 1986; Sperk, et al., 1983). Progesterone treatment reduces limbic seizures in a variety of experimental models (Edwards et al., 1999; Frye and Bayon, 1998; Frye and Scalise, 2000; Tauboll and Lindstrom, 1993) but it is unclear if the steroid has any neuroprotective effects of its own apart from its effects on seizure activity per se.

For estrogen, a few studies suggest that despite the potential for increased seizures, estrogen may reduce neuronal death from seizures (Azcoitia et al., 1999; Veliskova et al., 2000). However, those studies only used injected steroid (which produces variable hormone levels) and doses that often exceeded the physiological range. Thus, it is unclear if the effects of estrogen are dose-dependent. To fill those gaps, the studies presented in this manuscript sought to determine if maintained physiological levels of either estrogen or progesterone affected kainic acid (KA) seizure patterns and if these hormones could alter the relationship between seizure severity and brain injury.

Methods

Animal treatment

Adult female Sprague–Dawley rats (200–225 g) were maintained on 12:12 light:dark cycle (lights on at 3:30 EST). After a 1-week acclimation, rats were anesthetized with Metofane and ovariectomized under sterile conditions; 7 days later they were implanted with blank silastic capsules ($n = 18$; capsule length = 40 mm; OD = 0.125mm; ID = 0.078mm); estrogen pellets (estradiol-17β, 0.5mg/21 day, $n = 6$; or 0.1 mg/21 day, $n = 8$; Innovative Research of America, Sarasota, FL); or 1 ($n = 3$), 2 ($n = 9$), 4 ($n = 6$), or 6 ($n = 8$) silastic capsules containing crystalline progesterone (capsule length = 40 mm; OD = 0.125mm; ID = 0.078 mm; Sigma, St. Louis MO) designed to achieve progesterone plasma levels of 10–60 ng/ml.

Behavioral testing

Seven days after implants or pellets were inserted, half the control animals and the steroid-replaced animals were administered KA at a dose of 8.5 mg/kg, ip. The remaining control rats received an equal volume of saline vehicle. The behavior of the animals was monitored by an individual blind to the animal treatment for 6 h following saline or KA injection and assigned a score for seizure behaviors using the following scale modified from Lothman (Lothman and Collins, 1981):

1= minor behaviors such as catatonia, wet dog shakes (WDS), scratching, sniffing, and head bobbing;

2 = minor behaviors + chewing and salivation, rearing without loss of balance;

3 = minor behaviors + chewing and salivation, rearing with ataxia;

4 = biclonus seizure activity; and

5 = death. Following the observation period the animals were returned to the vivarium.

Tissue preparation and neuroanatomical analysis

Ninety-six hours after injection of KA or vehicle, each animal was anesthetized with an overdose of pentobarbital (100 mg/kg, ip), a blood sample was removed directly from the heart, and the animals were perfused transcardially with saline containing 2% sodium nitrite, followed by fixation with 2.5% acrolein in 4% paraformaldehyde in 0.05 M phosphate buffer, pH 6.8 (Hoffman et al., 2001). The brains were removed, sunk in 30% sucrose, and sectioned at 25 μm on a Leica freezing microtome (Bannockburn, IL). The sections were placed into antifreeze cryoprotectant solution (Watson et al., 1986) and stored at −20°C until immunocytochemical localization of NeuN (a neuron-specific marker that stains nuclei and frequently dendrites and soma (Mullen et al., 1992; Wolf et al., 1996)) was initiated.

Brain sections from each animal (1:6 series) that contained the entorhinal cortex and hippocampal formation were processed for NeuN immunoreactivity using standard immunocytochemical techniques (Hoffman et al., 2001). Following immunocytochemical staining, the slides were coded and examined for the number of separate regions that showed neuron loss (“spread of damage”). This parameter was chosen due to the variability in sites of hippocampal damage in less severely affected rats with respect to which particular CA subfield showed damage. Second, neuronal survival was assessed by measuring the area occupied by NeuN immunoreactivity within the CA subfields at the coronal level where the CA regions showed maximal length. To accomplish this, an image of the section was captured with a 4X objective on a Nikon Eclipse 800 microscope using a Sensys digital camera (Biovision Technologies, Exton, PA). With IP Spectrum software (Scanalytics, Fairfax, VA) operating on a Power Computing Macintosh computer, the CA area (in square micrometers) occupied by NeuN immunoreactive structures was determined. Reductions in NeuN area reflected the degree of neuron loss. To control for slight variation in hippocampal orientation, the total CA length was determined for each section and the NeuN area measurements were normalized for CA length (NeuN area/μm length).

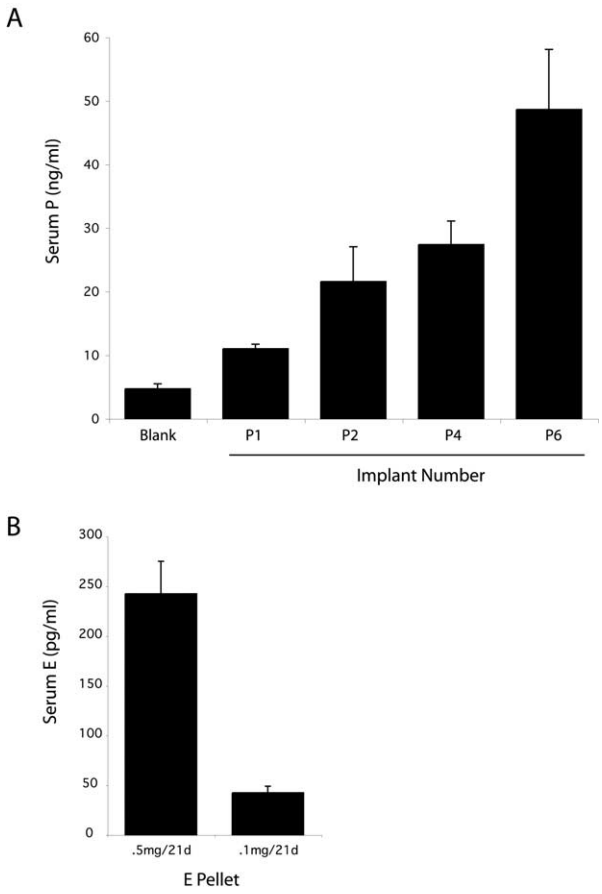

Fig. 1. (A) Serum levels of progesterone (P). Each bar represents the mean ± SEM for serum levels of P in nanograms per milliliter for animals that were ovariectomized and received blank capsules (pooling animals that later were administered saline with animals that received KA) or one, two, four, or six capsules containing P. (B) Plasma β-estradiol (E) levels (mean ± SEM) in picograms per milliliter for ovariectomized animals implanted with estradiol pellets containing either 0.5 mg/21 day release or 0.1 mg/21 day release. Ovariectomized animals had E values below detection in the assay.

Radioimmunoassay for estrogen and progesterone

Atrial blood was collected at the time of perfusion to determine serum progesterone and estrogen concentrations for the various treatment paradigms. After 2 h at room temperature to allow for clot formation, serum was separated by centrifugation. Samples were stored at −20°C until radioimmunoassays were initiated. For estradiol, samples were first extracted with diethyl ether. Serum progesterone and estrogen concentrations were determined using the Diagnostics Products Corporation Coat-A-Count kit (Estradiol, TKE25; Progesterone, TKPG2; Los Angeles, CA).

Statistical analysis

Significant differences among treatment groups were analyzed using the nonparametric Kruskall–Wallis test followed by post hoc Mann–Whitney U tests; $P < 0.05$ was considered significant. Correlations between the various measures were assessed using a simple regression analysis and GB-Stat software; $P < 0.05$ was considered significant.

Results

Hormone levels

The placement of one to six progesterone implants resulted in serum progesterone levels averaging from 11 to 48 ng/ml (Fig. 1A); these values are all within physiological ranges. Since the placement of two or four implants produced essentially the same progesterone levels, the data from those two groups were pooled in subsequent analyses. The 0.5 mg/21 day and 0.1 mg/21 day estrogen pellets produced hormone levels of 242.4 ± 32.6 pg/ml and 42.4 ± 6.6 pg/ml, respectively (Fig. 1B). Only the lower dose was within the physiological range.

Mortality

One striking feature of animals replaced with estrogens or progesterone was a reduction in the mortality rate. Seven of the 24 animals (29.2%) that received blank capsules and KA died, whereas for E, only 4 of 48 animals (8.3%) died and for P, 3 of 34 animals (8.8%) died. There was no obvious relationship of mortality to dose of replaced hormone (Table 1).

Seizure severity

Seizure severity was significantly reduced in progesterone-treated, but not estrogen-treated, rats (Fig. 2A). This reduction in seizure severity by progesterone was dose-dependent. In animals with one or two to four progesterone implants, seizure scores were significantly reduced compared with ovariectomized animals treated with KA that received blank capsules (for P1, $P = 0.05$; for P2–4, $P < 0.0005$). No significant difference in seizure severity was noted in animals that received six implants compared to blanks ($P > 0.05$). As a result, animals that had only mild

Table 1
Mortality after kainic acid seizures

Treatment group	No. died	Total	%
Blank + KA	7	24	29.2
E-0.1 mg/21 d + KA	2	25	8.0
E-0.5 mg/21 d + KA	2	23	8.7
E Combined	4	48	8.3
P1 + KA	0	6	0.0
P2–4 + KA	2	18	11.1
P6 + KA	1	10	10.0
P Combined	3	34	8.8

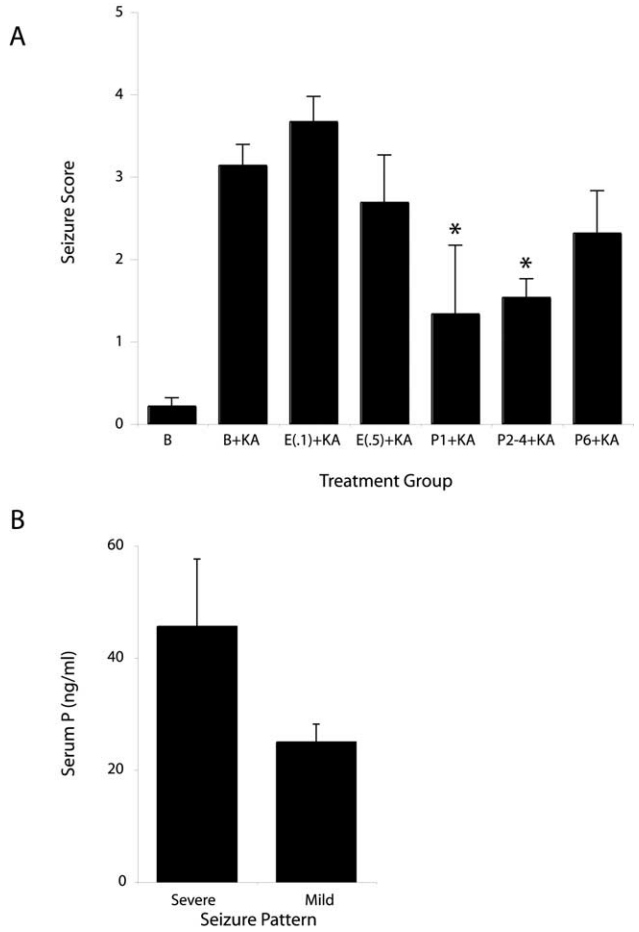

Fig. 2. (A) Effects of hormone treatment on KA-induced seizures. Animals fitted with one or two to four P implants showed significantly lower seizure scores (*$P \leq 0.05$) than animals treated with KA that received no hormone treatment (B+KA). In contrast, animals that received six P pellets showed no suppression of KA seizures as did animals fitted with E pellets. Values represent the mean ± SEM. (B) Comparison of plasma P levels in animals which displayed either severe (score > 2.0) or mild (score ≤ 2.0) seizures. P-implanted animals with severe seizures had significantly higher P levels than P-treated animals that had mild seizures ($P < 0.02$).

seizures in the progesterone-treated group (i.e., seizure scores ≤2.0) had significantly lower plasma P values (mean plasma P = 25.0 ± 3.2) than animals treated with P that had severe seizures with scores >2.0 (mean plasma P = 45.6 ± 12.0; $P < 0.05$; Fig. 2B).

Number of areas showing neuronal loss: spread of damage

On average, approximately three hippocampal areas showed neuronal loss in control animals after KA treatment (Fig. 3). This typically included the entorhinal cortex (not shown), CA1, CA3, or the hilus (Fig. 4B compared with controls, Fig. 4A). CA2 and the dentate gyrus were generally spared. The spread of damage after KA administration varied significantly with the level of seizure activity (Fig. 5A; $r^2 = 0.45$; $P < 0.02$).

In P-treated animals, the spread of damage induced by KA administration was independent of plasma P level (Fig. 3). Rather, in P-treated animals, spread of damage was directly influenced by seizure severity. Animals displaying a high level of seizure activity (score >2) after KA had a greater number of areas showing neuronal loss than animals with lower seizure activity (score ≤ 2) (Fig. 4C–E and Fig 5B, $r^2 = .665$; $P < .0001$; Fig. 6).

In estrogen-treated animals, fewer hippocampal regions showed signs of neuron loss after KA treatment than controls (Fig. 3, $P < 0.05$; Fig. 4F and **G**) despite the persistence of seizures (Fig. 2A). Therefore, unlike progesterone, the effect of estrogen on the spread of damage was not dose-dependent (Fig 3; $P > 0.05$) nor was it correlated with seizure severity (Fig. 5C; $r^2 = 0.049$, $P > 0.05$). Thus, even when animals displayed severe seizures following KA, estrogen administration (at either high or low doses) limited the number of hippocampal regions that showed any neuronal damage (Fig. 6).

Loss of neurons in CA subfields: area occupied by NeuN immunoreactivity

Compared with saline-treated control animals (blank capsules), KA-treated control rats with high seizure activity had significant losses of NeuN in the CA subfields ($p < 0.005$; Fig. 7). Overall, the losses in NeuN immunoreactivity in the Blank + KA group were highly correlated with seizure score (Fig. 8A; $r^2 = 0.47$, $P < 0.02$).

In animals treated with P, the animals with high seizure scores also had severe reductions in NeuN compared with controls (*$P < 0.005$; Fig. 7). The NeuN losses in P-treated

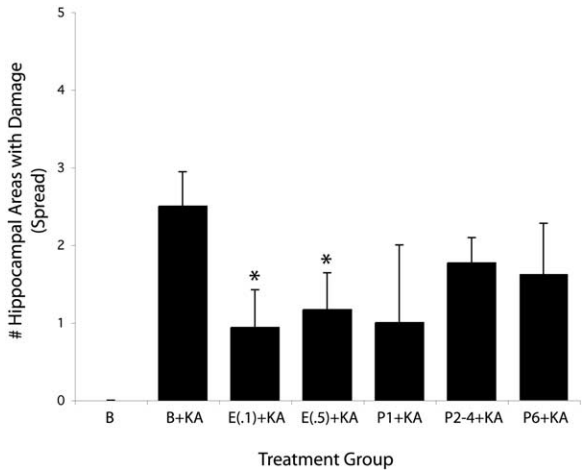

Fig. 3. Effects of hormonal treatment on the spread of damage to the hippocampal formation after KA treatment. Values represent the number of hippocampal formation regions (mean ± SEM) showing neuronal injury after KA treatment. P did not produce significant dose-dependent effects on spread of damage. Both low and high E treatment produced a significant reduction (*$P \leq 0.05$) in the number of regions showing neuronal damage after KA treatment despite the failure of the steroid to reduce seizure severity.

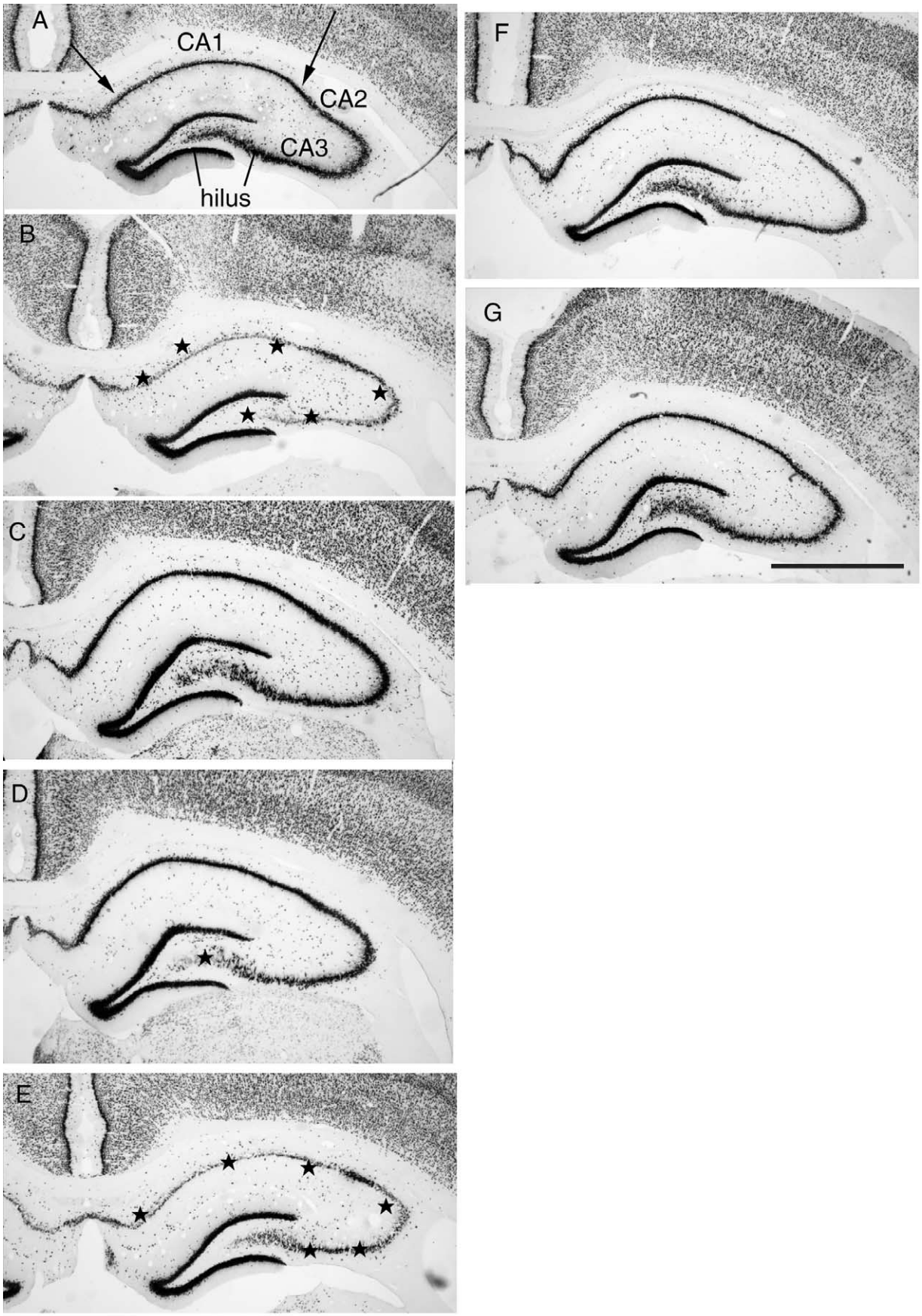
A
CA1
CA2
CA3
hilus
B
C
D
E
F
G

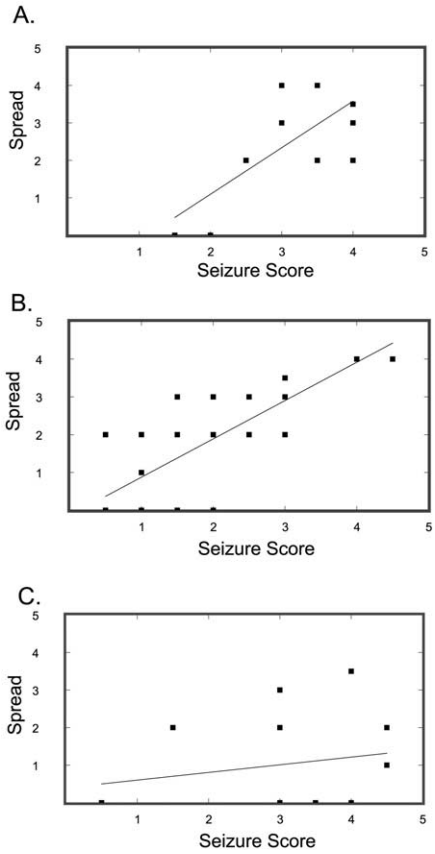

Fig. 5. Correlation of seizure score and spread of damage in KA-treated ovariectomized rats with (A) blank implants, (B) progesterone, or (C) estrogen replacement. The spread of damage was significantly correlated with seizure scores in animals with blank ($P < 0.02$) and P ($P < 0.001$) implants but in E-treated rats this relationship was lost ($P > 0.05$). Thus, despite increased seizures, damage to the hippocampus did not spread to many areas after E replacement.

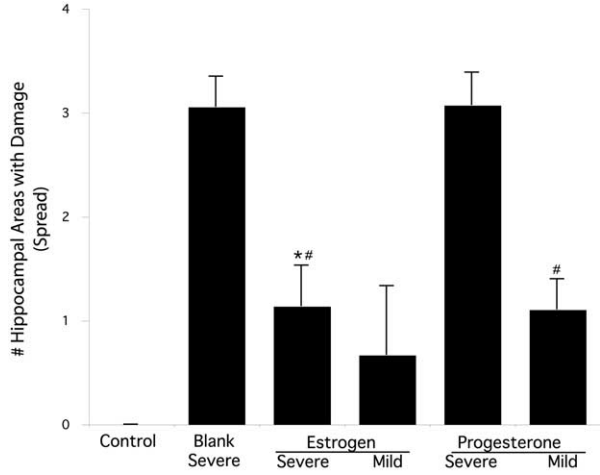

Fig. 6. Effects of estrogen or progesterone on spread of damage from KA in animals exhibiting mild (behavioral score ≤2) or severe (behavioral score >2) seizures. Animals treated with E that displayed severe seizures showed significantly fewer regions of neuronal damage after KA than severely affected animals that either did not receive hormone replacement (*$P < 0.005$) or received P treatment (#$P < 0.01$). The spread of damage in these E-treated rats was no different from that seen in animals that had only mild seizures. The spread of damage in severely affected rats that were treated with P was no different from that seen in severely affected KA-treated control animals (Blank, Severe).

animals with mild seizures after KA were significantly less than those seen in the severely affected P-treated rats ($P < 0.001$). Similar to what was noted in control animals, the losses of NeuN immunoreactivity within the CA subfields after KA treatment in P treated rats were significantly correlated with the seizure scores ($r^2 = 0.343$, $P < 0.005$; Fig. 8B). Thus, the higher the seizure score, the greater the degree of neuronal loss.

For estrogen-treated animals, no significant losses of NeuN immunoreactivity after KA treatment were noted. This was true even in animals displaying high seizure scores. As a result, estrogen-treated animals displaying severe seizures had significantly more NeuN-immunoreactive neurons than was seen in the animals treated with progesterone that had equally high seizure scores (Fig. 7; $P < 0.05$). No correlation was observed between seizure scores and NeuN immunoreactivity in the estrogen-treated rats (Fig. 8C; $r^2 = 0.018$; $P > 0.05$).

Discussion

The results of these studies indicate that progesterone produces its effect principally by reducing seizure behavior; by contrast, estrogen has little beneficial effect on seizure behavior but is capable of protecting the hippocampus from seizure damage. The majority of animal studies examining the effects of gonadal steroids on seizures reported that seizure susceptibility/activity was reduced by progesterone (Backstrom et al., 1985; Beyenburg et al., 2001; Edwards et al., 1999; Nicoletti et al., 1985). In addition, in women with catemenial epilepsy, the luteal phase, when progesterone levels are high relative to estrogen, is associated with a lower seizure incidence than the menstrual and follicular phases where estrogen and progesterone are both low or

Fig. 4. Hippocampal neuron patterns. Micrographs of the hippocampus from (A) control saline-treated ovariectomized rat with blank capsules shows the CA1, CA2, CA3, hilus, and dentate gyrus. (B) Blank + KA rat displaying a seizure score of 3.5 has marked neuronal losses in CA1, CA3, and the hilus (☆). This same animal also possessed damage to the entorhinal cortex (not shown). (C) P + KA-treated rat with a seizure score of 1.5 shows only slight neuron loss in the hilus; all other regions are normal. (D) P + KA-treated rat with a seizure score of 2.5 shows clear evidence of hilar neuronal loss (☆); (E) P + KA-treated rat with a seizure score of 3.5 had damage to the hippocampal CA fields (☆) that are quite similar to those in the blank + KA rats. (F) E-treated rat with a seizure score of 1.5 shows little or no hippocampal damage; (G) E treated rat with a seizure score of 3.5 also shows little evidence of neuronal loss.

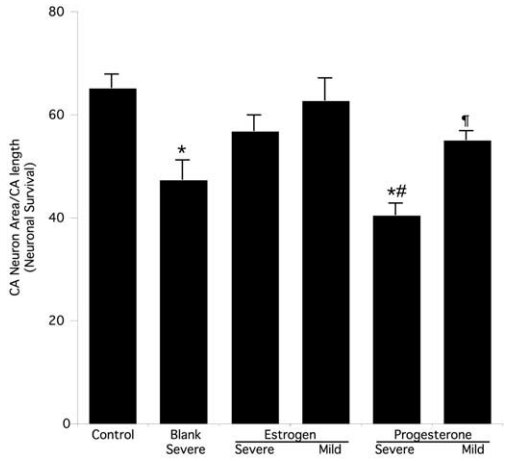

Fig. 7. Effects of estrogen or progesterone on neuron loss in KA-treated animals exhibiting mild (behavioral scores ≤2) or severe (behavioral scores >2) seizures. Ovariectomized animals that received blank capsules and showed severe seizures after KA had significant loss of NeuN immunoreactivity compared with control rats (*$P < 0.005$). Losses of NeuN immunoreactivity in P-treated rats were significantly different from control rats only when seizures were severe (*$P < 0.005$). Thus P-treated animals with high seizures had significantly more neuron losses than P-treated rats with mild seizures (#$P < 0.001$). In contrast, E-treated rats with either severe or mild seizures showed no significant differences in NeuN immunoreactivity (NeuN area/CA length) compared with controls.

estrogen is elevated relative to progesterone (Bauer, 2001; Bonuccelli et al., 1989; Herkes et al., 1993; Herzog et al., 1997; Lundberg, 1997; Morrell, 1992, 1999; Murri and Galli, 1997; Schachter, 1988; Zimmerman, 1986). Thus, it would logically follow that progesterone should reduce brain damage from seizures simply because there are fewer seizures. Indeed, in P-treated animals that exhibited reduced seizure severity, brain damage was reduced. What was surprising is that progesterone was only effective in reducing seizures at low physiological ranges. High doses of progesterone failed to reduce seizures or prevent brain damage.

Progesterone is metabolized to 3-α-hydroxy-5α-pregnan-20-one (allopregnanolone), a potent allosteric modulator of the $GABA_A$ receptor (Baulieu et al., 1996). Several studies have suggested allopregnanolone acting at the $GABA_A$ receptor is the mechanism whereby progesterone attenuates seizure activity (Beyenburg et al., 2001; Frye and Scalise, 2000; Frye et al., 1998; Galli et al., 2001; Morrell, 1992; Murri and Galli, 1997). Frye (1995), reported that subcutaneous administration of allopregnanolone 3 h prior to perforant path stimulation significantly reduced both seizure severity and the resulting hippocampal neuronal loss. What is difficult to explain is why higher plasma levels of progesterone failed to alter seizures or the brain damage from them. Levels of allopregnanolone and GABA receptor activity in vitro and in vivo are positively correlated with progesterone levels (Barbaccia et al., 1996; Corpechot et al., 1993), raising the expectation that increases in plasma progesterone should result in increased seizure suppression. In women suppression of brain excitability by progesterone is not universally effective. George and co-workers measured CSF levels of progesterone and its metabolites in women and their relationship to affective disorders (George et al., 1994). In that study, increased levels of allopregnanolone did not always accompany the increased progesterone levels seen during the luteal phase of the cycle, suggesting that biological variation in metabolism of progesterone could explain the variable effects of the steroid on seizures. Herzog (1995) too noted that of his female patients treated with progesterone, 28% did not respond to progesterone treatment. While that study did not speculate on the lack of effect in those women, altered conversion to allopregnanolone could be responsible. In our rats whether prolonged exposure to high, but not low, progesterone levels is capable of interfering with the synthesis of allopregnanolone remains to be determined.

It is also possible that after long-term exposure to allopregnanolone, the GABA receptor fails to respond or is downregulated. Studies examining GABA receptor function after withdrawal from chronic allopregnanolone or progesterone in pseudopregnant rats show that the receptor is desensitized and that expression of the alpha 4 subunit of

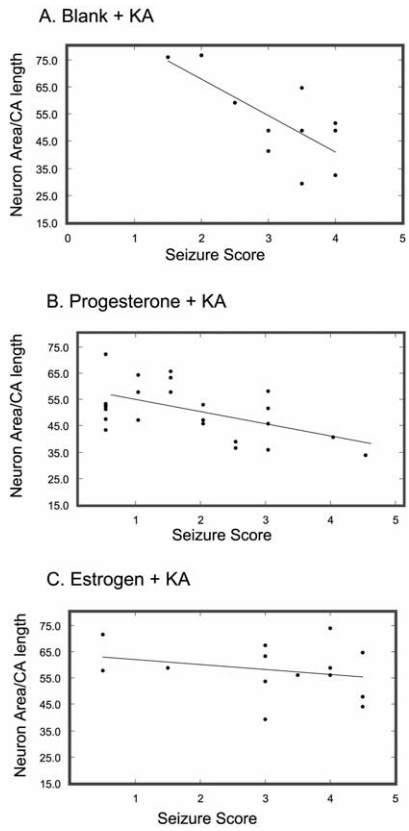

Fig. 8. Correlation of seizure severity and NeuN immunoreactivity in KA-treated ovariectomized rats with (A) blank implants, (B) progesterone, or (C) estrogen replacement. The NeuN immunoreactivity was negatively correlated with seizure scores in KA-treated animals with blank ($P < 0.02$) and P ($P < .005$) implants. In E-treated rats this relationship was lost ($P > 0.05$) owing to the fact that even when seizures were severe, neuron losses were reduced.

the $GABA_A$ receptor is reduced (Smith, 2002; Smith et al., 1998). The levels of the steroids were both relatively high prior to withdrawal. Since the studies did not examine GABA receptor function during pseudopregnancy when the hormone levels were still elevated, it is possible that the desensitization actually occurred prior to withdrawal. Indeed, in vitro, prolonged exposure of cortical neurons to allopregnanolone abolishes the potentiation of $GABA_A$ receptors by altering the allosteric interactions of allopregnanolone with the benzodiazepine binding sites (Friedman et al., 1993). Subsequent studies of cortical neurons in vitro determined that attenuation of $GABA_A$ receptor function was due to reduction in GABA receptor binding due to alterations in both beta and alpha receptor subunit expression (Yu et al., 1996). In vivo prolonged treatment with either progesterone or allopregnalonone produces similar desensitization of the GABA receptor and it was proposed that similar alterations in $GABA_A$ receptor subunit expression were responsible (Gulinello et al., 2001; Wohlfarth, et al., 2002). While none of the studies varied the dose of progesterone or allopregnanolone, if the desentization of the GABA receptor only occurs in conditions of high steroid levels, such changes in the $GABA_A$ receptor composition/function could explain why low but not high doses of progesterone reduced seizures after KA.

In the present study, administration of estrogen had no effect on KA seizure severity. A large number of studies in vivo and in vitro demonstrate that the steroid increases after discharge patterns and seizure thresholds (Backstrom et al., 1985; Buterbaugh, 1987, 1989; Buterbaugh and Hudson, 1991; Edwards et al., 1999; Gu and Moss, 1996; Hom and Buterbaugh, 1986; Hom et al., 1993; Kubo et al., 1975; Maggi and Perez, 1985; Nicoletti et al., 1985; Smith et al., 2002; Stitt and Kinnard, 1968; Teyler et al., 1980; Wong and Moss, 1991; Woolley, 2000). Thus, one would predict that under conditions of high estrogen concentrations KA would yield the strongest stimulatory effects thereby increasing the potential for excitotoxic brain damage. Yet, despite the persistence of seizures, estrogen replacement reduced mortality from KA seizures and significantly limited the overall spread of damage and amount of neuronal loss. Earlier studies examining hormonal effects on KA-induced brain damage are mixed. In intact females, injection of KA on proestrus (when estrogen levels are maximal) still produced substantial brain damage (Azcoitia et al., 1999). However, in that same study, animals that were ovariectomized and replaced with estrogen but not progesterone showed protection from damage, provided the steroid was administered 2 days prior to onset of seizures. Subcutaneous injections of 0.2 μg estrogen administered 48 and 24 h prior to KA reduced hippocampal brain damage (Veliskova et al., 2000), as did supraphysiological doses of estrogen (150 μg/rat) administered before or along with KA (Azcoitia et al., 1998, 1999). It would appear from these studies that reduction in damage from KA seizures by estrogen administration may not be strictly dose-dependent, but fluctuating hormone levels after steroid injection make that conclusion tenuous. Our data demonstrate more clearly that maintained doses of E in either the physiological range or supraphysiological range protect neurons from damage.

How estrogen protected the hippocampus from damage is not immediately clear. Initially it was thought that KA cell death was exclusively necrotic and there would be little basis for estrogen interfering in that process. More recent studies demonstrate that delayed cell death accompanied by DNA laddering (normally associated with apoptosis) after KA induced seizures (Fujikawa et al., 2000; Kondo et al., 1997; Kondratyev and Gale, 2001; Liu et al., 2001; Pollard et al., 1994a, 1994b; Venero et al., 1999). The proapoptotic molecule Bax is upregulated following KA seizures and concomitantly the prosurvival molecule Bcl-2 is downregulated (Gillardon et al., 1995). In a variety of models of neuronal injury estrogen upregulates expression of Bcl-2 (Choi et al., 2001; Dubal et al., 1999; Harms et al., 2001; Pike, 1999; Sawada et al., 2000; Singer et al., 1998) and, if acting similarly in our studies, this mechanism could explain estrogen's protective effects. There are also studies suggesting that antioxidant effects seen with high doses of estrogen protect neurons from cell death (Bae et al., 2000; Behl et al., 1995, 1997, 2000; Culmsee et al., 1999; Emilien et al., 2000; Goodman et al., 1996; Green et al., 1998; Green and Simpkins, 2000; Gridley et al., 1998; Inestrosa et al., 1998; Keller et al., 1997). The pellets we used generated plasma levels of estrogens high enough to produce antioxidant effects. The high progesterone levels in our animals should also have exerted antioxidant effects (Goodman et al., 1996); however, high levels of progesterone did nothing to protect the animals from seizures or neuronal cell death.

In summary, our data indicate that low but not high doses of progesterone reduce seizures and, in so doing, reduce damage to the hippocampus. Estrogen, on the other hand, at either physiological or supraphysiological levels, reduces neuronal cell death from seizures, but has little effect on seizure severity. It will be important to determine the mechanism whereby each of the steroids influences seizure activity and the ensuing brain injury. These results also raise the question of what effect combinations of both steroids might have. Possibly, when E + P are administered together, P would suppress seizure activity, but should some seizures still persist, E would then reduce the potential for brain damage. Studies examining this issue are currently underway.

Acknowledgments

The authors acknowledge Dr. Susan Zup and Ms. Takisha Schulderbrandt for their helpful editorial comments. This research was supported by DAMD1799-1-9483. Radioimmunoassays were supported by NICHD/NIH through cooperative agreement U54 HD28934 as part of the Specialized Cooperative Centers Program in Reproduction Research.

References

Azcoitia, I., Fernandez-Galaz, C., Sierra, A., Garcia-Segura, L.M., 1999. Gonadal hormones affect neuronal vulnerability to excitotoxin-induced degeneration. J. Neurocytol. 28, 699–710.

Azcoitia, I., Sierra, A., Garcia-Segura, L.M., 1998. Estradiol prevents kainic acid-induced neuronal loss in the rat dentate gyrus. NeuroReport 9, 3075–3079.

Azcoitia, I., Sierra, A., Garcia-Segura, L.M., 1999. Neuroprotective effects of estradiol in the adult rat hippocampus: interaction with insulin-like growth factor-I signalling. J. Neurosci. Res. 58, 815–822.

Backstrom, T., Bixo, M., Hammarback, S., 1985. Ovarian steroid hormones: effects on mood, behaviour and brain excitability. Acta Obstet. Gynecol. Scand. 130 (Suppl.), 19–24.

Bae, Y.H., Hwang, J.Y., Kim, Y.H., Koh, J.Y., 2000. Anti-oxidative neuroprotection by estrogens in mouse cortical cultures. J. Korean Med. Sci. 15, 327–336.

Barbaccia, M.L., Roscetti, G., Trabucchi, M., Mostallino, M.C., Concas, A., Purdy, R.H., Biggio, G., 1996. Time-dependent changes in rat brain neuroactive steroid concentrations and GABAA receptor function after acute stress. Neuroendocrinology 63, 166–172.

Bauer, J., 2001. Interactions between hormones and epilepsy in female patients. Epilepsia 42, 20–22.

Baulieu, E.E., Schumacher, M., Koenig, H., Jung-Testas, I., Akwa, Y., 1996. Progesterone as a neurosteroid: actions within the nervous system. Cell. Mol. Neurobiol. 16, 143–154.

Behl, C., Moosmann, B., Manthey, D., Heck, S., 2000. The female sex hormone oestrogen as neuroprotectant: activities at various levels. Novartis Found. Symp. 230, 221–234.

Behl, C., Skutella, T., Lezoualc'h, F., Post, A., Widmann, M., Newton, C.J., Holsboer, F., 1997. Neuroprotection against oxidative stress by estrogens: structure–activity relationship. Mol. Pharmacol. 51, 535–541.

Behl, C., Widmann, M., Trapp, T., Holsboer, F., 1995. 17-beta estradiol protects neurons from oxidative stress-induced cell death in vitro. Biochem. Biophys. Res. Commun. 216, 473–482.

Ben-Ari, Y., Tremblay, E., Ottersen, O.P., Meldrum, B.S., 1980. The role of epileptic activity in hippocampal and "remote" cerebral lesions induced by kainic acid. Brain Res. 191, 79–97.

Beyenburg, S., Stoffel-Wagner, B., Bauer, J., Watzka, M., Blumcke, I., Bidlingmaier, F., Elger, C.E., 2001. Neuroactive steroids and seizure susceptibility. Epilepsy Res. 44, 141–153.

Bonuccelli, U., Melis, G.B., Paoletti, A.M., Fioretti, P., Murri, L., Muratorio, A., 1989. Unbalanced progesterone and estradiol secretion in catamenial epilepsy. Epilepsy Res. 3, 100–106.

Buterbaugh, G.G., 1987. Acquisition of amygdala-kindled seizures in female rats: relationship between the effect of estradiol and intra-amygdaloid electrode location. Pharmacol. Biochem. Behav. 28, 291–297.

Buterbaugh, G.G., 1989. Estradiol replacement facilitates the acquisition of seizures kindled from the anterior neocortex in female rats. Epilepsy Res. 4, 207–215.

Buterbaugh, G.G., Hudson, G.M., 1991. Estradiol replacement to female rats facilitates dorsal hippocampal but not ventral hippocampal kindled seizure acquisition. Exp. Neurol. 111, 55–64.

Choi, K.C., Kang, S.K., Tai, C.J., Auersperg, N., Leung, P.C., 2001. Estradiol up-regulates antiapoptotic Bcl-2 messenger ribonucleic acid and protein in tumorigenic ovarian surface epithelium cells. Endocrinology 142, 2351–2360.

Corpechot, C., Young, J., Calvel, M., Wehrey, C., Veltz, J.N., Touyer, G., Mouren, M., Prasad, V.V., Banner, C., Sjovall, J., et al., 1993. Neurosteroids: 3 alpha-hydroxy-5 alpha-pregnan-20-one and its precursors in the brain, plasma, and steroidogenic glands of male and female rats. Endocrinology 133, 1003–1009.

Culmsee, C., Vedder, H., Ravati, A., Junker, V., Otto, D., Ahlemeyer, B., Krieg, J.C., Krieglstein, J., 1999. Neuroprotection by estrogens in a mouse model of focal cerebral ischemia and in cultured neurons: evidence for a receptor-independent antioxidative mechanism. J. Cereb. Blood Flow Metab. 19, 1263–1269.

Dubal, D.B., Shughrue, P.J., Wilson, M.E., Merchenthaler, I., Wise, P.M., 1999. Estradiol modulates bcl-2 in cerebral ischemia: a potential role for estrogen receptors. J. Neurosci. 19, 6385–6393.

Edwards, H.E., Burnham, W.M., Mendonca, A., Bowlby, D.A., MacLusky, N.J., 1999. Steroid hormones affect limbic afterdischarge thresholds and kindling rates in adult female rats. Brain Res. 838, 136–150.

Emilien, G., Beyreuther, K., Masters, C.L., Maloteaux, J.M., 2000. Prospects for pharmacological intervention in Alzheimer disease. Arch. Neurol. 57, 454–459.

Friedman, L., Gibbs, T.T., Farb, D.H., 1993. Gamma-aminobutyric acidA receptor regulation: chronic treatment with pregnanolone uncouples allosteric interactions between steroid and benzodiazepine recognition sites. Mol. Pharmacol. 44, 191–197.

Frye, C.A., 1995. The neurosteroid 3 alpha, 5 apha-THP has antiseizure and possible neuroprotective effects in an animal model of epilepsy. Brain Res. 696, 113–120.

Frye, C.A., Bayon, L.E., 1998. Seizure activity is increased in endocrine states characterized by decline in endogenous levels of the neurosteroid 3 alpha,5 alpha-THP. Neuroendocrinology 68, 272–280.

Frye, C.A., Scalise, T.J., 2000. Anti-seizure effects of progesterone and 3alpha,5alpha-THP in kainic acid and perforant pathway models of epilepsy. Psychoneuroendocrinology 25, 407–420.

Frye, C.A., Scalise, T.J., Bayon, L.E., 1998. Finasteride blocks the reduction in ictal activity produced by exogenous estrous cyclicity. J. Neuroendocrinol. 10, 291–296.

Fujikawa, D.G., Shinmei, S.S., Cai, B., 2000. Seizure-induced neuronal necrosis: implications for programmed cell death mechanisms. Epilepsia 41, S9–13.

Galli, R., Luisi, M., Pizzanelli, C., Monteleone, P., Casarosa, E., Iudice, A., Murri, L., 2001. Circulating levels of allopregnanolone, an anticonvulsant metabolite of progesterone, in women with partial epilepsy in the postcritical phase. Epilepsia 42, 216–219.

Gayoso, M.J., Primo, C., al-Majdalawi, A., Fernandez, J.M., Garrosa, M., Iniguez, C., 1994. Brain lesions and water-maze learning deficits after systemic administration of kainic acid to adult rats. Brain Res. 653, 92–100.

George, M.S., Guidotti, A., Rubinow, D., Pan, B., Mikalauskas, K., Post, R.M., 1994. CSF neuroactive steroids in affective disorders: pregnenolone, progesterone, and DBI. Biol. Psychiat. 35, 775–780.

Gillardon, F., Wickert, H., Zimmermann, M., 1995. Up-regulation of bax and down-regulation of bcl-2 is associated with kainate-induced apoptosis in mouse brain. Neurosci. Lett. 192, 85–88.

Goodman, Y., Bruce, A.J., Cheng, B., Mattson, M.P., 1996. Estrogens attenuate and corticosterone exacerbates excitotoxicity, oxidative injury, and amyloid beta-peptide toxicity in hippocampal neurons. J. Neurochem. 66, 1836–1844.

Green, P.S., Gridley, K.E., Simpkins, J.W., 1998. Nuclear estrogen receptor-independent neuroprotection by estratrienes: a novel interaction with glutathione. Neuroscience 84, 7–10.

Green, P.S., Simpkins, J.W., 2000. Neuroprotective effects of estrogens: potential mechanisms of action. Int. J. Dev. Neurosci. 18, 347–358.

Gridley, K.E., Green, P.S., Simpkins, J.W., 1998. A novel, synergistic interaction between 17 beta-estradiol and glutathione in the protection of neurons against beta-amyloid 25–35-induced toxicity in vitro. Mol. Pharmacol. 54, 874–880.

Gu, Q., Moss, R.L., 1996. 17 beta-Estradiol potentiates kainate-induced currents via activation of the cAMP cascade. J. Neurosci. 16, 3620–3629.

Gulinello, M., Gong, Q.H., Li, X., Smith, S.S., 2001. Short-term exposure to a neuroactive steroid increases alpha4 GABA(A) receptor subunit levels in association with increased anxiety in the female rat. Brain Res. 910, 55–66.

Harms, C., Lautenschlager, M., Bergk, A., Katchanov, J., Freyer, D., Kapinya, K., Herwig, U., Megow, D., Dirnagl, U., Weber, J.R., Hortnagl, H., 2001. Differential mechanisms of neuroprotection by 17 beta-estradiol in apoptotic versus necrotic neurodegeneration. J. Neurosci. 21, 2600–2609.

Herkes, G.K., Eadie, M.J., Sharbrough, F., Moyer, T., 1993. Patterns of seizure occurrence in catamenial epilepsy. Epilepsy Res. 15, 47–52.

Herzog, A.G., 1995. Progesterone therapy in women with complex partial and secondary generalized seizures. Neurology 45, 1660–1662.

Herzog, A.G., Klein, P., Ransil, B.J., 1997. Three patterns of catamenial epilepsy. Epilepsia 38, 1082–1088.

Hoffman, G.E., Le, W.W., Murphy, A.Z., Koski, C.L., 2001. Divergent effects of ovarian steroids on neuronal survival during experimental allergic encephalitis in Lewis rats. Exp. Neurol. 171, 272–284.

Holmes, L.B., Harvey, E.A., Coull, B.A., Huntington, K.B., Khoshbin, S., Hayes, A.M., Ryan, L.M., 2001. The teratogenicity of anticonvulsant drugs. N. Engl. J. Med. 344, 1132–1138.

Hom, A.C., Buterbaugh, G.G., 1986. Estrogen alters the acquisition of seizures kindled by repeated amygdala stimulation or pentylenetetrazol administration in ovariectomized female rats. Epilepsia 27, 103–108.

Hom, A.C., Leppik, I.E., Rask, C.A., 1993. Effects of estradiol and progesterone on seizure sensitivity in oophorectomized DBA/2J mice and C57/EL hybrid mice. Neurology 43, 198–204.

Inestrosa, N.C., Marzolo, M.P., Bonnefont, A.B., 1998. Cellular and molecular basis of estrogen's neuroprotection: potential relevance for Alzheimer's disease. Mol. Neurobiol. 17, 73–86.

Jarrard, L.E., 1983. Selective hippocampal lesions and behavior: effects of kainic acid lesions on performance of place and cue tasks. Behav. Neurosci. 97, 873–889.

Kalviainen, R., Salmenpera, T., Partanen, K., Vainio, P., Riekkinen, P., Pitkanen, A., 1998. Recurrent seizures may cause hippocampal damage in temporal lobe epilepsy. Neurology 50, 1377–1382.

Keller, J.N., Germeyer, A., Begley, J.G., Mattson, M.P., 1997. 17Beta-estradiol attenuates oxidative impairment of synaptic Na+/K+− ATPase activity, glucose transport, and glutamate transport induced by amyloid beta-peptide and iron. J. Neurosci. Res. 50, 522–530.

Kondo, T., Sharp, F.R., Honkaniemi, J., Mikawa, S., Epstein, C.J., Chan, P.H., 1997. DNA fragmentation and Prolonged expression of c-fos, c-jun, and hsp70 in kainic acid-induced neuronal cell death in transgenic mice overexpressing human CuZn-superoxide dismutase. J. Cereb. Blood Flow Metab. 17, 241–256.

Kondratyev, A., Gale, K., 2001. Temporal and spatial patterns of DNA fragmentation following focally or systemically-evoked status epilepticus in rats. Neurosci. Lett. 310, 13–16.

Kubo, K., Gorski, R.A., Kawakami, M., 1975. Effects of estrogen on neuronal excitability in the hippocampal–septal–hypothalamic system. Neuroendocrinology 18, 176–191.

Liu, W., Liu, R., Chun, J.T., Bi, R., Hoe, W., Schreiber, S.S., Baudry, M., 2001. Kainate excitotoxicity in organotypic hippocampal slice cultures: evidence for multiple apoptotic pathways. Brain Res. 916, 239–248.

Lothman, E.W., Collins, R.C., 1981. Kainic acid induced limbic seizures: metabolic behavioral, electroencephalographic, and neuropathological correlates. Brain Res. 218, 299–318.

Lundberg, P.O., 1997. Catamenial epilepsy: a review. Cephalalgia 17 (Suppl. 20), 42–45.

Maggi, A., Perez, J., 1985. Role of female gonadal hormones in the CNS: clinical and experimental aspects. Life Sci. 37, 893–906.

Mathern, G.W., Price, G., Rosales, C., Pretorius, J.K., Lozada, A., Mendoza, D., 1998. Anoxia during kainate status epilepticus shortens behavioral convulsions but generates hippocampal neuron loss and supragranular mossy fiber sprouting. Epilepsy Res. 30, 133–151.

Morrell, M.J., 1992. Hormones and epilepsy through the lifetime. Epilepsia 33, S49–S61.

Morrell, M.J., 1999. Epilepsy in women: the science of why it is special. Neurology 53(4), S42–S48.

Moshe, S.L., 1998. Brain injury with prolonged seizures in children and adults. J. Child Neurol. 13 (Suppl 1), S30–S32 S3–S6; discussion.

Mullen, R.J., Buck, C.R., Smith, A.M., 1992. NeuN, a neuronal specific nuclear protein in vertebrates. Development 116, 201–211.

Murri, L., Galli, R., 1997. Catamenial epilepsy, progesterone and its metabolites. Cephalalgia 17 (Suppl. 20), 46–47.

Nicoletti, F., Speciale, C., Sortino, M.A., Summa, G., Caruso, G., Patti, F., Canonico, P.L., 1985. Comparative effects of estradiol benzoate, the antiestrogen clomiphene citrate, and the progestin medroxyprogesterone acetate on kainic acid-induced seizures in male and female rats. Epilepsia 26, 252–257.

Olney, J.W., Collins, R.C., Sloviter, R.S., 1986. Excitotoxic mechanisms of epileptic brain damage. Adv. Neurol. 44, 857–877.

Olney, J.W., Fuller, T., de Gubareff, T., 1979. Acute dendrotoxic changes in the hippocampus of kainate treated rats. Brain Res. 176, 91–100.

Pike, C.J., 1999. Estrogen modulates neuronal Bcl-xL expression and beta-amyloid-induced apoptosis: relevance to Alzheimer's disease. J. Neurochem. 72, 1552–1563.

Pollard, H., Cantagrel, S., Charriaut-Marlangue, C., Moreau, J., Ben Ari, Y., 1994a. Apoptosis associated DNA fragmentation in epileptic brain damage. NeuroReport 5, 1053–1055.

Pollard, H., Charriaut-Marlangue, C., Cantagrel, S., Represa, A., Robain, O., Moreau, J., Ben-Ari, Y., 1994b. Kainate-induced apoptotic cell death in hippocampal neurons. Neuroscience 63, 7–18.

Salmenpera, T., Kalviainen, R., Partanen, K., Pitkanen, A., 2001. Hippocampal and amygdaloid damage in partial epilepsy: a cross-sectional MRI study of 241 patients. Epilepsy Res. 46, 69–82.

Sawada, H., Ibi, M., Kihara, T., Urushitani, M., Honda, K., Nakanishi, M., Akaike, A., Shimohama, S., 2000. Mechanisms of antiapoptotic effects of estrogens in nigral dopaminergic neurons. FASEB J. 14, 1202–1214.

Schachter, S.C., 1988. Hormonal considerations in women with seizures. Arch. Neurol. 45, 1267–1270.

Singer, C.A., Rogers, K.L., Dorsa, D.M., 1998. Modulation of Bcl-2 expression: a potential component of estrogen protection in NT2 neurons. NeuroReport 9, 2565–2568.

Smith, M.D., Jones, L.S., Wilson, M.A., 2002. Sex differences in hippocampal slice excitability: role of testosterone. Neuroscience 109, 517–530.

Smith, S.S., 2002. Withdrawal properties of a neuroactive steroid: implications for GABA(A) receptor gene regulation in the brain and anxiety behavior. Steroids 67, 519–528.

Smith, S.S., Gong, Q.H., Li, X., Moran, M.H., Bitran, D., Frye, C.A., Hsu, F.C., 1998. Withdrawal from 3alpha-OH-5alpha-pregnan-20-One using a pseudopregnancy model alters the kinetics of hippocampal GABAA-gated current and increases the GABAA receptor alpha4 subunit in association with increased anxiety. J. Neurosci. 18, 5275–5284.

Sperk, G., Lassmann, H., Baran, H., Kish, S.J., Seitelberger, F., Hornykiewicz, O., 1983. Kainic acid induced seizures: neurochemical and histopathological changes. Neuroscience 10, 1301–1315.

Stitt, S.L., Kinnard, W.J., 1968. The effect of certain progestins and estrogens on the threshold of electrically induced seizure patterns. Neurology 18, 213–216.

Tasch, E., Cendes, F., Li, L.M., Dubeau, F., Andermann, F., Arnold, D.L., 1999. Neuroimaging evidence of progressive neuronal loss and dysfunction in temporal lobe epilepsy. Ann. Neurol. 45, 568–576.

Tauboll, E., Lindstrom, S., 1993. The effect of progesterone and its metabolite 5 alpha-pregnan-3 alpha-ol-20-one on focal epileptic seizures in the cat's visual cortex in vivo. Epilepsy Res. 14, 17–30.

Teyler, T.J., Vardaris, R.M., Lewis, D., Rawitch, A.B., 1980. Gonadal steroids: effects on excitability of hippocampal pyramidal cells. Science 209, 1017–1018.

Theodore, W.H., Bhatia, S., Hatta, J., Fazilat, S., DeCarli, C., Bookheimer, S.Y., Gaillard, W.D.,, 1999. Hippocampal atrophy, epilepsy duration, and febrile seizures in patients with partial seizures. Neurology 52, 132–136.

Veliskova, J., Velisek, L., Galanopoulou, A.S., Sperber, E.F., 2000. Neuroprotective effects of estrogens on hippocampal cells in adult female rats after status epilepticus. Epilepsia 41, S30–S35.

Venero, J.L., Revuelta, M., Machado, A., Cano, J., 1999. Delayed apoptotic pyramidal cell death in CA4 and CA1 hippocampal subfields after a single intraseptal injection of kainate. Neuroscience 94, 1071–1081.

Watson, R.E., Wiegand, S.J., Clough, R.W., Hoffman, G.E., 1986. Use of cryoprotectant to maintain longterm peptide immunoreactivity and tissue morphology. Peptides 7, 155–159.

Wohlfarth, K.M., Bianchi, M.T., Macdonald, R.L., 2002. Enhanced neurosteroid potentiation of ternary GABA(A) receptors containing the delta subunit. J. Neurosci. 22, 1541–1549.

Wolf, H.K., Buslei, R., Schmidt-Kastner, R., Schmidt-Kastner, P.K., Pietsch, T., Wiestler, O.D., Bluhmke, I., 1996. NeuN: a useful neuronal marker for diagnostic histopathology. J. Histochem. Cytochem. 44, 1167–1171.

Wong, M., Moss, R.L., 1991. Electrophysiological evidence for a rapid membrane action of the gonadal steroid, 17 beta-estradiol, on CA1 pyramidal neurons of the rat hippocampus. Brain Res. 543, 148–152.

Woolley, C.S., 2000. Estradiol facilitates kainic acid-induced, but not flurothyl-induced, behavioral seizure activity in adult female rats. Epilepsia 41, 510–515.

Yu, R., Follesa, P., Ticku, M.K., 1996. Down-regulation of the GABA receptor subunits mRNA levels in mammalian cultured cortical neurons following chronic neurosteroid treatment. Brain Res. Mol. Brain Res. 41, 163–168.

Zimmerman, A.W., 1986. Hormones and epilepsy. Neurol. Clin. 4, 853–861.

Journal of Neurochemistry, 2003, **86**, 1101–1107 doi:10.1046/j.1471-4159.2003.01908.x

Regulation of brain mitochondrial H_2O_2 production by membrane potential and NAD(P)H redox state

Anatoly A. Starkov and Gary Fiskum

Department of Anesthesiology, University of Maryland School of Medicine, Baltimore, Maryland, USA

Abstract

Mitochondrial production of reactive oxygen species (ROS) at Complex I of the electron transport chain is implicated in the etiology of neural cell death in acute and chronic neurodegenerative disorders. However, little is known regarding the regulation of mitochondrial ROS production by NADH-linked respiratory substrates under physiologically realistic conditions in the absence of respiratory chain inhibitors. This study used Amplex Red fluorescence measurements of H_2O_2 to test the hypothesis that ROS production by isolated brain mitochondria is regulated by membrane potential ($\Delta\Psi$) and NAD(P)H redox state. $\Delta\Psi$ was monitored by following the medium concentration of the lipophilic cation tetraphenylphosphonium with a selective electrode. NAD(P)H autofluorescence was used to monitor NAD(P)H redox state. While the rate of H_2O_2 production was closely related to $\Delta\Psi$ and the level of NAD(P)H reduction at high values of $\Delta\Psi$, 30% of the maximal rate of H_2O_2 formation was still observed in the presence of uncoupler (*p*-trifluoromethoxycarbonylcyanide phenylhydrazone) concentrations that provided for maximum depolarization of $\Delta\Psi$ and oxidation of NAD(P)H. Our findings indicate that ROS production by mitochondria oxidizing physiological NADH-dependent substrates is regulated by $\Delta\Psi$ and by the NAD(P)H redox state over ranges consistent with those that exist at different levels of cellular energy demand.

Keywords: brain mitochondria, hydrogen peroxide, membrane potential, reactive oxygen species.

J. Neurochem. (2003) **86,** 1101–1107.

Mitochondrial production of reactive oxygen species (ROS) is involved in neural cell death associated with acute ischemic brain injury and with chronic neurodegenerative diseases (Fiskum 2000; Nicholls and Budd 2000). Several potential sites of ROS production exist within the mitochondrial electron transport chain. Recent attention has focused on respiratory chain Complex I as an important source of free radicals, due in part to the stimulation of ROS production and induction of oxidative stress caused by neurotoxins, e.g. 1-methyl-4-phenylpyridinium (MPP^+) and rotenone, that target Complex I and evoke a neuropathology similar to that of Parkinson's disease (Sherer *et al*. 2002). The molecular mechanism and regulation of ROS production by Complex I is, however, not well understood (reviewed in Turrens 1997).

As Complex I may be a primary site of mitochondrial ROS generation in the absence of toxins as well as in their presence, identification of physiological factors that control Complex I mediated ROS production is necessary. We hypothesized that such factors include mitochondrial membrane potential and NAD(P)H redox state. Both undergo substantial fluctuation in response to different levels of mitochondrial respiratory activity caused by, for example, different demand for ATP production. Modulation of these factors by the activities of mitochondrial uncoupling proteins and by the mitochondrial ATP-regulated potassium channel may also explain their apparent ability to reduce mitochondrial ROS production (Kim-Han *et al*. 2001; Echtay *et al*. 2002; Ferranti *et al*. 2003). The results of this study support the hypothesis that biologically relevant, NADH linked substrate-dependent mitochondrial ROS production is tightly controlled by membrane potential and NAD(P)H redox state in the physiological range.

Resubmitted manuscript received March 23, 2003; accepted April 29, 2003.

Address correspondence and reprint requests to Dr Gary Fiskum, Department of Anesthesiology, University of Maryland School of Medicine, 685 W. Baltimore St., MSTF-5.34, Baltimore, MD 21201, USA. E-mail: gfisk001@umaryland.edu

Abbreviations used: ACI, acceptor control index; $\Delta\Psi$, mitochondrial membrane potential; FCCP, *p*-trifluoromethoxycarbonylcyanide phenylhydrazone, MPP^+, 1-methyl-4-phenylpyridinium; ROS, reactive oxygen species; TPP^+, tetraphenylphosphonium.

Materials and methods

Isolation of brain mitochondria

All animal experiments were conducted in accordance with guidelines established by the Institutional Animal Care and Use Committee of the University of Maryland, Baltimore.

Brain mitochondria were isolated from adult male Sprague Dawley rats as described in Rosenthal *et al*. (1987), with the only modification that our isolation buffer did not contain Nagarse protease. This method utilizes digitonin to disrupt synaptosomal membranes, yielding mitochondria from both synaptosomal and non-synaptosomal origin. The functional quality of each mitochondrial preparation was estimated by measuring acceptor control index (ACI). For these experiments, incubation medium was composed of 125 mM KCl, 20 mM HEPES (pH 7.0), 2 mM KH_2PO_4, 0.8 mM ADP, 1 mM $MgCl_2$, 5 mM glutamate, and 5 mM malate. Oxygen consumption was recorded with a Clark-type oxygen electrode. The State 3 respiration was initiated by the addition of 0.5 mg/mL rat brain mitochondria to the incubation medium, and was terminated with 0.5 μg/mL oligomycin. The ratio of respiration rate in State 3 to that in the presence of oligomycin was defined as ACI. Preparations exhibiting values for ACI in the range of 8–12 were used for this study.

Experimental conditions and incubation medium

Incubation medium contained 125 mM KCl, 20 mM HEPES (pH 7.0), 2 mM KH_2PO_4, 1 mM $MgCl_2$, 0.5 mg/mL bovine serum albumin, and 0.25 mM EGTA, and was maintained at 37°C, unless stated otherwise.

Measurement of hydrogen peroxide

Hydrogen peroxide production was measured fluorimetrically employing the dye Amplex Red (Molecular Probes, Eugene, OR, USA) in combination with horseradish peroxidase (Kushnareva *et al*. 2002; Rosen *et al*. 2002). In these experiments, the incubation medium was supplemented with 1 μM amplex red, 5 U/mL horseradish peroxidase, and 40 U/mL Cu,Zn superoxide dismutase. The presence of superoxide dismutase prevents the auto-oxidation of Amplex Red that interferes with quantitative assessment of low rates of H_2O_2 production. The detection of H_2O_2 in mitochondrial suspensions was recorded as an increase in fluorescence of the dye at 585 nm with the excitation wavelength set at 550 nm. The dye response was calibrated either by sequential additions of known amounts of hydrogen peroxide solution, or by continuous infusion of H_2O_2 solution at 100–1000 pmol/min. The concentration of commercial 30% H_2O_2 solution was calculated from light absorbance at 240 nM employing $E^{240} = 43.6\ \text{M}^{-1}\ \text{cm}^{-1}$; the stock solution was diluted to 100 μM with de-ionized water and used for calibration immediately.

Measurement of mitochondrial membrane potential

Mitochondrial membrane potential ($\Delta\Psi$) was estimated from tetraphenylphosphonium (TPP^+) ion distribution measured with a custom-made TPP^+-selective electrode (Kamo *et al*. 1979). For these experiments, incubation medium was supplemented with 1.6 μM TPP^+Cl^-. Both the TPP^+-sensitive and the reference electrodes were inserted directly into the fluorimeter cuvette and data were collected using an amplifier and a two-channel data acquisition system. The electrode response was calibrated by sequential additions of TPP^+Cl^- in the range of concentrations 0.2–1.6 μM and $\Delta\Psi$ was calculated as described in Rolfe *et al*. (1994) utilizing the reported binding correction factor for brain mitochondria. Alternatively, $\Delta\Psi$ values were calculated by the procedure reported in Rottenberg (1984), assuming the matrix volume for brain mitochondria equal to 1.2 μL/mg protein. Both procedures gave essentially similar results. No attempt to correct for non-$\Delta\Psi$ dependent binding of TPP^+ was made (Hashimoto *et al*. 1984; Rottenberg 1984; Rolfe *et al*. 1994).

Measurement of NAD(P)H oxidation/reduction state

Reduced NAD(P)H was measured fluorimetrically using an excitation wavelength of 346 nm and an emission wavelength of 460 nm. Maximal NAD(P)H reduction was defined as the absorbance observed after the addition of the electron transport chain Complex I inhibitor rotenone (1 μM) and maximal oxidation defined as the absorbance obtained in the presence of the respiratory uncoupler *p*-trifluoromethoxycarbonylcyanide phenylhydrazone (FCCP) (0.1 μM).

Reagents

Oligomycin, FCCP, and rotenone were dissolved in ethanol, and Amplex Red was dissolved in dimethylsulfoxide. All reagents and ethanol were tested and exhibited no interference with H_2O_2 assay at the concentrations used in our experiments. All the reagents were purchased from Sigma (St Louis, MO, USA).

Results

The results shown in Fig. 1 illustrate the dependence of H_2O_2 production on mitochondrial $\Delta\Psi$ in the presence of NADH-linked respiratory substrates. Suspensions of rat brain mitochondria were exposed to various concentrations (0–80 nM) of the uncoupler FCCP to lower $\Delta\Psi$. Alternatively, mitochondria were exposed to ADP (0.8 mM) to reduce $\Delta\Psi$ as a consequence of activating State 3 respiration, i.e. oxidative phosphorylation. H_2O_2 production was measured fluorimetrically with the dye Amplex Red and $\Delta\Psi$ was calculated based on the medium/mitochondrial distribution of the lipophilic cation TPP^+, as measured with an electrode placed within the fluorometer cuvette. Malate plus glutamate or α-ketoglutarate were used as NADH-linked substrates.

In the presence of either set of NADH-linked oxidizable substrates, a reduction in $\Delta\Psi$ was accompanied by a decrease in H_2O_2 production (Fig. 1). This relationship between H_2O_2 production and $\Delta\Psi$ is qualitatively similar to that reported earlier for heart mitochondria oxidizing the Complex II respiratory substrate succinate (Korshunov *et al*. 1997). However, whereas a small, 10% reduction in $\Delta\Psi$ resulted in a 90% reduction in succinate-supported ROS production (Korshunov *et al*. 1997), approximately 30% of the maximal rate of NADH-linked substrate dependent ROS production was still present at a concentration of FCCP that caused maximal reduction of membrane potential (Fig. 1) and a maximal increase in O_2 consumption (not shown). Addition

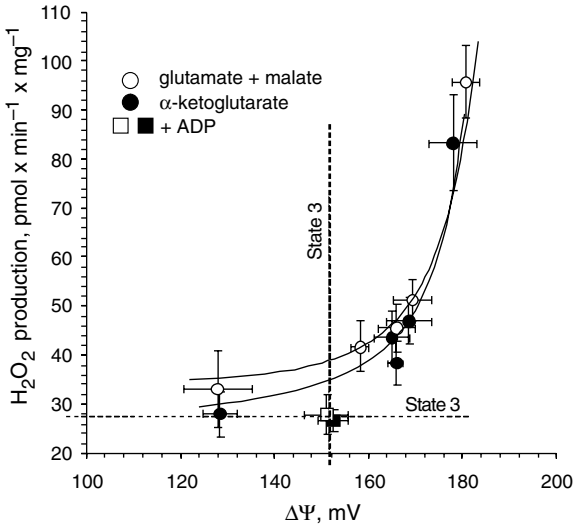

Fig. 1 Relationship between mitochondrial membrane potential and H_2O_2 production supported by NADH-linked respiratory substrates. Mitochondrial membrane potential was calculated based on the distribution of the lipophilic cation TPP^+, using an electrode to measure the medium [TPP^+] (1.2 μM initial concentration). H_2O_2 was measured simultaneously by monitoring the fluorescence of Amplex Red (1 μM) in the presence of horseradish peroxidase (5 U/mL) and 40 U/mL Cu/Zn superoxide dismutase. Incubation medium (see 'Materials and methods') maintained at 37°C also contained either 5 mM malate + 5 mM glutamate (○) or 5 mM α-ketoglutarate (●). Mitochondria were added at 0.5 mg/mL. Differences in membrane potential were generated by adding various concentrations of FCCP ranging from 0 to 80 nM (0–160 pmol/mg mitochondrial protein). Alternatively, a decrease in membrane potential was induced by adding 0.8 mM ADP to mitochondria respiring on malate + glutamate (□) or α-ketoglutarate (■). Values represent means ± SD for $n = 4$ experiments.

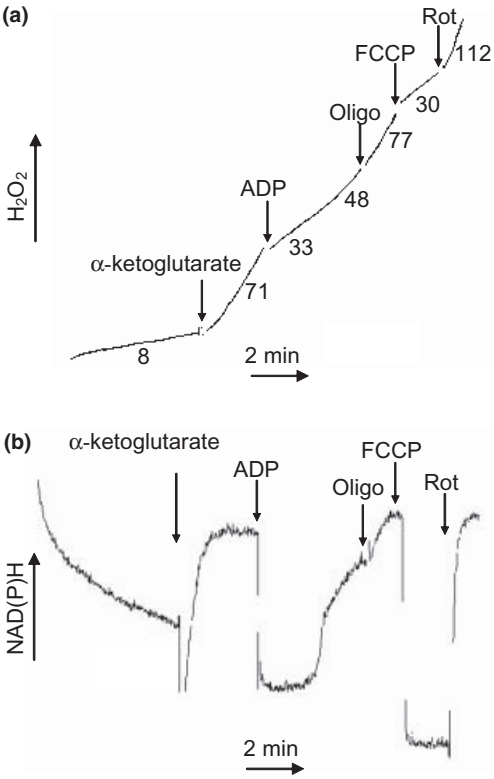

Fig. 2 Regulation of mitochondrial H_2O_2 production through metabolic modulation of NAD(P)H redox state. (a) H_2O_2 production by brain mitochondria. (b) Mitochondrial NAD(P)H autofluorescence. Incubation medium (see 'Materials and methods') maintained at 37°C was supplemented with 5 U/mL horseradish peroxidase, 1 μM Amplex red, and 40 U/mL SOD. Mitochondria were added at 0.5 mg/mL. Additions to the suspensions were α-ketoglutarate (5 mM), ADP (0.8 mM), oligomycin (0.5 μg/ml), FCCP (80 nM), and rotenone (0.5 μM).

of even greater FCCP concentrations had no further effect on either ROS production or TPP^+ distribution. As the TPP^+ procedure for monitoring ΔΨ is incapable of detecting potentials at less than approximately 120 mV, these observations indicate that a significant fraction of maximal NADH-dependent mitochondrial ROS production can occur in the absence of ΔΨ.

A 70% reduction in ROS generation was also observed in the absence of FCCP when ADP was added to initiate oxidative phosphorylation, thereby stimulating respiration (Fig. 1). Therefore, physiologically relevant NADH-linked respiration generates ROS in a manner that is tightly regulated by differences in ΔΨ over a range that occurs during normal fluctuations in energy metabolism. The approximately 70% reduction in ROS production during State 3 respiration was, however, observed at a level of ΔΨ that was approximately 20 mV greater than that present at the same rate of ROS generation evoked by the addition of FCCP.

The redox state of mitochondrial pyridine nucleotides is sensitive to changes in ΔΨ when respiration is supported by NADH-linked substrates. We therefore performed parallel measurements of H_2O_2 production and reduced NAD(P)H to determine their relationship (Fig. 2). Addition of brain mitochondria to medium in the absence of respiratory substrates resulted in a steady oxidized shift of pyridine nucleotides and a relatively very low rate of H_2O_2 production. In the absence of exogenous oxidizable substrates, respiration is also minimal. Thus the flow of electrons limits both ROS production and O_2 consumption under these conditions. Addition of the respiratory substrate α-ketoglutarate caused an abrupt increase in the level of reduced NAD(P)H and stimulated ROS production by almost 10-fold. Subsequent addition of 0.8 mM ADP resulted in an immediate and extensive oxidation of pyridine nucleotides and a > 50% reduction in H_2O_2 production. During the next 4 min, the pyridine nucleotide redox state underwent a partial reversal toward reduction, accompanied by an increase in ROS production. Independent measurements of O_2 consumption verify that this transition is due to the deceleration of State 3 respiration toward resting, State 4 respiration (data

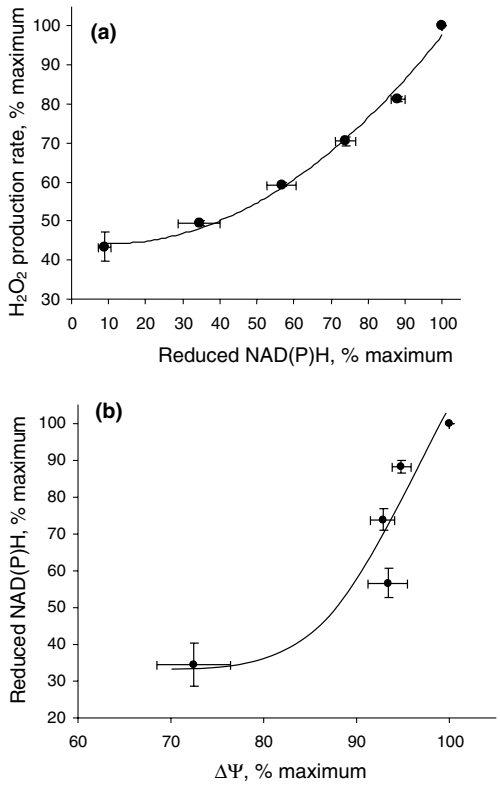

Fig. 3 Relationships between mitochondrial H_2O_2 production, NAD(P)H redox state, and membrane potential. Mitochondrial H_2O_2 production (a), NAD(P)H redox state (b), and membrane potential (b) were measured as described for Figs 1 and 2 in the presence of glutamate + malate and the uncoupler FCCP at concentrations of from 0 to 80 nM. Values represent means ± SD obtained from $n = 4$ experiments and are expressed as percentage of the maximal values obtained in the absence of FCCP.

not shown). In the presence of Mg^{2+}, post-State 3 respiration is limited by the rate of ATP cycling due to ATP hydrolysis by contaminating ATP hydrolases and by ATP synthesis by the mitochondrial F_1F_o ATP synthetase. Inhibition of the synthetase by the addition of oligomycin resulted in an additional shift toward reduction in the pyridine nucleotide redox state accompanied by a further stimulation of ROS generation. As expected, subsequent addition of the uncoupler FCCP resulted in maximal NAD(P)H oxidation and a decrease in ROS production to a level similar to that observed upon addition of ADP. Further verification that ROS generation is redox regulated came from the observation that subsequent addition of the Complex I inhibitor rotenone caused a maximal shift toward reduction of pyridine nucleotides and a maximal rate of H_2O_2 generation, even though $\Delta\Psi$ was already collapsed by the addition of FCCP.

The relationship between the rate of mitochondrial H_2O_2 production and NAD(P)H redox state was assessed by performing measurements of NAD(P)H autofluorescence in parallel to those of $\Delta\Psi$ described in Fig. 1. Thus the addition of increasing concentrations of the respiratory uncoupler FCCP was accompanied by increased NAD(P)H oxidation, consistent with greater membrane depolarization and accelerated respiration. As Fig. 3(a) demonstrates, FCCP-induced NAD(P)H oxidation is directly related to inhibition of H_2O_2 production. NAD(P)H oxidation is very sensitive to membrane depolarization, as shown in Fig. 3(b) where a 10% reduction in $\Delta\Psi$ is accompanied by an approximately 50% reduction in NAD(P)H fluorescence.

Discussion

The results of this study demonstrate that ROS production by isolated rat brain mitochondria respiring on NADH-dependent substrates is highly dependent on both mitochondrial membrane potential and NAD(P)H redox state. Moreover, this relationship is observed over a range of conditions that are consistent with those associated with normal fluctuations in cellular energy metabolism. Therefore, the rate of physiologically relevant mitochondrial ROS production can vary by several hundred percent, depending on whether energy demand is maximal (State 3 respiration) or ATP hydrolysis is minimal (State 4 respiration) (Fig. 1).

Relatively few measurements of mitochondrial ROS generation in the presence of NADH-linked respiratory substrates and in the absence of respiratory chain inhibitors have been reported, due to the low sensitivity of H_2O_2-sensitive indicators that were previously available. The utilization of Amplex Red enables detection of H_2O_2 at levels previously not considered significant (Starkov *et al.* 2002). The enhanced sensitivity of Amplex Red is also likely to be the explanation for why similar measurements using the fluorescent indicator scopoletin did not detect a relationship between $\Delta\Psi$ and H_2O_2 production in the presence of NADH-linked substrates (Votyakova and Reynolds 2001).

Mitochondrial ROS production is particularly sensitive to changes in $\Delta\Psi$ at the highest range of values (i.e. 170–185 mV) (Fig. 1). Quantification of this relationship can therefore only be accomplished with isolated mitochondria that are extremely well coupled and thus able to establish such high membrane potentials. We determined that including bovine serum albumin and EGTA in the incubation media helps mitochondria maintain high membrane potentials. Bovine serum albumin binds free fatty acids that can be generated from membrane lipids and that can uncouple mitochondria (Skulachev 1991). The Ca^{2+} chelator EGTA protects against any form of Ca^{2+}-induced mitochondrial dysfunction, including the membrane permeability transition that by definition results in uncoupling and membrane depolarization.

Although the relationship between $\Delta\Psi$, NAD(P)H redox state, and mitochondrial ROS production is apparent when these parameters are varied by the addition of either FCCP or ADP, the quantitative relationships are not identical. Thus,

the rates of ROS production with either saturating FCCP or ADP were approximately equal, but $\Delta\Psi$ was at least 20 mV higher with ADP (Fig. 1). Moreover, the NAD(P)H redox state was not as oxidized in the presence of ADP as it was in the presence of FCCP (Fig. 2). This apparent discrepancy may simply be due to a lack of control over ROS production at membrane potentials and pyridine nucleotide redox state at or below that maintained under State 3 respiration. Alternatively, differences in conditions present in the mitochondrial matrix during State 3 compared to uncoupled respiration might influence the site or sites responsible for ROS production. Additional evidence for the existence of membrane potential- and NAD(P)H/NAD(P)-independent ROS generation comes from the observation that the rate of H_2O_2 formation in the presence of rotenone was considerably greater than that observed in the presence of the ATP synthetase inhibitor oligomycin, even though the NAD(P)H autofluorescence was identical (Fig. 2). This difference could be due to a direct induction of ROS production by rotenone at Complex I in addition to its ability to induce a reduced shift in NAD(P)H and other redox sites proximal to the site at which rotenone inhibits electron transport (Ramsay and Singer 1992).

The site and the mechanism of ROS production by mitochondria oxidizing NADH-linked substrates in the absence of electron chain inhibitors are not fully characterized. Two fundamentally different mechanisms of ROS generation are possible. One mechanism involves the metabolism of NADH-dependent substrates to succinate and subsequent ROS production due to succinate oxidation by Complex II, and reversed electron flow through Complex I. The other mechanism is direct flow of electrons from NADH-dependent substrates to O_2 via one or more redox centers present within Complex I. In either case, the site of ROS generation within Complex I appears to be an iron-sulfur center within either the N2 or N1-a proteins (Genova *et al*. 2001; Kushnareva *et al*. 2002).

Dehydrogenases present in the mitochondrial matrix are functionally organized within the tricarboxylic acid cycle pathway and, with the aid of transaminases, allow for rapid interconversion of metabolic intermediates. Thus, metabolism of NADH-linked substrates can result in the formation of any TCA cycle intermediate, including (Von Korff *et al*. 1971; Von Korff and Kerpel-Fronius 1975; Beck *et al*. 1977; Kerpel-Fronius *et al*. 1977). Succinate oxidation stimulates ROS production at one or more sites located in Complex I via reverse electron transfer from Complex II through ubiquinone (Turrens 1997). Reversed electron transport is endergonic but can be driven by the energy present within a high membrane potential, as indicated by the complete inhibition of this process in the presence of uncouplers (Hansford *et al*. 1997; Korshunov *et al*. 1997; Votyakova and Reynolds 2001; Liu *et al*. 2002). The dependence of ROS production on $\Delta\Psi$ described in Fig. 1 might therefore be the consequence of metabolism to succinate and reversed electron flow to Complex I.

An alternative mechanism of ROS generation at Complex I specifically involves the redox state of NAD(P)H (Hansford *et al*. 1997*)*. Thus $\Delta\Psi$ may not affect ROS production directly but could regulate the rate of production through the close relationship between $\Delta\Psi$ and NAD(P)H redox state (Fig. 3). We propose that the ROS-producing site of Complex I is in redox equilibrium with mitochondrial pyridine nucleotides so that its degree of reduction depends on the $NADH/NAD^+$ ratio. This hypothesis is supported by the relationship between the rate of H_2O_2 production and the level of reduced pyridine nucleotides (Fig. 3), as has recently been described by Kushnareva *et al*. (2002). Additional evidence in support of this mechanism comes from the observation that superoxide production by rotenone-inhibited Complex I in submitochondrial particles also depends on the $NADH/NAD^+$ ratio and apparently originates from enzyme-bound reduced NADH (Krishnamoorthy and Hinkle 1988).

Although succinate-driven ROS production at Complex I is completely abolished by uncoupler-induced mitochondrial membrane depolarization (Hansford *et al*. 1997), we found that a significant fraction (30%) of H_2O_2 formation in the presence of NADH-linked substrates persists following maximal uncoupling (Fig. 1) and maximal NAD(P)H oxidation (Fig. 3). This observation supports the opinion that NADH-linked substrate-dependent ROS production is not indirectly due to succinate oxidation. The exact nature of this $\Delta\Psi$-independent ROS generation is unknown. However, preliminary results obtained with mitochondria and with isolated enzymes suggest that it could be mediated by the direct formation of superoxide by specific dehydrogenases, e.g. α-ketoglutarate dehydrogenase, and may be independent of Complex I mediated ROS production.

In conclusion, the results of this study emphasize the important role of ROS production by NADH-linked respiratory substrates in mitochondrial ROS generation. Mitochondrial ROS production in the presence of the Complex II substrate succinate is approximately 10 times greater than that of NADH-linked substrates at 5–10 mM substrate concentrations (Hansford *et al*. 1997; Korshunov *et al*. 1997; Votyakova and Reynolds 2001). Others have reported values for succinate-dependent ROS production that are comparable to the values we obtained for NADH-dependent generation (Barja and Herrero 1998; Herrero and Barja 1998). However, since succinate-dependent ROS generation is even more sensitive to a decline in $\Delta\Psi$ than is NADH-dependent ROS generation, variability among laboratories can be due to differences in $\Delta\Psi$ caused by different mitochondrial isolation procedures or incubation conditions. Although tissue succinate levels are normally much lower than the total concentration of NADH-linked respiratory substrates, concentrations of succinate do reach mM levels in

the brain and other tissues after periods of severe hypoxia induced by ischemia (Hoyer and Krier 1986; Camici *et al*. 1991). The redox state of pyridine nucleotides also shifts to a hyperoxidized level for up to 1 h during reperfusion following cerebral ischemia (Rosenthal *et al*. 1995). These conditions might allow for succinate-driven generation of ROS production at Complex I via reversed electron flow from Complex II (succinate dehydrogenase) and coenyzme Q. However, under normal conditions or when Complex I is inhibited by neurotoxins, e.g. MPP^+ or rotenone, ROS production at this site is far more likely to be fueled by the oxidation of NADH-dependent respiratory substrates (Sanchez-Ramos *et al*. 1988). We have now shown that NADH-dependent ROS generation is significant and regulated by physiological fluctuations in mitochondrial $\Delta\Psi$ and redox state. This finding provides further support for exploring neuroprotective interventions based on reducing mitochondrial ROS generation through limited respiratory uncoupling (Kim-Han *et al*. 2001; Ferranti *et al*. 2003).

Acknowledgements

This work was supported by USAMRMC Neurotoxin Initiative (DAMD 17-99-1-9483), NIH NS34152 and ES11838.

References

Barja G. and Herrero A. (1998) Localization at complex I and mechanism of the higher free radical production of brain nonsynaptic mitochondria in the short-lived rat than in the longevous pigeon. *J. Bioenerg. Biomembr.* **30**, 235–243.

Beck D. P., Broyles J. L. and Von Korff R. W. (1977) Role of malate transport in regulating metabolism in mitochondria isolated from rabbit brain. *J. Neurochem.* **29**, 487–493.

Camici P., Marraccini P., Lorenzoni R., Ferrannini E., Buzzigoli G., Marzilli M. and L'Abbate A. (1991) Metabolic markers of stress-induced myocardial ischemia. *Circulation* **83**, III8–13.

Echtay K. S. *et al.* (2002) Superoxide activates mitochondrial uncoupling proteins. *Nature* **415**, 96–99.

Ferranti R., da Silva M. M. and Kowaltowski A. J. (2003) Mitochondrial ATP-sensitive K^+ channel opening decreases reactive oxygen species generation. *FEBS Lett.* **536**, 51–55.

Fiskum G. (2000) Mitochondrial participation in ischemic and traumatic neural cell death. *J. Neurotrauma* **17**, 843–855.

Genova M. L., Ventura B., Giuliano G., Bovina C., Formiggini G., Parenti C. G. and Lenaz G. (2001) The site of production of superoxide radical in mitochondrial Complex I is not a bound ubisemiquinone but presumably iron-sulfur cluster N2. *FEBS Lett.* **505**, 364–368.

Hansford R. G., Hogue B. A. and Mildaziene V. (1997) Dependence of H_2O_2 formation by rat heart mitochondria on substrate availability and donor age. *J. Bioenerg. Biomembr.* **29**, 89–95.

Hashimoto K., Angiolillo P. and Rottenberg H. (1984) Membrane potential and surface potential in mitochondria. Binding of a cationic spin probe. *Biochim. Biophys. Acta* **764**, 55–62.

Herrero A. and Barja G. (1998) H_2O_2 production of heart mitochondria and aging rate are slower in canaries and parakeets than in mice: sites of free radical generation and mechanisms involved. *Mech. Ageing Dev.* **103**, 133–146.

Hoyer S. and Krier C. (1986) Ischemia and aging brain. Studies on glucose and energy metabolism in rat cerebral cortex. *Neurobiol. Aging* **7**, 23–29.

Kamo N., Muratsugu M., Hongoh R. and Kobatake Y. (1979) Membrane potential of mitochondria measured with an electrode sensitive to tetraphenyl phosphonium and relationship between proton electrochemical potential and phosphorylation potential in steady state. *J. Membr. Biol.* **49**, 105–121.

Kerpel-Fronius S., Beck D. P. and Von Korff R. W. (1977) Studies on the metabolism of glutamate and glutamine by mitochondria from rabbit brain: complications due to isotopic exchange reactions. *J. Neurochem.* **28**, 871–875.

Kim-Han J. S., Reichert S. A., Quick K. L. and Dugan L. L. (2001) BMCP1: a mitochondrial uncoupling protein in neurons which regulates mitochondrial function and oxidant production. *J. Neurochem.* **79**, 658–668.

Korshunov S. S., Skulachev V. P. and Starkov A. A. (1997) High protonic potential actuates a mechanism of production of reactive oxygen species in mitochondria. *FEBS Lett.* **416**, 15–18.

Krishnamoorthy G. and Hinkle P. C. (1988) Studies on the electron transfer pathway, topography of iron-sulfur centers, and site of coupling in NADH-Q oxidoreductase. *J. Biol. Chem.* **263**, 17566–17575.

Kushnareva Y. E., Murphy A. N. and Andreyev A. Y. (2002) Complex I mediated reactive oxygen species generation: Modulation by Cytochrome *c* and NAD(P)+ oxidation-reduction state. *Biochem. J.* **368**, 545–553.

Liu Y., Fiskum G. and Schubert D. (2002) Generation of reactive oxygen species by the mitochondrial electron transport chain. *J. Neurochem.* **80**, 780–787.

Nicholls D. G. and Budd S. L. (2000) Mitochondria and neuronal survival. *Physiol. Rev.* **80**, 315–360.

Ramsay R. R. and Singer T. P. (1992) Relation of superoxide generation and lipid peroxidation to the inhibition of NADH-Q oxidoreductase by rotenone, piericidin A, and MPP+. *Biochem. Biophys. Res. Commun* **189**, 47–52.

Rolfe D. F., Hulbert A. J. and Brand M. D. (1994) Characteristics of mitochondrial proton leak and control of oxidative phosphorylation in the major oxygen-consuming tissues of the rat. *Biochim. Biophys. Acta* **1188**, 405–416.

Rosen G. M., Tsai P., Weaver J. M., Porasuphatana S., Roman L. J., Starkov A. A., Fiskum G. and Pou S. (2002) Tetrahydrobiopterin: Its role in the regulation of neuronal nitric oxide synthase-generated superoxide. *J. Biol. Chem.* **277**, 40275–40280.

Rosenthal R. E., Hamud F., Fiskum G., Varghese P. J. and Sharpe S. (1987) Cerebral ischemia and reperfusion: prevention of brain mitochondrial injury by lidoflazine. *J. Cereb. Blood Flow Metab.* **7**, 752–758.

Rosenthal M., Feng Z. C., Raffin C. N., Harrison M. and Sick T. J. (1995) Mitochondrial hyperoxidation signals residual intracellular dysfunction after global ischemia in rat neocortex. *J. Cereb. Blood Flow Metab.* **15**, 655–665.

Rottenberg H. (1984) Membrane potential and surface potential in mitochondria: uptake and binding of lipophilic cations. *J. Membr. Biol.* **81**, 127–138.

Sanchez-Ramos J. R., Hollinden G. E., Sick T. J. and Rosenthal M. (1988) 1-Methyl-4-phenylpyridinium (MPP+) increases oxidation of cytochrome-*b* in rat striatal slices. *Brain Res.* **443**, 183–189.

Sherer T. B., Betarbet R. and Greenamyre J. T. (2002) Environment, mitochondria, and Parkinson's disease. *Neuroscientist* **8**, 192–197.

Skulachev V. P. (1991) Fatty acid circuit as a physiological mechanism of uncoupling of oxidative phosphorylation. *FEBS Lett.* **294**, 158–162.

Starkov A. A., Polster B. M. and Fiskum G. (2002) Regulation of hydrogen peroxide production by brain mitochondria by calcium and Bax. *J. Neurochem.* **83**, 220–228.

Turrens J. F. (1997) Superoxide production by the mitochondrial respiratory chain. *Biosci. Rep.* **17**, 3–8.

Von Korff R. W. and Kerpel-Fronius S. (1975) The effect of cosubstrates on tricarboxylic acid cycle dynamics during pyruvate oxidation: the formation of alpha-ketoglutarate and utilization of glutamate by mitochondria from rabbit brain. *J. Neurochem.* **25**, 767–778.

Von Korff R. W., Steinman S. and Welch A. S. (1971) Metabolic characteristics of mitochondria isolated from rabbit brain. *J. Neurochem.* **18**, 1577–1587.

Votyakova T. V. and Reynolds I. J. (2001) DeltaPsi(m)-Dependent and -independent production of reactive oxygen species by rat brain mitochondria. *J. Neurochem.* **79**, 266–277.

Free Radical Biology & Medicine, Vol. 37, No. 11, pp. 1845–1853, 2004

0891-5849/$-see front matter

ELSEVIER

doi:10.1016/j.freeradbiomed.2004.09.005

Original Contribution

BCL-2 FAMILY PROTEINS REGULATE MITOCHONDRIAL REACTIVE OXYGEN PRODUCTION AND PROTECT AGAINST OXIDATIVE STRESS

ALICIA J. KOWALTOWSKI,* ROBERT G. FENTON,† and GARY FISKUM‡

*Departamento de Bioquímica, Instituto de Química, Universidade de São Paulo, São Paulo, Brazil; and
†Greenbaum Cancer Center and ‡Department of Anesthesiology, University of Maryland School of Medicine, Baltimore, MD 21201, USA

(*Received* 25 *June* 2004; *Revised* 10 *August* 2004; *Accepted* 2 *September* 2004)
Available online 25 September 2004

Abstract—Bcl-2 family proteins protect against a variety of forms of cell death, including acute oxidative stress. Previous studies have shown that overexpression of the antiapoptotic protein Bcl-2 increases cellular redox capacity. Here we report that cell lines transfected with Bcl-2 paradoxically exhibit increased rates of mitochondrial H_2O_2 generation. Using isolated mitochondria, we determined that increased H_2O_2 release results from the oxidation of reduced nicotinamide adenine dinucleotide-linked substrates. Antiapoptotic Bcl-2 family proteins Bcl-xL and Mcl-1 also increase mitochondrial H_2O_2 release when overexpressed. Chronic exposure of cells to low levels of the mitochondrial uncoupler carbonyl cyanide 4-(triflouromethoxy)phenylhydrazone reduced the rate of H_2O_2 production by Bcl-xL overexpressing cells, resulting in a decreased ability to remove exogenous H_2O_2 and enhanced cell death under conditions of acute oxidative stress. Our results indicate that chronic and mild elevations in H_2O_2 release from Bcl-2, Bcl-xL, and Mcl-1 overexpressing mitochondria lead to enhanced cellular antioxidant defense and protection against death caused by acute oxidative stress.

Keywords—Free radicals, Hydrogen peroxide, Digitonin, Apoptosis, Necrosis, Complex I, Antioxidant

INTRODUCTION

The Bcl-2 protein inhibits cell death promoted by a wide variety of stimuli when overexpressed (for reviews see [1–3]). This protein is located predominantly in intracellular membranes, and most of its protective effects against cell death have been attributed to its mitochondrial location [1–3]. Mitochondria play essential roles in the regulation of key steps in both apoptotic and necrotic cell death by affecting energy metabolism, participating in intracellular Ca^{2+} homeostasis, regulating the activation of caspases, and releasing reactive oxygen species (ROS) [1,4–6]. Bcl-2 overexpression has been previously shown to act at multiple steps of mitochondrially regulated cell death such as increasing maximal mitochondrial Ca^{2+} uptake capacity [7], preventing the release of proapoptotic mitochondrial intermembrane proteins [8–10], and preventing oxidative stress following deadly stimuli [4,11–13].

The prevention of oxidative stress following cell-death-initiating stimuli is associated with an increase in the total antioxidant capacity of Bcl-2 overexpressing cells [13–15]. It has been hypothesized [12] that this enhanced antioxidant capacity is related to a chronic increase in cellular ROS under physiological conditions secondary to Bcl-2 overexpression. Indeed, many redox-related genes are activated by increased H_2O_2 levels [16,17] and can be determinant in the apoptotic process [13]. Data using a single Bcl-2-transfected cell line support the idea that Bcl-2 chronically increases ROS [12]. However, other groups [11,18] have not found changes in mitochondrial ROS release in Bcl-2 overexpressing cells under physiological conditions but have uncovered a protection against oxidative stress by Bcl-2 following apoptotic stimuli. It has been argued that the lack of detection of a Bcl-2 effect under physiological conditions is due to the use of less sensitive ROS probes [12].

Address correspondence to: Gary Fiskum, University of Maryland School of Medicine, 685 W. Baltimore St., MSTF-5.34, Baltimore, MD 21201, USA; Fax: +1 (410) 706 2550; E-mail: gfisk001@umaryland.edu.

If an effect of Bcl-2 on mitochondrial ROS release under physiological conditions is confirmed, the mechanism through which such a change could occur would be of great interest. We demonstrated [7,19] that Bcl-2 does not alter mitochondrial functional parameters such as respiration and the inner membrane potential, suggesting that these are not direct causes for any possible changes in ROS release by this organelle. Furthermore, a link between chronic increases in ROS release by Bcl-2 and protection against acute oxidative cell death has not been established.

In this study we evaluated the effects of Bcl-2 and antiapoptotic Bcl-2 family proteins Bcl-xL and Mcl-1 on mitochondrial ROS release using a H_2O_2 detection system that is more sensitive than techniques applied previously to similar comparisons. We additionally tested the relationship of endogenous mitochondrial ROS production with sensitivity to acute cell death caused by oxidative stress. Our findings support the hypothesis that these Bcl-2 family proteins protect against acute cell death by increasing cellular antioxidant capacity due to chronic changes in mitochondrial ROS release.

EXPERIMENTAL PROCEDURES

Cell cultures

PC12 pheochromocytoma and immortalized hypothalamic GT1-7 neuronal cell lines transfected with the human *bcl-2* gene (Bcl-2+) or with a control retroviral construct (Bcl-2−) were maintained as described previously [20]. Western blot analysis indicated that Bcl-2 levels were undetectable in Bcl-2- cells and that the protein was present at high levels in the mitochondrial fraction of Bcl-2+ preparations (not shown). Parental MM 8226 cells (control cells) were transfected with *bcl-xl* (Bcl-xL cells) and *mcl-1* (Mcl-1 cells) and cultured as previously described [21]. Western blots of control cells did not exhibit any detectable Bcl-xL or Mcl-1. Prior to experiments, the cells were suspended in growth medium supplemented with 10 mM Hepes, pH 7.0. Suspended cells were kept at room temperature for up to 5 h. Cell viability, as assessed by a cell count in the presence of trypan blue, was above 95% even after 5 h at room temperature. The suspended cells were centrifuged and resuspended in the medium used in the experiment just prior to each determination. Cell protein content was determined using the Biuret method. The protein/cell count ratio was not affected by the level of Bcl-2 family protein expression. All experiments were conducted at 37°C.

Mitochondrial isolation

Mitochondria were isolated from digitonin-permeabilized cells as described by Moreadith and Fiskum [22] in isolation buffer containing 210 mM mannitol, 75 mM sucrose, 1 mg/mL BSA, 5 mM Hepes, and 1 mM EGTA, pH 7.2 (KOH). Mitochondria isolated in this manner typically displayed respiratory control ratios between 3 and 6, when respiring on NADH-linked substrates.

H_2O_2 release

H_2O_2 was measured by following the oxidation of 50 μM amplex red (Molecular Probes A12222) in the presence of 1 U/mL horseradish peroxidase (HRP) [23,24] recorded on a temperature-controlled fluorescence spectrophotometer equipped with continuous stirring and operating at excitation and emission wavelengths of 563 and 587 nm, respectively. Because amplex red presents a slow rate of spontaneous oxidation in the presence of HRP (<2% of rates in the presence of cells or mitochondria), all traces were subtracted from a baseline trace recorded in the same media devoid of cells or mitochondria. Data were calibrated by adding known quantities of a freshly prepared H_2O_2 stock quantified by its absorbance at 240 nm ($E = 43.6\ M \cdot cm^{-1}$).

H_2O_2 removal

H_2O_2 removal was measured as described previously [25] from freshly isolated cell homogenates suspended in phosphate-buffered saline. Briefly, 0.5 mg/mL of total cell protein was incubated for 1 min with 1.0 μM H_2O_2 and a 1-μL aliquot was taken and diluted in 2 mL of suspension buffer with 50 μM amplex red and 1.0 U/mL horseradish peroxidase. A single fluorescence reading was taken at 563 nm emission and 587 nm excitation. Amplex red readings in samples untreated with H_2O_2 were negligible, indicating that oxidation of the dye by cytosolic components, e.g., NADH, did not significantly affect measurements under these conditions.

Lactate dehydrogenase (LDH) activity

LDH activity was measured using Sigma Diagnostics LDH kit No. 500 in 10 μL undiluted growth media from cells plated 2 h previously at 1 mg protein/mL in the presence of varying H_2O_2 concentrations. Total releasable LDH was measured by treating cells with 0.05% digitonin.

Reagents

Amplex red was purchased from Molecular Probes. Horseradish peroxidase (P8125), EGTA, digitonin, malate, glutamate, pyruvate, succinate, BSA, rotenone, antimycin A, and alamethicin were from Sigma–Aldrich. All other reagents were of analytical purity grades.

Data analysis

Traces are representative of data collected from at least three similar repetitions. Averages represented in scatter and bar graphs were calculated from data collected from three to nine repetitions using different preparations. Error bars indicate standard errors (SE) and significance was calculated using pairwise Tukey tests, conducted by SigmaStat.

RESULTS

Figure 1 shows H_2O_2 release from two distinct cell lines (GT1-7 hypothalamic tumor and PC12 pheochromocytoma cells), comparing the effects of Bcl-2 expression on cellular H_2O_2 production by following the time-dependent oxidation of amplex red in the presence of HRP [25]. This method is sensitive to physiological levels of H_2O_2 release and detects between 0.025 and 0.05 nmol $H_2O_2 \cdot min^{-1} \cdot mg^{-1}$ cell protein under normal growth conditions. In intact cells, no difference in H_2O_2 release between Bcl-2− and Bcl-2+ cells was apparent (left panels), a result consistent with previous findings [11,18].

Based on previous work showing that Bcl-2 overexpression increases mitochondrial H_2O_2 release in Burkitt's lymphoma and promyelocytic leukemia cell lines [12] and the finding that Bcl-2 overexpression enhances cytosolic antioxidant levels in the cell lines used in our study [14], we reevaluated H_2O_2 release in digitonin-permeabilized cells respiring in state 4 (non-phosphorylating) conditions. Low digitonin concentrations selectively permeabilize the plasma membrane, promoting a large dilution of cytosolic components (including intracellular antioxidants) while maintaining cell architecture and mitochondrial function unaltered [26]. This is the preferred method to study the effects of Bcl-2 in mitochondria from transfected cell lines, since mitochondrial isolation may promote damage to the organelle in a Bcl-2-inhibited manner [7,27]. Under these

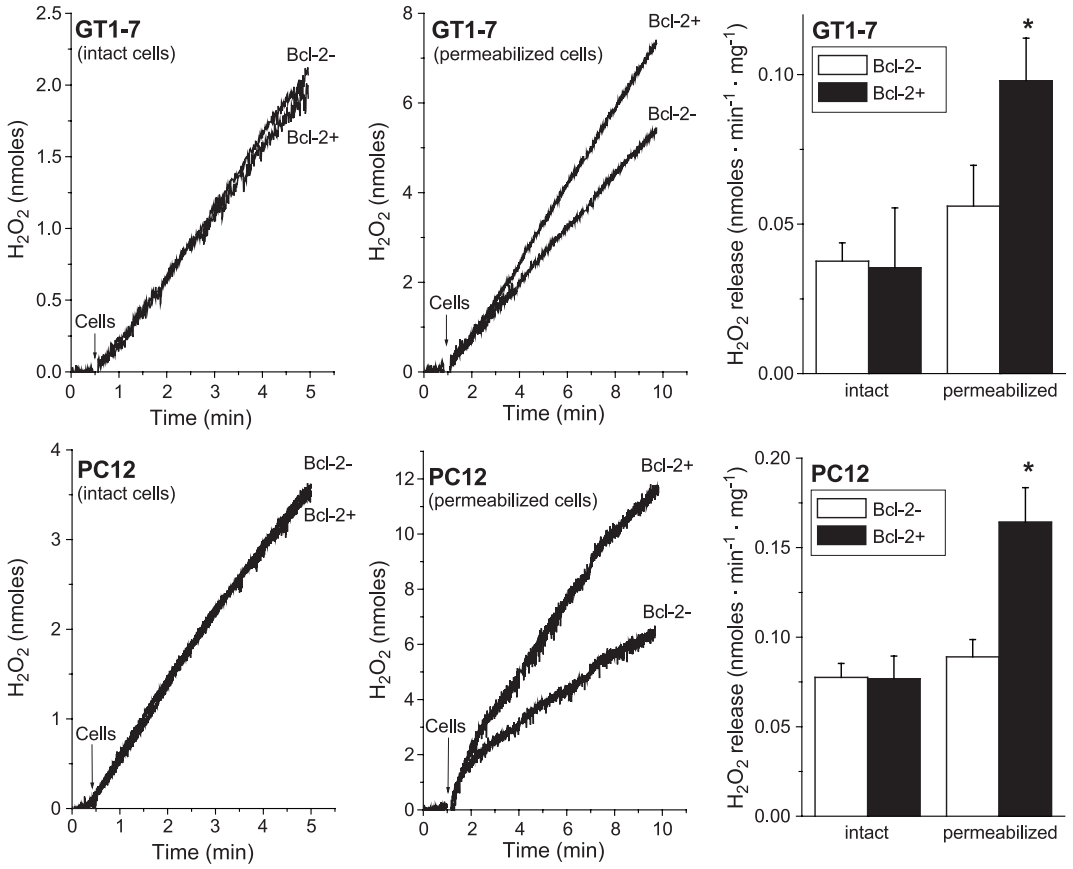

Fig. 1. Bcl-2 overexpression increases H_2O_2 generation in digitonin-permeabilized cells. GT1-7 or PC12 Bcl-2- and Bcl-2+ cells (as indicated) were added at a concentration of 10 mg protein/mL to 37°C media containing 1 U/mL HRP and 50 μM amplex red to measure H_2O_2 release (as described under Experimental Procedures). Intact cells were incubated in phenol red-free modified Eagle's medium supplemented with 10 mM Hepes, pH 7.2. Permeabilized cells were incubated at 37°C in 250 mM sucrose, 5 mM pyruvate, 5 mM malate, 5 mM glutamate, 100 μM EGTA, 1 mg/mL BSA, 0.001 or 0.004% digitonin (GT1-7 and PC12 cells, respectively), 1 μg/mL oligomycin, and 10 mM K^+-Hepes, pH 7.2. Leftmost and center panels depict representative tracings of intact and permeabilized cell measurements, respectively. The panels on the right show averages of at least three repetitions. *$p < 0.05$ compared to Bcl-2- cells.

conditions and in the presence of NADH-linked substrates, we found that both lines of Bcl-2+ cells generated significantly higher H_2O_2 levels than their respective control transfectants (Fig. 1, right panels).

To determine whether mitochondria are responsible for the Bcl-2-dependent differences in H_2O_2 release, we incubated permeabilized GT1-7 and PC12 cells in the absence of respiratory substrates (Fig. 2). Under these conditions, endogenous redox sources are rapidly depleted (1–2 min after the addition of the cells). The H_2O_2 detection rates after this period were similar in Bcl-2- and Bcl-2+ cells, but the increased H_2O_2 release rates observed in Bcl-2+ cells could be recovered by adding the mitochondrial NADH-linked substrate pyruvate, indicating that the difference in H_2O_2 release in Bcl-2+ cells is of mitochondrial origin.

There are several sites of mitochondrial ROS production including Complexes I and III of the electron transport chain and possibly several tricarboxylic acid cycle dehydrogenases [28,29]. Furthermore, mitochondrial ROS release is altered by changes in respiratory rates and the use of different respiratory inhibitors. While increasing respiration with uncouplers generally reduces ROS release, inhibiting specific respiratory complexes enhances electron leakage from sites upstream of the inhibition [30,31]. ROS production by Bcl-2+ and Bcl-2− mitochondria was compared using different respiratory substrates and inhibitors in an attempt to further identify the molecular basis for the effects of Bcl-2 on ROS generation. In these experiments, we used isolated GT1-7 and PC12 mitochondria to avoid amplex red oxidation by nonmitochondrial cellular components. Using isolated mitochondria, amplex red oxidation in the absence of respiratory substrates was negligible (results not shown). H_2O_2 release from isolated Bcl-2+ mitochondria was enhanced relative to Bcl-2- preparations in the presence

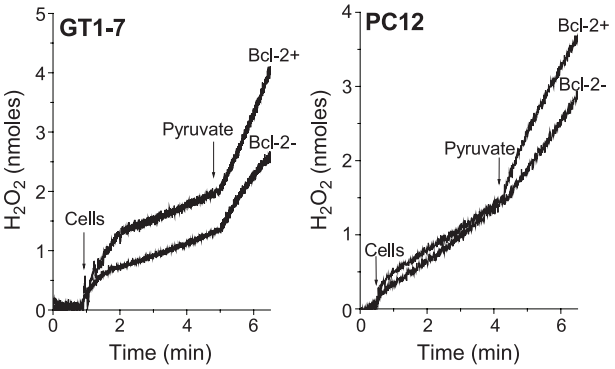

Fig. 2. Increased H_2O_2 release in Bcl-2+ cells is of mitochondrial origin. Permeabilized GT1-7 and PC12 cells were incubated under the conditions described in the legend to Fig. 1, except that the mitochondrial respiratory substrates pyruvate, malate, and glutamate were not present in the incubation buffer. Pyruvate (5 mM) was added where indicated.

of NADH-linked substrates malate plus glutamate (Mal + Glu) or pyruvate (Pyr). Rotenone (Rot), a Complex I inhibitor, enhanced H_2O_2 release in both Bcl-2+ and Bcl-2- preparations (Fig. 3), suggesting that the difference in ROS generation originates from an electron source upstream of rotenone inhibition, such as iron–sulfur centers in Complex I [28,32].

Support for a Complex-I-associated effect of Bcl-2 on mitochondrial ROS production came from experiments performed with the Complex II substrate succinate (Succ). GT1-7 Bcl-2+ and Bcl-2- mitochondria generated equal amounts of H_2O_2 when energized with succinate (Fig. 3). In PC12 mitochondria, H_2O_2 release rates supported by succinate were significantly higher in Bcl-2 transfectants unless antimycin A (AA), which increases ROS release at the level of coenzyme Q [33], was present. As these results argue against an involvement of coenzyme Q/Complex III in Bcl-2-regulated ROS production in the presence of succinate, we hypothesized that Bcl-2 affects ROS production by NADH-linked substrates, e.g., malate, that can be generated from succinate via matrix tricarboxylic acid cycle enzymes. To eliminate this potential contribution to succinate-driven ROS generation, we incubated mitochondria with alamethicin (Ala), which forms large pores in mitochondrial membranes resulting in organellar swelling, rupture, and release of soluble matrix components. Under these conditions, succinate oxidation via membrane-bound succinate dehydrogenase (Complex II) resulted in H_2O_2 release rates that were equal for Bcl-2- and Bcl-2+ mitochondria. Thus, increases in ROS release in Bcl-2+ mitochondria occur due to changes in NADH metabolism, and electron leakage leading to ROS release between Complexes II and IV is equal in cells with different levels of Bcl-2 expression. H_2O_2 release in alamethicin-permeabilized mitochondria was measured using only succinate as a substrate due to the interference of added NADH with the amplex red detection system.

Previous experiments by our group using the same cell lines have determined that Bcl-2 does not significantly change mitochondrial respiratory rates or membrane potential [7,19]. This suggests that changes in respiratory rates are not responsible for increases in ROS release in Bcl-2+ mitochondria. We have also found previously that Bcl-2+ mitochondria contain larger quantities of NAD(H) and an increased ability to maintain NAD(H) in its reduced state [34]. This effect could be related to the enhanced H_2O_2 generation promoted by Bcl-2 as mitochondrial ROS production is very sensitive to changes in NAD(H) redox state [35,36]. To investigate this possibility, we measured H_2O_2 release in the presence of different respiratory conditions that maintain NADH/NAD^+ ratios at either very high or low levels by, respectively, decreasing or maximizing elec-

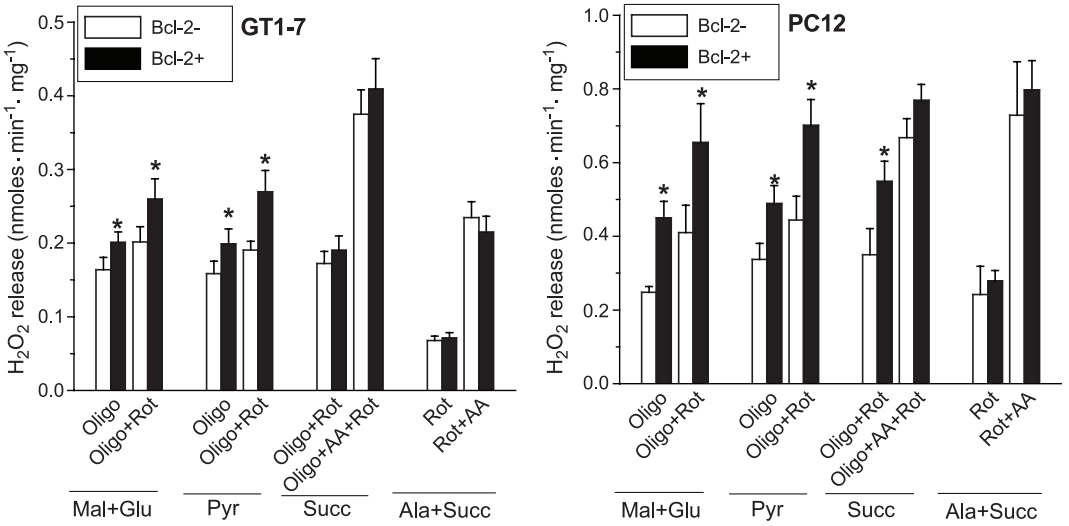

Fig. 3. NADH is the electron source for increased ROS release in Bcl-2+ cells. Isolated GT1-7 and PC12 cell mitochondria (0.5 mg/mL) were incubated at 37°C in 250 mM sucrose, 1 mM EGTA, 1 mg/mL BSA, 1 mM K^+-P_i, 5 mM Mg^{2+}, 2 mM ATP, and 10 mM K^+-Hepes, pH 7.2, containing 1 U/mL HRP and 50 μM amplex red. Malate plus glutamate (Mal + Glu, 5 mM each), 5 mM pyruvate (Pyr), 5 mM succinate (Succ), 100 nM alamethicin (Ala), 1 μg/mL oligomycin (Oligo), 100 nM rotenone (Rot), and/or 200 nM antimycin A (AA) were added where indicated. *$p < 0.05$ compared to Bcl-2-mitochondria.

tron transport (Fig. 4). We found that H_2O_2 release levels were higher in both Bcl-2+ cell types, regardless of whether respiration was maximized by oxidative phosphorylation (ADP) or uncoupler (FCCP), or decreased by the ATP synthetase inhibitor oligomycin (Oligo). These results demonstrate that the Bcl-2 effect on ROS production is independent of changes in NADH/NAD^+ ratios and is probably related to increased electron leakage at or prior to Complex I.

If the increase in mitochondrial H_2O_2 release promoted by Bcl-2 bears any relevance to ability to advance tumor generation or protect against cell death, similar effects should be observed with other antiapoptotic Bcl-2 family proteins. Thus, we worked with multiple myeloma cells (MM 8226) transfected with Bcl-xL and Mcl-1 antiapoptotic proteins. Bcl-xL is structurally similar to Bcl-2 , while Mcl-1 is a larger protein, lacking the BH4 homology region [2,21]. Both proteins are effective protectors against a variety of forms of cell death, including oxidative damage [2,21,37,38]. We found (Fig. 5) that Mcl-1 moderately increased cellular H_2O_2 release measured in intact cells, digitonin-permeabilized cells, or isolated mitochondria, while Bcl-xL presented a very strong H_2O_2-stimulating effect under these conditions. Again, increased H_2O_2 release was observed only using NADH-linked substrates. Parallel measure-

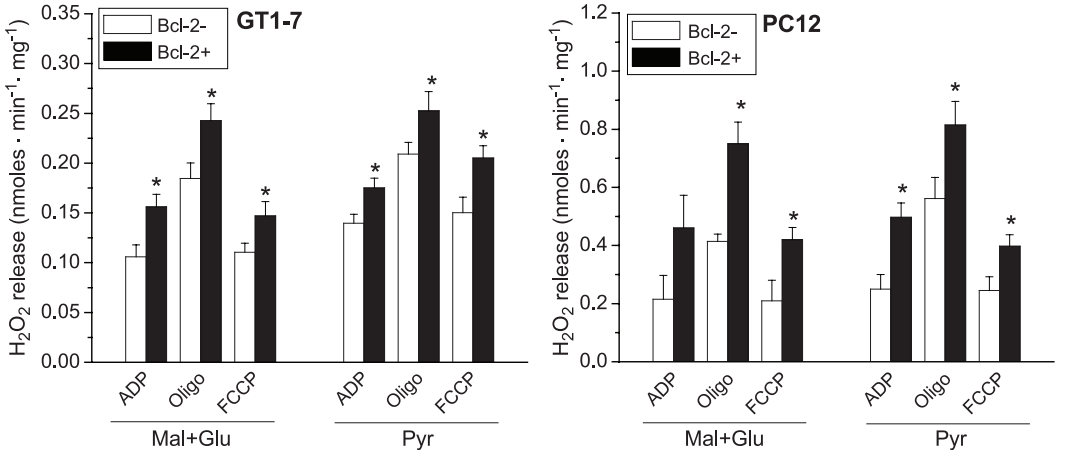

Fig. 4. Increased ROS release in Bcl-2+ cells is independent of respiratory energy coupling. Isolated GT1-7 and PC12 cell mitochondria (0.5 mg/mL) were incubated at 37°C in 250 mM sucrose, 1 mM EGTA, 1 mg/mL BSA, 1 mM K^+-P_i, 5 mM Mg^{2+}, and 10 mM K^+-Hepes, pH 7.2, containing 1 U/mL HRP and 50 μM amplex red. Malate plus glutamate (Mal + Glu, 5 mM each) or 5 mM pyruvate (Pyr). 200 μM ADP, 1 μg/mL oligomycin (Oligo), and 0.5 μM FCCP were added sequentially where indicated. *$p < 0.05$ compared to Bcl-2-mitochondria.

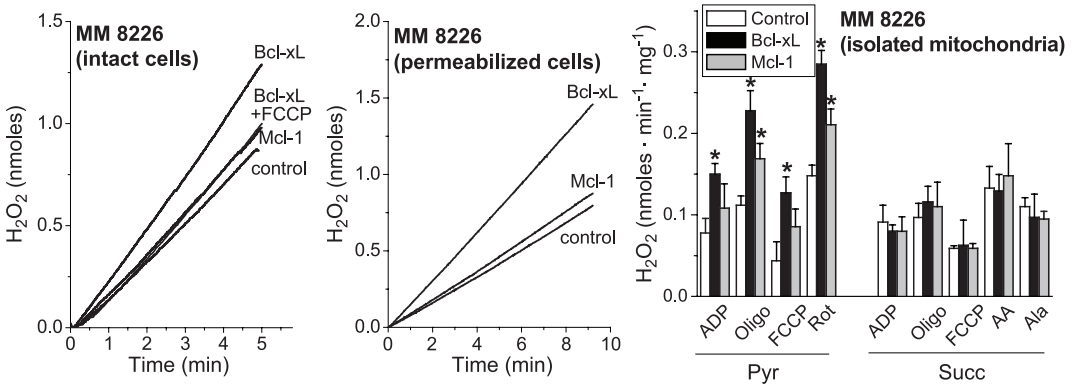

Fig. 5. Bcl-xL and Mcl-1 overexpression increases H_2O_2 generation. 10 mg/mL control, Bcl-xL, or Mcl-1 overexpressing MM 8226 cells (0.5 mg/mL) isolated MM 8226 mitochondria (as indicated) were added to 37°C media containing 1 U/ml HRP and 50 μM amplex red to measure H_2O_2 release (as described under Experimental Procedures). Intact cells were incubated in RPMI media supplemented with 5 U superoxide dismutase/mL and 10 mM Hepes, pH 7.2. FCCP (100 nM) was added where shown 15 min before the measurement. Permeabilized cells were incubated in 250 mM sucrose, 5 mM pyruvate, 5 mM malate, 5 mM glutamate, 100 μM EGTA, 1 mg/mL BSA, 0.005% digitonin, 1 μg/mL oligomycin, and 10 mM K^+-Hepes, pH 7.2. Experiments using isolated MM 8226 mitochondria were conducted under the conditions described in the legend to Fig. 3. *$p < 0.05$ compared to control mitochondria.

ments of respiratory rates and respiratory control ratios did not show any significant differences between transfected and untransfected cells (results not shown).

Since Bcl-xL-dependent differences in H_2O_2 release were detectable in intact MM 8226 cells, we used these cells to test the hypothesis that chronic increases in H_2O_2 generation are paradoxically related to protection against acute oxidative cell death. We found that H_2O_2 release in Bcl-xL cells could be reduced by mildly uncoupling mitochondria with nanomolar concentrations of FCCP (Fig. 5, far left). We cultured the cells in the presence of these concentrations of FCCP for 48 h, measured their ability to remove H_2O_2, and determined their resistance to H_2O_2-promoted cell death (Fig. 6). We found (Fig. 6, left) that Bcl-xL cell homogenates had a greater ability to remove H_2O_2 relative to controls, possibly reflecting enhanced catalase and peroxidase activity. Incubation with FCCP for 48 h reduced the H_2O_2 removal activity of Bcl-xL cells to levels more similar to those of controls. This effect was not due to a toxic effect of FCCP per se, since Bcl-xL cells treated with FCCP just prior to homogenization did not exhibit lower H_2O_2 removal activity. Thus, the decrease in H_2O_2 removal promoted by FCCP is dependent on long-term mild uncoupling and is associated with depressed mitochondrial ROS release.

In parallel to H_2O_2 removal experiments, we measured resistance to acute oxidative stress in these cell types. Intact cells were incubated in the presence of mM concentrations of exogenous H_2O_2 for 2 h, and cell damage was measured by determining lactate dehydro-

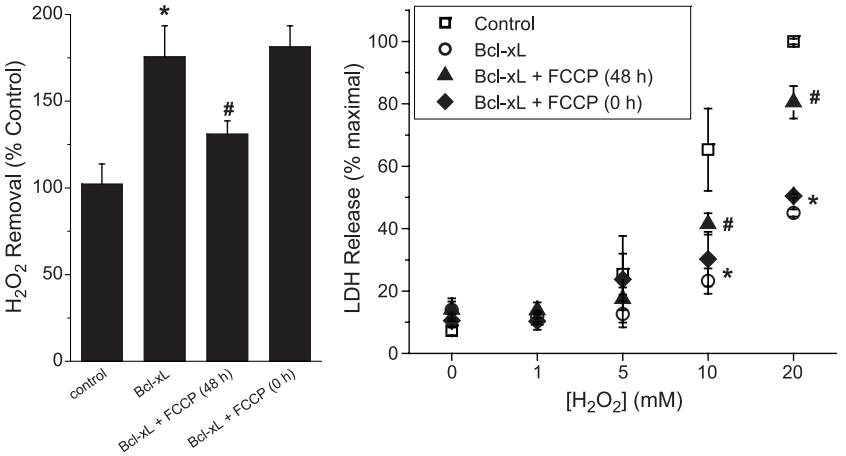

Fig. 6. Mild uncoupling decreases the effect of Bcl-xL overexpression on cellular H_2O_2 removal capacity and resistance to oxidative stress. Control or Bcl-xL cells were grown under control conditions or in the presence of 100 nM FCCP, as shown. H_2O_2 removal capacity (left) was determined in fresh cell homogenates as described under Experimental Procedures. Cell death, as indicated by LDH release (right), was determined in the growth medium after 2-h incubation in varying H_2O_2 concentrations, as shown. *$p < 0.05$ compared to control cells; $^{\#}p < 0.05$ compared to Bcl-xL cells.

genase activity in the growth media. We found (Fig. 6, right) that Bcl-xL cells were strongly resistant to damage under these conditions. However, Bcl-xL cells treated with FCCP for 48 h lost most of their resistance to H_2O_2-induced cell death. This increased sensitivity to H_2O_2 was not related to acute FCCP poisoning, since Bcl-xL cells treated with FCCP just prior to the addition of H_2O_2 exhibited injury similar to that of untreated cells. In addition, control cells treated with FCCP for 48 h or just prior to H_2O_2 exposure behaved similarly to untreated control cells (results not shown). Thus, increased mitochondrial ROS release, increased ability to remove H_2O_2, and resistance to oxidative stress are closely associated in Bcl-xL overexpressing cells.

DISCUSSION

One of the most intriguing properties of Bcl-2 family proteins is their ability to prevent both apoptotic and necrotic cell death. While the antiapoptotic effects of these proteins have been shown to be mediated by binding to proapoptotic proteins such as Bax, inhibiting their ability to oligomerize and form pores in the mitochondrial outer membrane through which soluble mitochondrial proapoptotic proteins are released into the cytosol [2,39,40], the mechanisms related to antinecrotic effects of Bcl-2 [41,42] are more poorly understood.

Several lines of evidence suggest that one of the mechanisms through which Bcl-2 family proteins protect against necrotic cell death involves enhanced antioxidant defenses in these cells: (i) these proteins protect against cell death induced by exogenous oxidants [11,37,38], (ii) depletion of intracellular antioxidants without affecting Bcl-2 levels can eliminate the protective effect of Bcl-2 or Bcl-xL [13,15,43,44], and (iii) Bcl-2 overexpressing cells contain higher levels of antioxidants [14,15]. However, the mechanism through which cells expressing Bcl-2 family proteins develop this increased resistance against oxidative stress was not established to date.

Redox-related genes are regulated by a variety of factors that include local oxygen tension and intracellular [H_2O_2] [16,17,45], parameters that could be altered by mitochondrial proteins such as Bcl-2. Since previous data from our group indicated that Bcl-2 does not alter normal mitochondrial respiration [7,19], it is unlikely that intracellular oxygen tension is affected by Bcl-2 levels. We therefore focused our attention on a possible effect of this protein on mitochondrial H_2O_2 release levels. We hypothesized that Bcl-2 could moderately increase mitochondrial ROS release under physiological conditions, leading to enhanced antioxidant expression levels and protection against acute oxidative stress-related cell death. Our hypothesis was supported by previous results suggesting higher mitochondrial H_2O_2 generation in Bcl-2-transfected cells [12,46] despite a lack of such a difference reported in other publications [11,18].

Using cell lines transfected with Bcl-2, Bcl-xL, and Mcl-1 and employing a highly sensitive H_2O_2 detection method, we found a significant 30–100% increase in mitochondrial H_2O_2 release relative to cells that express lower levels of these antiapoptotic proteins (Figs. 1–5). This effect is probably due to changes in electron leakage at the level of respiratory Complex I, since it could be observed only in the presence of NADH-linked substrates (Figs. 3 and 5). The promotion of ROS production by these Bcl-2 family proteins is not due to their effects on NAD(H) redox state, as indicated by the consistent results observed in the presence either of the uncoupler FCCP (oxidized redox state) or of the ATP synthetase inhibitor oligomycin (reduced redox state) (Figs. 4 and 5). We have not, at this juncture, identified the precise mechanism through which Bcl-2 family protein overexpression leads to enhanced ROS release from mitochondria. It is, however, possible that this effect of Bcl-2 proteins is due to changes in the composition or structure of Complex I, resulting in increased electron leakage but not enhanced electron transport. Alternatively, Bcl-2 family proteins may interact with Complex I, resulting in increased electron leakage. Furthermore, although our results suggest that Complex I is the main site for enhanced electron leakage in Bcl-2-family-protein-transfected mitochondria, they do not completely rule out a possibility for other electron leakage sites such as Complex III. Regardless of the site and mechanism through which the increase in ROS occurs, our results confirm and extend earlier reports suggesting elevated ROS generation with Bcl-2 overexpression [12] and are the first to demonstrate that three different anti-death Bcl-2 family proteins share the common characteristic of elevating basal rates of mitochondrial ROS production.

Despite the higher H_2O_2 release rate observed with Bcl-2 family protein expression and either isolated mitochondria or permeabilized cells, differences in H_2O_2 production measured with control vs overexpressing intact cells were either eliminated (Bcl-2, Fig. 1) or less evident (Bcl-xL, Fig. 5). These comparisons indicate that elevated mitochondrial ROS production is compensated by enhanced H_2O_2 removal capacities in the transfected cells. Our finding that the H_2O_2 removal rate of Bcl-xL cell homogenates is greater than that of control cells supports this interpretation (Fig. 6). Moreover, previous work with the same Bcl-2-transfected cells demonstrated elevated expression of catalase or glutathione reductase, two enzymes directly involved in the elimination of H_2O_2 [14]. These observations taken together suggest that the mild oxidative stress caused by elevated mitochondrial ROS production mediated by Bcl-2 family protein overexpression is responsible for inducing the expression of

one or more antioxidant systems. Our finding that 48 h exposure of Bcl-xL overexpressing cells to a level of a mitochondrial uncoupler that significantly lowers cellular H_2O_2 release also reduces the H_2O_2 removal capacity of cellular homogenates supports this hypothesis (Fig. 6).

Our results suggest that Bcl-2 family proteins may protect against oxidative cell death in a manner similar to that of ischemic preconditioning in which short nondamaging periods of ischemia protect against longer ischemic damage [47]. During preconditioning, mitochondrial ROS release is moderately increased, and this effect prevents large increases in ROS after ischemia [48,49]. The prevention of ROS release after ischemic preconditioning may be related to altered gene expression in delayed preconditioning [50] or, acutely, to redox activation of pathways capable of preventing mitochondrial ROS release such as ATP-sensitive K^+ channels [48,51].

Thus, while large increases in endogenous ROS accumulation are damaging to cells under many conditions, moderate increases in ROS such as those promoted by antiapoptotic Bcl-2 family members may be protective in a preconditioning-like manner, making cells better prepared to respond to acute oxidative stress. This effect explains the protective role of Bcl-2 family proteins against acute oxidative stress, in which the primary role of these proteins does not necessarily involve preventing the proapoptotic effects of proteins such as Bax or the prevention of caspase activation [37]. Indeed, protection against oxidative stress promoted by Bcl-2 family proteins may be vital to tumor cell survival since primary and metastatic tumors grow under a variety of oxygen tensions [52–54] and, presumably, intermittent periods of oxidative stress.

Acknowledgments—This project was supported by Fundação de Amparo à Pesquisa do Estado de São Paulo, Coordenação de Aperfeiçoamento de Pessoal de Nível Superior, Conselho Nacional de Desenvolvimento Científico e Tecnológico, the National Institutes of Health (NS34152 and ES11838), and the U.S. Army Medical Research and Material Command (DAMD 17-99-1-9483). The authors wish to acknowledge Edson A. Gomes and Camille C. da Silva for excellent technical assistance and Prof. A. Starkov for helpful discussions.

REFERENCES

[1] Green, D. R.; Reed, J. C. Mitochondria and apoptosis. *Science* **281:**1309–1312; 1998.
[2] Cory, S.; Huang, D. C.; Adams, J. M. The Bcl-2 family: roles in cell survival and oncogenesis. *Oncogene* **22:**8590–8607; 2003.
[3] Tsujimoto, Y. Cell death regulation by the Bcl-2 protein family in the mitochondria. *J. Cell Physiol.* **195:**158–167; 2003.
[4] Korsmeyer, S. J.; Yin, X. M.; Oltvai, Z. N.; Veis-Novack, D. J.; Linette, G. P. Reactive oxygen species and the regulation of cell death by the Bcl-2 gene family. *Biochim. Biophys. Acta* **1271:**63–66; 1995.
[5] Lemasters, J. J.; Qian, T.; Bradham, C. A.; Brenner, D. A.; Cascio, W. E.; Trost, L. C.; Nishimura, Y.; Nieminen, A. L.; Herman, B. Mitochondrial dysfunction in the pathogenesis of necrotic and apoptotic cell death. *J. Bioenerg. Biomembr.* **31:**305–319; 1999.
[6] Skulachev, V. P. Mitochondria in the programmed death phenomena; a principle of biology: "it is better to die than to be wrong." *IUBMB Life* **49:**365–373; 2000.
[7] Murphy, A. N.; Bredesen, D. E.; Cortopassi, G.; Wang, E.; Fiskum, G. Bcl-2 potentiates the maximal calcium uptake capacity of neural cell mitochondria. *Proc. Natl. Acad. Sci. USA* **93:**9893–9898; 1996.
[8] Susin, S. A.; Zamzami, N.; Castedo, M.; Hirsch, T.; Marchetti, P.; Macho, A.; Daugas, E.; Geuskens, M.; Kroemer, G. Bcl-2 inhibits the mitochondrial release of an apoptogenic protease. *J. Exp. Med.* **184:**1331–1341; 1996.
[9] Kluck, R. M.; Bossy-Wetzel, E.; Green, D. R.; Newmeyer, D. D. The release of cytochrome c from mitochondria: a primary site for Bcl-2 regulation of apoptosis. *Science* **275:**1132–1136; 1997.
[10] Yang, J.; Liu, X.; Bhalla, K.; Kim, C. N.; Ibrado, A. M.; Cai, J.; Peng, T. I.; Jones, D. P.; Wang, X. Prevention of apoptosis by Bcl-2: release of cytochrome c from mitochondria blocked. *Science* **275:**1129–1132; 1997.
[11] Hockenbery, D. M.; Oltvai, Z. N.; Yin, X. M.; Milliman, C. L.; Korsmeyer, S. J. Bcl-2 functions in an antioxidant pathway to prevent apoptosis. *Cell* **75:**241–251; 1993.
[12] Esposti, M. D.; Hatzinisiriou, I.; McLennan, H.; Ralph, S. Bcl-2 and mitochondrial oxygen radicals. New approaches with reactive oxygen species-sensitive probes. *J. Biol. Chem.* **274:** 29831–29837; 1999.
[13] Voehringer, D. W. BCL-2 and glutathione: alterations in cellular redox state that regulate apoptosis sensitivity. *Free Radic. Biol. Med.* **27:**945–950; 1999.
[14] Ellerby, L. M.; Ellerby, H. M.; Park, S. M.; Holleran, A. L.; Murphy, A. N.; Fiskum, G.; Kane, D. J.; Testa, M. P.; Kayalar, C.; Bredesen, D. E. Shift of the cellular oxidation-reduction potential in neural cells expressing Bcl-2. *J. Neurochem.* **67:**1259–1267; 1996.
[15] Rudin, C. M.; Yang, Z.; Schumaker, L. M.; VerWeele, D. J.; Newkirk, K.; Egorin, M. J.; Zuhowski, E. G.; Cullen, K. J. Inhibition of glutathione synthesis reverses Bcl-2-mediated cisplatin resistance. *Cancer Res.* **63:**312–318; 2003.
[16] Godon, C.; Lagniel, G.; Lee, J.; Buhler, J. M.; Kieffer, S.; Perrot, M.; Boucherie, H.; Toledano, M. B.; Labarre, J. The H_2O_2 stimulon in Saccharomyces cerevisiae. *J. Biol. Chem.* **273:**22480–22489; 1998.
[17] Demasi, A. P.; Pereira, G. A.; Netto, L. E. S. Cytosolic thioredoxin peroxidase I is essential for the antioxidant defense of yeast with dysfunctional mitochondria. *FEBS Lett.* **509:**430–434; 2001.
[18] Cai, J.; Jones, D. P. Superoxide in apoptosis. Mitochondrial generation triggered by cytochrome c loss. *J. Biol. Chem.* **273:**11401–11404; 1998.
[19] Kowaltowski, A. J.; Cosso, R. G.; Campos, C. B.; Fiskum, G. Effect of Bcl-2 overexpression on mitochondrial structure and function. *J. Biol. Chem.* **277:**42802–42807; 2002.
[20] Kane, D. J.; Sarafian, T. A.; Anton, R.; Hahn, H.; Gralla, E. B.; Valentine, J. S.; Ord, T.; Bredesen, D. E. Bcl-2 inhibition of neural death: decreased generation of reactive oxygen species. *Science* **262:**1274–1277; 1993.
[21] Zhang, B.; Gojo, I.; Fenton, R. G. Myeloid cell factor-1 is a critical survival factor for multiple myeloma. *Blood* **99:**1885–1893; 2002.
[22] Moreadith, R. W.; Fiskum, G. Isolation of mitochondria from ascites tumor cells permeabilized with digitonin. *Anal. Biochem.* **137:**360–367; 1984.
[23] Mohanty, J. G.; Jaffe, J. S.; Schulman, E. S.; Raible, D. G. A highly sensitive fluorescent micro-assay of H_2O_2 release from activated human leukocytes using a dihydroxyphenoxazine derivative. *J. Immunol. Methods* **202:**133–141; 1997.
[24] Zhou, M.; Diwu, Z.; Panchuk-Voloshina, N.; Haugl, R. P. A stable nonfluorescent derivative of resorufin for the fluorometric determination of trace hydrogen peroxide: applications in detecting the activity of phagocyte NADPH oxidase and other oxidases. *Anal. Biochem.* **253:**162–168; 1997.
[25] Barros, M. H.; Netto, L. E. S.; Kowaltowski, A. J. H_2O_2 generation in Saccharomyces cerevisiae respiratory pet mutants: effect of cytochrome c. *Free Radic. Biol. Med.* **35:**179–188; 2003.

[26] Fiskum, G.; Craig, S. W.; Decker, G.; Lehninger, A. L. The cytoskeleton of digitonin-treated rat hepatocytes. *Proc. Nat. Acad. Sci. USA* **77:**3430–3434; 1980.
[27] Fiskum, G.; Kowaltowski, A. J.; Andreyev, A. Y.; Kushnareva, Y. E.; Starkov, A. A. Apoptosis-related activities measured with isolated mitochondria and digitonin-permeabilized cells. *Methods Enzymol.* **322:**222–234; 2000.
[28] Turrens, J. F.; Boveris, A. Generation of superoxide anion by the NADH dehydrogenase of bovine heart mitochondria. *Biochem. J.* **191:**421–427; 1980.
[29] Starkov, A. A.; Fiskum, G.; Chinopoulos, C.; Lorenzo, B. J.; Browne, S. E.; Patel, M. S.; Beal, M. F. Mitochondrial alpha-ketoglutarate complex generates reactive oxygen species. *J. Neurosci.* **24:**7779–7788; 2004.
[30] Skulachev, V. P. Uncoupling: new approaches to an old problem of bioenergetics. *Biochim. Biophys. Acta* **1363:**100–124; 1998.
[31] St-Pierre, J.; Buckingham, J. A.; Roebuck, S. J.; Brand, M. D. Topology of superoxide production from different sites in the mitochondrial electron transport chain. *J. Biol. Chem.* **277:**44784–44790; 2002.
[32] Genova, M. L.; Ventura, B.; Giuliano, G.; Bovina, C.; Formiggini, G.; Parenti Castelli, G.; Lenaz, G. The site of production of superoxide radical in mitochondrial Complex I is not a bound ubisemiquinone but presumably iron-sulfur cluster N2. *FEBS Lett.* **505:**364–368; 2001.
[33] Turrens, J. F.; Alexandre, A.; Lehninger, A. L. Ubisemiquinone is the electron donor for superoxide formation by complex III of heart mitochondria. *Arch. Biochem. Biophys.* **237:**408–414; 1985.
[34] Kowaltowski, A. J.; Vercesi, A. E.; Fiskum, G. Bcl-2 prevents mitochondrial permeability transition and cytochrome c release via maintenance of reduced pyridine nucleotides. *Cell Death Differ.* **7:**903–910; 2000.
[35] Kushnareva, Y.; Murphy, A. N.; Andreyev, A. Complex I-mediated reactive oxygen species generation: modulation by cytochrome c and NAD(P)+ oxidation-reduction state. *Biochem. J.* **368:** 545–553; 2002.
[36] Starkov, A. A.; Fiskum, G. Regulation of brain mitochondrial H_2O_2 production by membrane potential and NAD(P)H redox state. *J. Neurochem.* **86:**1101–1107; 2003.
[37] Luetjens, C. M.; Lankiewicz, S.; Bui, N. T.; Krohn, A. J.; Poppe, J. H.; Prehn, J. H. Up-regulation of Bcl-xL in response to subtoxic beta-amyloid: role in neuronal resistance against apoptotic and oxidative injury. *Neuroscience* **102:**139–150; 2001.
[38] Chen, S. R.; Dunigan, D. D.; Dickman, M. B. Bcl-2 family members inhibit oxidative stress-induced programmed cell death in Saccharomyces cerevisiae. *Free Radic. Biol. Med.* **34:**1315–1325; 2003.
[39] Oltvai, Z. N.; Milliman, C. L.; Korsmeyer, S. J. Bcl-2 heterodimerizes in vivo with a conserved homolog, Bax, that accelerates programmed cell death. *Cell* **74:**609–619; 1993.
[40] Polster, B. M.; Kinnally, K. W.; Fiskum, G. BH3 death domain peptide induces cell type-selective mitochondrial outer membrane permeability. *J. Biol. Chem.* **276:**37887–37894; 2001.
[41] Myers, K. M.; Fiskum, G.; Liu, Y.; Simmens, S. J.; Bredesen, D. E.; Murphy, A. N. Bcl-2 protects neural cells from cyanide/aglycemia-induced lipid oxidation, mitochondrial injury, and loss of viability. *J. Neurochem.* **65:**2432–2440; 1995.
[42] Kane, D. J.; Ord, T.; Anton, R.; Bredesen, D. E. Expression of bcl-2 inhibits necrotic neural cell death. *J. Neurosci. Res.* **40:**269–275; 1995.
[43] Mirkovic, N.; Voehringer, D. W.; Story, M. D.; McConkey, D. J.; McDonnell, T. J.; Meyn, R. E. Resistance to radiation-induced apoptosis in Bcl-2-expressing cells is reversed by depleting cellular thiols. *Oncogene* **15:**1461–1470; 1997.
[44] Bojes, H. K.; Datta, K.; Xu, J.; Chin, A.; Simonian, P.; Nunez, G.; Kehrer, J. P. Bcl-xL overexpression attenuates glutathione depletion in FL5.12 cells following interleukin-3 withdrawal. *Biochem. J.* **325:**315–319; 1997.
[45] Zitomer, R. S.; Lowry, C. V. Regulation of gene expression by oxygen in Saccharomyces cerevisiae. *Microbiol. Rev.* **56:**1–11; 1992.
[46] Armstrong, J. S.; Jones, D. P. Glutathione depletion enforces the mitochondrial permeability transition and causes cell death in Bcl-2 overexpressing HL60 cells. *FASEB J.* **16:**1263–1265; 2002.
[47] Murry, C. E.; Jennings, R. B.; Reimer, K. A. Preconditioning with ischemia: a delay of lethal cell injury in ischemic myocardium. *Circulation* **74:**1124–1136; 1986.
[48] Vanden Hoek, T. L.; Becker, L. B.; Shao, Z.; Li, C.; Schumacker, P. T. Reactive oxygen species released from mitochondria during brief hypoxia induce preconditioning in cardiomyocytes. *J. Biol. Chem.* **273:**18092–18098; 1998.
[49] da Silva, M. M.; Sartori, A.; Belisle, E.; Kowaltowski, A. J. Ischemic preconditioning inhibits mitochondrial respiration, increases H_2O_2 release, and enhances K^+ transport. *Am. J. Physiol.* **285:**H154–H162; 2003.
[50] Stenzel-Poore, M. P.; Stevens, S. L.; Xiong, Z.; Lessov, N. S.; Harrington, C. A.; Mori, M.; Meller, R.; Rosenzweig, H. L.; Tobar, E.; Shaw, T. E.; Chu, X.; Simon, R. P. Effect of ischaemic preconditioning on genomic response to cerebral ischaemia: similarity to neuroprotective strategies in hibernation and hypoxia-tolerant states. *Lancet* **362:**1028–1037; 2003.
[51] Ferranti, R.; da Silva, M. M.; Kowaltowski, A. J. Mitochondrial ATP-sensitive K^+ channel opening decreases reactive oxygen species generation. *FEBS Lett.* **536:**51–55; 2003.
[52] Zetter, B. R. Angiogenesis and tumor metastasis. *Annu. Rev. Med.* **49:**407–424; 1998.
[53] Cristofanilli, M.; Charnsangavej, C.; Hortobagyi, G. N. Angiogenesis modulation in cancer research: novel clinical approaches. *Nat. Rev. Drug Discovery* **1:**415–426; 2002.
[54] Semenza, G. L. Angiogenesis in ischemic and neoplastic disorders. *Annu. Rev. Med.* **54:**17–28; 2003.

ABBREVIATIONS

AA — antimycin A
Ala — alamethicin
BSA — bovine serum albumin
EGTA — ethylene glycol-bis(2-aminoethylether)-N,N,N',N'-tetraacetic acid
FCCP — carbonyl cyanide 4-(trifluoromethoxy)phenylhydrazone
Glu — glutamate
HRP — horseradish peroxidase
LDH — lactate dehydrogenase
Mal — malate
Oligo — oligomycin
Pyr — pyruvate
ROS — reactive oxygen species
Rot — rotenone
Succ — succinate

Inhibition of glutamate-induced delayed calcium deregulation by 2-APB and La^{3+} in cultured cortical neurones

Christos Chinopoulos,*,†,[1] Akos A. Gerencser,*,[1] Judit Doczi,* Gary Fiskum† and Vera Adam-Vizi*

*Semmelweis University, Department of Medical Biochemistry, Neurobiochemical Group, Hungarian Academy of Sciences, Budapest, Hungary

†University of Maryland, Department of Anesthesiology, Baltimore, Maryland, USA

Abstract

Exposure of neurones in culture to excitotoxic levels of glutamate results in an initial transient spike in $[Ca^{2+}]_i$ followed by a delayed, irreversible $[Ca^{2+}]_i$ rise governed by rapid kinetics, with Ca^{2+} originating from the extracellular medium. The molecular mechanism responsible for the secondary Ca^{2+} rise is unknown. Here, we report that the delayed Ca^{2+} entry in cortical neurones is diminished by 2-aminoethoxydiphenyl borate (2-APB: $IC_{50} = 62 \pm 9$ μM) and La^{3+} ($IC_{50} = 7.2 \pm 3$ μM), both known to inhibit transient receptor potential (TRP) and store-operated Ca^{2+} (SOC) channels. Application of thapsigargin, however, failed to exacerbate the delayed Ca^{2+} deregulation, arguing against a store depletion event as the stimulus for induction of the secondary $[Ca^{2+}]_i$ rise. In addition, these neurones did not exhibit SOC entry. Unexpectedly, application of ryanodine or caffeine significantly inhibited glutamate-induced delayed Ca^{2+} deregulation. In basal Ca^{2+} entry experiments, La^{3+} and 2-APB modulated the rapid rise in $[Ca^{2+}]_i$ caused by exposure of neurones to Ca^{2+} after pre-incubating in a calcium-free medium. This basal Ca^{2+} influx was mitigated by extracellular Mg^{2+} but not aggravated by thapsigargin, ryanodine or caffeine. These results indicate that 2-APB and La^{3+} influence non-store-operated Ca^{2+} influx in cortical neurones and that this route of Ca^{2+} entry is involved in glutamate-induced delayed Ca^{2+} deregulation.

Keywords: 2-aminoethoxydiphenyl borate, delayed Ca^{2+} deregulation, excitotoxicity, La^{3+}, store-operated calcium entry, transient receptor potential.

J. Neurochem. (2004) 10.1111/j.1471-4159.2004.02732.x

Delayed calcium deregulation (DCD) is a phenomenon originally described by Manev and colleagues (Manev *et al*. 1989), further characterized by the groups of Thayer (Randall and Thayer 1992) and Tymianski (Tymianski *et al*. 1993b), addressing the latent loss of calcium homeostasis of cultured neurones upon exposure to glutamate. The phenomenon is invariably demonstrated in every neuronal cell type studied, i.e. spinal (Tymianski *et al*. 1993b), hippocampal (Randall and Thayer 1992), cerebellar granule (Budd and Nicholls 1996), striatal (Alano *et al*. 2002) and cortical neurones (Rajdev and Reynolds 1994). DCD is not observed if high extracellular K^+ is alternatively employed to elevate $[Ca^{2+}]_I$; this led to the proposal of a 'source specificity' hypothesis of Ca^{2+}-induced neurotoxicity (Tymianski *et al*. 1993b). However, this idea has been challenged by subsequent studies showing that activation of NMDA receptors produces much larger Ca^{2+} entry than activation of voltage-dependent Ca^{2+} channels by high extracellular K^+ (Hyrc *et al*. 1997). The initial spike in $[Ca^{2+}]_i$ induced by glutamate is due to opening of the ligand-gated glutamate receptors, in addition

Received May 6, 2004; revised manuscript received June 18, 2004; accepted July 4, 2004.

Address correspondence and reprint requests to Prof. Vera Adam-Vizi, Semmelweis University, Department of Medical Biochemistry, Budapest H-1444, P.O. Box 262, Hungary. E-mail: av@puskin.sote.hu

[1]Christos Chinopoulos and Akos A. Gerencser contributed equally to this work.

Abbreviations used: ANT, adenine nucleotide translocator; 2-APB, 2-aminoethoxydiphenyl borate; CCD, charged coupled device; CCE, capacitative calcium entry; CICR, Ca^{2+}-induced Ca^{2+} release; CNQX, 6-cyano-7-nitroquinoxaline-2,3-dione; DCD, delayed calcium deregulation; DHPG, S-3,5-dihydroxyphenylglycine; DMEM, Dulbecco's modified Eagle's essential medium; EGTA, ethylene glycol-bis(2-aminoethylether)-*N*,*N*,*N*′,*N*′-tetraacetic acid; hTRPC3, human TRP3; IP_3, inositol trisphosphate; IP_3R, inositol trisphosphate receptor; mGluR1, metabotropic glutamate receptor 1; MIC, Mg^{2+} inhibitable cation channel; NA, numerical aperture; NMDA, *N*-Methyl-D-aspartate; NMDAR, NMDA receptor; PMNCX, plasma membrane Na^+/Ca^{2+} exchanger; PTP, permeability transition pore; RyR, ryanodine receptor; SOCE, store-operated calcium entry; SOCs, store-operated calcium channels; TRP, transient receptor potential; TTX, tetrodotoxin; VDCCs, voltage-dependent calcium channels.

to secondary activation of the voltage-dependent calcium channels (VDCCs). DCD, however, is not attributed only to events downstream of NMDA receptor activation, but also to AMPA/kainate, as well as to tetrodotoxin (TTX)-sensitive channels activated by veratridine in combination with oxidative stress (Chinopoulos *et al*. 2000) or alone (Rego *et al*. 2001). Yet, the delayed $[Ca^{2+}]_i$ rise is not inhibitable by post-glutamate addition of antagonists of NMDA or non-NMDA receptors (Manev *et al*. 1989; Tymianski *et al*. 1993a), nor by blocking voltage-dependent Ca^{2+} or Na^+ channels (Hartley and Choi 1989; Manev *et al*. 1989; Randall and Thayer 1992; Tymianski *et al*. 1993a). A number of studies have shown that DCD is associated with the loss of mitochondrial membrane potential. Therefore, the secondary rise in $[Ca^{2+}]_i$ could result from the release of calcium previously sequestered by mitochondria (Nicholls and Ward 2000). In addition, the delayed $[Ca^{2+}]_i$ rise appears to be accompanied by mitochondrial sequestration, supported by *in vivo* studies (Dux *et al*. 1987) demonstrating ultra-structural alterations of the mitochondria suggestive of pore opening. However, to consign DCD and permeability transition pore (PTP) in the pragmatic order of events is not yet feasible (Nicholls *et al*. 2003). Several lines of evidence argue against the possible contribution of a reverse function of the plasma membrane Na^+/Ca^{2+} exchanger (PMNCX) to the delayed Ca^{2+} rise: (i) NMDA-induced (but not glutamate-induced) neurotoxicity is not affected by profound hypothermia (12°C) (Tymianski *et al*. 1998), a condition that diminishes the function of the exchanger dramatically (Schellenberg and Swanson 1982); (ii) the reverse function of the exchanger is eliminated upon exposure of neurones to glutamate within 3–5 min (Yu & Choi 1997); (iii) inhibition of the exchanger by KB-R7943 unveiled a trivial role for the expression of excitotoxic injury (Hoyt *et al*. 1998). However, DCD demands the existence of a discrete pathway as it precedes, and eventually leads to, plasma membrane leakiness (Tymianski *et al*. 1993a) and cell death (Tymianski *et al*. 1993a, b; Limbrick *et al*. 1995). It is firmly established that Ca^{2+} originates from the extracellular medium (Hartley and Choi 1989; Manev *et al*. 1989; Randall and Thayer 1992; Tymianski *et al*. 1993b), but DCD is not attributed to the 'traditionally' recognized Ca^{2+} channels, such as glutamate receptor-operated or voltage-gated Ca^{2+} channels (Limbrick *et al*. 2001). Along this line, it was shown that a secondary activation of a non-selective cation conductance, termed post-exposure current (I_{pe}), is induced subsequent to excitotoxic application of NMDA to hippocampal neurones and probably accounts for the delayed Ca^{2+} rise (Chen *et al*. 1997).

We explored the possibility that DCD is mediated by transient receptor potential (TRP) channels, which are abundant in nervous tissue (Montell *et al*. 2002). Currently, a few members of the TRP family are candidates for the so-called 'store-operated Ca^{2+} entry' [(SOCE) also known as capacitative calcium entry (CCE)]. SOCE is a process whereby the depletion of intracellular calcium stores (likely endoplasmic or sarcoplasmic reticulum) activates plasma membrane Ca^{2+} permeable channels (Putney 1986). SOCE is centrally positioned among signal transduction and $[Ca^{2+}]_i$ homeostasis in both excitable and non-excitable cells (Venkatachalam *et al*. 2002). However, unequivocal evidence showing that TRP channels account for SOCE is yet to be reported (Clapham 2003). In addition, several members of the TRP channel family operate in a store-independent manner (Braun *et al*. 2001; Obukhov and Nowycky 2002; Zitt *et al*. 2002).

Our results are consistent with the hypothesis that activation of TRP channels is responsible for the delayed $[Ca^{2+}]_i$ rise. However, they do not support a role for intracellular Ca^{2+} store depletion in triggering DCD. This hypothesis is supported by the recent demonstration that TRPM7, a member of the melastatin branch of the TRP family, is responsible for neuronal death (Aarts *et al*. 2003) caused by oxygen-glucose deprivation, a model previously reported to mediate neuronal demise through NMDA receptor (NMDAR) activation (Goldberg *et al*. 1987; Goldberg and Choi 1993).

Materials and methods

Preparation of cortical neurones

Primary cultures of cortical neurones were prepared from Sprague-Dawley rats (17th day *in utero*). All animal procedures were carried out in accordance with the National Institutes of Health and the University of Maryland, Baltimore, Animal Care and Use Committee Guidelines. Neurones were grown on 25 mm coverslips for 10–16 days *in vitro*, at a density of approximately 50 000 cells/coverslip, supplemented with Dulbecco's modified Eagle's essential medium (DMEM), glutamine, neurobasal medium and B27 supplement. Glial proliferation was prevented by adding cytosine-arabinofuranoside (5 μM) 24 h after plating. Immunocytochemical measurements of glial fibrillary acid protein (GFAP) confirmed that cultures contained < 1% glia.

$[Ca^{2+}]_i$ imaging

To measure $[Ca^{2+}]_i$, neurones were loaded with fura-2 AM, fura-6F AM or fura-FF AM (2 μM) at 37°C for 20 min, followed by a 10 min hydrolysis period. Single cell fluorescence of fura-2, fura-6F or fura-FF was ratio imaged by alternating excitation at 340 nm and 380 nm (Polychrome IV, Till, Munich, Germany), and emission at 510 nm. Image sequences (10 s/ratio frame, 50 ms exposure time, 2 × 2 binning) were acquired using an ORCA-ER cooled digital CCD camera (Hamamatsu Photonics, Hamamatsu, Japan) mounted on a Nikon Eclipse TE2000-S inverted microscope (SFluor 20 × 0.75 NA and 40× 1.2 numerical apeture (NA) for $[Ca^{2+}]_i$ and $[Ca^{2+}]_{ER}$ determinations, respectively; Nikon Corp., Tokyo, Japan). Image acquisition was controlled by Metafluor 5.0 (Universal Imaging Corp., West Chester, PA, USA). The sample holder and the perfusate (50 mL/h flow rate) were temperature controlled at 37°C at the side of

the recording. The composition of the perfusate was, in mM: NaCl 120, KCl 3.5, KH_2PO_4 0.4, HEPES 20, $NaHCO_3$ 5, glucose 15, $CaCl_2$ 1.3 (or 2.6 where indicated), $MgCl_2$ 1 (or nominally Mg^{2+}-free for DCD experiments in the absence or presence of inhibitors). Whenever $LaCl_3$ was used, KH_2PO_4 and $NaHCO_3$ were excluded from the medium; control experiments verified that the lack of these chemicals did not account for the effects of $LaCl_3$.

Delayed Ca^{2+} deregulation was assayed by counting the cells on fura-6F ratio plots, which exhibited a sudden, irreversible rise in fura-6F fluorescence ratio after the initial glutamate peak. Half-times ($t_{1/2}$) of $[Ca^{2+}]_i$ decay for basal Ca^{2+} entry experiments were calculated by fitting a single-exponential decay function on each trace, from the peak in 400 s length. Image analysis was carried out in Metafluor Analyst (Universal Imaging Corp.), and data analysis in Mathematica 4.2 (Wolfram Research, Champaign, IL, USA) and SigmaPlot 8 (SPSS Inc., Chicago, IL, USA).

$[Mg^{2+}]_i$ imaging

$[Mg^{2+}]_i$ determination was performed similarly to the $[Ca^{2+}]_i$ imaging. Neurones were loaded with Mag-fura red-AM (3 μM) at 37°C for 15 min, followed by a 5 min hydrolysis period. Single-cell fluorescence of Mag-fura red was ratio imaged by alternating excitation at 430 nm and 490 nm, and emission at > 570 nm. The affinity constant (K_d) of Mag-fura red was determined in a cuvette fluorimeter (PTI Deltascan, New Brunswick, NJ, USA) and estimated to be 2.4 mM (37°C; pH 7.05). Ratios were calibrated *in vitro* using the Grynkiewicz equation (Grynkiewicz *et al*. 1985) with a measured viscosity correction (Poenie 1990). Image sequences (30 s/ratio frame, 100 ms exposure time, 2 × 2 binning) were acquired by the CCD camera. The sample holder and the perfusate (50 mL/h flow rate) were temperature controlled at 37°C at the side of the recording. The composition of the perfusate was, in mM: NaCl 120, KCl 3.5, KH_2PO_4 0.4, HEPES 20, $NaHCO_3$ 5, glucose 15, $CaCl_2$ 1.3, $MgCl_2$ 1 (or nominally Mg^{2+}-free, where indicated).

IC_{50} determination of 2-APB and La^{3+}-mediated inhibition of DCD

Cortical neurones were plated in 96-well polystyrene dishes (Costar; Sigma, St Louis, MO, USA) at the same density as for the imaging experiments. To avoid background fluorescence of polystyrene, the red fluorescent mag-fura red was used for measuring $[Ca^{2+}]_i$. Cells were loaded with the AM dye (3 μM) for 20 min, followed by a 5 min hydrolysis period. Mag-fura-red has a low affinity for Ca^{2+} (K_d = 70 μM; measured in a cuvette fluorimeter, 37°C, pH 7.05; PTI Deltascan); it is therefore only responsive to large magnitude rises in Ca^{2+}, as occur during DCD, and is not the primary response for the glutamate stimulus. Macroscopic, cumulative fluorescence of Mag-fura red was ratioed with a plate reader fluorimeter (Victor^3; Perkin Elmer, Turku, Finland) using excitation filters at 420–430 nm and 490–500 nm (Omega Optical, Brattleboro, VT, USA) and emission at 660 nm. Fluorescence background of each well was determined before loading cells with the AM dye. Inhibition of DCD was assayed by end point measurement of the background-corrected Mag-fura red ratio increase relative to the baseline after 60 min of treatment with 100 μM glutamate + 10 μM glycine in the presence of 14–300 μM 2-APB or 0.4–200 μM La^{3+} (eight concentrations performed in triplicate). Experiments were carried out in buffers similar to those used in the imaging experiments but containing 44 mM $NaHCO_3$, and cultures were kept in a CO_2 incubator at 37°C during the treatment.

Materials

2-APB, $LaCl_3$, cyclosporin A, thapsigargin, ryanodine, caffeine, 4-Br-A23187, nifedipine, cytosine-arabinofuranoside, MK-801 and CNQX were from Sigma. Fura-2 AM, fura-6F AM, fura-FF AM, mag-fura-red-AM and fura-6F5K$^+$ salt were from Molecular Probes (Eugene, OR, USA). Bongkrekic acid was from Calbiochem (EMD Biosciences, Inc., Darmstadt, Germany). Standard laboratory chemicals were from Sigma.

Results

DCD is abolished by 2-APB and La^{3+}

Cortical neurones exposed to 100 μM glutamate + 10 μM glycine exhibit an abrupt increase in $[Ca^{2+}]_i$ attributed to activation of ligand-gated glutamate receptors (Fig. 1a, 100 s, Table 1). Although glutamate and glycine remain in the perfusate throughout the experiment, $[Ca^{2+}]_i$ plateaus at a level lower than the ligand-induced peak, due to desensitization of the NMDA receptors (Mayer and Westbrook 1985), as well as inhibition of the receptor by elevated $[Ca^{2+}]_i$ (Legendre *et al*. 1993). After ≥ 5 min, and over a period of 60 min, neurones lose the ability to maintain $[Ca^{2+}]_i$ at the newly established level and exhibit asynchronous, large and abrupt increases in fura-6F fluorescence ratio. Fura-6F has a relatively high K_d (2.47 μM) for Ca^{2+} and it measures $[Ca^{2+}]$ reliably in the range of 0.5–50 μM (Chinopoulos *et al*. 2003). Therefore, the dye is not saturated at the glutamate-induced Ca^{2+} spike, a phenomenon observed with high-affinity calcium indicators (Stout and Reynolds 1999). This also 'unmasks' the magnitude of the secondary Ca^{2+} rise. It is apparent that the majority of neurones undergo DCD, with a mean onset $t_{mean} = 910 \pm 160$ s after application of the glutamate stimulus (Table 1). While there is strong evidence that DCD is due to plasmalemmal Ca^{2+} influx (see introduction), the extent of the burden that it imposes on calcium extrusion (e.g. plasma membrane Ca^{2+} ATPase) and sequestering mechanisms (e.g. mitochondrial calcium uptake) has not yet been clarified. Therefore, in a separate set of experiments, $[Ca^{2+}]_e$ was removed from the perfusate by switching to a nominally Ca^{2+}-free medium plus 25 μM EGTA at 1500 s, which prevented further occurrence of DCD (Fig. 1b) and caused a decline of $[Ca^{2+}]_i$ in cells that were already deregulated. The slope of this decline was determined for each deregulated cell and was plotted against the time elapsed from the onset of DCD to the time of $[Ca^{2+}]_e$ washout (Fig. 1c). Linear regression analysis of this plot showed that removal of $[Ca^{2+}]_e$ shortly after the onset of DCD causes a rapid decrease in $[Ca^{2+}]_i$ but that subsequently, neurones lose the ability to rapidly restore resting $[Ca^{2+}]_i$. This finding raises the possibility that the delayed Ca^{2+} influx

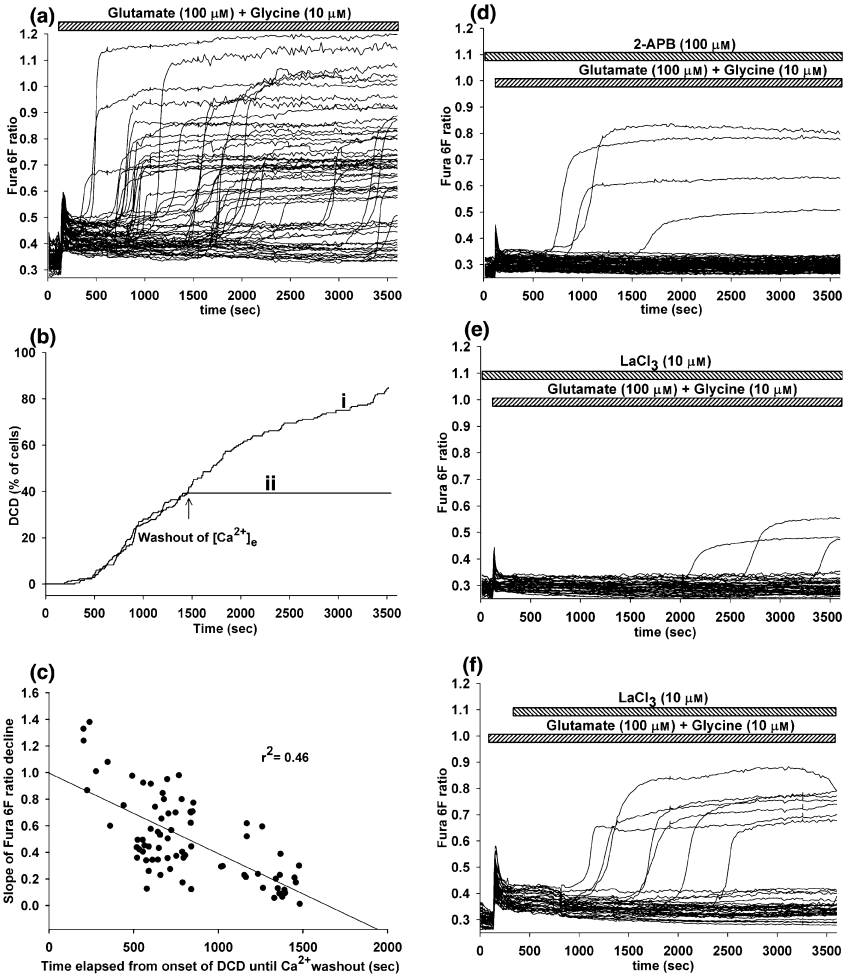

Fig. 1 DCD induced by glutamate (100 μM) plus glycine (10 μM) in cortical neurones and the effect of 2-APB and La^{3+}. a, d, e, f: Fura-6F ratio fluorescence of $[Ca^{2+}]_i$ upon exposure to glutamate plus glycine in the presence and absence of 2-APB (100 μM) or $LaCl_3$ (10 μM) recorded for 1 h. Glutamate plus glycine were added to the perfusion medium at 100 s and were present throughout the entire experiment. (a) No inhibitor present. Traces are representative of six independent experiments. 2-APB (d) or La^{3+} (e) were given 10 min prior to glutamate plus glycine exposure and were present throughout the entire experiment. Traces are representative of five (d) or three (e) independent experiments. (f) Effect of $LaCl_3$ added 300 s after the addition of glutamate plus glycine (representative of three independent experiments). (b) Percentage of cells that underwent DCD upon exposure to glutamate plus glycine (added at 100 s) versus time. Trace (i) was calculated from the data set corresponding to Table 1. In trace (ii) the perfusion was switched to Ca^{2+}-free medium + 25 μM EGTA containing glutamate plus glycine at 1500 s. (c) Linear regression analysis of slope of fura-6F ratio fluorescence (10^{-3} ratio units/s) versus time elapsed from DCD onset until removal of extracellular calcium, in s. Data pooled from three independent experiments.

elicits a sequence of events that gradually incapacitate calcium extrusion/sequestering mechanisms.

2-APB (100 μM) added 10 min prior to exposure to glutamate led to a dramatic decrease in the incidence of the secondary $[Ca^{2+}]_i$ rise (Fig. 1d, Table 1). The same phenomenon was observed if 10–100 μM $LaCl_3$ was applied, but 1 μM $LaCl_3$ was ineffective (Fig. 1e, Table 1). In an effort to determine the IC_{50} for 2-APB and La^{3+}, DCD was assayed by measuring the cumulative response of mag-fura red (used as a low affinity Ca^{2+} dye) -loaded cortical neurones cultured in 96-well dishes. Parallel imaging experiments using Mag-fura red and the standard DCD protocol (100 μM glutamate + 10 μM glycine for 1 h) were performed (not shown). Due to the low affinity ($K_d = 70$ μM) of Mag-fura red, the difference between the fluorescence ratio before, and 60 min after the addition of glutamate plus glycine reflects the fraction of cells that underwent DCD. 2-APB (14–300 μM) applied 10 min before, and La^{3+} (0.4–200 μM) applied together with glutamate, dose-dependently diminished the ratio increase evoked by the glutamate treatment. IC_{50} of 2-APB inhibition on DCD was estimated to be 62 ± 9 μM ($n = 4$ plates), whereas that for La^{3+} was 7.2 ± 3 μM ($n = 3$ plates).

Although $LaCl_3$ blocks voltage-dependent Ca^{2+} channels (Nelson *et al*. 1984), this pathway has previously been excluded as a candidate for the secondary $[Ca^{2+}]_i$ rise (see introduction). In addition to inhibiting DCD, 100 μM 2-APB and 10 μM $LaCl_3$ reduced the glutamate-induced $[Ca^{2+}]_i$ peak (Figs 1d and e, Table 1) and accelerated the decay to a newly established $[Ca^{2+}]_i$ plateau. The latter observation is similar to that of Baba and colleagues (Baba *et al*. 2003). However, in contrast to our results with glutamate, these authors did not detect an inhibitory effect of 2-APB or La^{3+} on the peak amplitude of the NMDA-induced $[Ca^{2+}]_i$ transients. This reflects the possibility that glutamate-induced non-NMDAR $[Ca^{2+}]_i$ influx encompasses 2-APB and La^{3+}-sensitive targets. Application of a lower concentration (30 μM) of 2-APB did not result in a decrease in glutamate-induced $[Ca^{2+}]_i$ peak, whereas the incidence of DCD was slightly decreased with an increase in the mean onset time of DCD (t_{mean}; Table 1). As Baba and colleagues demonstrated

Table 1 Characteristics of glutamate-induced DCD in the presence and absence of various compounds

	n	Total number of cells	DCD % of cells	Onset of DCD t_{mean} (s)	Baseline $[Ca]_i$ (fura-6F ratio fluorescence)	Glutamate + glycine induced $[Ca]_i$ peak (fura-6F ratio at 100 s, absolute value)
Control	6	332	84.5 ± 9.7	910 ± 160	0.31 ± < 0.001	0.397 ± < 0.001
2-APB (100 μM)	5	490	4.5 ± 1.0*[a]	917 ± 149 [n.s]	0.30 ± < 0.001	0.354 ± < 0.001*[b]
2-APB (30 μM)	3	189	77.8 ± 4.8*[a]	1366 ± 125*[b]	0.30 ± < 0.001	0.398 ± < 0.001 [n.s]
$MgCl_2$ (10 mM) (pre-incubation)	5	603	8.2 ± 3.0*[a]	894 ± 188 [n.s]	0.31 ± < 0.001	0.370 ± < 0.001 [n.s]
$LaCl_3$ (1 μM)	3	155	70.0 ± 6.9*[a]	902 ± 155 [n.s]	0.30 ± < 0.001	0.378 ± < 0.001 [n.s]
$LaCl_3$ (10 μM)	3	168	8.1 ± 1.2*[a]	2480 ± 182*[b]	0.30 ± < 0.001	0.357 ± < 0.001*[b]
$LaCl_3$ (10 μM) (after glutamate)	3	151	9.8 ± 3.2*[a]	1654 ± 111*[b]	0.30 ± < 0.001	0.399 ± < 0.001 [n.s]
$LaCl_3$ (100 μM)	3	199	2.02 ± 1.33*[a]	2607 ± 188*[b]	0.31 ± < 0.001	0.366 ± < 0.001 [n.s]
Ryanodine (1 μM)	3	204	28.4 ± 0.6*[a]	1816 ± 173*[b]	0.30 ± < 0.001	0.383 ± < 0.001 [n.s]
Caffeine (10 mM)	3	248	7.67 ± 1.7*[a]	1450 ± 292*[b]	0.30 ± < 0.001	0.368 ± < 0.001 [n.s]
SK&F 96365 (5 μM)	3	255	88.9 ± 10.4 [n.s]	780 ± 169 [n.s]	0.30 ± < 0.001	0.394 ± < 0.001 [n.s]
Cyclosporin A (1 μM)	3	198	86.7 ± 12.8 [n.s]	885 ± 168 [n.s]	0.31 ± < 0.001	0.431 ± 0.008*[b]
Bongkrekic acid (20 μM)	3	178	89.5 ± 13.9 [n.s]	931 ± 174 [n.s]	0.33 ± < 0.001	0.467 ± 0.009*[b]
Thapsigargin (1 μM)	3	158	87.1 ± 9.8 [n.s]	911 ± 160 [n.s]	0.30 ± < 0.001	0.404 ± < 0.001 [n.s]

2-APB, $LaCl_3$, ryanodine, caffeine, SK&F 96365, cyclosporin A, bongkrekic acid and thapsigargin were present for 10–30 min (as described in the text) prior to exposure to glutamate plus glycine and throughout the entire duration of the experiment. $MgCl_2$ was present only for 30 min prior to exposure to glutamate plus glycine. $LaCl_3$, where indicated, was applied 300 s after perfusion with glutamate plus glycine ($LaCl_3$ 10 μM after glutamate). *n* = number of independent experiments. Statistics: Mann–Whitney rank sum test.

[a]Significant compared to control, $p < 0.001$, [b]significant compared to control, $p < 0.005$, n.s: not significant compared to control, $p < 0.005$.

electrophysiologically that 2-APB and La^{3+} do not inhibit the NMDA receptor, our results are not attributable to a confounding inhibitory action on the NMDA receptor itself. Nevertheless, the moderately reduced glutamate-induced $[Ca^{2+}]_i$ peak and the accelerated return towards baseline values (Figs 1d and e, Table 1) may contribute to the diminished incidence and mean onset time of DCD by other means. Therefore, we applied the compounds 300 s after the start of perfusion with glutamate. It is apparent from Fig. 1(f) and Table 1 that application of $LaCl_3$ (10 μM) strongly inhibited DCD while the glutamate-induced $[Ca^{2+}]_i$ peak remained unchanged. The protective effect of 2-APB given after glutamate + glycine was, however, less pronounced, diminishing the incidence of DCD to approximately 55% (not shown).

Mitochondrial PTP inhibitors fail to ameliorate DCD

To address the role of PTP in our system, cortical neurones were treated with cyclosporin A (1 μM) for 30 min prior to exposure to glutamate; the inhibitor was also present in the perfusate for the entire duration of the experiment. As shown in Fig. 2(a) and Table 1, there was no statistical difference in the percentage of cells undergoing DCD, or in the mean time of onset in the presence or absence of cyclosporin A. It is noteworthy that DCD is an event usually demonstrated in the absence of Mg^{2+} to relieve the block of the NMDA receptor, and it has been shown that Mg^{2+} is critical for conferring cyclosporin A sensitivity of the permeability transition in rat liver mitochondria (Andreyev *et al*. 1994). In an effort to increase $[Mg^{2+}]_i$, neurones were pre-treated with 10 mM $MgCl_2$ for 30 min prior to glutamate exposure without cyclosporin A. This led to an increase in the baseline $[Mg^{2+}]_i$ from 0.65 ± 0.02 mM to 1.15 ± 0.03 mM, persisting for at least 1 h irrespective of perfusing with a $MgCl_2$-free buffer during the experiment. This regime resulted in a substantial reduction in the incidence of DCD without affecting the glutamate-induced $[Ca^{2+}]_i$ peak (Table 1). However, the exact mechanism underlying this protective effect was not further investigated. As with cyclosporin A, bongkrekic acid (20 μM) failed to decrease the incidence or the onset time of DCD, irrespective of whether it was present throughout the experiment (Fig. 2b, Table 1) or present only during a 10 min pre-incubation period (not shown). Notably, application of either cyclosporin A or bongkrekic acid led to a statistically significant increase in the glutamate-induced $[Ca^{2+}]_i$ peak (Figs 2a and 2b, respectively, and Table 1). The mechanism(s) for this peculiarity was not further investigated here.

Do cortical neurones exhibit store-operated Ca^{2+} entry?

We first investigated 'basal' Ca^{2+} entry, in which neurones were deprived of extracellular calcium ('Ca^{2+}-free' medium in the absence of Sarcoplasmic Reticulum Ca^{2+} ATPase (SERCA)

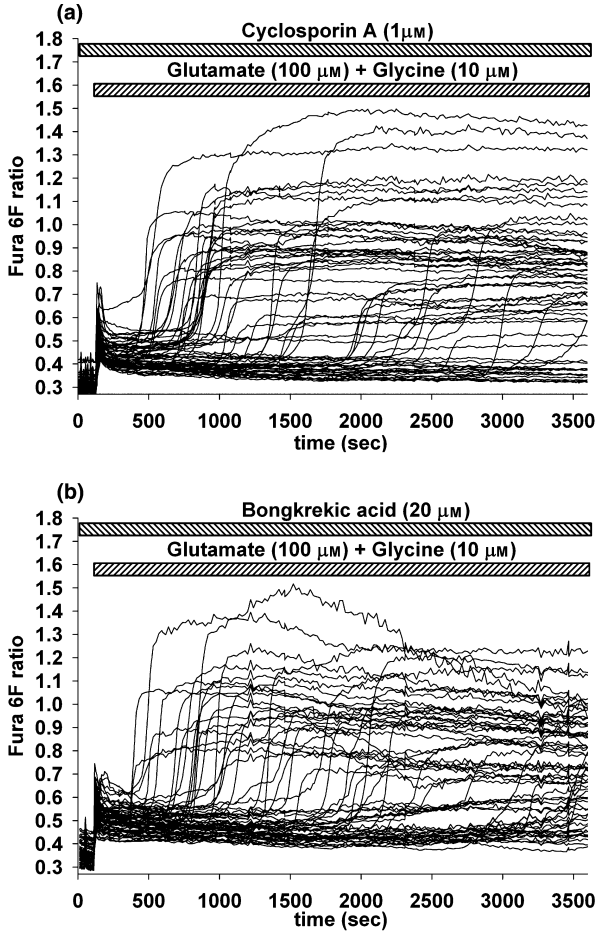

Fig. 2 Lack of effect of cyclosporin A and bongkrekic acid on glutamate induced DCD. Fura-6F ratio fluorescence of $[Ca^{2+}]_i$ of cortical neurones upon exposure to glutamate (100 μM) plus glycine (10 μM) is shown in the presence of cyclosporin A (1 μM) or bongkrekic acid (20 μM) recorded for 1 h. (a) Cyclosporin A was given 30 min prior to glutamate plus glycine exposure, and was present throughout the entire experiment. Traces are representative of three independent experiments. (b) Bongkrekic acid was present for 10 min prior to glutamate plus glycine exposure, as well as throughout the entire experiment. Traces are representative of three independent experiments.

inhibitors, containing 7.44 μM free Ca^{2+} measured by fura-6F $5K^+$ salt) for 8–10 min, followed by re-introduction of the cation to the perfusing medium. Prior to this, in order to demonstrate that the intracellular stores do contain Ca^{2+}, neurones were perfused with either Ca^{2+}-free medium (Fig. 3a, trace i), Ca^{2+}-free medium containing EGTA (25 μM) (Fig. 3a, trace i), Ca^{2+}-free medium plus thapsigargin (Tg; 1 μM) (Fig. 3a, trace iii), or Ca^{2+}-free medium containing EGTA plus Tg (Fig. 3a, trace iv). $[Ca^{2+}]_{ER}$ was estimated from the perinuclear fluorescence of fura-FF (Csordas and Hajnoczky 2001) under resting conditions when $[Ca^{2+}]_i$ is low. Therefore, the low affinity Ca^{2+} dye is unresponsive to changes in $[Ca^{2+}]_i$, but responsive to alterations in $[Ca^{2+}]$ in compartments where $[Ca^{2+}]$ is sufficiently high, such as the endoplasmic reticulum (ER). High magnification imaging revealed a perinuclear patchy pattern of higher ratios. In the presence of Tg ± EGTA, the fura-FF ratio dropped quickly (in 2–400 s) over these regions, indicating that the measured signal (at least partially) originates from the ER. In contrast, perfusing with Ca^{2+}-free medium did not cause a significant ratio change, but when EGTA was also present, a small and delayed decrease in the fura-FF ratio fluorescence was observed. To address the degree of the intracellular stores depletion upon Tg treatment, neurones were challenged with a cocktail consisting of 4-Br A23187 (10 μM), monensin (10 μM), nigericin (10 μM) and gramicidin (5 μM), applied at 200 s (trace v), or at 700 s (Fig. 3a, trace iv). It is apparent that 10 min of perfusing with EGTA + Tg depletes Tg-sensitive intracellular stores (compare trace iv with trace v at 800–900 s). To examine further the filling status of the intracellular stores, $[Ca^{2+}]_i$ was measured using fura-2 in neurones which were perfused with Ca^{2+}-free medium + EGTA ± Tg for various time intervals, followed by addition of the calcium ionophore 4-Br-A23187 (5 μM) (Fig. 3b). Under this condition, Ca^{2+} released exclusively from intracellular compartments would increase fura-2 fluorescence. Specifically, perfusion with Ca^{2+}-free medium + EGTA led to a moderately diminished response to ionophore added at 400 s (Fig. 3b, trace iv) compared with 100 s (Fig. 3b, trace ii) (0.24 ± 0.03 vs. 0.62 ± 0.03 slope ratio/min, significant, Mann–Whitney rank sum test, $p < 0.005$, 0.58 ± 0.03 vs. 0.70 ± 0.01 peak fura-2 ratio, significant, Mann–Whitney rank sum test, $p < 0.005$). When the perfusate was changed from Ca^{2+}-containing (1.3 mM) to Ca^{2+}-free medium + EGTA (< 100 nM $[Ca^{2+}]_e$) without any pre-incubation delay (Fig. 3b, trace i), the $[Ca^{2+}]_i$ transients elicited by the addition of ionophore were not different from those observed following a 100 s pre-incubation time (Fig. 3b, trace ii). Pre-treatment of the cultures with Tg (1 μM) prior to the addition of the ionophore failed to induce further increase in $[Ca^{2+}]_i$ (Fig. 3b, trace iii, 100–400 s). Application of Tg to neurones perfused with a medium containing 1.3 mM $CaCl_2$ also failed to elevate fura-2 fluorescence (not shown). Moreover, the presence of Tg did not alter significantly the $[Ca^{2+}]_i$ transients caused by addition of ionophore when cells were perfused with the EGTA-containing medium (Fig. 3b, trace iv vs. trace iii, not significant). The lack of effect of Tg is not inconsistent with the observation shown in Fig. 3a, where changes in the $[Ca^{2+}]_{ER}$ were estimated. 4Br-A23187 releases Ca^{2+} from all internal stores. Although the rise in fura-2 ratio elicited by the ionophore in the absence or presence of Tg pre-treatment was very similar, this could be explained by the existence of a relatively large Tg-insensitive compared with Tg-sensitive Ca^{2+} store. Collectively, these observations led us to conclude that Tg-sensitive intracellular stores in cultured cortical neurones contain releasable, sequestered Ca^{2+}. Perfusing the cells with Ca^{2+}-free medium does not lead to an alteration of their filling state, while chelating extracellular Ca^{2+} slightly depletes the stores,

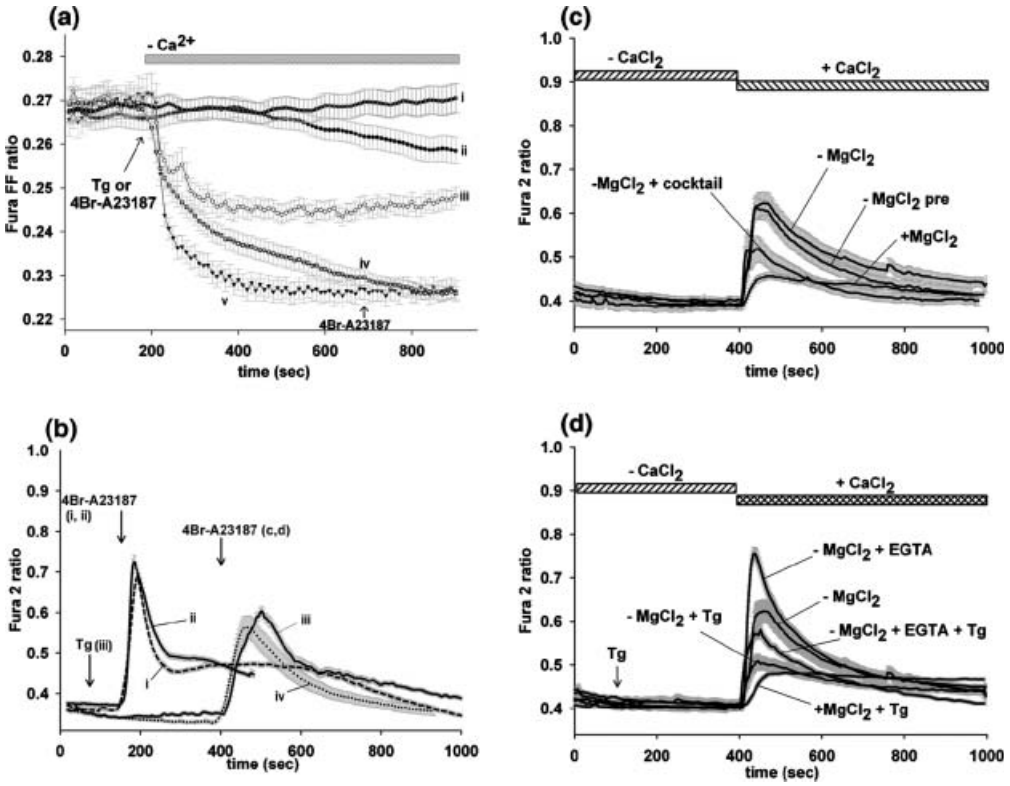

Fig. 3 (a) Effect of removal of extracellular Ca^{2+} on neuronal stores. $[Ca^{2+}]_{ER}$ was estimated as the perinuclear fluorescence ratio of fura-FF. Perfusion of neurones with Ca^{2+}-free medium (trace i), Ca^{2+}-free medium containing 25 μM EGTA (trace ii), Ca^{2+}-free medium plus 1 μM Tg (trace iii), or Ca^{2+}-free medium containing 25 μM EGTA plus 1 μM Tg (trace iv), Ca^{2+}-free medium containing 25 μM EGTA plus an ionophore cocktail consisting of 4-Br A23187 (10 μM), monensin (10 μM), nigericin (10 μM) and gramicidin (5 μM) (trace v), was started at 200 s as indicated. In trace (iv) the ionophore cocktail was applied at 700 s. Each trace represents mean ± SEM of cells from three independent experiments. (b) Neurones were perfused with Ca^{2+}-containing medium for 100 s (trace i), Ca^{2+}-free medium + EGTA for 100 s (trace ii) and 400 s (traces iii and iv). After these intervals, 5 μM 4-Br A23187 was added in the presence of EGTA. In trace (iii), Tg (1 μM) was added to the perfusate at 50 s. When 1.3 mM $CaCl_2$ was present throughout the entire duration of the experiment, fura-2 ratio plateaued at about 2.7 at 400 s (omitted from the graph). Traces are representative of three independent experiments. (c) Fura-2 ratio fluorescence of $[Ca^{2+}]_i$ of cortical neurones on basal Ca^{2+} entry. Cortical neurones were incubated in Ca^{2+}-free medium for 8–10 min (including the initial 400 s recording interval). $CaCl_2$ (2.6 mM) was re-introduced to the perfusing medium at 400 s. $-MgCl_2$ indicates absence of extracellular $MgCl_2$. + $MgCl_2$ signifies the presence of 1 mM $MgCl_2$ in the perfusate. $MgCl_2$ pre indicates that neurones were pre-exposed to 10 mM $MgCl_2$ for 30 min, but it was absent from the perfusate. Cocktail consisted of 10 μM MK-801, 10 μM CNQX and 1 μM nifedipine. The decay of $[Ca^{2+}]_i$ after the peak Ca^{2+} entry was quantified by the half-time ($t_{1/2}$ in s): $-MgCl_2$: 93 ± 11, $-MgCl_2$ + cocktail: 92 ± 12, + $MgCl_2$: 154 ± 40*, $MgCl_2$ pre: 96 ± 12. Traces are representative of three independent experiments. (d) Basal Ca^{2+} entry as measured by fura-2 ratio fluorescence of $[Ca^{2+}]_i$ in the presence and absence of Tg (1 μM). Cortical neurones were incubated in the absence of extracellular Ca^{2+} ± Tg for 8–10 min, in the presence and absence of EGTA. $CaCl_2$ (2.6 mM) was re-introduced to the perfusing medium at 400 s. $t_{1/2}$: $-MgCl_2$ + Tg: 134 ± 25*. $t_{1/2}$: $-MgCl_2$ + EGTA + Tg: 145 ± 13*, $t_{1/2}$: $-MgCl_2$ + EGTA: 84 ± 6*. Traces are representative of four independent experiments. One-way ANOVA, Tukey's post hoc analysis; *significant, compared to $-MgCl_2$, $p < 0.05$.

and a complete depletion can be achieved by inhibiting Ca^{2+} uptake through the SERCA pump.

Subsequently, basal Ca^{2+} entry was assessed by perfusing neurones with Ca^{2+}-free medium, followed by re-introduction of $[Ca^{2+}]_e$. It is apparent from Fig. 3(c) that re-introduction of Ca^{2+} to the medium induces a small increase in $[Ca^{2+}]_i$ in the presence of 1 mM extracellular Mg^{2+}, and a slow return towards basal $[Ca^{2+}]_i$ levels. DCD experiments were performed in the absence of Mg^{2+} in order to relieve the block of the NMDA receptor, otherwise the initial glutamate-induced $[Ca^{2+}]_i$ peak is severely blunted and DCD does not manifest itself. Therefore, basal Ca^{2+} entry was also investigated in the absence of extracellular Mg^{2+}. As shown in Fig. 3(c), the lack of Mg^{2+} in the medium led to a more robust increase in fura-2 ratio upon re-addition of Ca^{2+}. However, omission of extracellular Mg^{2+} may sensitize the NMDA receptor to activation. In addition, non-NMDARs and VDCCs, in a concerted action, could contribute to this Ca^{2+} influx related to the status of the plasma membrane potential, possibly affected by omission/re-introduction of

extracellular Ca^{2+}. Inclusion of a cocktail comprising the NMDA inhibitor MK-801 (10 μM), the AMPA/kainate inhibitor CNQX (10 μM) and the VDCC blocker nifedipine (1 μM) caused a reduction of the basal Ca^{2+} entry observed in the absence of Mg^{2+} (Fig. 3c). However, the peak of the $[Ca^{2+}]_i$ increase was still higher than when extracellular Mg^{2+} was present (fura-2 ratio = 0.21 ± 0.05 relative to baseline vs. 0.07 ± 0.01 in the presence of $MgCl_2$). These observations indicate that there is a basal Ca^{2+} entry in cultured cortical neurones that is unmasked in the absence of extracellular Mg^{2+}, which is influenced by, but not due to ligand and/or voltage-gated Ca^{2+} channels.

In order to investigate the spatial role of Mg^{2+} in the alleviation of basal Ca^{2+} entry, neurones were incubated in the presence of 10 mM $MgCl_2$ for 30 min. This treatment caused a rise in $[Mg^{2+}]_I$, from 0.65 ± 0.02 mM to 1.15 ± 0.03 mM, that persisted for at least 1 h even when the extracellular medium was subsequently switched to the $MgCl_2$-free perfusate. Pre-treatment of the cells in the absence of $[Mg^{2+}]_e$ (for 30 min) did not cause a significant drop in $[Mg^{2+}]_i$ (not shown). These neurones did not exhibit a significantly different peak amplitude of basal Ca^{2+} entry (0.33 ± 0.03 vs. 0.31 ± 0.03 in the presence of $MgCl_2$, one-way ANOVA Tukey's *post hoc* analysis).

Next, we investigated whether abolition of Ca^{2+} uptake by the SERCA pump using Tg (1 μM) results in capacitative calcium entry (CCE). Neurones were perfused with Ca^{2+}-free medium ± EGTA (25 μM) for 5–8 min, followed by addition of Tg, which failed to induce any change in $[Ca^{2+}]_i$ (Fig. 3d, 100–400 s). Re-introduction of extracellular Ca^{2+} caused a *decreased* Ca^{2+} entry compared with that observed in the absence of Tg, whether neurones were perfused with Ca^{2+}-free medium (fura-2 ratio = 0.11 ± 0.02 relative to baseline vs. 0.31 ± 0.03 in the absence of Tg) or with Ca^{2+}-free medium + EGTA (fura-2 ratio = 0.19 ± 0.01 relative to baseline vs. 0.36 ± 0.01 in the absence of Tg). This counterintuitive response contrasting the 'authentic' capacitative Ca^{2+} entry described for non-excitable as well as several excitable cell models (Elliott 2001; Putney 2003) is inconsistent with the possibility that in cortical neurones, depletion of Tg-sensitive Ca^{2+} stores activates Ca^{2+}-permeable non-voltage-gated cation channels located in the plasma membrane that mediate SOCE in other cell types. In support of this, the presence of a Ca^{2+} entry pathway in sympathetic, sensory and hippocampal neurones, distinct from voltage-dependent Ca^{2+} channels, was demonstrated and regulated by ryanodine-sensitive Ca^{2+} stores (Friel and Tsien 1992). Therefore, we examined the effect of ryanodine receptor agonists on Ca^{2+} entry.

Ryanodine receptor activation does not potentiate basal Ca^{2+} entry

Cortical neurones were perfused with Ca^{2+}-free medium for 5 min, followed by addition of ryanodine (1 μM) (Fig. 4a, 100–400 s) or caffeine (10 mM) (Fig. 4b, 100–400 s). Ryanodine or caffeine alone did not result in a measurable increase in $[Ca^{2+}]_i$. In addition, application of caffeine caused a minor decrease in baseline Fura 2 fluorescence. Ryanodine failed to potentiate basal Ca^{2+} entry, though it led to a slightly accelerated decay of $[Ca^{2+}]_i$ towards baseline values (Fig. 4a). The Ca^{2+} influx was strongly alleviated by extracellular Mg^{2+} and moderately decreased by concomitant inhibition of NMDARs/non-NMDARs/VDCCs by the cocktail (Fig. 4a). Likewise, caffeine did not lead to augmentation of basal Ca^{2+} entry and its effect on hastening $[Ca^{2+}]_i$ decay was not significant. These results do not support SOCE regulation by ryanodine-sensitive stores in cortical neurones.

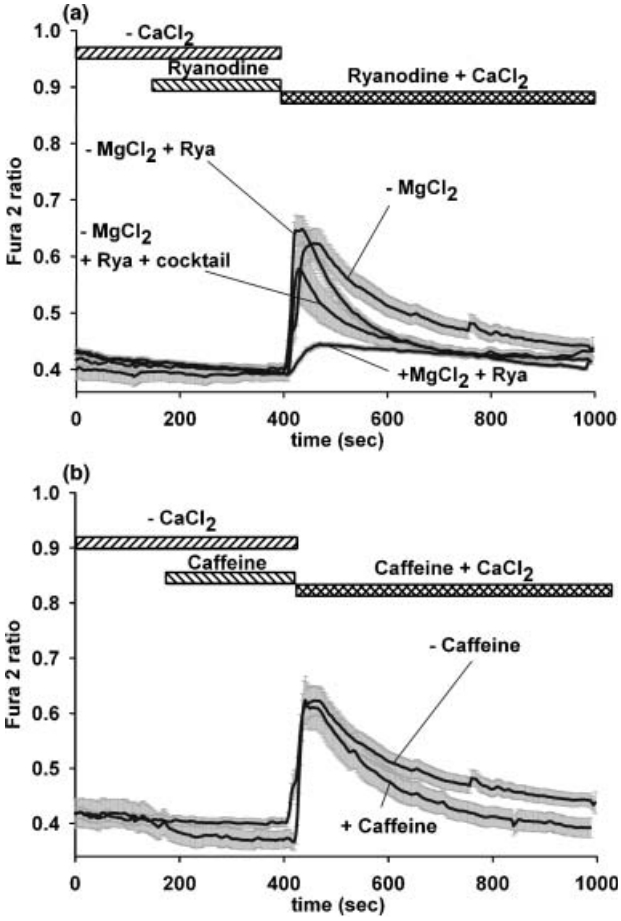

Fig. 4 Fura-2 ratio fluorescence of $[Ca^{2+}]_i$ of cortical neurones on Ca^{2+} entry in the presence of ryanodine 1 μM (a) or caffeine 10 mM (b). Cortical neurones were incubated in Ca^{2+}-free medium for 8–10 min (including the initial 400 s recording interval). $CaCl_2$ (2.6 mM) was re-introduced to the perfusing medium at 400 s. $-MgCl_2$ signifies absence of extracellular $MgCl_2$. + $MgCl_2$ signifies presence of 1 mM $MgCl_2$ in the perfusate. Rya: ryanodine. $t_{1/2}$: $-MgCl_2$ + Rya: 64 ± 4*, $t_{1/2}$: $-MgCl_2$ + Rya + cocktail: 57 ± 13*. + caffeine: 94 ± 10. Graphs are representative of three independent experiments. One-way ANOVA, Tukey's post hoc analysis; *significant, compared to Fig. 3(c) $-MgCl_2$, $p < 0.05$.

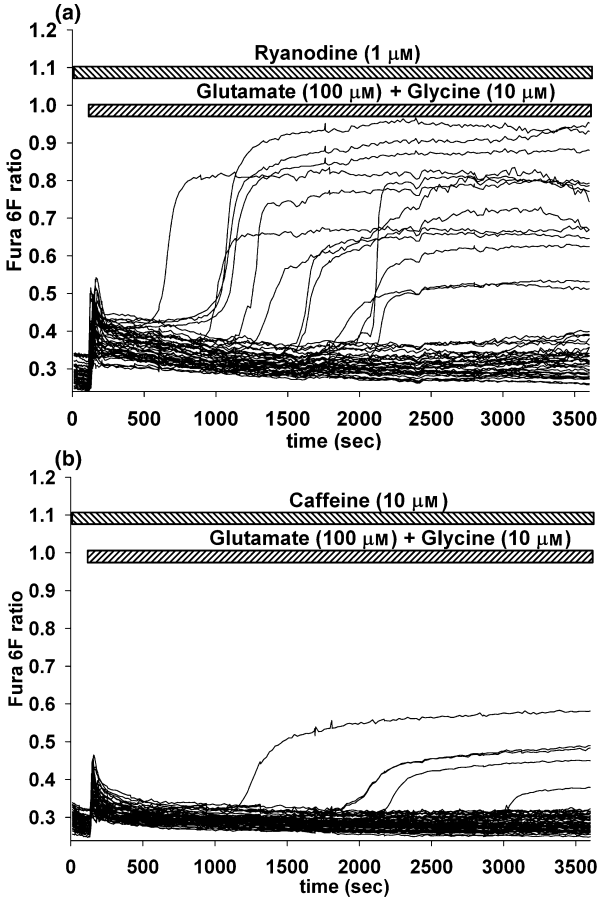

Fig. 5 Fura-6F ratio fluorescence of $[Ca^{2+}]_i$ of cortical neurones upon exposure to glutamate (100 μM) plus glycine (10 μM) in the presence of 1 μM ryanodine (a) or 10 mM caffeine (b) recorded for 1 h. Ryanodine/caffeine was present for 10 min prior to glutamate plus glycine exposure, as well as throughout the entire experiment. Traces are representative of three independent experiments.

Ryanodine and caffeine but not thapsigargin inhibit DCD

Neurones were incubated with ryanodine (1 μM) or caffeine (10 mM) for 10 min prior to exposure to glutamate; the compounds remained present in the perfusate for the entire duration of the experiments (Fig. 5). Exposure to glutamate caused an abrupt elevation in $[Ca^{2+}]_i$ level (Figs 5a and b, 100 s) followed by a return to a newly established plateau. Activation of RyR resulted in a significant decrease in the percentage of the number of cells undergoing DCD (Table 1). Application of Tg did not increase mean onset time or incidence of DCD (Table 1). Further information concerning the pharmacological profile of the mechanism underlying both events was obtained by 2-APB and La^{3+}.

2-APB and La^{3+} modulate basal Ca^{2+} entry

Neurones were perfused with Ca^{2+}-free medium for 8–10 min, followed by re-introduction of the cation to the perfusing medium. 2-APB (100 μM) or $LaCl_3$ (10 μM) was present for the entire duration of the experiment (Fig. 6). It is evident that 2-APB diminished the peak Ca^{2+} influx by about 50%, while La^{3+} did not affect peak amplitude but caused an accelerated return towards baseline $[Ca^{2+}]_i$. An inhibition of basal calcium entry by 2-APB in platelets was previously reported (Dobrydneva and Blackmore 2001).

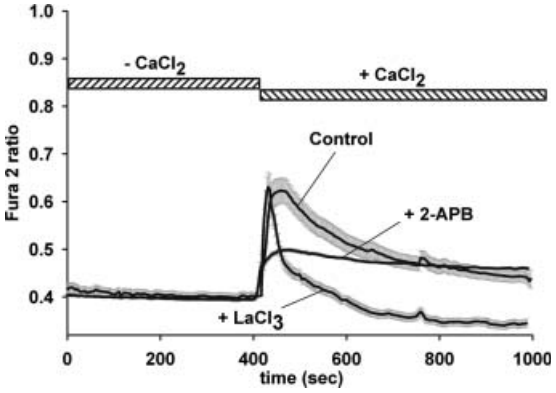

Fig. 6 Fura-2 ratio fluorescence of $[Ca^{2+}]_i$ of cortical neurones on basal Ca^{2+} entry. Cortical neurones were incubated in Ca^{2+}-free medium for 8–10 min (including the initial 400 s recording interval). $CaCl_2$ (2.6 mM) was re-introduced to the perfusing medium at 400 s. All curves were recorded in the absence of extracellular $MgCl_2$. 2-APB (100 μM) or $LaCl_3$ (10 μM) were present for the entire duration of the experiments. $t_{1/2}$: + $LaCl_3$: 78 ± 16*, + 2-APB: > 600 s*. Trace is representative of three independent experiments. One-way ANOVA, Tukey's post hoc analysis; *significant, compared to Fig. 3(c) –$MgCl_2$, $p < 0.05$.

Discussion

In the present study we demonstrated that the delayed Ca^{2+} deregulation induced by glutamate is diminished by 2-APB and La^{3+} in cultured cortical neurones. These agents are known to inhibit TRP and SOC channels. We did not find evidence for a thapsigargin or ryanodine-sensitive SOCE in these neurones. Furthermore, application of thapsigargin failed to aggravate mean onset time or the incidence of DCD (Table 1). In addition, activation of the RyR mitigated DCD.

Our results, excluding other obvious possibilities, could be consistent with the role of TRP channels operating in a manner independent of intracellular Ca^{2+} stores in inducing DCD. This notion is also supported by our observation that low concentration of 2-APB (30 μM) did not prevent DCD, arguing against the involvement of SOCE since at this concentration, the compound is a rapid and effective inhibitor of SOC channels (Dobrydneva and Blackmore 2001).

One of the proposed mechanisms of activation of SOC channels involves conformational coupling to the IP_3 receptor (Putney *et al*. 2001), and 2-APB was originally reported to block IP_3 receptors (Maruyama *et al*. 1997). However,

more recent studies have led to the consensus that the effect of this compound is due to a direct inhibition of SOC channels or proteins that mediate their activation (Dobrydneva and Blackmore 2001; Ma *et al*. 2002), rather than that of the IP_3 receptor itself (Bootman *et al*. 2002). SK&F 96365, an alternative SOC blocker (Merritt *et al*. 1990), did not prevent or delay DCD (Table 1).

The pharmacological promiscuity of 2-APB extends to many other targets, including the SERCA pump (at very high concentrations) (Bilmen *et al*. 2002), voltage-dependent K^+ channels (Wang *et al*. 2002), gap junctions (Harks *et al*. 2003) and the mitochondrial permeability transition pore (PTP) (Chinopoulos *et al*. 2003). Several lines of evidence prompted us to investigate the role of the PTP as a possible event upstream of the secondary Ca^{2+} rise: (i) application of the PTP inhibitor, cyclosporin A, or its non-immunosuppressant analogue, *N*-methyl-valine-4-cyclosporin, prevents the delayed Ca^{2+} rise in striatal (Alano *et al*. 2002) and hippocampal neurones (Vergun *et al*. 1999), but not in cerebellar granule cells (Castilho *et al*. 1998); (ii) 2-APB (and bongkrekic acid) inhibits high Ca^{2+}-induced PTP in isolated brain mitochondria (Chinopoulos *et al*. 2003); (iii) inhibition of the mitochondrial ANT with bongkrekic acid prevents NMDA receptor-mediated apoptosis of cerebrocortical neurones (Budd *et al*. 2000); (iv) a prerequisite for PTP induction is mitochondrial Ca^{2+} uptake (Zoratti and Szabo 1995) and DCD is eliminated when mitochondrial membrane potential is collapsed in the presence of the respiratory inhibitor, rotenone, plus the mitochondrial ATPase inhibitor, oligomycin (Nicholls and Budd 1998). Our results do not favour the involvement of PTP upstream of the occurrence of DCD, since neither cyclosporin A nor bongkrekic acid prevented or delayed DCD onset (Fig. 2, Table 1). Unfortunately, we were unable to obtain *N*-methyl-valine-4-cyclosporin, previously shown to inhibit PTP more effectively than cyclosporin A in mitochondria from nervous tissue (Khaspekov *et al*. 1999). In addition, brain mitochondria exhibit diminished sensitivity to inhibition of PTP by cyclosporin A in the presence of physiological concentrations of adenine nucleotides and Mg^{2+} but are responsive to bongkrekic acid (Chinopoulos *et al*. 2003).

In view of the fact that DCD is abolished by pharmacological inhibitors of TRP and SOC channels, the question arises as to whether DCD is a SOCE event. Relevant to this, it was previously reported that Ca^{2+} entering through either voltage- or receptor-operated channels provides a trigger to stimulate Ca^{2+} release from neuronal internal stores (Lipscombe *et al*. 1988). However, SOCE has not been demonstrated in every type of excitable cells originating from nervous tissue (Putney 2003). Our findings led us to conclude that cortical neurones do not exhibit authentic capacitative Ca^{2+} entry for the following reasons: (i) application of thapsigargin prior to and during re-introduction of $CaCl_2$ to the perfusing medium failed to potentiate the rise of fura-2 ratio compared with the absence of the SERCA inhibitor and, counter-intuitively, thapsigargin *decreased* Ca^{2+} influx (Fig. 3d). As a proof-of-protocol, astrocytes and endothelial cells subject to identical conditions exhibited robust CCE (not shown). However, neurones treated with thapsigargin in a Ca^{2+}-free medium in the absence or presence of EGTA exhibited reduction of $[Ca^{2+}]_{ER}$ and depletion of intracellular Ca^{2+} stores, respectively (Fig. 3a); (ii) neither ryanodine nor caffeine application prior to and during re-introduction of $CaCl_2$ to the perfusing medium led to SOCE, as compared with the absence of these agents (Fig. 4); (iii) cortical neurones exhibit 'basal Ca^{2+} entry' (Figs 3c and d) even when thapsigargin-sensitive intracellular stores are not emptied (Fig. 3a, top curve). This latter mode of Ca^{2+} entry merits further investigation.

Concerning the unexpected observations on the effects of ryanodine/caffeine on DCD, we cannot prove (or disprove) that in the presence of ryanodine there is a common mechanism underlying the amelioration of DCD and the moderate acceleration of decay of the $[Ca^{2+}]_i$ to the baseline seen in Fig. 4(a). Caffeine has been reported to inhibit the IP_3 receptor (Ehrlich *et al*. 1994). Indeed, it inhibited DHPG-induced $[Ca^{2+}]_i$ transients (not shown), which caused liberation of Ca^{2+} from intracellular stores mediated by the IP_3 receptor subsequent to activation of the mGluR1 (Nakamura *et al*. 2000) and therefore, a possible effect of caffeine on the IP_3R cannot be excluded. Although xestospongin C has been reported to inhibit the IP_3R (Gafni *et al*. 1997), it failed to abolish DCD or DHPG-induced $[Ca^{2+}]_i$ transients (10 μM xestospongin C, not shown). Inhibition of the SERCA pump by thapsigargin did not alter DCD incidence or mean onset time (Table 1). It is, however, possible that potentiation of DCD by thapsigargin was not detected under the conditions used in our experiments because over 85% of the cells underwent DCD in the absence of this modulator of intracellular Ca^{2+} stores.

Diverse pathological conditions of the central nervous system converge to excitotoxicity, a process characterized by excessive synaptic release of glutamate, which, in turn, activates post-synaptic glutamate receptors (Sattler and Tymianski 2001). As a consequence of the latter, severe neuronal Ca^{2+} and Na^+ loading occurs (Choi 1987), culminating in cell death (Arundine and Tymianski 2003). Events comparable with delayed calcium deregulation occur *in vivo* under pathological conditions (Silver and Erecinska 1992; Rothman and Olney 1995) and thus, investigation of DCD *in vitro* provides a model to study the events downstream to glutamate receptor activation. Although a profound increase in $[Ca^{2+}]_i$ unequivocally triggers early neurodegeneration (Tymianski *et al*. 1993c), the exact mechanism(s) responsible for the loss of $[Ca^{2+}]_i$ homeostasis remain obscure (Choi 1995). A large body of evidence (see introduction) supports the notion that the secondary rise is due to a Ca^{2+} influx pathway, supported by the discovery of a non-selective cation current appearing subsequent to NMDA application,

termed post-exposure current (I_{pe}) (Chen *et al*. 1997). In addition, it was recently demonstrated that anoxic neuronal death, which is linked to excitotoxicity (Goldberg *et al*. 1987; Goldberg and Choi 1993), is mediated through activation of TRPM7 (Aarts *et al*. 2003).

TRP channels emerge as obvious candidates for DCD on the basis of their intense expression in the central nervous system (Montell *et al*. 2002) and their high Ca^{2+} conductance (Zitt *et al*. 2002). Inexorably, the large number of TRP family members, together with their combinatorial co-assembling tendency and the lack of individually specific inhibitors, contributes to an inability to pinpoint the culprit channel in the present study. However, some of our results, together with the recent literature (Aarts *et al*. 2003), imply that DCD may be due to activation of TRPM7 (also known as LTRPC7/MIC/MagNuM) (Nadler *et al*. 2001; Clapham 2002). TRPM7 operates independently of store depletion (Prakriya and Lewis 2002b), is inhibited by 2-APB (Prakriya and Lewis 2002a) and La^{3+} (Runnels *et al*. 2001), is expressed in the mammalian brain (Runnels *et al*. 2001) and receives strong negative feedback by intracellular Mg^{2+} (Nadler *et al*. 2001). We could not achieve silencing of TRPM7 expression in cultured cortical neurones with RNA interference technology (tested by immunocytochemical detection on the cultures using a polyclonal antibody against TRPM7, not shown) based on the mouse sequence homologue (accession number: AY032951, GeneBank); unfortunately, the rat homologue sequence is not yet available.

The inability of La^{3+} to inhibit peak basal Ca^{2+} influx does not necessarily rule out the involvement of TRP channels in this effect, because at least two members of the TRP family (TRPC4 and 5) exhibit potentiation of their current by micromolar levels of La^{3+}, while other members are inhibited (Clapham *et al*. 2003). Given the complex combinatorial co-assembly of individual TRP channels within the same cell (Hofmann *et al*. 2002; Strubing *et al*. 2003), the effect of La^{3+} might reflect the combined result of two effects. In addition, the same TRP channel (hTRPC3) exhibits a cell-type-specific mode of activation and response to pharmacological inhibition (Trebak *et al*. 2002).

The potential identification of a novel molecular target amenable to pharmacological manipulation greatly expands the prospects for treating acute and chronic neurological disorders associated with excitotoxicity (Montell 2001; Wissenbach *et al*. 2004). This approach avoids excitatory neurotransmission blockade and therefore, lacks the serious drawbacks of glutamate receptor antagonists that contributed to the failure of clinical trials concerning stroke treatment (Ikonomidou and Turski 2002; Muir and Lees 2003). A more challenging field will be to understand why cortical neurones express Ca^{2+}-permeable, non-selective cation channels while they are so well equipped with VDCCs and ligand-gated cation receptors.

Acknowledgements

We gratefully acknowledge Drs Indu Ambudkar, Vera Golovina and Bill Shuttleworth for valuable comments during the preparation of this manuscript, and to Ms Irene Hopkins and Zolde Katalin for excellent technical assistance. Grants are acknowledged from OTKA, MTA and ETT to VA-V, and grant NIH NS34152 and USAMRMC Neurotoxin Initiative Grant DAMD 17-99-1-9483, to GF.

References

Aarts M., Iihara K., Wei W. L., Xiong Z. G., Arundine M., Cerwinski W., MacDonald J. F. and Tymianski M. (2003) A key role for TRPM7 channels in anoxic neuronal death. *Cell* **115**, 863–877.

Alano C. C., Beutner G., Dirksen R. T., Gross R. A. and Sheu S. S. (2002) Mitochondrial permeability transition and calcium dynamics in striatal neurons upon intense NMDA receptor activation. *J. Neurochem.* **80**, 531–538.

Andreyev A. Y., Mikhaylova L. M., Starkov A. A. and Kushnareva Y. (1994) Ca(2+)-loading modulates potencies of cyclosporin A, Mg2+ and ADP to recouple permeabilized rat liver mitochondria. *Biochem. Mol. Biol. Int.* **34**, 367–373.

Arundine M. and Tymianski M. (2003) Molecular mechanisms of calcium-dependent neurodegeneration in excitotoxicity. *Cell Calcium* **34**, 325–337.

Baba A., Yasui T., Fujisawa S., Yamada R. X., Yamada M. K., Nishiyama N., Matsuki N. and Ikegaya Y. (2003) Activity-evoked capacitative Ca2+ entry: implications in synaptic plasticity. *J. Neurosci.* **23**, 7737–7741.

Bilmen J. G., Wootton L. L., Godfrey R. E., Smart O. S. and Michelangeli F. (2002) Inhibition of SERCA Ca2+ pumps by 2-aminoethoxydiphenyl borate (2-APB). *Eur. J. Biochem.* **269**, 3678–3687.

Bootman M. D., Collins T. J., Mackenzie L., Roderick H. L., Berridge M. J. and Peppiatt C. M. (2002) 2-aminoethoxydiphenyl borate (2-APB) is a reliable blocker of store-operated Ca2+ entry but an inconsistent inhibitor of InsP3-induced Ca2+ release. *FASEB J.* **16**, 1145–1150.

Braun F. J., Broad L. M., Armstrong D. L. and Putney J. W. Jr (2001) Stable activation of single Ca2+ release-activated Ca2+ channels in divalent cation-free solutions. *J. Biol. Chem.* **276**, 1063–1070.

Budd S. L. and Nicholls D. G. (1996) Mitochondria, calcium regulation, and acute glutamate excitotoxicity in cultured cerebellar granule cells. *J. Neurochem.* **67**, 2282–2291.

Budd S. L., Tenneti L., Lishnak T. and Lipton S. A. (2000) Mitochondrial and extramitochondrial apoptotic signaling pathways in cerebrocortical neurons. *Proc. Natl Acad. Sci. USA* **97**, 6161–6166.

Castilho R. F., Hansson O., Ward M. W., Budd S. L. and Nicholls D. G. (1998) Mitochondrial control of acute glutamate excitotoxicity in cultured cerebellar granule cells. *J. Neurosci.* **18**, 10 277–10 286.

Chen Q. X., Perkins K. L., Choi D. W. and Wong R. K. (1997) Secondary activation of a cation conductance is responsible for NMDA toxicity in acutely isolated hippocampal neurons. *J. Neurosci.* **17**, 4032–4036.

Chinopoulos C., Tretter L., Rozsa A. and Adam-Vizi V. (2000) Exacerbated responses to oxidative stress by an Na(+) load in isolated nerve terminals: the role of ATP depletion and rise of [Ca(2+)](i). *J. Neurosci.* **20**, 2094–2103.

Chinopoulos C., Starkov A. A. and Fiskum G. (2003) Cyclosporin A-insensitive permeability transition in brain mitochondria: inhibition by 2-aminoethoxydiphenyl borate. *J. Biol. Chem.* **278**, 27 382–27 389.

Choi D. W. (1987) Ionic dependence of glutamate neurotoxicity. *J. Neurosci.* **7**, 369–379.

Choi D. W. (1995) Calcium: still center-stage in hypoxic-ischemic neuronal death. *Trends Neurosci.* **18**, 58–60.

Clapham D. E. (2002) Sorting out MIC, TRP, and CRAC ion channels. *J. Gen. Physiol.* **120**, 217–220.

Clapham D. E. (2003) TRP channels as cellular sensors. *Nature* **426**, 517–524.

Clapham D. E., Montell C., Schultz G. and Julius D. (2003) International Union of Pharmacology. XLIII. Compendium of voltage-gated ion channels: transient receptor potential channels. *Pharmacol. Rev.* **55**, 591–596.

Csordas G. and Hajnoczky G. (2001) Sorting of calcium signals at the junctions of endoplasmic reticulum and mitochondria. *Cell Calcium* **29**, 249–262.

Dobrydneva Y. and Blackmore P. (2001) 2-Aminoethoxydiphenyl borate directly inhibits store-operated calcium entry channels in human platelets. *Mol. Pharmacol.* **60**, 541–552.

Dux E., Mies G., Hossmann K. A. and Siklos L. (1987) Calcium in the mitochondria following brief ischemia of gerbil brain. *Neurosci. Lett.* **78**, 295–300.

Ehrlich B. E., Kaftan E., Bezprozvannaya S. and Bezprozvanny I. (1994) The pharmacology of intracellular Ca(2+)-release channels. *Trends Pharmacol. Sci.* **15**, 145–149.

Elliott A. C. (2001) Recent developments in non-excitable cell calcium entry. *Cell Calcium* **30**, 73–93.

Friel D. D. and Tsien R. W. (1992) A caffeine- and ryanodine-sensitive Ca2+ store in bullfrog sympathetic neurones modulates effects of Ca2+ entry on [Ca2+]i. *J. Physiol.* **450**, 217–246.

Gafni J., Munsch J. A., Lam T. H., Catlin M. C., Costa L. G., Molinski T. F. and Pessah I. N. (1997) Xestospongins: potent membrane permeable blockers of the inositol 1,4,5-trisphosphate receptor. *Neuron* **19**, 723–733.

Goldberg M. P. and Choi D. W. (1993) Combined oxygen and glucose deprivation in cortical cell culture: calcium-dependent and calcium-independent mechanisms of neuronal injury. *J. Neurosci.* **13**, 3510–3524.

Goldberg M. P., Weiss J. H., Pham P. C. and Choi D. W. (1987) *N*-methyl-D-aspartate receptors mediate hypoxic neuronal injury in cortical culture. *J. Pharmacol. Exp. Ther.* **243**, 784–791.

Grynkiewicz G., Poenie M. and Tsien R. Y. (1985) A new generation of Ca2+ indicators with greatly improved fluorescence properties. *J. Biol. Chem.* **260**, 3440–3450.

Harks E. G., Camina J. P., Peters P. H., Ypey D. L., Scheenen W. J., Van Zoelen E. J. and Theuvenet A. P. (2003) Besides affecting intracellular calcium signaling, 2-APB reversibly blocks gap junctional coupling in confluent monolayers, thereby allowing measurement of single-cell membrane currents in undissociated cells. *FASEB J.* **17**, 941–943.

Hartley D. M. and Choi D. W. (1989) Delayed rescue of *N*-methyl-D-aspartate receptor-mediated neuronal injury in cortical culture. *J. Pharmacol. Exp. Ther.* **250**, 752–758.

Hofmann T., Schaefer M., Schultz G. and Gudermann T. (2002) Subunit composition of mammalian transient receptor potential channels in living cells. *Proc. Natl Acad. Sci. USA* **99**, 7461–7466.

Hoyt K. R., Arden S. R., Aizenman E. and Reynolds I. J. (1998) Reverse Na+/Ca2+ exchange contributes to glutamate-induced intracellular Ca2+ concentration increases in cultured rat forebrain neurons. *Mol. Pharmacol.* **53**, 742–749.

Hyrc K., Handran S. D., Rothman S. M. and Goldberg M. P. (1997) Ionized intracellular calcium concentration predicts excitotoxic neuronal death: observations with low-affinity fluorescent calcium indicators. *J. Neurosci.* **17**, 6669–6677.

Ikonomidou C. and Turski L. (2002) Why did NMDA receptor antagonists fail clinical trials for stroke and traumatic brain injury? *Lancet Neurol.* **1**, 383–386.

Khaspekov L., Friberg H., Halestrap A., Viktorov I. and Wieloch T. (1999) Cyclosporin A and its nonimmunosuppressive analogue N-Me-Val-4-cyclosporin A mitigate glucose/oxygen deprivation-induced damage to rat cultured hippocampal neurons. *Eur. J. Neurosci.* **11**, 3194–3198.

Legendre P., Rosenmund C. and Westbrook G. L. (1993) Inactivation of NMDA channels in cultured hippocampal neurons by intracellular calcium. *J. Neurosci.* **13**, 674–684.

Limbrick D. D. Jr, Churn S. B., Sombati S. and DeLorenzo R. J. (1995) Inability to restore resting intracellular calcium levels as an early indicator of delayed neuronal cell death. *Brain Res.* **690**, 145–156.

Limbrick D. D. Jr, Pal S. and DeLorenzo R. J. (2001) Hippocampal neurons exhibit both persistent Ca2+ influx and impairment of Ca2+ sequestration/extrusion mechanisms following excitotoxic glutamate exposure. *Brain Res.* **894**, 56–67.

Lipscombe D., Madison D. V., Poenie M., Reuter H., Tsien R. W. and Tsien R. Y. (1988) Imaging of cytosolic Ca2+ transients arising from Ca2+ stores and Ca2+ channels in sympathetic neurons. *Neuron* **1**, 355–365.

Ma H. T., Venkatachalam K., Parys J. B. and Gill D. L. (2002) Modification of store-operated channel coupling and inositol trisphosphate receptor function by 2-aminoethoxydiphenyl borate in DT40 lymphocytes. *J. Biol. Chem.* **277**, 6915–6922.

Manev H., Favaron M., Guidotti A. and Costa E. (1989) Delayed increase of Ca2+ influx elicited by glutamate: role in neuronal death. *Mol. Pharmacol.* **36**, 106–112.

Maruyama T., Kanaji T., Nakade S., Kanno T. and Mikoshiba K. (1997) 2APB, 2-aminoethoxydiphenyl borate, a membrane-penetrable modulator of Ins (1,4,5), P3-induced Ca2+ release. *J. Biochem. (Tokyo)* **122**, 498–505.

Mayer M. L. and Westbrook G. L. (1985) The action of *N*-methyl-D-aspartic acid on mouse spinal neurones in culture. *J. Physiol.* **361**, 65–90.

Merritt J. E., Armstrong W. P., Benham C. D., Hallam T. J., Jacob R., Jaxa-Chamiec A., Leigh B. K., McCarthy S. A., Moores K. E. and Rink T. J. (1990) SK&F 96365, a novel inhibitor of receptor-mediated calcium entry. *Biochem. J.* **271**, 515–522.

Montell C. (2001) Physiology, phylogeny, and functions of the TRP superfamily of cation channels. *Sci. STKE* **2001**, RE1.

Montell C., Birnbaumer L. and Flockerzi V. (2002) The TRP channels, a remarkably functional family. *Cell* **108**, 595–598.

Muir K. W. and Lees K. R. (2003) Excitatory amino acid antagonists for acute stroke. *Cochrane Database Syst. Rev.* CD001244.

Nadler M. J., Hermosura M. C., Inabe K. *et al.* (2001) LTRPC7 is a Mg.ATP-regulated divalent cation channel required for cell viability. *Nature* **411**, 590–595.

Nakamura T., Nakamura K., Lasser-Ross N., Barbara J. G., Sandler V. M. and Ross W. N. (2000) Inositol 1,4,5-trisphosphate (IP3)-mediated Ca2+ release evoked by metabotropic agonists and backpropagating action potentials in hippocampal CA1 pyramidal neurons. *J. Neurosci.* **20**, 8365–8376.

Nelson M. T., French R. J. and Krueger B. K. (1984) Voltage-dependent calcium channels from brain incorporated into planar lipid bilayers. *Nature* **308**, 77–80.

Nicholls D. G. and Budd S. L. (1998) Mitochondria and neuronal glutamate excitotoxicity. *Biochim. Biophys. Acta* **1366**, 97–112.

Nicholls D. G. and Ward M. W. (2000) Mitochondrial membrane potential and neuronal glutamate excitotoxicity: mortality and millivolts. *Trends Neurosci.* **23**, 166–174.

Nicholls D. G., Vesce S., Kirk L. and Chalmers S. (2003) Interactions between mitochondrial bioenergetics and cytoplasmic calcium in cultured cerebellar granule cells. *Cell Calcium* **34**, 407–424.

Obukhov A. G. and Nowycky M. C. (2002) TRPC4 can be activated by G-protein-coupled receptors and provides sufficient Ca(2+) to trigger exocytosis in neuroendocrine cells. *J. Biol. Chem.* **277**, 16 172–16 178.

Poenie M. (1990) Alteration of intracellular Fura-2 fluorescence by viscosity: a simple correction. *Cell Calcium* **11**, 85–91.

Prakriya M. and Lewis R. S. (2002a) Separation and characterization of currents through store-operated CRAC channels and Mg(2+)-inhibited cation (MIC) channels. *J. Gen. Physiol.* **119**, 487–507.

Prakriya M. and Lewis R. S. (2002b) Separation and characterization of currents through store-operated CRAC channels and Mg2+-inhibited cation (MIC) channels. *J. Gen. Physiol.* **119**, 487–507.

Putney J. W. Jr (1986) A model for receptor-regulated calcium entry. *Cell Calcium* **7**, 1–12.

Putney J. W. (2003) Capacitative calcium entry in the nervous system. *Cell Calcium* **34**, 339–344.

Putney J. W. Jr, Broad L. M., Braun F. J., Lievremont J. P. and Bird G. S. (2001) Mechanisms of capacitative calcium entry. *J. Cell Sci.* **114**, 2223–2229.

Rajdev S. and Reynolds I. J. (1994) Glutamate-induced intracellular calcium changes and neurotoxicity in cortical neurons *in vitro*: effect of chemical ischemia. *Neuroscience* **62**, 667–679.

Randall R. D. and Thayer S. A. (1992) Glutamate-induced calcium transient triggers delayed calcium overload and neurotoxicity in rat hippocampal neurons. *J. Neurosci.* **12**, 1882–1895.

Rego A. C., Ward M. W. and Nicholls D. G. (2001) Mitochondria control ampa/kainate receptor-induced cytoplasmic calcium deregulation in rat cerebellar granule cells. *J. Neurosci.* **21**, 1893–1901.

Rothman S. M. and Olney J. W. (1995) Excitotoxicity and the NMDA receptor – still lethal after eight years. *Trends Neurosci.* **18**, 57–58.

Runnels L. W., Yue L. and Clapham D. E. (2001) TRP-PLIK, a bifunctional protein with kinase and ion channel activities. *Science* **291**, 1043–1047.

Sattler R. and Tymianski M. (2001) Molecular mechanisms of glutamate receptor-mediated excitotoxic neuronal cell death. *Mol. Neurobiol.* **24**, 107–129.

Schellenberg G. D. and Swanson P. D. (1982) Solubilization and reconstitution of membranes containing the Na+–Ca2+ exchange carrier from rat brain. *Biochim. Biophys. Acta* **690**, 133–144.

Silver I. A. and Erecinska M. (1992) Ion homeostasis in rat brain *in vivo*: intra- and extracellular [Ca2+] and [H+] in the hippocampus during recovery from short-term, transient ischemia. *J. Cereb. Blood Flow Metab.* **12**, 759–772.

Stout A. K. and Reynolds I. J. (1999) High-affinity calcium indicators underestimate increases in intracellular calcium concentrations associated with excitotoxic glutamate stimulations. *Neuroscience* **89**, 91–100.

Strubing C., Krapivinsky G., Krapivinsky L. and Clapham D. E. (2003) Formation of novel TRPC channels by complex subunit interactions in embryonic brain. *J. Biol. Chem.* **278**, 39 014–39 019.

Trebak M., Bird G. S., McKay R. R. and Putney J. W. Jr (2002) Comparison of human TRPC3 channels in receptor-activated and store-operated modes. Differential sensitivity to channel blockers suggests fundamental differences in channel composition. *J. Biol. Chem.* **277**, 21 617–21 623.

Tymianski M., Charlton M. P., Carlen P. L. and Tator C. H. (1993a) Secondary Ca2+ overload indicates early neuronal injury which precedes staining with viability indicators. *Brain Res.* **607**, 319–323.

Tymianski M., Charlton M. P., Carlen P. L. and Tator C. H. (1993b) Source specificity of early calcium neurotoxicity in cultured embryonic spinal neurons. *J. Neurosci.* **13**, 2085–2104.

Tymianski M., Wallace M. C., Spigelman I., Uno M., Carlen P. L., Tator C. H. and Charlton M. P. (1993c) Cell-permeant Ca2+ chelators reduce early excitotoxic and ischemic neuronal injury *in vitro* and *in vivo*. *Neuron* **11**, 221–235.

Tymianski M., Sattler R., Zabramski J. M. and Spetzler R. F. (1998) Characterization of neuroprotection from excitotoxicity by moderate and profound hypothermia in cultured cortical neurons unmasks a temperature-insensitive component of glutamate neurotoxicity. *J. Cereb. Blood Flow Metab.* **18**, 848–867.

Venkatachalam K., van Rossum D. B., Patterson R. L., Ma H. T. and Gill D. L. (2002) The cellular and molecular basis of store-operated calcium entry. *Nat. Cell Biol.* **4**, E263–E272.

Vergun O., Keelan J., Khodorov B. I. and Duchen M. R. (1999) Glutamate-induced mitochondrial depolarisation and perturbation of calcium homeostasis in cultured rat hippocampal neurones. *J. Physiol.* **519**, 451–466.

Wang Y., Deshpande M. and Payne R. (2002) 2-Aminoethoxydiphenyl borate inhibits phototransduction and blocks voltage-gated potassium channels in Limulus ventral photoreceptors. *Cell Calcium* **32**, 209–216.

Wissenbach U., Niemeyer B. A. and Flockerzi V. (2004) TRP channels as potential drug targets. *Biol. Cell* **96**, 47–54.

Yu S. P. and Choi D. W. (1997) Na(+)–Ca2+ exchange currents in cortical neurons: concomitant forward and reverse operation and effect of glutamate. *Eur. J. Neurosci.* **9**, 1273–1281.

Zitt C., Halaszovich C. R. and Luckhoff A. (2002) The TRP family of cation channels: probing and advancing the concepts on receptor-activated calcium entry. *Prog. Neurobiol.* **66**, 243–264.

Zoratti M. and Szabo I. (1995) The mitochondrial permeability transition. *Biochim. Biophys. Acta* **1241**, 139–176.

Journal of Neurochemistry, 2004, **90**, 1281–1289 doi:10.1111/j.1471-4159.2004.02572.x

REVIEW

Mitochondrial mechanisms of neural cell apoptosis

Brian M. Polster* and Gary Fiskum†

*W. Harry Feinstone Department of Microbiology and Molecular Immunology, The Johns Hopkins University School of Public Health, Baltimore, Maryland, USA

†Department of Anesthesiology, University of Maryland School of Medicine, Baltimore, Maryland, USA

Abstract

The importance of calcium overload, mitochondrial dysfunction, and free radical generation to neuropathological processes has been recognized for many years. Only more recently has evidence accumulated that the programmed cell death process of apoptosis plays an integral role not only in the development of the nervous system, but in the loss of cells following acute neurological insults and chronic disease. In 1996 came the landmark discovery that cytochrome *c*, an evolutionary old and essential component of the respiratory chain, has a second and deadly function when it escapes the mitochondrion: triggering the cell death cascade. A flurry of activity has since ensued in an effort to understand the mechanistic events associated with mitochondrial permeabilization during apoptosis and regulation by an enigmatic family of proteins characterized by homology to the proto-oncogene Bcl-2. This review discusses the evidence for various release mechanisms of apoptotic proteins (e.g. cytochrome *c*) from neural cell mitochondria, focusing particularly on roles for calcium, Bax, p53, and oxidative stress. The need for new drugs that act at the level of the mitochondrion to prevent apoptosis is also highlighted.

Keywords: Bax, Bcl-2, cytochrome *c*, membrane permeability transition, oxidative stress, p53.

J. Neurochem. (2004) **90,** 1281–1289.

Death pathways in neurodevelopment and degeneration

The significance of cytochrome *c* to the apoptotic process was revealed by the finding that mitochondrially released cytochrome *c* combines with apoptosis protease activating factor-1 (Apaf-1), procaspase-9, and dATP in the cytosol, producing active caspase-9 (Zou *et al*. 1997; Li *et al*. 1998). The activation of this initiator caspase then leads to the proteolytic activation of caspase-3, the primary effector caspase of the cell (Fig. 1). This pathway is referred to as the mitochondrial pathway or 'intrinsic pathway' of caspase activation, and often involves the release of additional mitochondrial proteins such as second mitochondrial-derived activator of caspase/direct IAP-associated binding protein with low PI (Smac/DIABLO) and HtrA2/Omi, which antagonize inhibitor of apoptosis (IAP) proteins, and apoptosis inducing factor (AIF) and Endonuclease G (EndoG), which contribute to DNA fragmentation. A second, 'extrinsic' pathway of caspase activation exists where the binding of a death ligand such as Fas to its death receptor triggers auto-processing of caspase-8 to its active form, which then directly activates caspase-3 (Muzio *et al*. 1996). The pro-apoptotic Bcl-2 family protein Bid bridges the two pathways by translocating to mitochondria and releasing cytochrome *c* after truncation by caspase-8 (Fig. 2) (Li *et al*. 1998; Luo *et al*. 1998). The intrinsic pathway of cell death appears to be the primary mode of cell elimination during synaptic development (Chang *et al*. 2002) while both pathways can be recruited in neurodestructive processes, e.g. ischemic brain injury.

Received February 1, 2004; revised manuscript received February 28, 2004; accepted March 4, 2004.

Address correspondence and reprint requests to: Dr Gary Fiskum, Department of Anesthesiology, University of Maryland School of Medicine, 685 W. Baltimore Street, MSTF-5.34, Baltimore MD 21201 USA. E-mail: gfisk001@umaryland.edu

Abbreviations used: AIF, apoptosis-inducing factor; ANT, adenine nucleotide translocase; BIP, Bax inhibitory peptide; DIABLO, direct IAP-associated binding protein with low PI; IAP, inhibitor of apoptosis protein; MAC, mitochondria apoptosis-induced channel; NGF, nerve growth factor; NMDA, N-methyl-D-aspartate; PARP-1, Poly(ADP) ribose polymerase-1; PTP, permeability transition pore; ROS, reactive oxygen species; Smac, second mitochondria-derived activator of caspase; TUDCA, tauroursodeoxycholic acid; VDAC, voltage-dependent anion channel.

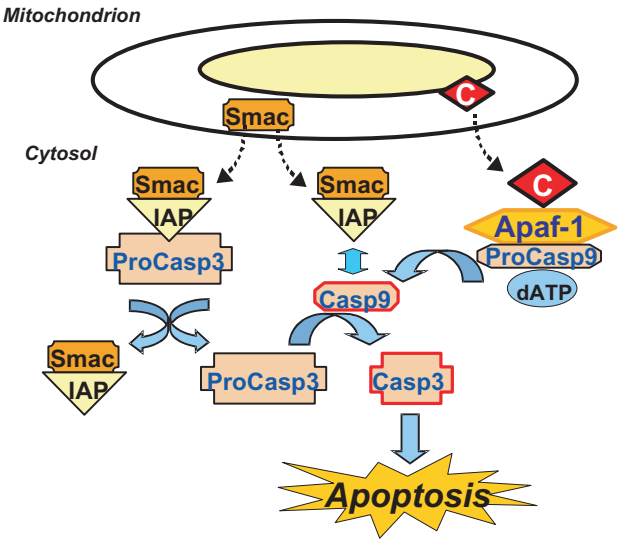

Fig. 1 Intrinsic pathway of caspase activation. Cytochrome *c* (C) released from mitochondria combines with apoptosis protease activating factor-1 (Apaf-1) and procaspase-9 (ProCasp9) in the cytosol to produce active caspase-9 (Casp9). Caspase-9 cleaves procaspase-3 to activate caspase-3 (Casp3) and initiates apoptosis. The release of Smac (Second Mitochondria-derived Activator of Caspase)/DIABLO (direct IAP-associated binding protein with Low PI) from mitochondria relieves caspase-inhibition by inhibitor of apoptosis proteins (IAP), allowing caspase activation by cytochrome *c*.

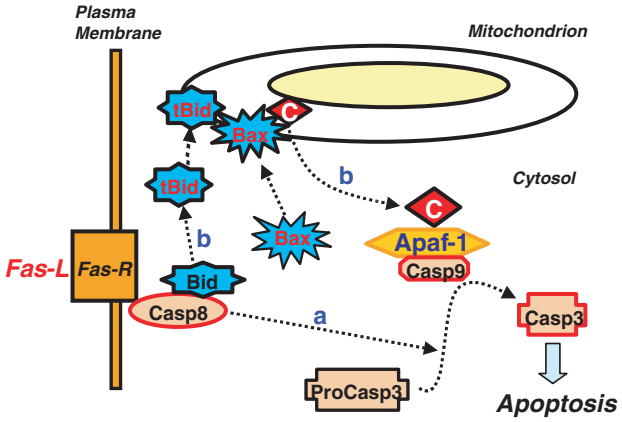

Fig. 2 Recruitment of the intrinsic mitochondrial apoptotic pathway following death receptor ligation by caspase-8 cleaved Bid. In the death receptor pathway (i.e. Fas), Fas ligand (Fas-L) binding to Fas receptor (Fas-R) activates caspase-8 (Casp8). In some cell types (Type I cells), caspase-8 activation is sufficient to cleave procaspase-3 (ProCasp3) to active caspase-3 (Casp3) and induce apoptosis (path a). However many cell types (Type II cells) require amplification of the caspase cascade by cytochrome *c* (C) release initiated by caspase-cleaved Bid (path b). Caspase-3 is proteolytically activated by the initiator caspase-9 (Casp9).

In addition to the well-characterized caspase-mediated intrinsic and extrinsic apoptotic pathways, mitochondrial AIF release mediates a caspase-independent cell death cascade that is also important in neurons. AIF translocation from mitochondria to the nucleus has been observed in photoreceptors following retinal detachment (Hisatomi *et al*. 2001), in rat cortex and hippocampus following traumatic brain injury (Zhang *et al*. 2002), in neonatal rat brain following hypoxia-ischemia (Zhu *et al*. 2003), in rat hippocampal CA1 neurons following transient global ischemia (Cao *et al*. 2003), in cortical neurons following N-methyl-D-aspartate (NMDA) treatment (Yu *et al*. 2002), peroxynitrite treatment (Zhang *et al*. 2002), or oxygen/glucose deprivation (Cao *et al*. 2003), and in primary neuronal and microglial cells following exposure to pneumococcus (Braun *et al*. 2001). Poly(ADP-ribose) polymerase-1 (PARP-1) inhibitors or genetic deletion of PARP-1 prevents AIF-mediated death of NMDA-treated cortical neurons, indicating that AIF release lies downstream of PARP-1 activation in this excitotoxicity model (Yu *et al*. 2002). Although caspase inhibitors had no effect on PARP-1 mediated cell death, AIF release in response to various apoptotic stimuli appears to be a separate event from cytochrome *c* release and requires caspase activation (Arnoult *et al*. 2002), suggesting that AIF release may be differentially regulated in caspase-independent versus caspase-dependent cell death. Interestingly, the recently described Harlequin mouse mutant has an 80% reduction in AIF expression yet displays progressive degeneration of terminally differentiated cerebellar and retinal neurons associated with oxidative stress (Klein *et al*. 2002). This finding is contrary to what would be expected if AIF functions solely as an apoptotic factor in the nervous system. Overexpression of AIF in cerebellar granule neurons was protective against peroxide-mediated cell death suggesting that, in addition to its pro-death function in the nucleus, AIF may also function as a free radical scavenger at the mitochondria (Klein *et al*. 2002).

Genetic lesion studies in mice and mouse embryos have provided strong evidence for the contribution of Bcl-2 family proteins to naturally occurring cell death during nervous system development. Pro-apoptotic Bax is required for the cell death program in many populations of neurons, including peripheral ganglia, motor neurons in the spinal cord, neurons in the trigeminal brainstem nuclear complex, and some neurons in the cerebellum, retina, and hippocampus (Deckwerth *et al*. 1996; White *et al*. 1998; Fan *et al*. 2001). Mouse embryos deficient in anti-apoptotic Bcl-X display massive cell death of immature neurons of the brain, spinal cord, and dorsal root ganglia that is largely rescued by codeletion of Bax, providing evidence that Bcl-X is an essential negative regulator of the Bax-mediated programmed cell death pathway *in vivo* (Motoyama *et al*. 1995; Shindler *et al*. 1997). *In vitro* experiments using wild type and Bax deficient cerebellar granule neurons

demonstrated involvement of the intrinsic pathway by showing that BH3-only protein-mediated Bax activation, cytochrome *c* release, and caspase activation was responsible for eliciting developmental-like apoptosis following withdrawal of depolarizing concentrations of potassium chloride (Harris & Johnson 2001).

Although brain mitochondria have been extensively investigated as a primary target of excitotoxic calcium loads and reactive oxygen species leading to acute energy failure, new evidence reveals that the BH3-only signal transduction cascade mediating programmed cell removal also contributes substantially to neural injury. The BH3-only protein Bid is cleaved during focal ischemia in a caspase-8 dependent fashion and Bid-deficient mice display a significant reduction in infarct volume that coincides with protection against cytochrome *c* release and impaired caspase-3 activation (Plesnila *et al*. 2001). Bad, another member of the BH3-only subgroup of Bcl-2 family proteins, regulates the threshold for mitochondrial cytochrome *c* release in neurons by inactivating anti-apoptotic Bcl-2 proteins (Datta *et al*. 2002). Although normally held in check by survival kinase-mediated phosphorylation, excitotoxic elevation of intraneuronal calcium can lead to Bad dephosphorylation and activation through the Ca^{2+}-dependent phosphatase calcineurin (Wang *et al*. 1999). *In vivo* evidence suggests that Bad activation contributes to apoptotic death following traumatic spinal cord injury (Springer *et al*. 2000) and kainic acid-induced seizures (Henshall *et al*. 2002). Studies using double-knockout mice of Bax and its close relative Bak revealed that BH3-only proteins such as Bid require these multidomain Bcl-2 homologs for their cytochrome *c*-releasing and killing ability (Wei *et al*. 2001); however, the precise biochemical actions of these proteins has been a subject of considerable debate.

The mitochondrial permeability transition hypothesis

A phenomenon called the mitochondrial permeability transition was the initial mechanism proposed to mediate the release of mitochondrial intermembrane constituents. Identified as early as the 1960s, mitochondria undergo swelling following exposure to high calcium and oxidative stress. The swelling results from the opening of the mitochondrial permeability transition pore (PTP) in the inner membrane. Solute entry ($\leq$ 1500 Da) precipitates water influx, leading to expansion of the matrix space within the highly convoluted inner membrane and dissipation of the electrochemical gradient. The comparatively rigid outer mitochondrial membrane eventually ruptures, releasing the contents of the intermembrane space including cytochrome *c*. Reconstitution of the inner membrane adenine nucleotide translocator (ANT) together with the matrix protein cyclophilin D and the outer membrane voltage-dependent anion channel (VDAC) in proteoliposomes mimics mitochondrial permeability transition pore activity observed in isolated mitochondria (Crompton *et al*. 1998). Co-purification, co-immunoprecipitation, and yeast-two-hybrid screening have demonstrated an interaction of Bax with the ANT (Marzo *et al*. 1998b) and some investigators have found evidence supporting induction of the mitochondrial PTP as the mechanism for Bax-mediated apoptosis (Marzo *et al*. 1998a; Pastorino *et al*. 1998) although many find that Bax-induced cytochrome *c* release and apoptosis occurs in the absence of mitochondrial permeability transition (Eskes *et al*. 1998; Polster *et al*. 2003). New evidence suggests that Bax and Bak may contribute indirectly to mitochondrial permeability transition by controlling endoplasmic reticulum-to-mitochondria calcium signaling in some apoptotic paradigms (Scorrano *et al*. 2003; Zong *et al*. 2003).

PTP inhibitors, such as cyclosporine A and bongkrekic acid, have been used to investigate the involvement of the mitochondrial permeability transition in neural cell death. Although PTP inhibitors are protective in some models (Budd *et al*. 2000; Cao *et al*. 2001), in most cases inhibition of cytochrome *c* release was not demonstrated and non-PTP effects were not excluded, such as protective general inhibition of protein synthesis (Wigdal *et al*. 2002). Detailed analysis from our lab and others using both biochemical and imaging techniques have excluded a role for the PTP in the mechanism of Bax-induced cytochrome *c* release from isolated brain mitochondria (Brustovetsky *et al*. 2003; Polster *et al*. 2003). Nevertheless, the PTP may still play a role in neural cell death, perhaps by signaling Bax translocation to mitochondria (De Giorgi *et al*. 2002), participating in intracellular Ca^{2+} or ROS signaling, or regulating the release of larger mitochondrial apoptogenic proteins that occurs downstream of cytochrome *c* release. Recently it was shown that both Bax and Bak are dispensible for NMDA-induced death of cerebellar granule neurons (Lindsten *et al*. 2003), perhaps suggesting a comparatively greater role for calcium in forms of neuronal death that are not purely apoptotic. However, whether PTP is a cause or the result of irreversible excitotoxic neuronal injury is, at this juncture, unclear.

The outer membrane channel hypothesis

As an alternative to non-selective mitochondrial outer membrane permeabilization due to membrane breakage, it is possible that a discrete outer membrane protein-conducting channel forms to allow cytochrome *c* and its death-promoting cohorts to escape the intermembrane space during apoptosis. One proposal is that Bax combines with the outer membrane, non-selective metabolite channel VDAC to increase its permeability or form hybrid channels that are large enough to flux cytochrome *c*. Bax and VDAC but neither protein alone was capable of passing cytochrome *c* across planar lipid bilayers (Shimizu *et al*. 1999). Also, Bax was co-immunoprecipitated with VDAC, and antibodies that blocked ^{14}C-sucrose uptake by VDAC-containing liposomes also blocked mammalian apoptosis (Shimizu *et al*. 1999;

Shimizu *et al*. 2001). However, although Tsujimoto and colleagues first proposed that Bax and Bak mediate cytochrome *c* release by modulating the conductance state of VDAC in 1999, independent studies have yet to reproduce their findings. Conflicting results, e.g. the findings that Bax expression in VDAC-deficient yeast induces large conductance mitochondrial channels and cytochrome *c* release (Pavlov *et al*. 2001), lead many to favor the hypothesis that Bax does not require native mitochondrial proteins for outer membrane permeabilization.

N-terminal epitope-specific Bax antibodies and trypsin digestion patterns were used to demonstrate that active Bid can induce a conformation change in Bax or Bak (Desagher *et al*. 1999; Wei *et al*. 2000) that precedes the formation of higher order complexes (Eskes *et al*. 2000). Associated with this conformational change was a shift in mitochondrially associated Bax from a loosely bound, alkali-extractable form to an alkali-resistant form that is characteristic of integral membrane proteins. The formation of oligomers is required for the ability of Bax to release entrapped molecules from liposomes in cell-free assays (Antonsson *et al*. 2000) and endogenous high molecular weight Bax oligomer/complexes have been found in mitochondrial membranes of apoptotic cells (Antonsson *et al*. 2001) supporting a physiological role for Bax multimerization. Inhibition of cytochrome *c* efflux by size-specific dextrans from protein-free liposomes treated with Bax estimated a Bax pore size of ~30 Angstroms that was consistent with a Bax tetramer (Saito *et al*. 2000). However, in contrast to larger Bax complexes that have been detected within cells (Antonsson *et al*. 2001; Nechushtan *et al*. 2001), proteinaceous channels formed by more than four Bax molecules could not be detected in this liposomal system. Furthermore, the predicated size of tetrameric Bax channels was insufficient to account for the release of large mitochondrial proteins observed during apoptosis, although there is also now evidence that the release of several mitochondrial intermembrane space proteins (e.g. Smac/DIABLO and AIF) occurs by more than one mechanism, or is at least differentially regulated by various pro-apoptotic proteins (Adrain *et al*. 2001; Arnoult *et al*. 2002; Kandasamy *et al*. 2003).

The lipid pore hypothesis

A substantial shift in the thinking in the field occurred when investigators began considering a role for mitochondrial lipids in the permeabilization process. The hypothesis of Bax-induced lipid pore formation was first proposed but largely ignored in 1999, when Basañez and co-workers found that Bax decreased planar phospholipid bilayer stability and diminished membrane linear tension, corresponding to a lowered energy requirement for the formation of a lipidic pore (Basanez *et al*. 1999). Newmeyer's group recently revisited this hypothesis by demonstrating that mitochondrial lipids, particularly cardiolipin, are essential for Bax-induced permeabilization of vesicles and showing remarkably that 2000 kilodalton dextran molecules could be released from liposomes without visible changes in structure (Kuwana *et al*. 2002). However, they were not able to exclude the possibility that the liposome membrane resealed during the process of preparation for electron microscopy. Additional support for a lipid pore-mediated mechanism of Bax permeabilization came from observations that altering intrinsic membrane curvature in lipid vesicles can inhibit or promote Bax activity (Basanez *et al*. 2002) and that amphiphilic cations that interact strongly with mitochondrial lipids can prevent Bax-induced permeabilization of isolated mitochondria or liposomes without affecting the ability of Bax to integrate into membranes (Polster *et al*. 2003). Atomic force microscopy was used to directly visualize a toroidal-shaped pore formed by oligomeric Bax in synthetic lipid bilayers, demonstrating proof-of-concept in an artificial system (Epand *et al*. 2002). Assessing the ability of dibucaine and propranolol to inhibit MAC (mitochondria apoptosis-induced channel), a novel high conductance channel that was electrophysiologically characterized on mitochondrial outer membranes of apoptotic cells (Pavlov *et al*. 2001), will aid in bridging the gap between events detected in isolated systems and intact cells. Intriguing new observations that Bax and Bak colocalize with proteins involved in mitochondrial fission and fusion at mitochondrial constriction sites in apoptotic cells suggest a role for regulation of lipid dynamics *in vivo* (Karbowski *et al*. 2002). Antagonism of the mitochondrial fission protein Drp1 inhibits Bax-mediated cytochrome *c* release and apoptosis in cells (Frank *et al*. 2001) by a process that is still unknown and may prove difficult to address in simplified systems, e.g. isolated mitochondria or liposomes.

Regulation by p53

Induction of the transcriptional activating factor p53 by oxidative stress, hypoxia, etc. results in apoptosis mediated by the intrinsic (mitochondrial) pathway (Miller *et al*. 2000). p53 stimulates the expression of several Bcl-2 family genes including Bax and multiple BH3-only proteins, e.g. Bid, Noxa, and PUMA (Sax and El Deiry 2003). In addition to elevating the levels of proteins that mediate release of cytochrome *c*, p53 stimulates apoptosis by a transcription–independent pathway (Caelles *et al*. 1994). The molecular mechanism by which p53 activates apoptosis independent of transcription apparently involves the direct binding of p53 to one or more anti-apoptotic mitochondrial proteins, e.g. Bcl-X_L, thereby inhibiting their ability to suppress Bax- or Bak-mediated pore formation and cytochrome *c* release (Fig. 3) (Chipuk *et al*. 2003; Mihara *et al*. 2003). The ability of other nuclear factors such as TR3/nur77 and histone H1.2 to directly stimulate cytochrome *c* release from mitochondria has also been described (Li *et al*. 2000; Konishi *et al*. 2003), indicating that nuclear-to-mitochondrial signaling may be a

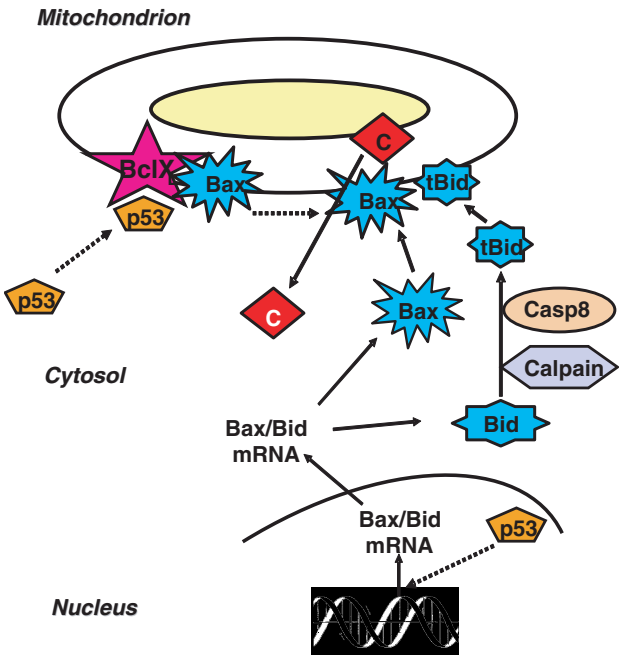

Fig. 3 Regulation of the intrinsic mitochondrial apoptotic pathway by p53. Various stressful stimuli associated with neurologic disorders, e.g. oxidative stress, stimulate the expression of p53. This gene product transcriptionally activates several pro-apoptotic genes, including Bax, Bid, Noxa, and PUMA. In addition, p53 stimulates apoptosis by a non-transcriptional mechanism involving direct binding to anti-apoptotic mitochondrial proteins, e.g. Bcl-X_L, inhibiting their ability to block outer membrane pore formation by Bax and Bak.

common theme in apoptotic death. However the importance of these nuclear instigators of the mitochondrial death pathway has yet to be investigated in neural cells.

Role of reactive oxygen species

A significant rise in reactive oxygen species (ROS) occurs in both apoptotic and necrotic neural cell death. Examination of Bax deficient and Bax heterozygous mouse sympathetic neurons revealed that the amount of ROS produced subsequent to nerve growth factor (NGF) withdrawal directly correlates with Bax gene dosage (Kirkland *et al*. 2002). In Bax –/– neurons, no elevation of ROS occurred and cytochrome *c* release in response to growth factor deprivation was completely suppressed. The complex I inhibitor rotenone abrogated the increase in ROS, indicating a mitochondrial source for the reactive oxygen species.

Cai and Jones initially proposed that intracellular redistribution of cytochrome *c* is responsible for the oxidative stress that often accompanies apoptosis (Cai and Jones 1998). We have found that Bax-induced release of cytochrome *c* from isolated brain mitochondria causes increased production of ROS (Starkov *et al*. 2002), likely via stimulation of superoxide production at Complex I of the electron transport chain (Kushnareva *et al*. 2002). This observation supports the hypothesis that Bax-dependent mitochondrial ROS generation lies downstream of cytochrome *c* release. This concept is challenged by measurements of the timing of stimulated ROS production in mouse sympathetic neurons, which was found to precede the release of cytochrome *c,* as measured by immunofluorescence (Kirkland *et al*. 2002). However, evidence in rat sympathetic neurons suggests that partial cytochrome *c* release may be detectable by subcellular fractionation and immunoblotting earlier than when the change in immunostaining pattern becomes apparent (Martinou *et al*. 1999). Lipid peroxidation, particularly of cardiolipin, can cause dissociation of cytochrome *c* from its electrostatic interaction with the inner mitochondrial membrane (Ott *et al*. 2002). Thus, release of the intermembrane soluble pool of cytochrome *c* by Bax could potentially lead to ROS generation that would then enhance cytochrome *c* release, further enhancing the production of ROS. Activated caspase-3 was also reported to enhance mitochondrial ROS downstream of cytochrome *c* release by damaging complexes I and II (Ricci *et al*. 2003). Although the mechanism of mitochondrial ROS generation by Bax is not clear, a membrane-permeant form of reduced glutathione was able to limit the ROS burst and cytochrome *c* release in Bax+/+neurons deprived of NGF (Kirkland *et al*. 2002), pointing to an important role of ROS and possibly lipid or protein oxidation in the mitochondrial permeabilization process.

Neuroprotective interventions

As the apoptotic pathway has become better defined and its contribution to neurodegenerative disorders irrefutable, the development of anti-apoptotic therapeutics has predictably become a focus of investigation. Suppression of apoptosis at the level of caspases via caspase inhibitors is one approach that has been actively explored with modest success (Bilsland and Harper 2002). A factor complicating this strategy, however, is that mitochondrial dysfunction often occurs even in the presence of caspase inhibition, leading to an impairment in ATP production and an increase in the generation of reactive oxygen species (Chang *et al*. 2002). Thus, caspase inhibitors may merely delay cell death. Alternatively, neurons surviving injury in the presence of caspase inhibitors may still be functionally impaired and contribute to poor neurologic outcome.

In contrast to the inhibition of caspases, genetic deletion of Bax and Bak confers long-term resistance to apoptosis in cultured cells and prevents upstream apoptotic changes in mitochondria, e.g. loss of apoptogenic factors and membrane potential (Wei *et al*. 2001). Thus, the challenge is to develop or identify pharmacologic agents capable of inhibiting apoptosis at steps upstream of Bax and Bak-induced mitochondrial changes (Fig. 4). In neurons, the relocalization of Bax from the cytosol to the mitochondria represents one of the first steps in programmed cell death (Putcha *et al*. 1999). Although Bax has an N-terminal mitochondrial targeting

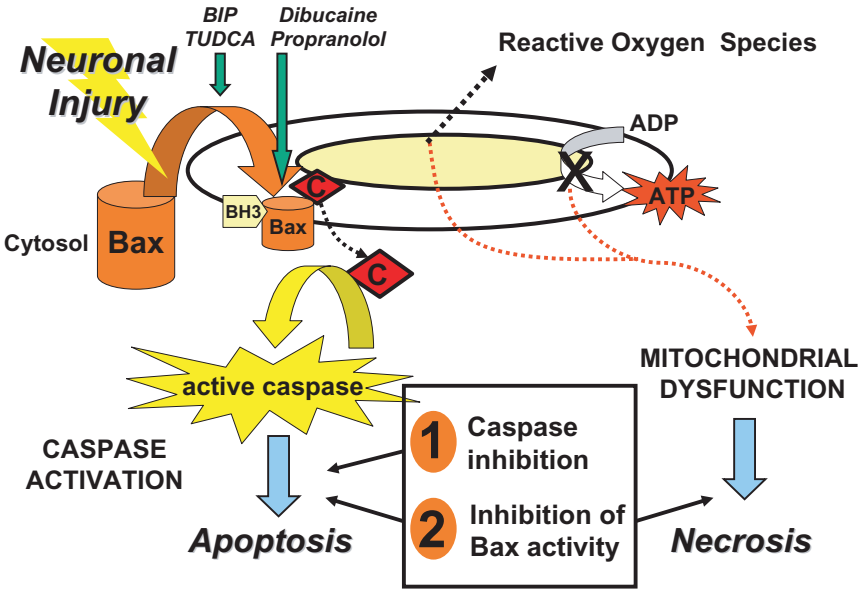

Fig. 4 Neuroprotection strategies targeting the intrinsic pathway of apoptosis. Until recently, the development of caspase inhibitors that cross the blood–brain barrier has been the major focus of neuroprotective studies that target apoptosis. However, because mitochondrial damage occurring upstream of caspase activation can lead to necrotic cell death due to oxidative stress and energy failure, inhibition of Bax function at the mitochondria is potentially a more effective therapeutic strategy. Bax-inhibiting Peptide (BIP) and tauroursodeoxycholic acid (TUDCA) prevent Bax translocation and association with mitochondria, while dibucaine and propranolol inhibit Bax-induced cytochrome *c* release downstream of Bax membrane insertion.

signal (Cartron *et al*. 2003), in healthy cells it is largely retained in the cytosol either by binding to a 24 amino acid anti-apoptotic peptide called humanin (Guo *et al*. 2003), or through an interaction with the DNA repair protein Ku70 (Sawada *et al*. 2003b). A cell permeable five amino acid peptide BIP (Bax-inhibiting peptide) designed from the Bax binding domain of Ku70 protected cells against Bax-dependent apoptotic stimuli in multiple cell types (Sawada *et al*. 2003a), demonstrating the possibility of inhibiting Bax-induced death at the initial stage of activation. Tauroursodeoxycholic acid limits Bax association with mitochondria (Rodrigues *et al*. 2003) while dibucaine and propranolol inhibit Bax-induced cytochrome *c* release downstream of Bax mitochondrial insertion (Polster *et al*. 2003), showing promise for the development of drugs that interfere with the membrane permeabilizing activity of Bax.

In contrast to Bax, Bak is constitutively present at mitochondria in healthy cells, and although Bax and Bak are often considered to have redundant pro-death functions, recent experiments with isolated rat brain mitochondria implicate distinct mechanisms in the release of cytochrome *c* (Brustovetsky *et al*. 2003). VDAC2 was recently shown to inhibit mitochondrial outer membrane permeabilization by Bak but not Bax (Cheng *et al*. 2003), while humanin and Ku70 appear to be specific Bax antagonists (Guo *et al*. 2003; Sawada *et al*. 2003b), demonstrating distinct mechanisms of regulation as well. Calcium-induced permeability transition is also likely to contribute to neuronal cell death under many circumstances and new permeability transition pore inhibitors are being developed (Walter *et al*. 2000; Cesura *et al*. 2003; Chinopoulos *et al*. 2003). Thus, therapeutics focused solely on suppressing Bax translocation or function may display incomplete efficacy due to the existence of alternate, parallel, or compensatory death pathways.

Bcl-2 and Bcl-X_L are two prominent native inhibitors of apoptosis and Bax and Bak function. Early investigations focused on the ability of Bcl-2 to regulate inner mitochondrial permeability transition, cellular redox state, and oxidative damage-induced cell death (Hockenbery *et al*. 1993; Susin *et al*. 1996; Kowaltowski *et al*. 2000). This approach was followed by research on binding interactions between Bcl-2 or Bcl-X_L and Bax/Bak or BH3-only proteins, and regulation of mitochondrial outer membrane permeability (Wei *et al*. 2001). The ability of Bcl-2 and Bcl-X_L to strengthen antioxidant defenses, to inhibit mitochondrial permeability transition, and to inhibit permeability transition pore-independent cytochrome *c* release makes these proteins attractive multitarget neuroprotective candidates. Early attempts to deliver the Bcl-X_L protein directly to the brain via fusion to a protein transduction-conferring TAT peptide have been fruitful, with several studies demonstrating protection in rodent ischemic injury models (Cao *et al*. 2002; Kilic *et al*. 2002). Because of the multifaceted nature of cell death pathways in the nervous system, it is likely that a cocktail of

therapeutics will ultimately prove most effective in treating both acute and chronic neurodegenerative disorders.

Conclusions

Although mitochondrial inner membrane permeability transition contributes to acute necrotic neural cell death, the selective permeabilization of the outer membrane caused by Bax and other Bcl-2 family proteins is likely to play a more causative role in apoptosis. Mitochondrial lipids are thought to play an important role in the outer membrane permeabilization process, although the nature of Bax- or Bak-induced protein or lipid pores in intact cells remains to be defined. Adding to the complexity, it is now apparent that mitochondrial apoptotic proteins are not always released in synchrony, for instance, Smac/DIABLO and AIF release are sometimes seen only after caspase activation has occurred downstream of cytochrome *c* redistribution. Thus, although considerable progress has been made toward unravelling the mechanism(s) of release of apoptotic proteins from mitochondria during programmed cell death, our understanding of the process is far from complete. Various mechanisms discussed in this review may be recruited by different stimuli or in different neural cell types, and undoubtedly additional players remain to be discovered. Further characterization of events that occur at mitochondrial membranes during apoptosis will provide novel targets for upstream therapeutic interventions in the apoptotic pathway that may prove effective in the treatment of both acute neurologic disorders and chronic neurodegenerative diseases.

Acknowledgements

The authors are supported by National Institutes of Health (NIH) grants R01 NS34152, P01 HD016596, and R21 NS45038 to G.F and F32 NS44791 to B.M.*p*., and U.S. Army Medical Research and Material Command grant DAMD 17-99-1-9483 to G.F.

References

Adrain C., Creagh E. M. and Martin S. J. (2001) Apoptosis-associated release of Smac/DIABLO from mitochondria requires active caspases and is blocked by Bcl-2. *EMBO J.* **20**, 6627–6636.

Antonsson B., Montessuit S., Lauper S., Eskes R. and Martinou J. C. (2000) Bax oligomerization is required for channel-forming activity in liposomes and to trigger cytochrome *c* release from mitochondria. *Biochem. J.* **345**, 271–278.

Antonsson B., Montessuit S., Sanchez B. and Martinou J. C. (2001) Bax is present as a high molecular weight oligomer/complex in the mitochondrial membrane of apoptotic cells. *J. Biol. Chem.* **276**, 11615–11623.

Arnoult D., Parone P., Martinou J. C., Antonsson B., Estaquier J. and Ameisen J. C. (2002) Mitochondrial release of apoptosis-inducing factor occurs downstream of cytochrome *c* release in response to several proapoptotic stimuli. *J. Cell Biol.* **159**, 923–929.

Basanez G., Nechushtan A., Drozhinin O., Chanturiya A., Choe E., Tutt S., Wood K. A., Hsu Y., Zimmerberg J. and Youle R. J. (1999) Bax, but not Bcl-xL, decreases the lifetime of planar phospholipid bilayer membranes at subnanomolar concentrations. *Proc. Natl Acad. Sci. USA* **96**, 5492–5497.

Basanez G., Sharpe J. C., Galanis J., Brandt T. B., Hardwick J. M. and Zimmerberg J. (2002) Bax-type apoptotic proteins porate pure lipid bilayers through a mechanism sensitive to intrinsic monolayer curvature. *J Biol Chem*. **277**, 49360–49365.

Bilsland J. and Harper S. (2002) Caspases and neuroprotection. *Curr. Opin. Invest Drugs* **3**, 1745–1752.

Braun J. S., Novak R., Murray P. J., Eischen C. M., Susin S. A., Kroemer G., Halle A., Weber J. R., Tuomanen E. I. and Cleveland J. L. (2001) Apoptosis-inducing factor mediates microglial and neuronal apoptosis caused by pneumococcus. *J. Infect Dis* **184**, 1300–1309.

Brustovetsky N., Dubinsky J. M., Antonsson B. and Jemmerson R. (2003) Two pathways for tBID-induced cytochrome *c* release from rat brain mitochondria: BAK- versus BAX-dependence. *J. Neurochem.* **84**, 196–207.

Budd S. L., Tenneti L., Lishnak T. and Lipton S. A. (2000) Mitochondrial and extramitochondrial apoptotic signaling pathways in cerebrocortical neurons. *Proc. Natl Acad. Sci. USA* **97**, 6161–6166.

Caelles C., Helmberg A. and Karin M. (1994) p53-dependent apoptosis in the absence of transcriptional activation of p53-target genes. *Nature* **370**, 220–223.

Cai J. and Jones D. P. (1998) Superoxide in apoptosis. Mitochondrial generation triggered by cytochrome *c* loss. *J. Biol. Chem.* **273**, 11401–11404.

Cao G., Minami M., Pei W., Yan C., Chen D., O'Horo C., Graham S. H. and Chen J. (2001) Intracellular Bax translocation after transient cerebral ischemia: implications for a role of the mitochondrial apoptotic signaling pathway in ischemic neuronal death. *J. Cereb Blood Flow Metab* **21**, 321–333.

Cao G., Pei W., Ge H., Liang Q., Luo Y., Sharp F. R., Lu A., Ran R., Graham S. H. and Chen J. (2002) In Vivo Delivery of a Bcl-xL Fusion Protein Containing the TAT Protein Transduction Domain Protects against Ischemic Brain Injury and Neuronal Apoptosis. *J. Neurosci.* **22**, 5423–5431.

Cao G., Clark R. S., Pei W., Yin W., Zhang F., Sun F. Y., Graham S. H. and Chen J. (2003) Translocation of apoptosis-inducing factor in vulnerable neurons after transient cerebral ischemia and in neuronal cultures after oxygen-glucose deprivation. *J. Cereb Blood Flow Metab* **23**, 1137–1150.

Cartron P. F., Priault M., Oliver L., Meflah K., Manon S. and Vallette F. M. (2003) The N-terminal end of Bax contains a mitochondrial-targeting signal. *J. Biol. Chem.* **278**, 11633–11641.

Cesura A. M., Pinard E., Schubenel R., Goetschy V., Friedlein A., Langen H., Polcic P., Forte M. A., Bernardi P. and Kemp J. A. (2003) The voltage-dependent anion channel is the target for a new class of inhibitors of the mitochondrial permeability transition pore. *J. Biol. Chem.* **278**, 49812–49818.

Chang L. K., Putcha G. V., Deshmukh M. and Johnson E. M. Jr (2002) Mitochondrial involvement in the point of no return in neuronal apoptosis. *Biochimie* **84**, 223–231.

Cheng E. H., Sheiko T. V., Fisher J. K., Craigen W. J. and Korsmeyer S. J. (2003) VDAC2 inhibits BAK activation and mitochondrial apoptosis. *Science* **301**, 513–517.

Chinopoulos C., Starkov A. A. and Fiskum G. (2003) Cyclosporin A-insensitive permeability transition in brain mitochondria: Inhibition by 2-aminoethoxydiphenyl borate. *J. Biol. Chem.* **278**, 27382–27389.

Chipuk J. E., Maurer U., Green D. R. and Schuler M. (2003) Pharmacologic activation of p53 elicits Bax-dependent apoptosis in the absence of transcription. *Cancer Cell* **4**, 371–381.

Crompton M., Virji S. and Ward J. M. (1998) Cyclophilin-D binds strongly to complexes of the voltage-dependent anion channel and the adenine nucleotide translocase to form the permeability transition pore. *Eur. J. Biochem.* **258**, 729–735.

Datta S. R., Ranger A. M., Lin M. Z., Sturgill J. F., Ma Y. C., Cowan C. W., Dikkes P., Korsmeyer S. J. and Greenberg M. E. (2002) Survival factor-mediated BAD phosphorylation raises the mitochondrial threshold for apoptosis. *Dev. Cell* **3**, 631–643.

De Giorgi F., Lartigue L., Bauer M. K., Schubert A., Grimm S., Hanson G. T., Remington S. J., Youle R. J. and Ichas F. (2002) The permeability transition pore signals apoptosis by directing Bax translocation and multimerization. *FASEB J.* **16**, 607–609.

Deckwerth T. L., Elliott J. L., Knudson C. M., Johnson E. M. J., Snider W. D. and Korsmeyer S. J. (1996) BAX is required for neuronal death after trophic factor deprivation and during development. *Neuron* **17**, 401–411.

Desagher S., Osen-Sand A., Nichols A., Eskes R., Montessuit S., Lauper S., Maundrell K., Antonsson B. and Martinou J. C. (1999) Bid-induced conformational change of Bax is responsible for mitochondrial cytochrome *c* release during apoptosis. *J. Cell Biol.* **144**, 891–901.

Epand R. F., Martinou J. C., Montessuit S., Epand R. M. and Yip C. M. (2002) Direct evidence for membrane pore formation by the apoptotic protein Bax. *Biochem. Biophys. Res. Commun* **298**, 744–749.

Eskes R., Antonsson B., Osen-Sand A., Montessuit S., Richter C., Sadoul R., Mazzei G., Nichols A. and Martinou J. C. (1998) Bax-induced cytochrome *c* release from mitochondria is independent of the permeability transition pore but highly dependent on Mg^{2+} ions. *J. Cell Biol.* **143**, 217–224.

Eskes R., Desagher S., Antonsson B. and Martinou J. C. (2000) Bid induces the oligomerization and insertion of bax into the outer mitochondrial membrane. *Mol Cell Biol.* **20**, 929–935.

Fan H., Favero M. and Vogel M. W. (2001) Elimination of Bax expression in mice increases cerebellar purkinje cell numbers but not the number of granule cells. *J. Comp Neurol.* **436**, 82–91.

Frank S., Gaume B., Bergmann-Leitner E. S., Leitner W. W., Robert E. G., Catez F., Smith C. L. and Youle R. J. (2001) The role of dynamin-related protein 1, a mediator of mitochondrial fission, in apoptosis. *Dev Cell* **1**, 515–525.

Guo B., Zhai D., Cabezas E., Welsh K., Nouraini S., Satterthwait A. C. and Reed J. C. (2003) Humanin peptide suppresses apoptosis by interfering with Bax activation. *Nature* **423**, 456–461.

Harris C. A. and Johnson E. M. Jr (2001) Bh3-only bcl-2 family members are coordinately regulated by the jnk pathway and require bax to induce apoptosis in neurons. *J. Biol. Chem.* **276**, 37754–37760.

Henshall D. C., Araki T., Schindler C. K., Lan J. Q., Tiekoter K. L., Taki W. and Simon R. P. (2002) Activation of Bcl-2-associated death protein and counter-response of Akt within cell populations during seizure-induced neuronal death. *J. Neurosci.* **22**, 8458–8465.

Hisatomi T., Sakamoto T., Murata T., Yamanaka I., Oshima Y., Hata Y., Ishibashi T., Inomata H., Susin S. A. and Kroemer G. (2001) Relocalization of apoptosis-inducing factor in photoreceptor apoptosis induced by retinal detachment in vivo. *Am. J. Pathol* **158**, 1271–1278.

Hockenbery D. M., Oltvai Z. N., Yin X. M., Milliman C. L. and Korsmeyer S. J. (1993) Bcl-2 functions in an antioxidant pathway to prevent apoptosis. *Cell* **75**, 241–251.

Kandasamy K., Srinivasula S. M., Alnemri E. S., Thompson C. B., Korsmeyer S. J., Bryant J. L. and Srivastava R. K. (2003) Involvement of proapoptotic molecules Bax and Bak in tumor necrosis factor-related apoptosis-inducing ligand (TRAIL)-induced mitochondrial disruption and apoptosis: differential regulation of cytochrome c and Smac/DIABLO release. *Cancer Res.* **63**, 1712–1721.

Karbowski M., Lee Y. J., Gaume B., Jeong S. Y., Frank S., Nechushtan A., Santel A., Fuller M., Smith C. L. and Youle R. J. (2002) Spatial and temporal association of Bax with mitochondrial fission sites, Drp1, and Mfn2 during apoptosis. *J. Cell Biol.* **159**, 931–938.

Kilic E., Dietz G. P., Hermann D. M. and Bahr M. (2002) Intravenous TAT-Bcl-Xl is protective after middle cerebral artery occlusion in mice. *Ann. Neurol.* **52**, 617–622.

Kirkland R. A., Windelborn J. A., Kasprzak J. M. and Franklin J. L. (2002) A Bax-induced pro-oxidant state is critical for cytochrome c release during programmed neuronal death. *J. Neurosci.* **22**, 6480–6490.

Klein J. A., Longo-Guess C. M., Rossmann M. P., Seburn K. L., Hurd R. E., Frankel W. N., Bronson R. T. and Ackerman S. L. (2002) The harlequin mouse mutation downregulates apoptosis-inducing factor. *Nature* **419**, 367–374.

Konishi A., Shimizu S., Hirota J. *et al.* (2003) Involvement of histone H1.2 in apoptosis induced by DNA double-strand breaks. *Cell* **114**, 673–688.

Kowaltowski A. J., Vercesi A. E. and Fiskum G. (2000) Bcl-2 prevents mitochondrial permeability transition and cytochrome c release via maintenance of reduced pyridine nucleotides. *Cell Death Differ* **7**, 903–910.

Kushnareva Y. E., Murphy A. N. and Andreyev A. Y. (2002) Complex I mediated reactive oxygen species generation: Modulation by Cytochrome c and NAD (P) + oxidation-reduction state. *Biochem. J.* **368**, 545–553.

Kuwana T., Mackey M. R., Perkins G., Ellisman M. H., Latterich M., Schneiter R., Green D. R. and Newmeyer D. D. (2002) Bid, Bax, and lipids cooperate to form supramolecular openings in the outer mitochondrial membrane. *Cell* **111**, 331–342.

Li H., Zhu H., Xu C. J. and Yuan J. (1998) Cleavage of BID by caspase 8 mediates the mitochondrial damage in the Fas pathway of apoptosis. *Cell* **94**, 491–501.

Li H., Kolluri S. K., Gu J. *et al.* (2000) Cytochrome c release and apoptosis induced by mitochondrial targeting of nuclear orphan receptor TR3. *Science* **289**, 1159–1164.

Lindsten T., Golden J. A., Zong W. X., Minarcik J., Harris M. H. and Thompson C. B. (2003) The proapoptotic activities of Bax and Bak limit the size of the neural stem cell pool. *J. Neurosci.* **23**, 11112–11119.

Luo X., Budihardjo I., Zou H., Slaughter C. and Wang X. (1998) Bid, a Bcl2 interacting protein, mediates cytochrome c release from mitochondria in response to activation of cell surface death receptors. *Cell* **94**, 481–490.

Martinou I., Desagher S., Eskes R., Antonsson B., Andre E., Fakan S. and Martinou J. C. (1999) The release of cytochrome c from mitochondria during apoptosis of NGF- deprived sympathetic neurons is a reversible event. *J. Cell Biol.* **144**, 883–889.

Marzo I., Brenner C., Zamzami N., Jurgensmeier J. M., Susin S. A., Vieira H. L., Prevost M. C., Xie Z., Matsuyama S., Reed J. C. and Kroemer G. (1998a) Bax and adenine nucleotide translocator cooperate in the mitochondrial control of apoptosis. *Science* **281**, 2027–2031.

Marzo I., Brenner C., Zamzami N., Susin S. A., Beutner G., Brdiczka D., Remy R., Xie Z. H., Reed J. C. and Kroemer G. (1998b) The permeability transition pore complex: a target for apoptosis regulation by caspases and bcl-2-related proteins. *J. Exp Med.* **187**, 1261–1271.

Mihara M., Erster S., Zaika A., Petrenko O., Chittenden T., Pancoska P. and Moll U. M. (2003) p53 has a direct apoptogenic role at the mitochondria. *Mol Cell* **11**, 577–590.

Miller F. D., Pozniak C. D. and Walsh G. S. (2000) Neuronal life and death: an essential role for the p53 family. *Cell Death Differ* **7**, 880–888.

Motoyama N., Wang F., Roth K. A., Sawa H., Nakayama K., Nakayama K., Negishi I., Senju S., Zhang Q. and Fujii S. (1995) Massive cell death of immature hematopoietic cells and neurons in Bcl-x-deficient mice. *Science* **267**, 1506–1510.

Muzio M., Chinnaiyan A. M., Kischkel F. C. *et al.* (1996) FLICE, a novel FADD-homologous ICE/CED-3-like protease, is recruited to the CD95 (Fas/APO-1) death – inducing signaling complex. *Cell* **85**, 817–827.

Nechushtan A., Smith C. L., Lamensdorf I., Yoon S. H. and Youle R. J. (2001) Bax and Bak coalesce into novel mitochondria-associated clusters during apoptosis. *J. Cell Biol.* **153**, 1265–1276.

Ott M., Robertson J. D., Gogvadze V., Zhivotovsky B. and Orrenius S. (2002) Cytochrome c release from mitochondria proceeds by a two-step process. *Proc. Natl Acad. Sci. USA* **99**, 1259–1263.

Pastorino J. G., Chen S. T., Tafani M., Snyder J. W. and Farber J. L. (1998) The overexpression of Bax produces cell death upon induction of the mitochondrial permeability transition. *J. Biol. Chem.* **273**, 7770–7775.

Pavlov E. V., Priault M., PietkiewicZ. D., Cheng E. H., Antonsson B., Manon S., Korsmeyer S. J., Mannella C. A. and Kinnally K. W. (2001) A novel, high conductance channel of mitochondria linked to apoptosis in mammalian cells and Bax expression in yeast. *J. Cell Biol.* **155**, 725–731.

Plesnila N., Zinkel S., Le D. A., Amin-Hanjani S., Wu Y., Qiu J., Chiarugi A., Thomas S. S., Kohane D. S., Korsmeyer S. J. and Moskowitz M. A. (2001) BID mediates neuronal cell death after oxygen/ glucose deprivation and focal cerebral ischemia. *Proc. Natl Acad. Sci. USA* **98**, 15318–15323.

Polster B. M., Basanez G., Young M., Suzuki M. and Fiskum G. (2003) Inhibition of Bax-induced cytochrome C release from neural cell and brain mitochondria by dibucaine and propranolol. *J. Neurosci.* **23**, 2735–2743.

Putcha G. V., Deshmukh M. and Johnson E. M. J. (1999) BAX translocation is a critical event in neuronal apoptosis: regulation by neuroprotectants, BCL-2, and caspases. *J. Neurosci.* **19**, 7476–7485.

Ricci J. E., Gottlieb R. A. and Green D. R. (2003) Caspase-mediated loss of mitochondrial function and generation of reactive oxygen species during apoptosis. *J. Cell Biol.* **160**, 65–75.

Rodrigues C. M., Sola S., Sharpe J. C., Moura J. J. and Steer C. J. (2003) Tauroursodeoxycholic acid prevents bax-induced membrane perturbation and cytochrome C release in isolated mitochondria. *Biochemistry* **42**, 3070–3080.

Saito M., Korsmeyer S. J. and Schlesinger P. H. (2000) BAX-dependent transport of cytochrome c reconstituted in pure liposomes. *Nat Cell Biol.* **2**, 553–555.

Sawada M., Hayes P. and Matsuyama S. (2003a) Cytoprotective membrane-permeable peptides designed from the Bax-binding domain of Ku70. *Nat Cell Biol.* **5**, 352–357.

Sawada M., Sun W., Hayes P., Leskov K., Boothman D. A. and Matsuyama S. (2003b) Ku70 suppresses the apoptotic translocation of Bax to mitochondria. *Nat Cell Biol.* **5**, 320–329.

Sax J. K. and El Deiry W. S. (2003) p53 downstream targets and chemosensitivity. *Cell Death Differ* **10**, 413–417.

Scorrano L., Oakes S. A., Opferman J. T., Cheng E. H., Sorcinelli M. D., Pozzan T. and Korsmeyer S. J. (2003) BAX and BAK regulation of endoplasmic reticulum Ca2+: a control point for apoptosis. *Science* **300**, 135–139.

Shimizu S., Narita M. and Tsujimoto Y. (1999) Bcl-2 family proteins regulate the release of apoptogenic cytochrome c by the mitochondrial channel VDAC. *Nature* **399**, 483–487.

Shimizu S., Matsuoka Y., Shinohara Y., Yoneda Y. and Tsujimoto Y. (2001) Essential role of voltage-dependent anion channel in various forms of apoptosis in mammalian cells. *J. Cell Biol.* **152**, 237–250.

Shindler K. S., Latham C. B. and Roth K. A. (1997) Bax deficiency prevents the increased cell death of immature neurons in bcl-x-deficient mice. *J. Neurosci.* **17**, 3112–3119.

Springer J. E., Azbill R. D., Nottingham S. A. and Kennedy S. E. (2000) Calcineurin-mediated BAD dephosphorylation activates the caspase-3 apoptotic cascade in traumatic spinal cord injury. *J. Neurosci.* **20**, 7246–7251.

Starkov A. A., Polster B. M. and Fiskum G. (2002) Regulation of hydrogen peroxide production by brain mitochondria by calcium and Bax. *J. Neurochem.* **83**, 220–228.

Susin S. A., Zamzami N., Castedo M., Hirsch T., Marchetti P., Macho A., Daugas E., Geuskens M. and Kroemer G. (1996) Bcl-2 inhibits the mitochondrial release of an apoptogenic protease. *J. Exp Med.* **184**, 1331–1341.

Walter L., Nogueira V., Leverve X., Heitz M. P., Bernardi P. and Fontaine E. (2000) Three classes of ubiquinone analogs regulate the mitochondrial permeability transition pore through a common site. *J. Biol. Chem.* **275**, 29521–29527.

Wang H. G., Pathan N., Ethell I. M., Krajewski S., Yamaguchi Y., Shibasaki F., McKeon F., Bobo T., Franke T. F. and Reed J. C. (1999) Ca2+-induced apoptosis through calcineurin dephosphorylation of BAD. *Science* **284**, 339–343.

Wei M. C., Lindsten T., Mootha V. K., Weiler S., Gross A., Ashiya M., Thompson C. B. and Korsmeyer S. J. (2000) tBID, a membrane-targeted death ligand, oligomerizes BAK to release cytochrome c. *Genes Dev* **14**, 2060–2071.

Wei M. C., Zong W. X., Cheng E. H., Lindsten T., Panoutsakopoulou V., Ross A. J., Roth K. A., MacGregor G. R., Thompson C. B. and Korsmeyer S. J. (2001) Proapoptotic BAX and BAK: a requisite gateway to mitochondrial dysfunction and death. *Science* **292**, 727–730.

White F. A., Keller-Peck C. R., Knudson C. M., Korsmeyer S. J. and Snider W. D. (1998) Widespread elimination of naturally occurring neuronal death in Bax-deficient mice. *J. Neurosci.* **18**, 1428–1439.

Wigdal S. S., Kirkland R. A., Franklin J. L. and Haak-Frendscho M. (2002) Cytochrome c release precedes mitochondrial membrane potential loss in cerebellar granule neuron apoptosis: lack of mitochondrial swelling. *J. Neurochem.* **82**, 1029–1038.

Yu S. W., Wang H., Poitras M. F., Coombs C., Bowers W. J., Federoff H. J., Poirier G. G., Dawson T. M. and Dawson V. L. (2002) Mediation of poly (ADP-ribose) polymerase-1-dependent cell death by apoptosis-inducing factor. *Science* **297**, 259–263.

Zhang X., Chen J., Du Graham S. H. L., Kochanek P. M., Draviam R., Guo F., Nathaniel P. D., Szabo C., Watkins S. C. and Clark R. S. (2002) Intranuclear localization of apoptosis-inducing factor (AIF) and large scale DNA fragmentation after traumatic brain injury in rats and in neuronal cultures exposed to peroxynitrite. *J. Neurochem.* **82**, 181–191.

Zhu C., Qiu L., Wang X., Hallin U., Cande C., Kroemer G., Hagberg H. and Blomgren K. (2003) Involvement of apoptosis-inducing factor in neuronal death after hypoxia-ischemia in the neonatal rat brain. *J. Neurochem.* **86**, 306–317.

Zong W. X., Li C., Hatzivassiliou G., Lindsten T. YuQ. C., Yuan J. and Thompson C. B. (2003) Bax and Bak can localize to the endoplasmic reticulum to initiate apoptosis. *J. Cell Biol.* **162**, 59–69.

Zou H., Henzel W. J., Liu X., Lutschg A. and Wang X. (1997) Apaf-1, a human protein homologous to C. elegans CED-4, participates in cytochrome c-dependent activation of caspase-3. *Cell* **90**, 405–413.

Neurobiology of Disease

Mitochondrial α-Ketoglutarate Dehydrogenase Complex Generates Reactive Oxygen Species

Anatoly A. Starkov,[1] Gary Fiskum,[2] Christos Chinopoulos,[2] Beverly J. Lorenzo,[1] Susan E. Browne,[1] Mulchand S. Patel,[3] and M. Flint Beal[1]

[1]Department of Neurology and Neuroscience, Weill Medical College, Cornell University, New York, New York 10021, [2]Department of Anesthesiology, University of Maryland School of Medicine, Baltimore, Maryland 21202, and [3]Department of Biochemistry, School of Medicine and Biomedical Sciences, State University of New York at Buffalo, Buffalo, New York 14214

Mitochondria-produced reactive oxygen species (ROS) are thought to contribute to cell death caused by a multitude of pathological conditions. The molecular sites of mitochondrial ROS production are not well established but are generally thought to be located in complex I and complex III of the electron transport chain. We measured H_2O_2 production, respiration, and NADPH reduction level in rat brain mitochondria oxidizing a variety of respiratory substrates. Under conditions of maximum respiration induced with either ADP or carbonyl cyanide *p*-trifluoromethoxyphenylhydrazone, α-ketoglutarate supported the highest rate of H_2O_2 production. In the absence of ADP or in the presence of rotenone, H_2O_2 production rates correlated with the reduction level of mitochondrial NADPH with various substrates, with the exception of α-ketoglutarate. Isolated mitochondrial α-ketoglutarate dehydrogenase (KGDHC) and pyruvate dehydrogenase (PDHC) complexes produced superoxide and H_2O_2. NAD^+ inhibited ROS production by the isolated enzymes and by permeabilized mitochondria. We also measured H_2O_2 production by brain mitochondria isolated from heterozygous knock-out mice deficient in dihydrolipoyl dehydrogenase (Dld). Although this enzyme is a part of both KGDHC and PDHC, there was greater impairment of KGDHC activity in Dld-deficient mitochondria. These mitochondria also produced significantly less H_2O_2 than mitochondria isolated from their littermate wild-type mice. The data strongly indicate that KGDHC is a primary site of ROS production in normally functioning mitochondria.

Key words: **mitochondria; reactive oxygen species; lipoamide dehydrogenase; ketoglutarate dehydrogenase; Parkinson; Alzheimer**

Introduction

Reactive oxygen species (ROS) are thought to contribute to neuronal cell death caused by ischemia, excitotoxicity, and various acute and chronic neurological disorders (Dykens, 1994; Fiskum et al., 1999; Murphy et al., 1999; Fiskum, 2000; Nicholls and Budd, 2000). A compelling body of evidence indicates that mitochondria are the major source of ROS in normal tissues and under a variety of neurodegenerative conditions (Murphy et al., 1999). However, the mechanism and the sites of ROS production in mitochondria require additional research. The vast majority of studies on mitochondrial ROS generation have used heart mitochondria and respiratory chain inhibitors as tools to maximize ROS production and to identify potential sites of ROS generation. These studies revealed that inhibiting complexes I and III of the mitochondrial respiratory chain with specific mitochondrial toxins, such as rotenone and antimycin A, resulted in high rates of ROS production (Turrens, 1997; Murphy et al., 1999; Lenaz, 2001). Similar approaches have been used successfully to study ROS production by isolated (Kwong and Sohal, 1998) and *in situ* (Sipos et al., 2003) brain mitochondria, but no information is yet available regarding the specific sites or mechanisms of ROS generation in the absence of respiratory chain inhibitors (Sorgato et al., 1974; Patole et al., 1986; Cino and Del Maestro, 1989; Ramsay and Singer, 1992; Hensley et al., 1998; Kwong and Sohal, 1998; Sims et al., 1998; Tretter and Adam-Vizi, 2000; Sipos et al., 2003).

Previously, we suggested that mitochondrial matrix dehydrogenases other than complex I [e.g., α-ketoglutarate dehydrogenase enzyme complex (KGDHC)] can contribute to the observed ROS production in the absence of inhibitors of the mitochondrial respiratory chain (Starkov and Fiskum, 2002). It is known that reduced flavins (Massey, 1994) and flavoproteins (Chan and Bielski, 1974, 1980; Zhang et al., 1998; Bunik and Sievers, 2002) can generate superoxide in aqueous oxygenated solutions. Isolated lactate dehydrogenase (Chan and Bielski, 1974) and glyceraldehyde-3-phosphate dehydrogenase (Chan and Bielski, 1980) were shown to catalyze NADH-dependent superoxide production, whereas malate and isocitrate dehydrogenase did not produce superoxide (Chan and Bielski, 1974). The isolated dehydrogenase component of mitochondrial succinate dehydrogenase (SDH) complex was also capable of flavin-dependent superoxide production in the absence of an electron acceptor (Zhang et al.,

Received May 15, 2004; revised July 14, 2004; accepted July 18, 2004.

This work was supported in part by National Institutes of Health Grants ES11838 and NS34152 (G.F.) and AG14930 (M.F.B.) and by the United States Army Medical Research and Materiel Command Neurotoxin Initiative, Mitochondrial Collaborative Group (DAMD17-99-1-9483 to G.F. and DAMD17-98-1-8620 to S.E.B.). We are grateful to Drs. John P. Blass, Gary E. Gibson, and Bill Nicklas for very helpful discussion of portions of this manuscript.

Correspondence should be addressed to Dr. M. Flint Beal, Department of Neurology and Neuroscience, Weill Medical College of Cornell University, New York Presbyterian Hospital, 525 East 68th Street, New York, NY 10021. E-mail: fbeal@med.cornell.edu.

DOI:10.1523/JNEUROSCI.1899-04.2004

 0270-6474/04/247779-10$15.00/0

1998). It has also been recently demonstrated that the flavin of the dihydrolipoamide dehydrogenase (Dld) component (EC 1.8.1.4) of isolated KGDHC can generate superoxide (Bunik and Sievers, 2002). The latter is of particular interest with regard to the mechanisms and sites of ROS production in mitochondria because the flavin of the Dld subunit is abundant in mitochondria (Kunz and Gellerich, 1993) and has a sufficiently negative redox potential (E_m 7.4 = −283 mV) (Kunz and Kunz, 1985) to allow for superoxide production.

The data presented here demonstrate that KGDHC represents a significant source of ROS in brain mitochondria. The reduced Dld subunit of KGDHC is the most likely source of ROS in the mitochondrial matrix under conditions of an elevated NADPH/$NADP^+$ ratio in the matrix of mitochondria. Preliminary results have been reported previously (Starkov and Fiskum, 2002).

Materials and Methods

Reagents. Oligomycin, antimycin A3, and rotenone (Sigma, St. Louis, MO) were dissolved in ethanol, and Amplex Red (10-acetyl-3,7-dihydroxyphenoxazine; Molecular Probes, Eugene, OR) was dissolved in dimethylsulfoxide. All other reagents were purchased from Sigma. All reagents and ethanol were tested and exhibited no interference with the H_2O_2 assay at the concentrations used in our experiments.

Mouse and rat forebrain mitochondria were isolated as described previously (Rosenthal et al., 1987; Starkov and Fiskum, 2001, 2003), with modifications as follows. Sprague Dawley rats and knock-out Dld-deficient mice (Johnson et al., 1997) and their littermate controls were used. Animals were decapitated, and the brain was excised and placed into ice-cold isolation buffer containing 225 mM mannitol, 75 mM sucrose, 5 mM HEPES-KOH, pH 7.4, 1 mM EGTA, and 1 gm/l bovine serum albumin. Two mouse brains or a single rat brain were used per isolation. The cerebellum was removed, and the rest of the brain tissue was placed in a 15 ml Dounce homogenizer and homogenized manually with eight strokes of pestle A, followed by eight strokes of pestle B. The homogenate was diluted with 15 ml of isolation buffer, distributed into four centrifuge tubes, and centrifuged at 3000 × *g* for 4 min. The supernatant was separated and centrifuged again at 14,000 × *g* for 10 min. The pellet was resuspended in 15 ml of the ice-cold isolation buffer without BSA and kept on ice, and 30 μl of digitonin (10% stock solution in DMSO) was added. After a 4 min incubation with occasional stirring by slow inversion of tubes, the suspension was diluted with 15 ml of ice-cold isolation buffer containing BSA and centrifuged at 14,000 × *g* for 10 min. The pellet was resuspended in 8 ml of ice-cold isolation buffer containing neither BSA nor EGTA and centrifuged again at 14,000 × *g* for 10 min. The final pellet containing mitochondria of both synaptosomal and nonsynaptosomal origin was resuspended in isolation buffer without EGTA and BSA to a concentration of 25–30 mg of protein/ml, stored on ice, and used within 5 hr.

Alternatively, nonsynaptosomal rat and mouse forebrain mitochondria were isolated by the Percoll gradient separation method as described (Sims, 1990), and measurements of H_2O_2 production and respiration were performed. The Percoll gradient-isolated mitochondria generally exhibited higher H_2O_2 and respiration rates than digitonin-isolated mitochondria when expressed per milligram of mitochondrial protein, however the difference was not qualitative and would not justify repeating all the experiments reported here with mitochondria isolated by both methods. Therefore, only the data obtained with mitochondria isolated by the digitonin procedure are presented here, unless indicated otherwise.

Respiration of isolated mitochondria was measured at 37°C with a commercial Clark-type oxygen electrode (Hansatech, Norfolk, UK). The incubation medium composition and respiratory substrates are indicated in the legends to the figures.

The quality of the mitochondrial preparation was estimated by measuring the acceptor control ratio (ACR) defined as ADP-stimulated (state 3) respiration divided by resting (state 4) respiration. For these experiments, the incubation medium consisted of (in mM) 125 KCl, 20 HEPES, pH 7.0, 2 KH_2PO_4, 1 $MgCl_2$, 5 glutamate, 5 malate, and 0.8 ADP. State 3 respiration was initiated by the addition of 0.5 mg/ml brain mitochondria to the incubation medium. State 3 respiration was terminated, and state 4 was initiated by the addition of 1 μM carboxyatractylate, an inhibitor of the ADP/ATP transporter. Only mitochondrial preparations that exhibited an ACR of >8 were used in this study.

Membrane potentials of isolated mitochondria were estimated using the fluorescence of safranine O (3 μM) with excitation and emission wavelengths of 495 and 586 nm, respectively (Votyakova and Reynolds, 2001; Starkov et al., 2002).

KGDHC activity in mouse mitochondria was measured fluorimetrically. The reaction medium was composed of 50 mM KCl, 10 mM HEPES, pH 7.4, 20 μg/ml alamethicin, 0.3 mM thiamine pyrophosphate (TPP), 10 μM $CaCl_2$, 0.2 mM $MgCl_2$, 5 mM α-ketoglutarate, 1 μM rotenone, and 0.2 mM NAD^+. The reaction was started by adding 0.14 mM CoASH to permeabilized mitochondria (0.1–0.25 mg/ml). Reduction of NAD^+ was followed at 460 nm emission after excitation at 346 nm. The scale was calibrated by adding known amounts of freshly prepared NADPH. KGDHC and pyruvate dehydrogenase complex (PDHC) activity in rat brain mitochondria were measured in the same way, except that reduction of NAD^+ was followed by absorbance changes at 340 nm using the extinction coefficient, $E^{340}mM = 6.22\ cm^{-1}$.

Succinate dehydrogenase activity was measured spectrophotometrically as described previously (Arrigoni and Singer, 1962). The reaction medium was composed of 50 mM KCl, 10 mM HEPES, pH 7.4, 20 μg/ml alamethicin, 10 mM succinate, 2 mM KCN, 1 μM rotenone, 50 μM 2,3-dimethoxy-5-methyl-6-decyl-1,4-benzoquinone, 50 μM 2,6-dichlorophenol indophenol, and 20 μM EDTA; reaction was monitored at 600 nm, and the activity was calculated using $E^{600}mM = 21\ cm^{-1}$ for 2,6-dichlorophenol indophenol.

Measurement of hydrogen peroxide was performed as follows. The incubation medium contained 125 mM KCl, 20 mM HEPES, pH 7.0, 2 mM KH_2PO_4, 4 mM ATP, 5 mM $MgCl_2$, 1 μM Amplex Red, 5 U/ml horseradish peroxidase (HRP), and 20 U/ml Cu,ZnSOD and was maintained at 37°C. A change in the concentration of H_2O_2 in the medium was detected as an increase in Amplex Red fluorescence using excitation and emission wavelengths of 585 and 550 nm, respectively. The response of Amplex Red to H_2O_2 was calibrated either by sequential additions of known amounts of H_2O_2 or by continuous infusion of H_2O_2 at 100–1000 pmol/min. The concentration of commercial 30% H_2O_2 solution was calculated from light absorbance at 240 nM using $E^{240}mM = 43.6\ cm^{-1}$; the stock solution was diluted to 100 μM with water and used for calibration immediately.

It is to be noted that HRP catalyzes the oxidation of NADH that might result in an underestimation of H_2O_2 in an HRP-dependent assay, such as a classical scopoletin–HRP assay or Amplex Red–HRP assay used in our study. However, it was found that although NADH can react with the oxidized form of HRP, it cannot effectively compete with scopoletin in an HRP–scopoletin H_2O_2 assay (Marquez and Dunford, 1995). Furthermore, rat brain mitochondria contain ~5 nmol of total NAD/mg protein (C. Chinopoulos, unpublished observations) similar to the amount found in mitochondria from other tissues (3–7 nmol of total NAD/mg mitochondrial protein) (Tischler et al., 1977; Di Lisa et al., 2001). We have previously demonstrated that under the experimental conditions used in this study, rat brain mitochondria did not release more than ~15% of their total NAD content (Chinopoulos et al., 2003). Similar amounts of NADH added exogenously did not affect the H_2O_2 rates detected by the Amplex Red–HRP assay (data not shown).

Superoxide production was followed spectrophotometrically with partially acetylated cytochrome *c* (Azzi et al., 1975) and calculated from cytochrome *c* absorbance at 550-540 nm using extinction coefficient $E^{550\text{-}540}mM = 19.2\ cm^{-1}$.

The mitochondrial NADPH reduction state was measured fluorimetrically using an excitation wavelength of 346 nm and an emission wavelength of 460 nm. Maximal NADPH reduction was defined as the absorbance observed after the addition of the electron transport chain complex I inhibitor rotenone (1 μM), and maximal oxidation was defined as the absorbance obtained in the presence of the saturating

amounts of respiratory uncoupler carbonyl cyanide *p*-trifluoromethoxyphenylhydrazone (FCCP) (120–160 pmol/mg mitochondria).

Ubiquinones were extracted from frozen–thawed and sonicated mitochondrial samples into hexane using coenzyme Q6 as an internal standard. Samples were analyzed by HPLC using an MDA-50 (ESA, Chelmsford, MA) column and gradient separation. The detector was an eight-channel electrochemical array detector (CoulArray 5600; ESA) consisting of a series of five increasing oxidation potentials (ending with +800 mV) before a reducing channel of −800 mV and two additional oxidizing channels at +5 and +200 mV. Measurements were made on the final +200 mV channel (Gamache, 1999).

Mitochondrial protein was estimated by the Biuret method.

Statistical analysis. Data are expressed as mean ± SEM. Statistical analysis was performed using Student's *t* test.

Results

Previous attempts to understand the mechanisms of ROS production by mitochondria have been hampered by the low sensitivity of ROS detection methods and have therefore used inhibitors of either complex I or III of the respiratory chain to maximize ROS production. Recently, a novel fluorescent probe for H_2O_2, Amplex Red (10-acetyl-3,7-dihydroxyphenoxazine) (Zhou et al., 1997), has become available that is suitable for measurements with isolated mitochondria (Votyakova and Reynolds, 2001; Kushnareva et al., 2002). We have determined that it is sufficiently sensitive and its fluorescent response is linearly related to H_2O_2 even at levels that are generated by mitochondria in the absence of respiratory chain inhibitors (data not shown). With Amplex Red, it was possible to perform reliable measurements of H_2O_2 emission rates with the NAD^+-dependent respiratory substrates malate, pyruvate, citrate, glutamate, and α-ketoglutarate and with succinate and compare them with rates of O_2 consumption and the level of NADPH reduction of isolated rat and mouse brain mitochondria.

Figure 1 shows typical fluorescent recordings of H_2O_2 production by isolated rat brain mitochondria oxidizing NAD^+-dependent substrates or succinate. H_2O_2 generation was dependent on the addition of a respiratory substrate (succinate) (Fig. 1, curve a) or α-ketoglutarate (Fig. 1, curves b, c) and was suppressed by mitochondrial uncoupler FCCP (Fig. 1, curves a, b).

With NAD^+-dependent substrates, H_2O_2 production was stimulated by rotenone, which inhibits NADH oxidation at complex I (Fig. 1, curves b, c). However, rotenone inhibited succinate-supported H_2O_2 production, indicating that it was fueled by reverse electron transfer from succinate to a site in complex I (Turrens, 1997). With both types of substrates, H_2O_2 production was stimulated by an inhibitor of complex III (antimycin A) that increases the coenzyme Q semiquinone level (Turrens, 1997). With both types of substrates, H_2O_2 production was unaffected by the addition of NAD^+ (only the data with α-ketoglutarate is presented) (Fig. 1, curve c). It is well known that the inner mitochondrial membrane is impermeable to NAD^+.

It is important to note that H_2O_2 production in the presence of a complex I inhibitor (rotenone) was two to three times higher with α-ketoglutarate than that with succinate (Fig. 1). Previously, we (Korshunov et al., 1997; Starkov et al., 2002; Starkov and Fiskum, 2003) and others (Hansford et al., 1997; Votyakova and Reynolds, 2001) demonstrated that regardless of the nature of the respiratory substrate, rates of H_2O_2 production were directly related to the magnitude of the membrane potential of mitochondria. However, the difference in H_2O_2 production demonstrated in Figure 1 cannot be explained by the difference in the membrane potential because the concentration of FCCP (120 pmol/mg mitochondria) used in these experiments was selected

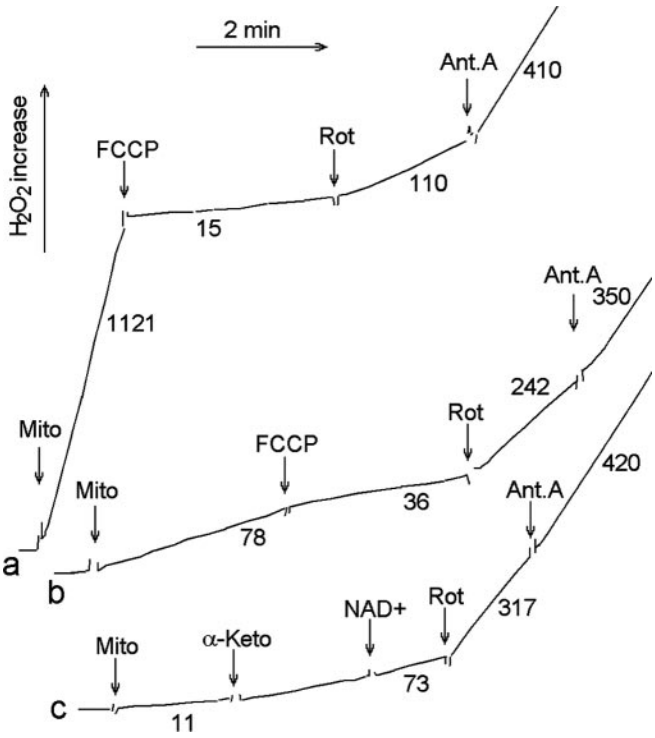

Figure 1. H_2O_2 production by rat brain mitochondria oxidizing α-ketoglutarate or succinate. Medium (37°C) contained 125 mM KCl, 2 mM $MgCl_2$, 0.2 mM EGTA, 2 mM KH_2PO_4, 10 mM HEPES, pH 7.2, 5 U/ml HRP, 20 U/ml superoxide dismutase, and 1 μM Amplex Red. Curve a, Rat brain mitochondria oxidizing succinate (10 mM); curves b and c, rat brain mitochondria oxidizing α-ketoglutarate. Additions included 0.25 mg/ml rat brain mitochondria (Mito), 5 mM α-ketoglutarate (α-Keto), 0.5 μM rotenone (Rot), 1 mM NAD^+, 120 pmol/mg FCCP, and 1 μM antimycin (Ant.A). Numbers near the tracings indicate the rates of H_2O_2 production in picomoles per minute per milligram of mitochondrial protein. Typical tracings are shown.

to completely uncouple mitochondria so that no membrane potential could be detected under these conditions by either the TPP^+ electrode or safranine fluorescence method, and no additional increase in FCCP concentration would stimulate the respiration of brain mitochondria (data not presented). Previously, we demonstrated that at such low values the membrane potential no longer affects the H_2O_2 production supported by either succinate (Korshunov et al., 1997) or a NAD-dependent substrate (Starkov and Fiskum, 2003).

We (Starkov and Fiskum, 2003) and others (Kushnareva et al., 2002) also observed that with a NAD^+-dependent substrate, the rate of H_2O_2 production was apparently modulated by the level of NADPH reduction in mitochondria. However, it is obvious that such a modulation could not explain the finding that rotenone inhibition of complex I induced much higher H_2O_2 production when α-ketoglutarate was the substrate (Fig. 1, traces b, c) compared with succinate-supported H_2O_2 production (Fig. 1, trace a). In these experiments, a sufficiently high concentration of rotenone was used (0.5 μM) that completely inhibited NADH oxidation (judging by the complete inhibition of respiration with pyruvate plus malate or glutamate plus malate; data not shown). Intuitively, one would expect essentially similar levels of the intramitochondrial NADPH reduction state when the oxidation of NADH is completely inhibited with rotenone, as in our experiments. If mitochondrial complex I is a sole source of H_2O_2 under such conditions, it seems difficult to understand why rotenone-inhibited complex I produces less H_2O_2 when its substrate NADH was reduced by succinate rather than by α-ketoglutarate.

It appeared that rates of H_2O_2 production varied significantly among different NAD^+-linked substrates both in the absence (Fig. 2*A*) and in the presence (Fig. 2*B*) of the complex I inhibitor rotenone. The rates of H_2O_2 generation were not directly related to relative rates of state 4 (Fig. 2*C*) or state 3 (Fig. 2*D*) respiration. With most NAD^+-dependent substrates, there was a reasonably good correlation between the level of NADPH reduction and the rate of H_2O_2 emission. However, α-ketoglutarate-supported H_2O_2 production was higher than expected under both conditions and did not correlate with the level of reduction of matrix pyridine nucleotides in either the presence or absence of rotenone (Fig. 2*A*,*B*). We therefore hypothesized that KGDHC itself could be a significant source of ROS.

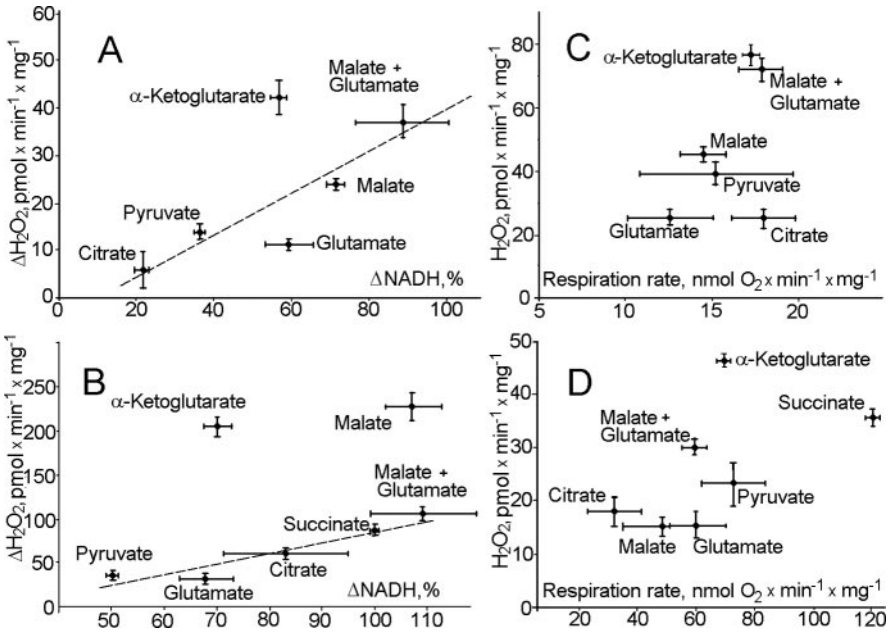

Figure 2. A typical relationship between H_2O_2 production rates by rat brain mitochondria oxidizing various substrates and the corresponding levels of reduction mitochondrial pyridine nucleotides and the rates of respiration. *A*, ΔH_2O_2 production by rat brain mitochondria in state 4. ΔNADPH was obtained by measuring the difference in NADPH fluorescence both in the absence and in the presence of 160 pmol/mg FCCP. ΔNADPH in the presence of succinate was taken as 100%. H_2O_2 production in the presence of succinate was 1123 ± 71 pmol/min/mg (data not shown). The H_2O_2 production rate in the presence of FCCP was subtracted from that in the absence of the uncoupler and presented as ΔH_2O_2. *B*, ΔH_2O_2 production rate plotted against ΔNADPH in the presence of 1 μM rotenone. *C*, H_2O_2 production rate plotted against the rate of respiration by mitochondria in state 4. *D*, H_2O_2 production rate plotted against the rate of respiration by mitochondria in state 3. Incubation medium (see Fig. 1) was maintained at 37°C. For *D* only, state 3 respiration was initiated by adding 0.4 mM ADP to mitochondrial suspension. Substrates were present at the following concentrations: malate and glutamate, 5 mM plus 5 mM; α-ketoglutarate, 7 mM; succinate, 5 mM; citrate, 5 mM; pyruvate, 10 mM; glutamate, 5 mM; malate, 5 mM. Mitochondria were added at 0.5 mg/ml.

In intact mitochondria, the activity of all dehydrogenases can affect each other through the common pool of pyridine nucleotides and through the inter-conversion of tricarboxylic acid (TCA) cycle metabolic intermediates. To test whether the rate of H_2O_2 production is substrate selective in the absence of this interconversion, we made mitochondria freely permeable to metabolites and other small molecules by the addition of the pore-forming peptide alamethicin (Gostimskaya et al., 2003). This treatment did not result in loss of malate dehydrogenase, pyruvate dehydrogenase, or KGDHC activities from the mitochondria (data not shown). Figure 3 shows that adding α-ketoglutarate stimulated H_2O_2 production in both alamethicin-permeabilized (Fig. 3, curves a, c) and intact (Fig. 3, curve b) rat brain mitochondria. Coenzyme A (CoA), a cofactor of KGDHC, stimulated H_2O_2 production only in alamethicin-treated mitochondria (Fig. 3, curves a, c) because it is impermeable to the inner membrane of intact mitochondria (Fig. 3, curve b); the addition of alamethicin stimulated H_2O_2 production in intact mitochondria by rendering their inner membrane permeable to CoA (Fig. 3, curve b). Catalase almost completely suppresses H_2O_2 production (Fig. 3, curve c). Under these conditions, the now-permeant NAD^+ inhibited H_2O_2 production (Fig. 3, curves a–c), whereas rotenone (Fig. 3, curves a, b) stimulated production because its ability to inhibit complex I of the mitochondrial electron transport chain does not require an intact inner membrane. It causes net reduction of NAD^+ to NADH and thereby overreduction of complex I and complex I-mediated ROS production in both intact and permeabilized mitochondria.

Results shown in Figure 4 indicate that both PDHC and KGDHC produce superoxide. The maximum superoxide production rate was obtained in the presence of all the same enzyme cofactors and substrates as needed for a normal enzymatic reaction catalyzed by these enzyme complexes. However, KGDHC produced approximately twice as much superoxide as PDHC (Fig. 4). As with permeabilized mitochondria (Fig. 3), NAD^+ inhibited superoxide production (Fig. 4). Malate dehydrogenase in the presence of either malate or oxaloacetate did not produce detectable amounts of superoxide (data not shown).

Both PDHC and KGDHC also produced H_2O_2. We explored

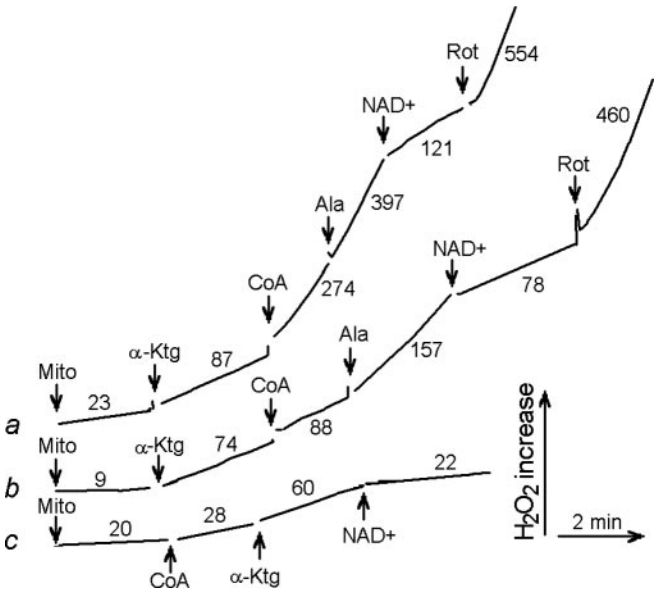

Figure 3. H_2O_2 production by permeabilized rat brain mitochondria. Incubation medium was composed of 225 mM mannitol, 75 mM sucrose, 10 mM HEPES-KOH, pH 7.4, 2 mM KH_2PO_4, 1 mM $MgCl_2$, 0.25 mM EGTA, 48 μM thiamine, 5 U/ml HRP, 20 U/ml superoxide dismutase, and 1 μM Amplex Red ($t = 37$°C). Curve a, Mitochondria (Mito; 1 mg) were incubated for 5 min with 20 μg/mg alamethicin, then centrifuged at 20,000 × *g* for 10 min and resuspended at 0.5 mg/ml for H_2O_2 measurement; curve b, intact rat brain mitochondria; curve c, mitochondria were pretreated as in curve a; 0.25 mg/ml catalase was included into the incubation medium. Additions included 10 mM α-ketoglutarate (α-Ktg), 0.2 mM NAD^+, 0.12 mM CoASH (CoA), 1 μM rotenone (Rot), and 20 μg/mg alamethicin (Ala).

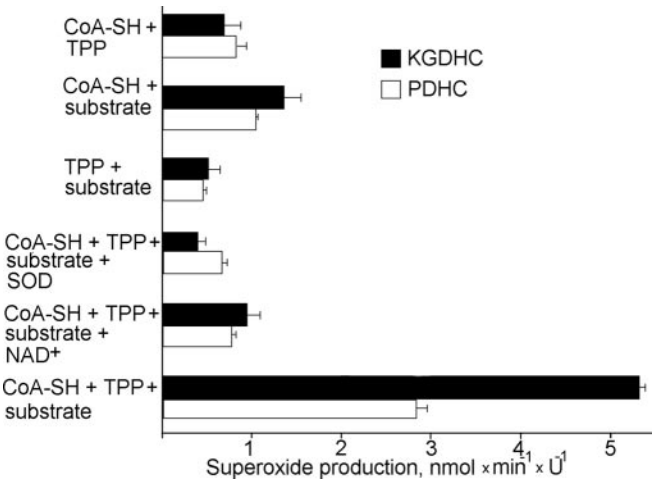

Figure 4. Cofactor and substrate dependence of superoxide production by isolated KGDHC and PDHC. Superoxide production was measured as described in Materials and Methods. Incubation medium contained 50 mM KH_2PO_4 buffer, pH 7.8, 50 μM acetylated cytochrome *c*, 10 μM $CaCl_2$, and 0.2 mM $MgCl_2$, maintained at $t = 37$°C. Where indicated, 0.12 mM CoASH, 0.3 mM TPP, 40 U/ml superoxide dismutase (SOD), 2 mM NAD^+, and either 10 mM ketoglutarate (for KGDHC) or 7 mM pyruvate (for PDHC) were included into the incubation medium (substrate). Reaction was started by adding 0.9–3.6 U/ml PDHC or 0.6–2.4 U/ml KGDHC.

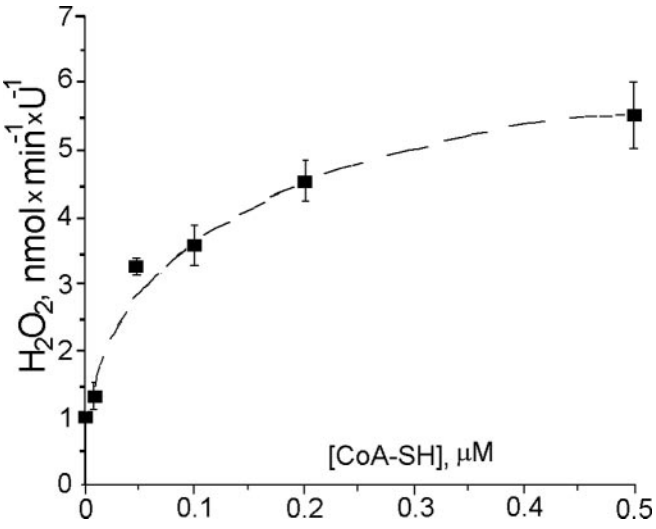

Figure 5. CoA-SH dependence of H_2O_2 production by isolated KGDHC. H_2O_2 production was measured as described in Materials and Methods. Incubation medium contained 50 mM KH_2PO_4 buffer, pH 7.8, 10 μM $CaCl_2$, 0.2 mM $MgCl_2$, 0.3 mM TPP, 40 U/ml superoxide dismutase (SOD), 5 U/ml HRP, and 1 μM Amplex Red, maintained at $t = 37$°C. Medium was supplemented with 10 mM ketoglutarate.

the substrate and cofactor dependence for H_2O_2 production and for NAD^+ reduction catalyzed by KGDHC. The H_2O_2 production rate by isolated KGDHC exhibited hyperbolic dose dependence to concentrations of CoA-SH (Fig. 5) and α-ketoglutarate (data not shown; more details can be found in an accompanying report by Tretter and Adam-Vizi, 2004). However, CoA-SH requirements for maximum H_2O_2 production appeared to be much lower than that for maximum NAD^+ reduction; the apparent K_m for CoASH was ~0.03 μM for H_2O_2 production (Fig. 5), whereas the K_m for NAD^+ reduction was ~30 μM (data not shown).

We also measured enzymatic activities of PDHC and KGDHC in alamethicin-permeabilized rat brain mitochondria (see Materials and Methods). We found that PDHC activity was 0.245 U/mg mitochondria and that of KGDHC was 0.215 U/mg. Assuming that PDHC and KGDHC produce superoxide (Fig. 4) as their primary ROS, and that two superoxide molecules dismutate to produce one H_2O_2 molecule, we calculated that mitochondria produce a maximum of ~560 pmol of H_2O_2/mg protein with α-ketoglutarate as substrate and ~330 pmol of H_2O_2/mg protein with pyruvate, whereas minimum rates (in the presence of NAD^+) are ~70 and ~90 pmol of H_2O_2/mg protein, respectively. These values are remarkably similar to the actual rates of H_2O_2 production observed with rat brain mitochondria, particularly for α-ketoglutarate (Figs. 1–3). Altogether, these results indicate that the Dld component of KGDHC, and to a lesser degree of PDHC, may be an important constitutive source of ROS in mitochondria.

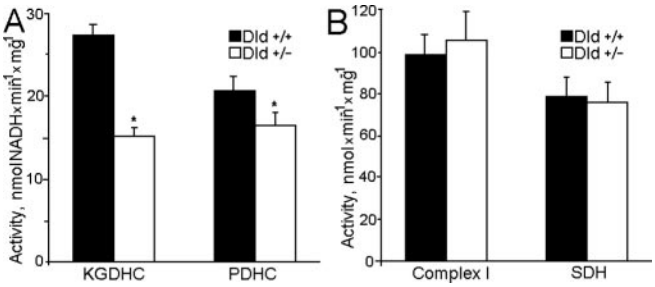

Figure 6. Activity of selected mitochondrial enzymes in brain mitochondria isolated from Dld-deficient mice compared with their littermate controls. *A*, Activity of KGDHC and PDHC. *B*, Activity of complex I (NADH:Q1 reductase) and SDH. KGDHC, PDHC, and SDH activities were measured as described in Materials and Methods. Mitochondrial complex I was measured with frozen–thawed mitochondrial samples fluorimetrically by following coenzyme Q1-induced rotenone-sensitive NADH oxidation at 346 nm excitation and 460 nm emission. Incubation medium was composed of 125 mM KCl, 2 mM $MgCl_2$, 2 mM KH_2PO_4, 0.2 mg/ml BSA, 10 μM $CaCl_2$, 2 mM KCN, 50 μM NADH, 20 μg/ml alamethicin, and 0.08–0.09 mg/ml mitochondria, at $t = 37$°C. Reaction was started by adding 40 μM coenzyme Q1 and terminated by adding 1 μM rotenone. Complex I activity was calculated as the difference between the NADH oxidation rate in the presence and in the absence of rotenone and presented in nanomole of NADH per minute per milligram. The scale was calibrated by adding known amounts of freshly prepared NADH.

Additional experiments used brain mitochondria isolated from knock-out heterozygous mice deficient in Dld ($Dld^{+/-}$). Although Dld is shared between PDHC and KGDHC, a deficiency in Dld affected primarily mitochondrial KGDHC enzyme activity (Fig. 6*A*). As expected, maximum respiration rates were reduced only when α-ketoglutarate was oxidized; there was no significant difference in maximum respiration rates or respira-

Table 1. Respiration of mouse brain mitochondria with different substrates

Substrate	State 3	State 4	ACR
Pyruvate plus malate			
Dld+/+	95.6 ± 9.7	6.2 ± 1.1	16.1 ± 1.3
Dld+/−	96.7 ± 5.7	6.7 ± 0.4	14.5 ± 1.0
Glutamate plus malate			
Dld+/+	98.4 ± 11.8	7.4 ± 0.9	13.4 ± 1.1
Dld−/+	87.4 ± 8.3	6.6 ± 0.8	13.5 ± 1.0
α-Ketoglutarate			
Dld+/+	40.2 ± 6.7	8.4 ± 1.4	4.9 ± 0.4
Dld−/+	26.8 ± 1.6	6.7 ± 0.7	4.1 ± 0.2
Succinate			
Dld+/+	38.7 ± 3.2	23.0 ± 2.6	1.7 ± 0.1
Dld−/+	36.2 ± 4.7	21.8 ± 1.4	1.6 ± 0.1

Mitochondria were isolated from brains of Dld-deficient mice and their littermate wild-type mice. Incubation medium was as in Figure 7. Substrates were added at the following concentrations: pyruvate plus malate, 7 plus 1 mM; glutamate plus malate, 5 plus 5 mM; α-ketoglutarate, 5 mM; succinate (in the absence of rotenone), 5 mM. State 4 was induced by carboxyatractylate. Respiration was measured as described in Materials and Methods. The numbers represent respiration rates expressed in nanomoles of O_2 per minute per milligram of mitochondria. ACR, Acceptor control index.

tory control index when mitochondria oxidized pyruvate plus malate, glutamate plus malate, or succinate (Table 1). Therefore, Dld deficiency apparently did not indirectly affect other parts of the respiratory chain, such as complex I or complex III. Measurements of complex I and complex II activity in alamethicin-permeabilized mitochondria supported this conclusion (Fig. 6*B*). However, H_2O_2 production rates by Dld $^{+/-}$ mitochondria were significantly reduced with either succinate or α-ketoglutarate during state 4 respiration (Fig. 7*A*) and were similarly reduced in the presence of the respiratory chain inhibitors rotenone (Fig. 7*B*) and antimycin A (Fig. 7*C*).

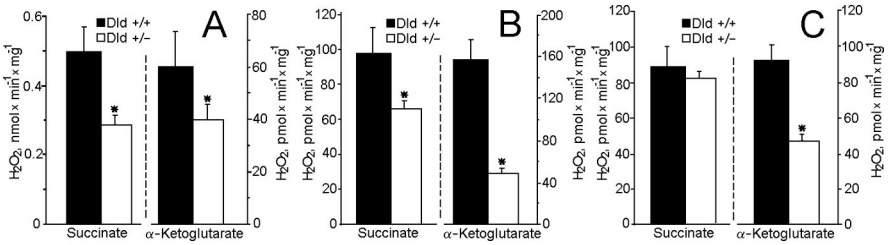

Figure 7. Hydrogen peroxide production by brain mitochondria isolated from Dld-deficient mice compared with their littermate wild-type mice. Incubation medium was as in Figure 1, except that EGTA was omitted and 0.4 mM ADP and 0.2 mg/ml BSA were included. Where indicated, 5 mM succinate or 5 mM α-ketoglutarate A were included into the medium. The sequence of additions was as follows: mitochondria (0.125 mg/ml) were added into the incubation medium and incubated for 2 min, then phosphorylation was inhibited with 1.2 μM carboxyatractylate and H_2O_2 production was measured as described in Materials and Methods (state 4); then 1 μM rotenone and, finally, 1 μM antimycin A were added into the incubation medium. *A*, H_2O_2 production in state 4. *B*, H_2O_2 production induced by rotenone. *C*, H_2O_2 production induced by antimycin A. In *B* for α-ketoglutarate only and in *C* for both α-ketoglutarate and succinate, the presented rate of H_2O_2 production was obtained by subtracting the rate of H_2O_2 production in state 4 from the rate induced by rotenone (*B*) and the rate in the presence of rotenone from that was induced by antimycin A (*C*).

Generally, the rate of H_2O_2 generation depends on the magnitude of the mitochondrial membrane potential (Hansford et al., 1997; Korshunov et al., 1997; Votyakova and Reynolds, 2001; Starkov et al., 2002; Starkov and Fiskum, 2003), which in turn depends on the metabolic state and the quality ("coupling") of mitochondria. Dld $^{+/-}$ mitochondria are deficient in KGDHC and therefore may possess lower membrane potential than Dld $^{+/+}$ mitochondria. The Percoll isolation procedure yields very tightly coupled, mostly nonsynaptic mitochondria possessing high membrane potential. Therefore, we used Percoll-isolated (see Materials and Methods) mitochondria to measure the membrane potential and H_2O_2 production by mouse brain mitochondria. It appeared that the amplitude of the membrane potential was virtually identical in both Dld $^{+/+}$ and Dld $^{+/-}$ mitochondria oxidizing either succinate (Fig. 8*A*) or α-ketoglutarate (Fig. 8*B*) either in the presence of ADP or in the resting state. Nevertheless, Dld $^{+/-}$ mitochondria produced significantly less H_2O_2 (Fig. 9) than Dld $^{+/+}$ mitochondria under all metabolic conditions, except state 3 (Fig. 9*A*).

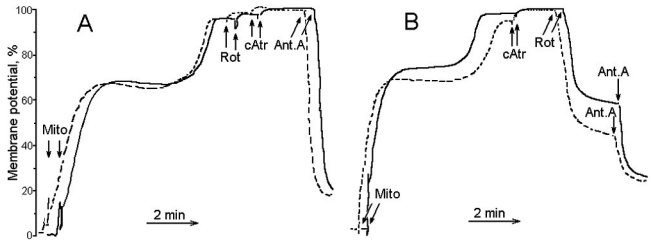

Figure 8. The membrane potential of mouse brain mitochondria oxidizing succinate or α-ketoglutarate. Mouse brain mitochondria were isolated by the Percoll gradient procedure (see Materials and Methods). Incubation medium contained 125 mM KCl, 2 mM $MgCl_2$, 2 mM KH_2PO_4, 10 mM HEPES, pH 7.2, 0.2 mg/ml BSA, 0.2 mM ADP, 5 mM succinate (*A*) or 5 mM α-ketoglurate (*B*), and 1 μM safranin O. Additions included 0.25 mg/ml mouse brain mitochondria (Mito), 1 μM rotenone (Rot), 1 μM carboxyatractylate (cAtr), and 1 μM antimycin A (Ant A). Typical tracings are shown. Solid lines, Dld $^{+/+}$ mitochondria; dotted lines, Dld $^{+/-}$ mitochondria.

We also measured the content and composition of coenzymes Q in mitochondrial membrane because there are several reports that the Q9/Q10 ratio and the total amount of coenzyme Q can affect ROS production (Boveris and Chance, 1973; Lass et al., 1997; Lass and Sohal, 1999, 2000). There was no difference in the Q9/Q10 ratio or coenzymes Q content in mitochondria from Dld $^{+/-}$ mice compared with their littermate controls (Fig. 10).

Discussion

Our data suggest that complex I of the mitochondrial electron transport chain is not the exclusive source of H_2O_2 and that the Dld components of KGDHC and PDHC are substantial constitutive sources of free radicals in rat and mouse brain mitochondria under conditions of the elevated mitochondrial NADPH/NADP $^+$ ratio.

Complex I of the mitochondrial electron transport chain has been viewed as a major site of mitochondrial ROS production (Barja, 1999; Herrero and Barja, 2000; Lenaz, 2001; Sipos et al., 2003). However, there are no data yet that demonstrate that complex I is the major site of ROS production in intact mitochondria, in the absence of respiratory chain inhibitors. There are three principal types of experiments that contributed to the concept that complex I is a major ROS-producing site: (1) experiments demonstrating that isolated complex I preparations generate ROS in the presence of NADH; (2) experiments with rotenone-inhibited mitochondria oxidizing NAD-dependent substrates; and (3) experiments with isolated mitochondria under conditions favoring reverse electron transfer from succinate to complex I. The latter reaction generates large amounts of ROS (Fig. 1, curve a) (Turrens, 1997; Lenaz, 2001; Votyakova and Reynolds, 2001). However, the possibility of reverse electron transfer under physiological conditions is not yet established. The interpretation of such experiments may be complicated because the source of ROS could be anything that is in a redox equilibrium with intramitochondrial NADPH. This difficulty also applies to experiments demonstrating the dependence of mitochondrial ROS production on the amplitude of the membrane potential (Hansford et al., 1997; Korshunov et al., 1997; Votyakova and Reynolds, 2001; Starkov and Fiskum, 2003) or intramitochondrial NADPH/NADP $^+$ ratio (Kushnareva et al., 2002; Starkov and Fiskum, 2003).

Several research groups have demonstrated that isolated complex I preparations can generate ROS when reduced with NADH, although there is no consensus about the site of ROS production in complex I (Lenaz, 2001; Kushnareva et al., 2002; Liu et al., 2002).

However, some evidence argues against the concept that complex I in mitochondria, or in submitochondrial particles, can generate ROS in the absence or even in the presence of its inhibitors. The absence of a correlation between the inhibition of complex I activity by rotenone and other inhibitors and the production of ROS by submitochondrial particles was interpreted as an

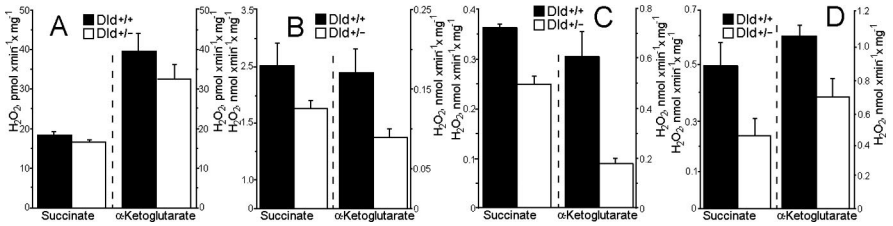

Figure 9. Hydrogen peroxide production by brain mitochondria isolated by the Percoll procedure from Dld-deficient mice compared with their littermate wild-type mice. Mouse brain mitochondria were isolated by the Percoll gradient procedure (see Materials and Methods). Incubation medium was as in Figure 8, except that safranin O was omitted and 5 U/ml HRP, 20 U/ml superoxide dismutase, and 1 μM Amplex Red were included. Where indicated, 5 mM succinate or 5 mM α-ketoglutarate A were included into the medium. The sequence of additions was as follows: mitochondria (0.1–0.125 mg/ml) were added into the incubation medium and incubated for 2 min, then phosphorylation was inhibited with 1.2 μM carboxyatractylate, then 1 μM rotenone and, finally, 1 μM antimycin A were added into the incubation medium. *A*, H_2O_2 production in state 3. *B*, H_2O_2 production in state 4. *C*, H_2O_2 production induced by rotenone. *D*, H_2O_2 production induced by antimycin A. In *C* for α-ketoglutarate only and in *D* for both α-ketoglutarate and succinate, the presented rate of H_2O_2 production was obtained by subtracting the rate of H_2O_2 production in state 4 from the rate induced by rotenone (*C*) and the rate in the presence of rotenone from that induced by antimycin A (*D*).

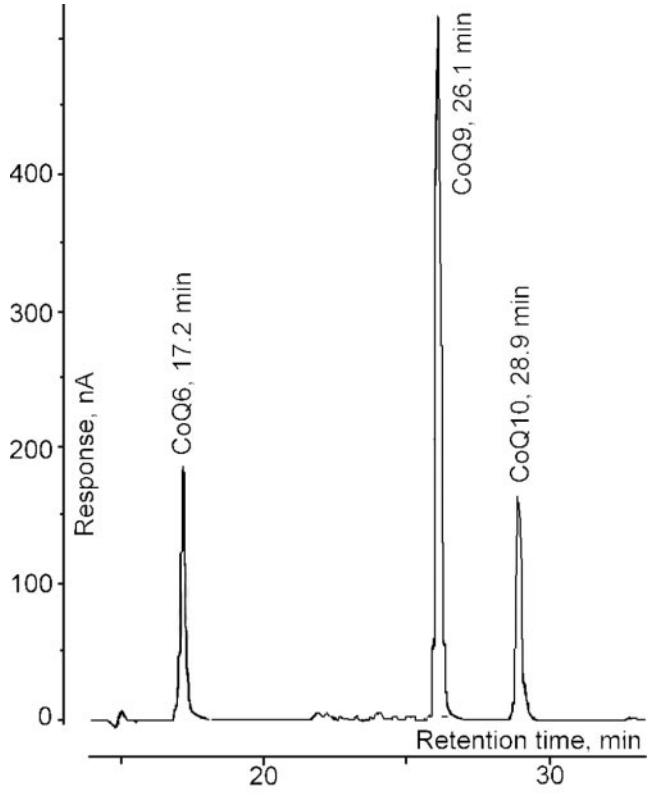

	Dld$^{+/+}$	Dld$^{+/-}$
CoQ9	0.66 ± 0.10	0.64 ± 0.12
CoQ10	0.22 ± 0.03	0.21 ± 0.03
Q9:Q10	2.95 ± 0.20	2.93 ± 0.20

Figure 10. Coenzyme Q9 and coenzyme Q10 content in brain mitochondria isolated from Dld-deficient mice compared with their littermate wild-type mice. Coenzymes Q9 and Q10 were measured by HPLC as described in Materials and Methods. Data are presented in picomole of quinone per milligram of mitochondria.

indication of the presence of a superoxide-producing rotenone-binding site other than complex I (Ramsay and Singer, 1992). The finding that H_2O_2 production is frequently reported as being almost absent in the presence of succinate and rotenone (Barja, 1999; Liu et al., 2002) is intriguing because the intramitochondrial NADPH/NADP$^+$ ratio under such conditions is high. Stimulatory effects of ADP (Barja, 1999) and Ca^{2+} (Dykens, 1994; Kowaltowski et al., 1995, 1996, 1998a,b) on mitochondrial ROS production are also puzzling because both Ca^{2+} uptake/retention and ADP-induced oxidative phosphorylation dissipate energy and would be expected to decrease the level of reduction of complex I and hence the ROS production. It also appears that the stimulatory effect of the complex I inhibitor rotenone on ROS production that possibly originates from a site within complex I is species and tissue dependent; ROS stimulation by rotenone varies from ~300% in guinea pig to 0% in horse heart submitochondrial particles (Herrero and Barja, 2000) and in whole intact rat heart mitochondria (Chen et al., 2003) to inhibition of ROS production in mouse kidney mitochondria (Kwong and Sohal, 1998).

Our data indicate that KGDHC may be a major ROS-producing site in mitochondria. Mammalian KGDHC is composed of multiple copies of three enzymes: α-ketoglutarate dehydrogenase (E1; EC 1.2.4.2), dihydrolipoamide succinyltransferase (E2; EC 2.3.1.12), and Dld (E3 or Dld; EC 1.6.4.3). E1 and E3 are noncovalently bound to a core formed by E2 (Wagenknecht et al., 1983; Sheu and Blass, 1999). Dld is also a part of other multienzyme complexes such as PDHC, branched chain ketoacid dehydrogenase complex, and glycine cleavage complex (Koike et al., 1974; Patel and Roche, 1990; Reed and Hackert, 1990). Dld is a flavoenzyme, the redox center of which is formed by a disulfide bridge coupled with a flavin ring. The catalyzed reaction proceeds via the formation of a charge transfer complex between those two groups (Matthews et al., 1977; Templeton et al., 1980). The catalytic mechanism of α-ketoacid dehydrogenase complexes was reviewed by Bunik (2003).

In the context of the enzymatic mechanism, results of experiments with isolated PDHC and KGDHC point to the flavin or the neighboring disulfide bridge in the catalytic center of the Dld component as an electron donor for superoxide formation. This explanation is in agreement with another recently published study (Bunik and Sievers, 2002) indicating that the flavin of the Dld component of KGDHC is involved in superoxide generation.

It is not clear yet why α-ketoglutarate-supported (and presumably, KGDHC-mediated) ROS production is much higher than pyruvate-supported production (Fig. 2) because both KGDHC and PDHC share the Dld component that generates ROS (Zhang et al., 1998). The reason for this discrepancy may be related to differing composition and molecular organization of these large enzyme complexes.

KGDHC activity is regulated by multiple mechanisms. The enzyme is inhibited by its own product, succinyl–CoA, by a high NADH/NAD$^+$ ratio as well as by a high dihydrolipoate/lipoate ratio, thereby playing an important role in cellular redox regulation (Bunik, 2003). KGDHC is activated by low concentrations of Ca^{2+} and matrix ADP (Hamada et al., 1975; McMinn and Ottaway, 1977; LaNoue et al., 1983; Wan et al., 1989; Kiselevsky et al., 1990). Considering that KGDHC-mediated ROS production requires a fully active complex with all the cofactors and substrates (except NAD$^+$) (Figs. 4, 5), the fact that the enzyme

activity is stimulated by Ca^{2+} and ADP may perhaps account for previous findings that mitochondrial ROS production was increased by Ca^{2+} (Dykens, 1994; Kowaltowski et al., 1995, 1996, 1998a,b), Ca^{2+} in the presence of rotenone and succinate (Starkov et al., 2002), and by ADP (Barja, 1999). The results presented in the accompanying report by Tretter and Adam-Vizi (2004) demonstrate that Ca^{2+} activated ROS production by isolated KGDHC both in the presence and in the absence of pyridine nucleotides.

It is well known that the activity of KGDHC is severely reduced in a variety of neurodegenerative diseases associated with impaired mitochondrial functions, including Alzheimer's and Parkinson's diseases. However, the relationship between KGDHC activity and mitochondrial damage per se is much less clear. KGDHC is an integral mitochondrial enzyme tightly bound to the inner mitochondrial membrane on the matrix side (Maas and Bisswanger, 1990). It binds (specifically) to complex I of the mitochondrial respiratory chain (Sumegi and Srere, 1984) and may form a part of the TCA cycle enzyme supercomplex (Lyubarev and Kurganov, 1989). The mitochondrial TCA cycle enzymes aconitase, succinate dehydrogenase (SDH), and KGDHC itself are sensitive to oxidative inactivation both *in vitro* and *in vivo* (Tretter and Adam-Vizi, 2000; Gibson et al., 2002; Sadek et al., 2002). The close spatial and functional relationship of KGDHC to sensitive TCA cycle enzymes may result in specific targeting and damage to these enzymes by KGDHC-originated ROS. Mitochondria from different brain regions possess different amounts of KGDHC (Calingasan et al., 1994; Park et al., 2000), which may account for regional vulnerability. For instance, the cholinergic neurons of the nucleus basalis of Meynert have high levels of KGDHC, and these neurons are particularly vulnerable in Alzheimer's disease (Gibson et al., 1988). The conditions promoting KGDHC-mediated ROS production may be any that increase the intramitochondrial NADH/NAD^+ ratio (e.g., inhibition of oxidative phosphorylation or inhibition of any segment of the mitochondrial electron transport chain). This hypothesis is strongly supported by the results presented in the accompanying report by Tretter and Adam-Vizi (2004) that demonstrated that ROS production by isolated KGDHC is strongly dependent on the NADH/NAD^+ ratio. It also agrees well with the recent demonstration of a selective loss of KGDHC-enriched neurons in human brains with Alzheimer's disease (Ko et al., 2001). [Alternatively, as Dr. John Blass pointed out (personal communication), a regulatory mechanism might be in place decreasing the expression and/or assembly of a functional KGDH complex in response to the oxidative stress induced by either damage to mitochondria leading to an increase in their overall reduction potential, or by an oxidants external to mitochondria.]

In this respect, it is very interesting that the *DLST* gene encoding the E2 component of KGDHC also encodes truncated mRNA for another protein designated MIRTD that localizes to mitochondria, where it regulates the biogenesis of the mitochondrial respiratory chain (Kanamori et al., 2003).

In conclusion, we emphasize that although results presented here, and particularly those with Dld-deficient mice (Fig. 7), indicate that the Dld component of KGDHC may be a significant source of ROS in mitochondria, they do not rule out complex I (or other potential sites) as important sources of ROS. In fact, results of substrate-dependent ROS production experiments (Fig. 2*B*) indicate that some other dehydrogenases might also be involved in ROS production. The results presented here challenge the idea of a single "major" site of ROS production in mitochondria, whether it be complexes I, II, and III or the Dld component, and emphasize the necessity of additional systematic research on the mechanisms and regulation of mitochondrial ROS production.

References

Arrigoni O, Singer TP (1962) Limitations of the phenazine methosulphate assay for succinic and related dehydrogenases. Nauchni Tr Vissh Med Inst Sofiia 193:1256–1258.

Azzi A, Montecucco C, Richter C (1975) The use of acetylated ferricytochrome c for the detection of superoxide radicals produced in biological membranes. Biochem Biophys Res Commun 65:597–603.

Barja G (1999) Mitochondrial oxygen radical generation and leak: sites of production in states 4 and 3, organ specificity, and relation to aging and longevity. J Bioenerg Biomembr 31:347–366.

Boveris A, Chance B (1973) The mitochondrial generation of hydrogen peroxide. General properties and effect of hyperbaric oxygen. Biochem J 134:707–716.

Bunik VI (2003) 2-Oxo acid dehydrogenase complexes in redox regulation. Eur J Biochem 270:1036–1042.

Bunik VI, Sievers C (2002) Inactivation of the 2-oxo acid dehydrogenase complexes upon generation of intrinsic radical species. Eur J Biochem 269:5004–5015.

Calingasan NY, Baker H, Sheu KF, Gibson GE (1994) Distribution of the alpha-ketoglutarate dehydrogenase complex in rat brain. J Comp Neurol 346:461–479.

Chan PC, Bielski BH (1974) Enzyme-catalyzed free radical reactions with nicotinamide adenine nucleotides. II. Lactate dehydrogenase-catalyzed oxidation of reduced nicotinamide adenine dinucleotide by superoxide radicals generated by xanthine oxidase. J Biol Chem 249:1317–1319.

Chan PC, Bielski BH (1980) Glyceraldehyde-3-phosphate dehydrogenase-catalyzed chain oxidation of reduced nicotinamide adenine dinucleotide by perhydroxyl radicals. J Biol Chem 255:874–876.

Chen Q, Vazquez EJ, Moghaddas S, Hoppel CL, Lesnefsky EJ (2003) Production of reactive oxygen species by mitochondria: central role of complex III. J Biol Chem 278:36027–36031.

Chinopoulos C, Starkov AA, Fiskum G (2003) Cyclosporin A-insensitive permeability transition in brain mitochondria: inhibition by 2-aminoethoxydiphenyl borate. J Biol Chem 278:27382–27389.

Cino M, Del Maestro RF (1989) Generation of hydrogen peroxide by brain mitochondria: the effect of reoxygenation following postdecapitative ischemia. Arch Biochem Biophys 269:623–638.

Di Lisa F, Menabo R, Canton M, Barile M, Bernardi P (2001) Opening of the mitochondrial permeability transition pore causes depletion of mitochondrial and cytosolic NAD+ and is a causative event in the death of myocytes in postischemic reperfusion of the heart. J Biol Chem 276:2571–2575.

Dykens JA (1994) Isolated cerebral and cerebellar mitochondria produce free radicals when exposed to elevated CA2+ and Na+: implications for neurodegeneration. J Neurochem 63:584–591.

Fiskum G (2000) Mitochondrial participation in ischemic and traumatic neural cell death. J Neurotrauma 17:843–855.

Fiskum G, Murphy AN, Beal MF (1999) Mitochondria in neurodegeneration: acute ischemia and chronic neurodegenerative diseases. J Cereb Blood Flow Metab 19:351–369.

Gamache PH, Freeto SM, Acworth IN (1999) Coulometric array HPLC analysis of lipid-soluble vitamins and antioxidants. Amer Clin Lab 18:18–19.

Gibson GE, Sheu KF, Blass JP, Baker A, Carlson KC, Harding B, Perrino P (1988) Reduced activities of thiamine-dependent enzymes in the brains and peripheral tissues of patients with Alzheimer's disease. Arch Neurol 45:836–840.

Gibson GE, Zhang H, Xu H, Park LC, Jeitner TM (2002) Oxidative stress increases internal calcium stores and reduces a key mitochondrial enzyme. Biochim Biophys Acta 1586:177–189.

Gostimskaya IS, Grivennikova VG, Zharova TV, Bakeeva LE, Vinogradov AD (2003) In situ assay of the intramitochondrial enzymes: use of alamethicin for permeabilization of mitochondria. Anal Biochem 313:46–52.

Hamada M, Koike K, Nakaula Y, Hiraoka T, Koike M (1975) A kinetic study of the alpha-keto acid dehydrogenase complexes from pig heart mitochondria. J Biochem (Tokyo) 77:1047–1056.

Hansford RG, Hogue BA, Mildaziene V (1997) Dependence of H2O2 for-

mation by rat heart mitochondria on substrate availability and donor age. J Bioenerg Biomembr 29:89–95.
Hensley K, Pye QN, Maidt ML, Stewart CA, Robinson KA, Jaffrey F, Floyd RA (1998) Interaction of alpha-phenyl-*N*-tert-butyl nitrone and alternative electron acceptors with complex I indicates a substrate reduction site upstream from the rotenone binding site. J Neurochem 71:2549–2557.
Herrero A, Barja G (2000) Localization of the site of oxygen radical generation inside the complex I of heart and nonsynaptic brain mammalian mitochondria. J Bioenerg Biomembr 32:609–615.
Johnson MT, Yang HS, Magnuson T, Patel MS (1997) Targeted disruption of the murine dihydrolipoamide dehydrogenase gene (Dld) results in perigastrulation lethality. Proc Natl Acad Sci USA 94:14512–14517.
Kanamori T, Nishimaki K, Asoh S, Ishibashi Y, Takata I, Kuwabara T, Taira K, Yamaguchi H, Sugihara S, Yamazaki T, Ihara Y, Nakano K, Matuda S, Ohta S (2003) Truncated product of the bifunctional DLST gene involved in biogenesis of the respiratory chain. EMBO J 22:2913–2923.
Kiselevsky YV, Ostrovtsova SA, Strumilo SA (1990) Kinetic characterization of the pyruvate and oxoglutarate dehydrogenase complexes from human heart. Acta Biochim Pol 37:135–139.
Ko LW, Sheu KF, Thaler HT, Markesbery WR, Blass JP (2001) Selective loss of KGDHC-enriched neurons in Alzheimer temporal cortex: does mitochondrial variation contribute to selective vulnerability? J Mol Neurosci 17:361–369.
Koike K, Hamada M, Tanaka N, Otsuka KI, Ogasahara K, Koike M (1974) Properties and subunit composition of the pig heart 2-oxoglutarate dehydrogenase. J Biol Chem 249:3836–3842.
Korshunov SS, Skulachev VP, Starkov AA (1997) High protonic potential actuates a mechanism of production of reactive oxygen species in mitochondria. FEBS Lett 416:15–18.
Kowaltowski AJ, Castilho RF, Vercesi AE (1995) Ca(2+)-induced mitochondrial membrane permeabilization: role of coenzyme Q redox state. Am J Physiol 269:C141–C147.
Kowaltowski AJ, Castilho RF, Vercesi AE (1996) Opening of the mitochondrial permeability transition pore by uncoupling or inorganic phosphate in the presence of Ca2+ is dependent on mitochondrial-generated reactive oxygen species. FEBS Lett 378:150–152.
Kowaltowski AJ, Netto LE, Vercesi AE (1998a) The thiol-specific antioxidant enzyme prevents mitochondrial permeability transition. Evidence for the participation of reactive oxygen species in this mechanism. J Biol Chem 273:12766–12769.
Kowaltowski AJ, Naia-da-Silva ES, Castilho RF, Vercesi AE (1998b) Ca2+-stimulated mitochondrial reactive oxygen species generation and permeability transition are inhibited by dibucaine or Mg2+. Arch Biochem Biophys 359:77–81.
Kunz WS, Gellerich FN (1993) Quantification of the content of fluorescent flavoproteins in mitochondria from liver, kidney cortex, skeletal muscle, and brain. Biochem Med Metab Biol 50:103–110.
Kunz WS, Kunz W (1985) Contribution of different enzymes to flavoprotein fluorescence of isolated rat liver mitochondria. Biochim Biophys Acta 841:237–246.
Kushnareva Y, Murphy AN, Andreyev A (2002) Complex I-mediated reactive oxygen species generation: modulation by cytochrome c and NAD(P)+ oxidation-reduction state. Biochem J 368:545–553.
Kwong LK, Sohal RS (1998) Substrate and site specificity of hydrogen peroxide generation in mouse mitochondria. Arch Biochem Biophys 350:118–126.
LaNoue KF, Schoolwerth AC, Pease AJ (1983) Ammonia formation in isolated rat liver mitochondria. J Biol Chem 258:1726–1734.
Lass A, Sohal RS (1999) Comparisons of coenzyme Q bound to mitochondrial membrane proteins among different mammalian species. Free Radic Biol Med 27:220–226.
Lass A, Sohal RS (2000) Effect of coenzyme Q(10) and alpha-tocopherol content of mitochondria on the production of superoxide anion radicals. FASEB J 14:87–94.
Lass A, Agarwal S, Sohal RS (1997) Mitochondrial ubiquinone homologues, superoxide radical generation, and longevity in different mammalian species. J Biol Chem 272:19199–19204.
Lenaz G (2001) The mitochondrial production of reactive oxygen species: mechanisms and implications in human pathology. IUBMB Life 52:159–164.
Liu Y, Fiskum G, Schubert D (2002) Generation of reactive oxygen species by the mitochondrial electron transport chain. J Neurochem 80:780–787.
Lyubarev AE, Kurganov BI (1989) Supramolecular organization of tricarboxylic acid cycle enzymes. Biosystems 22:91–102.
Maas E, Bisswanger H (1990) Localization of the alpha-oxoacid dehydrogenase multienzyme complexes within the mitochondrion. FEBS Lett 277:189–190.
Marquez LA, Dunford HB (1995) Transient and steady-state kinetics of the oxidation of scopoletin by horseradish peroxidase compounds I, II and III in the presence of NADH. Eur J Biochem 233:364–371.
Massey V (1994) Activation of molecular oxygen by flavins and flavoproteins. J Biol Chem 269:22459–22462.
Matthews RG, Ballou DP, Thorpe C, Williams Jr CH (1977) Ion pair formation in pig heart lipoamide dehydrogenase: rationalization of pH profiles for reactivity of oxidized enzyme with dihydrolipoamide and 2-electron-reduced enzyme with lipoamide and iodoacetamide. J Biol Chem 252:3199–3207.
McMinn CL, Ottaway JH (1977) Studies on the mechanism and kinetics of the 2-oxoglutarate dehydrogenase system from pig heart. Biochem J 161:569–581.
Murphy AN, Fiskum G, Beal MF (1999) Mitochondria in neurodegeneration: bioenergetic function in cell life and death. J Cereb Blood Flow Metab 19:231–245.
Nicholls DG, Budd SL (2000) Mitochondria and neuronal survival. Physiol Rev 80:315–360.
Park LC, Calingasan NY, Sheu KF, Gibson GE (2000) Quantitative alpha-ketoglutarate dehydrogenase activity staining in brain sections and in cultured cells. Anal Biochem 277:86–93.
Patel MS, Roche TE (1990) Molecular biology and biochemistry of pyruvate dehydrogenase complexes. FASEB J 4:3224–3233.
Patole MS, Swaroop A, Ramasarma T (1986) Generation of H2O2 in brain mitochondria. J Neurochem 47:1–8.
Ramsay RR, Singer TP (1992) Relation of superoxide generation and lipid peroxidation to the inhibition of NADH-Q oxidoreductase by rotenone, piericidin A, and MPP+. Biochem Biophys Res Commun 189:47–52.
Reed LJ, Hackert ML (1990) Structure-function relationships in dihydrolipoamide acyltransferases. J Biol Chem 265:8971–8974.
Rosenthal RE, Hamud F, Fiskum G, Varghese PJ, Sharpe S (1987) Cerebral ischemia and reperfusion: prevention of brain mitochondrial injury by lidoflazine. J Cereb Blood Flow Metab 7:752–758.
Sadek HA, Humphries KM, Szweda PA, Szweda LI (2002) Selective inactivation of redox-sensitive mitochondrial enzymes during cardiac reperfusion. Arch Biochem Biophys 406:222–228.
Sheu KF, Blass JP (1999) The alpha-ketoglutarate dehydrogenase complex. Ann NY Acad Sci 893:61–78.
Sims NR (1990) Rapid isolation of metabolically active mitochondria from rat brain and subregions using Percoll density gradient centrifugation. J Neurochem 55:698–707.
Sims NR, Williams VK, Zaidan E, Powell JA (1998) The antioxidant defences of brain mitochondria during short-term forebrain ischemia and recirculation in the rat. Brain Res Mol Brain Res 60:141–149.
Sipos I, Tretter L, Adam-Vizi V (2003) Quantitative relationship between inhibition of respiratory complexes and formation of reactive oxygen species in isolated nerve terminals. J Neurochem 84:112–118.
Sorgato MC, Sartorelli L, Loschen G, Azzi A (1974) Oxygen radicals and hydrogen peroxide in rat brain mitochondria. FEBS Lett 45:92–95.
Starkov A, Fiskum G (2002) Generation of reactive oxygen species by brain mitochondria mediated by alpha-ketoglutarate dehydrogenase. Soc Neurosci Abstr 28:194.17.
Starkov AA, Fiskum G (2001) Myxothiazol induces H(2)O(2) production from mitochondrial respiratory chain. Biochem Biophys Res Commun 281:645–650.
Starkov AA, Fiskum G (2003) Regulation of brain mitochondrial H2O2 production by membrane potential and NAD(P)H redox state. J Neurochem 86:1101–1107.
Starkov AA, Polster BM, Fiskum G (2002) Regulation of hydrogen peroxide production by brain mitochondria by calcium and Bax. J Neurochem 83:220–228.
Sumegi B, Srere PA (1984) Complex I binds several mitochondrial NAD-coupled dehydrogenases. J Biol Chem 259:15040–15045.
Templeton DM, Hollebone BR, Tsai CS (1980) Magnetic circular dichroism studies on the active-site flavin of lipoamide dehydrogenase. Biochemistry 19:3868–3873.
Tischler ME, Hecht P, Williamson JR (1977) Effect of ammonia on mito-

chondrial and cytosolic NADH and NADPH systems in isolated rat liver cells. FEBS Lett 76:99–104.

Tretter L, Adam-Vizi V (2000) Inhibition of Krebs cycle enzymes by hydrogen peroxide: a key role of [alpha]-ketoglutarate dehydrogenase in limiting NADH production under oxidative stress. J Neurosci 20:8972–8979.

Tretter L, Adam-Vizi V (2004) Generation of reactive oxygen species in the reaction catalyzed by α-ketoglutarate dehydrogenase. J Neurosci 24:7771–7778.

Turrens JF (1997) Superoxide production by the mitochondrial respiratory chain. Biosci Rep 17:3–8.

Votyakova TV, Reynolds IJ (2001) DeltaPsi(m)-dependent and -independent production of reactive oxygen species by rat brain mitochondria. J Neurochem 79:266–277.

Wagenknecht T, Francis N, DeRosier DJ (1983) Alpha-ketoglutarate dehydrogenase complex may be heterogeneous in quaternary structure. J Mol Biol 165:523–539.

Wan B, LaNoue KF, Cheung JY, Scaduto Jr RC (1989) Regulation of citric acid cycle by calcium. J Biol Chem 264:13430–13439.

Zhang L, Yu L, Yu CA (1998) Generation of superoxide anion by succinate-cytochrome c reductase from bovine heart mitochondria. J Biol Chem 273:33972–33976.

Zhou M, Diwu Z, Panchuk-Voloshina N, Haugland RP (1997) A stable nonfluorescent derivative of resorufin for the fluorometric determination of trace hydrogen peroxide: applications in detecting the activity of phagocyte NADPH oxidase and other oxidases. Anal Biochem 253:162–168.

Journal of Bioenergetics and Biomembranes, Vol. 36, No. 4, August 2004 (© 2004)

Protection Against Ischemic Brain Injury by Inhibition of Mitochondrial Oxidative Stress

Gary Fiskum,[1,2,6] Robert E. Rosenthal,[1,2] Viktoria Vereczki,[1] Erica Martin,[1,2] Gloria E. Hoffman,[2,4] Christos Chinopoulos,[1] and Alicia Kowaltowski[5]

Received March 14, 2004; accepted May 7, 2004

Mitochondria are both targets and sources of oxidative stress. This dual relationship is particularly evident in experimental paradigms modeling ischemic brain injury. One mitochondrial metabolic enzyme that is particularly sensitive to oxidative inactivation is pyruvate dehydrogenase. This reaction is extremely important in the adult CNS that relies very heavily on carbohydrate metabolism, as it represents the sole bridge between anaerobic and aerobic metabolism. Oxidative injury to this enzyme and to other metabolic enzymes proximal to the electron transport chain may be responsible for the oxidized shift in cellular redox state that is observed during approximately the first hour of cerebral reperfusion. In addition to impairing cerebral energy metabolism, oxidative stress is a potent activator of apoptosis. The mechanisms responsible for this activation are poorly understood but likely involve the expression of p53 and possibly direct effects of reactive oxygen species on mitochondrial membrane proteins and lipids. Mitochondria also normally generate reactive oxygen species and contribute significantly to the elevated net production of these destructive agents during reperfusion. Approaches to inhibiting pathologic mitochondrial generation of reactive oxygen species include mild uncoupling, pharmacologic inhibition of the membrane permeability transition, and simply lowering the concentration of inspired oxygen. Antideath mitochondrial proteins of the Bcl-2 family also confer cellular resistance to oxidative stress, paradoxically through stimulation of mitochondrial free radical generation and secondary upregulation of antioxidant gene expression.

KEY WORDS: Superoxide; nitric oxide; peroxynitrite; pyruvate dehydrogenase; calcium; apoptosis.

MITOCHONDRIAL TARGETS OF OXIDATIVE STRESS

Several lines of evidence indicate that oxidative stress is a primary mediator of neurologic injury following cerebral ischemia. The extent of delayed neuronal death correlates well with prelethal markers of oxidative molecular alterations. Neuroprotection is observed following the use of antioxidants and inhibitors of free radical producing enzymes, e.g., nitric-oxide synthetase. In addition, neuroprotection is evident in genetic animal models where genes coding for enzymes that promote oxidative stress are knocked down or out, and where genes coding for antioxidant enzymes, e.g., superoxide dismutase (SOD) are overexpressed (see (Lewen *et al*., 2000) for review).

Virtually every cellular and extracellular molecular component is potentially sensitive to damage caused by oxidative stress. Oxidative modification to DNA, RNA, proteins, lipids, and small metabolites occur during ischemia/reperfusion. Our research focuses on the mitochondrion and its components as both targets and mediators of oxidative reperfusion injury (Fiskum *et al*., 1999; Murphy *et al*., 1999). From both in vitro studies with

[1] Department of Anesthesiology, University of Maryland School of Medicine, 685 W. Baltimore St., MSTF 5.34, Baltimore, Maryland 21201.
[2] Program in Neuroscience, University of Maryland School of Medicine, Baltimore, Maryland.
[3] Program in Trauma Department of Surgery, University of Maryland School of Medicine, Baltimore, Maryland.
[4] Department of Anatomy and Neurobiology, University of Maryland School of Medicine, Baltimore, Maryland.
[5] Departamento de Bioquímica, Instituto de Química, Universidade de São Paulo, SP, Brazil.
[6] To whom correspondence should be addressed; e-mail: gfisk001@umaryland.edu.

0145-479X/04/0800-0347/0

neural cells (Myers *et al*., 1995) and animal models of global cerebral ischemia (Liu *et al*., 1998), we conclude that mitochondrial energy metabolism is extremely sensitive to impairment by reactive oxygen and nitrogen species (ROS/RNS) and that mitochondrial oxidative stress limits metabolic recovery and promotes the intrinsic pathway of apoptosis.

One hypothesis we are testing is that during reperfusion, pyruvate dehydrogenase (PDH) is oxidatively modified and inactivated (Bogaert *et al*., 2000; Rosenthal *et al*., 1992), resulting in impaired oxidative energy metabolism and exacerbation of postischemic brain lactic acidosis (Rosenthal *et al*., 1992). PDH enzyme activity is lost when purified enzyme is exposed to systems that generate hydroxyl radicals (Bogaert *et al*., 1994) or peroxynitrite (E. Martin, unpublished), two ROS/RNS species strongly implicated in reperfusion brain injury. In addition to inactivation of PDH, the activity of the electron transport chain Complex I (NADH-CoQ oxidoreductase) is also depressed during reperfusion (Almeida *et al*., 1995), which could be particularly important since this complex is normally the rate-limiting step of the electron transport chain (Davey *et al*., 1997). The relative importance of damage to components of the electron transport chain compared to upstream metabolic enzymes, e.g., PDH, is at this juncture unknown. However, decreased production of NADH by PDH and TCA cycle dehydrogenases may be responsible for the hyperoxidized redox state of NAD(H) and components of the mitochondrial electron transport chain that occurs during the first hour of reperfusion after global cerebral ischemia (Rosenthal *et al*., 1995). If the electron transport chain was metabolically rate limiting during reperfusion, the NAD(H) redox state should be relatively reduced rather than oxidized. Postischemic oxidation of NAD(H) may therefore constitute an important clue for the identification of the most important metabolic targets of reperfusion injury.

Other possible explanations for the effect of ischemia/reperfusion on NAD(H) redox state include depletion of pyridine nucleotides through PARP activation (Wang *et al*., 2002), and release of mitochondrial NAD(H) and NADP(H) from the mitochondrial matrix into the cytosol, e.g., what occurs following activation of the mitochondrial membrane permeability transition (MPT) (Chinopoulos *et al*., 2003). In addition to inhibiting PDH and other mitochondrial enzyme activities, ROS/RNS are potent activators of both PARP and the MPT(Kowaltowski *et al*., 2000; Prabhakaran *et al*., 2004). Moreover, the metabolism of H_2O_2 and other peroxides via the glutathione peroxidase/reductase system can contribute to the oxidative shift in pyridine nucleotide redox state. Irrespective of the mechanism by which cerebral reperfusion causes this shift in redox state, the associated decrease in reducing power could limit detoxification of peroxides and maintenance of reduced protein sulfhydryl groups, thereby contributing to the prolonged oxidative stress characteristic of reperfusion tissue injury.

While oxidative damage to cerebral energy metabolism is a critical contributor to delayed, necrotic neuronal death, oxidative stress is also a powerful initiator of apoptosis, which also contributes significantly to ischemic neural cell death (DeGracia *et al*., 2002; Hou and MacManus, 2002). The mechanism by which oxidative stress promotes apoptosis is far from understood. Possible mechanisms include increased expression of p53, a redox-sensitive transcriptional activator of several proapoptotic genes that also directly induces release of mitochondrial cytochrome *c* (CytC) through its interaction with the antiapoptotic mitochondrial protein Bcl-X_L (Chipuk *et al*., 2003; Miller *et al*., 2000; Soengas *et al*., 1999). Reactive oxygen and nitrogen species can also induce the release of CytC from mitochondria through promotion of the MPT (Kowaltowski *et al*., 2000; Borutaite *et al*., 1999), although this event is more likely to cause necrosis due to the devastating effects of the MPT on mitochondrial energy metabolism. Oxidative alterations to mitochondrial membrane lipids or apoptotic proteins might also promote the release of CytC and other proapoptotic mitochondrial proteins through both MPT-dependent and independent mechanisms.

NEUROPROTECTION BY AVOIDING HYPEROXIA DURING CEREBRAL REPERFUSION

Intracellular conditions that exist early during reperfusion, e.g., low pH and high [Ca^{2+}], can promote the generation of ROS by mitochondria and other sources (Fiskum, 1997). Microdialysis measurements demonstrate high levels of hydroxyl radical production during the first 30–45 min of reperfusion (Piantadosi and Zhang, 1996). During this same period, hyperoxia exacerbates the oxidized shift in mitochondrial redox state and delays recovery of evoked potentials compared to what is observed with normoxic animals (Feng *et al*., 1998). Several other studies have compared hyperoxic to normoxic reperfusion using histopathology as the outcome measure. Halsey implanted O_2 electrodes in the brains of rats before subjecting them to a 20 min global ischemic insult and found a positive correlation between reoxygenation level and severity of neuronal damage (Halsey *et al*., 1991). Gerbils treated with 100% O_2 after 15 min bilateral carotid occlusion sustained increased white matter damage (Mickel *et al*., 1990). A study using 15 min of cardiac arrest in

dogs followed by hyperoxic resuscitation found a significant increase in the total number of injured neurons in the brain stem and spinal cord within 1 h of resuscitation (Marsala *et al*., 1992). Our preliminary results using a 10 min canine cardiac arrest model and sterologic cell counting indicate a significant reduction in hippocampal neuronal death using normoxic compared to hyperoxic resuscitation (V. Vereczki, unpublished). In contrast, Agardh used a rat model of transient global ischemia and failed to demonstrate differences in 7 day neuronal damage after resuscitation with 100% O_2 compared to normoxia or hypoxia (Agardh *et al*., 1991). Lipinski *et al*. also found no difference in hippocampal neuronal death 72 h following cardiac arrest in rats ventilated on 100 or 21% O_2 (Lipinski *et al*., 1999). This model is, however, significantly different from the canine cardiac arrest model or from most human cardiac arrest scenarios as the animals experience severe hypoxia prior to cardiac arrest.

The few reported comparisons of neurologic outcome following hyperoxic and normoxic reperfusion strongly suggest that hyperoxic resuscitation is detrimental. Using a 9 min canine cardiac arrest model, Zwemer found that resuscitation with 100%-inspired O_2 resulted in worsened 12 and 24 h neurologic outcome when compared to animals receiving 21% O_2 (Zwemer *et al*., 1994). This difference was eliminated when animals were pretreated with an antioxidant prior to the arrest and hyperoxic resuscitation. In our canine experiments using 10 min cardiac arrest, neurologic impairment measured at 24 h was significantly worse in animals ventilated on 100% O_2 during and for 1 h after resuscitation than that exhibited by dogs resuscitated on 21% O_2 and subsequently ventilated on 21–30% O_2 to maintain normal PaO2 (Liu *et al*., 1998). The one published negative study is the Lipinski report where no difference in 72 h neurologic impairment was observed following asphyxia-induced cardiac arrest in rats (Lipinski *et al*., 1999). The only long-term outcome study focused on mortality and used the gerbil bilateral carotid occlusion model. Mickel and colleagues found that animals exposed to 100% O_2 for 3–6 h after 15 min global cerebral ischemia experienced a threefold increase in 14 day mortality compared with those allowed to breathe room air after ischemia (Mickel *et al*., 1987).

MITOCHONDRIA AS SOURCES OF REACTIVE OXYGEN SPECIES

Superoxide is a normal byproduct of mitochondrial respiration and accounts for ~1% of O_2 consumed by mitochondria. Because of its extremely high reactivity and short half-life, it normally dismutates to H_2O_2 either spontaneously or via catalysis by mitochondrial or cytosolic superoxide dismutases. While the metabolism of H_2O_2 via peroxidases can, under some circumstances, lead to oxidative stress due to an oxidized shift in cellular redox state, the primary toxicity of elevated superoxide and H_2O_2 production is exerted by other metabolites (Fig. 1). These products include the hydroxyl radical, generated by metal-catalyzed reduction of H_2O_2, and peroxynitrite, generated by the reaction of superoxide with nitric oxide. Both of these reactive agents are capable of oxidatively modifying proteins, lipids, RNA, and DNA. As there are no known enzymatic systems for detoxifying either hydroxyl radical or peroxynitrite, endogenous interventions are limited primarily to those that reduce the production of superoxide or nitric oxide, or that promote the nontoxic metabolism of H_2O_2 to H_2O via peroxidase activities. A number of additional exogenous antioxidant approaches are available, including the use of iron chelators, spin-traps, and other natural and artificial antioxidant compounds.

While the role of mitochondrial ROS production in ischemia/reperfusion injury is often touted as important, little direct evidence is available from in vivo experiments. Existing evidence is based on the effects of mitochondrial respiratory inhibitors or uncouplers on markers of oxidative injury. Additional support for a critical role of mitochondrial oxidative stress in acute neuronal cell death comes from in vitro experiments using cultured neurons and other neural cell lines exposed to hypoxia and glucose deprivation, or to toxic levels of excitatory neurotransmitters or their agonists. From these and more recent studies, it appears that initial entry of Ca^{2+} through glutamate receptors is accumulated into mitochondria, causing an increase in mitochondrial ROS production that then causes a secondary irreversible entry of Ca^{2+} through redox-sensitive transient receptor potential (Trp) channels (Aarts *et al*., 2003).

One controversial topic in this field is the involvement of the MPT in Ca^{2+}-induced mitochondrial ROS production. MPT-mediated release of CytC can certainly stimulate mitochondrial generation of ROS by causing a reduced shift in mitochondrial redox sites associated with superoxide production. The MPT also causes a drop in mitochondrial membrane potential ($\Delta\Psi$) and a loss of mitochondrial pyridine nucleotides, both of which should depress mitochondrial generation of ROS. Recent work suggests, however, that even if mitochondrial NAD(H) were released into the cytosol in response to the MPT, the residual concentration in the mitochondrial matrix in equilibrium with the cytosolic pool could be sufficient to support substantial ROS production (Batandier *et al*., 2004). The use of MPT inhibitors like cyclosporin A as neuroprotectants both in vivo and in vitro has met with

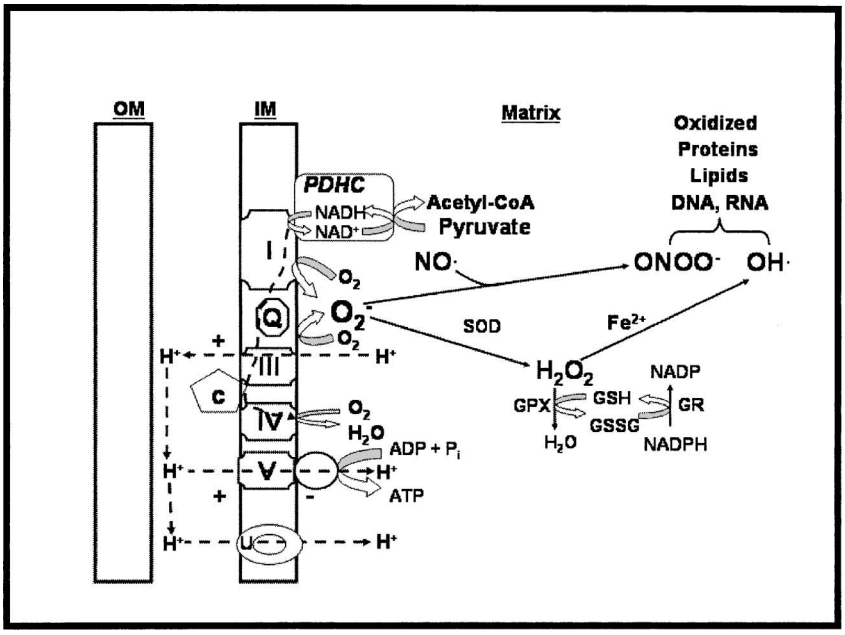

Fig. 1. Mitochondrial production and metabolism of reactive oxygen species. Superoxide (O_2^-) is produced at one or more sites within the electron transport chain and possibly via one or more matrix dehydrogenases. Superoxide is converted to hydrogen peroxide via superoxide dismutase (SOD), that is subsequently metabolized to water via the glutathione peroxidase (GPX)/glutathione reductase (GR) system. During abnormally high rates of hydrogen peroxide production and in the presence of transition metals, e.g., iron, the highly toxic hydroxyl radical is generated. Peroxynitrite can also be produced via the reaction of superoxide and nitric oxide. These metabolites can oxidize mitochondrial proteins, lipids, RNA, and DNA, contributing to oxidative stress and ultimately cell death.

mixed success (Domanska-Janik *et al.*, 2004; Kaminska *et al.*, 2001; Maciel *et al.*, 2003; Scheff and Sullivan, 1999; Uchino *et al.*, 2002). Evidence indicates that cyclosporin A is ineffective at blocking the MPT under many conditions and in certain cell types, including neurons (Fiskum *et al.*, 2003). Development of more broadly effective MPT inhibitors is therefore needed. One agent that exhibits superior inhibition of the MPT in brain mitochondria is 2-aminoethoxydiphenylborate (2-APB) (Chinopoulos *et al.*, 2003). This drug also inhibits capacitative Ca^{2+} entry associated with Trp channels and may therefore provide a multipotent approach to neuroprotection (Iwasaki *et al.*, 2001).

Several mechanism other than, or in addition to the MPT could stimulate mitochondrial ROS production during ischemia/reperfusion. Thermodynamically, any inhibition of electron flow distal to redox sites of superoxide production would promote these reactions. Thus, inhibition of electron transfer in Complex I distal to the putative iron sulfur site of superoxide generation, as occurs with rotenone, greatly stimulates ROS production with NADH-linked respiratory substrates. Inhibition at the distal points in the electron chain, as occurs with nitric oxide at Complex IV, stimulates ROS production at both Complex I and at the Coenzyme Q/Complex III redox site (Brown and Borutaite, 2001). A similar situation occurs when CytC is released during apoptosis via Bax-mediated formation of pores in the outer membrane (Starkov *et al.*, 2002). When electron flow is only partially inhibited, the redox-mediated stimulation of ROS production can be counteracted by mild uncoupling, either with exogenous uncoupling agents, e.g., FCCP, or via increased expression or activity of mitochondrial uncoupling proteins. Mitochondrial ROS production is extremely sensitive to inhibition by slight depolarization and oxidized shift in redox state at high membrane potentials (Starkov and Fiskum, 2003). Thus a drop in $\Delta\Psi$ of only 15 mV reduces the rate of NADH-linked, substrate-dependent ROS formation by 50% with little effect on ATP production. Mild uncoupling may therefore constitute an effective means of immediately reducing oxidative stress in acute CNS injury paradigms (Ferranti *et al.*, 2003; Kim-Han *et al.*, 2001).

In addition to inhibiting mitochondrial superoxide production, the net production of ROS can also be reduced by promoting its detoxification to H_2O_2 and then to

H_2O. Bcl-2, an antideath protein normally thought to act by binding to outer membrane pore-forming-proapoptotic proteins, e.g., Bax, also exhibits an indirect antioxidant activity that is apparent even at the mitochondrial level (Ellerby *et al*., 1996). We demonstrated that the inhibition of pro-oxidant-induced MPT by Bcl-2 overexpression is due to increased resistance of pyridine nucleotides to oxidation rather than a direct effect on MPT proteins (Kowaltowski *et al*., 2000). In an attempt to explain this phenomenon, we explored the effects of Bcl-2 and other antiapoptotic Bcl-2 family members on mitochondrial bioenergetics. Through careful calibration techniques, we found that mitochondria from Bcl-2-overexpressing cells do not exhibit higher membrane potential, in contrast to previous reports indicating a difference in $\Delta\Psi$. In agreement with other investigators, we found that overexpression of Bcl-2 was associated with an increase in basal mitochondrial ROS (H_2O_2) production. This counterintuitive phenotype was also observed in cells overexpressing Bcl-X_L and Mcl-1, two additional cytoprotective Bcl-2 family members (A. Kowaltowski, unpublished). Most importantly, when the overexpressing cells were treated for 48 h with low levels of uncoupler that eliminate the elevated level of mitochondrial ROS production, the cells lose their abnormally high peroxidase activity and their resistance to acute necrotic cell death caused by exposure to high concentrations of exogenous H_2O_2. It therefore appears that the antioxidant activity of at least three antiapoptotic Bcl-2 family members is similar to preconditioning paradigms where sublethal levels of stress cause upregulation of proteins that protect against normally lethal levels of stressful stimuli. While overexpression of Bcl-2 increases basal ROS production, this effect stimulates the expression of one or more antioxidant enzymes resulting in a net resistance to oxidative stress.

ACKNOWLEDGMENTS

These authors are supported by NIH Grants R01 NS34152, P01 HD016596, and R21 NS45038, and the U.S. Army Medical Research and Material Command Grant DAMD 17-99-1-9483.

REFERENCES

Aarts, M., Iihara, K., Wei, W. L., Xiong, Z. G., Arundine, M., Cerwinski, W., MacDonald, J. F., and Tymianski, M. (2003). *Cell* **115**, 863–877.

Agardh, C. D., Zhang, H., Smith, M. L., and Siesjo, B. K. (1991). *Int. J. Dev. Neurosci.* **9**, 127–138.

Almeida, A., Allen, K. L., Bates, T. E., and Clark, J. B. (1995). *J. Neurochem.* **65**, 1698–1703.

Batandier, C., Leverve, X., and Fontaine, E. (2004). *J. Biol. Chem.* **279**, 17197–17204.

Bogaert, Y. E., Rosenthal, R. E., and Fiskum, G. (1994). *Free Radic. Biol. Med.* **16**, 811–820.

Bogaert, Y. E., Sheu, K. F., Hof, P. R., Brown, A. M., Blass, J. P., Rosenthal, R. E., and Fiskum, G. (2000) *Exp. Neurol.* **161**, 115–126.

Borutaite, V., Morkuniene, R., and Brown, G. C. (1999). *Biochim. Biophys. Acta* **1453**, 41–48.

Brown, G. C., and Borutaite, V. (2001). *IUBMB Life* **52**, 189–195.

Chinopoulos, C., Starkov, A. A., and Fiskum, G. (2003). *J. Biol. Chem.* **278**, 27382–27389.

Chipuk, J. E., Maurer, U., Green, D. R., and Schuler, M. (2003). *Cancer Cell* **4**, 371–381.

Davey, G. P., Canevari, L., and Clark, J. B. (1997). *J. Neurochem.* **69**, 2564–2570.

DeGracia, D. J., Kumar, R., Owen, C. R., Krause, G. S., and White, B. C. (2002). *J. Cereb. Blood Flow Metab.* **22**, 127–141.

Domanska-Janik, K., Buzanska, L., Dluzniewska, J., Kozlowska, H., Sarnowska, A., and Zablocka, B. (2004). *Brain Res. Mol. Brain Res.* **121**, 50–59.

Ellerby, L. M., Ellerby, H. M., Park, S. M., Holleran, A. L., Murphy, A. N., Fiskum, G., Kane, D. J., Testa, M. P., Kayalar, C., and Bredesen, D. E. (1996). *J. Neurochem.* **67**, 1259–1267.

Feng, Z. C., Sick, T. J., and Rosenthal, M. (1998). *Resuscitation* **37**, 33–41.

Ferranti, R., da Silva, M. M., and Kowaltowski, A. J. (2003). *FEBS Lett.* **536**, 51–55.

Fiskum, G. (1997). In *Neuroprotection* (Blanck, T. J. J., ed.), Williams and Wilkins, Baltimore, pp. 1–14.

Fiskum, G., Bambrick, L., Kristian, T., Chandrasekaran, K., and Chinopoulos, C. (2003). *J. Neurochem.* **85**(Supppl. 1), 56.

Fiskum, G., Murphy, A. N., and Beal, M. F. (1999). *J. Cereb. Blood Flow Metab.* **19**, 351–369.

Halsey, J. H., Jr., Conger, K. A., Garcia, J. H., and Sarvary, E. (1991). *J. Cereb. Blood Flow Metab.* **11**, 994–1000.

Hou, S. T., and MacManus, J. P. (2002). *Int. Rev. Cytol.* **221**, 93–148.

Iwasaki, H., Mori, Y., Hara, Y., Uchida, K., Zhou, H., and Mikoshiba, K. (2001). *Receptors Channels* **7**, 429–439.

Kaminska, B., Figiel, I., Pyrzynska, B., Czajkowski, R., and Mosieniak, G. (2001). *Br. J. Pharmacol.* **133**, 997–1004.

Kim-Han, J. S., Reichert, S. A., Quick, K. L., and Dugan, L. L. (2001). *J. Neurochem.* **79**, 658–668.

Kowaltowski, A. J., Vercesi, A. E., and Fiskum, G. (2000). *Cell Death Differ.* **7**, 903–910.

Lewen, A., Matz, P., and Chan, P. H. (2000). *J. Neurotrauma* **17**, 871–890.

Lipinski, C. A., Hicks, S. D., and Callaway, C. W. (1999). *Resuscitation* **42**, 221–229.

Liu, Y., Rosenthal, R. E., Haywood, Y., Miljkovic-Lolic, M., Vanderhoek, J. Y., and Fiskum, G. (1998). *Stroke* **29**, 1679–1686.

Maciel, E. N., Kaminski Schierle, G. S., Hansson, O., Brundin, P., and Castilho, R. F. (2003). *Exp. Neurol.* **183**, 430–437.

Marsala, J., Marsala, M., Vanicky, I., Galik, J., and Orendacova, J. (1992). *Neurosci. Lett.* **146**, 121–124.

Mickel, H. S., Kempski, O., Feuerstein, G., Parisi, J. E., and Webster, H. D. (1990). *Acta Neuropathol. (Berl.)* **79**, 465–472.

Mickel, H. S., Vaishnav, Y. N., Kempski, O., von Lubitz, D., Weiss, J. F., and Feuerstein, G. (1987). *Stroke* **18**, 426–430.

Miller, F. D., Pozniak, C. D., and Walsh, G. S. (2000). *Cell Death Differ.* **7**, 880–888.

Murphy, A. N., Fiskum, G., and Beal, M. F. (1990). *J. Cereb. Blood Flow Metab.* **19**, 231–245.

Myers, K. M., Fiskum, G., Liu, Y., Simmens, S. J., Bredesen, D. E., and Murphy, A. N. (1995). *J. Neurochem.* **65**, 2432–2440.

Piantadosi, C. A., and Zhang, J. (1996). *Stroke* **27**, 327–331.

Prabhakaran, K., Li, L., Borowitz, J. L., and Isom, G. E. (2004). *Toxicol. Appl. Pharmacol.* **195**, 194–202.

Rosenthal, M., Feng, Z. C., Raffin, C. N., Harrison, M., and Sick, T. J. (1995). *J. Cereb. Blood Flow Metab* **15**, 655–665.

Rosenthal, R. E., Williams, R., Bogaert, Y. E., Getson, P. R., and Fiskum, G. (1992). *Stroe* **23**, 1312–1317.

Scheff, S. W., and Sullivan, P. G. (1999). *J. Neurotrauma* **16**, 783–792.

Soengas, M. S., Alarcon, R. M., Yoshida, H., Giaccia, A. J., Hakem, R., Mak, T. W., and Lowe, S. W. (1999). *Science* **284**, 156–159.

Starkov, A. A., and Fiskum, G. (2003) Regulation of brain mitochondrial H_2O_2 production by membrane potential and NAD(P)H redox state. *J. Neurochem.* **86**, 1101–1107.

Starkov, A. A., Polster, B. M., and Fiskum, G. (2002). *J. Neurochem.* **83**, 220–228.

Uchino, H., Minamikawa-Tachino, R., Kristian, T., Perkins, G., Narazaki, M., Siesjo, B. K., and Shibasaki, F. (2002). *Neurobiol. Dis.* **10**, 219–233.

Wang, J. Y., Shum, A. Y., and Wang, J. Y. (2002) *Neurosci. Lett.* **322**, 187–191.

Zwemer, C. F., Whitesall, S. E., and D'Alecy, L. G. (1994). *Resuscitation* **27**, 159–170.

TOXICOLOGICAL SCIENCES **88(2)**, 495–504 (2005)
doi:10.1093/toxsci/kfi334
Advance Access publication September 21, 2005

Methoxychlor Inhibits Brain Mitochondrial Respiration and Increases Hydrogen Peroxide Production and CREB Phosphorylation

Rosemary A. Schuh,*,†,‡ Tibor Kristián,* Rupesh K. Gupta,†,‡ Jodi A. Flaws,†,‡ and Gary Fiskum*,‡,[1]

*Department of Anesthesiology, University of Maryland School of Medicine, Baltimore, Maryland 21201; †Department of Epidemiology and Preventive Medicine, University of Maryland School of Medicine, Baltimore, Maryland 21201; ‡Program in Toxicology, University of Maryland School of Medicine, Baltimore, Maryland 21201

Received July 28, 2005; accepted September 14, 2005

The organochlorine insecticide methoxychlor (mxc) is an established reproductive toxicant that affects other systems including the central nervous system (CNS), possibly by mechanisms involving oxidative stress. This study tested the hypothesis that mxc inhibits brain mitochondrial respiration, resulting in increased production of reactive oxygen species (ROS). Oxygen electrode measurements of mitochondrial respiration and Amplex Red measurements of H_2O_2 production were performed with rat brain mitochondria exposed *in vitro* to mxc (0–10 μg/ml) and with brain mitochondria from mice chronically exposed *in vivo* to mxc (0–64 mg/kg/day) for 20 days by intraperitoneal injection. *In vitro* mxc exposure inhibited ADP-dependent respiration (state 3) using both complex I- and II-supported substrates. Similarly, state 3 respiration was inhibited following *in vivo* mxc exposure using complex I substrates. H_2O_2 production was stimulated after *in vitro* mxc treatment in the presence of complex I substrates, but not in mitochondria isolated from *in vivo* mxc-treated mice. Because previous studies demonstrated a relationship between oxidative stress and CREB phosphorylation, we also tested the hypothesis that mxc elevates phosphorylated CREB (pCREB) in mitochondria. Enzyme-linked immunosorbent assay (ELISA) measurements demonstrated that pCREB immunoreactivity was elevated by *in vitro* mxc exposure in the presence or absence of respiratory substrates, indicating that stimulation of H_2O_2 production is not necessary for this effect. These multiple effects of mxc on mitochondria may play an important role in its toxicity, particularly in the CNS.

Key Words: **methoxychlor; mitochondria; CREB; oxidative stress.**

INTRODUCTION

Organochlorines are a diverse group of synthetic chemicals including pesticides and industrial products that are persistent environmental pollutants due to their high lipophilicity and subsequent bioaccumulation in the food chain. The organochlorine pesticides dichlorodiphenoxytrichloroethane (DDT) and 1,1,1-trichloro-2,2-bis(*p*-methoxyphenyl)ethane (methoxychlor, mxc) have been shown in several studies to possess estrogenic properties resulting in adverse effects on the reproductive system in both animal models (Borgeest *et al.*, 2002; Cummings, 1997; Gray *et al.*, 1989) and cell lines (Chedrese and Feyles, 2001; Hodges *et al.*, 2000; Okubo *et al.*, 2004; Shekhar *et al.*, 1997). These studies indicate that exposure to organochlorine pesticides and related compounds are of concern in terms of human health.

Botella *et al.* (2004) determined the levels of several organochlorine pesticide residues in adipose tissue and blood samples from 200 women living in Southern Spain. The highest concentrations found were for 1,1-dichloro-2,2-bis(*p*-chlorophenyl)ethylene (*p,p′*-DDE), the major metabolite of DDT. Methoxychlor residues were also identified in this study, but at lower levels than the other pesticides tested. In addition, a recent study by Rudel *et al.*, (2003) determined the levels of 89 target chemicals including pesticides, designated as endocrine disruptors in urine samples, house dust, and indoor air from 120 homes in Cape Cod, MA. The results from the study indicate that DDT and mxc were present in at least 50% of the homes tested at relatively high concentrations.

In addition to their estrogenic properties, certain organochlorines including hexachlorocyclohexane (Sahoo and Chainy, 1998) and endosulfan (Kannan and Jain, 2003) have been demonstrated to play a role in cellular oxidative stress. Studies by Latchoumycandane and Mathur (2002) demonstrated depletion of antioxidant enzymes in mitochondria and microsomes from rat testis following exposure to mxc. Additionally, Chen *et al.* (1999) demonstrated increased superoxide production in rat liver mitochondria following exposure to the synthetic estrogen ethinyl estradiol. Other pesticides, including paraquat and rotenone, inhibit mitochondrial respiration and stimulate mitochondrial production of reactive oxygen species (ROS) in rat brain (Meyer *et al.*, 2004; Starkov *et al.*, 2004; Tawara *et al.*, 1996). The mitochondrial effects of environmental toxicants, *e.g.,* rotenone, are likely responsible for their

[1] To whom correspondence should be addressed at Department of Anesthesiology, University of Maryland School of Medicine, 685 W. Baltimore Street, MSTF 5–34, Baltimore, MD 21201. Fax: (410) 706-2550. E-mail: gfisk001@umaryland.edu.

induction of neurodegeneration (Greenamyre *et al.*, 1999). Considering the epidemiological evidence that pesticide exposure may be linked to Parkinson's disease, a more extensive assessment of the effects of these toxicants on mitochondrial functions, including ROS production is needed.

Many studies have identified oxidative stress as an inducer of post-translational protein modification, resulting in transcriptional activation. For example, some studies indicate that oxidative stress during ischemia/reperfusion causes phosphorylation of Ca^{2+}/cAMP response element binding protein (pCREB) (Mabuchi *et al.*, 2001; Tanaka, 2001). In an earlier study, we determined that exposure of rat primary cortical and hippocampal neurons to the organophosphate insecticide chlorpyrifos increases pCREB immunoreactivity via a non-cholinesterase mechanism (Schuh *et al.*, 2002). CREB phosphorylation is implicated in the induction of transcriptional activity that stimulates the expression of antioxidant genes (Bedogni *et al.*, 2003). In addition to the effects of pCREB on nuclear gene transcription, mitochondrial gene expression may be under the control of mitochondrial-localized pCREB (Ryu *et al.*, 2003). pCREB is present in mitochondria from different tissues, including brain, and its phosphorylation state is regulated by Ca^{2+}, an important intracellular modulator of gene expression (Schuh *et al.*, 2005).

Although mxc and other endocrine disruptive compounds have been clearly identified as reproductive toxicants, other systems including the central nervous system (CNS) may also be targeted (Cooper *et al.*, 1999; Gore, A. C., 2002; Lafuente *et al.*, 2003). Furthermore, the mechanism(s) of action of these compounds within the CNS have not been fully investigated at the organelle level. Therefore, the primary objective of the present study was to determine the effects of *in vitro* and *in vivo* mxc exposure on brain mitochondrial respiration and ROS production. Considering the recent identification of mitochondrial CREB, we also tested the hypothesis that mxc increases mitochondrial CREB phosphorylation, possibly via stimulation of ROS production. The results of this study provide new insight into non-estrogenic effects of mxc that alter mitochondrial bioenergetics, producing oxidative stress. Mitochondrial pCREB is also identified as a new potential target of organochlorines.

MATERIALS AND METHODS

Chemicals and reagents. 1,1,1-trichloro-2,2-bis(*p*-methoxyphenyl)ethane (methoxychlor, mxc) was purchased from ChemService (West Chester, PA) in a powdered form and was 99% pure. All other reagents were purchased from Sigma (St. Louis, MO) unless otherwise stated.

Animals. Female CD-1 mice (25 g, 39 days old) were housed five animals per cage, and male Sprague-Dawley rats (300 g, 90 days old) were housed three animals per cage at the University of Maryland School of Medicine Central Animal Facility and provided food and water *ad libitum*. Animals were subjected to 12-h light:dark cycles. Mice were dosed via intraperitoneal injection with 16, 32, or 64 mg/kg/day mxc, or sesame oil (vehicle) for 20 continuous days. The mice were sacrificed when in estrus to minimize variability due to hormonal fluctuations within 24–72 h after the final mxc treatment. The *in vivo* mxc doses were selected based on earlier studies showing deleterious effects in the ovaries (Borgeest *et al*., 2002, 2004). The University of Maryland School of Medicine Institutional Animal Use and Care Committee approved all procedures involving animal care, euthanasia, and tissue collection.

Mitochondrial isolation. Male Sprague-Dawley rat brains and female CD-1 mouse brains were rapidly dissected then further processed to isolate non-synaptosomal mitochondria using the Percoll isolation method described by Sims (1990). Briefly, after decapitation, the forebrain was rapidly removed and placed in ice-cold mannitol-sucrose (MS) buffer pH 7.4 (225 mM mannitol, 75 mM sucrose, 5 mM Hepes, 1 mg/ml fatty acid free BSA, 1 mM EGTA). The brain was homogenized then centrifuged twice at 1317 × *g* for 3 min. After a further 10 min centrifugation at 21,074 × *g,* the pellet was resuspended in 15% Percoll (Amersham Biosciences, Piscataway, NJ) then layered on a discontinuous Percoll gradient and spun at 29,718 × *g* for 8 min. The mitochondrial fraction was centrifuged at 16,599 × *g* for 10 min then spun at 6668 × *g* for 10 min. The mitochondrial pellet was resuspended in the above buffer but without BSA or EGTA. Protein concentrations were determined by the method described by Lowry *et al.* (1951).

Mitochondrial oxygen consumption. Oxidizable respiratory substrates consisting of either 5 mM L-malate plus 5 mM L-glutamate, 5 mM succinate plus 1 μM rotenone, or 0.02 mM N,N,N′,N′-tetramethyl-*p*-phenylenediamine (TMPD) plus 2 mM ascorbate and 1 μM antimycin A in potassium chloride buffer (30°C) containing 125 mM KCl ultrapure (Merck, Whitehouse Station, NJ), 20 mM Hepes, 2 mM K_2HPO_4, 0.01 mM EGTA, and 1 mM $MgCl_2$ (pH 7.0) were placed in a thermostatically controlled Clarke-type O_2 electrode (Hansatech Instruments, Norfolk, England). Isolated non-synaptosomal rat or mouse brain mitochondria (0.25 mg/ml) were added to the chamber and the rates of oxygen consumption were measured. For the *in vitro* mxc treatment studies, mxc (0–10 μg/ml) in dimethyl sulfoxide (DMSO) was added prior to mitochondrial addition. State 3 respiration was initiated 2 min after the addition of mitochondria by the addition of 0.8 mM ADP. Approximately 2 min later, state 3 respiration was terminated and state 4_o respiration (resting) was initiated with addition of 1.25 μg/ml oligomycin, an inhibitor of the mitochondrial ATP synthase. While the state 4_o respiration measured in the presence of oligomycin is not equivalent to the classical state 4 rate obtained after a small bolus of ADP is almost completely converted to ATP, the use of oligomycin eliminates the contribution of ATP cycling via hydrolysis by contaminating ATPases and resynthesis by the mitochondrial ATP synthase to state 4 respiration. The oligomycin-induced state 4_o rate of respiration is therefore a more specific indicator of the inner membrane proton leakiness. The maximal rate of uncoupled respiration was subsequently measured by titration with 54 nM carbonyl cyanide *p*-(trifluoromethoxy)phenylhydrazone (FCCP). The mitochondrial suspensions were centrifuged at 18,522 × *g* for 3 min and the pellet resuspended in lysis buffer (pH 7.4) containing 0.5% NP40 (USB, Cleveland, OH), 1% Triton X-100, 150 mM NaCl, 10 mM Tris, and 1% protease inhibitor cocktail (Calbiochem, San Diego, CA). The aliquots were stored at −70°C.

Mitochondrial membrane potential. Mitochondrial membrane potential changes in isolated non-synaptosomal brain mitochondria (0.25 mg/ml) were followed qualitatively by monitoring the fluorescence of tetramethyl rhodamine methyl ester (TMRM, Molecular Probes, Eugene, OR), a cationic lipid-soluble probe that accumulates in energized mitochondria. Fluorescence intensity was measured in a Hitachi F-2500 fluorescence spectrophotometer (Tokyo, Japan) using the 549 nm wavelength for excitation and the emission wavelength set at 580 nm. An increase in fluorescence represents dequenching of TMRM when the probe is released into the medium upon mitochondrial depolarization. Briefly, the potassium chloride buffer (30°C) mentioned above was used, with addition of TMRM (100 nM) and oxidizable respiratory substrates consisting of 5 mM L-malate plus 5 mM L-glutamate. Following mitochondrial addition, sequential mxc (total amount 10 μg/ml) and FCCP (54 nM) were added.

Mitochondrial hydrogen peroxide production. Hydrogen peroxide (H_2O_2) production from isolated non-synaptosomal mitochondria from rat

and mouse brains was measured fluorimetrically utilizing Amplex Red (Molecular Probes, Eugene, OR) as previously described (Starkov and Fiskum, 2003). Briefly, the potassium chloride buffer (30°C) mentioned above was used, with addition of 5 U/ml horseradish peroxidase, 40 U/ml Cu, Zn superoxide dismutase, and 1 μM Amplex Red. Measurements were initiated prior to addition of mxc and mitochondria to identify background rates. Methoxychlor (0–10 μg/ml) in DMSO was added to the cuvette prior to mitochondria in studies using rat brain mitochondria. After mitochondrial addition, the oxidizable substrates 5 mM L-malate plus 5 mM L-glutamate were added. Adenosine diphosphate (0.8 mM) was added a minute later, followed by oligomycin (1.25 μg/ml). When malate/glutamate were used as substrates, 1 μM rotenone was added, following oligomycin treatment. For experiments using alternative substrates, 1 μM rotenone was added followed by 5 mM succinate and 1 μM antimycin A addition after the oligomycin. Detection of H_2O_2 production was measured as an increase in fluorescence of Amplex Red dye at 585 nm with the excitation wavelength set at 550 nm. The dye response was calibrated with addition of a known amount of H_2O_2 (1 nmol). The concentration of the H_2O_2 stock was calculated from light absorbance at 240 nm employing $E_{240} = 43.6\ M^{-1}\ cm^{-1}$.

Experiments using DMSO (vehicle control) alone were performed for all the procedures mentioned above and DMSO was determined to have no effect on the parameters measured. The DMSO concentrations in all experiments were kept below 0.5% (data not shown).

pCREB immunoreactivity. Mitochondrial samples were assessed using an enzyme-linked immunosorbent assay (ELISA kit; BioSource International, Camarillo, CA) that recognized pCREB phosphorylated at serine 133. pCREB levels were determined according to the manufacturer's protocol.

Statistical analysis. Data are expressed as means ± SE, and the comparisons between experimental groups were made with SPSS statistical software (SPSS, Inc., Chicago, IL) using a regression analysis (test for trend). Statistical significance was assumed at $p < 0.05$.

RESULTS

Methoxychlor Alters Rat Brain Mitochondrial Respiration and Membrane Potential

After isolation of non-synaptosomal mitochondria from rat forebrain, we determined whether and how mxc affects respiration. In untreated mitochondria, ADP addition to the mitochondrial suspension in the presence of the oxidizable substrates malate and glutamate initiated state 3 respiration (Fig. 1A). Addition of the mitochondrial ATP synthase inhibitor oligomycin reduced the rate of O_2 consumption to that of state 4_o respiration, limited by the proton permeability of the inner membrane. In a few experiments, the rate of respiration was measured in the presence of the protonophore uncoupler FCCP, which stimulated respiration due to rapid futile cycling of protons across the inner membrane and collapse of the electrochemical gradient (Fig. 1A). The rate of respiration in the presence of FCCP is limited by the rate of electron transport rather than the ATP synthase or adenine nucleotide translocase activities, which can, under some circumstances, limit the rate of state 3 respiration. The lower trace in Figure 1A details control conditions without mxc addition, whereas the upper trace demonstrates that the presence of mxc (10 μg/ml) resulted in a 48% inhibition of state 3 respiration and a 43% increase in the state 4_o rate. Methoxychlor also inhibited

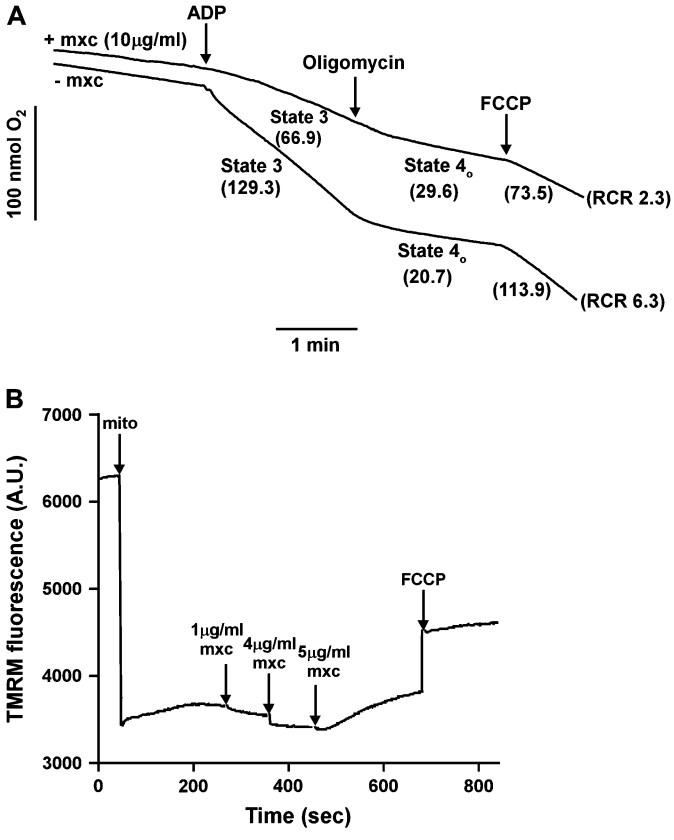

FIG. 1. Oxygen electrode measurements of respiration and fluorescence measurements of membrane potential using isolated rat brain mitochondria. A. Representative traces of mitochondrial oxygen consumption ± *in vitro* methoxychlor (mxc, 10 μg/ml) treatment in the presence of L-malate (5 mM), L-glutamate (5 mM), ADP (0.8 mM) to initiate state 3 respiration, and oligomycin (1.25 μg/ml) to induce state 4_o respiration. Maximal, uncoupled respiration was initiated with the protonophore carbonyl cyanide *p*-(trifluoromethoxy)phenylhydrazone (FCCP, 54 nM). The traces are representative of three to six separate experiments. B. Representative trace of changes in mitochondrial membrane potential ($\Delta\Psi$) following sequential additions of mxc (total amount 10 μg/ml) in the presence of L-malate (5 mM) plus L-glutamate (5 mM). Maximal $\Delta\Psi$ in uncoupled mitochondria was initiated with FCCP (54 nM). The trace is representative of three separate experiments. A.U., arbitrary units.

FCCP-stimulated respiration by 35%, suggesting a site of action at the electron transport chain rather than the ATP synthase.

The finding that 10 μg/ml mxc both inhibits state 3 respiration and stimulates state 4_o respiration suggests that mitochondrial membrane potential could be impaired. Qualitative, fluorescent TMRM measurements of mitochondrial membrane potential were performed under the same conditions used for the respiratory measurements, except that ADP was absent (Fig. 1B). Using suspensions of isolated mitochondria, depolarization causes an increase in TMRM fluorescence due to dequenching upon release of the fluorophore from mitochondria into the medium. After sequential additions of mxc totaling 10 μg/ml, the TMRM fluorescence increased toward

the level obtained in the presence of FCCP; however, no mitochondrial depolarization was apparent at total doses of either 1 or 5 μg/ml.

The dose–response relationships for mxc and mitochondrial respiration are shown in Figure 2. The mxc doses used in these experiments were based on the studies of Miller *et al.* (2005) assessing the effects of mxc on apoptosis *in vitro*. Exposure to mxc (0–10 μg/ml) significantly reduced state 3 respiration when electron transport chain complex I substrates malate and glutamate were present ($p < 0.001$ compared to vehicle control) (Fig. 2A). In the presence of the complex II substrate succinate and the complex I inhibitor rotenone, mxc also demonstrated significant inhibition of state 3 respiration ($p < 0.001$) (Fig. 2A). Complex I-dependent respiration appeared more sensitive to inhibition than that of complex II (5 μg/ml mxc resulted in a 40% inhibition of respiration on malate plus glutamate compared to a 19% inhibition for succinate plus rotenone). Ascorbate plus TMPD were used to donate electrons to cytochrome c and then through complex IV to O_2 to probe for any effects of mxc on this distal portion of the electron transport chain. No significant effect on state 3 respiration following addition of mxc was observed under these conditions ($p = 0.61$, Fig. 2A).

After addition of oligomycin, *in vitro* mxc treatment produced a small but significant increase in state 4_o respiration in the presence of the complex II-linked substrate succinate ($p < 0.001$ as compared to vehicle control; Fig. 2B). No significant effects of mxc on state 4_o respiration were observed when using either malate plus glutamate or ascorbate/TMPD as oxidizable substrates ($p = 0.147$ and $p = 0.333$, respectively; Fig. 2B). Despite the lack of an effect on state 4_o respiration in the presence of malate plus glutamate, mxc caused a dose-dependent reduction in the respiratory control ratio (RCR) ($p < 0.001$ compared to vehicle control; Fig. 2C). For example, in the presence of mxc at 1 and 10 μg/ml, the RCR values were 3.38 ± 1.04 and 2.21 ± 0.54, respectively, compared to 6.41 ± 1.22 in the absence of mxc (Fig. 2C).

In Vitro *Methoxychlor Treatment Increases ROS Production by Rat Brain Mitochondria*

Because inhibition of mitochondrial respiration can, under some circumstances, result in increased production of ROS, we next determined whether mxc stimulated mitochondrial ROS production. As described previously (Starkov and Fiskum, 2003), fluorescent Amplex Red measurements of H_2O_2 were made with isolated brain mitochondria exposed to subsequent additions of malate plus glutamate, ADP, oligomycin, and rotenone (Fig. 3A and B). The presence of 10 μg/ml mxc resulted in an approximately sevenfold increase in H_2O_2 production during state 3 respiration (Fig. 3B) as compared with control (Fig. 3A).

Since mxc inhibition of respiration was greatest in the presence of complex I substrates, we hypothesized that the

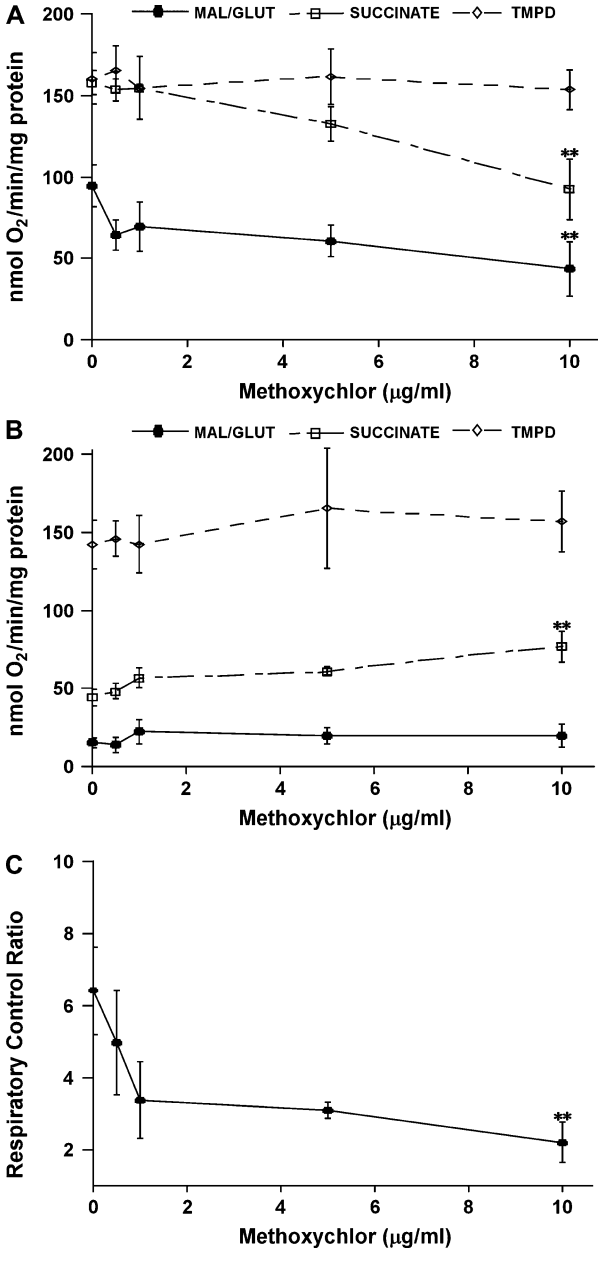

FIG. 2. Dose-dependent effects of *in vitro* methoxychlor treatment on rat brain mitochondria respiring on different oxidizable substrates. A. Mean state 3 oxygen consumption rates following exposure of isolated mitochondria to *in vitro* mxc (0–10 μg/ml) in the presence of either L-malate (5 mM) plus L-glutamate (5 mM); succinate (5 mM) and rotenone (1 μM); or N,N,N′,N′-Tetramethyl-*p*-phenylenediamine (TMPD, 0.02 mM), ascorbate (2 mM), and antimycin A (1 μM), measured as shown in Figure 1A. (B) Mean state 4_o oxygen consumption rates following addition of 1.25 μg/ml oligomycin were as shown in Figure 1A. Data are expressed as mean oxygen consumption rates (nmol oxygen/min/mg mitochondrial protein) and represent the mean ± SEM of three to six separate experiments. **Significantly different ($p < 0.001$) from control. C. Mean respiratory control ratios following exposure of isolated mitochondria to *in vitro* mxc (0–10 μg/ml) in the presence of L-malate (5 mM) plus L-glutamate (5 mM). Data are expressed as the ratio of state 3 rates:state 4_o rates and represent the mean ± SEM of three to six separate experiments. **Significantly different ($p < 0.001$) from control.

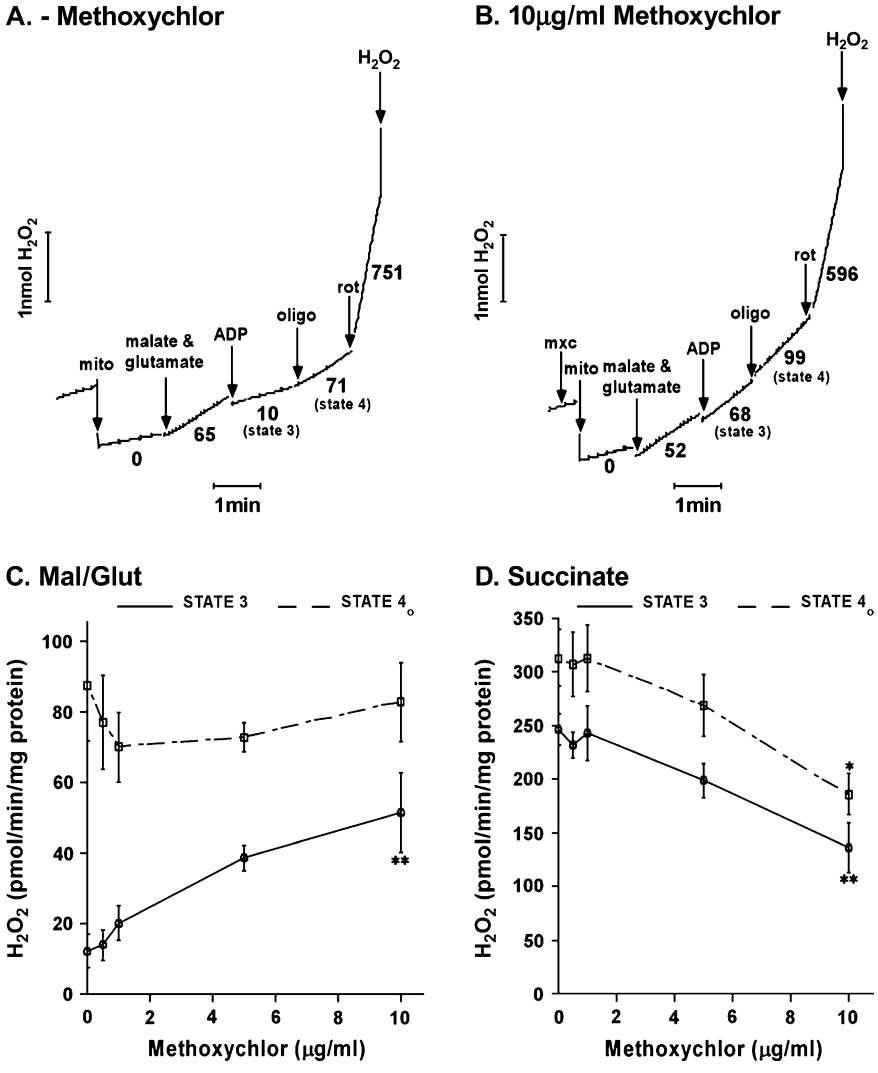

FIG. 3. Fluorescent Amplex Red measurements of H_2O_2 production in isolated rat brain mitochondria exposed *in vitro* to methoxychlor. Representative spectrofluorometer measurements of H_2O_2 production (A) without mxc or (B) plus mxc (10 μg/ml) in the presence of L-malate (5 mM) plus L-glutamate (5 mM), ADP (0.8 mM) to initiate state 3 respiration, and oligomycin (1.25 μg/ml) to induce state 4_o respiration. Mean H_2O_2 production rates after exposure of actively respiring mitochondria to mxc (0–10 μg/ml) in the presence of complex I-linked substrates (C) or complex II-linked substrates (D). Values represent mean H_2O_2 production rates (pmol/min/mg mitochondrial protein) ± SEM of three to four separate experiments. *Significantly different ($p < 0.01$); **significantly different ($p < 0.001$) from control.

effect of mxc on ROS production would be more pronounced with malate plus glutamate than with succinate in the presence of rotenone. The rate of H_2O_2 production at state 3 respiration with malate plus glutamate as substrates increased significantly with increasing doses of mxc as compared with vehicle control ($p < 0.001$; Fig. 3C). In the presence of oligomycin (state 4_o), mxc had no significant effect on mitochondrial H_2O_2 generation ($p = 0.65$; Fig. 3C). In contrast to the stimulatory effect of mxc on ROS production with malate plus glutamate, mxc caused a significant reduction in succinate-supported ROS generation under both state 3 and state 4_o respiration ($p < 0.001$ and $p < 0.01$, respectively; Fig. 3D).

Effect of Chronic Methoxychlor Exposure in Mice on Brain Mitochondrial Respiration and H_2O_2 Production

Considering the effects of mxc on mitochondrial respiration and ROS production *in vitro*, experiments were performed to probe for possible effects of mxc on brain mitochondria *in vivo*. Female CD-1 mice were treated with mxc (0–64 mg/kg/day) in sesame oil via ip injection for 20 consecutive days prior to the mitochondrial isolation. This dose range was used because it produces follicular atresia (Borgeest *et al.*, 2002, 2004) and oxidative injury to the testes (Latchoumycandane and Mathur, 2002). State 3 respiration with the complex I-linked substrates malate and glutamate was significantly lower for brain mitochondria isolated from the mxc-treated mice compared

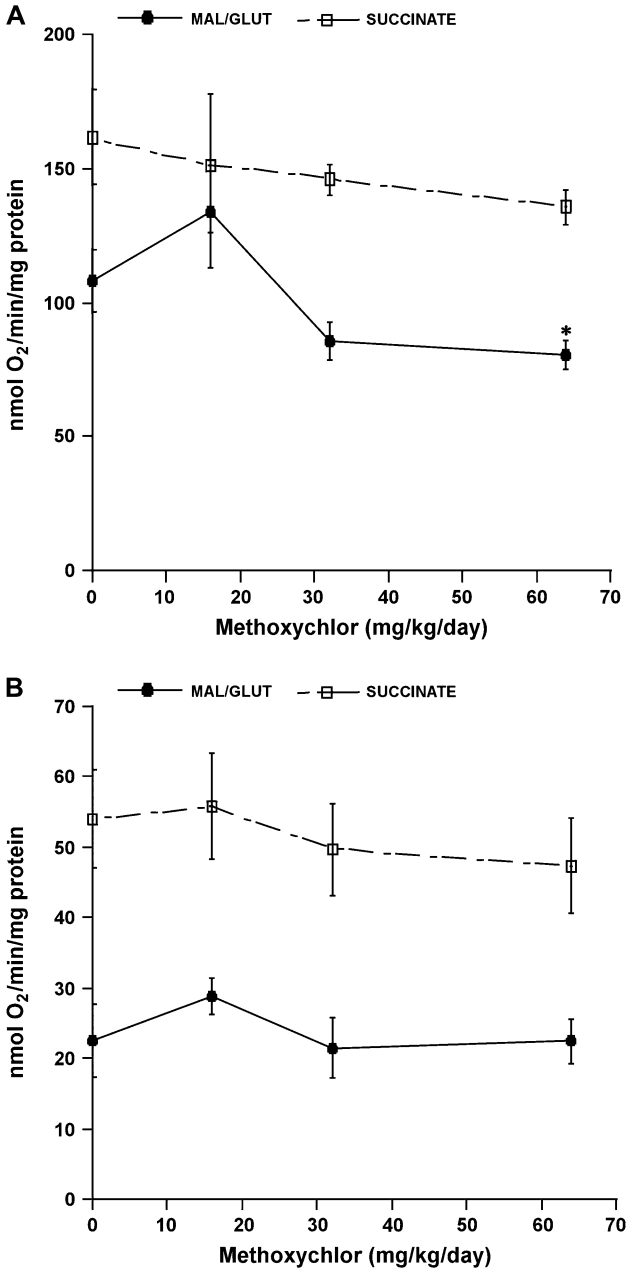

FIG. 4. Effects of *in vivo* methoxychlor treatment on mouse brain mitochondria respiring on different oxidizable substrates. A. Mean state 3 oxygen consumption rates in the presence of either L-malate (5 mM) plus L-glutamate (5 mM) or succinate (5 mM) and rotenone (1 μM) following *in vivo* mxc treatment (0–64 mg/kg/day) prior to mitochondrial isolation. B. Mean state 4_o oxygen consumption rates following addition of 1.25 μg/ml oligomycin. Data are expressed as mean oxygen consumption rates (nmol oxygen/min/mg mitochondrial protein) and represent the mean ± SEM of four separate experiments per treatment group. *Significantly different ($p < 0.05$) from control.

to those treated with the drug vehicle ($p < 0.05$; Fig. 4A). There was a similar trend toward inhibition for respiration using the complex II-linked substrate succinate with rotenone ($p = 0.08$; Fig. 4A). No significant changes in state 4_o respiration were observed with either complex I- or complex II-linked substrates ($p = 0.19$ and $p = 0.56$, respectively; Fig. 4B).

Because *in vivo* mxc treatment resulted in the inhibition of brain mitochondrial respiration, we then determined whether *in vivo* treatment also results in stimulation of H_2O_2 production by isolated mitochondria. No significant differences in H_2O_2 production were observed across treatment groups with either complex I-linked (Fig. 5A), or complex II-linked substrates (Fig. 5B).

In Vitro *Methoxychlor Treatment Increases the Phosphorylation State of Brain Mitochondrial Ca^{2+}/cAMP Response Element Binding Protein (CREB)*

Since it is well established in the literature that CREB can be phosphorylated and therefore activated following oxidative stress, we tested the hypothesis that CREB is a downstream target following mxc inhibition of mitochondrial respiration and stimulation of ROS production. At the end of the experiments measuring the effects of mxc on respiration, the mitochondrial suspensions were centrifuged and the mitochondrial pellet retrieved for ELISA measurements that are specific for the phosphorylated form of CREB (pCREB). As anticipated based on the stimulation of ROS production by mxc in the presence of malate plus glutamate, mxc also caused a significant increase in mitochondrial pCREB immunoreactivity ($p < 0.05$; Fig. 6A). Methoxychlor also caused a significant elevation of pCREB immunoreactivity in the presence of succinate plus rotenone, even though it did not stimulate ROS production under these conditions ($p < 0.001$; Fig. 6A).

To further assess the effect of mxc on CREB phosphorylation, mitochondria were incubated in the absence and presence of mxc in the absence of exogenous respiratory substrates, a condition that virtually eliminates mitochondrial ROS formation (Fig. 3A and B). Additionally, ATP (3 mM) was present to act as a phosphate source for CREB phosphorylation. In the presence of ATP and the absence of respiratory substrates, pCREB immunoreactivity was significantly elevated by mxc ($p < 0.001$, Fig. 6B), whereas mxc had no effect on pCREB in the absence of ATP. These results indicate that while mxc increases mitochondrial pCREB immunoreactivity, the stimulation of mitochondrial ROS production by mxc is not required to trigger this response.

Similar measurements were performed with the mitochondrial samples obtained from the *in vivo* mxc-treated mouse experiments. No significant effects of *in vivo* mxc treatment on pCREB immunoreactivity were present following incubation of mitochondria in the presence of complex I- or complex II-linked substrates ($p = 0.124$ and $p = 0.897$, respectively; Fig. 6C).

DISCUSSION

This study is, to our knowledge, the first to demonstrate the effects of methoxychlor on brain mitochondrial respiration and

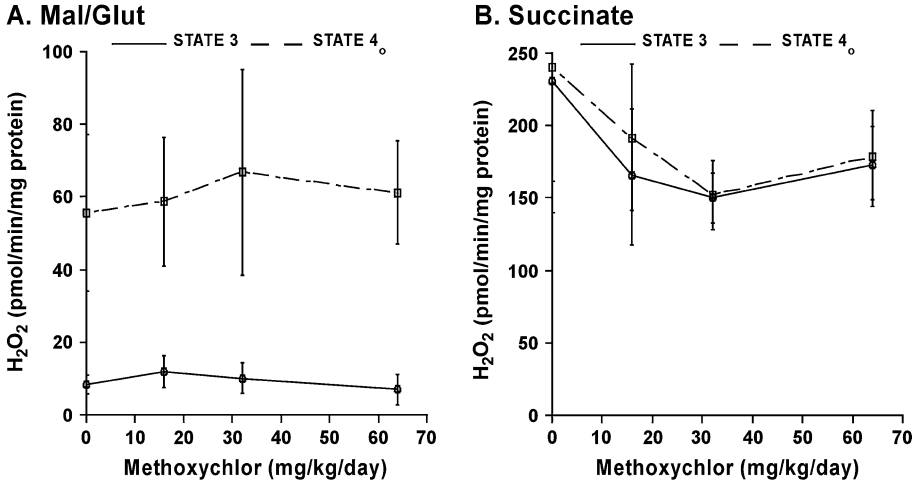

FIG. 5. Fluorescent Amplex Red measurements of H_2O_2 production in isolated mouse brain mitochondria treated *in vivo* with methoxychlor. Mean H_2O_2 production rates following *in vivo* mxc treatment (0–64 mg/kg/day) prior to mitochondrial isolation in the presence of actively respiring mitochondria utilizing complex I-linked substrates (A) or complex II-linked substrates (B). Values represent mean H_2O_2 production rates (pmol/min/mg mitochondrial protein) ± SEM for four separate experiments per treatment group. No significant differences were observed between treatment groups and vehicle controls.

production of ROS. Our results comparing the effects of mxc on mitochondrial O_2 consumption using oxidizable substrates that deliver electrons to different locations within the electron transport chain further define the regions of this pathway that are most affected by mxc. *In vitro*, mxc treatment significantly inhibits ADP-stimulated (state 3) respiration in the presence of the complex I-linked substrates malate plus glutamate and the complex II-linked substrate succinate (Fig. 2A), but it has no effect on O_2 consumption when measured in the presence of ascorbate plus TMPD, which deliver electrons to complex IV via cytochrome c (Fig. 2A). In addition, non-synaptosomal mitochondria isolated from mxc-treated mice exhibit significantly inhibited state 3 respiration in the presence of complex I-linked substrates but not in the presence of succinate plus rotenone (Fig. 4A). Thus, electron flow through complex I and, to a lesser extent complex II or III, is sensitive to inhibition by mxc treatment *in vitro* whereas only flow through complex I is affected by mxc treatment *in vivo.*

In addition to the respiratory inhibition most evident using complex I-dependent substrates, *in vitro* mxc treatment significantly increases state 4_o respiration in the presence of succinate plus rotenone (Fig. 2B). However, no significant effect on state 4_o respiration was observed across treatment groups in mitochondria isolated from *in vivo* mxc-treated mice (Fig. 4B). Thus, because state 4_o mitochondrial O_2 consumption in the presence of the ATP synthase inhibitor oligomycin is limited by the rate of H^+ influx across the inner membrane, stimulation of state 4_o respiration by mxc is likely due to a nonspecific increase in the ion permeability of the inner membrane caused by this lipophilic compound. This uncoupling effect is not as apparent in the presence of malate plus glutamate, because it is counteracted by more extensive respiratory inhibition. This interpretation is supported by the finding that mxc significantly lowers the respiratory control ratio measured in the presence of these substrates. The effects of mxc on respiratory coupling are also reflected by the partial loss of mitochondrial membrane potential observed at 10 μg/ml mxc (Fig. 1B). In summary, mxc is a respiratory inhibitor, particularly in the presence of complex I-linked substrates, and it is also a relatively mild respiratory uncoupler. The dual adverse actions of mxc on mitochondrial respiration indicate that it has the potential to induce cell death through metabolic failure or through adverse effects on respiration-linked activities, *e.g.*, superoxide formation.

Other toxicants, *e.g.*, DDT and paraquat, which inhibit the normal flow of electrons through the mitochondrial electron transport chain, also have the potential for increasing mitochondrial ROS production (Byczkowski and Tluczkiewicz, 1978; Tawara *et al.*, 1996). In our experiments, the rate of mitochondrial H_2O_2 production in the presence of malate plus glutamate and ADP was increased by more than 300% in the presence of 10 μg/ml mxc (Fig. 3C). The stimulation observed under state 3, but not state 4_o conditions is consistent with the state 3–specific respiratory inhibition observed with mxc. Maximal ROS production in the presence of complex I–dependent substrates is observed in the presence of a saturating concentration of the pesticide rotenone (Fig. 3A). The observation that mxc slightly inhibits the ROS production in the presence of rotenone (Fig. 3B) indicates that the sites of action of these toxicants within complex I are different and mxc acts at a redox site proximal to the site targeted by rotenone. Methoxychlor inhibits rather than stimulates H_2O_2 production when using the complex II substrate succinate (Fig. 3D). As mitochondrial ROS generation is regulated by the mitochondrial membrane potential through its influence of the redox state of mitochondrial electron transport chain components,

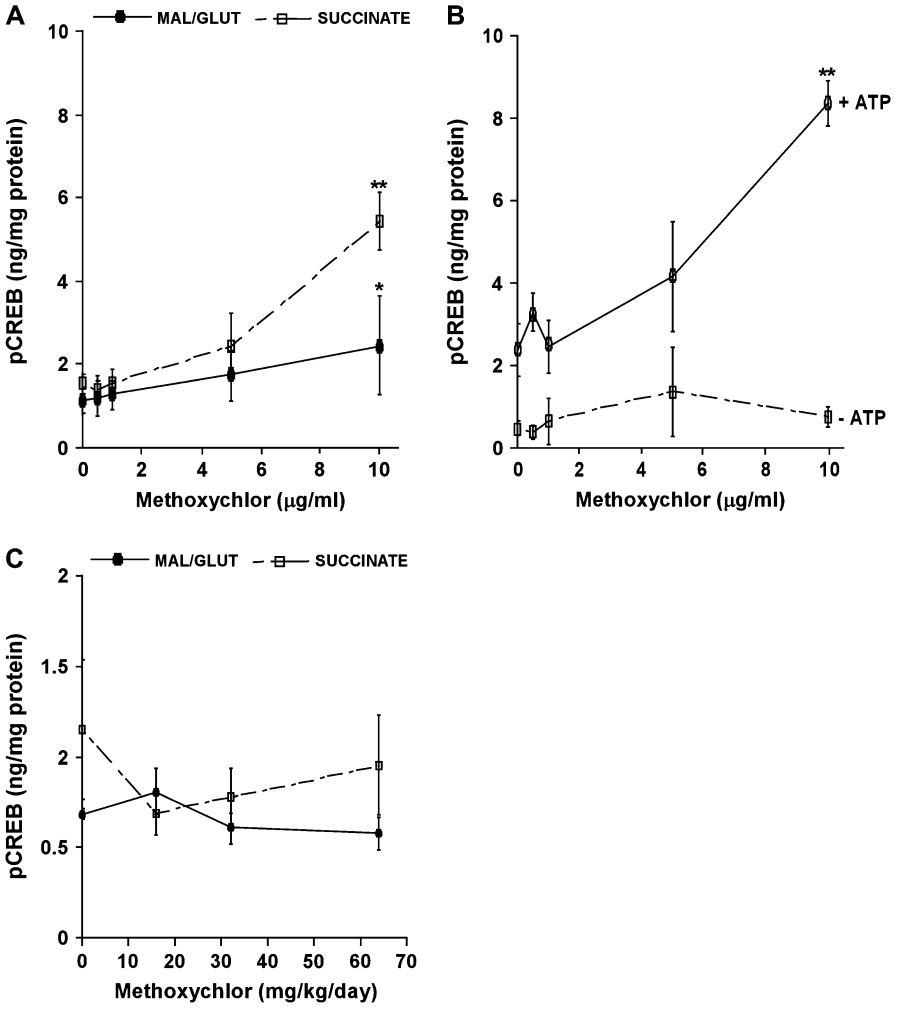

FIG. 6. Effects of methoxychlor on mitochondrial pCREB. A. pCREB levels (ng/mg mitochondrial protein) as assessed by ELISA following exposure of respiring rat brain mitochondria to *in vitro* mxc (0–10 μg/ml) treatment in experiments such as those shown in Figure 2A and B. Mitochondrial pCREB levels after incubation of rat brain mitochondria with mxc (0–10 μg/ml) in the absence of respiratory substrates and in the absence or presence of ATP (3 mM). C. pCREB levels (ng/mg mitochondrial protein) as assessed by ELISA after *in vivo* mxc (0–64 mg/kg/day) treatment in respiration experiments shown in Figure 4A. Values represent the means ± SEM for three to six separate experiments. *Significantly different ($p < 0.05$); **significantly different ($p < 0.001$) from control.

inhibition of succinate-supported H_2O_2 production is explained by the mild membrane depolarization known to inhibit ROS formation (Starkov and Fiskum, 2003). In summary, our direct measurements of the effect of mxc on H_2O_2 production by isolated brain mitochondria support the hypothesis that the toxicity of mxc is due in part to oxidative stress caused by its inhibition of electron flow through complex I of the electron transport chain. Moreover, our results extend the findings of Latchoumycandane and Mather (2002) by demonstrating that mxc-induced oxidative stress is not limited to the male reproductive system.

Although mxc stimulates mitochondrial ROS production *in vitro*, the rate of H_2O_2 production by mitochondria isolated from mice following *in vivo* mxc treatment was unchanged compared to vehicle-treated controls (Fig. 5). The presence of BSA in the mitochondrial isolation medium likely depletes the mitochondria of any residual mxc present *in situ* at the time the brain is removed. Thus, any mitochondrial alterations observed following isolation are the sequelae from the effects of mxc *in vivo*. Because complex I is sensitive to inhibition by ROS (Hillered and Ernster, 1983), stimulation of mitochondrial ROS formation by mxc present in the brains of chronically treated mice may result in oxidative modifications to complex I that are manifested as inhibition of state 3 respiration in the presence of malate plus glutamate. The absence of elevated H_2O_2 production by mitochondria isolated from mxc-treated animals indicates that the degree or nature of respiratory inhibition observed after mitochondrial isolation is insufficient to cause a detectable stimulation of ROS production. It is also possible that the metabolites of mxc generated *in vivo* have direct or indirect effects on brain mitochondria that are different from what we characterized for mxc *in vitro*. Further

studies are therefore necessary to determine the mechanisms of action of mxc on brain mitochondria *in vivo*.

A unique finding of this study is that *in vitro* mxc treatment increases the immunoreactivity of phosphorylated CREB within mitochondria at mxc concentrations similar to those that both inhibit respiration and stimulate mitochondrial ROS production. Several labs have documented the presence of CREB and pCREB in mitochondria (Cammarota *et al*., 1999; Schuh *et al.*, 2005; Ryu *et al.*, 2003), and we recently demonstrated how the mitochondrial CREB phosphorylation state is regulated by both physiological and pathological levels of Ca^{2+} (Schuh *et al.*, 2005). As oxidative stress can stimulate nuclear gene expression via an increase in cellular CREB phosphorylation, we hypothesized that the mitochondrial oxidative stress caused by mxc increases mitochondrial pCREB levels *in vitro*. After measurements of respiration, pCREB present within isolated brain mitochondria was measured. pCREB levels were significantly elevated in the presence of *in vitro* mxc-treated mitochondria respiring on either malate and glutamate or succinate (Fig. 6A). Because mxc inhibits ROS production with succinate as electron donor, we measured the effects of mxc on pCREB levels in the absence of oxidizable substrates where mitochondrial H_2O_2 production is negligible (Starkov and Fiskum, 2003). Methoxychlor increases mitochondrial pCREB immunoreactivity in the absence of respiration and ROS production, and the degree to which pCREB is elevated is greater than that observed in the presence of oxidizable substrates (Fig. 6B).

Because the results do not support the hypothesis that mxc-induced oxidative stress is responsible for increased mitochondrial CREB phosphorylation *in vitro*, the effect of mxc is likely due either to inhibition of a phosphatase or to activation of a kinase. We did not observe an effect of *in vivo* mxc treatment on mitochondrial pCREB immunoreactivity; however, the conditions used during the mitochondrial isolation procedure are not sufficient to clamp CREB phosphorylation at the state in which it exists *in vivo*. As studies implicate the cellular CREB pathway in the response of tissues other than brain to mxc and other organochlorines (Chuang and Chuang, 1998; Zhang and Teng, 2002), future experiments will determine if the phosphorylation state of mitochondrial and non-mitochondrial CREB in the brain are affected by mxc at the *in vivo* doses we found influence brain mitochondrial respiration.

The range of mxc concentrations that produce direct effects on mitochondrial respiration, ROS production, and CREB phosphorylation state are within the range of those that could feasibly exist *in vivo* at doses that elicit oxidative stress and cell death. The doses used *in vivo* range from approximately 20 to 200 mg/kg/day (Gray *et al.*, 1989). If the tissue concentrations generated at these doses are only 1% of these levels, the total concentration is in the range of 0.2–2.0 μg/ml, *i.e.*, comparable to the range of 0.5–10.0 μg/ml used in the *in vitro* mitochondrial experiments. It is impossible at this juncture to relate these levels to those that exist in humans, as virtually no data on mxc levels in human tissue are available.

It is well established that compromised mitochondrial respiration plays a role in initiation of apoptotic cascades. Additionally, several studies have suggested a relationship between defective energy metabolism and neurodegenerative diseases including Alzheimer's disease (Mutisya *et al.*, 1994) and Parkinson's disease (Greenamyre *et al.*, (1999). Thus, the findings that mxc inhibits brain mitochondrial respiration, stimulates ROS production, and increases mitochondrial CREB phosphorylation warrant further investigation into the role that endocrine-disruptive compounds may play utilizing non-estrogenic mechanisms of action, including those present within mitochondria.

ACKNOWLEDGMENTS

This work was supported by National Institute of Environmental Health Sciences (NIEHS) grant ES07263 to R.A.S., NIEHS grant ES13061–01 to J.A.F., National Institutes of Health (NIH) grant R21NS050653 to T.K., and NIH grants NS34152, HD016596, and U.S. Army Medical Research and Material Command Neurotoxin Research Program grant DAMD 17–99–1–9483 to G.F.

REFERENCES

Bedogni, B., Pani, G., Colavitti, R., Riccio, A., Borello, S., Murphy, M., Smith, R., Eboli, M. L., and Galeotti, T. (2003). Redox regulation of cAMP-responsive element-binding protein and induction of manganous superoxide dismutase in nerve growth factor-dependent cell survival. *J. Biol. Chem.* **278,** 16510–16519.

Borgeest, C., Symonds, D., Mayer, L. P., Hoyer, P. B., and Flaws, J. A. (2002). Methoxychlor may cause ovarian follicular atresia and proliferation of the ovarian epithelium in the mouse. *Toxicol. Sci.* **68,** 473–478.

Borgeest, C., Miller, K. P., Gupta, R., Greenfeld, C., Hruska, K. S., Hoyer, P., and Flaws, J. A. (2004). Methoxychlor-induced atresia in the mouse involves Bcl-2 family members, but not gonadotropins or estradiol. *Biol. Reprod.* **70,** 1828–1835.

Botella, B., Crespo, J., Rivas, A., Cerrillo, I., Olea-Serrano, M. F., and Olea, N. (2004). Exposure of women to organochlorine pesticides in Southern Spain. *Environ. Res.* **96,** 34–40.

Byczkowski, J. Z., and Tluczkiewicz, J. (1978). Comparative study of respiratory chain inhibition by DDT and DDE in mammalian and plant mitochondria. *Bull. Environ. Contam. Toxicol.* **20,** 505–512.

Cammarota, M., Paratcha, G., Bevilaqua, L., Levi de Stein, M., Lopez, M., Pellegrino de Iraldi, A., Izquierdo, I., and Medina, J. H. (1999). Cyclic AMP-responsive element binding protein in brain mitochondria. *J. Neurochem.* **72,** 2272–2277.

Chedrese, P. J., and Feyles, F. (2001). The diverse mechanism of action of dichlorodiphenyldichloroethylene (DDE) and methoxychlor in ovarian cells *in vitro*. *Reprod. Toxicol.* **15,** 693–698.

Chen, J., Li, Y., Lavigne, J. A., Trush, M. A., and Yager, J. D. (1999). Increased mitochondrial superoxide production in rat liver mitochondria, rat hepatocytes and HepG2 cells following ethinyl estradiol treatment. *Toxicol. Sci.* **51,** 224–235.

Chuang, L. F., and Chuang, R. Y. (1998). Heptachlor and the mitogen-activated protein kinase module in human lymphocytes. *Toxicology* **128,** 17–23.

Cooper, R. L., Goldman, J. M., and Stoker, T. E. (1999). Neuroendocrine and reproductive effects of contemporary-use pesticides. *Toxicol. Ind. Health* **15,** 26–36.

Cummings, A. M. (1997). Methoxychlor as a model for environmental estrogens. *Crit. Rev. Toxicol.* **27,** 367–379.

Gore, A. C. (2002). Organochlorine pesticides directly regulate gonadotropin-releasing hormone gene expression and biosynthesis in the GT1-7 hypothalamic cell line. *Mol. Cell. Endocrinol.* **192,** 157–170.

Gray, L. E., Jr., Ostby, J., Ferrell, J., Rehnberg, G., Linder, R., Cooper, R., Goldman, J., Slott, V., and Laskey, J. (1989). A dose–response analysis of methoxychlor-induced alterations of reproductive development and function in the rat. *Fundam. Appl. Toxicol.* **12,** 92–108.

Greenamyre, J. T., MacKenzie, G., Peng, T. I., and Stephans, S. E. (1999). Mitochondrial dysfunction in Parkinson's disease. *Biochem. Soc. Symp.* **66,** 85–97.

Hillered, L., and Ernster, L. (1983). Respiratory activity of isolated rat brain mitochondria following *in vitr*o exposure to oxygen radicals. *J. Cereb. Blood Flow Metabol.* **3,** 207–214.

Hodges, L. C., Bergerson, J. S., Hunter, D. S., and Walker, C. L. (2000). Estrogenic effects of organochlorine pesticides on uterine leiomyoma cells *in vitro*. *Toxicol. Sci.* **54,** 355–364.

Kannan, K., and Jain, S. K. (2003). Oxygen radical generation and endosulfan toxicity in Jurkat T-cells. *Mol. Cell. Biochem.* **247,** 1–7.

Lafuente, A., González-Carracedo, A., Romero, A., and Esquifino, A. I. (2003). Methoxychlor modifies the ultradian excretory pattern of prolactin and affects its TRH response. *Med. Sci. Monit.* **9,** P155–P160.

Latchoumycandane, C., and Mathur, P. P. (2002). Effect of methoxychlor on the antioxidant system in mitochondrial and microsome-rich fractions of rat testis. *Toxicology* **176,** 67–75.

Lowry, O. H., Rosebrough, N. J., Farr, A. L., and Randall, R. J. (1951). Protein measurement with the folin phenol reagent. *J. Biol. Chem.* **193,** 265–275.

Mabuchi, T., Kitagawa, K., Kuwabara, K., Takasawa, K., Ohtsuki, T., Xia, Z., Storm, D., Yanagihara, T., Hori, M., and Matsumoto, M. (2001). Phosphorylation of cAMP response element-binding protein in hippocampal neurons as a protective response after exposure to glutamate *in vitro* and ischemia *in vivo*. *J. Neurosci.* **21,** 9204–9213.

Meyer, M. J., Mosely, D. E., Amarnath, V., and Picklo, M. J. (2004). Metabolism of 4-hydroxy-trans-2-nonenal by central nervous system mitochondria is dependent on age and NAD^+ availability. *Chem. Res. Toxicol.* **17,** 1272–1279.

Miller, K. P., Gupta, R. K., Greenfeld, C. R., Babus, J. K., and Flaws, J. A. (2005). Methoxychlor directly affects ovarian antral follicle growth and atresia through Bcl-2- and Bax-mediated pathways. *Toxicol. Sci.* Epub Aug. 4, 2005.

Mutisya, E. M., Bowling, A. C., and Beal, M. F. (1994). Cortical cytochrome oxidase activity is reduced in Alzheimer's disease. *J. Neurochem.* **63,** 2179–2184.

Okubo, T., Yokoyama, Y., Kano, K., Soya, Y., and Kano, I. (2004). Estimation of estrogenic and antiestrogenic activities of selected pesticides by MCF-7 cell proliferation assay. *Arch. Environ. Contam. Toxicol.* **46,** 445–453.

Rudel, R. A., Camann, D. E., Spengler, J. D., Korn, L. R., and Brody, J. G. (2003). Phthalates, alkylphenols, pesticides, polybrominated diphenyl ethers, and other endocrine-disrupting compounds in indoor air and dust. *Environ. Sci. Technol.* **37,** 4543–4553.

Ryu, H., Lee, J., Simon, D. K., Aminova, A., Andreyev, A., Murphy, A., Ginty, D., Ferrante, R. J., and Ratan, R. R. (2003). Mitochondrial CREB regulates mitochondrial gene expression and neuronal survival. *Soc. Neurosci.* 207.3 (abstract).

Sahoo, A., and Chainy, G. B. (1998). Acute hexachlorocyclohexane-induced oxidative stress in rat cerebral hemisphere. *Neurochem. Res.* **23,** 1079–1084.

Schuh, R. A., Kristían, T., and Fiskum, G. (2005). Calcium-dependent dephosphorylation of brain mitochondrial calcium/cAMP response element binding protein (CREB). *J. Neurochem.* **92,** 388–394.

Schuh, R. A., Lein, P. J., Beckles, R. A., and Jett, D. A. (2002). Non-cholinesterase mechanisms of chlorpyrifos neurotoxicity: Altered phosphorylation of Ca^{2+}/cAMP response element binding protein in cultured neurons. *Toxicol. Appl. Pharmacol.* **182,** 176–185.

Shekhar, P. V., Werdell, J., and Basrur, V. S. (1997). Environmental estrogen stimulation of growth and estrogen receptor function in preneoplastic and cancerous human breast cell lines. *J. Natl. Cancer Inst.* **89,** 1774–1782.

Sims, N. R. (1990). Rapid isolation of metabolically active mitochondria from rat brain and subregions using percoll density gradient centrifugation. *J. Neurochem.* **55,** 698–707.

Starkov, A. A., and Fiskum, G. (2003). Regulation of brain mitochondrial H_2O_2 production by membrane potential and NAD(P)H redox state. *J. Neurochem.* **86,** 1101–1107.

Starkov, A. A., Fiskum, G., Chinopoulos, C., Lorenzo, B. J., Browne, S. E., Patel, M. S., and Beal, M. F. (2004). Mitochondrial α-ketoglutarate dehydrogenase complex generates reactive oxygen species. *J. Neurosci.* **24,** 7779–7788.

Tanaka, K. (2001) Alteration of second messengers during acute cerebral ischemia—Adenylate cyclase, cyclic AMP-dependent protein kinase, and cyclic AMP response element binding protein. *Prog. Neurobiol.* **65,** 173–207.

Tawara, T., Fukushima, T., Hojo, N., Isobe, A., Shiwaku, K., Setogawa, T., and Yamane, Y. (1996). Effects of paraquat on mitochondrial electron transport system and catecholamine contents in rat brain. *Arch. Toxicol.* **70,** 585–589.

Zhang, Z., and Teng, C. T. (2002). Methoxychlor stimulates the mouse lactoferrin gene promoter through a GC-rich element. *Biochem. Cell. Biol.* **80,** 23–26.

Journal of Neuroscience Research 79:240–247 (2005)

Pyruvate Dehydrogenase Complex: Metabolic Link to Ischemic Brain Injury and Target of Oxidative Stress

Erica Martin,[1,2] **Robert E. Rosenthal,**[1,3] **and Gary Fiskum**[1,2]*

[1]Department of Anesthesiology, University of Maryland School of Medicine, Baltimore, Maryland
[2]Program in Neuroscience, University of Maryland School of Medicine, Baltimore, Maryland
[3]Department of Surgery Program in Trauma, University of Maryland School of Medicine, Baltimore, Maryland

The mammalian pyruvate dehydrogenase complex (PDHC) is a mitochondrial matrix enzyme complex (greater than 7 million Daltons) that catalyzes the oxidative decarboxylation of pyruvate to form acetyl CoA, nicotinamide adenine dinucleotide (the reduced form, NADH), and CO_2. This reaction constitutes the bridge between anaerobic and aerobic cerebral energy metabolism. PDHC enzyme activity and immunoreactivity are lost in selectively vulnerable neurons after cerebral ischemia and reperfusion. Evidence from experiments carried out in vitro suggests that reperfusion-dependent loss of activity is caused by oxidative protein modifications. Impaired enzyme activity may explain the reduced cerebral glucose and oxygen consumption that occurs after cerebral ischemia. This hypothesis is supported by the hyperoxidation of mitochondrial electron transport chain components and NAD(H) that occurs during reperfusion, indicating that NADH production, rather than utilization, is rate limiting. Additional support comes from the findings that immediate postischemic administration of acetyl-L-carnitine both reduces brain lactate/pyruvate ratios and improves neurologic outcome after cardiac arrest in animals. As acetyl-L-carnitine is converted to acetyl CoA, the product of the PDHC reaction, it follows that impaired production of NADH is due to reduced activity of either PDHC or one or more steps in glycolysis. Impaired cerebral energy metabolism and PDHC activity are associated also with neurodegenerative disorders including Alzheimer's disease and Wernicke-Korsakoff syndrome, suggesting that this enzyme is an important link in the pathophysiology of both acute brain injury and chronic neurodegeneration.

Key words: mitochondria; peroxynitrite; acetyl-L-carnitine; lactate; acidosis

PYRUVATE DEHYDROGENASE ENZYME COMPLEX

The pyruvate dehydrogenase complex (PDHC), located in the mitochondrial matrix, plays a major role in aerobic energy metabolism. This enzyme serves as the critical link between glycolysis (anaerobic metabolism) and the tricarboxylic acid cycle by catalyzing the oxidative decarboxylation of pyruvate to form acetyl CoA (Fig. 1) (Reed, 1981, 2001). The PDHC is a multisubunit complex composed of three major subunits: E1, E2, and E3 (Fig. 1). The E1 subunit (pyruvate dehydrogenase) is a tetramer that contains two α and two β subunits with molecular weights of 41 and 36 kDa, respectively. The entire PDHC contains approximately 30 copies of E1 and 60 copies of the 74-kDa E2 (dihydrolipoyl transacetylase) subunit. The 55-kDa E3 (dihydrolipoyl dehydrogenase) subunit is also found in α-ketoglutarate dehydrogenase (α-KGDH) (Patel and Harris, 1995). This shared homology makes many of the pathologies observed in PDHC also relevant to α-KGDH. Six copies of E3 are found within the PDHC. The enzyme complex also requires a variety of substrates and cofactors. Pyruvate, nicotinamide adenine dinucleotide (NAD^+), thiamine pyrophosphate (TPP), and coenzyme A (CoA) are all required for PDHC activity, as are flavin adenine dinucleotide (FAD) and lipoic acid (Reed, 2001). Activity of this complex enzyme is regulated by a host of factors, including phosphorylation state, Ca^{2+} concentration ($[Ca^{2+}]$), $[Mg^{2+}]$ (Huang et al., 1998), and [ATP/ADP] ratio (Fig. 2). PDHC is phosphorylated and therefore inactivated by PDH kinase, whereas PDH phosphatase activates the enzyme complex. Four isozymes of mammalian PDH kinase have been identified (PDK1–4). Although these isozymes differ in tissue-specific expression (Bowker-Kinley et al., 1998), they are all activated by elevated [acetyl-CoA/CoA] and [NADH/NAD^+] ratios (Bowker-Kinley, et al., 1998; Baker et al., 2000; Sugden and Holness, 2003) and inhibited by elevated ADP levels (Roche et al., 2003) and the drug

Contract grant sponsor: NIH; Contract grant number: NS34152, ES11838, HD16596; Contract grant sponsor: US Army Medical Research and Material Command; Contract grant number: DAMD 1799-1-9483, AHA 0215331U.

*Correspondence to: Dr. Gary Fiskum, Department of Anesthesiology, University of Maryland School of Medicine, 685 W. Baltimore St., MSTF 5.34, Baltimore, MD 21201. E-mail: gfisk001@umaryland.edu

Received 9 July 2004; Revised 10 August 2004; Accepted 10 August 2004

Published online 23 November 2004 in Wiley InterScience (www.interscience.wiley.com). DOI: 10.1002/jnr.20293

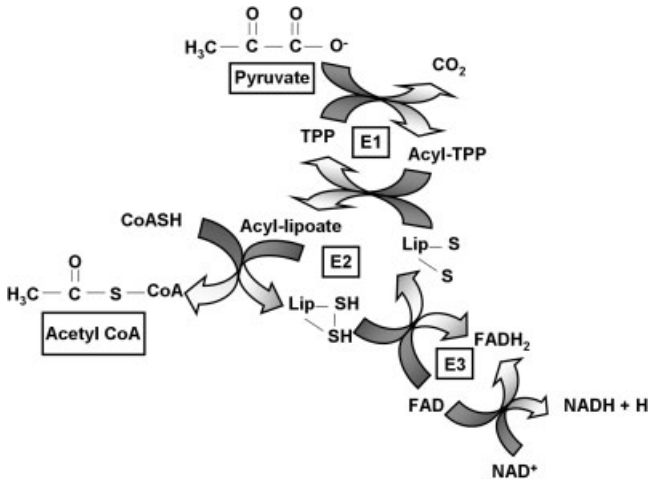

Fig. 1. Partial reactions of the PDHC. The PDHC catalyzes the oxidative decarboxylation of pyruvate to form acetyl CoA. The enzyme complex is composed of three major subunits: pyruvate dehydrogenase (E1), dihydrolipoyl transacetylase (E2), and dihydrolipoyl dehydrogenase (E3). In addition to pyruvate and coenzyme A (CoASH), PDHC also requires a host of cofactors, including thiamine pyrophosphate (TPP), nicotinamide adenine dinucleotide (NAD^+), flavin adenine dinucleotide (FAD), and lipoic acid (LIP).

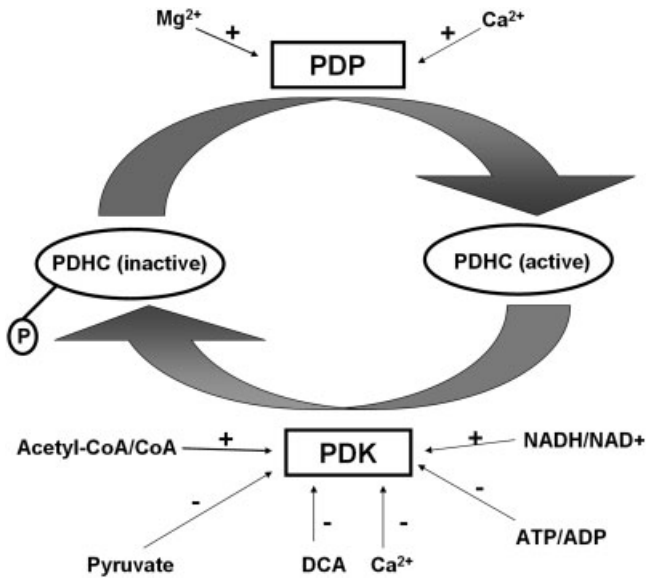

Fig. 2. Regulation of PDHC by phosphatase and kinase activities. PDHC is inactivated when phosphorylated by PDH kinase (PDK). PDK is activated by elevated $NADH/NAD^+$ and acetyl CoA/CoA ratios and is inactivated by pyruvate, dichloroacetate (DCA), Ca^{2+}, and elevated ATP/ADP ratios. PDHC is activated when dephosphorylated by PDH phosphatase (PDP). Although less characterized than PDK, PDP is stimulated by both Mg^{2+} and Ca^{2+}. Four isozymes of PDH kinase (PDK1–4) and two isozymes of PDH phosphatase (PDP1c and PDP2c) have been identified. These isozymes differ in tissue specificity, as well as relative sensitivity to the effectors depicted in the figure.

dichloroacetate (Whitehouse et al., 1974; Baker et al., 2000; Wilson et al., 2003). Some PDH phosphatase isoforms are stimulated by Ca^{2+} (Huang et al., 1998; Karpova et al., 2003; Roche et. al., 2003). The complexity of the multitude of subunits, strict cofactor requirements, and stringent regulation of the PDHC make it a possible target for damage and subsequent inactivation during pathologic conditions including ischemia and neurodegenerative disorders.

EFFECTS OF ISCHEMIA/REPERFUSION ON CEREBRAL ENERGY METABOLISM AND PDHC ACTIVITY

Measurements of cerebral glucose metabolism and oxygen utilization after global ischemia/reperfusion indicate that cerebral energy metabolism is impaired markedly during postischemic recirculation (Pulsinelli et al., 1982). A significant decrease in glucose oxidation develops within the first hour of reperfusion and remains for many hours thereafter (Sims, 1995). Oxidative glucose metabolism is also reduced after focal cerebral ischemia in a time-dependent manner (Pascual et al., 1998). Although aerobic glucose metabolism is impaired, the oxidative metabolism of other fuels, e.g., glutamate, γ-aminobutyric acid (GABA), and glutamine, can accelerate after focal ischemia (Pascual et al., 1998).

One possible explanation for reduced cerebral glucose metabolism after ischemia is decreased PDHC activity (Fukuchi et al., 1998; Schoder et al., 1998). In the rat dorsolateral striatum after short-term forebrain ischemia, PDHC activity is reduced, particularly in selectively vulnerable neurons (Zaidan and Sims, 1997). Reduced

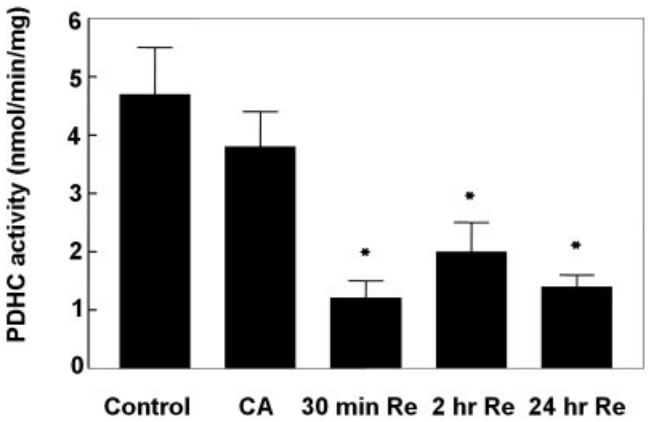

Fig. 3. Effects of cardiac arrest and resuscitation on canine frontal cortex PDHC enzyme activity. PDHC activity remains unchanged after 10 min of cardiac arrest (CA) alone. Activity is decreased significantly, however, as early as 30 min of reperfusion (Re) and remains depressed through 24 hr. PDHC activity was measured using a radioisotopic assay that monitors CO_2 production from [1-^{14}C] pyruvate. PDHC activity is reported in nmol/min/mg total brain protein. Reprinted from Free Radical Biology and Medicine, Vol 16, Bogaert et al., Postischemic inhibition of cerebral cortex pyruvate dehydrogenase, p 811–820, ©1994 with permission from Elsevier.

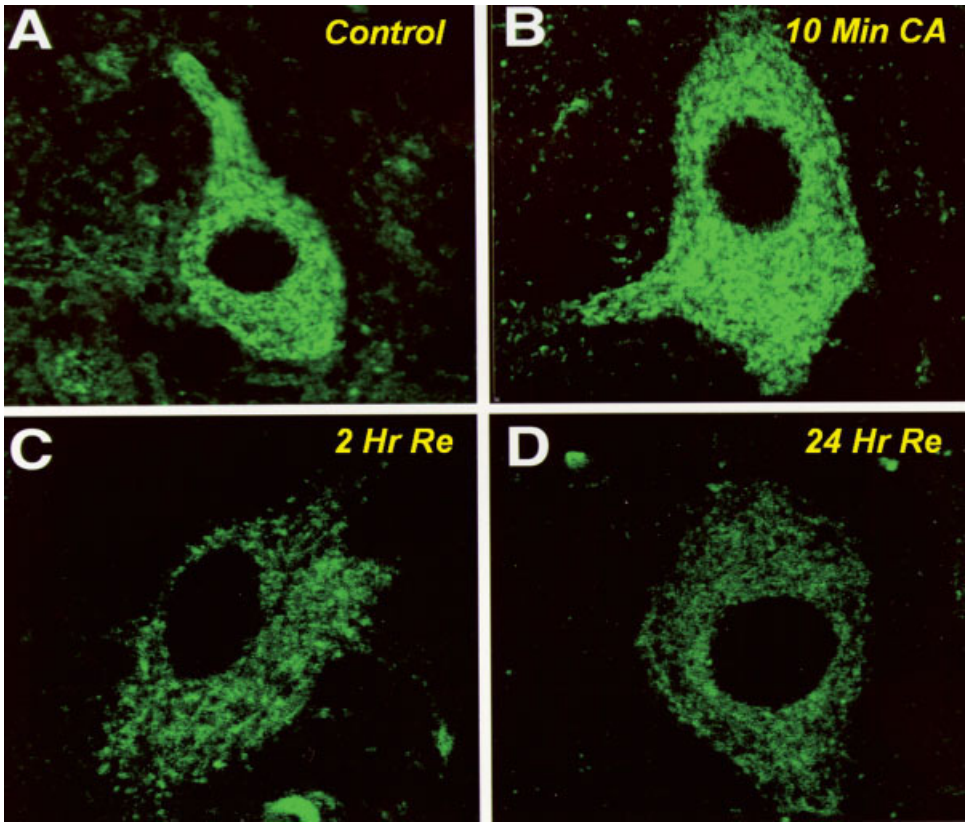

Fig. 4. Effects of cardiac arrest and resuscitation on canine frontal cortex PDHC immunoreactivity. Canine frontal cortex neuronal PDHC immunoreactivity remains unchanged after 10-min cardiac arrest (**A, B**). Confocal fluorescent imaging, using a polyclonal antibody to the entire PDHC complex, reveals diminished immunoreactivity after 2-hr reperfusion (**C**), which remains low at 24 hr reperfusion (**D**). Reprinted from Experimental Neurology, Vol 161, Bogaert et al., Neuronal subclass-selective loss of pyruvate dehydrogenase immunoreactivity following canine cardiac arrest and resuscitation, p 115-126, ©2000 with permission from Elsevier.

PDHC activity is observed in other locations, such as the frontal cortex, and is evident with reperfusion times as short as 30 min and as long as 24 hr (Zaidan and Sims, 1993; Bogaert et al., 1994). This decrease in enzyme activity is reperfusion dependent, as no change in activity is detected after ischemia alone (Fig. 3). It is unlikely that these changes are attributed to changes in cofactor levels, as the activity assays were carried out with saturating levels of required substrates and cofactors. PDHC immunoreactivity is also lost after ischemia/reperfusion. After a 10-min canine cardiac arrest with either 2 or 24 hr of reperfusion, both Western immunoblot and immunohistochemical analysis indicate a significant decrease in PDHC immunoreactivity (Fig. 4) (Bogaert et al., 2000). It is unlikely that the decline in PDHC activity or immunoreactivity is due to changes in the phosphorylation of the complex, as the phosphorylation state of PDHC does not change appreciably, at least in some models of ischemia/reperfusion (Zaidan and Sims, 1993). The decreased PDHC immunoreactivity, however, could be due to effects of ischemia/reperfusion-mediated damage to one or more of the PDHC required substrates or cofactors. A more likely explanation is site-specific protein oxidation, which may cause the decreased PDHC immunoreactivity by marking the affected regions for proteolytic degradation after an ischemia/reperfusion event (Stadtman, 1990).

At this juncture, direct evidence for a reduction in PDHC activity being responsible for impaired postischemic cerebral energy metabolism is lacking; however, several observations support this hypothesis. One such finding is that immediate intravenous administration of acetyl-L-carnitine (ALCAR; 100 mg/kg) reduces brain lactate levels and improves neurologic outcome after cardiac arrest (Table I) (Rosenthal et al., 1992). These effects are not observed with administration of equimolar equivalent levels of acetate and free carnitine, indicating that ALCAR possesses unique neuroprotective characteristics. Medium- and long-chain acylcarnitines are not well metabolized in the adult brain due to relatively very low acylcarnitine-CoA transferase activities. Acetylcarnitine-CoA transferase is present, however, allowing for possible entry of ALCAR acetyl units into the tricarboxylic acid (TCA) cycle of astrocytes or neurons (Bresolin et al., 1982). By providing a source of fuel alternative to pyruvate, ALCAR may stimulate aerobic energy metabolism, thereby reducing the rate of glycolytic lactate production and the tissue acidosis that accompanies anaerobic metabolism (Fig. 5). ALCAR also acts at least indirectly as an antioxidant, reducing protein carbonyl formation during reperfusion (Liu et al., 1993), and cerebrospinal fluid protein nitration in multiple sclerosis patients (Calabrese et al., 2003). This protection against oxidative stress may explain its ability to protect against the loss of PDHC activity in the cardiac arrest model (Bogaert et al., 1994), which in turn may help explain its ability to lower tissue lactate levels. ALCAR can also ameliorate some metabolic ab-

TABLE I. Effects of Acetyl-L-Carnitine and Acetate Plus Carnitine on 2-hr Neurochemical Outcome and 24-hr Neurologic Outcome After 10-min Canine Cardiac Arrest

	Vehicle[a]	Acetyl-L-carnitine[a]	Acetate + carnitine[b]
Lactate (μmol/g wet wt)	4.3 ± 0.2	2.0 ± 0.4*	5.7 ± 2.2
Pyruvate (nmol/g wet wt)	160 ± 41	197 ± 24	139.2 ± 51
Lactate/pyruvate	34.3 ± 6.9	9.5 ± 1.1**	51.3 ± 22
Neurodeficit score[c]	48.4 ± 5.4	22.3 ± 5.2***	41.0 ± 3.1

[a]Values for vehicle- and acetyl-L-carnitine-treated animals reprinted with permission from Rosenthal et al. 1992. Prevention of postischemic canine neurological injury through potentiation of brain energy metabolism by acetyl-L-carnitine. Stroke 23:1312–1318.

[b]Animals treated with acetate plus carnitine at levels equimolar to that of acetyl-L-carnitine administered at 100 mg/kg intravenously immediately after resuscitation, then at 50 mg/kg every 6 hr. Samples were obtained from canine frontal cortex, immediately placed into liquid nitrogen, and stored at −80°C until analyzed for lactate and pyruvate. Values represent means ± standard error for $n = 5$–7 animals per group.

[c]Neurodefecit score evaluated on a scale from 0 (normal) to 100 (braindead).

*$P < 0.01$ compared to vehicle group.

**$P < 0.05$ compared to vehicle group.

***$P < 0.002$ compared to vehicle group.

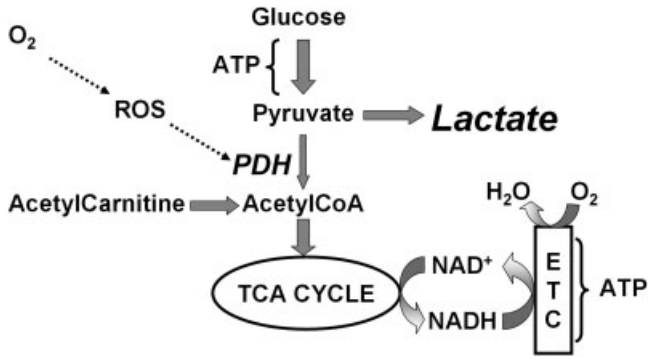

Fig. 5. PDHC serves as the bridge between anaerobic and aerobic metabolism. The PDHC is a target of oxidative stress and is inhibited after cerebral ischemia. Such inhibition may be responsible for chronically elevated brain lactate levels after ischemic episodes as PDHC constitutes the bridge between aerobic and anaerobic cerebral energy metabolism. Acetyl-L-carnitine (ALCAR) may serve as an exogenous, alternative source of acetyl CoA, thereby reducing tissue acidosis and improving neurologic outcome.

normalities induced by chronic excessive alcohol consumption, which is also associated with impaired brain PDHC activity (Calabrese et al., 2002).

Another observation implicating the role of PDHC in brain injury resulting from ischemia/reperfusion is the hyperoxidation of NAD(H) and components of the mitochondrial electron transport chain during reperfusion (Rosenthal et al., 1995). If damage to the electron transport chain was the major factor in ischemia/reperfusion injury, the redox state of NAD(H) would undergo a shift toward a more reduced state. The limiting factor in reperfusion injury therefore seems to be proximal to the electron transport chain. The rate-limiting site could include various TCA cycle enzymes, e.g., α-KGDH. According to the direct metabolic hypothesis for neuroprotection by ALCAR, however, inhibition of metabolism at points distal to acetyl CoA would not be alleviated by ALCAR administration. Experiments are in progress using ^{13}C nuclear magnetic resonance (NMR) spectroscopy to study the metabolism of ALCAR, and the effects it has on glucose metabolism to help, determine the significance of altered PDHC activity in ischemic brain injury.

ROLE OF PYRUVATE DEHYDROGENASE COMPLEX IN THE PATHOPHYSIOLOGY OF NEURODEGENERATIVE DISORDERS

In addition to ischemic brain injury, PDHC is affected also in other neurologic disorders. Wernicke-Korsakoff Syndrome (WKS) is a disease characterized by a triad of mental confusion, ataxia, and ophthalmoplegia. This disorder is commonly associated with chronic alcoholism, although other nutritional deficits resulting in low dietary thiamine can also cause onset of disease symptoms. The main etiologic factor is known to be lack of thiamine, but the biochemical mechanisms involved remain unclear. Thiamine-dependent enzymes such as PDHC and αKGDH are thought to play a role in the pathogenesis of WKS. Decreased PDHC and αKGDH enzyme activities are found in alcoholics diagnosed with WKS, whereas alcoholic patients without WKS display normal levels of thiamine-dependent enzyme activities (Butterworth et al., 1993). Although decreased αKGDH activity has also been shown in an animal model of thiamine deficiency, the effects of thiamine depletion on PDHC activity in vitro remain controversial (Parker et al., 1984; Butterworth and Heroux, 1989; Munujos et al., 1996). PDHC activity is also affected in Alzheimer's disease (AD) (Sheu et al., 1985). Brain lipid peroxidation and decreased brain glucose utilization are characteristic of this neurodegenerative disease. Acrolein, a byproduct of lipid peroxidation that accumulates within the brain during AD, decreases PDHC activity. Specifically, acrolein binds lipoic acid, a component of both PDHC and αKGDH (Pocernich and Butterfield, 2003). Inactivation of PDHC by acrolein or other mechanisms may be at least partially responsible for mito-

chondrial dysfunction and impaired cerebral energy metabolism associated with AD.

MOLECULAR MECHANISMS OF ENZYME INACTIVATION

The PDHC inactivation that occurs during acute brain injuries and in neurodegenerative disorders could be due to any one or a combination of several mechanisms. In addition to depletion of the enzyme cofactors TPP and lipoic acid, the protein subunits may also be direct targets of oxidative stress. Purified porcine heart PDHC is highly sensitive to inactivation when exposed to a hydroxyl radical ($OH^{\bullet}$) generating system composed of H_2O_2 and Fe^{2+} (Bogaert et al., 1994). PDHC activity is not lost in the presence of H_2O_2 alone, as activity is retained in the presence of the iron chelator diethylenetriaminepentacetic acid (DTPA; 2 mM) (Fig. 6). Recent findings in our laboratory suggest that PDHC is also targeted by peroxynitrite ($ONOO^-$). Peroxynitrite is formed when superoxide reacts with NO (Beckman et al., 1990; Goldstein and Czapski, 1995; Beckman, 1996; Murphy et al., 1998). Both substrates are generated by 3-morpholinosydnonomine (SIN-1) (Feelisch et al., 1989), which when incubated with purified PDHC results in a loss of enzyme activity that is partially inhibited by the presence of superoxide dismutase (Fig. 6). Further experiments are planned to determine the relative contribution of $ONOO^-$, compared to NO or $O_2^{-\bullet}$, to the impairment of enzyme activity observed in this system.

In addition to the aforementioned in vitro effects of free radicals on PDHC activity, decreased activity of other mitochondrial proteins has also been identified in vivo. Hypoxia–reoxygenation paradigms decrease aconitase and succinate dehydrogenase activities, a finding attributed to excess $O_2^{-\bullet}$ production (Powell and Jackson, 2003). Additionally, αKGDH and aconitase activities are decreased during reperfusion of ischemic myocardial tissue (Sadek et al., 2002). As evidence indicates that production of superoxide, hydroxyl radical, nitric oxide, and peroxynitrite are elevated during reperfusion (Metodiewa and Koska, 2000), these results support the hypothesis that oxidative stress is responsible for reperfusion-dependent loss of brain PDHC activity.

Further support for oxidative stress as a mechanism responsible for PDHC damage during ischemia reperfusion comes from comparison of protein immunoreactivity between cardiac arrest animal groups resuscitated with relatively high and low concentrations of ventilatory O_2. Hippocampal PDHC E1α subunit immunostaining is reduced by up to 90% within 2 hr of reperfusion in dogs resuscitated on 100% O_2 compared to that in nonischemic animals, whereas no significant reduction in hippocampal E1α immunoreactivity is observed in animals resuscitated with 21% O_2 (room air). Double labeling with neuron-specific nuclear protein antibody (NeuN) indicates the PDHC loss is partially neuronal, but astrocytic involvement remains undetermined. Moreover, hippocampal nitrotyrosine immunoreactivity is greater in the hyperoxic resuscitation group (Vereczki et al., 2003). These results, taken together with our previous findings that hyperoxic resuscitation causes increased brain lipid peroxidation and worse neurologic outcome (Liu et al., 1998), suggest that PDHC is one important target of oxidative stress and that its inactivation may contribute to neuronal injury and neurologic impairment.

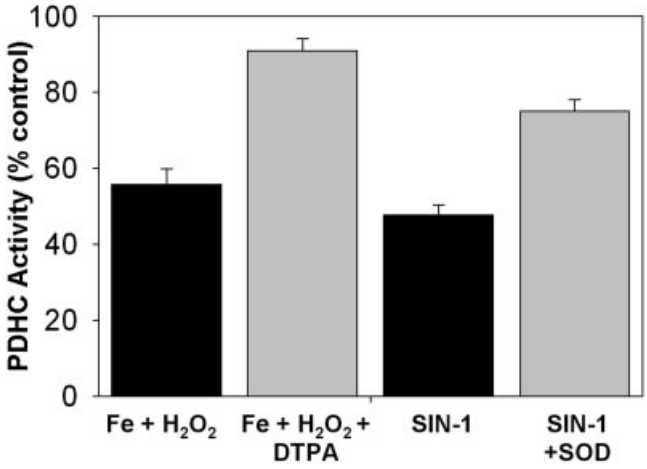

Fig. 6. Inhibition of PDHC activity by hydroxyl radical and peroxynitrite. Results obtained with exposure of purified porcine heart mitochondria for 10 min at 37°C to a Fenton reagent consisting of 0.25 mM $FeSO_4$ plus 0.5 mM H_2O_2 in the absence and presence of 2.5 mM diethylenetriaminepentacetic acid (DTPA). Reprinted from Free Radical Biology and Medicine, Vol 16, Bogaert et al., Postischemic inhibition of cerebral cortex pyruvate dehydrogenase, p 811–820, ©1994 with permission from Elsevier. Additional results were obtained under similar conditions but using 0.6 mM of the peroxynitrite generator 3-morpholinosydnonomine (SIN-1) in the absence and presence of superoxide dismutase (SOD; 20 U/ml). Enzyme activity after the preincubations was measured either radioisotopically by determining the $^{14}CO_2$ production from [1-^{14}C] pyruvate (Fenton reagent; Bogaert et al., 1994), or spectrophotometrically by measuring NADH production at 340 nm (SIN-1). Dithiothreitol (9 mM) was present during all preincubations to eliminate possible inactivation due to thiol oxidations or S-nitrosylation. Experimental conditions for experiments involving SIN-1 were modified from Hinman and Blass (1981) and consisted of 50 mM potassium phosphate buffer (37°C), 2.06 U/ml PDHC, 5 mM pyruvate, 0.3 mM thiamine pyrophosphate (TPP), 1 mM magnesium chloride, 0.01 mM calcium chloride, and 1 mM NAD^+. The reaction was initiated by the addition of 0.12 mM coenzyme A whereas the reactions after exposure to the Fenton reagent were initiated with the addition of 2 mM pyruvate.

POTENTIAL THERAPEUTIC INTERVENTIONS

Based on the hypothesis that impairment of PDHC activity contributes to the pathophysiology of ischemic brain injury, interventions that either protect against PDHC inactivation or compensate for the metabolic disruption should be neuroprotective. Dichloroacetate (DCA) is a pharmacologic agent that stimulates maximal PDHC activity by inhibiting PDH kinase. It is used as a treatment for patients with PDHC deficiency, a condition that presents clinical symptoms during the first months of

life. PDHC activity is increased in PDHC-deficient patients treated with 5 mM DCA (Fouque et al., 2003). DCA administration has also been demonstrated to decrease brain lactate and to improve outcome in small and large animal models of both global and focal cerebral ischemia (Biros et al., 1986; Cardell et al., 1989; Katayama and Welsh, 1989; Chang et al., 1992; Corbett et al., 1998; Chandy and Ravindra, 2000). Moreover, one clinical study using proton magnetic resonance spectroscopy indicates that administration of DCA within the first 2 days of ischemic stroke lowers brain lactate (Graham et al., 2000). Administration of lipoic acid is also neuroprotective and although its mechanisms of action are ascribed to either direct antioxidant activity or regulation of gene transcription, promotion of PDHC activity has not been addressed (Wolz and Krieglstein, 1996; Packer, 1998; Clark et al., 2001; Garcia-Estrada et al., 2003). Thiamine replacement therapy is used for patients with thiamine deficiency but has not been tested for neuroprotection after acute brain injury.

As mentioned earlier, immediate postischemic infusion of acetyl-L-carnitine is neuroprotective, possibly by providing alternative oxidative fuel in the presence of reduced conversion of pyruvate to acetyl CoA. Other researchers have demonstrated neuroprotection by administration of ketone bodies, e.g., β-hydroxybutyrate, in animal models of ischemia, trauma, and Parkinson's disease (Lundy et al., 1984, 1987; Marie et al., 1987; Sims and Heward, 1994; Kashiwaya et al., 2000; Ottani et al., 2003; Tieu et al., 2003; Yosunkaya et al., 2004). Although the mechanism of neuroprotection by ketone bodies is not characterized, they similarly bypass the PDHC reaction and provide fuel to the TCA cycle.

Although interventions that compensate for a loss of PDHC activity may prove clinically effective, an alternative approach is to inhibit those mechanisms responsible for damage to the enzyme complex. Based on the hypothesis that oxidative stress is the primary culprit, antioxidants should prove useful. Indeed, many preclinical studies with antioxidants have demonstrated neuroprotection (Chan, 2001; Floyd and Hensley, 2002); however, results from the few clinical trials testing antioxidants are disappointing (van der Worp et al., 2002). An alternative approach to minimizing oxidative stress during postischemic reperfusion is to limit the delivery of oxygen to the brain. The few reported comparisons of neurologic outcome after hyperoxic and normoxic reperfusion strongly suggest that hyperoxic resuscitation is detrimental. Using a 9-min canine cardiac arrest (CA) model, Zwemer et al. (1994) found that resuscitation with 100% inspired O_2 resulted in worsened 12- and 24-hr neurologic outcome when compared to that in animals receiving 21% O_2. This difference was eliminated when animals were pretreated with an antioxidant before the CA and hyperoxic resuscitation. In our canine experiments using 10-min CA, neurologic impairment measured at 24 hr was significantly worse in animals ventilated on 100% O_2 during and for 1 hr after resuscitation than that exhibited by dogs resuscitated on 21% O_2 and subsequently ventilated on 21–30% O_2 to maintain normal PaO_2 (Rosenthal et al., 2003). The one negative study is the report mentioned earlier where no difference in neurologic impairment was observed 72 hr after asphyxia-induced CA in rats (Lipinski et al., 1999). The only published long-term outcome study focused on mortality and used the gerbil bilateral carotid occlusion model. Mickel et al. (1987) found that animals exposed to 100% O_2 for 3–6 hr after 15-min global cerebral ischemia experienced a threefold increase in 14-day mortality compared to those allowed to breathe room air after ischemia. As mentioned earlier, our recent results comparing hippocampal PDHC immunoreactivity between hyperoxic and normoxic resuscitated animals indicate that normoxic ventilation preserves this PDHC immunostaining (Vereczki et al., 2003). Studies are in progress to determine if normoxic resuscitation also preserves PDHC enzyme activity and, in turn, aerobic cerebral energy metabolism.

SUMMARY

PDHC plays a critical role in cerebral aerobic energy metabolism. Its vast size, strict cofactor requirements, and stringent regulation make it a potential target of injury during times of neurologic stress, such as ischemia or trauma. Indirect evidence suggests that loss of PDHC enzyme activity after cardiac arrest and resuscitation contributes to the prolonged elevation of brain lactate levels. More direct evidence that impaired PDHC activity limits cerebral energy metabolism during reperfusion awaits quantitative analysis of metabolic flux. Although evidence obtained in vitro indicates that PDHC is sensitive to inactivation when exposed to reactive oxygen and nitrogen species, further work is necessary to conclude that oxidative alterations are responsible for its inactivation in vivo.

REFERENCES

Baker JC, Yan X, Peng T, Kasten S, Roche TE. 2000. Marked differences between two isoforms of human pyruvate dehydrogenase kinase. J Biol Chem 275:15773–15781.

Beckman JS. 1996. Oxidative damage and tyrosine nitration from peroxynitrite. Chem Res Toxicol 9:836–844.

Beckman JS, Beckman TW, Chen J, Marshall PA, Freeman BA. 1990. Apparent hydroxyl radical production by peroxynitrite: implications for endothelial injury from nitric oxide and superoxide. Proc Natl Acad Sci USA 87:1620–1624.

Biros MH, Dimlich RV, Barsan WG. 1986. Postinsult treatment of ischemia-induced cerebral lactic acidosis in the rat. Ann Emerg Med 15:397–404.

Bogaert YE, Rosenthal RE, Fiskum G. 1994. Postischemic inhibition of cerebral cortex pyruvate dehydrogenase. Free Radic Biol Med 16:811–820.

Bogaert YE, Sheu KF, Hof PR, Brown AM, Blass JP, Rosenthal RE, Fiskum G. 2000. Neuronal subclass-selective loss of pyruvate dehydrogenase immunoreactivity following canine cardiac arrest and resuscitation. Exp Neurol 161:115–126.

Bowker-Kinley MM, Davis WI, Wu P, Harris RA, Popov KM. 1998. Evidence for existence of tissue-specific regulation of the mammalian pyruvate dehydrogenase complex. Biochem J 329:191–196.

Bresolin N, Freddo L, Vergani L, Angelini C. 1982. Carnitine, carnitine acyltransferases, and rat brain function. Exp Neurol 78:285–292.

Butterworth RF, Heroux M. 1989. Effect of pyrithiamine treatment and subsequent thiamine rehabilitation on regional cerebral amino acids and thiamine-dependent enzymes. J Neurochem 52:1079–1084.

Butterworth RF, Kril JJ, Harper CG. 1993. Thiamine-dependent enzyme changes in the brains of alcoholics: relationship to the Wernicke-Korsakoff syndrome. Alcohol Clin Exp Res 17:1084–1088.

Calabrese V, Scapagnini G, Latteri S, Colombrita C, Ravagna A, Catalano C, Pennisi G, Calvani M, Butterfield DA. 2002. Long-term ethanol administration enhances age-dependent modulation of redox state in different brain regions in the rat: protection by acetyl carnitine. Int J Tissue React 24:97–104.

Calabrese V, Scapagnini G, Ravagna A, Bella R, Butterfield DA, Calvani M, Pennisi G, Giuffrida Stella AM. 2003. Disruption of thiol homeostasis and nitrosative stress in the cerebrospinal fluid of patients with active multiple sclerosis: evidence for a protective role of acetylcarnitine. Neurochem Res 28:1321–1328.

Cardell M, Koide T, Wieloch T. 1989. Pyruvate dehydrogenase activity in the rat cerebral cortex following cerebral ischemia. J Cereb Blood Flow Metab 9:350–357.

Chan PH. 2001. Reactive oxygen radicals in signaling and damage in the ischemic brain. J Cereb Blood Flow Metab 21:2–14.

Chandy MJ, Ravindra J. 2000. Effect of dichloracetate on infarct size in a primate model of focal cerebral ischaemia. Neurol India 48:227–230.

Chang LH, Shimizu H, Abiko H, Swanson RA, Faden AI, James TL, Weinstein PR. 1992. Effect of dichloroacetate on recovery of brain lactate, phosphorus energy metabolites, and glutamate during reperfusion after complete cerebral ischemia in rats. J Cereb Blood Flow Metab 12:1030–1038.

Clark WM, Rinker LG, Lessov NS, Lowery SL, Cipolla MJ. 2001. Efficacy of antioxidant therapies in transient focal ischemia in mice. Stroke 32: 1000–1004.

Corbett R, Laptook A, Gee J, Garcia D, Silmon S, Tollefsbol G. 1998. Age-related differences in the effect of dichloroacetate on postischemic lactate and acid clearance measured in vivo using magnetic resonance spectroscopy and microdialysis. J Neurochem 71:1205–1214.

Feelisch M, Ostrowski J, Noack E. 1989. On the mechanism of NO release from sydnonimines. J Cardiovasc Pharmacol 14(Suppl):13–22.

Floyd RA, Hensley K. 2002. Oxidative stress in brain aging. Implications for therapeutics of neurodegenerative diseases. Neurobiol Aging 23:795–807.

Fouque F, Brivet M, Boutron A, Vequaud C, Marsac C, Zabot MT, Benelli C. 2003. Differential effect of DCA treatment on the pyruvate dehydrogenase complex in patients with severe PDHC deficiency. Pediatr Res 53:793–799.

Fukuchi T, Katayama Y, Kamiya T, McKee A, Kashiwagi F, Terashi A. 1998. The effect of duration of cerebral ischemia on brain pyruvate dehydrogenase activity, energy metabolites, and blood flow during reperfusion in gerbil brain. Brain Res 792:59–65.

Garcia-Estrada J, Gonzalez-Perez O, Gonzalez-Castaneda RE, Martinez-Contreras A, Luquin S, de la Mora PG, Navarro-Ruiz A. 2003. An alpha-lipoic acid-vitamin E mixture reduces post-embolism lipid peroxidation, cerebral infarction, and neurological deficit in rats. Neurosci Res 47:219–224.

Goldstein S, Czapski G. 1995. The reaction of NO. with O2.− and HO2.: a pulse radiolysis study. Free Radic Biol Med 19:505–510.

Graham GD, Barker PB, Brooks WM, Morris DC, Ahmed W, Bryniarski E, Hearshen DO, Sanders JA, Holshouser BA, Turkel CC. 2000. MR spectroscopy study of dichloroacetate treatment after ischemic stroke. Neurology 55:1376–1378.

Hinman LM, Blass JP. 1981. An NADH-linked spectrophotometric assay for pyruvate dehydrogenase complex in crude tissue homogenates. J Biol Chem 256:6583–6586.

Huang B, Gudi R, Wu P, Harris RA, Hamilton J, Popov KM. 1998. Isoenzymes of pyruvate dehydrogenase phosphatase. DNA-derived amino acid sequences, expression, and regulation. J Biol Chem 273:17680–17688.

Karpova T, Danchuk S, Kolobova E, Popov KM. 2003. Characterization of the isozymes of pyruvate dehydrogenase phosphatase: implications for the regulation of pyruvate dehydrogenase activity. Biochim Biophys Acta 1652:126–135.

Kashiwaya Y, Takeshima T, Mori N, Nakashima K, Clarke K, Veech RL. 2000. D-beta-hydroxybutyrate protects neurons in models of Alzheimer's and Parkinson's disease. Proc Natl Acad Sci USA 97:5440–5444.

Katayama Y, Welsh FA. 1989. Effect of dichloroacetate on regional energy metabolites and pyruvate dehydrogenase activity during ischemia and reperfusion in gerbil brain. J Neurochem 52:1817–1822.

Lipinski CA, Hicks SD, Callaway CW. 1999. Normoxic ventilation during resuscitation and outcome from asphyxial cardiac arrest in rats. Resuscitation 42:221–229.

Liu Y, Rosenthal RE, Haywood Y, Miljkovic-Lolic M, Vanderhoek JY, Fiskum G. 1998. Normoxic ventilation after cardiac arrest reduces oxidation of brain lipids and improves neurological outcome. Stroke 29: 1679–1686.

Liu Y, Rosenthal RE, Starke-Reed P, Fiskum G. 1993. Inhibition of postcardiac arrest brain protein oxidation by acetyl-L-carnitine. Free Radic Biol Med 15:667–670.

Lundy EF, Klima LD, Huber TS, Zelenock GB, D'Alecy LG. 1987. Elevated blood ketone and glucagon levels cannot account for 1,3-butanediol induced cerebral protection in the Levine rat. Stroke 18:217–222.

Lundy EF, Luyckx BA, Combs DJ, Zelenock GB, D'Alecy LG. 1984. Butanediol induced cerebral protection from ischemic-hypoxia in the instrumented Levine rat. Stroke 15:547–552.

Marie C, Bralet AM, Bralet J. 1987. Protective action of 1,3-butanediol in cerebral ischemia. A neurologic, histologic, and metabolic study. J Cereb Blood Flow Metab 7:794–800.

Metodiewa D, Koska C. 2000. Reactive oxygen species and reactive nitrogen species: relevance to cyto(neuro)toxic events and neurologic disorders. An overview. Neurotox Res 1:197–233.

Mickel HS, Vaishnav YN, Kempski O, von Lubitz D, Weiss JF, Feuerstein G. 1987. Breathing 100% oxygen after global brain ischemia in Mongolian gerbils results in increased lipid peroxidation and increased mortality. Stroke 18:426–430.

Munujos P, Coll-Canti J, Beleta J, Gonzalez-Sastre F, Gella FJ. 1996. Brain pyruvate oxidation in experimental thiamin-deficiency encephalopathy. Clin Chim Acta 255:13–25.

Murphy MP, Packer MA, Scarlett JL, Martin SW. 1998. Peroxynitrite: a biologically significant oxidant. Gen Pharmacol 31:179–186.

Ottani A, Saltini S, Bartiromo M, Zaffe D, Renzo BA, Ferrari A, Bertolini A, Genedani S. 2003. Effect of γ-hydroxybutyrate in two rat models of focal cerebral damage. Brain Res 986:181–190.

Packer L. 1998. alpha-Lipoic acid: a metabolic antioxidant which regulates NF-kappa B signal transduction and protects against oxidative injury. Drug Metab Rev 30:245–275.

Parker WD, Haas R, Stumpf DA, Parks J, Eguren LA, Jackson C. 1984. Brain mitochondrial metabolism in experimental thiamine deficiency. Neurology 34:1477–1481.

Pascual JM, Carceller F, Roda JM, Cerdan S. 1998. Glutamate, glutamine, and GABA as substrates for the neuronal and glial compartments after focal cerebral ischemia in rats. Stroke 29:1048–1056.

Patel MS, Harris RA. 1995. Mammalian alpha-keto acid dehydrogenase complexes: gene regulation and genetic defects. FASEB J 9:1164–1172.

Pocernich CB, Butterfield DA. 2003. Acrolein inhibits NADH-linked mitochondrial enzyme activity: implications for Alzheimer's disease. Neurotox Res 5:515–520.

Powell CS, Jackson RM. 2003. Mitochondrial complex I, aconitase, and succinate dehydrogenase during hypoxia-reoxygenation: modulation of enzyme activities by MnSOD. Am J Physiol Lung Cell Mol Physiol 285:189–198.

Pulsinelli WA, Levy DE, Duffy TE. 1982. Regional cerebral blood flow and glucose metabolism following transient forebrain ischemia. Ann Neurol 11:499–502.

Reed LJ. 1981. Regulation of mammalian pyruvate dehydrogenase complex by a phosphorylation-dephosphorylation cycle. Curr Top Cell Regul 18:95–106.

Reed LJ. 2001. A trail of research from lipoic acid to alpha-keto acid dehydrogenase complexes. J Biol Chem 276:38329–38336.

Roche TE, Hiromasa Y, Turkan A, Gong X, Peng T, Yan X, Kasten SA, Bao H, Dong J. 2003. Essential roles of lipoyl domains in the activated function and control of pyruvate dehydrogenase kinases and phosphatase isoform 1. Eur J Biochem 270:1050–1056.

Rosenthal M, Feng ZC, Raffin CN, Harrison M, Sick TJ. 1995. Mitochondrial hyperoxidation signals residual intracellular dysfunction after global ischemia in rat neocortex. J Cereb Blood Flow Metab 15:655–665.

Rosenthal RE, Silbergleit R, Hof PR, Haywood Y, Fiskum G. 2003. Hyperbaric oxygen reduces neuronal death and improves neurological outcome after canine cardiac arrest. Stroke 34:1311–1316.

Rosenthal RE, Williams R, Bogaert YE, Getson PR, Fiskum G. 1992. Prevention of postischemic canine neurological injury through potentiation of brain energy metabolism by acetyl-L-carnitine. Stroke 23:1312–1317.

Sadek HA, Humphries KM, Szweda PA, Szweda LI. 2002. Selective inactivation of redox-sensitive mitochondrial enzymes during cardiac reperfusion. Arch Biochem Biophys 406:222–228.

Schoder H, Knight RJ, Kofoed KF, Schelbert HR, Buxton DB. 1998. Regulation of pyruvate dehydrogenase activity and glucose metabolism in post-ischaemic myocardium. Biochim Biophys Acta 1406:62–72.

Sheu KF, Kim YT, Blass JP, Weksler ME. 1985. An immunochemical study of the pyruvate dehydrogenase deficit in Alzheimer's disease brain. Ann Neurol 17:444–449.

Sims NR. 1995. Calcium, energy metabolism and the development of selective neuronal loss following short-term cerebral ischemia. Metab Brain Dis 10:191–217.

Sims NR, Heward SL. 1994. Delayed treatment with 1,3-butanediol reduces loss of CA1 neurons in the hippocampus of rats following brief forebrain ischemia. Brain Res 662:216–222.

Stadtman ER. 1990. Covalent modification reactions are marking steps in protein turnover. Biochemistry 29:6323–6331.

Sugden MC, Holness MJ. 2003. Recent advances in mechanisms regulating glucose oxidation at the level of the pyruvate dehydrogenase complex by PDKs. Am J Physiol Endocrinol Metab 284:855–862.

Tieu K, Perier C, Caspersen C, Teismann P, Wu DC, Yan SD, Naini A, Vila M, Jackson-Lewis V, Ramasamy R, Przedborski S. 2003. D-beta-Hydroxybutyrate rescues mitochondrial respiration and mitigates features of Parkinson disease. J Clin Invest 112:892–901.

van der Worp HB, Kappelle LJ, Algra A, Bar PR, Orgogozo JM, Ringelstein EB, Bath PM, van Gijn J. 2002. The effect of tirilazad mesylate on infarct volume of patients with acute ischemic stroke. Neurology 58:133–135.

Vereczki V, Martin E, Rosenthal RE, Hof PR, Sherwood CC, Chinopoulos C, Hu W, Hoffman GE, Fiskum G. 2003. Normoxic versus hyperoxic ventilation after cardiac arrest: hippocampal protein nitration, pyruvate dehydrogenase immunoreactivity, and cell death. Soc Neurosci Abstr 739.8.

Whitehouse S, Cooper RH, Randle PJ. 1974. Mechanism of activation of pyruvate dehydrogenase by dichloroacetate and other halogenated carboxylic acids. Biochem J 141:761–774.

Wilson JS, Rushing G, Johnson BL, Kline JA, Back MR, Bandyk DF. 2003. Dichloroacetate increases skeletal muscle pyruvate dehydrogenase activity during acute limb ischemia. Vasc Endovascular Surg 37:191–195.

Wolz P, Krieglstein J. 1996. Neuroprotective effects of alpha-lipoic acid and its enantiomers demonstrated in rodent models of focal cerebral ischemia. Neuropharmacology 35:369–375.

Yosunkaya A, Ak A, Bariskaner H, Ustun ME, Tuncer S, Gurbilek M. 2004. Effect of γ-hydroxybutyric acid on lipid peroxidation and tissue lactate level in experimental head trauma. J Trauma 56:585–590.

Zaidan E, Sims NR. 1993. Selective reductions in the activity of the pyruvate dehydrogenase complex in mitochondria isolated from brain subregions following forebrain ischemia in rats. J Cereb Blood Flow Metab 13:98–104.

Zaidan E, Sims NR. 1997. Reduced activity of the pyruvate dehydrogenase complex but not cytochrome c oxidase is associated with neuronal loss in the striatum following short-term forebrain ischemia. Brain Res 772:23–28.

Zwemer CF, Whitesall SE, D'Alecy LG. 1994. Cardiopulmonary-cerebral resuscitation with 100% oxygen exacerbates neurological dysfunction following nine minutes of normothermic cardiac arrest in dogs. Resuscitation 27:159–170. Erratum in: Resuscitation 27:267.

 doi:10.1111/j.1471-4159.2005.03066.x

Regulation of mitochondrial gene expression by energy demand in neural cells

Zara Mehrabian,* Li-Ing Liu,† Gary Fiskum,* Stanley I. Rapoport† and Krish Chandrasekaran*

**Department of Anesthesiology, University of Maryland School of Medicine, Baltimore, Maryland, USA*

†*Section on Brain Physiology and Metabolism, National Institute on Aging, National Institutes of Health, Bethesda, Maryland, USA*

Abstract

Mitochondrial DNA (mtDNA) encodes critical subunit proteins of the oxidative phosphorylation (OXPHOS) complex that generates ATP. This study tested the hypothesis that mitochondrial gene expression in neural cells is regulated by energy demand, as modified via stimulation of cellular sodium transport. Exposure of PC12S cells to the sodium ionophore monensin (250 nM) for 1–6 h caused a 13–60% decrease in cellular ATP (from 15 to 5 nmol per mg protein at 6 h). Levels of mitochondrial DNA-encoded mRNAs (mt-mRNAs) increased significantly (150%) within the first hour of exposure to monensin, and then decreased significantly (50%) at 3–4 h. Levels of mtDNA-encoded 12S rRNA and nuclear DNA-encoded OXPHOS subunit mRNAs were not significantly affected. Exposure of primary cerebellar neuronal cultures to the excitatory amino acid glutamate caused a similar rapid and significant increase followed by a significant decrease in cell mt-mRNA levels. The monensin-induced initial increase in mt-mRNA levels was abolished by pretreatment with actinomycin D or by reducing extracellular sodium ion concentration. The monensin-induced delayed reduction in mt-mRNA levels was accelerated in the presence of actinomycin D, and was accompanied by a 67% reduction in the half-life (from 3.6 to 1.2 h). Exposure of PC12S cells to 2-deoxy-D-glucose significantly decreased cellular ATP levels (from 14.2 to 7.1 nmol per mg protein at 8 h), and increased mt-mRNA levels. These results suggest a physiological transcriptional mechanism of regulation of mitochondrial gene expression by energy demand and a post-transcriptional regulation that is independent of energy status of the cell.

Keywords: mitochondrial DNA, monensin, mRNA half-life, post-transcription, RNase-L, transcription.

J. Neurochem. (2005) 10.1111/j.1471-4159.2005.03066.x

The mammalian brain is characterized by a high rate of glucose consumption, high content of carriers and enzymes for glucose transport and metabolism, a high rate of oxidative phosphorylation (OXPHOS) in mitochondria, and a high ATP consumption (Erecinska and Silver 1989; Wong-Riley 1989). Furthermore, the rates of glucose utilization and activities of the OXPHOS enzymes that generate ATP correlate with neuronal activity (Hevner *et al*. 1995). ATP is the energy source for active ion pumping to maintain resting membrane potential, fast axoplasmic transport, membrane phospholipid turnover, synthesis of macromolecules and neurotransmitters, and other cellular processes (Erecinska and Silver 1989; Wong-Riley 1989; Purdon *et al*. 2002). Active ion pumping at synapses and dendrites by far consumes the most ATP (Erecinska and Silver 1989).

The mitochondrial respiratory chain responsible for generation of cellular ATP consists of five multisubunit OXPHOS enzyme complexes. Four of these, Complexes I, III, IV and V, are bipartite and consist of subunits derived from both mitochondrial DNA (mtDNA) and nuclear DNA (nDNA). MtDNA encodes 13 polypeptides, all of which are necessary for electron transport and OXPHOS. The remaining subunits are specified by the nuclear genome. Both mtDNA and nDNA-encoded subunits are required to form active enzyme complexes (Attardi and Schatz 1988).

Received September 27, 2004; revised manuscript received December 17, 2004; accepted December 23, 2004.

Address correspondence and reprint requests to Dr Krish Chandrasekaran, Department of Anesthesiology, University of Maryland School of Medicine, Medical School Teaching Facility 5–34, 685 West Baltimore Street, Baltimore, MD 21201, USA.

E-mail: kchandra@anesthlab.umm.edu

Abbreviations used: $[Ca^{2+}]_i$, intracellular calcium concentration; COX, cytochrome oxidase; cyt, cytochrome; DMEM, Dulbecco's modified Eagle's medium; DPBS, Dulbecco's phosphate-buffered saline; mtDNA, mitochondrial DNA, mt-mRNA, mitochondrial DNA-encoded mRNA; $[Na^+]_e$, extracellular sodium concentration; $[Na^+]_i$, intracellular sodium concentration; ND, NADH dehydrogenase; nDNA, nuclear DNA; NRF, nuclear respiratory factor; OXPHOS, oxidative phosphorylation; SDH, succinate dehydrogenase.

Changes in levels of mtDNA-encoded mRNA (mt-mRNA) occur rapidly in response to changes in energy requirement of the cell. Decreased neuronal activity, induced by afferent impulse blockade, decreases neuronal mt-mRNA (Wong-Riley *et al*. 1997), whereas removal of the afferent impulse blockade restores basal mRNA levels (Hevner and Wong-Riley 1993), suggesting feedback regulation of mitochondrial gene expression by energy demand (Wong-Riley *et al*. 1997). Consistent with this reasoning, an *in organello* method demonstrated that high intramitochondrial ATP levels suppress transcription of mtDNA, suggesting how energy demand can regulate mtDNA transcription (Gaines and Attardi 1984; Enriquez *et al*. 1996; DasGupta *et al*. 2001). Apart from transcriptional control, mitochondrial gene expression depends on differences in RNA stability (Gelfand and Attardi 1981; Attardi *et al*. 1990). Although mitochondrial gene expression is a major component in the regulation of energy metabolism of the cell, the contributions of transcriptional and post-transcriptional mechanisms to this regulation are not known (Kagawa and Ohta 1990).

The aim of our present study was to investigate the mechanism(s) of regulation of mitochondrial gene expression under conditions of increasing energy demand. Cellular energy demand was increased by exposing rat pheochromocytoma PC12 cultures to the Na^+ ionophore monensin (Pressman and Fahim 1982), or by exposing primary neuronal cultures to the excitatory amino acid glutamate (Ankarcrona *et al*. 1995), then measuring ATP and levels of mtDNA-encoded and nDNA-encoded OXPHOS mRNAs. Our results indicate a selective initial increase and a subsequent decrease in mt-mRNA in both monensin- and glutamate-treated cells. The initial increase is due to transcriptional regulation dependent on the energy status of the cell, whereas the subsequent decrease is due to post-transcriptional regulation that is independent of the cell's energy status. Part of this work has been published as an abstract (Liu *et al*. 1999).

Materials and methods

Chemicals

Reagents and chemicals were of the highest grade available from Sigma Chemical Co. (St Louis, MO, USA). Stock solutions of ouabain and actinomycin D were prepared in water, whereas monensin and ionomycin were dissolved in 95% ethanol. When ethanol was used as a solvent, appropriate control experiments were conducted using the vehicle alone. Ethanol concentrations were always < 0.1%.

Culture of PC12S cells

A morphological variant of rat pheochromocytoma PC12 cells (PC12S) that has the ability to grow in tissue culture dishes without polylysine treatment was used in the experiments (Fukuyama *et al*. 1993). The PC12S cells were maintained in Dulbecco's modified Eagle's medium (DMEM) containing 2 mM glutamine, 7.5% heat-inactivated fetal calf serum, 7.5% heat-inactivated horse serum and penicillin–streptomycin.

Primary rat cerebellar cultures

Procedures involving animals and their care were conducted in conformity with institutional guidelines that are in compliance with national and international laws and policies (National Institutes of Health (NIH) Guide for the Care and Use of Laboratory Animals, NIH publication no. 85–23, 1985).

Cerebellar granule neurons were prepared from brains of 7-day-old Sprague–Dawley rats using a standard method (Schousboe *et al*. 1989). Neurons were plated at a density of 2×10^5 cells/cm^2 in six-well tissue culture chambers coated with poly-L-lysine (MW 30 000–700 000) and were cultured in Eagle's basal medium supplemented with Earle's salts, 10% inactivated fetal calf serum, 25 mM KCl and gentamicin (50 ng/mL). Neuronal cultures were incubated at 37°C in a humidified atmosphere containing 5% CO_2/95% air. Twenty-four hours after plating, cytosine arabinoside (10 μM) was added to the cultures to prevent growth of glial cells. To ensure sensitivity to glutamate, we routinely used 8-day-old cerebellar neuronal cultures.

Exposure to monensin, ouabain, ionomycin or 2-deoxy-D-glucose

PC12S cells grown in 100 × 15 mm dishes were treated with vehicle, monensin (final concentration 250 nM), ouabain (final concentration 1 mM) or ionomycin (final concentration 3 μM). At timed points over a 6–8-h period, cells were washed with Dulbecco's phosphate-buffered saline (DPBS) without calcium and magnesium, and total RNA was isolated using RNA-Bee reagent as recommended by the manufacturer (TEL-TEST Inc., Friendswood, TX, USA). Total RNA was subjected to northern blot analysis as described below.

For experiments with 2-deoxy-D-glucose, this reagent was added at a concentration of 4.5 g/L to glucose-free DMEM containing pyruvate (110 mg/L). At timed points over an 8-h period, the cells were exposed to this medium and total RNA was isolated.

The effect of extracellular sodium ($[Na^+]_e$) on monensin-induced changes in mt-mRNA levels was studied by changing $[Na^+]_e$ from 125 mM to 62.5 mM or 31.25 mM. Briefly, the amount of sodium chloride in constituted culture medium was decreased and replaced with a corresponding concentration of choline chloride (Choi 1987).

The effect of monensin on the stability of mtDNA- and nDNA-encoded transcripts was determined by adding the transcriptional inhibitor actinomycin D to the cultures at a final concentration of 5 μg/mL. After 1 h, either vehicle or monensin was added. Total RNA was isolated at various times over timed periods and processed for northern blot analysis.

Exposure of neurons to glutamate

On day 8 in culture, the cell culture medium was removed and stored. Neuronal cultures were washed once with prewarmed (37°C) Locke solution (134 mM NaCl, 5 mM KCl, 4 mM $NaHCO_3$, 5 mM HEPES, pH 7.4, 2.3 mM $CaCl_2$ and 5 mM glucose) and incubated for 15 min. Immediately thereafter, L-glutamate (100 μM) and glycine (10 μM) were added, and the cells were further incubated for 30 min at room temperature (24°C). The cells then were washed

and kept in the old culture medium without glutamate for up to 24 h. Control cultures were treated with vehicle over the same time period as that of glutamate-treated cells. At timed points over an 8-h period, neuronal cultures were washed with DPBS; total RNA was isolated and subjected to northern blot analysis.

Cell viability

Cell viability was determined using a two-color fluorescence assay based on the simultaneous determination of live and dead cells. Two probes were employed that measure two recognized parameters of cell viability: intracellular esterase activity and plasma membrane integrity. Viable cells were quantified after staining of cells with cell-permeant dye calcein AM (2 μM). Non-viable cells were quantified with cell-impermeant propidium iodide (10 μg/mL). The ratio of the number of cells that displayed propidium iodide fluorescence (non-viable) to the total number of cells in a field was determined.

RNA analysis

Some 2–10 μg total RNA was run on a 1.2% formaldehyde agarose gel, stained with ethidium bromide. 28S rRNA and 18S rRNA were imaged and quantified to confirm equal loading of RNA, and the gel was then transferred on to a GeneScreen Plus membrane as described by the manufacturer (Dupont, New England Nuclear, MA, USA). Prehybridization and hybridization were done with Hybridizol reagent (Hybridizol I and II in a ratio of 3 : 2; Serologicals Corporation, Norcross, GA, USA). The blots were prehybridized at 37°C for 16 h and hybridized with ^{32}P-labeled mtDNA- and nDNA-encoded gene probes at 37°C for 48 h (Chandrasekaran *et al*. 1994). The blots were washed with increasing stringency and the final wash was performed at 65°C with 0.2 × SSC (1 × SSC contains 150 mM sodium chloride and 15 mM sodium citrate) and 1% sodium dodecyl sulfate. The blots were exposed to X-ray film (Bio-max MS, Kodak, Rochester, NY, USA) with an intensifying screen for 45 min to 2 days at − 70°C. The probes were removed from the blots by placing them in boiling Diethyl Pyrocarbonate (DEPC)-treated water for 10 min. The blots were then rehybridized with a ^{32}P-labeled control β-actin probe as described above. Finally the blots were hybridized with 12S rRNA probe. The level of RNA hybridized was quantified using an image analysis program. To maintain measured intensities within the linear range, the blots hybridized with different probes were exposed for different periods of time. The level of RNA was quantified from autoradiograms of lower exposure than was used for photography. Ratios of mt-mRNA to β-actin mRNA or 12S rRNA to β-actin mRNA were calculated (Chandrasekaran *et al*. 1994).

Probe preparation and labeling

Mitochondrial DNA probes that simultaneously detect several mt-mRNAs were used (Murdock *et al*. 1999). The probes were created by amplifying nucleotides (nt) 3351–7570 of mtDNA (probe 1) and nt 8861–14 549 of mtDNA (probe 2). Probe 1 hybridized to mtDNA-encoded NADH dehydrogenase (ND) subunit 1 (ND1), ND2, cytochrome oxidase (COX) subunit I (COX I) and COX II mRNAs. Probe 2 hybridized to ND5, ND4 and ND4L, cytochrome *b* (cyt *b*) and COX III mRNAs. cDNA inserts of β-actin cDNA and 12S rRNA clones were used as probes. In the case of nDNA-encoded cytochrome *c* (cyt *c*), COX IV and succinate dehydrogenase (SDH) subunit B (SDH B), probes were prepared by RT–PCR using gene-specific primers and were confirmed by sequencing. The probes were radiolabeled by the random primer method.

Estimation of half-lives of mt-mRNAs, 12S rRNA and β-actin mRNA

Some 2–10 μg total RNA from cells treated with either vehicle or monensin in the presence of actinomycin D was subjected to northern blot analysis. The blots were hybridized with mtDNA probe 2, 12S rRNA, β-actin, COX IV and COX VIII probes, and the levels of respective RNA species quantified. Levels of β-actin mRNA are expressed as a percentage of the β-actin mRNA remaining at each experimental time compared with time zero. Levels of mt-mRNA, 12S rRNA, COX IV mRNA and COX VIII mRNA were calculated as the ratio of the respective species to the level of β-actin mRNA. At each experimental time, the RNA ratios are expressed as a percentage of the ratio at time zero. The half-lives were determined from the equation $t_{1/2} = 0.301/\text{slope}$ of the best fit line ($\log_{10}$ remaining RNA vs. time).

Measurement of ATP and intracellular sodium ($[Na^+]_i$)

Cellular ATP levels were determined luminometrically (Victor^3, Shelton, CT, USA); Perkin-Elmer Instruments using an ATP Bioluminescence Assay Kit (Boehringer Ingelheim, Ridgefield, CT, USA) according to the protocol provided. Briefly, after exposing PC12S cells to vehicle, monensin or 2-deoxy-D-glucose, the medium was withdrawn, the cells were exposed to lysis buffer mixed with dilution buffer for 5 min and were then harvested by scraping. Aliquots of cellular extracts were assayed for ATP content using the ATP dependency of the light-emitting luciferase/luciferin reagent. ATP concentration was determined from a standard curve. Results were normalized with respect to cell protein concentration.

The culture medium was replaced with medium containing ^{22}Na (5 μCi or 185 KBq per ml). Measurement of intracellular ^{22}Na showed that equilibration between added radioactive label and 'cold' sodium in the medium was achieved within 24 h. The cells were then treated for various time periods with either the vehicle or monensin (250 nM). The reaction was terminated by aspiration of the medium, and the cells were quickly washed twice with ice-cold DPBS and digested for 1 h in 0.2 mL 1 M NaOH at room temperature. Cell digests were assayed for ^{22}Na content by scintillation counting.

Statistical analysis and replication of results

The results presented are representative of at least three to five independent experiments. Where indicated, statistical analysis was carried out using one-way ANOVA followed by Tukey's test for multiple comparisons. Mean ± SEM values are presented. Differences were considered significant when $p < 0.05$.

Results

Treatment of PC12S cells with monensin reduces cellular ATP levels

Exposure of PC12S cell cultures to monensin (250 nM) caused a sustained 13–60% decrease in total cellular ATP levels, from 15 ± 2 nmol per mg protein at time zero, to

13 ± 1.5, 10 ± 1, 8 ± 0.7 and 5 ± 0.5 nmol per mg protein at 0.5, 1, 3 and 6 h respectively. Exposure of PC12S cells to monensin for 6 h resulted in a 500% increase in intracellular ^{22}Na ($[Na^+]_i$) from 30 ± 5 to 150 ± 12 pmol per μg protein. Determination of cell viability using calcein AM and propidium iodide showed no decrease in viability (> 95% propidium iodide negative) with exposure to monensin for up to 6 h. Our interpretation of these results is that exposure to monensin in PC12S cells causes an influx of Na^+, which in turn activates Na/K-ATPase, leading to increased consumption of ATP and decreased cellular ATP levels.

Biphasic changes in expression of mt-mRNAs induced by exposure of PC12S cells to monensin

To examine the effects of increased $[Na^+]_I$ on mt-mRNA expression, monensin (250 nM) was added to PC12S cell cultures. At different periods of exposure to monensin total cellular RNA was isolated and subjected to northern blotting. Blots of RNA were probed with mtDNA-derived probes (probes 1 and 2), 12S rRNA, nDNA-derived cDNA encoding cyt *c*, COX IV, SDH (Complex II of OXPHOS) subunits A and B (SDH A and B), and β-actin. Levels of β-actin mRNA were determined as a reference to ensure that equivalent amounts of RNA were loaded and transferred into each lane in northern blot analyses (Fig. 1).

Exposure of PC12S cells to monensin increased the mt-mRNA levels during the first hour of treatment (Fig. 1). Continued exposure to monensin caused a significant decrease in mt-mRNAs at 4–6 h (Fig. 1). Levels of mtDNA-encoded 12S rRNA and nDNA-encoded cyt *c*, COX IV, SDH A, SDH B and β-actin mRNA were unaffected by monensin treatment. Quantification of the mt-mRNA levels showed a biphasic response following exposure to monensin; a significant 1.5-fold increase in mt-mRNAs during the first 30 min of exposure followed by a significant (50%) decrease at 4–6 h after exposure (Figs 1a and b).

Biphasic changes in expression of mt-mRNAs induced by exposure of rat cerebellar granule neurons to glutamate

Although PC12 pheochromacytoma cells represent a cell line commonly used to model neuronal activities, it is possible that the response of mt-mRNA to increased $[Na^+]_i$ is not the same as in primary cultures of neurons. We therefore tested the effects of the excitatory neurotransmitter glutamate on primary cultures of rat cerebellar granule neurons. Glutamate-induced excitotoxicity in primary neuronal cultures is associated with increases in $[Na^+]_i$ and intracellular calcium concentration $[Ca^{2+}]_I$, and decreased cellular ATP levels (Ankarcrona *et al*. 1995). Rat cerebellar neurons were treated with glutamate (100 μM) for 30 min, followed by normal culture conditions. Total cellular RNA was isolated and subjected to northern blot analysis with mtDNA probes at the end of the glutamate exposure and at several times during the 8-h after treatment. An autoradiogram and quantitative data are shown in Fig. 2. Immediately following exposure of neurons to glutamate, levels of mt-mRNA rose significantly (150%). This increase was followed by a significant decrease

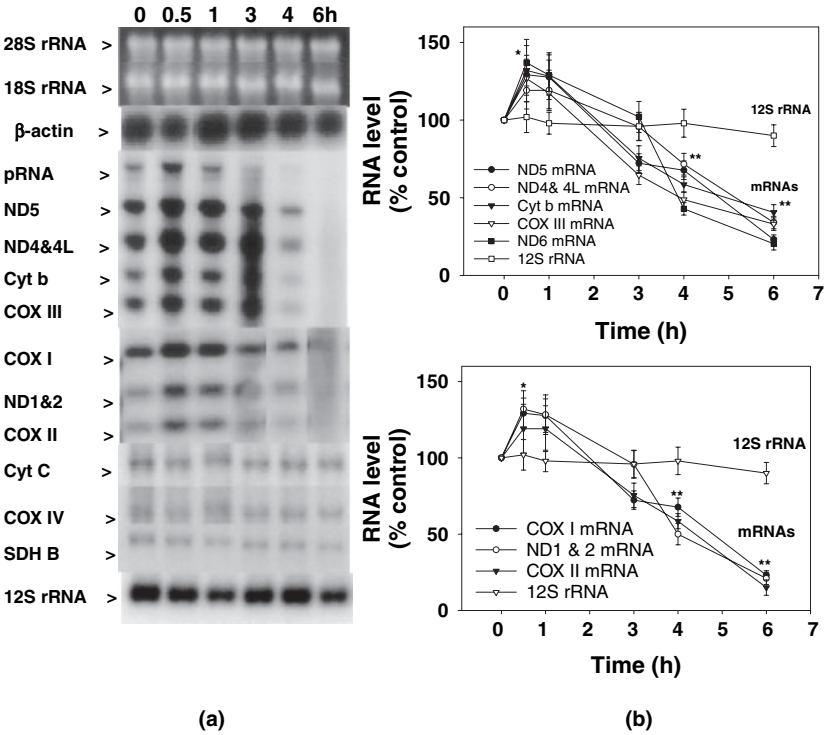

Fig. 1 Effect of monensin on mtDNA- and nDNA-encoded RNA expression in PC12S cells. PC12S cells were exposed to monensin (final concentration 250 nM) for the indicated periods and total RNA was isolated. (a) Northern blot analysis for mtDNA- and nDNA-encoded RNAs. (b) The intensity of the hybridization signal was quantified by image analysis of the autoradiograms. The ratio of individual mtDNA-encoded mRNA and 12S rRNA to β-actin mRNA was calculated at each time point. The percentage RNA change with respect to time zero is shown. Each point represents the mean ± SEM of five separate experiments. No significant changes were observed with mtDNA-encoded 12S rRNA or with nDNA-encoded cyt *c*, COX IV and SDH B mRNAs. pRNA, precursor RNA. $^*p < 0.05$, $^{**}p < 0.01$ versus time zero samples (one-way ANOVA followed by Tukey's test for multiple comparisons).

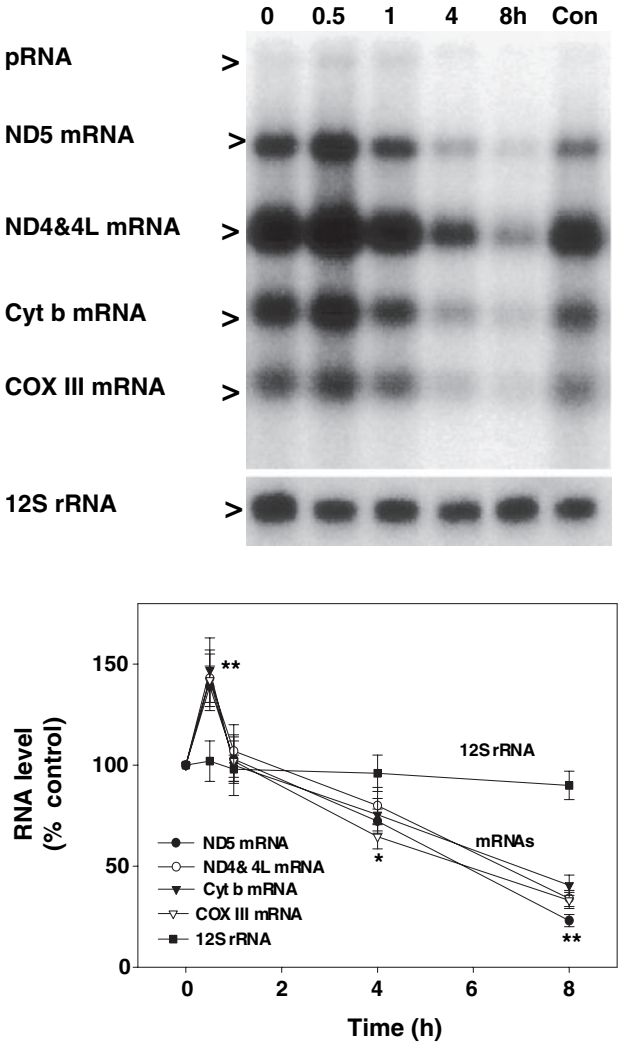

Fig. 2 Effect of glutamate exposure on mtDNA-encoded RNA expression in rat cerebellar neurons. Rat cerebellar granule neurons cultured for 8 days *in vitro* were exposed to glutamate (100 μM) for 30 min in Locke solution. The cells were then washed and kept in the old culture medium without glutamate for up to 8 h. At indicated times, total RNA was isolated and subjected to northern blot analysis with mtDNA probes. The intensity of the hybridization signal was quantified by image analysis of the autoradiograms. The ratio of individual mt-mRNA and 12S rRNA to β-actin mRNA was calculated at each time point. The percentage RNA change with respect to time zero is shown. Each point represents the mean ± SEM of three separate experiments. pRNA, precursor RNA. $^*p < 0.05$, $^{**}p < 0.01$ versus time zero (one-way ANOVA followed by Tukey's test for multiple comparisons). Con = 8 h control without glutamate exposure.

at 4–8 h (< 25% compared with level at time zero). These results suggest that there are two mechanisms operating in the regulation of mt-mRNA expression in neuronal cells under conditions of ATP depletion and ionic stress: an early increase in mt-mRNA levels and a decrease at later time periods (> 4 h). We therefore studied the molecular basis of these two mechanisms.

Monensin-induced increase in mt-mRNA levels is abolished by decreasing $[Na^+]_e$

To understand the relation between the monensin-induced increase in mt-mRNA and changes in $[Na^+]_i$ or cellular ATP levels, we exposed the PC12S cell cultures to varying concentrations of $[Na^+]_e$ in the presence of monensin and measured changes in mt-mRNA levels. $[Na^+]_e$ was decreased from 125 mM to 62.5 mM or to 31.25 mM. Monensin (250 nM) was added to the culture medium and at various times, total cellular RNA was isolated and subjected to northern blot analysis with mtDNA probe. The results shown in Fig. 3 show that when $[Na^+]_e$ was reduced from 125 mM to either 62.5 or 31.25 mM, the rapid increase and the subsequent decrease in mt-mRNA was eliminated. The effects of monensin on levels of mt-mRNA are therefore sodium dependent.

Addition of ouabain or the calcium ionophore ionomycin does not increase mt-mRNAs

Further experiments were conducted to determine whether the effects of monensin on mt-mRNA levels are due to increased $[Na^+]_i$ *per se*, or to the reduction in ATP caused by increased sodium cycling. In addition, the possible secondary effect of increased $[Ca^{2+}]_i$ caused by raised $[Na^+]_i$ through Na^+/Ca^{2+} exchange was investigated (Fasolato *et al*. 1991). To assess the effect of $[Na^+]_i$, PC12S cells were treated with the Na/K-ATPase inhibitor ouabain (1 mM), which increases $[Na^+]_i$ without decreasing ATP (Taurin *et al*. 2003). The possible effects of raised $[Ca^{2+}]_i$ were assessed by the addition of the calcium ionophore ionomycin (3 μM) (Fasolato *et al*. 1991). Total RNA was isolated and subjected to northern blot analysis with mtDNA probes. The results are shown in Fig. 4.

Addition of ouabain decreased steady-state levels of mt-mRNA. Mitochondrial DNA-encoded 12S rRNA, however, was unaffected by ouabain. Exposure to ouabain for 2 h increased $[Na^+]_i$ from 30 ± 5 to 75 ± 9 pmol per μg protein and increased cellular ATP from 15 ± 2 to 23 ± 3 nmol per mg protein. Exposure to ionomycin for up to 2 h caused no significant change in cellular ATP (14.1 ± 2 to 12.2 ± 3 nmol per mg protein) and no significant change in the levels of mt-mRNA. These results indicate that the initial increase in mt-mRNA synthesis in response to monensin is not due to the increase in $[Na^+]_i$ or $[Ca^{2+}]_i$ but probably results from decreased cellular ATP levels.

A decrease in cellular ATP does not decrease mt-mRNAs

To determine whether the delayed decrease in mt-mRNA is also due to a decrease in cellular ATP levels, we exposed PC12S cells to 2-deoxy-D-glcose (4.5 g/L) in glucose-free DMEM containing sodium pyruvate (110 mg/L). Cellular ATP levels were determined at several times during the 8 h after treatment. Exposure of PC12S cell cultures to 2-deoxy-D-glcose in glucose-free medium caused a

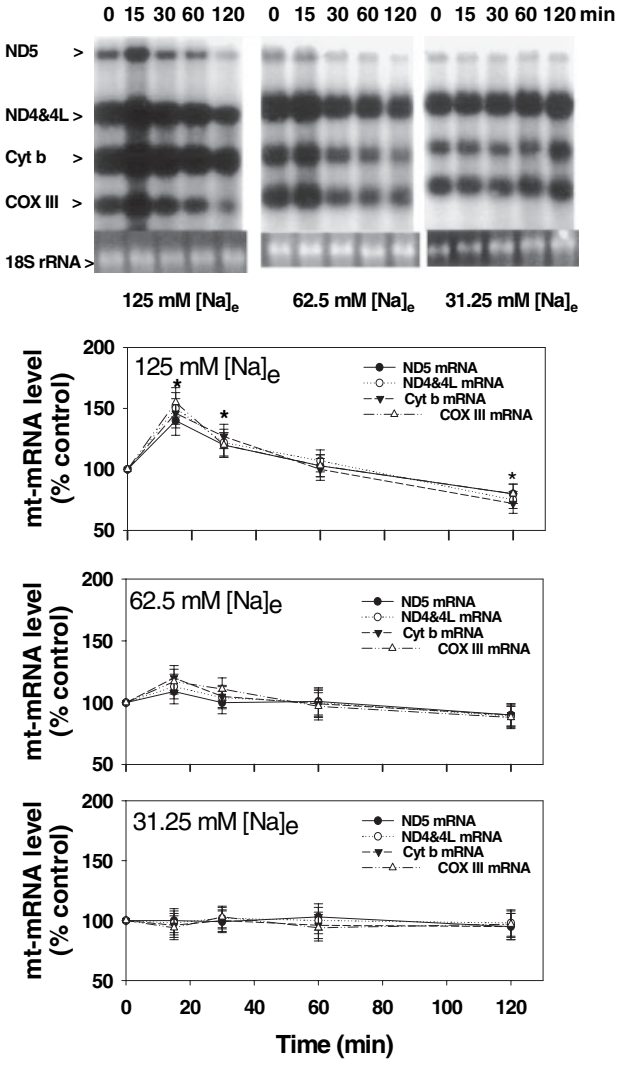

Fig. 3 Effect of changes in extracellular sodium on mtDNA-encoded RNA expression. PC12S cells were exposed to monensin (final concentration 250 nM) in the presence of decreasing $[Na^+]_e$. At indicated times, total RNA was isolated and subjected to northern blot analysis with mtDNA-encoded probes. The intensity of the hybridization signal was quantified by image analysis of the autoradiograms. The ratio of individual mt-mRNA to β-actin mRNA was calculated at each time point. The percentage RNA change with respect to time zero is shown. Note no significant increase was seen at 15 min when the $[Na^+]_e$ was decreased from 125 to 31.2 mM. Each point represents the mean ± SEM of three separate experiments. pRNA, precursor RNA. $^*p < 0.05$ versus time zero (one-way ANOVA followed by Tukey's test for multiple comparisons).

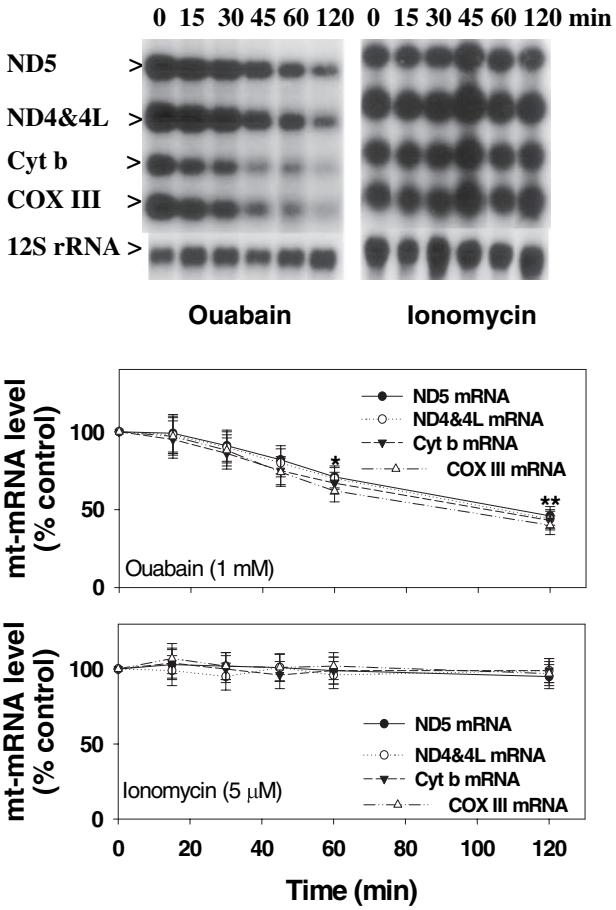

Fig. 4 Effect of ouabain or ionomycin on mtDNA-encoded RNA expression. PC12S cells were exposed to ouabain (final concentration 1 mM) or ionomycin (final concentration 3 μM) for the indicated time periods. Total RNA was isolated and subjected to northern blot analysis with mtDNA-encoded probes. The intensity of the hybridization signal was quantified by image analysis of the autoradiograms. The ratio of individual mt-mRNA and 12S rRNA to β-actin mRNA was calculated at each time point. The percentage RNA change with respect to time zero is shown. Mt-mRNA levels decreased in ouabain-treated cells, whereas no significant changes were observed with mtDNA-encoded 12S rRNA. Exposure to ionomycin did not alter the levels of mt-mRNA and 12S rRNA during the 2-h period. Each point represents the mean ± SEM of three separate experiments. $^*p < 0.05$, $^{**}p < 0.01$ versus time zero (one-way ANOVA followed by Tukey's test for multiple comparisons).

sustained 10–50% decrease in total cellular ATP levels, from 14.2 ± 1.7 nmol per mg protein at time zero, to 13 ± 1, 10.5 ± 0.9, 8.1 ± 0.8 and 7.1 ± 0.8 nmol per mg protein at 1, 3, 5 and 8 h respectively (Fig. 5). To examine the effects of decreased cellular ATP levels on mt-mRNA expression, total cellular RNA was isolated from 2-deoxy-D-glucose-treated cells, subjected to northern blotting, and probed with mtDNA-derived probe 2. The autoradiograms of northern blots and the quantification of changes in mt-RNA levels are shown in Fig. 5. Exposure to 2-deoxy-D-glcose increased the levels of mt-mRNA by 20–32% at 5 and 8 h after treatment and there was no evidence of a decrease in mt-mRNA levels. Thus, the late decrease in mt-mRNA levels in monensin-treated cells appears to be independent of cellular ATP decline.

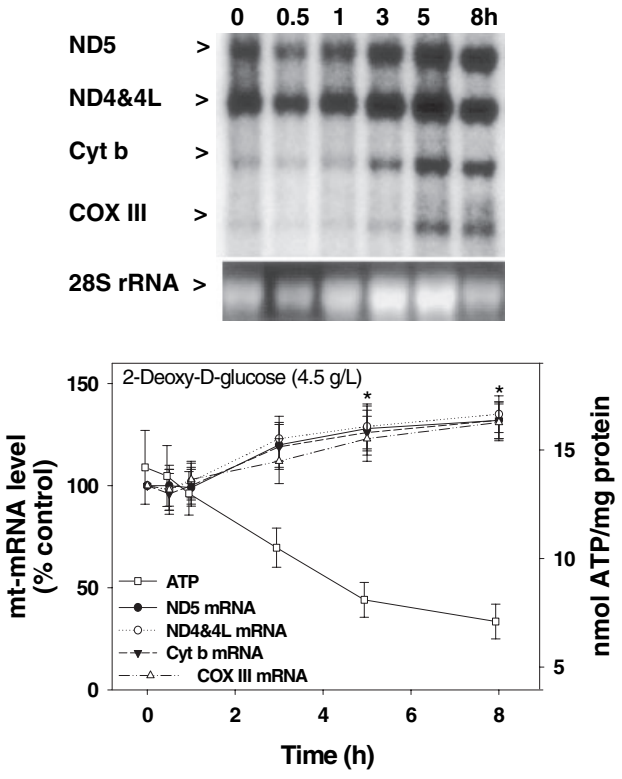

Fig. 5 Effect of 2-deoxy-D-glucose on mtDNA-encoded RNA expression in PC12S cells. PC12S cells were exposed to 2-deoxy-D-glucose (final concentration 4.5 g/L) for the indicated periods, and total RNA was isolated and subjected to northern blot analysis with mtDNA-encoded probes. The intensity of the hybridization signal was quantified by image analysis of the autoradiograms. The ratio of individual mt-mRNA to 18S rRNA was calculated at each time point. The percentage RNA change with respect to time zero is shown. Each point represents the mean ± SEM of five separate experiments. No significant changes were observed with mt-mRNA at earlier time points (< 3 h), whereas there was a significant increase at later time points (> 5 h). $*p < 0.05$ versus time zero (one-way ANOVA followed by Tukey's test for multiple comparisons).

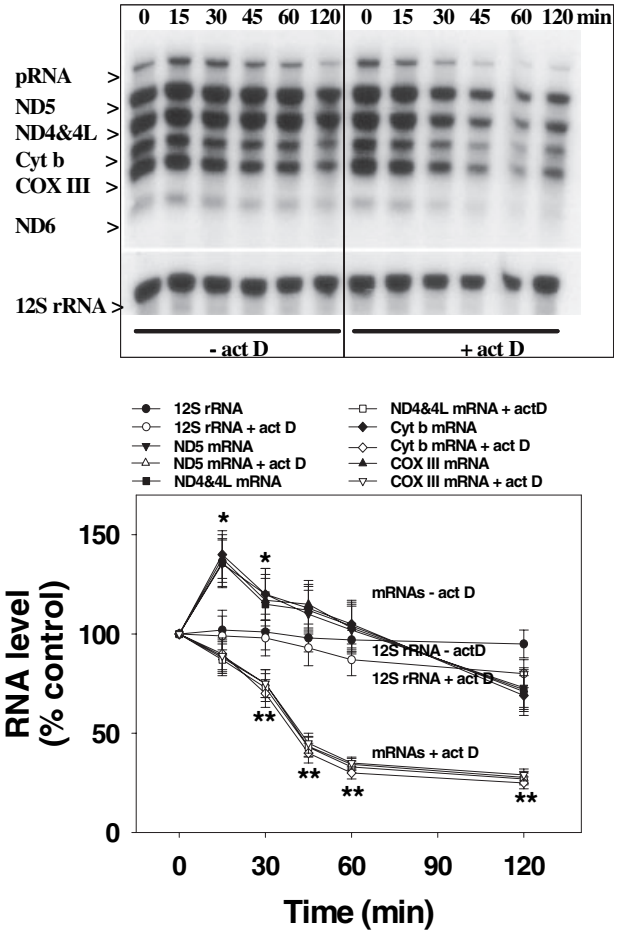

Fig. 6 Effect of termination of transcription with actinomycin D (act D) on monensin-induced increase in mtDNA-encoded RNA levels. PC12S cells were exposed to monensin in the presence or absence of actinomycin D (5 μg/mL). Total RNA was isolated at indicated times and 2-μg aliquots were subjected to northern blot analysis. Hybridization was quantified by image analysis of autoradiograms. The ratio of individual mt-mRNA and 12S rRNA to β-actin mRNA was calculated at each time point. The percentage RNA change with respect to time zero is shown. Each point represents the mean ± SEM of three separate experiments. pRNA, precursor RNA. $*p < 0.05$, $**p < 0.01$ versus time zero (one-way ANOVA followed by Tukey's test for multiple comparisons).

Addition of actinomycin D abolishes the monensin-induced initial increase in mt-mRNAs

To test whether the initial increase in mt-mRNAs in monensin-treated cells observed during the first hour is due to increased transcription or decreased mRNA turnover, we determined the effects of adding actinomycin D, an inhibitor of cellular transcription (Chrzanowska-Lightowlers *et al.* 1994), on mt-mRNA levels. Actinomycin D (5 μg/mL) was added to the culture medium and monensin was added 1 h later. Total cellular RNA was isolated at 15, 30, 45, 60 and 120 min, and subjected to northern blot analysis with mtDNA probe 2 (Fig. 6). Throughout this period, cell viability was not compromised and there was no substantial reduction in total RNA yield. The autoradiograms of northern blots probed with mtDNA probe 2 and 12S rRNA, and the quantification of changes in mt-mRNA levels, are shown in Fig. 6. In the absence of actinomycin D, levels of mt-mRNAs increased as early as 15 min after addition of monensin (Fig. 6). In the presence of actinomycin D, the monensin-induced increase was abolished (Fig. 6). This result suggests that the monensin-induced early increase in mt-mRNA levels is due to increased mtDNA transcription.

Addition of actinomycin D accelerates monensin-induced delayed decrease in mt-mRNAs

To test whether the delayed decrease in mt-mRNA in monensin-treated cells is due to increased degradation or

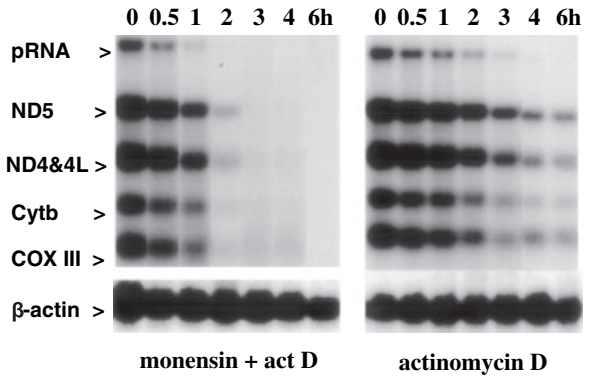

Fig. 7 Effect of actinomycin D on β-actin mRNA and mtDNA- encoded mRNAs in control and monensin-treated PC12S cells. Total RNA was isolated from control and monensin-treated cells at indicated times after termination of transcription by actinomycin D, and 10-μg aliquots were subjected to northern blot analysis. Hybridization was quantified by image analysis of autoradiograms and normalized to that of β-actin mRNA. Calculated half-lives are shown in Table 1.

Table 1 Estimation of half-lives for β-actin mRNA, 12S rRNA and mtDNA- and nDNA-encoded mRNAs in control and monensin-treated PC12S cells

Transcript	Estimated $t_{1/2}$		Relative $t_{1/2}$ (control/monensin)
	Control	+ Monensin	
Encoded by nDNA			
COX IV	23.4 ± 5 (3)	20.0 ± 4 (3)	1.2
COX VIII	24.0 (1)	20.0 (1)	1.2
β-Actin	24.6 ± 5 (5)	22.0 ± 5 (5)	1.2
Encoded by mtDNA			
pRNA	3.6 ± 1 (3)	1.1 ± 0.2 (3)*	3.3
COX I	3.8 (2)	1 (2)*	3.8
COX II	3.7 (2)	1.1 (2)*	3.4
COX III	3.5 ± 0.5 (5)	1 ± 0.1 (5)*	3.5
ND5	3.5 ± 0.5 (3)	1 ± 0.2 (3)*	3.5
ND4 and ND4L	3.5 ± 0.5 (3)	1 ± 0.2 (3)*	3.5
Cyt *b*	3.0 ± 0.25 (3)	1 ± 0.2 (3)*	3.0
12S rRNA	20 ± 4 (5)	18 ± 3 (5)*	1.1

Total RNA was isolated from control and monensin-treated cells at various times after termination of transcription by actinomycin D, and 10-μg aliquots were subjected to northern blot analysis. Hybridization was quantified by image analysis of autoradiograms and normalized to that of β-actin mRNA. The half-lives were determined from the equation $t_{1/2} = 0.301$/slope of the best fit line ($\log_{10}$ remaining RNA vs. time). Each point represents the mean ± SEM of three separate experiments. pRNA, precursor RNA. *$p < 0.01$ versus control (one-way ANOVA followed by Tukey's test for multiple comparisons).

decreased synthesis, we determined the half-lives of mt-mRNA, mtDNA-encoded 12S rRNA, nDNA-encoded COX IV, COX VIII and β-actin mRNA in control and monensin-treated PC12S cells. Actinomycin D (5 μg/mL) was added to the culture medium and after 1 h monensin was added. Total cellular RNA was isolated at 0.5, 1, 2, 3, 4 and 6 h after adding monensin, and subjected to northern blot analysis. Hybridization results with mtDNA probe 2 and β-actin are shown in Fig. 7. The half-life of other RNAs is shown in Table 1. In monensin-treated cells, half-lives of mtDNA-encoded ND5, ND4, ND4L, cyt *b* and COX III mRNAs were significantly shortened from approximately 3.5 h to 1 h. No significant reductions in half-life were observed with mtDNA-encoded 12S rRNA and nDNA-encoded COX IV, COX VIII and β-actin mRNA in monensin-treated cells. It is also clear that the half-life of mt-mRNA is much shorter (3.5 h) than that of mtDNA-encoded 12S rRNA, nDNA-encoded OXPHOS mRNA and β-actin mRNA (~20 h).

Discussion

This study examined the involvement of transcriptional and post-transcriptional mechanisms in the regulation of mitochondrial gene expression. The data show that exposure of PC12S cells to the sodium ionophore monensin, or exposure of cerebellar granule neurons to the excitatory amino acid glutamate, induces a selective initial increase followed by a delayed decrease in mt-mRNAs. A similar biphasic response in mt-mRNA levels was also observed when human neuroblastoma SH-SY5Y cells were exposed to monensin or primary cortical neuronal cultures were exposed to glutamate. These results suggest the existence of two pathways that regulate the levels of mt-mRNAs in cells.

Investigation into whether mtDNA-encoded structural or non-mitochondrial RNAs are also regulated in response to monensin revealed that the regulation is specific to mt-mRNAs. Exposure of PC12S cells to monensin or exposure of cerebellar neurons to glutamate caused no change in mtDNA-encoded 12S rRNA levels. These RNA subtype-specific effects may reflect differences in the transcriptional regulation of mtDNA-encoded rRNA and mt-mRNA, as well as differences in their half-lives (20 vs. 3.6 h). Quantification of mtDNA by Southern blot analysis showed similar levels in PC12S cells with or without monensin treatment, suggesting that the changes in mt-mRNA are not due to mitochondrial turnover. We measured the levels of three nDNA-encoded OXPHOS mRNAs (cyt *c*, COX IV and SDH B) as well as β-actin mRNA, to determine whether the mt-mRNA changes were specific or represented a general adaptation to the increased energy demand resulting from exposure to monensin. Transcriptional regulators of nuclear-encoded mitochondrial proteins such as nuclear respiratory factors (NRFs) 1 and 2 have been shown to regulate nDNA-encoded cyt *c*, COX IV, SDH B, and the mitochondrial transcription factor Tfam (Virbasius *et al.* 1993; Kelly and Scarpulla 2004). SDH B of OXPHOS complex II was also chosen because this complex is entirely

coded by nDNA, whereas other OXPHOS complexes (I, III, IV and V) consist of subunits encoded by both mtDNA and nDNA (Attardi and Schatz 1988). Our northern blot results showed no significant changes in the levels of nDNA-encoded OXPHOS and non-OXPHOS mRNAs (β-actin) after exposure to monensin. They suggest that the monensin-induced response is specific to mt-mRNAs. Levels of all mt-mRNAs were altered in a similar manner in both monensin- and glutamate-treated cells. This similarity may reflect the transcriptional mechanism by which each strand of mtDNA is transcribed as a single polycistronic message, following which the message is processed to individual mRNAs by post-transcriptional mechanisms (Attardi *et al*. 1990).

Increasing or decreasing energy demand has been shown, respectively, to up-regulate or down-regulate both mtDNA- and nDNA-encoded OXPHOS genes (Hevner and Wong-Riley 1993; Heddi *et al*. 1999; Murdock *et al*. 1999; Wiesner *et al*. 1999; Zhang and Wong-Riley 2000). For example, under conditions of decreased neuronal activity induced by afferent impulse blockade with monocular tetrodotoxin injection in monkeys, mRNA levels of OXPHOS subunit genes encoded by mtDNA and nDNA were decreased in lateral geniculate nucleus and primary visual cortex within days (Hevner and Wong-Riley 1993; Wong-Riley *et al*. 1997). Removal of the blockade restored basal mRNA levels within days (Hevner and Wong-Riley 1993; Wong-Riley *et al*. 1997). However, in these studies the changes in mt-mRNA were disproportionately larger and occurred earlier than changes in mRNA encoded by nDNA, suggesting that changes in mt-mRNA are more tightly regulated by neuronal activity and energy demand (Hevner and Wong-Riley 1993; Wong-Riley *et al*. 1997). On the other hand, the changes in nDNA-encoded OXPHOS mRNA probably represent compensatory mechanisms that operate more slowly. Because we measured changes over a period of 6 h, we interpret the immediate increase in mt-mRNA in response to monensin or glutamate as representing a mechanism that couples increasing energy demand directly with up-regulated mitochondrial gene expression. Consistent with this interpretation are the results that show increased levels of mtDNA- and nDNA-encoded COX subunit mRNA in primary neuronal cultures in response to KCl-induced depolarization (Zhang and Wong-Riley 2000). It would appear that both NRF-2α and NRF-2β respond to increased neuronal activity by translocating from the cytoplasm to the nucleus, where they engage in transcriptional activation of target genes such as Tfam (Zhang and Wong-Riley 2000; Yang *et al*. 2004).

Investigations into the molecular component of this rapid coupling suggested that the monensin-induced decrease in cellular ATP level is probably responsible for the stimulation of mitochondrial transcription. *In organello* transcription experiments with isolated mitochondria show that mitochondrial RNA synthesis is regulated in response to changes in intramitochondrial ATP levels (Gaines *et al*. 1987; Enriquez *et al*. 1996; DasGupta *et al*. 2001). A low level of intramitochondrial ATP stimulates mtDNA transcription, whereas a high level suppresses mtDNA transcription, possibly by inhibiting mitochondrial RNA polymerase. This sensitivity to ATP levels represents a mechanism by which energy demand could regulate mtDNA transcription (Enriquez *et al*. 1996; DasGupta *et al*. 2001). Moreover, *in organello* studies using [α-^{32}P]UTP showed that at low intramitochondrial ATP levels, mRNA species are labeled to a substantial extent, whereas there is minimal labeling of the rRNA species (Gaines *et al*. 1987). This observation may explain our finding of an increase in mt-mRNA levels but not 12S rRNA in monensin-treated cells. The results demonstrating a reduction in mt-mRNA levels associated with increased ATP levels in ouabain-treated cells are also consistent with this mechanism of gene regulation. Thus, the initial increase in mt-mRNA in monensin-treated cells may represent a physiological coupling mechanism that operates at the transcriptional level, allowing mtDNA to generate optimal levels of mRNA in response to energy demands.

Our results demonstrating a rapid positive effect of monensin on transcription of mt-mRNAs and a negative effect of ouabain suggest that the metabolic pathways are uniquely organized in mammalian brain so that dynamic local energy demand can be met rapidly by increased OXPHOS (Rapoport 1970; Kato and Lowry 1973; Sokoloff 1991; Wong-Riley *et al*. 1998). At sites of high energy demand, such as at postsynaptic dendrites and axon terminals where Na/K-ATPase and mitochondria are enriched, increased electrical activity causes an increase in $[Na^+]_i$ which in turn stimulates Na/K-ATPase to consume ATP. Reduced ATP and increased ADP and AMP level can be sensed by mitochondria to stimulate the transcription and translation of mtDNA-encoded subunits. These changes provide a framework for the import and integration of nuclear-encoded subunits, which are entirely synthesized in cell bodies. Dynamic local energy demand can be met when mtDNA- and nDNA-encoded subunits are assembled to form functional OXPHOS complexes.

The decrease in mt-mRNA at 4–6 h of exposure to monensin suggests the presence of a slower-acting mechanism for inhibiting mitochondrial gene expression, which is independent of the cell energy status and overrides the normal rapid regulation by energy demand. The independence of the decrease in mt-mRNA levels with cellular ATP decline was substantiated by the observation that exposure to 2-deoxy-D-glucose decreased cellular ATP levels with no evidence of any mt-mRNA decrease. Decreases in mt-mRNA levels under pathological conditions have been observed. For example, the level of mtDNA-encoded COX I mRNA decreases within hours in CA1 neurons of gerbils after transient forebrain ischemia (Abe *et al*. 1993). This decrease occurs in the absence of a decrease in mtDNA, suggesting impaired transcription and/or turnover of mt-mRNA (Abe *et al*. 1993).

In this model, the decrease in COX I mRNA occurs when energy demand is high on these cells to restore ionic gradients to resting levels and to maintain neuronal activity (Arai *et al*. 1986; Abe *et al*. 1993). A disproportionate decrease in mtDNA-encoded COX subunit mRNA in the absence of a change in mtDNA-encoded 12S rRNA has also been noted in brains of patients with Alzheimer's disease (Chandrasekaran *et al*. 1994, 1998; Hatanpaa *et al*. 1996).

Our actinomycin D experiments suggest that a post-transcriptional mechanism is responsible for the observed decrease in mt-mRNA in monensin-treated cells. Half-lives of mt-mRNA, 12S rRNA, COX IV, COX VIII and β-actin mRNA in the presence and absence of monensin were calculated after inhibition of *de novo* mitochondrial and nuclear transcription by actinomycin D. The estimated half-life of mt-mRNAs in control cells was ∼3.6 h, whereas that of mtDNA-encoded 12S rRNA and of nDNA-encoded COX IV, COX VIII and β-actin mRNA was greater than 20 h. The half-lives of mt-mRNAs in PC12S cells are similar to those reported in other cell culture systems (Gelfand and Attardi 1981; Chrzanowska-Lightowlers *et al*. 1994). In monensin-treated cells, the estimated half-life of mt-mRNA decreased from 3.6 to ∼1 h, representing a 3.5-fold decrease in the stability of mt-mRNA in monensin-treated cells. This post-transcriptional mechanism involving Rnase(s) probably accounts for the accelerated degradation of mt-mRNA.

Although we have not identified a specific Rnase responsible for the accelerated degradation of mt-mRNA in PC12S cells, an Rnase-L has been reported to degrade a number of mitochondrial mRNAs in human H9 cells in response to interferon-α treatment (Le Roy *et al*. 2001). This Rnase-L pathway is activated in models of ischemia–reperfusion injury (Paschen *et al*. 1999). A comparison of the half-life of mt-mRNA in monensin-treated mouse embryo fibroblasts showed greater stability in Rnase-L–/– cells compared with Rnase-L+/+ cells (Chandrasekaran *et al*. 2004). Thus, activation of Rnase-L may be responsible for the accelerated degradation of mt-mRNA in monensin-treated cells.

In summary, our results suggest a physiological transcriptional mechanism of regulation of mitochondrial gene expression by energy demand and a pathological post-transcriptional regulation that is independent of energy status of the cell. The post-transcriptional mechanism is likely to be pathological because it overrides the normal regulation by energy demand, causes accelerated degradation of transcripts and undermines the actual energy demand of the cell.

Acknowledgements

This work was supported by grants from the NIH (NS045081) to KC, American Heart Association (AHA) (0256383U) to KC and the US Army (DAMD17-99-1-9483) to GF.

References

Abe K., Kawagoe J. and Kogure K. (1993) Early disturbance of a mitochondrial DNA expression in gerbil hippocampus after transient forebrain ischemia. *Neurosci. Lett.* **153**, 173–176.

Ankarcrona M., Dypbukt J. M., Bonfoco E., Zhivotovsky B., Orrenius S., Lipton S. A. and Nicotera P. (1995) Glutamate-induced neuronal death: a succession of necrosis or apoptosis depending on mitochondrial function. *Neuron* **15**, 961–973.

Arai H., Passonneau J. V. and Lust W. D. (1986) Energy metabolism in delayed neuronal death of CA1 neurons of the hippocampus following transient ischemia in the gerbil. *Metab. Brain Dis.* **1**, 263–278.

Attardi G. and Schatz G. (1988) Biogenesis of mitochondria. *Annu. Rev. Cell Biol.* **4**, 289–333.

Attardi G., Chomyn A., King M. P., Kruse B., Polosa P. L. and Murdter N. N. (1990) Regulation of mitochondrial gene expression in mammalian cells. *Biochem. Soc. Trans.* **18**, 509–513.

Chandrasekaran K., Giordano T., Brady D. R., Stoll J., Martin L. J. and Rapoport S. I. (1994) Impairment in mitochondrial cytochrome oxidase gene expression in Alzheimer disease. *Brain Res. Mol. Brain Res.* **24**, 336–340.

Chandrasekaran K., Hatanpaa K., Brady D. R., Stoll J. and Rapoport S. I. (1998) Downregulation of oxidative phosphorylation in Alzheimer disease: loss of cytochrome oxidase subunit mRNA in the hippocampus and entorhinal cortex. *Brain Res.* **796**, 13–19.

Chandrasekaran K., Mehrabian Z., Li X. L. and Hassel B. (2004) RNase-L regulates the stability of mitochondrial DNA-encoded mRNAs in mouse embryo fibroblasts. *Biochem. Biophys. Res. Commun.* **325**, 18–23.

Choi D. W. (1987) Ionic dependence of glutamate neurotoxicity. *J. Neurosci.* **7**, 369–379.

Chrzanowska-Lightowlers Z. M., Preiss T. and Lightowlers R. N. (1994) Inhibition of mitochondrial protein synthesis promotes increased stability of nuclear-encoded respiratory gene transcripts. *J. Biol. Chem.* **269**, 27 322–27 328.

DasGupta S. F., Rapoport S. I., Gerschenson M., Murphy E., Fiskum G., Russell S. J. and Chandrasekaran K. (2001) ATP synthesis is coupled to rat liver mitochondrial RNA synthesis. *Mol. Cell. Biochem.* **221**, 3–10.

Enriquez J. A., Fernandez-Silva P., Perez-Martos A., Lopez-PereZ. M. J. and Montoya J. (1996) The synthesis of mRNA in isolated mitochondria can be maintained for several hours and is inhibited by high levels of ATP. *Eur. J. Biochem.* **237**, 601–610.

Erecinska M. and Silver I. A. (1989) ATP and brain function. *J. Cereb. Blood Flow Metab.* **9**, 2–19.

Fasolato C., Zottini M., Clementi E., Zacchetti D., Meldolesi J. and Pozzan T. (1991) Intracellular Ca^{2+} pools in PC12 cells. Three intracellular pools are distinguished by their turnover and mechanisms of Ca^{2+} accumulation, storage, and release. *J. Biol. Chem.* **266**, 20 159–20 167.

Fukuyama R., Chandrasekaran K. and Rapoport S. I. (1993) Nerve growth factor-induced neuronal differentiation is accompanied by differential induction and localization of the amyloid precursor protein (APP) in PC12 cells and variant PC12S cells. *Brain Res. Mol. Brain Res.* **17**, 17–22.

Gaines G. and Attardi G. (1984) Highly efficient RNA-synthesizing system that uses isolated human mitochondria: new initiation events and *in vivo*-like processing patterns. *Mol. Cell. Biol.* **4**, 1605–1617.

Gaines G., Rossi C. and Attardi G. (1987) Markedly different ATP requirements for rRNA synthesis and mtDNA light strand transcription versus mRNA synthesis in isolated human mitochondria. *J. Biol. Chem.* **262**, 1907–1915.

Gelfand R. and Attardi G. (1981) Synthesis and turnover of mitochondrial ribonucleic acid in HeLa cells: the mature ribosomal and messenger ribonucleic acid species are metabolically unstable. *Mol. Cell. Biol.* **1**, 497–511.

Hatanpaa K., Brady D. R., Stoll J., Rapoport S. I. and Chandrasekaran K. (1996) Neuronal activity and early neurofibrillary tangles in Alzheimer's disease. *Ann. Neurol.* **40**, 411–420.

Heddi A., Stepien G., Benke P. J. and Wallace D. C. (1999) Coordinate induction of energy gene expression in tissues of mitochondrial disease patients. *J. Biol. Chem.* **274**, 22 968–22 976.

Hevner R. F. and Wong-Riley M. T. (1993) Mitochondrial and nuclear gene expression for cytochrome oxidase subunits are disproportionately regulated by functional activity in neurons. *J. Neurosci.* **13**, 1805–1819.

Hevner R. F., Liu S. and Wong-Riley M. T. (1995) A metabolic map of cytochrome oxidase in the rat brain: histochemical, densitometric and biochemical studies. *Neuroscience* **65**, 313–342.

Kagawa Y. and Ohta S. (1990) Regulation of mitochondrial ATP synthesis in mammalian cells by transcriptional control. *Int. J. Biochem.* **22**, 219–229.

Kato T. and Lowry O. H. (1973) Enzymes of energy-converting systems in individual mammalian nerve cell bodies. *J. Neurochem.* **20**, 151–163.

Kelly D. P. and Scarpulla R. C. (2004) Transcriptional regulatory circuits controlling mitochondrial biogenesis and function. *Genes Dev.* **18**, 357–368.

Le Roy F., Bisbal C., Silhol M., Martinand C., Lebleu B. and Salehzada T. (2001) The 2–5A/RNase L/RNase L Inhibitor (RLI) pathway regulates mitochondrial mRNAs stability in interferon alpha-treated H9 cells. *J. Biol. Chem.* **276**, 48 473–48 482.

Liu L. I., Rapoport S. I. and Chandrasekaran K. (1999) Regulation of mitochondrial gene expression in differentiated PC12 cells. *Ann. N. Y. Acad. Sci.* **893**, 341–344.

Murdock D. G., Boone B. E., Esposito L. A. and Wallace D. C. (1999) Up-regulation of nuclear and mitochondrial genes in the skeletal muscle of mice lacking the heart/muscle isoform of the adenine nucleotide translocator. *J. Biol. Chem.* **274**, 14 429–14 433.

Paschen W., Althausen S. and Doutheil J. (1999) Ischemia-induced changes in 2′-5′-oligoadenylate synthethase mRNA levels in rat brain: comparison with changes produced by perturbations of endoplasmic reticulum calcium homeostasis in neuronal cell cultures. *Neurosci. Lett.* **263**, 109–112.

Pressman B. C. and Fahim M. (1982) Pharmacology and toxicology of the monovalent carboxylic ionophores. *Annu. Rev. Pharmacol. Toxicol.* **22**, 465–490.

Purdon A. D., Rosenberger T. A., Shetty H. U. and Rapoport S. I. (2002) Energy consumption by phospholipid metabolism in mammalian brain. *Neurochem. Res.* **27**, 1641–1647.

Rapoport S. I. (1970) The sodium–potassium exchange pump: relation of metabolism to electrical properties of the cell. I. Theory. *Biophys. J.* **10**, 246–259.

Schousboe A., Meier E., Drejer J. and Hertz L. (1989) Preparation of primary cultures of mouse (rat) cerebellar granule cells, in *A Dissection and Tissue Culture Manual of the Nervous System* (Shahar A., de Vellis J., Vernadakis A. and Haber B., eds), pp. 203–206. Alan R. Liss, Inc., New York.

Sokoloff L. (1991) Measurement of local cerebral glucose utilization and its relation to local functional activity in the brain. *Adv. Exp. Med. Biol.* **291**, 21–42.

Taurin S., Hamet P. and Orlov S. N. (2003) Na/K pump and intracellular monovalent cations: novel mechanism of excitation–transcription coupling involved in inhibition of apoptosis. *Mol. Biol. (Mosk.)* **37**, 371–381.

Virbasius C. A., Virbasius J. V. and Scarpulla R. C. (1993) NRF-1, an activator involved in nuclear–mitochondrial interactions, utilizes a new DNA-binding domain conserved in a family of developmental regulators. *Genes Dev.* **7**, 2431–2445.

Wiesner R. J., Hornung T. V., Garman J. D., Clayton D. A., O'Gorman E. and Wallimann T. (1999) Stimulation of mitochondrial gene expression and proliferation of mitochondria following impairment of cellular energy transfer by inhibition of the phosphocreatine circuit in rat hearts. *J. Bioenerg. Biomembr.* **31**, 559–567.

Wong-Riley M. T. (1989) Cytochrome oxidase: an endogenous metabolic marker for neuronal activity. *Trends Neurosci.* **12**, 94–101.

Wong-Riley M. T., Mullen M. A., Huang Z. and Guyer C. (1997) Brain cytochrome oxidase subunit complementary DNAs: isolation, subcloning, sequencing, light and electron microscopic *in situ* hybridization of transcripts, and regulation by neuronal activity. *Neuroscience* **76**, 1035–1055.

Wong-Riley M., Anderson B., Liebl W. and Huang Z. (1998) Neurochemical organization of the macaque striate cortex: correlation of cytochrome oxidase with Na^+K^+ATPase, NADPH-diaphorase, nitric oxide synthase, and *N*-methyl-D-aspartate receptor subunit 1. *Neuroscience* **83**, 1025–1045.

Yang S. J., Liang H. L., Ning G. and Wong-Riley M. T. (2004) Ultrastructural study of depolarization-induced translocation of NRF-2 transcription factor in cultured rat visual cortical neurons. *Eur. J. Neurosci.* **19**, 1153–1162.

Zhang C. and Wong-Riley M. T. (2000) Synthesis and degradation of cytochrome oxidase subunit mRNAs in neurons: differential bigenomic regulation by neuronal activity. *J. Neurosci. Res.* **60**, 338–344.

Synthes Award for Resident Research on Brain and Craniofacial Injury: Normoxic Ventilatory Resuscitation After Controlled Cortical Impact Reduces Peroxynitrite-Mediated Protein Nitration in the Hippocampus

Edward S. Ahn, M.D., Courtney L. Robertson, M.D., Viktoria Vereczki, M.D., Gloria E. Hoffman, Ph.D., and Gary Fiskum, Ph.D.

ABSTRACT

Resuscitation with 100% ventilatory oxygen is routinely initiated after severe traumatic brain injury (TBI). Despite the objective to improve oxygenation of the injured brain, there are concerns about the increased production of reactive oxygen species (ROS), which can lead to further neuronal damage. 3-nitrotyrosine (3-NT), the product of peroxynitrite-meditated tyrosine residue nitration, has been used as a marker for ROS-induced oxidative damage to proteins. We hypothesized that posttraumatic resuscitation with hyperoxic ventilation with a fraction of inspired oxygen (Fio_2, 100%) results in increased ROS-induced damage to proteins compared with resuscitation with normoxic ventilation or room air (Fio_2, 21%).

Male Sprague-Dawley rats underwent controlled cortical impact (CCI) and were resuscitated with either normoxic or hyperoxic ventilation for 1 hour after injury (n = 5 per group). Sham-operated control groups received 1 hour of normoxic or hyperoxic ventilation without CCI (n = 4–5 per group). Twenty-four hours after injury, rats were perfused with fixative, and hippocampi were evaluated for levels of 3-NT immunostaining. In a second experiment, for a delayed assessment of neuronal survival, another set of rats similarly underwent CCI and normoxic or hyperoxic ventilation for 1 hour (n = 4 per group), and a sham-operated group was used as a control (n = 4). One week after injury, neuronal cell counts and abnormal cell quantification were performed after staining with the neuron-specific NeuN antibody.

Quantification of 3-NT staining revealed significantly increased levels in the ipsilateral hippocampus in the hyperoxic CCI group. The normoxic group showed a 51.0% reduction of staining in CA1 when compared with those rats resuscitated with hyperoxia and a 50.8% reduction in CA3 (both $P < 0.05$). There was no significant difference in staining between the injured normoxic group and the sham-operated groups. In the delayed analysis of neuronal survival, although neuronal counts were reduced in the hippocampus on the injured side in both injured groups, there was no significant difference between hyperoxic and normoxic groups. Similarly, abnormal cell counts were not significantly different between groups.

In this clinically relevant model of TBI, normoxic resuscitation significantly reduced levels of oxidative damage to proteins compared with hyperoxic resuscitation. Delayed neuronal counts showed no beneficial effect of hyperoxic resuscitation. These findings indicate that hyperoxic ventilation in the early stages after severe TBI may exacerbate oxidative damage to proteins. Future studies should examine the relationship between protein oxidation and histologic and neurologic outcome in TBI.

Improvement of cerebral oxygenation after human TBI is one of the main therapeutic goals in the attempt to prevent secondary brain injury. After severe TBI, there is cerebral edema and often decreased cerebral blood flow (CBF), which causes a shift from aerobic to anaerobic metabolism. The presence of impaired oxidative metabolism is suggested by increased brain tissue lactate levels after TBI and reduction of lactate levels with increased inspired oxygen concentration (Fio_2 100%).[30] In fact, in the prehospital setting, endotracheal intubation and initial resuscitation with an Fio_2 of 100% is routinely used in patients after severe TBI. In an effort to prevent hypoxia and secondary brain injury, it is recommended as a guideline to avoid oxygen saturation <90% in the field or a Pao_2 <60 mm Hg.[6] However, often large concentrations of oxygen are continually given during resuscitation and throughout the first 24 hours after injury, which results in Pao_2 levels well above physiologic conditions.

Despite the seemingly beneficial effect of increased Fio_2 or normobaric hyperoxia on cerebral metabolism after

0148-703/05/5201-0001

TBI,[44] the potential adverse effects must be considered. First, the generation of ROS occurs by a reaction without saturation at the inner mitochondrial membrane in the presence of large concentrations of oxygen. These products can result in oxidized proteins, lipids, DNA, and RNA, which can, in turn, impair cell metabolism and cell viability. Second, the harmful effects of hyperoxia on the lungs, including atelectasis, proinflammatory processes, fibrosis, and pulmonary hypertension have been well demonstrated.[22,39] Underlying this issue, there is also a question of how much oxygen, when delivered at large concentrations to the lungs and blood stream, is actually effectively delivered to the brain tissue.[23,28,38]

The aim of this study is to determine the effect of hyperoxic (Fio_2 100%) versus normoxic (Fio_2 21%) ventilatory resuscitation after TBI on the production of ROS by using an experimental model of CCI. Peroxynitrite is formed from a reaction between the ROS nitric oxide and superoxide. 3-NT is the product of peroxynitrite-mediated nitration of tyrosine residues and has been used as a marker for oxidative stress. We designed this study to determine the levels of 3-NT in animals treated with hyperoxic versus normoxic ventilatory resuscitation after CCI.

MATERIALS AND METHODS

The subjects were 31 male Sprague-Dawley rats with a mean age of 10.6 weeks (range, 9.6–12.3) and a mean weight of 326.7 g (range, 262–432). All experiments were performed in accordance with the Institutional Animal Care and Use Committee at the University of Maryland School of Medicine.

Surgery

Rats were placed in a Plexiglas chamber, and anesthesia was induced by 4.5% inhaled isoflurane in pressurized room air for 2 to 3 minutes. They were then endotracheally intubated with a 14-gauge Angiocath and placed on positive pressure ventilation on a small animal ventilator (Harvard Apparatus, Holliston, MA). Maintenance anesthesia was delivered with 3% isoflurane. The animal was placed in a stereotactic frame. A rectal temperature probe and a heating blanket (Henry Schein, Melville, NY) were used to maintain the body temperature at 37°C. The mean temperature at time of CCI was 36.9 ± 0.1°C (range, 34.4–37.7).

After a midline scalp incision, the left parietal bone was exposed. A left parietal craniotomy was performed with the aide of a surgical microscope and a dental drill (Fine Science, Foster City, CA). Then, the CCI device was calibrated with respect to the exposed dura within the craniotomy. The parameters of impact in injured rats were a depth of 1.5 mm, a mean velocity of 5.62 ± 0.04 m/s (range, 5.24–5.88), and a duration of 50 ms. After impact, the hyperoxic rats were ventilated with 100% O_2 for 1 hour. Normoxic rats were continued on ventilation with room air (Fio_2 21%) for 1 hour. The craniotomy site was covered with dental acrylic, and the scalp incision was closed with silk suture. Sham-operated groups received a craniotomy without CCI and were ventilated with either hyperoxia or normoxia for 1 hour. Arterial blood gas analysis was performed in all rats 30 minutes after injury with blood obtained from the tail artery. The Po_2, pH value, and Pco_2 of the groups analyzed for 3-NT are shown in *Table 45.1* and those analyzed for NeuN in *Table 45.2*. After 1 hour of resuscitation, the isoflurane was stopped. The rats were extubated after exhibiting spontaneous respiration and movement. T1 T2

IMMUNOHISTOCHEMISTRY

3-NT

Twenty-four hours after injury, rats were injected with a lethal dose of intraperitoneal sodium pentobarbital. Rats were perfused first with intracardiac saline and then with 4% paraformaldehyde. The brains were removed and postfixed in a 2.5% acrolein (Polysciences, EM grade, Warrington, PA) solution in 4% paraformaldehyde, pH 6.8, for 1 hour, and kept in 4% paraformaldehyde for 1 day. The brains were then sliced to isolate 3-mm coronal blocks that included the hippocampi. These blocks were then transferred to a 30% sucrose solution and left until they sank. Using a freezing microtome, blocks were cut into 25-μm sections in a 1:6 series for staining. Sections were stored at −20°C in a cryoprotectant polyethylene glycol for at least 1 week before staining.[47]

TABLE 45.1. Arterial blood gas analysis during ventilatory resuscitation after CCI for rats analyzed for 3-NT[a,b]

Subject group	Po_2	Pco_2	pH value
Injured hyperoxic (n = 5)	396.5 ± 26.9[c]	32.0 ± 3.6	7.51 ± 0.04
Injured normoxic (n = 5)	105.6 ± 4.3	31.4 ± 6.1	7.46 ± 0.06
Sham hyperoxic (n = 5)	346.0 ± 30.5[c]	30.6 ± 2.6	7.52 ± 0.03
Sham normoxic (n = 4)	102.8 ± 8.7	33.4 ± 2.6	7.49 ± 0.03

[a]Values are expressed as mean ± SE.
[b]CCI, controlled cortical impact; 3-NT, 3-nitrotyrosine; Po_2, partial pressure of oxygen; Pco_2, partial carbon dioxide pressure.
[c]$P < 0.05$ compared with normoxic group counterparts.

TABLE 45.2. Arterial blood gas analysis during ventilatory resuscitation after CCI for rats analyzed for NeuN[a,b]

Subject group	P_{O_2}	P_{CO_2}	pH value
Injured hyperoxic (n = 4)	306.8 ± 25.6[c]	35.4 ± 1.9	7.48 ± 0.02
Injured normoxic (n = 4)	128.1 ± 16.8	32.7 ± 4.3	7.50 ± 0.04
Sham hyperoxic (n = 4)	346.7 ± 28.7[c]	34.2 ± 2.6	7.52 ± 0.03

[a]Values are expressed as mean ± SE.
[b]CCI, controlled cortical impact; NeuN, neuron-specific antibody; P_{O_2}, partial pressure of oxygen; P_{CO_2}, partial carbon dioxide pressure.
[c]$P < 0.05$ compared with normoxic group counterparts.

Sections were then washed in 0.1 M of Tris buffer solution, pH 7.6, six times, 10 minutes each, to rinse out the cryoprotectant. They were then incubated in a 1% sodium borohydride solution for 20 minutes and rinsed multiple times with Tris buffer. The following staining method was adapted from a protocol previously described by Lorch et al.[26] Sections were mounted on glass slides and allowed to dry overnight. The next day, slides were rehydrated in Tris buffer and treated in a 5% H_2O_2/methanol solution for 30 minutes to kill endogenous peroxidase activity. They were then washed in tap water for 10 minutes. Slides were then submerged in a boiling citrate solution for 10 minutes and then allowed to soak in the hot solution for another 10 minutes. They were then washed in distilled H_2O for 5 minutes and Tris buffer three times, 5 minutes each. Slices were blocked with a 50% goat serum Tris buffer solution for 1 hour in a moist chamber. Next, slices were treated with a 5% goat serum Tris buffer solution with rabbit anti-3-nitrotyrosine antibody (1:500; Upstate, Waltham, MA) overnight at 4°C. Slices were then washed in Tris buffer two times, 5 minutes each, and treated with biotinylated goat anti-rabbit antibody in Tris buffer (1:1000) for 1 hour at room temperature in a moist chamber. After washing again in Tris buffer two times, 5 minutes each, slices were stained with Nickel-diaminobenzidine (Ni-DAB) chromogen using the VectorStain Elite ABC kit (Vector Laboratories, Burlingame, CA).

Stained slices were analyzed for intensity of 3-NT staining. Quantitative analyses were performed with computer-assisted image analysis system, which consisted of a Nikon Eclipse 800 photomicroscope, a Retiga 1300 cooled CCD digital camera (Biovision Technologies, Inc., Exton, PA), and a Macintosh G4 computer with IP Spectrum software (Scientific Image Processing, Version: 3.9.3 r2, Mac OS 10.3.3; Scanalytics, Fairfax, VA). The total area of staining was determined in regions of the hippocampus under 40× magnification. For each subject, an equivalent slice through the hippocampus was analyzed in the CA1, CA 2/3, and dentate gyrus (DG) regions in both sides ipsilateral and contralateral to the injury. For each region of the hippocampus, three fields under 40× magnification were analyzed. The stage of the microscope was adjusted so that the cell layer was centered in the field and was oriented horizontally in the captured image. The amount of staining was expressed as the average area occupied by the black reaction product, which represented 3-NT immunoreactivity within the microscopic field. For each image analysis, segmentation values were set to eliminate any background staining, and the total area of staining (in square micrometers) was determined. All slices were analyzed by the same examiner for consistency.

NeuN

For delayed analysis of neuronal survival 7 days after injury, rats were perfused and brain slices were prepared using the same method described above for the 3-NT antibody. After storing sections at −20°C in polyethylene glycol for at least 1 week, they were stained using a free-floating double label immunocytochemistry protocol, previously described by Hoffman et al.[19] Briefly, sections were washed in 0.05 M of potassium phosphate buffered saline (KPBS) six times, 10 minutes each, to rinse out the cryoprotectant. They were then incubated in a sodium borohydride solution, as described above, and rinsed multiple times in KPBS. The slices were then incubated with the primary antibody, mouse monoclonal anti-NeuN (1:120,000; Chemicon, Temecula, CA) in KPBS with 0.4% Triton-X for 1 hour at room temperature and then for 24 hours at 4°C. Sections were then rinsed again in KPBS six times, 10 minutes each. They were incubated with the secondary antibody, biotinylated horse anti-mouse antibody (1:600) in KPBS with 0.4% Triton-X for 1 hour. After rinsing again in KPBS five times, 10 minutes each, sections were prepared with the VectorStain Elite ABC kit. Sections were then rinsed in KPBS three times, 5 minutes each, then 0.175M sodium acetate three times, 5 minutes each, and then KPBS three times, 5 minutes each. The sections were then placed into a Ni-DAB H_2O_2 chromogen solution (250 mg of Ni sulfate, 2 mg of DAB, and 8.3 μL of 3% H_2O_2 /10 L of 10.175 sodium acetate solution). Sections were left in solution for 10 minutes and staining was then terminated by transferring to the sodium acetate solution. Stained sections were then mounted on glass slides, dehydrated, and coverslipped with Histomount (Zymed Laboratories, South San Francisco, CA).

For neuronal quantification, the same computer-assisted image analysis system described above for 3-NT was used. For each subject, an equivalent section through the hippocampus was analyzed for neuronal counts in the CA1 and CA3 regions in both sides ipsilateral and contralateral to the injury. In each hippocampal region, two high-power fields under 40× magnification were analyzed. The number of normal neurons was determined. In addition, abnormal neu-

rons that exhibited fragmented, pyknotic, or absent nuclei were also counted. All slices were analyzed by the same examiner for consistency.

Statistics

One way analysis of variance (ANOVA, Student-Newman-Keuls method) was used for data analysis. All comparisons with $P < 0.05$ are considered significant. All values are expressed as mean ± SEM.

RESULTS

Arterial Blood Gas Analysis

Mean Po_2, Pco_2, and pH values obtained from the tail arterial blood after 30 minutes of ventilatory resuscitation after CCI for the rats analyzed for 3-NT are shown in *Table 45.1*. In the 3-NT immunohistochemistry experiment, the mean Po_2 values for the hyperoxic ventilated rats were 396.5 ± 26.9 for the injured rats and 346.0 ± 30.5 for the sham-operated rats. These values were significantly increased when compared to the normoxic counterparts with po_2 values of 105.6 ± 4.3 and 102.8 ± 8.7, with ($P < 0.001$). Arterial blood gas analysis for rats analyzed for NeuN are shown in *Table 45.2*. Similarly, rats that received hyperoxic resuscitation had Po_2 values of 306.8 ± 25.6 for the injured rats and 346.7 ± 28.7 for the sham-operated rats. These values were significantly increased compared with the normoxic rats with a mean Po_2 of 128.1 ± 16.8 ($P < 0.001$). In both experiments, there was no significant difference in Pco_2 or pH values between groups.

Nitrotyrosine Analysis

In this experiment, rats were subject to one of four conditions: injury with hyperoxic resuscitation (n = 5), injury with normoxic resuscitation (n = 5), sham operation with hyperoxic resuscitation (n = 5), or sham operation with normoxic resuscitation (n = 4). To determine levels of oxidative stress, brain slices through the hippocampus were obtained 24 hours after CCI and stained with the 3-NT antibody (*Fig. 45.1*). Quantification of 3-NT staining in the hippocampus ipsilateral to the injured cortex is displayed in *Figure 45.2*. In the hippocampal region of CA1, rats resuscitated with normoxia showed a 51.0% reduction of staining when compared with those rats resuscitated with hyperoxia ($P < 0.05$). In CA3, normoxic rats showed a 50.8% reduction in staining when compared with hyperoxic rats ($P < 0.05$). Furthermore, there was increased staining in the CA1 and CA3 regions of the injured hyperoxic group when compared with equivalent regions of both sham-operated groups ($P < 0.05$). In contrast, there was no difference in staining in these regions among the injured normoxic group and both sham-operated groups. There was also no difference in the staining of the DG between all groups. Of note, the sham-operated hyperoxic group showed increased staining in all hippocampal regions compared with the sham-operated normoxic group, but there was no statistical significance ($P = 0.679$ in CA1; $P = 0.475$ in CA3; $P = 0.271$ in DG).

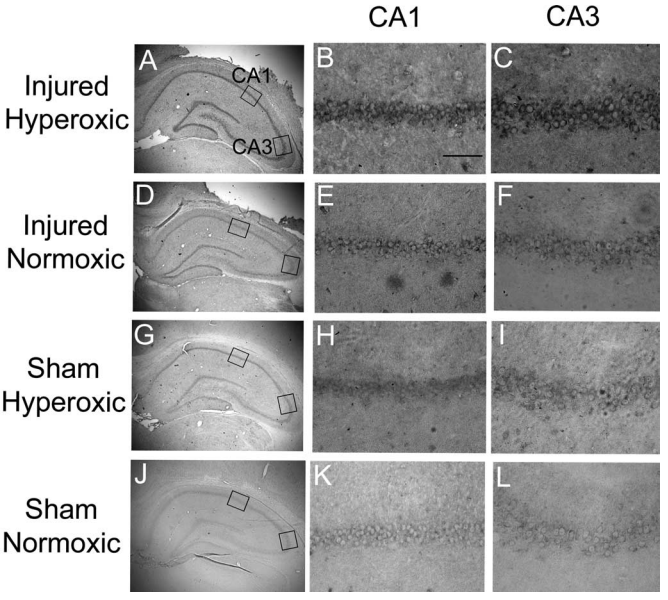

FIGURE 45.1 Sample photomicrographs of the hippocampus underlying the injured cortex with 3-NT (1:500) staining 24 hours after CCI for each of the subject groups: injured hyperoxic, *A–C*, injured normoxic, *D–F*, sham hyperoxic, *G–I*, and sham normoxic, *J–L*. Photomicrographs in the first column, *A, D, G, and J,* are low-power views of the hippocampus. The damaged cortex can be seen in both injured rats, *A and D*. Black boxes indicate the CA1 and CA3 regions, which are shown to the right at 40× magnification (CA1, *B, E, H, and K,* and CA3, *C, F, I, and L*). The injured hyperoxic group showed the most intense staining in the CA1 and CA3 regions of the hippocampus. The least intense staining was seen in the sham-operated normoxic group. Scale bar = 50 μm.

In the hyperoxic group, the hippocampus on the injured side of the brain demonstrated increased staining when compared with the hippocampus on the contralateral side. There was a mean 43.0 ± 18.7% increase in CA1 and a mean 86.6 ± 27.5% increase in CA3. Comparatively, the normoxic group did not display the same magnitude of increased staining on the injured side. There was a mean 22.6 ± 8.2% decrease in CA1 and a mean 21.5 ± 33.3% increase in CA3. There was no consistent pattern between the ipsilateral and contralateral hippocampal regions in either of the sham-operated groups. There was no significant difference in staining in the contralateral hippocampus among all four groups.

NeuN Analysis

For delayed immunohistochemical analysis, brain slices through the hippocampus were obtained from rats 1 week after exposure to one of three different conditions: injury with hyperoxic resuscitation (n = 4), injury with

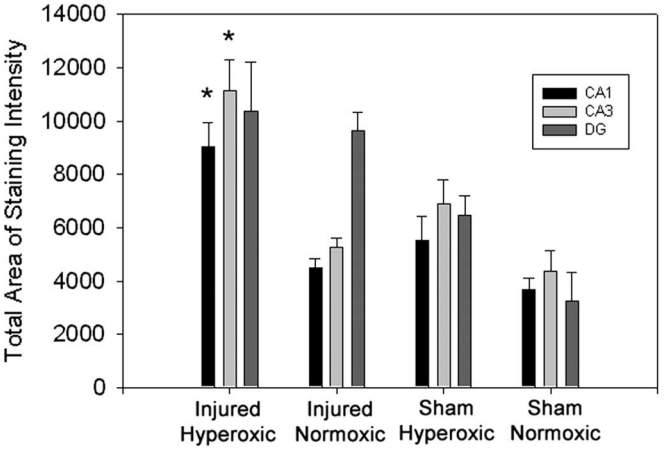

FIGURE 45.2 Quantification of 3-NT (1:500) staining 24 hours after CCI in regions of the hippocampus underlying the injured cortex. Staining area is quantified for each high-power field (40×) in square micrometers. In the CA1 and CA3 regions of the hippocampus of the injured hyperoxic group, there is a significant increase in 3-NT staining when compared with equivalent regions in the injured normoxic group and both sham-operated groups ($P < 0.05$). *$P < 0.05$ in equivalent regions of the other groups.

normoxic resuscitation (n = 4), and sham operation with hyperoxic resuscitation (n = 4). Slices were stained with the NeuN antibody (1:120,000). A sample photomicrograph from an injured hyperoxic rat is shown in *Figure 45.3A*. CA1 and CA3 regions of the hippocampus both ipsilateral and contralateral to the injury were analyzed under high-power magnification at 40×. There were two types of neurons counted: normal and abnormal. Normal neurons had the expected pyramidal shape with round nuclei. Abnormal neurons possessed vacuolated, pyknotic, or disrupted nuclei that were likely damaged cells in the process of dying (*Fig. 45.3B*).

Neuronal counts in the CA1 and CA3 regions of the hippocampus ipsilateral to injury are displayed in *Figure 45.4*. There was a significant reduction in CA1 neurons in both hyperoxic and normoxic injured rats when compared with the sham-operated rats ($P < 0.05$). However, there was no significant difference between the two injured groups. In CA3, there was no significant difference in neuronal counts between all groups.

The ratios between hippocampal neuronal counts on the injured side versus the noninjured side were determined to assess neuronal loss from injury (*Fig. 45.5*). In CA1, there was a mean cell loss of 22.3% in the hyperoxic group and 26.4% in the normoxic group. In CA3, the cell loss was less appreciable, with a mean of 9.9% in the hyperoxic group and 4.6% in the normoxic group. However, there was no significant difference between the hyperoxic and normoxic groups in CA1 or CA3.

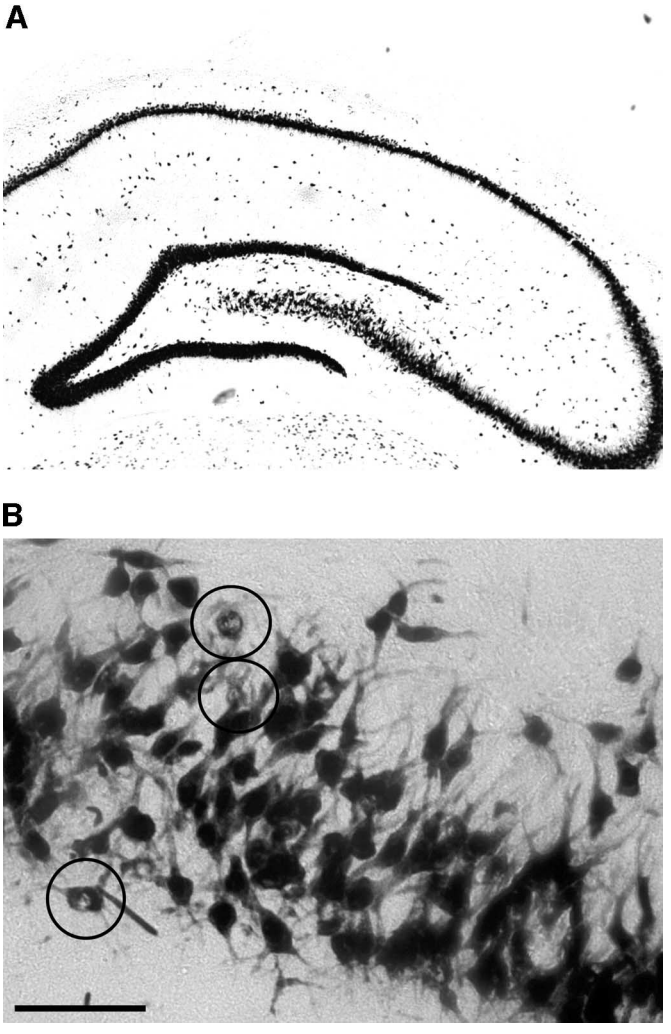

FIGURE 45.3 Sample photomicrographs of the hippocampus of an injured rat with NeuN staining (1:120,000) 7 days after CCI. *A*, A low-power view of the hippocampus is shown. *B*, a 40× magnification of the CA3 region is shown. Black circles indicate abnormal neurons with vacuolated nuclei, which likely represent neurons in the process of cell death. Scale bar = 50 μm.

Abnormal cell counts in the CA1 region of the hippocampus ipsilateral to the injury revealed 10.1 ± 1.4% abnormal cells in the hyperoxic group and 10.8 ± 1.1% in the normoxic group. In CA3, there were 8.1 ± 1.1% abnormal cells in the hyperoxic group and 12.4 ± 2.1% in the normoxic group. In both CA1 and CA3 regions, there was no significant difference in abnormal cell counts between the hyperoxic and normoxic groups.

DISCUSSION

Traumatic Brain Injury and Metabolic Dysfunction

Prospectively collected data from the Traumatic Coma Data Bank demonstrated that early hypoxemia in the field

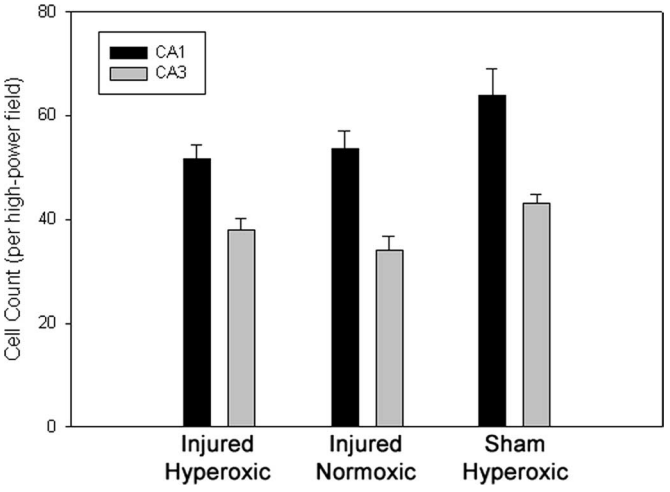

FIGURE 45.4 Neuronal counts per high-power field in the CA1 and CA3 regions of the hippocampus ipsilateral to injured cortex with NeuN staining 7 days after CCI. There is a significant reduction of neurons in the CA1 region of the hippocampus in both injured groups compared with the sham-operated group ($P < 0.05$). However, there is no significant difference between the hyperoxic- and normoxic-injured groups. In CA3, there is no significant difference in cell counts among groups.

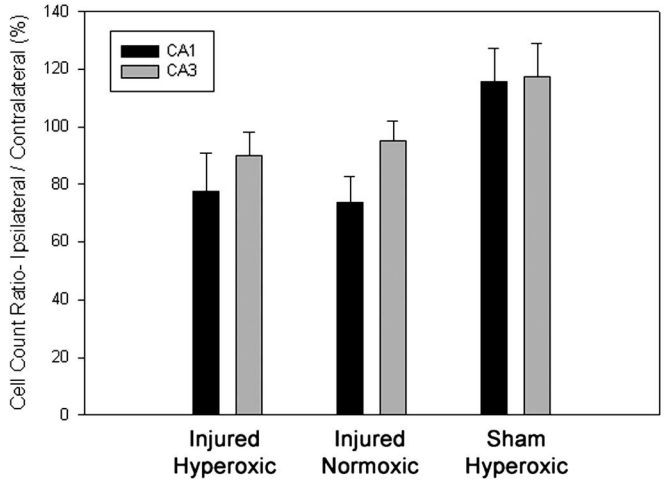

FIGURE 45.5 Ratio of neuronal counts of the ipsilateral versus contralateral hippocampus with NeuN staining 7 days after CCI. There is cell loss in the CA1 and CA3 regions of the injured hippocampus compared with the contralateral side in both injured groups. However, there is no significant difference in ratios between groups.

after severe TBI with Pao_2 <60 mm Hg is associated with an increased morbidity and mortality.[7] Therefore, recommendations from the Brain Trauma Foundation are to oxygenate to keep O_2 saturation >90% or Pao_2 >60 mm Hg to prevent hypoxia and secondary brain injury.[6,15] In practice, ventilatory resuscitation with $Fio_2$100% is routinely used after severe traumatic brain injury both during the prehospital management and during initial resuscitation while in the trauma center.

Recently, there have been clinical[30,34,44] and laboratory[35] investigations that support the use of normobaric hyperoxia as a therapeutic measure in the initial treatment of severe TBI. This thought emanates from the fact that there is an increased metabolic demand of brain tissue after TBI, during which there is a shift from aerobic to anaerobic metabolism, as suggested by an increase in brain tissue lactate.[5,48] The aim of hyperoxic ventilatory resuscitation is to restore aerobic metabolism and to ameliorate the mismatch between CBF and metabolic stimulation.

In an experimental model of TBI, animals resuscitated with an Fio_2 100% had significantly decreased brain lactate levels compared with animals resuscitated with Fio_2 21% as measured by microdialysis.[35] In a clinical study, Menzel et al.[30] measured brain tissue lactate and glucose levels in patients who received Fio_2 100% for 6 hours after severe TBI. Brain tissue lactate levels decreased by 40% from baseline during this hyperoxic period. Tolias et al.[44] confirmed these results in their multicenter study where patients with severe TBI were given Fio_2 100% for 24 hours, which resulted in a significant decrease in lactate and glutamate levels, as measured by microdialysis, when compared with a historical control group. Comparatively, in another clinical study of severe TBI using microdialysis, Magnoni et al.[28] found reduced levels of lactate with ventilation with $Fio_2$100% and reduced levels of pyruvate whereby the lactate/pyruvate ratio did not change. Therefore, they concluded that hyperoxia did not change the redox status of injured cells, and thus, there was no improvement in glucose metabolism. However, in the study by Tolias et al.,[44] there was a significant decrease in the lactate/pyruvate ratio with hyperoxia. The difference in the two studies is suggested to be attributable to the delayed initiation of hyperoxia in the Magnoni et al.[28] study.

Furthermore, there have been reports about the benefit of using hyperbaric oxygen therapy in an effort to increase brain tissue Po_2 after severe TBI.[11,36,43] Similar to the use of normobaric hyperoxia, the therapeutic aim is to improve oxidative metabolism; however, with the use of these enhanced concentrations of oxygen, there must be further concern about oxidative damage to the injured cells.

Stroke and Cardiac Arrest

Previous studies on the effect of hyperoxia on ischemic brain injury from stroke are precursors to the experiments described in this article. Hyperoxia has been shown to be beneficial in experimental models of focal cerebral ischemia.[13,40,41] One hundred percent O_2 is routinely administered to patients after an acute stroke, as a recommended intervention from the American Heart Association.[1] However, in a measure of patient survival after acute stroke of

various severities, Rønning et al.[37] demonstrated that supplemental 100% O_2 administered to patients with minor to moderate strokes for 24 hours reduced survival when compared with those who did not receive supplemental oxygen. In a canine model of cardiac arrest, dogs resuscitated with 21% O_2 demonstrated lower levels of oxidized brain lipids and improved neurological outcome compared with those resuscitated with 100% O_2.[25] These studies, in addition to other animal studies of global cerebral ischemia,[32,49] caution the empiric usage of 100% O_2 after an acute stroke.

Previously, in our laboratory, the hypothesis that resuscitation with 100% O_2 after global cerebral ischemia results in increased ROS-induced damage was tested with the canine cardiac arrest model. 3-NT has been established as a marker for oxidative damage to proteins after peroxynitrite-mediated nitration of tyrosine.[3,4,20,21] When the hippocampus was stained with the 3-NT antibody 2 hours after cardiac arrest, those animals resuscitated with 100% O_2 showed a significant increase in staining in all regions of the hippocampus compared with those resuscitated with normoxia.[46] Understanding that this model of global cerebral ischemia has many differences with models of TBI, our experiments were designed to address the possibility that exacerbation of ROS-induced protein damage in the hippocampus with hyperoxia could also be present after TBI.

Oxidative Stress

This study is consistent with previous studies in which there is increased production of ROS after experimental TBI.[2,12,16–18,24,29,33] ROS, such as peroxynitrite, exhibit toxicity to the brain by way of their modification of macromolecules, especially DNA, and the induction of apoptotic and necrotic cell death pathways.[27] Investigators have described the time course of peroxynitrite-mediated oxidative damage to proteins using the 3-NT antibody in experimental models of TBI.[18,31] Hall et al.[18] showed that the highest intensity of staining was within the first 48 hours after injury in the neuronal perikarya and processes and microvessels. Our findings of significant 3-NT immunostaining 24 hours after CCI are consistent with the findings of Hall et al.[18] Those rats in our study with hyperoxic resuscitation had an increased staining intensity on the injured side compared with the noninjured side of 43.0% in CA1 and 86.6% in CA3. However, this increased staining on the injured side was not as pronounced in the normoxic group. Moreover, the total amount of staining on the injured side in the normoxic group was no different than in the sham-operated groups. In contrast, there was a significantly increased amount of staining in the injured hippocampus of the hyperoxic group. Our findings suggest that normoxic ventilatory resuscitation provides significant protection against oxidative damage to proteins as measured at 24 hours after TBI when compared with hyperoxic ventilatory resuscitation.

In addition to the differences seen among the injured rats, there was also a noticeable difference between the sham-operated groups. Although not a statistically significant difference, the hyperoxic sham-operated rats had increased levels of 3-NT staining in the hippocampus when compared with the normoxic sham-operated rats, which suggests that hyperoxic ventilation alone may increase levels of oxidative stress. Similarly, in the study of ROS production from subdural hematoma induction, Doppenberg et al.[12] found increased levels of hydroxyl radical degradation products in noninjured animals after increasing the Fio_2 to 100%. These results support the hypothesis that in the presence of high oxygen tension, even under normobaric conditions and in the noninjured brain, there is increased ROS production. These findings in sham-operated animals warrant additional caution with respect to the administration of large concentrations of ventilatory oxygen.

Delayed neuronal counts at 1 week after injury were consistent with previous studies using the CCI model. The CA1 and CA3 regions of the hippocampus showed appreciable cell loss on the injured side. In our analysis, the CA1 region was affected more than the CA3 region. These results differ from previous studies using the CCI model where the CA3 region was the more affected population of neurons.[8,14,42,45] The difference may be due to the parameters of the impact: depth of injury and impact velocity. Our CCI parameters allowed for a more shallow depth and a higher impact velocity, which may have resulted in an increased susceptibility of CA1 neurons to cell death. The appearance of neurons with pyknotic or vacuolated nuclei in the hippocampus on the side of injury is also consistent with past studies using the CCI model.[9,10] These neurons, which have been found to be present up to 2 weeks after injury, are likely destined to die by either necrosis or apoptosis.

Studies have supported the use of normobaric hyperoxia in the initial treatment after TBI because of the favorable shift from anaerobic to aerobic metabolism.[30,34,35,44] However, our analysis of neuronal cell loss and abnormal cell counts did not show any beneficial effect of hyperoxic resuscitation. At 1 week after injury, rats that were ventilated with Fio_2 100% for 1 hour after CCI showed no significant difference in neuronal loss and abnormal cell morphology than those that were ventilated with room air. Perhaps a lengthier period of hyperoxic ventilation after CCI may have been required to establish a more favorable environment for aerobic metabolism in the injured tissue; however, as demonstrated by our findings with 3-NT staining, one would also expect a significantly heightened level of oxidative damage with extended hyperoxic ventilation. It is possible that as a consequence of hyperoxia, there are at least two major processes, a shift toward aerobic metabolism and oxidative damage, both of which may affect neuronal survival; there-

fore, further investigation is required to define their respective roles in delayed neuronal function and survival after TBI.

Clinical Implications

With early hypoxemia as a reliable predictor for morbidity and mortality after severe TBI, endotracheal intubation and supplemental oxygenation is indeed a crucial intervention in the early resuscitation of a patient after severe TBI. However, when ventilation with Fio_2f 100% becomes prolonged, this administration of normobaric hyperoxia then moves beyond an early intervention to become a deliberate treatment. As with any treatment, a dose-response curve and consideration for treatment toxicity is essential. In light of the findings by Magnoni et al.[28] that demonstrate a lack of improvement in cerebral metabolism with hyperoxic resuscitation, the benefit of normobaric hyperoxia after severe TBI is at least debatable. Moreover, our finding of a significant increase in oxidative damage to proteins with just 1 hour of hyperoxic ventilation in an experimental TBI model demonstrates the potential toxicity of the purported treatment with normobaric hyperoxia. This concern for ROS-mediated damage to the brain with hyperoxia compounds what has already been established about oxygen toxicity to the lungs.

In the prehospital setting, ventilatory resuscitation with 100% O_2 may be the most effective method of avoiding early hypoxemia after severe TBI. However, if efforts toward ameliorating ROS-mediated damage are to be made, this large concentration of oxygen can rapidly and easily be adjusted. Because pulse oximetry and arterial blood gas analyses are routinely monitored for early hypoxemia, the same modalities could also be used to monitor for the potential toxicity of hyperoxia. These modalities could be monitored with a predetermined set of parameters to avoid the harmful effects of either extreme in oxygenation. Similar parameters could also be applied to brain tissue oximetry. Nevertheless, further investigation into hyperoxic ventilation after severe TBI is required to establish how its potential metabolic benefit and its potential for oxidative damage impact neuronal survival and neurological outcome.

CONCLUSION

Ventilatory resuscitation with 100% O_2 is routinely administered after severe TBI to prevent early hypoxemia. In addition, the use of normobaric hyperoxia after severe TBI has recently been supported for the main therapeutic goal of shifting from anaerobic metabolism to aerobic metabolism in the injured brain. Other investigators have called into question this metabolic benefit. Furthermore, the use of normobaric hyperoxia heightens the concern for oxygen toxicity and ROS-mediated damage to the brain. Our results show that rats administered 100% O_2 for 1 hour after CCI had significantly increased levels of ROS-mediated damage to proteins in the CA1 and CA3 regions of the hippocampus when compared with rats administered room air. Levels of ROS-mediated protein nitration in the normoxic group were no different than those of noninjured rats. Additionally, there was no beneficial effect of hyperoxic resuscitation on neuronal survival or abnormal neuronal morphology 1 week after injury. These results warrant additional caution in the empiric use of hyperoxic resuscitation in the treatment of severe TBI. If future studies support this concern for increased ROS-mediated damage with hyperoxia, then efforts will need to be made toward early adjustments in the O_2 concentration administered during resuscitation after severe TBI.

ACKNOWLEDGMENTS

This work was supported by DAMD 17-99-1-9483 (G.F.) and the National Institutes of Health K08NS 42805 (C.L.R.). We would also like to thank Robert E. Rosenthal, M.D., Manda Saraswati, Peter Baab, and Erica Martin, Ph.D., for work that was instrumental in the completion of this project.

REFERENCES

1. Adams HP Jr, Brott TG, Crowell RM, Furlan AJ, Gomez CR, Grotta J, Helgason CM, Marler JR, Woolson RF, Zivin JA: Guidelines for the management of patients with acute ischemic stroke: A statement for healthcare professionals from a special writing group of the Stroke Council, American Heart Association. **Stroke** 25:1901–1914, 1994.
2. Althaus JS, Andrus PK, Williams CM, VonVoigtlander PF, Cazers AR, Hall ED: The use of salicylate hydroxylation to detect hydroxyl radical generation in ischemic and traumatic brain injury: Reversal by tirilazad mesylate (U-74006F). **Mol Chem Neuropathol** 20:147–162, 1993.
3. Beckman JS, Carson M, Smith CD, Koppenol WH: ALS, SOD and peroxynitrite. **Nature** 364:584, 1993.
4. Beckman JS, Koppenol WH. Nitric oxide, superoxide, and peroxynitrite: The good, the bad, and ugly. **Am J Physiol** 271:C1424–C1436, 1996.
5. Bergsneider M, Hovda DA, Shalmon E, Kelly DF, Vespa PM, Martin NA, Phelps ME, McArthur DL, Caron MJ, Kraus JF, Becker DP: Cerebral hyperglycolysis following severe traumatic brain injury in humans: a positron emission tomography study. **J Neurosurg** 86:241–251, 1997.
6. The Brain Trauma Foundation, The American Association of Neurological Surgeons, The Joint Section on Neurotrauma and Critical Care: Guidelines for the management of severe traumatic brain injury: Resuscitation of blood pressure and oxygenation. **J Neurotrauma** 17:471–478, 2000.
7. Chesnut RM, Marshall LF, Klauber MR, Blunt BA, Baldwin N, Eisenberg HM, Jane JA, Marmarou A, Foulkes MA: The role of secondary brain injury in determining outcome from severe head injury. **J Trauma** 34:216–222, 1993.
8. Clark RS, Kochanek PM, Dixon CE, Chen M, Marion DW, Heineman S, DeKosky ST, Graham SH: Early neuropathologic effects of mild or moderate hypoxemia after controlled cortical impact injury in rats. **J Neurotrauma** 14:179–189, 1997.
9. Colicos MA, Dash PK: Apoptotic morphology of dentate gyrus granule cells following experimental cortical impact injury in rats: possible role in spatial memory deficits. **Brain Res** 739:120–131, 1996.
10. Colicos MA, Dixon CE, Dash PK: Delayed, selective neuronal death following experimental cortical impact injury in rats: possible role in memory deficits. **Brain Res** 739:111–119, 1996.
11. Daugherty WP, Levasseur JE, Sun D, Rockswold GL, Bullock MR: Effects of hyperbaric oxygen therapy on cerebral oxygenation and mitochondrial function following moderate lateral fluid-percussion injury in rats. **J Neurosurg** 101:499–504, 2004.
12. Doppenberg EM, Rice MR, Di X, Young HF, Woodward JJ, Bullock R:

Increased free radical production due to subdural hematoma in the rat: effect of increased inspired oxygen fraction. **J Neurotrauma** 15:337–347, 1998.
13. Flynn EP, Auer RN: Eubaric hyperoxemia and experimental cerebral infarction. **Ann Neurol** 52:566–572, 2002.
14. Forbes ML, Clark RS, Dixon CE, Graham SH, Marion DW, DeKosky ST, Schiding JK, Kochanek PM: Augmented neuronal death in CA3 hippocampus following hyperventilation early after controlled cortical impact. **J Neurosurg** 88:549–556, 1998.
15. Gabriel EJ, Ghajar J, Jagoda A, Pons PT, Scalea T, Walters BC, Brain Trauma Foundation: Guidelines for prehospital management of traumatic brain injury. **J Neurotrauma** 19:111–174, 2002.
16. Globus MY, Alonso O, Dietrich WD, Busto R, Ginsberg MD: Glutamate release and free radical production following brain injury: effects of posttraumatic hypothermia. **J Neurochem** 65:1704–1711, 1995.
17. Hall ED, Andrus PK, Yonkers PA: Brain hydroxyl radical generation in acute experimental head injury. **J Neurochem** 60:588–594, 1993.
18. Hall ED, Detloff MR, Johnson K, Kupina NC: Peroxynitrite-mediated protein nitration and lipid peroxidation in a mouse model of traumatic brain injury. **J Neurotrauma** 21:9–20, 2004.
19. Hoffman GE, Smith MS, Fitzsimmons MD: Detecting steroidal effects on immediate early gene expression in the hypothalamus. **Neuroprotocols** 1:52–66, 1992.
20. Ischiropoulos H: Biological tyrosine nitration: a pathophysiological function of nitric oxide and reactive oxygen species. **Arch Biochem Biophys** 356:1–11, 1998.
21. Ischiropoulos H, Zhu L, Chen J, Tsai M, Martin JC, Smith CD, Beckman JS: Peroxynitrite-mediated tyrosine nitration catalyzed by superoxide dismutase. **Arch Biochem Biophys** 298:431–437, 1992.
22. Jackson RM: Molecular, pharmacologic, and clinical aspects of oxygen-induced lung injury. **Clin Chest Med** 11:73–86, 1990.
23. Jacobson I, Harper AM, McDowall DG: The effects of oxygen at 1 and 2 atmospheres on the blood flow and oxygen uptake of the cerebral cortex. **Surg Gynecol Obstet** 119:737–742, 1964
24. Kwon TH, Chao DL, Malloy K, Sun D, Alessandri B, Bullock MR: Tempol, a novel stable nitroxide, reduces brain damage and free radical production, after acute subdural hematoma in the rat. **J Neurotrauma** 20:337–345, 2003.
25. Liu Y, Rosenthal RE, Haywood Y, Miljkovic-Lolic M, Vanderhoek JY, Fiskum G: Normoxic ventilation after cardiac arrest reduces oxidation of brain lipids and improves neurological outcome. **Stroke** 29:1679–1686, 1998.
26. Lorch S, Lightfoot R, Ohshima H, Virag L, Chen Q, Hertkorn C, Weiss M, Souza J, Ischiropoulos H, Yermilov V, Pignatelli B, Masuda M, Szabo C: Detection of peroxynitrite-induced protein and DNA modifications. **Methods Mol Biol** 196:247–275, 2002.
27. Love S: Oxidative stress in brain ischemia. **Brain Pathol** 9:119–131, 1999.
28. Magnoni S, Ghisoni L, Locatelli M, Caimi M, Colombo A, Valeriani V, Stocchetti N: Lack of improvement in cerebral metabolism after hyperoxia in severe head injury: a microdialysis study. **J Neurosurg** 98:952–958, 2003.
29. Marklund N, Lewander T, Clausen F, Hillered L: Effects of the nitrone radical scavengers PBN and S-PBN on in vivo trapping of reactive oxygen species after traumatic brain injury in rats. **J Cereb Blood Flow Metab** 21:1259–1267, 2001.
30. Menzel M, Doppenberg EM, Zauner A, Soukup J, Reinert MM, Bullock R: Increased inspired oxygen concentration as a factor in improved brain tissue oxygenation and tissue lactate levels after severe human head injury. **J Neurosurg** 91:1–10, 1999.
31. Mesenge C, Charriaut-Marlangue C, Verrecchia C, Allix M, Boulu RR, Plotkine M: Reduction of tyrosine nitration after N(omega)-nitro-L-arginine-methyl ester treatment of mice with traumatic brain injury. **Eur J Pharmacol** 353:53–57, 1998.
32. Mickel HS, Vaishnav YN, Kempski O, von Lubitz D, Weiss JF, Feuerstein G: Breathing 100% oxygen after global brain ischemia in Mongolian Gerbils results in increased lipid peroxidation and increased mortality. **Stroke** 18:426–430, 1987.
33. Nakamura H, Uzura M, Uchida K, Nakayama H, Furuya Y, Hayashi T, Sekino H, Ominato M, Owada S: Effects of edaravone on experimental brain injury in view of free radical reaction. **Acta Neurochir Suppl** 86:309–311, 2003.
34. Reinert M, Barth A, Rothen HU, Schaller B, Takala J, Seiler RW: Effects of cerebral perfusion pressure and increased fraction of inspired oxygen on brain tissue oxygen, lactate and glucose in patients with severe head injury. **Acta Neurochir (Wien)** 145:341–349, 2003.
35. Reinert M, Schaller B, Widmer HR, Seiler R, Bullock R: Influence of oxygen therapy on glucose-lactate metabolism after diffuse brain injury. **J Neurosurg** 101:323–329, 2004.
36. Rockswold GL, Ford SE, Anderson DC, Bergman TA, Sherman RE: Results of a prospective randomized trial for treatment of severely brain-injured patients with hyperbaric oxygen. **J Neurosurg** 76:929–934, 1992.
37. Rønning OM, Guldvog B: Should stroke victims routinely receive supplemental oxygen? A quasi-randomized controlled trial. **Stroke** 30: 2033–2037, 1999.
38. Rossi S, Stocchetti N, Longhi L, Balestreri M, Spagnoli D, Zanier ER, Bellinzona G: Brain oxygen tension, oxygen supply, and oxygen consumption during arterial hyperoxia in a model of progressive cerebral ischemia. **J Neurotrauma** 18:163–174, 2001. **AQ: A**
39. Singer MM, Wright F, Stanley LK, Roe BB, Hamilton WK: Oxygen toxicity in man: A prospective study in patients after open-heart surgery. **N Engl J Med** 283:1473–1478, 1970.
40. Singhal AB, Dijkhuizen RM, Rosen BR, Lo EH: Normobaric hyperoxia reduces MRI diffusion abnormalities and infarct size in experimental stroke. **Neurology** 58:945–952, 2002.
41. Singhal AB, Wang X, Sumii T, Mori T, Lo EH: Effects of normobaric hyperoxia in a rat model of focal cerebral ischemia-reperfusion. **J Cereb Blood Flow Metab** 22:861–868, 2002.
42. Smith DH, Soares HD, Pierce JS, Perlman KG, Saatman KE, Meaney DF, Dixon CE, McIntosh TK: A model of parasagittal controlled cortical impact in the mouse: Cognitive and histopathologic effects. **J Neurotrauma** 12:169–178, 1995.
43. Sukoff MH: Effects of hyperbaric oxygenation. **J Neurosurg** 95:544–546, 2001.
44. Tolias CM, Reinert M, Seiler R, Gilman C, Scharf A, Bullock MR: Normobaric hyperoxia-induced improvement in cerebral metabolism and reduction in intracranial pressure in patients with severe head injury: A prospective historical cohort-matched study. **J Neurosurg** 101:435–444, 2004.
45. Varma MR, Dixon CE, Jackson EK, Peters GW, Melick JA, Griffith RP, Vagni VA, Clark RS, Jenkins LW, Kochanek PM: Administration of adenosine receptor agonists or antagonists after controlled cortical impact in mice: Effects on function and histopathology. **Brain Res** 951: 191–201, 2002.
46. Vereczki V, Martin E, Rosenthal RE, Hof PR, Sherwood CC, Chinopoulos C, Hu W, Hoffman GE, Fiskum G: Normoxic versus hyperoxic ventilation after cardiac arrest: Hippocampal protein nitration, pyruvate dehydrogenase immunoreactivity, and cell death. Program No. 739.8. 2003 Abstract Viewer/Itinerary Planner. Washington, DC, **Society for Neuroscience**, 2003. Online (abstr).
47. Watson RE Jr, Wiegand SJ, Clough RW, Hoffman GE: Use of cryoprotectant to maintain long-term peptide immunoreactivity and tissue morphology. **Peptides** 7:155–159, 1986.
48. Yoshino A, Hovda DA, Kawamata T, Katayama Y, Becker DP: Dynamic changes in local cerebral glucose utilization following cerebral conclusion in rats: Evidence of a hyper- and subsequent hypometabolic state. **Brain Res** 561:106–119, 1991.
49. Zwemer CF, Whitesall SE, D'Alecy LG: Cardiopulmonary-cerebral resuscitation with 100% oxygen exacerbates neurological dysfunction following nine minutes of normothermic cardiac arrest in dogs. **Resuscitation** 27:159–170, 1994.

AUTHOR QUERIES

AUTHOR PLEASE ANSWER ALL QUERIES **1**

A—AU: Reference number 39 was skipped; thus, references have been renumbered

---

Journal of Bioenergetics and Biomembranes, Vol. 37, No. 4, August 2005 (© 2005)
DOI: 10.1007/s10863-005-6634-0

Diacylglycerols Activate Mitochondrial Cationic Channel(s) and Release Sequestered Ca^{2+}

Christos Chinopoulos,[1] Anatoly A. Starkov,[2] Sergey Grigoriev,[3] Laurent M. Dejean,[3] Kathleen W. Kinnally,[3] Xibao Liu,[4] Indu S. Ambudkar,[4] and Gary Fiskum[1,5]

Received May 18, 2005; accepted May 31, 2005

Mitochondria contribute to cytosolic Ca^{2+} homeostasis through several uptake and release pathways. Here we report that 1,2-sn-diacylglycerols (DAGs) induce Ca^{2+} release from Ca^{2+}-loaded mammalian mitochondria. Release is not mediated by the uniporter or the Na^+/Ca^{2+} exchanger, nor is it attributed to putative catabolites. DAGs-induced Ca^{2+} efflux is biphasic. Initial release is rapid and transient, insensitive to permeability transition inhibitors, and not accompanied by mitochondrial swelling. Following initial rapid release of Ca^{2+} and relatively slow reuptake, a secondary progressive release of Ca^{2+} occurs, associated with swelling, and mitigated by permeability transition inhibitors. The initial peak of DAGs-induced Ca^{2+} efflux is abolished by La^{3+} (1 mM) and potentiated by protein kinase C inhibitors. Phorbol esters, 1,3-diacylglycerols and 1-monoacylglycerols do not induce mitochondrial Ca^{2+} efflux. Ca^{2+}-loaded mitoplasts devoid of outer mitochondrial membrane also exhibit DAGs-induced Ca^{2+} release, indicating that this mechanism resides at the inner mitochondrial membrane. Patch clamping brain mitoplasts reveal DAGs-induced slightly cation-selective channel activity that is insensitive to bongkrekic acid and abolished by La^{3+}. The presence of a second messenger-sensitive Ca^{2+} release mechanism in mitochondria could have an important impact on intracellular Ca^{2+} homeostasis.

KEY WORDS: Mitochondria; calcium; diacylglycerol; mitoplast; cation channel; permeability transition pore; protein kinase C; transient receptor potential; OAG.

INTRODUCTION

A plethora of cellular signaling cascades converge to the production of diacylglycerols (DAGs), leading to the activation of various target proteins regulating cellular processes of extraordinary diversity (Brose *et al*., 2004). Depending on the identity of the stimulated receptor, different PLC isoforms are activated resulting in the immediate formation of DAG from inositol phospholipids, most rapidly from P1-4,5-bisphosphate (PIP_2). This DAG molecule disappears quickly; however, a second wave of DAG emerges with a relatively slow onset persisting for minutes or hours. This latent increase in DAG is partially attributed to the subsequent action of phospholipase D (PLD) on phosphatidylcholine (PC) to yield phosphatidate plus choline followed by phosphatidate phosphatase generating DAG and orthophosphate (Nishizuka, 1992,

[1] Department of Anesthesiology, University of Maryland, Baltimore, Maryland.
[2] Department of Neurology, Weill Medical College, Cornell University, New York, New York.
[3] Division of Basic Sciences, New York University College of Dentistry, New York, New York.
[4] Secretory Physiology Section, Gene Therapy and Therapeutics Branch, NIDCR, National Institutes of Health, Bethesda, Maryland.
[5] To whom correspondence should be addressed at Department of Anesthesiology, University of Maryland School of Medicine, 685 West Baltimore Street, MSTF 5-34, Baltimore, Maryland 21201; e-mail: gfisk001@umaryland.edu.

Abbreviations used: 1,2-DGs, 1,2-Diacylglycerols; 1,3-DGs, 1,3-Diacylglycerols; 2-MGs, 2-Monoacylglycerols; 1-MGs, 1-Monoacylglycerols; ALM, Alamethicin; BKA, Bongkrekic acid; Cys A, Cyclosporin A; PTP, Permeability Transition Pore; OAG, 1-oleoyl-acetyl-sn-glycerol; DOL, 1,2-Dioleoylglycerol (18:1); DDC, 1,2-Didecanoylglycerol (10:0); SAG, 1-stearoyl-2-arachidonoyl-sn-glycerol; DOG, 1,2-Dioctanoyl-sn-glycerol (8:0); HDAG, 1-O-Hexadecyl-2-arachidonoyl-sn-glycerol.

1995). An additional pathway contributing to this latency is substantiated by the slow degradation of DAG by DAG lipase; this DAG is produced from PC hydrolysis by phosphatidylcholine-specific phospholipase C and is a poor substrate for the fast-acting enzyme DAG kinase (Ford and Gross, 1990; Lee *et al*., 1991). DAG kinase rapidly catabolizes DAG produced from phosphatidylinositol hydrolysis converting it to phosphatidate at the expense of ATP (Florin-Christensen *et al*., 1992).

Downstream effects of DAGs are commonly attributed to activation of PKCs. There are, however, additional important targets of DAGs including protein kinase D (PKD), DAG kinases α, β, and γ, RasGRPs, chimaerins, Munc13s, and channels of the transient receptor potential (TRP) family, namely TRPC3, 6, and 7 (Brose *et al*., 2004; Brose and Rosenmund, 2002; Hofmann *et al*., 1999; Kazanietz, 2002; Okada *et al*., 1999; Yang and Kazanietz, 2003).

Upon PIP_2 hydrolysis, DAGs are formed in a membrane-delimited manner both on the plasma membrane and on intracellular membranes (Irvine, 2002; Panagia *et al*., 1991; Rebecchi and Pentyala, 2000), serving as hydrophobic anchors to recruit their targets to the membrane (Brose *et al*., 2004). The other product, IP_3, diffuses in the cytosol to activate IP_3 receptors on the ER releasing Ca^{2+} to the cytoplasm followed by triggering of Ca^{2+} influx from the extracellular space (Mikoshiba and Hattori, 2000). Within the context of intracellular Ca^{2+} homeostasis, mechanisms and effectors downstream of the IP_3 signaling pathway received the vast majority of attention, culminating in a spark of interest on the so-called "store-operated Ca^{2+} entry" (SOCE) (Nilius, 2004; Penner and Fleig, 2004; Venkatachalam *et al*., 2002). SOCE is a process whereby the depletion of intracellular Ca^{2+} stores (likely ER or SR) activates plasma membrane Ca^{2+} permeable channels (Putney, 1986). Members of the TRP family are candidates for SOCE; however, unequivocal evidence demonstrating that TRP channels account for this phenomenon is yet to be reported (Clapham, 2003; Nilius, 2004). Conversely, it has been shown that at least three members of the TRP family are activated by DAGs but not through PKC (Clapham *et al*., 2003). These channels (TRPC3, 6, and 7) do not possess the DAG-binding C1 domain (Gudermann *et al*., 2004), while TRPC3 plus two additional TRP channels, TRPC4 and TRPC5, are inhibited upon activation of PKC (Venkatachalam *et al*., 2003).

Enzymes and macromolecules participating in the formation of DAGs have been reported to reside or translocate to mitochondria. PIP_2 is found in mitochondria (Watt *et al*., 2002) and a brain-specific isomer may exist (Bothmer *et al*., 1992); PLCδ is found in mitochondria from liver (Knox *et al*., 2004), yeast (Vaena de *et al*., 2004), and kidney (Nishihira and Ishibashi, 1986). PLD and phosphatidate phosphatase exist in intestinal and myocardial mitochondria (Freeman and Mangiapane, 1989; Liscovitch *et al*., 1999). The same is true for DAG targets: mitochondrial translocation of PKCδ is a critical proapoptotic event in cardiac responses following ischemia and reperfusion (Murriel *et al*., 2004), as well as in phorbol ester-induced apoptosis in human myeloid leukemia cells (Majumder *et al*., 2000) and keratinocytes (Li *et al*., 1999). An alternative isoform PKCε, confers beneficial effects upon translocation to mitochondria by inhibiting the permeability transition (Baines *et al*., 2003), while others, such as PKCα, phosphorylate mitochondrial Bcl-2 suppressing apoptosis (Ruvolo *et al*., 1998) or promote cardioprotection at least partially due to modulation of mitochondrial K^+_{ATP} channels (Korge *et al*., 2002; Sato *et al*., 1998). With the exception of mitochondrial PKD (Storz *et al*., 2000), the presence of other non-PKC targets of DAG has not been reported.

Based on the involvement of DAGs on multiple mitochondrial functions, we tested the hypothesis that this second messenger affects mitochondrial Ca^{2+} handling. We show that DAGs release Ca^{2+} from Ca^{2+}-loaded mitochondria in conjunction with activation of novel channel(s) present on the inner mitochondrial membrane.

MATERIALS AND METHODS

Isolation of Mitochondria

All animal procedures were carried out according to the National Institutes of Health and the University of Maryland, Baltimore animal care and use committee guidelines. Adult male Sprague-Dawley rats and C57BL/6 mice were used. Nonsynaptic adult rat brain mitochondria were isolated on a Percoll gradient exactly as described previously (Chinopoulos *et al*., 2003). Mouse heart, kidney, and liver mitochondria were prepared as described previously (Starkov and Fiskum, 2001). Mitochondria from sweet potato (*Ipomoea batatas*) were isolated as detailed previously (Chen and Lehninger, 1973).

Mitochondrial Ca^{2+} Uptake in Mammalian Mitochondria

Rat Brain

Mitochondrial or mitoplast-dependent (0.275 mg/mL) removal of medium Ca^{2+} was followed using

the impermeant pentapotassium salt of the ratiometric dye Fura 6F (Molecular Probes, Portland, OR, USA) as previously described in a KCl-based medium containing malate plus glutamate as respiratory substrates (Chinopoulos *et al*., 2003). All experiments were performed at 37°C.

Rat Liver

The experiments were conducted as for rat brain mitochondria, with the exception that these mitochondria (0.5 mg/ml) were suspended in 250 mM sucrose, 20 mM Hepes, 2 mM KH_2PO_4, 1 mM $MgCl_2$, 5 mM succinate, 1 μM rotenone, 1 mg/ml bovine serum albumin (BSA, fatty acid-free), pH 7.2.

Mouse Heart and Kidney

These experiments were performed similar to the ones for rat brain, but at room temperature (~23°C), the fluorescent dye used was the hexapotassium salt of Calcium Green-5N (200 nM, $K_d = 4.3\ \mu$M) (Rajdev and Reynolds, 1993), and the mitochondria (0.25 mg/mL) were suspended in 225 mM mannitol, 75 mM sucrose, 2 mM KH_2PO_4 5 mM HEPES, 0.2 mg/mL BSA (fatty acid-free) 5 mM glutamate, 5 mM malate, pH 7.4.

Mitochondrial Ca^{2+} Uptake in Sweet Potato Mitochondria

1 mg/mL of mitochondria was used; the experimental conditions were similar to those for mammalian mitochondria but performed at room temperature (~23°C) in 300 mM mannitol, 10 mM Hepes, 2 mM KH_2PO_4, 10 mM succinate, 0.5 mM ADP, 2 mM ATP, plus 1 mg/mL BSA (fatty acid-free), pH 7.4.

Preparation of Mitoplasts From Rat Brain Mitochondria for Ca^{2+} Uptake Studies

Mitoplasts were prepared as described previously (Schnaitman *et al*., 1967), with minor modifications: Upon isolation of mitochondria, protein determination was performed (Biuret); afterwards, 450–500 μL of 20 mg/mL mitochondria were suspended in 2.5 mL of buffer "A" containing 10 mM TRIS and 2 mM $MgCl_2$, pH = 7.8 for 20 min in ice while shaking. Subsequently, 3 mL of 1.8 M Sucrose plus 2 mM $MgCl_2$ was added and left in ice while shaking for an additional 20 min. Next, 12 mL of buffer A plus 45 μg of digitonin (>99% pure) was added to the suspension and left in ice while shaking for 15 min. At the end of this step, the suspension was diluted 5-fold with buffer "B" containing: 225 mM mannitol, 75 mM sucrose, 5 mM Hepes, 1 mM EGTA, 0.5 mg/mL BSA (fatty acid-free), pH = 7.4, and were centrifuged at 12, 000 × g for 10 min. This centrifugation step was repeated once, and the resulting pellet was suspended in buffer B without EGTA. To evaluate the efficiency of the removal of the outer mitochondrial membranes, mitoplasts were tested for the presence of adenylate kinase, as described previously (Schmidt *et al*., 1984); >95% of adenylate kinase activity was lost with this method. These mitoplasts retained a respiratory control ratio of 5 ± 1 over a period of 45 min (in the presence of externally added cyt *c*).

Preparation of Mitoplasts From Rat Brain Mitochondria for Patch Clamp Studies

Upon isolation of mitochondria, the organelles were suspended in a hypertonic buffer consisting of 460 mM Mannitol, 140 mM Sucrose, 10 mM HEPES, pH 7.4 for 10 min. Subsequently, they were subjected to 1500 psi with a French press (American Instruments Company, Silver Springs, MD, USA). The suspension was diluted with 2 volumes of 230 mM Mannitol, 70 mM Sucrose, 5 mM HEPES, pH 7.4. Mitoplasts were pelleted at 12, 000 × g for 10 min and resuspended in 100 μL of the same buffer.

Oxygen Consumption

Mitochondrial respiration was recorded at 37°C with a Clark-type oxygen electrode (Hansatech, UK) as described previously (Chinopoulos *et al*., 2003).

Mitochondrial Swelling

Swelling of isolated liver mitochondria was assessed by measuring light scatter at 540 nm (37°C) in a Beckman Coulter DU 7500 spectrophotometer (Fullerton, CA, USA) as detailed previously (Bernardi *et al*., 1992).

Patch Clamp of Rat Brain Mitoplasts

Membrane patches were excised from rat brain mitoplasts after formation of a giga-seal (2–5 GΩ) using

glass electrodes made of borosilicate and resistances of 10–30 MΩ. The solution in the electrodes and bath was 150 mM KCl, 5 mM HEPES, pH 7.4. This buffer contained 10 μM free Ca^{2+}. Experiments were carried out at room temperature (~23°C). Voltage clamp was established with the inside-out excised configuration and currents were amplified using an Axopatch 200 amplifier (Union city, CA, USA). Current traces were sampled at 5 kHz with 2 kHz filtration and analyzed with WinEDR version v2.4.3 program (Strathclyde Electrophysiological Software courtesy of J. Dempster, Univ. of Strathelyde, UK). Ion selectivity was measured by a 1:5 gradient by perfusion of the bath with 30 mM KCl, 184 mM mannitol, 56 mM sucrose, 5 mM HEPES, pH 7.4.

Reagents

Standard laboratory chemicals were from Sigma. 2-APB (Sigma), CGP 37157 (Calbiochem), cyclosporin A (Sigma), bongkrekic acid (Calbiochem), alamethicin (Sigma), BSA (Sigma), Digitonin (Spectrum, New Brunswick, NJ, USA), PMA (Sigma), RHC 80267 (Calbiochem), DAG kinase inhibitor II (Sigma), all PKC inhibitors (Calbiochem, PKC inhibitor set), all 1,2-DGs and MGs were from Sigma or Biomol, all 1,3-DGs were from ICN Biomedicals (Aurora, OH, USA).

RESULTS

Release of Sequestered Ca^{2+} in Mammalian but Not Sweet Potato Mitochondria by OAG

Ca^{2+}-loaded mitochondria from rat brain (Fig. 1(A)), mouse kidney (Fig. 1(B)), mouse heart (Fig. 1(C)), and rat liver (Fig. 1(E)) release Ca^{2+} upon exposure to the putative, cell-permeable diacylglycerol analogue, OAG. After the initial rapid release, Ca^{2+} was re-accumulated, followed by a secondary slow net release. In contrast to OAG, phorbol 12-myristate 13-acetate (PMA) failed to induce Ca^{2+} efflux (Fig. 1(A), trace *b*). Sweet potato mitochondria loaded with Ca^{2+} did not exhibit OAG-induced Ca^{2+} release (Fig. 1(D), trace *b*). Liver mitochondria pretreated with Cys A (Fig. 1(E), trace *b*) display an almost identical OAG-induced Ca^{2+} release and a moderate extent in the lag time until the spontaneous secondary efflux. Using identical conditions, swelling was not observed upon addition of OAG to Ca^{2+}-loaded liver mitochondria (Fig. 1(G)); however, they exhibit spontaneous large amplitude swelling coincident with the secondary Ca^{2+} efflux in the absence (trace *a*) or presence (trace *b*) of Cys A. Cys A moderately extends the threshold of PTP induction. In the

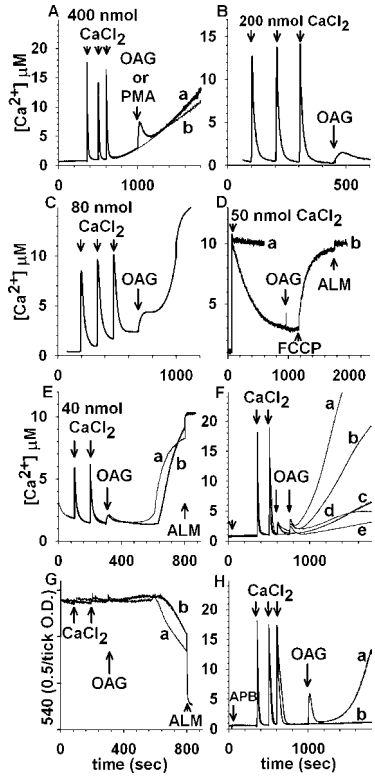

Fig. 1. OAG induces mitochondrial Ca^{2+} efflux and its relation to the permeability transition. Release of sequestered Ca^{2+} from rat brain (A, trace *a*), mouse kidney (B), mouse heart (C), and rat liver (E), but not sweet potato (D) mitochondria by the diacylglycerol analogue, OAG (100 μM). The phorbol ester PMA (1 μM) fails to induce Ca^{2+} release (A, trace *b*). In (D) trace *a*, Ru360 (165 nM) was present before addition of $CaCl_2$; in trace *b*, 1 μM FCCP was added at 1200 s. (E): Rat liver mitochondria are loaded with two pulses of $CaCl_2$ (100 and 200 s, 40 nmol each) in the absence (trace *a*) or presence of Cys A (1 μM, trace *b*), followed by addition of 100 μM OAG at 300 s. At approximately 600 s, mitochondria spontaneously release Ca^{2+}. Alamethicin (40 μg/ml) was added at 800 s. (F): PTP inhibitors do not affect the initial OAG-induced Ca^{2+} efflux, but modulate the secondary rise: Rat brain mitochondria were loaded with two pulses of $CaCl_2$ (350 and 500 s, 400 nmol each) followed by addition of OAG (50 μM) in the presence and absence of Cys A (2 μM) or BKA (20 μM) or 2-APB (100 μM) (each added at 50 s, small arrow). In trace *a*, mitochondria were not pretreated with either PTP inhibitor; trace *b*, Cys A is present; trace *c*, mitochondria were not challenged by OAG (replaced with vehicle); trace *d*, mitochondria were pretreated with 2-APB; trace *e*, mitochondria were pretreated with BKA. (G): OAG does not evoke an immediate large-amplitude swelling in Ca^{2+}-loaded rat liver mitochondria: Mitochondria were loaded with Ca^{2+} exactly as in (A) in the absence (trace *a*) or presence of Cys A (1 μM, trace *b*), followed by addition of 100 μM OAG at 300 s, and light scatter was followed spectrophotometrically. At approximately 600 s, mitochondria spontaneously swell. Alamethicin (40 μg/mL) was added at 800 s. (H): 2-APB does not inhibit the initial OAG-induced Ca^{2+} release. Rat brain mitochondria were loaded with three pulses of $CaCl_2$ (350, 500, and 600 s, 400 nmol each) followed by addition of OAG at 1000 s in the presence of 2-APB (100 μM, added at 50 s). Trace *a*, OAG (100 μM) was added at 1000 s; in trace *b*, no OAG was added (replaced by vehicle). Traces for this and all subsequent figures are representative of at least four independent experiments unless otherwise indicated.

absence of OAG, Cys A elevated the threshold for PTP induction by $CaCl_2$ in rat liver mitochondria from 160 nmol/mg protein to 1280 nmol/mg protein. PTP inhibitors didn't affect the first or the second pulse of OAG-induced Ca^{2+} efflux (Fig. 1(F)); however, Cys A partially inhibited the secondary Ca^{2+} rise, while BKA and 2-APB conferred substantial protection (Fig. 1(F) and (H)).

OAG-Induced Ca^{2+} Release Is Not Mediated by the Uniporter or the Mitochondrial Na^+/Ca^{2+} Exchanger

Inhibition of the uniporter by Ru360 fails to inhibit OAG-induced mitochondrial Ca^{2+} release and actually potentiates it (Fig. 2(A), trace *d*). Inhibition of the Na^+/Ca^{2+} exchanger by CGP-37157 had no effect on modulating the OAG-induced Ca^{2+} release mechanism (Fig. 2(A), trace *e*). Addition of FCCP (Fig. 2(A), trace *c*), or antimycin A_3 plus oligomycin (trace *b*) in Ca^{2+}-loaded mitochondria pretreated with Ru360 caused only a minor increase in the rate of Ca^{2+} efflux. La^{3+} abolishes OAG-induced Ca^{2+} release completely, but only moderately affects the reversal of the uniporter (Fig. 2(B)). Fura 6F reacts to La^{3+} similar to Ca^{2+}, however the K_d of the dye for the trivalent is different (not quantified). Its presence also alters the K_d for Ca^{2+}; therefore only qualitative measures of Ca^{2+} flux are possible after the addition of $LaCl_3$. La^{3+} is sequestered very slowly by mitochondria, competing with Ca^{2+} (Reed and Bygrave, 1974) and blocking the uniporter (Gunter and Pfeiffer, 1990). In trace *a*, addition of antimycin A_3 plus oligomycin induced slow Ca^{2+} efflux followed by faster release upon subsequent addition of FCCP. In trace *b* where no mitochondrial inhibitors were added, OAG-induced Ca^{2+} release was inhibited by $LaCl_3$. To address the directionality of the OAG-induced Ca^{2+} flux, mitochondria were not preloaded with $CaCl_2$, and Ru360 was added to eliminate Ca^{2+} uptake through the uniporter (Fig. 2(C), trace *a*). After subsequent addition of $CaCl_2$, there was no mitochondrial Ca^{2+} uptake and subsequent addition of OAG (trace *a*) had no effect on Fura 6F fluorescence. In contrast, Ca^{2+}-loaded mitochondria subsequently exposed to Ru360 still exhibited OAG-induced Ca^{2+} efflux (trace *b*).

Effect of OAG on Mitochondrial Sr^{2+} Handling

Rat brain mitochondria were loaded with $SrCl_2$ (Fig. 3(A)) and flux of Sr^{2+} was monitored with Fura 6F. This dye responds to Sr^{2+} similarly to Ca^{2+}; however, the K_d for Sr^{2+} is different (not quantified). In the absence of added OAG (trace *a*) mitochondria retain their Sr^{2+} load for the duration of the experiment. Addition of OAG (trace *b*) leads to an abrupt elevation of Fura 6F fluorescence, indicating release of sequestered Sr^{2+}. The increase in Fura 6F fluorescence is not due to efflux of endogenous mitochondrial Ca^{2+} as addition of OAG (or FCCP, not shown) to freshly isolated mitochondria that have not been loaded with Ca^{2+} does not lead to an increase in Fura 6F fluorescence (Fig. 4(D)). Similar to the effect of La^{3+} on Ca^{2+} efflux, La^{3+} completely blocked OAG-induced Sr^{2+} release (Fig. 3(B)).

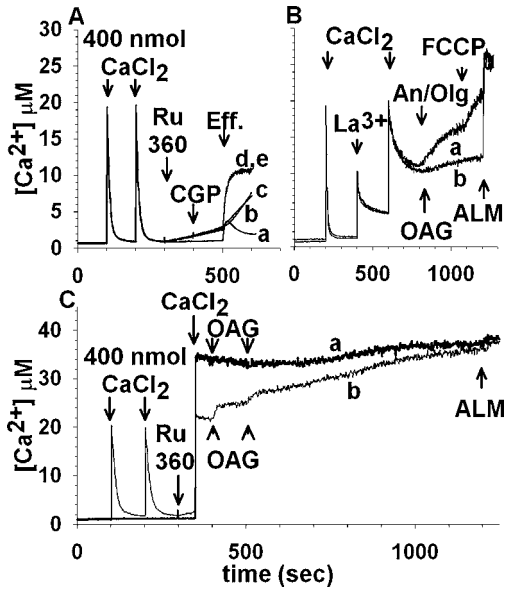

Fig. 2. OAG-induced Ca^{2+} efflux from rat brain mitochondria is not mediated by known Ca^{2+} uptake and release pathways. (A): Mitochondria are loaded by exogenously added Ca^{2+} (each pulse is 400 nmol $CaCl_2$) and the following compounds are administered: trace *a*, OAG (100 μM) at 500 s; trace *b*, 165 nM Ru360 at 300 s, 1 μM antimycin A_3 plus 2 μM oligomycin at 500 s; trace *c*, 165 nM Ru360 at 300 s, 0.5 μM FCCP at 500 s; trace *d*, 165 nM Ru360 at 300 s, 100 μM OAG at 500 s; trace *e*, 165 nM Ru360 at 300 s, 20 μM CGP-37157 at 400 s, 100 μM OAG at 500 s; traces *d* and *e* are superimposed. "Eff.": effectors. (B): 1 mM $LaCl_3$ abolishes OAG-induced Ca^{2+} efflux, without affecting the reverse function of the uniporter: mitochondria are treated with 400 nmol $CaCl_2$ at 350 and 600 s and 1 mM $LaCl_3$ in between (500 s). Subsequently 1 μM antimycin A_3 plus 2 μM oligomycin are administered at 800 s (trace *a*) or 100 μM OAG at 800 s (trace *b*). In trace *a* 0.5 μM FCCP was also added at 1100 s. In both traces, alamethicin (40 μg/ml) is added at 1200 s. (C): In trace *a*, rat brain mitochondria are not preloaded with Ca^{2+}, and Ru360 (165 nM) is added at 300 s; subsequently, 800 nmol of $CaCl_2$ is added at 350 s, followed by two pulses of OAG (100 μM each) at 400 and 500 s. In trace *b*, mitochondria are preloaded with two pulses of exogenously added $CaCl_2$ (100 and 200 s, 400 nmol each); 165 nM Ru360 is added at 300 s, followed by an additional pulse of 400 nmol $CaCl_2$ at 350 s. Subsequently OAG (two pulses of 100 μM each) are added at 400 and 500 s. In both traces, alamethicin (40 μg/mL) is added at 1200 s.

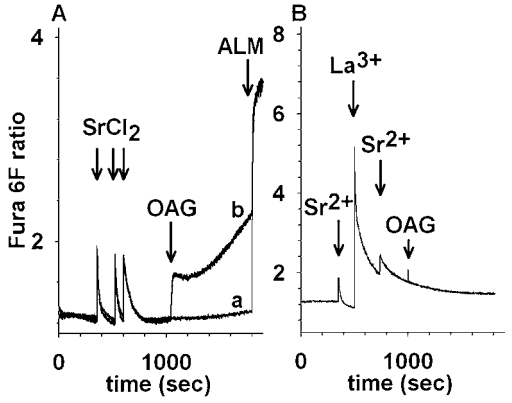

Fig. 3. OAG-induced Sr^{2+} efflux from rat brain mitochondria and inhibition by La^{3+}. (A): Mitochondria are loaded with three pulses of $SrCl_2$ (400 nmol each, trace *a*). In trace *b*, subsequent to Sr^{2+} loading, OAG is added (100 μM) at 1000 s causing an immediate increase in Fura 6F ratio fluorescence. In both traces, alamethicin (40 μg/ml) is added at 1800 s. (B): Mitochondria are treated with 400 nmol $SrCl_2$ at 350 and 750 s and 1 mM $LaCl_3$ in between (500 s). OAG is added (100 μM) at 1000 s causing no further increase in Fura 6F ratio fluorescence.

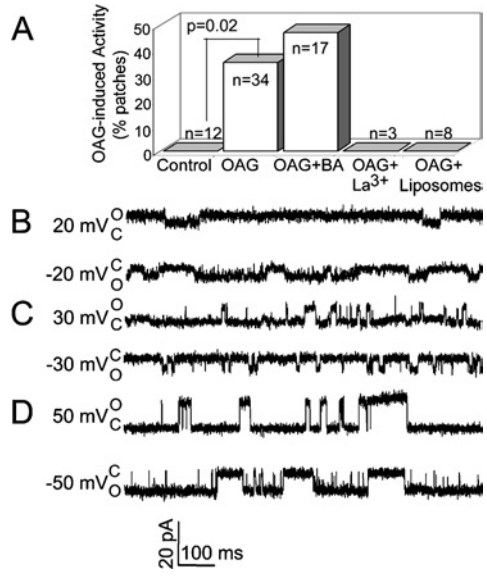

Fig. 4. OAG-induced mitoplast channel activity. (A): The frequency of detecting OAG-induced channel activity in rat brain mitoplasts is shown in the absence (Control) and presence (OAG) of 100 μM OAG, and presence of 100 μM OAG plus 20 μM BKA (OAG + BA). The frequency is statistically different in the absence and presence of OAG ($p = 0.02$) and is not statistically different in the presence and absence of BKA ($p = 0.4$, Fisher's test). The frequency of detecting OAG-induced activity in patches from giant liposomes is also shown (OAG + liposomes). "*n*" indicates the number of independent patches. (B–D). Current traces from three different excised patches from mitoplasts show 202 ± 33 pS (SD) transitions in the presence of 100 μM OAG at indicated voltages. O and C indicate open and closed current levels.

OAG Induces Cationic Channel Activity in Rat Brain Mitoplasts

In the absence of OAG, no channel activity was recorded from mitoplasts in 9 patches and conductances characteristic of PTP were observed in 3 other patches. Seventeen out of 34 patches showed no channel activity of any kind in the presence of OAG. Multiple conductance levels were observed in patches that were slightly cation-selective in the presence of OAG in 12 of 34 patches. These patches were scored positive for the presence of OAG-induced activity in the bar graph (Fig. 4(A), $p < 0.05$). While other transition sizes were observed, current traces recorded in the presence of OAG typically exhibited transitions of 202 ± 33 pS; ($n = 8$ patches, Fig. 4(B)–(D)). PTP and Tim23 channels with conductances of ~1200 and 750 pS, respectively, were recorded from 5 patches, which may have obscured the smaller OAG-induced activity (not shown). While the frequency of observing the OAG-induced activity increased slightly to 8 of 17 patches in the presence of the PTP inhibitor BKA, this increase was not statistically significant ($p = 0.4$). Unlike BKA, perfusing the excised patches that exhibited OAG-induced activity with 1 mM $LaCl_3$ led to a blockade of this channel activity ($n = 3$ patches). We did not observe any current upon exposure of OAG to patches excised from liposomes (Type IV, phosphatidylcholine, prepared as in (Guo *et al.*, 2004), Fig. 4(A)).

DAGs Release Mitochondrial Ca^{2+} Through a Mechanism Independent of DAG Metabolism or Activation of PKC

1,2-diacylglycerols other than OAG, release Ca^{2+} from Ca^{2+}-loaded mitochondria, (Fig. 5(A), traces *b*–*f*), while 1,3-diacylglycerols are inactive (Fig. 6(A)). Inhibition of PKC using five different PKC inhibitors (Fig. 5(B)) *potentiated* the OAG-induced initial Ca^{2+} efflux. No inhibitor exhibited statistically significant respiratory inhibition and/or uncoupling, except Myristoylated Protein Kinase C Inhibitor 20–28 (15% increase in state 4 respiration, not shown). The DAG lipase inhibitor RHC 80267 (Fig. 5(C), trace *b*) or the DAG kinase inhibitor II (Fig. 5(C), trace *c*) didn't influence significantly the initial OAG-induced Ca^{2+} efflux; RHC 80267 only slightly potentiated the initial OAG-induced Ca^{2+} efflux while the DAG kinase inhibitor II potentiated the delayed Ca^{2+} rise. Neither inhibitor exhibited respiratory inhibition or uncoupling (not shown). Addition of OAG to mitochondria prior to loading with $CaCl_2$ did not inhibit subsequent Ca^{2+} uptake; however, the time elapsed

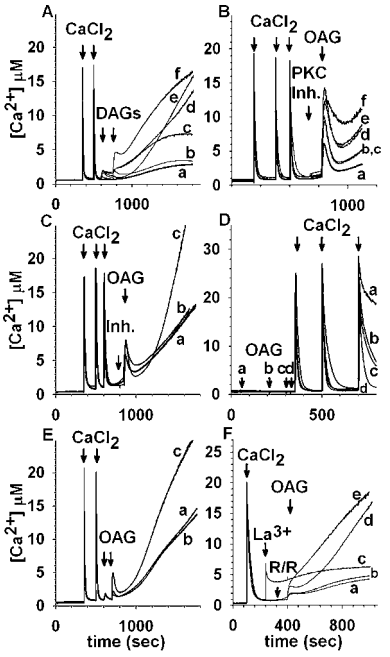

Fig. 5. Diacylglycerol-induced release of sequestered Ca^{2+} in rat brain mitochondria (A–E) and mitoplasts (F): Relationship to putative targets and catabolites. (A): Mitochondria are loaded with two pulses of $CaCl_2$ (400 nmol each at 350 and 500 s) followed by addition of the following DAG at 600 and 750 s (50 μM each pulse): trace *a*, vehicle (2 μl 96% ethanol [or DMSO, not shown]); trace *b*, DOL; trace *c*, DDC; trace *d,* SAG; trace *e,* DOG; trace *f*, HDAG. (B): PKC inhibitors potentiate the OAG-induced mitochondrial Ca^{2+} release: Mitochondria are loaded with three pulses of 400 nmol $CaCl_2$ (350, 500 and 600 s) and prior to addition of 100 μM OAG (850 s) the following PKC inhibitor is added at 800 s: trace *a*, vehicle (2 μl 96% ethanol); trace *b*, Ro-32-0432 (200 nM); trace *c*, Gö 6976 (100 nM); trace *d*, myristoylated PKC Inhibitor 20–28 (10 microM); trace *e*, chelerythrine chloride (1 microM) trace *f*, Bisindolylmaleimide I (30 nM). (C): Inhibition of OAG catabolism does not mitigate OAG-induced Ca^{2+} release: Mitochondria are loaded with three pulses of 400 nmol $CaCl_2$ (350, 500, and 600 s) and prior to addition of 100 μM OAG (850 s), inhibitors of DAG lipase and DAG lipase are added at 800 s. In trace *a*, no inhibitor is present, in trace *b* the DAG lipase inhibitor RHC 80267 (10 μM) is present; in trace *c*, the DAG kinase inhibitor "DAG kinase inhibitor II" (1 μM) was added at 800 s. (D): Addition of OAG to mitochondria that have not been loaded with Ca^{2+} does not abolish subsequent Ca^{2+} uptake. OAG (100 μM) was added at different time points at 50 s (trace *a*), 200 s (trace *b*), 300 s (trace *c*), 325 s (trace *d*), prior to challenging mitochondria with three pulses of $CaCl_2$ (at 350, 500, and 700 s, 400 nmol each). (E): Effect of phospholipids on the OAG-induced Ca^{2+} release: Mitochondria are loaded with two pulses of $CaCl_2$ (400 nmol each at 350 and 500 s) followed by addition of 25 μM OAG at 600 and 700 s in the presence of PS (10 μg/mg mitochondrial protein, trace *b*) or PE (10 μg/mg mitochondrial protein, trace *c*). In trace *a*, ethanol was added instead of a phospholipid. (F): OAG releases sequestered Ca^{2+} from rat brain mitoplasts: In all traces, mitoplasts are loaded with a single pulse of 400 nmol $CaCl_2$ (100 s), and OAG (100 μM unless otherwise indicated) is added at 400 s. In trace *a*, no further additions were made. In trace *b*, RHC 80267 (10 μM) was added at 320 s; in trace *c*, 1 mM $LaCl_3$ was added at 240 s; in trace *d*, 200 μM OAG was added at 400 s; in trace *e*, 165 nM Ru360 was added at 320 s, followed by 200 μM OAG at 400 s. "R/R" signifies RHC 80267 or Ru360.

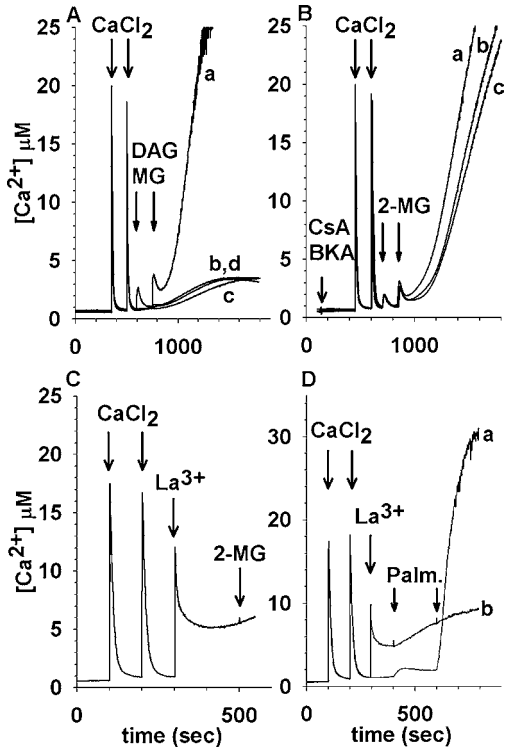

Fig. 6. Di- and Monoacylglycerol induced mitochondrial Ca^{2+} release: Effects of permeability transition inhibition and La^{3+}. (A): Mitochondria are loaded with two pulses of $CaCl_2$ (400 nmol each at 350 and 500 s) followed by addition of the following DAG or MG at 600 and 750 s (100 μM each pulse): trace *a*, 2-Monooleoylglycerol (C18:1, [*cis*]-9); trace *b*, 1,3-Di-([*cis*]-9-octadecenoyl)-rac-glycerol; trace *c*, vehicle; trace *d*, 1-Monooleoyl-rac-glycerol (C18:1, [*cis*]-9). (B): Mitochondria are pretreated with a PTP inhibitor (at 50 s) and challenged with two pulses of $CaCl_2$ (400 nmol each at 350 and 500 s) followed by addition of 2-Monooleoylglycerol at 600 and 750 s (50 μM each pulse); trace *a*, no PTP inhibitor; trace *b*, 2 μM Cys A; trace *c*, 20 μM BKA. (C): $LaCl_3$ inhibits the 2-MG induced Ca^{2+} efflux: Mitochondria are loaded with two pulses of $CaCl_2$ (400 nmol each at 100 and 200 s) followed by addition of 1 mM $LaCl_3$ at 300 s; subsequently, 100 μM 2-Monooleoylglycerol is added at 500 s. (D): $LaCl_3$ inhibits the palmitic acid- induced Ca^{2+} efflux: In trace *a*, mitochondria are loaded with two pulses of $CaCl_2$ (400 nmol each at 100 and 200 s); subsequently, 10 μM palmitic acid is added at 400 and 600 s; in trace *b*, mitochondria are loaded with two pulses of $CaCl_2$ (400 nmol each at 100 and 200 s) followed by addition of 1 mM $LaCl_3$ at 300 s; subsequently, 10 μM palmitic acid is added at 400 and 600 s.

before the addition of OAG to the point of Ca^{2+} challenge influenced the maximal Ca^{2+} uptake capacity of mitochondria (Fig. 5(D), traces *a–d*). Various PLC inhibitors (U-73122, Edelfosine, D609, neomycin) were tested for their effects on maximal Ca^{2+} uptake capacity with the exception of neomycin with these drugs inhibited uptake due to the finding that they are potent respiratory uncouplers (not shown). Inclusion of phospholipids

(phosphatidylethanolamine [PE] vs. phosphatidylserine [PS]) in the medium enhanced the potency of the second pulse of OAG-induced Ca^{2+} efflux from Ca^{2+}-loaded mitochondria (Fig. 5(E)). Addition of OAG to mitoplasts caused release of sequestered Ca^{2+} (Fig. 5(F), trace *a)*. The presence of RHC 80267 did not alter the initial OAG-induced Ca^{2+} efflux. The effect of OAG was further potentiated in the presence of Ru360 (Fig. 5(F), trace *e*). Pretreatment of Ca^{2+}-loaded mitoplasts with 1 mM $LaCl_3$ prior to addition of OAG blocked the effect of the diacylglycerol on releasing stored Ca^{2+} (Fig. 5(F), trace *c*).

Additional Characteristics of DAG-Induced Release of Mitochondrial Ca^{2+}

We compared the effect of OAG to 1,3-diolein (1,3-Di-([*cis*]-9-octadecenoyl)-rac-glycerol, (Fig. 6(A), trace *b*), 2-MG (2-Monooleoylglycerol (C18:1, [*cis*]-9) (trace *a*) and 1-MG (1-Monooleoyl-rac-glycerol (C18:1, [cis]-9), (trace *d*). Only 2-MG induced an initial Ca^{2+} efflux from Ca^{2+}-loaded rat brain mitochondria, followed by a robust delayed Ca^{2+} rise (Fig. 6(A), trace *a*). Neither the initial 2-MG-induced Ca^{2+} release nor the delayed Ca^{2+} efflux was sensitive to PTP inhibitors (Fig. 6(B), traces *b and c*). The 2-MG-induced Ca^{2+} release was, however, completely abolished by 1 mM $LaCl_3$ (Fig. 6(C)). 1 mM $LaCl_3$ also inhibited release of sequestered Ca^{2+} from rat brain mitochondria induced by palmitic acid (Fig. 6(D)). Moreover, $LaCl_3$ mitigated the uncoupling effect of this fatty acid (not shown). 2-MG exhibited both significant uncoupling and inhibition of state 3 respiration (Table I). Among the DAGs, DOG exhibited significant uncoupling. The other tested DAGs, including OAG, exhibited little or no inhibition of state 3 respiration.

DISCUSSION

The novel observations of the current study point to a potential mode of Ca^{2+} release in mitochondria that can be synchronized with physiological events inducing elevation of cytosolic [Ca^{2+}] either throughout the cell or in microdomains. Our primary finding is that OAG releases Ca^{2+} sequestered by mitochondria isolated from rodent tissues but not from sweet potato. Plants do possess multiple pathways that ultimately result in DAGs production (Wang, 2004). The importance of the lack of effect of OAG on sweet potato mitochondria is twofold: (i) it demonstrates biological diversity and (ii) it weakens the possibility of an artifact of OAG on lipid membranes, implicated previously (Allan *et al*., 1978; Leikin *et al*., 1996; Szule *et al*., 2002).

Additional lines of evidence argue against a Ca^{2+}-ionophoretic activity of the diacylglycerol or an unspecific effect on bilayers leading to ion permeability: (i) following Ca^{2+} release upon exposure to OAG in mammalian mitochondria, extramitochondrial [Ca^{2+}] returns to baseline values; an ionophore would lead to the establishment of a new steady-state [Ca^{2+}]; (ii) OAG does not cause any swelling during the initial Ca^{2+} release, excluding the possibility of an unspecific hole-forming effect or activation of the PTP; (iii) several effective 1,2-DAGs do not exhibit any uncoupling properties that would be obvious if they nonselectively permeabilize the mitochondrial inner membrane; (iv) application of OAG to the patches

Table I. Effects of Di- and Monoacylglycerols and Farnesyl Thiotriazole (FTT) on Rat Brain Mitochondrial Oxygen Consumption

	State 3	State 4 (effector added before oligomycin)	State 4 (effector added after oligomycin)
Vehicle, ($n = 12$)	131 ± 3	16 ± 1	16 ± 1
OAG ($n = 6$)	$102 \pm 4^{*}$	16 ± 1^{ns}	16 ± 1^{ns}
2-MG ($n = 5$)	$110 \pm 9^{*}$	$29 \pm 2^{*}$	15 ± 1^{ns}
DDC ($n = 3$)	$125 \pm 6^{n.s.}$	15 ± 1^{ns}	14 ± 1^{ns}
DOL ($n = 3$)	$113 \pm 6^{*}$	15 ± 1^{ns}	14 ± 1^{ns}
DOG ($n = 3$)	$130 \pm 9^{n.s.}$	$21 \pm 2^{*}$	17 ± 1^{ns}
FTT ($n = 3$)	$48 \pm 4^{*}$	$34 \pm 2^{*}$	$29 \pm 2^{*}$
HDAG ($n = 3$)	$96 \pm 5^{*}$	14 ± 1^{ns}	15 ± 1^{ns}
SAG ($n = 3$)	$126 \pm 7^{n.s.}$	15 ± 1^{ns}	14 ± 1^{ns}

Note. All di- and monoacylglycerols and FTT were tested at 100 μM concentration. *n*: number of independent experiments. Statistics: Mann-Whitney rank sum test; *: significant compared to control (vehicle), $p < 0.001$, ns: not significant compared to control. Values are given as nmol/min/mg protein and expressed as standard errors of the mean, rounded to the nearest integer.

does not always result in channel activity, arguing against a nonspecific membrane stressing effect; (v) no currents are observed with patched liposomes upon exposure to the diacylglycerol.

To test the hypothesis that OAG induces Ca^{2+} efflux through previously described mitochondrial flux pathways, we blocked independently the uniporter, the Na^+/Ca^{2+} exchanger, and the PTP. Blocking the uniporter with Ru360 preventing bidirectional Ca^{2+} transport by this pathway (Matlib *et al*., 1998) does not inhibit and, as expected, actually potentiates the OAG-induced Ca^{2+} release from mitochondria or mitoplasts; the amplitude of the release is greater in the presence of Ru360 due to the inability of the uniporter to reaccumulate Ca^{2+}, hence also the lack of post-OAG extramitochondrial $[Ca^{2+}]$ decay. This observation also argues against an uncoupling mode of action of OAG since uncoupler-induced calcium efflux occurs via reversal of the mitochondrial uniporter (Bernardi *et al*., 1984). In addition, the uniporter is relatively impermeable to K^+ while our electrophysiological recordings were made using symmetrical KCl solutions. Moreover, single uniporter channels have multiple subconductance states between 2.6 pS and 5.2 pS at -160 mV, but the OAG-induced conductances are $\sim$200 pS. Therefore, it is clear that the OAG-induced channel is not the uniporter characterized recently (Kirichok *et al*., 2004). La^{3+} inhibits completely the OAG response, while in our hands, La^{3+} (1 mM) does not eliminate the release of Ca^{2+} from mitochondria induced by respiratory inhibition or uncoupling. Blockade of the Na^+/Ca^{2+} exchanger with CGP-37157 does not antagonize the OAG effect; moreover, the fast kinetics of the initial OAG-induced Ca^{2+} efflux argue against the involvement of a slow exchanger. In addition, the absence of Na^+ in the medium eliminates the Na^+/Ca^{2+} exchanger as the mechanism.

We furthermore conclude that the initial rapid Ca^{2+} efflux induced by OAG is not due to PTP opening because: (i) it is insensitive to any PTP inhibitor tested; (ii) OAG-induced channel activity exhibits conductances $\sim$6 times lower than those characteristics of PTP (Loupatatzis *et al*., 2002); (iii) OAG induces Sr^{2+} release from Sr^{2+}-loaded mitochondria, whereas Sr^{2+} does not promote PTP formation (Hunter *et al*., 1976); (iv) OAG does not induce any large-amplitude swelling during the initial Ca^{2+} release and, in accordance with our observations, DAGs were shown earlier not to induce swelling of liver mitochondria (Pastorino *et al*., 1999). In contrast, the delayed Ca^{2+} rise exhibits robust evidence of PTP, including sensitivity to PTP inhibitors and large-amplitude mitochondrial swelling. At least one component leading to the delayed formation of PTP is the intense Ca^{2+} cycling substantiated by the OAG-induced Ca^{2+} channel(s) and the uniporter; however, in rat liver mitochondria, the presence of Cys A did not extend significantly the threshold for PTP induction in the presence of OAG, in spite of the immensely protecting effect of the immunophilin against high-Ca^{2+} mitochondrial loading in the absence of the diacylglycerol. Since DAGs activate PLA_2 which is also found in mitochondria (Nachbaur and Vignais, 1968), the OAG induced secondary phase of Ca^{2+} release could be due to activation of this enzyme, which is known to contribute to induction and/or maintenance of PTP (Broekemeier and Pfeiffer, 1989; Rustenbeck *et al*., 1996); however, neither aristolochic acid, nor bromoenol lactone (both inhibitors of PLA_2) inhibited mitochondrial Ca^{2+}-induced Ca^{2+} release (mCICR) under the exact conditions in the absence of OAG (Chinopoulos *et al*., 2003).

Phorbol esters can substitute for diacylglycerol in activating both protein kinase C (Nishizuka, 1995) and non-PKCs (Brose *et al*., 2004). Substitution of OAG for PMA fails to induce Ca^{2+} efflux. Moreover, inclusion of five different PKC inhibitors does not ameliorate the OAG effect and even potentiates it. Such a scenario has been reported for DAG-sensitive TRP channels on the plasma membrane (Venkatachalam *et al*., 2003). However, the possibility of TRP channels being present in mitochondria has been previously excluded (Chinopoulos *et al*., 2003). A caveat here is that contemporary pharmacological PKC antagonists targeting the C1 domain bind with similar affinities to non-PKCs possessing the same domain activated by DAG/phorbol esters (Yang and Kazanietz, 2003). The question arises, as to why would there be PKC in our isolated mitochondria preparations, since it translocates to the organelles as a reaction to cell stress; probably, the mitochondrial isolation procedure is damaging enough (decapitation of the animal, transient hypoxia of the tissue) to cause PKC translocation.

To characterize further the mode of action of DAGs on mitochondria, we tested di- and monoacylglycerols by varying the position of the acyl groups. Only 1,2-sn-DAGs induce release of Ca^{2+}, while 1,3-sn-DAGs are inactive. Among monoacylglycerols, 1-MG is not effective, as opposed to 2-MG that releases Ca^{2+} vigorously. As a comparison, PKC is not activated by 1,3-DAGs nor monoacylglycerols, but is activated by 1,2-DAGs (Nishizuka, 1995). 2-MG induces powerful uncoupling in addition to causing Ca^{2+} efflux that is insensitive to PTP inhibitors. At this juncture, it is not known if 2-MGs and 1,2-DAGs share the same target(s) on mitochondria or if 2-MG has an alternative mode of action. La^{3+} inhibits the 2-MG-induced Ca^{2+} release completely; however, La^{3+} also inhibits palmitic acid-induced PTP (Sultan and Sokolove, 2001) and Ca^{2+} flux through the uniporter. The universal ability of La^{3+} to block all forms of mitochondrial Ca^{2+}

release therefore limits its usefulness in delineating the individual mechanism involved in OAG-induced release.

In addition to regulation by diacylglycerol or phorbol esters, DAG targets require Ca^{2+} and PS (Bell and Burns, 1991). Inclusion of PS to the suspension does not have an effect on the OAG-induced Ca^{2+} efflux; however, PE potentiates the OAG response. At this juncture, we cannot attribute the PE potentiating effect on a biologically relevant mechanism or on the possibility that PE is a better vehicle for OAG in solution. Concerning the requirement of matrix Ca^{2+}, our experiments demonstrate that OAG causes release of Ca^{2+} from Ca^{2+}-loaded mitochondria but does not allow Ca^{2+} influx in mitochondria treated with Ru360. It is therefore possible that the target molecule(s) of OAG on the inner mitochondrial membrane possess binding site(s) for Ca^{2+} located at the inner leaflet of the membrane. This is a very similar scenario to the one involving PKC: Ca^{2+} increases the affinity of conventional PKCs for negatively charged lipids and this increase varies linearly with Ca^{2+} concentration in the low μM to submillimolar range (Mosior and Epand, 1994). OAG also releases sequestered strontium; however, due to the almost identical molecular radius of Sr^{2+} to Ca^{2+}, Sr^{2+} may substitute for Ca^{2+} for whatever means. The requirement for accumulated intramitochondrial Ca^{2+} for DAGs-induced Ca^{2+} release can be envisioned as a mechanism preventing mitochondria from buffering all the Ca^{2+} coming from other sources during PIP_2 hydrolysis. The necessity of an obligatory metabolite (DAG) sets the mechanism in synchrony.

It is clear that mitochondria host DAG targets (see Introduction), though the two major DAG clearance pathways, DAG kinase and DAG lipase, have not been unequivocally identified these organelles (Bothmer *et al*., 1992); nevertheless, 1,2-diacyl-sn-glycerol is a reactant or product in 23 reactions, spanning among four different biochemical pathways (for a complete description of the involvement of DAGs in biochemical pathways, see: http://www.genome.jp/dbget-bin/www_bget?compound±C00641), leaving multiple candidates for DAG clearance; parts from the overall reactions in all four pathways are hosted by mitochondrial membranes or take place in the matrix (Murray, 2003).

In summary, DAGs release sequestered Ca^{2+} from isolated mitochondria, most likely mediated through novel channels located on the inner mitochondrial membrane, or a single channel with multiple substates. It remains to be determined if DAGs are the physiological inducers for this channel activity during signal transduction in cells associated with activation of phospholipase C. This is an exciting possibility linking the triad of signal transduction, intracellular Ca^{2+} homeostasis, and mitochondrial bioenergetics.

ACKNOWLEDGMENTS

We thank Dr. Alicia J. Kowaltowski for help with the sweet potato mitochondrial isolation and Prof. Miklós Tóth and Dr. György Báthori for comments during the preparation of the manuscript. This work was supported by NIH grant GM57249 and NSF grant MCB-0235834 to K.W.K. and NIH grant NS34152 and USAMRMC grant DAMD 17-99-1-9483 to G.F.

REFERENCES

Allan, D., Thomas, P., and Michell, R. H. (1978). *Nature* **276**, 289–290.
Baines, C. P., Song, C. X., Zheng, Y. T., Wang, G. W., Zhang, J., Wang, O. L., Guo, Y., Bolli, R., Cardwell, E. M., and Ping, P. (2003). *Circ. Res.* **92**, 873–880.
Bell, R. M., and Burns, D. J. (1991). *J. Biol. Chem.* **266**, 4661–4664.
Bernardi, P., Paradisi, V., Pozzan, T., and Azzone, G. F. (1984). *Biochemistry* **23**, 1645–1651.
Bernardi, P., Vassanelli, S., Veronese, P., Colonna, R., Szabo, I., and Zoratti, M. (1992). *J. Biol. Chem.* **267**, 2934–2939.
Bothmer, J., Markerink, M., and Jolles, J. (1992). *Biochem. Biophys. Res. Commun.* **187**, 1077–1082.
Broekemeier, K. M., and Pfeiffer, D. R. (1989). *Biochem. Biophys. Res. Commun.* **163**, 561–566.
Brose, N., Betz, A., and Wegmeyer, H. (2004). *Curr. Opin. Neurobiol.* **14**, 328–340.
Brose, N., and Rosenmund, C. (2002). *J. Cell Sci.* **115**, 4399–4411.
Chen, C. H., and Lehninger, A. L. (1973). *Arch. Biochem. Biophys.* **157**, 183–196.
Chinopoulos, C., Starkov, A. A., and Fiskum, G. (2003). *J. Biol. Chem.* **278**, 27382–27389.
Clapham, D. E. (2003). *Nature* **426**, 517–524.
Clapham, D. E., Montell, C., Schultz, G., and Julius, D. (2003). *Pharmacol. Rev.* **55**, 591–596.
Florin-Christensen, J., Florin-Christensen, M., Delfino, J. M., Stegmann, T., and Rasmussen, H. (1992). *J. Biol. Chem.* **267**, 14783–14789.
Ford, D. A., and Gross, R. W. (1990). *J. Biol. Chem.* **265**, 12280–12286.
Freeman, M., and Mangiapane, E. H. (1989). *Biochem. J.* **263**, 589–595.
Gudermann, T., Hofmann, T., Schnitzler, M., and Dietrich, A. (2004). *Novartis Found. Symp.* **258**, 103–118.
Gunter, T. E., and Pfeiffer, D. R. (1990). *Am. J. Physiol.* **258**, C755–C786.
Guo, L., Pietkiewicz, D., Pavlov, E. V., Grigoriev, S. M., Kasianowicz, J. J., Dejean, L. M., Korsmeyer, S. J., Antonsson, B., and Kinnally, K. W. (2004). *Am. J. Physiol. Cell Physiol.* **286**, C1109–C1117.
Hofmann, T., Obukhov, A. G., Schaefer, M., Harteneck, C., Gudermann, T., and Schultz, G. (1999). *Nature* **397**, 259–263.
Hunter, D. R., Haworth, R. A., and Southard, J. H. (1976). *J. Biol. Chem.* **251**, 5069–5077.
Irvine, R. F. (2002). *Sci. STKE* 2002, RE13.
Kazanietz, M. G. (2002). *Mol. Pharmacol.* **61**, 759–767.
Kirichok, Y., Krapivinsky, G., and Clapham, D. E. (2004). *Nature* **427**, 360–364.
Knox, C. D., Belous, A. E., Pierce, J. M., Wakata, A., Nicoud, I. B., Anderson, C. D., Pinson, C. W., and Chari, R. S. (2004). *Am. J. Physiol. Gastrointest. Liver Physiol.* **287**, G533–G540.
Korge, P., Honda, H. M., and Weiss, J. N. (2002). *Proc. Natl. Acad. Sci. U.S.A* **99**, 3312–3317.
Lee, C., Fisher, S. K., Agranoff, B. W., and Hajra, A. K. (1991). *J. Biol. Chem.* **266**, 22837–22846.
Leikin, S., Kozlov, M. M., Fuller, N. L., and Rand, R. P. (1996). *Biophys. J.* **71**, 2623–2632.

Li, L., Lorenzo, P. S., Bogi, K., Blumberg, P. M., and Yuspa, S. H. (1999). *Mol. Cell Biol.* **19**, 8547–8558.
Liscovitch, M., Czarny, M., Fiucci, G., Lavie, Y., and Tang, X. (1999). *Biochim. Biophys. Acta* **1439**, 245–263.
Loupatatzis, C., Seitz, G., Schonfeld, P., Lang, F., and Siemen, D. (2002). *Cell. Physiol. Biochem.* **12**, 269–278.
Majumder, P. K., Pandey, P., Sun, X., Cheng, K., Datta, R., Saxena, S., Kharbanda, S., and Kufe, D. (2000). *J. Biol. Chem.* **275**, 21793–21796.
Matlib, M. A., Zhou, Z., Knight, S., Ahmed, S., Choi, K. M., Krause-Bauer, J., Phillips, R., Altschuld, R., Katsube, Y., Sperelakis, N., and Bers, D. M. (1998). *J. Biol. Chem.* **273**, 10223–10231.
Mikoshiba, K., and Hattori, M. (2000). *Sci. STKE* 2000, E1.
Mosior, M., and Epand, R. M. (1994). *J. Biol. Chem.* **269**, 13798–13805.
Murray, R. K. (2003). *Harper's Illustrated Biochemistry*, Lange Medical Books/McGraw-Hill, New York.
Murriel, C. L., Churchill, E., Inagaki, K., Szweda, L. I., and Mochly-Rosen, D. (2004). *J. Biol. Chem.* **279**, 47985–47991.
Nachbaur, J., and Vignais, P. M. (1968). *Biochem. Biophys. Res. Commun.* **33**, 315–320.
Nilius, B. (2004). *Sci. STKE.* 2004, e36.
Nishihira, J., and Ishibashi, T. (1986). *Lipids* **21**, 780–785.
Nishizuka, Y. (1992). *Science* **258**, 607–614.
Nishizuka, Y. (1995). *FASEB J.* **9**, 484–496.
Okada, T., Inoue, R., Yamazaki, K., Maeda, A., Kurosaki, T., Yamakuni, T., Tanaka, I., Shimizu, S., Ikenaka, K., Imoto, K., and Mori, Y. (1999). *J. Biol. Chem.* **274**, 27359–27370.
Panagia, V., Ou, C., Taira, Y., Dai, J., and Dhalla, N. S. (1991). *Biochim. Biophys. Acta* **1064**, 242–250.
Pastorino, J. G., Tafani, M., Rothman, R. J., Marcinkeviciute, A., Hoek, J. B., Farber, J. L., and Marcineviciute, A. (1999). *J. Biol. Chem.* **274**, 31734–31739.
Penner, R., and Fleig, A. (2004). *Sci. STKE* 2004, e38.
Putney, J. W. Jr. (1986). *Cell Calcium* **7**, 1–12.
Rajdev, S., and Reynolds, I. J. (1993). *Neurosci. Lett.* **162**, 149–152.
Rebecchi, M. J., and Pentyala, S. N. (2000). *Physiol. Rev.* **80**, 1291–1335.
Reed, K. C., and Bygrave, F. L. (1974). *Biochem. J.* **140**, 143–155.
Rustenbeck, I., Munster, W., and Lenzen, S. (1996). *Biochim. Biophys. Acta* **1304**, 129–138.
Ruvolo, P. P., Deng, X., Carr, B. K., and May, W. S. (1998). *J. Biol. Chem.* **273**, 25436–25442.
Sato, T., O'Rourke, B., and Marban, E. (1998). *Circ. Res.* **83**, 110–114.
Schmidt, B., Wachter, E., Sebald, W., and Neupert, W. (1984). *Eur. J. Biochem.* **144**, 581–588.
Schnaitman, C., Erwin, V. G., and Greenawalt, J. W. (1967). *J. Cell Biol.* **32**, 719–735.
Starkov, A. A., and Fiskum, G. (2001). *Biochem. Biophys. Res. Commun.* **281**, 645–650.
Storz, P., Hausser, A., Link, G., Dedio, J., Ghebrehiwet, B., Pfizenmaier, K., and Johannes, F. J. (2000). *J. Biol. Chem.* **275**, 24601–24607.
Sultan, A., and Sokolove, P. M. (2001). *Arch. Biochem. Biophys.* **386**, 52–61.
Szule, J. A., Fuller, N. L., and Rand, R. P. (2002). *Biophys. J.* **83**, 977–984.
Vaena de, A. S., Okamoto, Y., and Hannun, Y. A. (2004). *J. Biol. Chem.* **279**, 11537–11545.
Venkatachalam, K., van Rossum, D. B., Patterson, R. L., Ma, H. T., and Gill, D. L. (2002). *Nat. Cell Biol.* **4**, E263–E272.
Venkatachalam, K., Zheng, F., and Gill, D. L. (2003). *J. Biol. Chem.* **278**, 29031–29040.
Wang, X. (2004). *Curr. Opin. Plant Biol.* **7**, 329–336.
Watt, S. A., Kular, G., Fleming, I. N., Downes, C. P., and Lucocq, J. M. (2002). *Biochem. J.* **363**, 657–666.
Yang, C., and Kazanietz, M. G. (2003). *Trends Pharmacol. Sci.* **24**, 602–608.

Journal of Bioenergetics and Biomembranes, Vol. 37, No. 3, June 2005 (© 2005)
DOI: 10.1007/s10863-005-6590-8

Inhibition of Mitochondrial Neural Cell Death Pathways by Protein Transduction of Bcl-2 Family Proteins

Lucian Soane[1] and Gary Fiskum[1,2]

P1

Received ; accepted

Bcl-2 and other closely related members of the Bcl-2 family of proteins inhibit the death of neurons and many other cells in response to a wide variety of pathogenic stimuli. Bcl-2 inhibition of apoptosis is mediated by its binding to pro-apoptotic proteins, e.g., Bax and tBid, inhibition of their oligomerization, and thus inhibition of mitochondrial outer membrane pore formation, through which other pro-apoptotic proteins, e.g., cytochrome *c*, are released to the cytosol. Bcl-2 also exhibits an indirect antioxidant activity caused by a sub-toxic elevation of mitochondrial production of reactive oxygen species and a compensatory increase in expression of antioxidant gene products. While classic approaches to cytoprotection based on Bcl-2 family gene delivery have significant limitations, cellular protein transduction represents a new and exciting approach utilizing peptides and proteins as drugs with intracellular targets. The mechanism by which proteins with transduction domains are taken up by cells and delivered to their targets is controversial but usually involves endocytosis. The effectiveness of transduced proteins may therefore be limited by their release from endosomes into the cytosol.

KEY WORDS: Apoptosis; Bcl-2; mitochondria; protein transduction; endocytosis.

Bcl-2 AND NEUROPROTECTION

Bcl-2 is a 26 kDa protein that protects many different types of cells from death caused by a wide variety of insults. Although generally described as an anti-apoptotic protein, we and other investigators find it to also be effective against rapid, necrotic cell death, including that associated with in vitro ischemia (chemical hypoxia plus glucose deprivation) (Myers *et al*., 1995; Kane *et al*., 1995). Bcl-2 is a membrane protein located at mitochondria, the endoplasmic reticulum and the nuclear envelope. Bcl-2 is expressed at low basal levels in neurons in the adult brain (Merry and Korsmeyer, 1997), but is induced in many neurons following ischemia (Chen *et al*., 1995), and is elevated in aged animals (Kaufmann *et al*., 2001). Upregulation of Bcl-2 following brief, sublethal cerebral ischemia increases the resistance of neurons to a subsequent longer period of ischemia (Shimizu *et al*., 2001). In addition, Bcl-2 overexpression in neurons ameliorates cerebral ischemic injury (Martinou *et al*., 1994). *Bcl-2* gene deletion (Hata *et al*., 1999) or antisense treatment increases brain damage following ischemia/reperfusion (Chen *et al*., 2000). Studies demonstrating that delivery of the *bcl-2* gene to the brain via Adenoviral or Herpes virus vectors, or by liposome-mediated transfer, reduces the severity of ischemic injury suggest that Bcl-2 could be used therapeutically (Shimazaki *et al*., 2000; Linnik *et al*., 1995).

[1] Department of Anesthesiology, School of Medicine, University of Maryland, Baltimore, Maryland.
[2] To whom correspondence should be addressed at Department of Anesthesiology, School of Medicine, University of Maryland, 685 W. Baltimore St., MSTF 5-34, Baltimore, Maryland 21201; e-mail: gfisk001@umaryland.edu.

Abbreviations: Antp, Antennapedia; Bcl, B-cell lymphoma; BH domain, Bcl-2 homology domain; CPP, cell penetrating peptide; ER, endoplasmic reticulum; HIV, human immunodefficiency virus; HS, heparan sulfate; HSPG, heparan sulfate proteoglycan; PTD, protein transduction domain; STS, staurosporine; TAT, transactivator of transcription

Mitochondrial Mechanisms of Action of Anti-Apoptotic Bcl-2 Family Proteins

Murphy *et al*. (1996a, 1996b) were the first to report a direct effect of Bcl-2 on mitochondrial function, namely that overexpression increases mitochondrial Ca^{2+} buffering capacity and protects against Ca^{2+}-induced mitochondrial respiratory dysfunction (Murphy *et al*., 1996a). These observations were extended to demonstrate protection by Bcl-2 against cell death caused by elevated intracellular Ca^{2+} (Murphy and Fiskum, 1999). Kowaltowski and Fiskum then demonstrated inhibition by Bcl-2 of the mitochondrial inner membrane permeability transition (MPT) induced by Ca^{2+} together with oxidative stress elicited by the addition of hydroperoxides (Kowaltowski *et al*., 2000). The MPT results in uncoupling of oxidative phosphorylation, mitochondrial swelling, and release of cytochrome *c* through the disrupted outer membrane. Bcl-2 inhibits the MPT through its influence over NAD(P)H and glutathione redox state as it is not effective when the MPT is activated by direct chemical oxidation of protein thiols (Fig. 1) (Kowaltowski *et al*., 2000). This effect may be specific for neural cells, as it was not observed in liver mitochondria from Bcl-2 transgenic mice (Yang *et al*., 2000). The redox mode of MPT inhibition by Bcl-2 is consistent with the findings that Bcl-2 overexpressing neural cells display a relatively reduced redox state and a resistance to mitochondrial injury and cell death induced by oxidative/metabolic stress (Myers *et al*., 1995; Murphy *et al*., 1996b; Ellerby *et al*., 1996). When such stress is excessive, Bcl-2 protects against acute necrotic cell death, while when the duration of stress is limited, Bcl-2 protects against delayed, apoptotic cell death (Myers *et al*., 1995). While for many years the MPT was widely touted as a pro-apoptotic event (Zamzami and Kroemer, 2001), recent results obtained with tissues from knockout animals that do not express the MPT-associated protein cyclophilin D indicate that MPT is important for necrotic but not for many forms of apoptotic cell death (Nakagawa *et al*., 2005; Basso *et al*., 2005).

In contrast to the mechanism by which Bcl-2 protects against Ca^{2+}-induced mitochondrial cytochrome *c* release, we and other investigators found that inhibition by Bcl-2 of cytochrome *c* release induced by Bax in the presence of BH3 death domain only proteins, e.g., tBid, is independent of MPT inhibition (Polster *et al*., 2001; Jurgensmeier *et al*., 1998). Bax-mediated cytochrome *c* release occurs by a selective increase in the permeability of the mitochondrial outer membrane with no necessity for an increase in inner membrane permeability (Polster *et al*., 2001). Bax oligomerization and insertion in the outer membrane results in the formation of pores sufficiently large to allow the escape of cytochrome *c*, SMAC-Diablo, and other pro-apoptotic proteins from the mitochondrial intermembrane space into the cytosol. The Bax mechanism of release is insensitive to changes in mitochondrial redox state (Fiskum *et al*., 2000), whereas the MPT mechanism is highly sensitive to activation by an oxidized shift in redox state.

Considerable evidence indicates that Bcl-2 inhibits Bax-mediated cytochrome *c* release by heterodimerizing with Bax via the BH3 "death domain" common to all Bcl-2 family proteins and by sequestering BH3 only proteins (Shangary and Johnson, 2002). Different BH3 domain only proteins have different affinities for Bcl-2 and Bcl-X_L (Chen *et al*., 2005) and some, e.g., BimEL, may stimulate Bax-induced cytochrome *c* release independent of their ability to interact with Bcl-2 or Bcl-X_L (Yamaguchi and Wang, 2002). According to a recent model, activator BH3-only proteins, e.g., tBid, can directly bind and induce Bax oligomerization and mitochondrial outer membrane permeabilization, while sensitisers (e.g., Bad) bind to Bcl-2 and disrupt its heterodimerization with Bax (Fig. 1) (Letai *et al*., 2002).

THERAPEUTIC TARGETING OF Bcl-2 FAMILY PROTEINS

Extensive experimental evidence supports the concept of targeting Bcl-2 family proteins to modulate cell death in diverse pathologic conditions such as cancer or acute and chronic neurodegeneration. Despite substantial progress in understanding the molecular mechanisms of action of Bcl-2 family proteins, translation of this knowledge into effective therapies is limited. While useful in experimental settings, the therapeutic use of gene-based strategies is currently limited. Poor delivery, unequal rates of expression, toxicity and safety are several problems associated with this approach (Ferber, 2001).

Several other approaches are pursued, mostly for targeting anti-apoptotic Bcl-2/Bcl-X_L proteins, and hold promise for generating efficient therapeutic tools for many forms of cancer (reviewed in Reed and Pellecchia, 2005). An important recent development is the discovery of several classes of small-molecular inhibitors of Bcl-2 and Bcl-X_L through structure-based computer database screening and high-throughput screening of small-molecule libraries (reviewed in O'Neill *et al*., 2004; Reed and Pellecchia, 2005).

Therapeutic delivery of "information-rich" macromolecular compounds is another promising approach explored for delivery of full-length Bcl-2 family proteins and delivery of related peptides. Delivery of biologically active peptides or proteins has until recently been limited

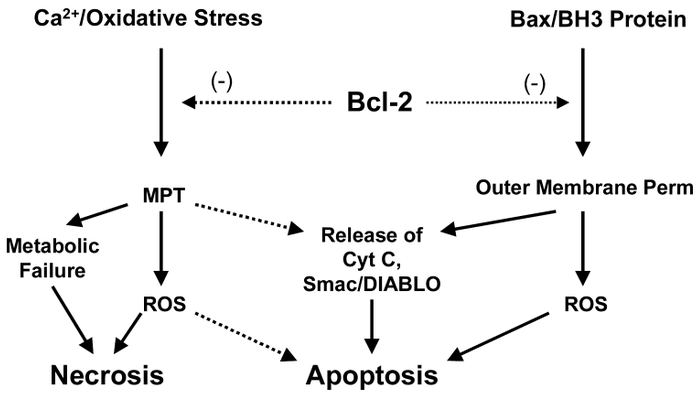

Fig. 1. Mitochondrial mechanisms of cytoprotection by Bcl-2. Expression of Bcl-2 causes upregulation of antioxidant gene expression resulting in protection from oxidative stress. One consequence of this form of protection is inhibition of the mitochondrial permeability transition (MPT), thus protection cells against MPT-induced metabolic failure, generation of reactive O_2 species (ROS), and rupture of the outer membrane resulting in loss of cytochrome *c*, Smac/DIABLO, and other intermembrane pro-apoptotic proteins. In addition, by binding to Bax and BH3-only proteins, e.g., tBid, Bcl-2 inhibits mitochondrial outer membrane pore formation, thereby inhibiting release of apoptotic proteins and mitochondrial ROS formation.

by their poor bioavailability imposed by the plasma membrane barrier. Several strategies, including linkage to non-toxic fragments of cell-penetrating toxins and receptor ligands such as transferrin, and incorporation into liposomes or other lipid-based delivery systems, have been explored to overcome this barrier (Dalkara *et al*., 2004; Stenmark *et al*., 1991). Delivery of the anti-apoptotic Bcl-X_L (Liu *et al*., 1999), or pro-apoptotic proteins such as Bad have been reported using these proteins as fusion proteins with diphtheria toxin (DT) fragments (Ichinose *et al*., 2002).

Protein transduction is a strategy developed during the last decade that allows the delivery of various membrane-impermeable cargoes in a receptor-independent manner in virtually any cell type, including primary cell cultures, and in vivo in various tissues including the brain (reviewed in Wadia and Dowdy, 2003; Joliot and Prochiantz, 2004). This new technology has a tremendous potential for overcoming the barrier imposed by the plasma membrane to deliver therapeutic macromolecules.

Protein Transduction

The concept of protein transduction originated from observations that certain proteins, e.g., the HIV-1 TAT (Frankel and Pabo, 1988; Green and Loewenstein, 1988) and the homeodomain protein Antennapedia (Antp) (Derossi *et al*., 1994) can enter cells in a receptor independent-manner. Based on work with homeodomain proteins, the concept of "messenger" proteins was proposed, according to which these proteins would regulate neighboring cells in a paracrine mode (Joliot and Prochiantz, 2004). The ability of Antp and TAT to enter cells was mapped to short domains, named protein transduction domains (PTD). PTDs, also known as cell-penetrating peptides (CPPs), are comprised of short basic peptides of various origins that can cross biological membranes. When fused to other molecules, some of these PTDs promote the delivery of attached cargoes (protein and non-protein) into cells. The highly cationic HIV-1 TAT-PTD, the third helix of Antennapedia homeodomain protein and polyarginine are the best characterized PTDs.

The TAT(47–57) PTD is a 10 aminoacids (YGRKKRRQRR) peptide derived from the human immunodefficiency virus (HIV)-1 transactivator of transcription (TAT) protein. In 1988, two groups reported independently that the HIV-1 TAT protein can translocate inside cells (Frankel and Pabo, 1988; Green and Loewenstein, 1988). Fawell *et al*. showed that heterologous proteins can be delivered into cells when chemically cross-linked with a 36 aminoacids peptide from HIV-1 TAT(37–72) and demonstrated the applicability of this approach to deliver proteins in vivo in mice (Fawell *et al*., 1994). Vives *et al*., determined that the basic domain (residues 49–60) in the HIV-1 TAT retains the transduction potential (Vives *et al*., 1997). Using the TAT(47–57) PTD, Dowdy's group developed a convenient method for transduction of proteins based on a in frame fusion strategy

that facilitated the delivery of a large variety of proteins. Delivery of large protein cargoes (up to 120 kDa) occurs both in cells, and in vivo in mice, and most tissues including the brain are transduced without toxic effects (Schwarze *et al*., 1999).

The third helix of the *Drosophila melanogaster* homeodomain protein Antennapedia also translocates inside cells in a receptor and energy-independent manner (Derossi *et al*., 1994). The 16 aminoacids transduction domain of Antennapedia (aminoacids 43–58; pAntp), also known as Penetratin, was used to deliver various cargoes such as peptides, proteins and antisense oligonucleotides (Dietz and Bahr, 2004; Joliot and Prochiantz, 2004). The *Herpes simplex virus* tegument protein VP22 is another cell translocating protein. Unlike the TAT-PTD and Antennapedia, VP22 mediates intercellular transport upon being secreted from cells (Elliott and O'Hare, 1997).

Numerous other PTDs have been reported and are derived from viral and cellular proteins or antibacterial peptides; synthetic CPPs have also been designed (Dietz and Bahr, 2004; Futaki, 2002). On the basis of observation that PTDs such as TAT-PTD and pAntp are highly enriched in basic aminoacids, especially arginine, arginine polymers of various lengths were tested and the R_8 and R_9 oligomers were found to transduce cells even more efficiently than the original TAT-PTD peptide (Wender *et al*., 2000; Futaki, 2002). To facilitate protein delivery without the need of covalent linkage to the cargo, Morris *et al*. designed the 21-mer Pep-1 peptide that can bind proteins and promote cellular transduction (Morris *et al*., 2001). One study indicated that Pep-1 is also efficient when used as a fusion protein and transduces superoxide dismutase into the brains of mice (Sik *et al*., 2004).

Transduction of both PTDs and attached cargoes was initially reported to occur rapidly (minutes) in a receptor and temperature-independent manner. Other studies examining the transduction of protein cargoes reported a much slower rate of uptake (hours) (Fittipaldi *et al*., 2003). PTD-mediated delivery is dose-dependent and cellular uptake occurs uniformly in close to 100% of the cells exposed. While transduction occurs into almost all cell types, internalization is not observed in some cell types (MDCK, CaCo-2) (Violini *et al*., 2002; Kramer and Wunderli-Allenspach, 2003). PTDs are usually used at μM concentrations (1–10 μM) and most applications with fused proteins use nM concentrations ($\sim$100 nM). Transduction of a biologically active modified Bcl-X_L can occur even at pM concentrations (Asoh *et al*., 2002). Most of the PTDs lack toxic effects at these doses. Toxicity occurs only at very high doses of TAT basic domain and pAntp (Jia *et al*., 2001; Bolton *et al*., 2000) and might be a concern for CPPs derived from pore-forming antibacterial peptides (Takeshima *et al*., 2003).

The list of cargoes delivered and the number of potential applications is continually increasing, and was recently reviewed in detail by Dietz and Bahr (2004). Beside proteins, other notable examples of cargoes include plasmid DNA complexed with TAT monomers or TAT oligomers and antisense oligonucleotides. Other small non-protein cargoes such as drugs, doxorubicin, cyclosporin A or large cargoes such as liposomes, phage particles and even nanoparticles were also delivered. In addition, the TAT-PTD can facilitate viral-mediated gene expression (Dietz and Bahr, 2004).

MODULATION OF MITOCHONDRIA-DEPENDENT CELL DEATH THROUGH PROTEIN TRANSDUCTION

Delivery of Pro-Apoptotic and Anti-Apoptotic Peptides

The ability of PTDs to facilitate intracellular delivery has been utilized to modulate apoptotic cell death by transduction of small PTD-linked peptides. The BH3 domain, encompassing an amphipathic α-helix, is shared by all Bcl-2 family proteins and is required for the dimerization and death-inducing ability of pro-apoptotic Bcl-2 proteins, especially the BH3-only proteins. The BH3 domain of pro-apoptotic proteins binds to the hydrophobic groove created by the BH3, BH2 and BH1 domains of anti-apoptotic Bcl-2-like proteins (reviewed in Petros *et al*., 2004). Synthetic BH3 peptides ($\sim$16-mer) can mimic the functionality of BH3-only proteins, induce Bax/Bak oligomerization, and antagonize anti-apoptotic Bcl-2 and Bcl-X_L proteins by disrupting their complexes with pro-apoptotic Bax and Bak. The functionality of several BH3 peptides was demonstrated in cells and in isolated mitochondria, where they are able to trigger the release of apoptogenic factors (Cyt C, EndoG, Smac/DIABLO and AIF) from the mitochondrial intermembrane space (sPolster *et al*., 2001; Letai *et al*., 2002).

Unlike the BH3 peptides alone, BH3 domain peptides fused to TAT-PTD, pAntp or polyarginine are rapidly internalized into cells through protein transduction, and subsequently induce apoptosis (Letai *et al*., 2002; Holinger *et al*., 1999). While useful experimental tools, cell-penetrating BH3 peptides derived from pro-apoptotic Bcl-2 proteins are also explored as a potential treatment for various forms of cancer. Using a hydrocarbon stapling strategy, Korsmeyer's group generated BH3 peptides with

improved stability and affinity that are effective at inhibiting the growth of leukemia xenografts in vivo (Walensky *et al*., 2004). The stapled peptides are internalized through macropinocytosis, a mechanism shown recently to mediate internalization of the TAT-PTD (Wadia *et al*., 2004) and polyarginine (Nakase *et al*., 2004).

PTD-mediated delivery of small peptides is also used to inhibit apoptotic cell death. The BH4 domain, shared only by anti-apoptotic Bcl-2 proteins, is required for interaction with several non-Bcl-2 family proteins and for anti-apoptotic activity. Shimizu *et al*. reported that a synthetic peptide corresponding to the BH4 domain of Bcl-X_L can enter cells and inhibit etoposide-induced apoptotic death when fused to TAT-PTD (Shimizu *et al*., 2000). TAT-BH4 is also effective in vivo and inhibits X-ray-induced apoptosis, Fas-induced fulminant hepatitis in mice, and ischemia-reperfusion injury in isolated rat heart (Sugioka *et al*., 2003; Chen *et al*., 2002). The BH4 domain of the anti-apoptotic Bcl-2 is also effective at protecting coronary endothelial cells against oxidative stress-induced death (Cantara *et al*., 2004).

Activation of the multidomain Bax/Bak proteins is required for activation of the intrinsic, mitochondria-dependent cell death pathway. Cells lacking both these proteins display long-term protection against multiple apoptotic stimuli (Wei *et al*., 2001). While protein–protein interaction and structural studies of Bcl-2 proteins provide a strong support for use of BH3 peptides as death inducers, no such candidate protein domains emerged, until recently, for inhibition of Bax/Bak activation. Recent studies revealed that Bax translocation from cytosol to mitochondria is suppressed by the DNA repair protein Ku70 (Sawada *et al*., 2003) and a similar role was demonstrated for the short peptide humanin (Guo *et al*., 2003). A pentapeptide derived from the Bax-binding sequence of Ku70, termed BIP (Bax inhibitory peptide), was tested for potential suppression of Bax activity. The BIP peptide is cell-permeable and protects against cell death induced by cytotoxic drugs (Sawada *et al*., 2003).

Humanin, a 24 aminoacids endogenous peptide, initially discovered as an inhibitor of amyloid-β induced neuronal death (Hashimoto *et al*., 2001), binds and stabilizes Bax in the cytosol in an inactive conformation (Guo *et al*., 2003). Reed's group also demonstrated that in addition to Bax, humanin binds to and inhibits the pro-apoptotic activity of the BH3-only proteins Bid (Zhai *et al*., 2005) and Bim-EL (Luciano *et al*., 2005). The ability of humanin to target and antagonize the activity of multiple pro-apoptotic proteins makes it an attractive candidate for cytoprotection. These studies also demonstrated that polyarginine-mediated transduction of the humanin peptide into cells is effective at inhibiting Bid and BimEL-induced death (Zhai *et al*., 2005; Luciano *et al*., 2005).

Delivery of Bcl-2 Family Proteins

The anti-death Bcl-2 family members Bcl-2 and Bcl-X_L inhibit apoptosis and are also effective at protecting against necrotic forms of cell death (Myers *et al*., 1995; Kane *et al*., 1995). Korsmeyer's group proposed over a decade ago the rheostat model, according to which the anti-apoptotic Bcl-2/Bcl-X_L bind and neutralize pro-apoptotic Bcl-2 family proteins and their relative balance determines cell death or survival (Korsmeyer *et al*., 1993). In addition to antagonizing the pro-apoptotic activity of multidomain Bax/Bak and to sequester BH3-only proteins (Bid, Bim, Bad and others), early studies indicated that the cytoprotective activity of Bcl-2 and more recently that of Bcl-X_L and Mcl-1, is at least in part due to additional mechanisms including their ability to increase protection against oxidative stress (Hockenbery *et al*., 1993; Kowaltowski *et al*., 2000, 2004). The multitasking nature of Bcl-2 cytoprotective activity cannot be mimicked by small drugs or peptide domains. Therefore delivery of "information-rich" macromolecules, i.e., full-length proteins, should be the most effective approach at cytoprotection.

Several groups have employed protein transduction to deliver anti-apoptotic Bcl-2 family proteins into cultured cells and in vivo into the brain in models of neural cell death. A TAT-PTD fused Bcl-X_L was efficiently transduced and protected retinal ganglion cells following optic nerve transsection (Dietz *et al*., 2002). This group also demonstrated that pretreatment with TAT-Bcl-X_L by intravenous injection reduces ischemia/reperfusion brain injury in mice (Kilic *et al*., 2002). Using a TAT-fused Bcl-X_L construct, Cao *et al*. also showed that transduction and neuroprotection can be achieved both in vitro and in vivo. In this study, a significant protection against brain ischemia/reperfusion was observed even when the protein was injected intraperitoneally after the ischemic period (Cao *et al*., 2002). Another study used TAT-mediated transduction of a mutated Bcl-X_L (FNK) with increased anti-apoptotic activity and showed greater protection in cultured cells and in vivo against ischemia/reperfusion than that obtained with PTD-Bcl-X_L (Asoh *et al*., 2002). The same approach was also used to deliver Bcl-X_L to pancreatic islets (Embury *et al*., 2001) and FNK to chondrocytes in cartilage slice culture (Ozaki *et al*., 2004).

While these studies indicate that protein transduction of Bcl-2 family proteins or peptides could become an effective therapeutic tool, a detailed understanding of

the mechanisms of intracellular delivery of functional proteins is needed, as several practical limitations have emerged. We recently explored the transduction of a modified Bcl-2 protein in neural cells, and investigated the mechanisms involved in intracellular delivery. For this purpose, a TAT-fusion protein was generated with a loop deleted Bcl-2 protein. Transducible TAT-Bcl-2Δloop protein confers significant protection in several neuronal cell lines against staurosporine or trophic factor withdrawal-induced death (Fig. 3 and unpublished results). Similar to recent findings from other laboratories, our results indicate that transduction of Bcl-2 in neuronal cell lines is mediated through an endocytotic pathway rather than through transduction mechanism.

MECHANISM OF PTD-MEDIATED PROTEIN DELIVERY

Direct Membrane Translocation of PTDs

The mechanism of PTD-mediated transduction is not entirely understood. The full-length HIV-1 TAT enters cells through adsorptive endocytosis in a receptor-independent manner (Mann and Frankel, 1991). In contrast, internalization of TAT-PTD and pAntp involves a distinct process named "transduction". Early reports indicated that transduction is effective even at 4°C, in the absence of endocytosis, and is energy and receptor-independent (Vives *et al*., 1997; Derossi *et al*., 1994). While it is known that polybasic peptides, e.g., lysine polymers, stimulate the uptake of cargoes into cells through adsorptive endocytosis (Ryser *et al*., 1978), the energy and receptor-independent characteristics of PTD uptake, appeared to distinguish transduction from most classic forms of internalization.

The numerous biochemical and biophysical studies aimed at elucidating the process of PTD internalization suggest that transduction is a multistep process initiated by interaction of CPPs with the cell surface (either with membrane lipids or negatively charged cell surface constituents). Binding is followed by internalization through either an undefined mechanism involving a direct membrane translocation step or by the better characterized process of endocytosis (Fig. 2). Although exhibiting diverse structures, most CPP share a high content of basic amino acids. The polycationic character of CPP is one of the most important structural requirements, as indicated by the correlation between the number of basic residues and efficiency of transduction (Wender *et al*., 2000). While positive charge is important, arginine appears to play a unique role. The guanidium group of arginine, rather than simply a positive charge, is required for efficient internalization, and replacement by an ammonium group reduces translocation (Wender *et al*., 2000). The uptake of oligoarginine is consistently more efficient than that of lysine or histidine oligomers (Mitchell *et al*., 2000). The presence of arginine may facilitate a transduction mechanism, while lysine-rich CPPs promote endocytosis (Zaro and Shen, 2003). Hydrophobicity and amphipathicity also play a role in transduction of some CPPs. Unlike the TAT-PTD and polyarginine, pAntp contains several hydrophobic residues. The central hydrophobic core composed of the W6, F7 aminoacids appears critical for transduction (Dom *et al*., 2003).

Several models have been proposed to explain the apparent ability of PTDs to translocate across cellular membranes (Fig. 2). Transient formation of inverted micelles initiated by binding of the basic PTDs to negatively charged membrane lipids is suggested for pAntp, TAT-PTD and Pep-1 (Derossi *et al*., 1994; Vives *et al*., 1997; Henriques and Castanho, 2004). Another mechanism involves formation of a pore allowing passage of small peptides through membranes, as proposed for Pep-1 and for CPPs derived from pore-forming antimicrobial peptides (Deshayes *et al*., 2004; Takeshima *et al*., 2003). However, PTDs such as TAT-PTD and polyarginine are highly charged and do not contain hydrophobic residues required for formation of inverted micelles. It is also difficult to explain through these models the internalization of very large cargoes as shown for the TAT-PTD. While TAT-PTD can interact with negatively charged lipids, binding to negatively charged heparan sulfate proteoglycans (HSPG) at the cell surface appears more likely (Ziegler *et al*., 2003). Partial insertion of pAntp into lipid membranes is also documented (Joliot and Prochiantz, 2004). Despite evidence for binding to membrane lipids, actual translocation across model lipid membranes or intact plasma membrane of cells was not observed for TAT-PTD (Kramer and Wunderli-Allenspach, 2003). For pAntp and for Pep-1, a few studies support a direct translocation model (Dom *et al*., 2003), while others indicate that actual internalization occurs through endocytosis (Drin *et al*., 2003).

PTD-Mediated Endocytosis

Studies performed in living cells without fixation indicate that contrary to initial reports, PTDs (TAT-PTD, polyarginine and pAntp) and PTD-fused proteins are unable to enter cells at 4°C (Richard *et al*., 2003; Lundberg *et al*., 2003; Drin *et al*., 2003). Strong cell-surface association of polycationic PTDs and artifactual redistribution following fixation result in apparent uptake at 4°C and cytosolic or nuclear staining. Moreover, PTDs and fused

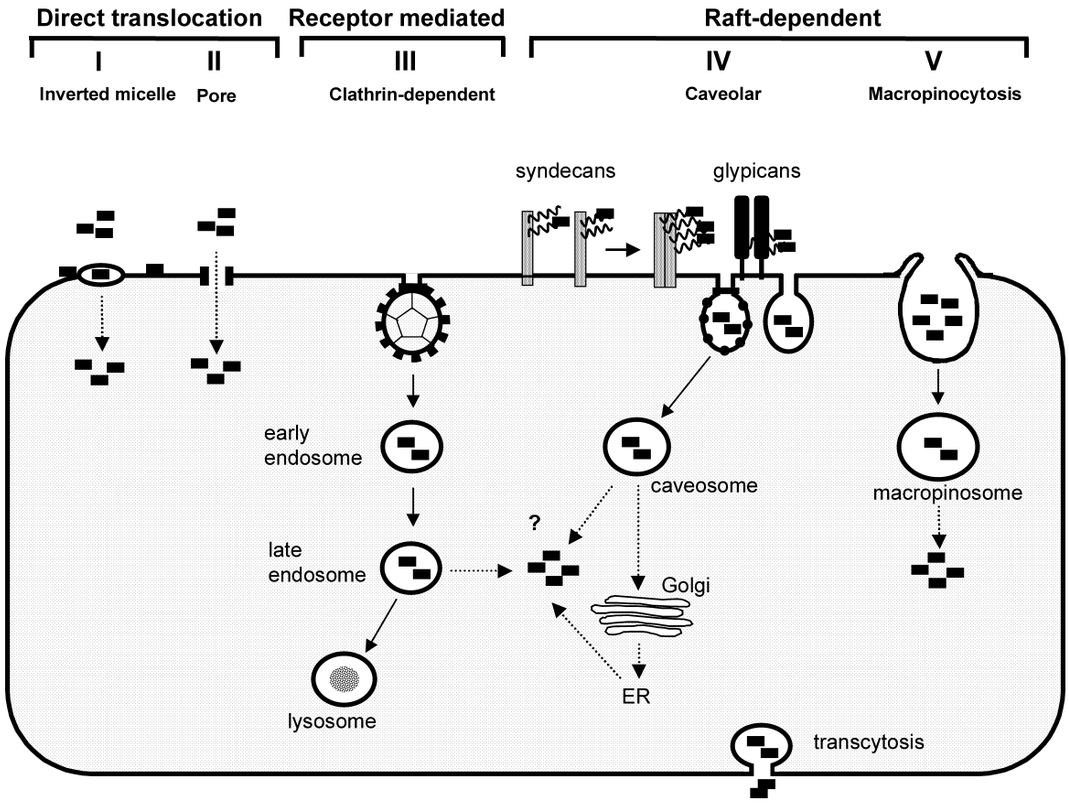

Fig. 2. Mechanism of protein transduction. Direct membrane translocation. Cationic PTDs bind to negatively charged membrane lipids and translocate across plasma membrane into cytosol. Direct translocation occurs through either (I) transient formation of inverted micelles or (II) formation of a pore-like structure allowing direct cytosolic delivery. *Endocytotic uptake*. Binding to the negatively charged cell-surface HSPG (syndecans or glypicans) is followed by endocytotic uptake of PTDs through (III) a clathrin-dependent, receptor-mediated pathway or a lipid raft-dependent pathway. Lipid raft-dependent endocytosis can occur either through (IV) a caveolar/caveolar-like pathway or (V) through raft-dependent macropinocytosis. Cytosolic delivery of PTDs (dotted line) might involve a direct translocation process where in this case the mechanisms (I) and (II) might take place at the endosomal membrane. PTD-induced endosome disruption or constitutive endosomal leakage could also mediate cytosolic delivery. Another possible pathway involves retrograde transport to Golgi and ER with subsequent cytosolic release.

proteins have been detected in vesicular structures inside the cells, suggesting endocytotic uptake (Richard *et al*., 2003; Lundberg *et al*., 2003; Drin *et al*., 2003).

The clathrin-dependent, receptor-mediated endocytotic pathway is the best-characterized form of internalization of membranes and proteins. Clathrin-independent endocytotic pathways include caveolar-endocytosis and macropinocytosis. Unlike clathrin-dependent endocytosis, most of these internalization pathways are sensitive to disruption of the plasma membrane lipid rafts (Nichols and Lippincott-Schwartz, 2001). The lipid-raft dependent caveolar pathway is involved in internalization of the full length HIV-1 TAT and of a TAT-PTD fused GFP protein in HeLa cells (Fittipaldi *et al*., 2003). Caveolae, first identified in endothelial cells (Palade, 1953), are found in many other cell types, although they have not been detected in lymphocytes and neurons (Razani *et al*., 2002), suggesting that endocytosis of TAT-fusion proteins might occur in a cell-specific manner. For instance, in lymphoid cells, an alternate, lipid raft-dependent, macropinocytotic pathway is involved in the internalization of both TAT-PTD and TAT-fusion proteins (Wadia *et al*., 2004; Kaplan *et al*., 2005). In neurons, internalization of full-length HIV-1 TAT occurs through a LRP receptor-dependent pathway, but the mechanism of TAT-PTD mediated uptake has not been examined. Since binding of full length TAT to LRP occurs through a different domain of TAT (34–47) than its PTD (47–57) (Liu *et al*., 2000), it is likely that such a receptor-mediated pathway is not

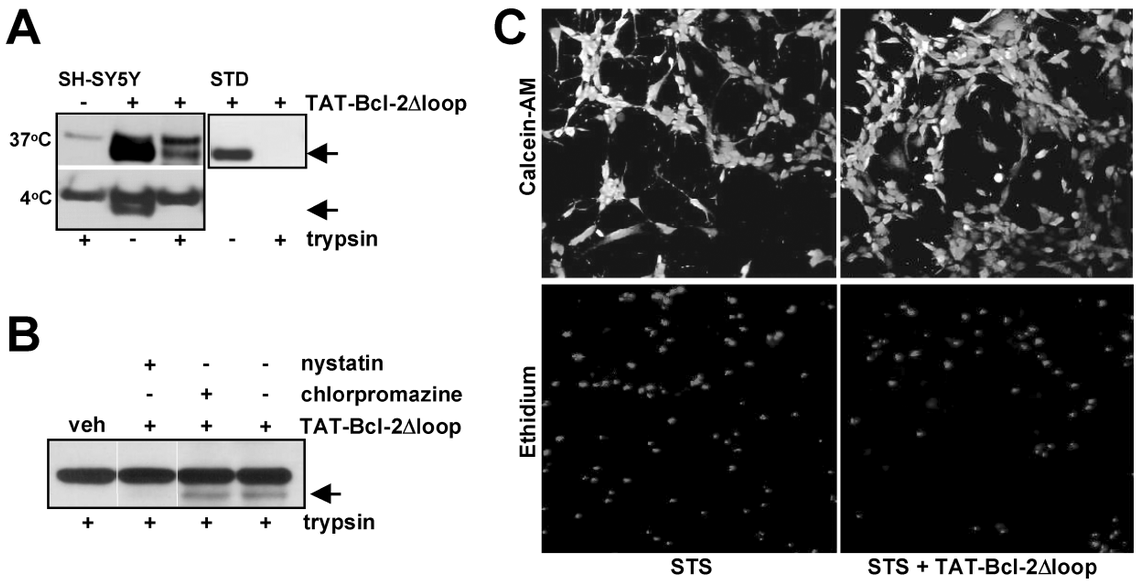

Fig. 3. Transduction of TAT-Bcl-2Δloop protein. (A) Transduction of TAT-Bcl-2Δloop was examined in SH-SY5Y neuroblastoma cells incubated with the protein (200 nM) for 1 h at 37°C or 4°C. TAT-Bcl-2Δloop uptake was examined by immunoblotting with an anti-Bcl-2 antibody and was detected as an additional band with a lower molecular weight than endogenous Bcl-2 (upper band). Trypsin treatment was performed at the end of incubation to eliminate the cell-surface bound protein and indicated that TAT-Bcl-2Δloop is internalized at 37°C but not at 4°C. A control protein (STD) was completely digested in the same conditions in the absence of cells. (B) The cells were pretreated with an inhibitor of clathrin-dependent endocytosis (chlorpromazine, 10 μM) or with the lipid raft disrupting agent nystatin (50 μg/ml) and the internalization of TAT-Bcl-2Δloop (100 nM; 1 h, 37°C) examined as in (A). Disruption of lipid rafts but not of clathrin-dependent endocytosis inhibited internalization of TAT-Bcl-2Δloop. (C) SH-SY5Y cells pretreated with TAT-Bcl-2Δloop (100 nM) were exposed to staurosporine (STS; 100 nM) for 18 h then cell survival examined by the live/dead assay by staining the cells with Calcein-AM (viable cells; upper panel) and ethidium homodimer (dead cells; lower panel). Pretreatment with TAT-Bcl-2Δloop resulted in significant protection (48.15%) against STS-induced death ($n = 4$, $p < 0.05$).

involved in internalization of TAT-PTD or of TAT-fusion proteins.

We recently examined the mechanisms involved in TAT-mediated internalization of Bcl-2 using neural cells. Using trypsinization to eliminate the cell-surface bound protein, we found that internalization of TAT-Bcl-2Δloop protein (35% of total cellular) occurs at 37°C but not at 4°C (Fig. 3A). Since all forms of endocytosis are inhibited at 4°C, this finding suggests that an endocytotic process rather than a temperature-independent transduction mechanism is involved. Consistent with this hypothesis, fluorescence microscopy of live cells transduced with both an FITC-labeled TAT-Bcl-2Δloop protein or a TAT-YFP protein reveal a vesicular distribution (Soane and Fiskum, unpublished).

The lipid raft-disrupting agent nystatin, that sequesters plasma membrane cholesterol, was used to test for possible involvement of a lipid raft-dependent endocytotic pathway in internalization of TAT-Bcl-2Δloop. A marked inhibition of internalization was observed in SH-SY5Y neuroblastoma cells (Fig. 3B). In addition, inhibition of clathrin-mediated endocytosis with the specific inhibitor chlorpromazine does not affect the internalization of TAT-Bcl-2Δloop (Fig. 3B). Fluorescence microscopy of transduced TAT-YFP also indicates that the protein does not colocalize with transferrin, a marker of clathrin-mediated endocytosis. Moreover, significant colocalization was observed with 70 kDa Dextran, a marker of fluid phase endocytosis (Soane and Fiskum, unpublished). Thus, like in other cells, TAT-mediated protein internalization of Bcl-2 in neural cells also occurs through a clathrin-independent and raft-dependent pathway.

While the direct membrane translocation mechanism might still be involved in internalization of PTDs and small cargoes, the delivery of protein cargoes is most likely mediated through endocytosis. Internalization of TAT-fusion proteins is apparently mediated in most cell types through endocytotic pathways originating at the plasma membrane lipid rafts, and can follow a caveolar or non-caveolar route, e.g., macropinocytosis or other less well characterized raft-dependent pathways (Fig. 2). Raft dependence of internalization was also noted in some cell

types for other cargoes transduced by TAT-PTD, such as plasmid DNA and phage particles (Ignatovich *et al*., 2003; Eguchi *et al*., 2001). In addition, similar to the TAT-PTD, polyarginine was also shown recently to be internalized through macropinocytosis in HeLa cells (Nakase *et al*., 2004).

Contrary to this model, however, are observations of partial colocalization with markers of clathrin-dependent endocytosis as reported for PTDs (Richard *et al*., 2003; Potocky *et al*., 2003) and for fusion proteins (Sengoku *et al*., 2004). In this later study, however, the proteins appeared inactive and sequestered in endosomes. Some studies also report a lack of inhibition of TAT-PTD or pAntp uptake by cholesterol-sequestering agents and suggest that internalization of PTDs is not limited to raft-dependent pathways (Drin *et al*., 2003; Richard *et al*., 2005). Consistent with this interpretation, TAT-PTD can enter at least HeLa cells through a clathrin-mediated pathway (Richard *et al*., 2005). However, in lymphoid cells, macropinocytosis is involved in internalization of both TAT-PTD and TAT-Cre fusion protein (Wadia *et al*., 2004; Kaplan *et al*., 2005). On the other hand, using the same cell type (HeLa cells) different endocytotic mechanisms are involved in internalization of TAT-PTD (clathrin-mediated) (Richard *et al*., 2005) and polyarginine (macropinocytosis) (Nakase *et al*., 2004).

The characteristics of PTD-mediated internalization are reminiscent of the cholera toxin can be internalized by both clathrin-dependent and independent pathways. However, cholera toxin is active only when it is endocytosed through non-clathrin and raft-dependent endocytosis, leading to Golgi localization and subsequent cytosolic delivery (Nichols and Lippincott-Schwartz, 2001). Sequence similarities between the TAT-PTD and several bacterial toxins that use the retrograde transport system to reach the ER and Golgi were noted recently (Fischer *et al*., 2004). Most of these arginine-rich motifs belong to toxins or proteins known to utilize a non-clathrin-mediated and cholesterol-sensitive endocytotic pathway for internalization. Currently, no explanation is available for these differences in the endocytotic pathways mediating transduction, other than the possible influence of the attached cargo and differences in the structure of the PTDs used. One possibility is that the internalization pathway is modulated by specific interaction of PTDs with cell-surface proteoglycans.

Role of Heparan Sulfate Proteoglycans

Heparan sulfate proteoglycans (HSPG) can mediate endocytotic uptake of various endogenous ligands, including basic fibroblast growth factor (FGF), lipoproteins, or pathogens, e.g., bacteria (Belting *et al*., 2003). Reports indicating that heparin, a structural analogue of heparan sulfate, inhibits internalization of HIV-1 TAT and that the TAT-PTD can bind heparin suggest a possible role of HSPG in PTD-mediated internalization (Mann and Frankel, 1991; Hakansson *et al*., 2001). Using CHO cells defective in heparan sulfate (HS) synthesis, Tyagi *et al*. clearly demonstrated that internalization of TAT and TAT-PTD fused proteins is dependent on binding to HSPG. Heparan sulfate but not chondroitin sulfate (CS) was required for internalization (Tyagi *et al*., 2001). Other studies have shown that binding to HSPG is also required for internalization of the TAT-PTD and polyarginine (Suzuki *et al*., 2002; Richard *et al*., 2005).

HS is present on cells mainly on two classes of membrane-anchored proteoglycans (PG), i.e., syndecans and glypicans. Expression of PG is affected by multiple factors and is developmentally regulated (Bandtlow and Zimmermann, 2000). Most cells contain PG of both types and their ubiquitous distribution might explain the ability of PTDs to transduce virtually any cell type. Glypicans are enriched in lipid rafts and are therefore logical candidates for raft-dependent internalization of TAT-delivered Bcl-2 or other proteins and PTDs. However, ligand binding to the HS chains of syndecans can also induce their clustering and raft-dependent endocytosis (Fuki *et al*., 2000). The TAT-PTD was shown to induce aggregates on the cell surface in an HS-dependent manner (Ziegler *et al*., 2005). The presence and binding of HSPG is not necessarily equivalent with internalization, as indicated by studies in MDCK and CaCo-2 cells in which no intracellular/transcellular TAT-PTD transport could be detected, despite the presence of HSPGs (Violini *et al*., 2002).

Cytosolic Delivery of Transduced Proteins

Despite recent evidence for involvement of endocytosis in protein transduction, demonstration of specific biologic effects of transduced proteins indicates that at least a fraction of the PTD-fused proteins are released from endosomes. Among Bcl-2 family proteins, both Bcl-2 (Fig. 3C and unpublished results) and Bcl-X_L are transduced in a functional form (Cao *et al*., 2002; Kilic *et al*., 2002; Asoh *et al*., 2002).

For the full length HIV-1 TAT protein, endocytotic internalization leads to endosomal localization and subsequent cytosolic release through a mechanism requiring acidification and relying on Hsp90 (Vendeville *et al*., 2004). The mechanisms of endosomal release of PTDs and attached cargoes are, however, unclear. Some of the

potential endosome release mechanisms involve a direct translocation or transport of PTDs across endosomal membranes, or formation of inverted micelle or pore-like structures in endosomes rather than in the plasma membrane (Fig. 2). Endosomal escape might also involve PTD-induced endosome disruption, or constitutive release from a fraction of leaky endosomes, e.g., macropinosomes (Wadia *et al*., 2004). Similar to cholera toxin, the retrograde transport to Golgi/ER and subsequent cytosolic exit through retro-translocation could also be involved. An acidification-dependent release from endosomes was suggested for TAT-PTD by the observation that neutralization of endosomal pH inhibits its cytosolic delivery (Potocky *et al*., 2003). Studies using brefeldin A, that disrupts Golgi trafficking, provide support for the possibility that the transduced proteins are released following retrograde transport to Golgi (Fischer *et al*., 2004; Fittipaldi *et al*., 2003). Another possible explanation is that the endosomal release is facilitated by some of the protein cargoes and not by the PTDs. Bcl-2 family proteins are a class of cargoes that could induce their own endosomal escape, since they can form ion channels or pores in membranes. Channel formation by Bcl-2 proteins is augmented by low pH (Schendel *et al*., 1998) and might therefore be activated in endosomes after acidification. This suggests that endosomal escape of TAT-delivered Bcl-2 or Bcl-X_L can occur in a manner similar to that of the pH-dependent pore-forming toxin Diphtheria toxin (DT), with which Bcl-2 proteins share structural homology. Yet another possibility is that Bcl-2 proteins delivered through transduction reach the ER through the retrograde transport mechanism and exert their effect at the ER without being released into the cytosol and localize to mitochondria. This possibility was also suggested by the studies on the DTR fused Bcl-X_L (Liu *et al*., 1999).

Recognition of the involvement of endocytosis in PTD-mediated transduction indicates that efficient delivery will only be achieved if this barrier is eliminated. The efficacy of PTDs to promote endosomal escape, at least for protein cargoes, appears quite limited in some cases (Sengoku *et al*., 2004). Several studies demonstrate that enhancing endosomal escape results in increased functional activity of transduced proteins. Chloroquine, known to enhance transactivation by full-length TAT and sucrose, was used to disrupt endosomes, resulting in an increase in the activity of a TAT-Cre protein (Caron *et al*., 2004; Wadia *et al*., 2004). Photo-acceleration of PTD release (TAT-PTD, polyarginine and pAntp) from endosomes following exposure to fluorescent light (480 nm) was also reported. The same method was efficient at increasing the cytosolic release of a polyarginine-transduced p53 protein (Matsushita *et al*., 2004). Similarly, laser illumination was also reported to increase redistribution of CPPs from endosomes to cytosol (Maiolo *et al*., 2004).

pH-sensitive toxins or fusogenic peptides can enhance endosomal escape through pH-induced endosomolysis and are used to increase the efficiency of non-viral DNA delivery methods (Cho *et al*., 2003). The utility of such a strategy at improving PTD-mediated delivery and endosomal escape was demonstrated by Wadia *et al*. by using a TAT-HA2 pH-sensitive fusogenic peptide that was co-transduced with a TAT-Cre protein, resulting in increased TAT-Cre activity (Wadia *et al*., 2004). This approach was also utilized for generation of a p53 fusion protein with both the TAT and HA2 peptides, and resulted in improved activity of transduced p53 (Michiue *et al*., 2005). The mechanism of endosomal release of transduced proteins remains one of the critical issues for PTD-mediated transduction and further improvement of cytosolic delivery might greatly enhance the therapeutic potential of this approach.

ACKNOWLEDGMENTS

The authors and some of their work described in this article were supported by grants from the NIH (NS34152 and NS45038) and by the U.S. Department of Defense (DAMD 17-99-1-9483).

REFERENCES

Asoh, S., Ohsawa, I., Mori, T., Katsura, K., Hiraide, T., Katayama, Y., Kimura, M., Ozaki, D., Yamagata, K., and Ohta, S. (2002). *Proc. Natl. Acad. Sci. U.S.A.* **99**, 17107–17112.

Bandtlow, C. E., and Zimmermann, D. R. (2000). *Physiol. Rev.* **80**, 1267–1290.

Basso, E., Fante, L., Fowlkes, J., Petronilli, V., Forte, M. A., and Bernardi, P. (2005). *J. Biol. Chem.* [Epub ahead of print].

Belting, M., Mani, K., Jonsson, M., Cheng, F., Sandgren, S., Jonsson, S., Ding, K., Delcros, J. G., and Fransson, L. A. (2003). *J. Biol. Chem.* **278**, 47181–47189.

Bolton, S. J., Jones, D. N., Darker, J. G., Eggleston, D. S., Hunter, A. J., and Walsh, F. S. (2000). *Eur. J. Neurosci.* **12**, 2847–2855.

Cantara, S., Donnini, S., Giachetti, A., Thorpe, P. E., and Ziche, M. (2004). *J. Vasc. Res.* **41**, 202–207.

Cao, G., Pei, W., Ge, H., Liang, Q., Luo, Y., Sharp, F. R., Lu, A., Ran, R., Graham, S. H., and Chen, J. (2002). *J. Neurosci.* **22**, 5423–5431.

Caron, N. J., Quenneville, S. P., and Tremblay, J. P. (2004). *Biochem. Biophys. Res. Commun.* **319**, 12–20.

Chen, J., Graham, S. H., Chan, P. H., Lan, J., Zhou, R. L., and Simon, R. P. (1995). *Neuroreport* **6**, 394–398.

Chen, J., Simon, R. P., Nagayama, T., Zhu, R., Loeffert, J. E., Watkins, S. C., and Graham, S. H. (2000). *J. Cereb. Blood Flow Metab.* **20**, 1033–1039.

Chen, L., Willis, S. N., Wei, A., Smith, B. J., Fletcher, J. I., Hinds, M. G., Colman, P. M., Day, C. L., Adams, J. M., and Huang, D. C. (2005). *Mol. Cell* **17**, 393–403.

Chen, M., Won, D. J., Krajewski, S., and Gottlieb, R. A. (2002). *J. Biol. Chem.* **277**, 29181–29186.

Cho, Y. W., Kim, J. D., and Park, K. (2003). *J. Pharm. Pharmacol.* **55**, 721–734.
Dalkara, D., Zuber, G., and Behr, J. P. (2004). *Mol. Ther.* **9**, 964–969.
Derossi, D., Joliot, A. H., Chassaing, G., and Prochiantz, A. (1994). *J. Biol. Chem.* **269**, 10444–10450.
Deshayes, S., Heitz, A., Morris, M. C., Charnet, P., Divita, G., and Heitz, F. (2004). *Biochemistry* **43**, 1449–1457.
Dietz, G. P., and Bahr, M. (2004). *Mol. Cell Neurosci.* **27**, 85–131.
Dietz, G. P., Kilic, E., and Bahr, M. (2002). *Mol. Cell Neurosci.* **21**, 29–37.
Dom, G., Shaw-Jackson, C., Matis, C., Bouffioux, O., Picard, J. J., Prochiantz, A., Mingeot-Leclercq, M. P., Brasseur, R., and Rezsohazy, R. (2003). *Nucleic Acids Res.* **31**, 556–561.
Drin, G., Cottin, S., Blanc, E., Rees, A. R., and Temsamani, J. (2003). *J. Biol. Chem.* **278**, 31192–31201.
Eguchi, A., Akuta, T., Okuyama, H., Senda, T., Yokoi, H., Inokuchi, H., Fujita, S., Hayakawa, T., Takeda, K., Hasegawa, M., and Nakanishi, M. (2001). *J. Biol. Chem.* **276**, 26204–26210.
Ellerby, L. M., Ellerby, H. M., Park, S. M., Holleran, A. L., Murphy, A. N., Fiskum, G., Kane, D. J., Testa, M. P., Kayalar, C., and Bredesen, D. E. (1996). *J. Neurochem.* **67**, 1259–1267.
Elliott, G., and O'Hare, P. (1997). *Cell* **88**, 223–233.
Embury, J., Klein, D., Pileggi, A., Ribeiro, M., Jayaraman, S., Molano, R. D., Fraker, C., Kenyon, N., Ricordi, C., Inverardi, L., and Pastori, R. L. (2001). *Diabetes* **50**, 1706–1713.
Fawell, S., Seery, J., Daikh, Y., Moore, C., Chen, L. L., Pepinsky, B., and Barsoum, J. (1994). *Proc. Natl. Acad. Sci. U.S.A.* **91**, 664–668.
Ferber, D. (2001). *Science* **294**, 1638–1642.
Fischer, R., Kohler, K., Fotin-Mleczek, M., and Brock, R. (2004). *J. Biol. Chem.* **279**, 12625–12635.
Fiskum, G., Polster, B. M., and Kowaltowski, A. J. (2000). In *Pharmacology of Cerebral Ischemia 2000* (Krieglstein, J., and Klumpp, S., eds.), Medpharm Scientific Publishers, Stuttgart.
Fittipaldi, A., Ferrari, A., Zoppe, M., Arcangeli, C., Pellegrini, V., Beltram, F., and Giacca, M. (2003). *J. Biol. Chem.* **278**, 34141–34149.
Frankel, A. D., and Pabo, C. O. (1988). *Cell* **55**, 1189–1193.
Fuki, I. V., Meyer, M. E., and Williams, K. J. (2000). *Biochem. J.* **351**, 607–612.
Futaki, S. (2002). *Int. J. Pharm.* **245**, 1–7.
Green, M., and Loewenstein, P. M. (1988). *Cell* **55**, 1179–1188.
Guo, B., Zhai, D., Cabezas, E., Welsh, K., Nouraini, S., Satterthwait, A. C., and Reed, J. C. (2003). *Nature* **423**, 456–461.
Hakansson, S., Jacobs, A., and Caffrey, M. (2001). *Protein Sci.* **10**, 2138–2139.
Hashimoto, Y., Ito, Y., Niikura, T., Shao, Z., Hata, M., Oyama, F., and Nishimoto, I. (2001). *Biochem. Biophys. Res. Commun.* **283**, 460–468.
Hata, R., Gillardon, F., Michaelidis, T. M., and Hossmann, K. A. (1999). *Metab. Brain Dis.* **14**, 117–124.
Henriques, S. T., and Castanho, M. A. (2004). *Biochemistry* **43**, 9716–9724.
Hockenbery, D. M., Oltvai, Z. N., Yin, X. M., Milliman, C. L., and Korsmeyer, S. J. (1993). *Cell* **75**, 241–251.
Holinger, E. P., Chittenden, T., and Lutz, R. J. (1999). *J. Biol. Chem.* **274**, 13298–13304.
Ichinose, M., Liu, X. H., Hagihara, N., and Youle, R. J. (2002). *Cancer Res.* **62**, 1433–1438.
Ignatovich, I. A., Dizhe, E. B., Pavlotskaya, A. V., Akifiev, B. N., Burov, S. V., Orlov, S. V., and Perevozchikov, A. P. (2003). *J. Biol. Chem.* **278**, 42625–42636.
Jia, H., Lohr, M., Jezequel, S., Davis, D., Shaikh, S., Selwood, D., and Zachary, I. (2001). *Biochem. Biophys. Res. Commun.* **283**, 469–479.
Joliot, A., and Prochiantz, A. (2004). *Nat. Cell Biol.* **6**, 189–196.
Jurgensmeier, J. M., Xie, Z., Deveraux, Q., Ellerby, L., Bredesen, D., and Reed, J. C. (1998). *Proc. Natl. Acad. Sci. U.S.A.* **95**, 4997–5002.
Kane, D. J., Ord, T., Anton, R., and Bredesen, D. E. (1995). *J. Neurosci. Res.* **40**, 269–275.
Kaplan, I. M., Wadia, J. S., and Dowdy, S. F. (2005). *J. Control Release* **102**, 247–253.
Kaufmann, J. A., Bickford, P. C., and Taglialatela, G. (2001). *J. Neurochem.* **76**, 1099–1108.
Kilic, E., Dietz, G. P., Hermann, D. M., and Bahr, M. (2002). *Ann. Neurol.* **52**, 617–622.
Korsmeyer, S. J., Shutter, J. R., Veis, D. J., Merry, D. E., and Oltvai, Z. N. (1993). *Semin. Cancer Biol.* **4**, 327–332.
Kowaltowski, A. J., Fenton, R. G., and Fiskum, G. (2004). *Free Radic. Biol. Med.* **37**, 1845–1853.
Kowaltowski, A. J., Vercesi, A. E., and Fiskum, G. (2000). *Cell Death Differ.* **7**, 903–910.
Kramer, S. D., and Wunderli-Allenspach, H. (2003). *Biochim. Biophys. Acta* **1609**, 161–169.
Letai, A., Bassik, M. C., Walensky, L. D., Sorcinelli, M. D., Weiler, S., and Korsmeyer, S. J. (2002). *Cancer Cell* **2**, 183–192.
Linnik, M. D., Zahos, P., Geschwind, M. D., and Federoff, H. J. (1995). *Stroke* **26**, 1670–1674.
Liu, X. H., Castelli, J. C., and Youle, R. J. (1999). *Proc. Natl. Acad. Sci. U.S.A.* **96**, 9563–9567.
Liu, Y., Jones, M., Hingtgen, C. M., Bu, G., Laribee, N., Tanzi, R. E., Moir, R. D., Nath, A., and He, J. J. (2000). *Nat. Med.* **6**, 1380–1387.
Luciano, F., Zhai, D., Zhu, X., Bailly-Maitre, B., Ricci, J. E., Satterthwait, A., and Reed, J. C. (2005). *J. Biol. Chem.* **280**, 15825–15835.
Lundberg, M., Wikstrom, S., and Johansson, M. (2003). *Mol. Ther.* **8**, 143–150.
Maiolo, J. R., Ottinger, E. A., and Ferrer, M. (2004). *J. Am. Chem. Soc.* **126**, 15376–15377.
Mann, D. A., and Frankel, A. D. (1991). *EMBO J.* **10**, 1733–1739.
Martinou, J. C., Dubois-Dauphin, M., Staple, J. K., Rodriguez, I., Frankowski, H., Missotten, M., Albertini, P., Talabot, D., Catsicas, S., and Pietra, C. (1994). *Neuron* **13**, 1017–1030.
Matsushita, M., Noguchi, H., Lu, Y. F., Tomizawa, K., Michiue, H., Li, S. T., Hirose, K., Bonner-Weir, S., and Matsui, H. (2004). *FEBS Lett.* **572**, 221–226.
Merry, D. E., and Korsmeyer, S. J. (1997). *Annu. Rev. Neurosci.* **20**, 245–267.
Michiue, H., Tomizawa, K., Wei, F. Y., Matsushita, M., Lu, Y. F., Ichikawa, T., Tamiya, T., Date, I., and Matsui, H. (2005). *J. Biol. Chem.* **280**, 8285–8289.
Mitchell, D. J., Kim, D. T., Steinman, L., Fathman, C. G., and Rothbard, J. B. (2000). *J. Pept. Res.* **56**, 318–325.
Morris, M. C., Depollier, J., Mery, J., Heitz, F., and Divita, G. (2001). *Nat. Biotechnol.* **19**, 1173–1176.
Murphy, A. N., Bredesen, D. E., Cortopassi, G., Wang, E., and Fiskum, G. (1996a). *Proc. Natl. Acad. Sci. U.S.A.* **93**, 9893–9898.
Murphy, A. N., and Fiskum, G. (1999). *Biochem. Soc. Symp.* **66**, 33–41.
Murphy, A. N., Myers, K. M., and Fiskum, G. (1996b). In *Pharmacology of Cerebral Ischemia* (Krieglstein, J., ed.), Wissenschaftliche Verlugsgesellschaft, Stuttgart, Germany, pp. 163–172.
Myers, K. M., Fiskum, G., Liu, Y., Simmens, S. J., Bredesen, D. E., and Murphy, A. N. (1995). *J. Neurochem.* **65**, 2432–2440.
Nakagawa, T., Shimizu, S., Watanabe, T., Yamaguchi, O., Otsu, K., Yamagata, H., Inohara, H., Kubo, T., and Tsujimoto, Y. (2005). *Nature* **434**, 652–658.
Nakase, I., Niwa, M., Takeuchi, T., Sonomura, K., Kawabata, N., Koike, Y., Takehashi, M., Tanaka, S., Ueda, K., Simpson, J. C., Jones, A. T., Sugiura, Y., and Futaki, S. (2004). *Mol. Ther.* **10**, 1011–1022.
Nichols, B. J., and Lippincott-Schwartz, J. (2001). *Trends Cell Biol.* **11**, 406–412.
O'Neill, J., Manion, M., Schwartz, P., and Hockenbery, D. M. (2004). *Biochim. Biophys. Acta* **1705**, 43–51.
Ozaki, D., Sudo, K., Asoh, S., Yamagata, K., Ito, H., and Ohta, S. (2004). *Biochem. Biophys. Res. Commun.* **313**, 522–527.
Palade, G. E. (1953). *J. Appl. Phys.* **24**, 1424–1436.
Petros, A. M., Olejniczak, E. T., and Fesik, S. W. (2004). *Biochim. Biophys. Acta* **1644**, 83–94.

Polster, B. M., Kinnally, K. W., and Fiskum, G. (2001). *J. Biol. Chem.* **276**, 37887–37894.
Potocky, T. B., Menon, A. K., and Gellman, S. H. (2003). *J. Biol. Chem.* **278**, 50188–50194.
Razani, B., Woodman, S. E., and Lisanti, M. P. (2002). *Pharmacol. Rev.* **54**, 431–467.
Reed, J. C. and Pellecchia, M. (2005). *Blood* [Epub ahead of print], 2004–2007.
Richard, J. P., Melikov, K., Brooks, H., Prevot, P., Lebleu, B., and Chernomordik, L. V. (2005). *J. Biol. Chem.* **280**, 15300–15306.
Richard, J. P., Melikov, K., Vives, E., Ramos, C., Verbeure, B., Gait, M. J., Chernomordik, L. V., and Lebleu, B. (2003). *J. Biol. Chem.* **278**, 585–590.
Ryser, H. J., Shen, W. C., and Merk, F. B. (1978). *Life Sci.* **22**, 1253–1260.
Sawada, M., Hayes, P., and Matsuyama, S. (2003). *Nat. Cell Biol.* **5**, 352–357.
Schendel, S. L., Montal, M., and Reed, J. C. (1998). *Cell Death Differ.* **5**, 372–380.
Schwarze, S. R., Ho, A., Vocero-Akbani, A., and Dowdy, S. F. (1999). *Science* **285**, 1569–1572.
Sengoku, T., Bondada, V., Hassane, D., Dubal, S., and Geddes, J. W. (2004). *Exp. Neurol.* **188**, 161–170.
Shangary, S., and Johnson, D. E. (2002). *Biochemistry* **41**, 9485–9495.
Shimazaki, K., Urabe, M., Monahan, J., Ozawa, K., and Kawai, N. (2000). *Gene Ther.* **7**, 1244–1249.
Shimizu, S., Konishi, A., Kodama, T., and Tsujimoto, Y. (2000). *Proc. Natl. Acad. Sci. U.S.A.* **97**, 3100–3105.
Shimizu, S., Nagayama, T., Jin, K. L., Zhu, L., Loeffert, J. E., Watkins, S. C., Graham, S. H., and Simon, R. P. (2001). *J. Cereb. Blood Flow Metab.* **21**, 233–243.
Sik, E. W., Won, K. D., Koo, H. I., Yoo, K. Y., Kang, T. C., Ho, J. S., Soon, C. H., Hyun, C. S., Hoon, K. Y., Young, K. S., Yil, K. H., Hoon, K. J., Kwon, O. S., Cho, S. W., Soo, L. K., Park, J., Ho, W. M., and Young, C. S. (2004). *Free Radic. Biol. Med.* **37**, 1656–1669.
Stenmark, H., Moskaug, J. O., Madshus, I. H., Sandvig, K., and Olsnes, S. (1991). *J. Cell Biol.* **113**, 1025–1032.
Sugioka, R., Shimizu, S., Funatsu, T., Tamagawa, H., Sawa, Y., Kawakami, T., and Tsujimoto, Y. (2003). *Oncogene* **22**, 8432–8440.
Suzuki, T., Futaki, S., Niwa, M., Tanaka, S., Ueda, K., and Sugiura, Y. (2002). *J. Biol. Chem.* **277**, 2437–2443.
Takeshima, K., Chikushi, A., Lee, K. K., Yonehara, S., and Matsuzaki, K. (2003). *J. Biol. Chem.* **278**, 1310–1315.
Tyagi, M., Rusnati, M., Presta, M., and Giacca, M. (2001). *J. Biol. Chem.* **276**, 3254–3261.
Vendeville, A., Rayne, F., Bonhoure, A., Bettache, N., Montcourrier, P., and Beaumelle, B. (2004). *Mol. Biol. Cell* **15**, 2347–2360.
Violini, S., Sharma, V., Prior, J. L., Dyszlewski, M., and Piwnica-Worms, D. (2002). *Biochemistry* **41**, 12652–12661.
Vives, E., Brodin, P., and Lebleu, B. (1997). *J. Biol. Chem.* **272**, 16010–16017.
Wadia, J. S., and Dowdy, S. F. (2003). *Curr. Protein Pept. Sci.* **4**, 97–104.
Wadia, J. S., Stan, R. V., and Dowdy, S. F. (2004). *Nat. Med.* **10**, 310–315.
Walensky, L. D., Kung, A. L., Escher, I., Malia, T. J., Barbuto, S., Wright, R. D., Wagner, G., Verdine, G. L., and Korsmeyer, S. J. (2004). *Science* **305**, 1466–1470.
Wei, M. C., Zong, W. X., Cheng, E. H., Lindsten, T., Panoutsakopoulou, V., Ross, A. J., Roth, K. A., MacGregor, G. R., Thompson, C. B., and Korsmeyer, S. J. (2001). *Science* **292**, 727–730.
Wender, P. A., Mitchell, D. J., Pattabiraman, K., Pelkey, E. T., Steinman, L., and Rothbard, J. B. (2000). *Proc. Natl. Acad. Sci. U.S.A.* **97**, 13003–13008.
Yamaguchi, H., and Wang, H. G. (2002). *J. Biol. Chem.* **277**, 41604–41612.
Yang, J. C., Kahn, A., and Cortopassi, G. (2000). *Toxicology* **151**, 65–72.
Zamzami, N., and Kroemer, G. (2001). *Nat. Rev. Mol. Cell Biol.* **2**, 67–71.
Zaro, J. L., and Shen, W. C. (2003). *Biochem. Biophys. Res. Commun.* **307**, 241–247.
Zhai, D., Luciano, F., Zhu, X., Guo, B., Satterthwait, A. C., and Reed, J. C. (2005). *J. Biol. Chem.* **280**, 15815–15824.
Ziegler, A., Blatter, X. L., Seelig, A., and Seelig, J. (2003). *Biochemistry* **42**, 9185–9194.
Ziegler, A., Nervi, P., Durrenberger, M., and Seelig, J. (2005). *Biochemistry* **44**, 138–148.

Queries to Publisher:

P1. Pub: Please provide received and accepted date in this article.

Journal of Neurochemistry, 2005, **92**, 388–394 doi:10.1111/j.1471-4159.2004.02873.x

Calcium-dependent dephosphorylation of brain mitochondrial calcium/cAMP response element binding protein (CREB)

Rosemary A. Schuh,*,† Tibor Kristián* and Gary Fiskum*,†

*Department of Anesthesiology and †Toxicology Program, University of Maryland School of Medicine, Baltimore, Maryland, USA

Abstract

Calcium-mediated signaling regulates nuclear gene transcription by calcium/cAMP response element binding protein (CREB) via calcium-dependent kinases and phosphatases. This study tested the hypothesis that CREB is also present in mitochondria and subject to dynamic calcium-dependent modulation of its phosphorylation state. Antibodies to CREB and phosphorylated CREB (pCREB) were used to demonstrate the presence of both forms in isolated mitochondria and mitoplasts from rat brain. When energized mitochondria were exposed to increasing concentrations of Ca^{2+} in the physiological range, pCREB was lost while total CREB remained constant. In the presence of Ru360, an inhibitor of the mitochondrial Ca^{2+} uptake uniporter, calcium-dependent loss of pCREB levels was attenuated, suggesting that intramitochondrial calcium plays an important role in pCREB dephosphorylation. pCREB dephosphorylation was not, however, inhibited by the phosphatase inhibitors okadaic acid and Tacrolimus. In the absence of Ca^{2+}, CREB phosphorylation was elevated by the addition of ATP to the mitochondrial suspension. Exposure of mitochondria to the pore-forming molecule alamethicin that causes osmotic swelling and release of intermembrane proteins enriched mitochondrial pCREB immunoreactivity. These results further suggest that mitochondrial CREB is located in the matrix or inner membrane and that a kinase and a calcium-dependent phosphatase regulate its phosphorylation state.

Keywords: adenosine triphosphate, kinase, phosphatase, transcription.

J. Neurochem. (2005) **92,** 388–394.

Calcium-mediated signaling cascades play an important role in many cellular processes, including secretion of certain neurotransmitters and hormones, cell cycle control and muscle contraction. Regulation of these signaling cascades by Ca^{2+} is often as a result of activation of kinases, including protein kinase C (PKC) and calmodulin kinase (CAMK). Conversely, activation of phosphatases by Ca^{2+} also results in altering the balance of phosphorylated and non-phosphorylated target proteins. The Ca^{2+}/cAMP response element binding protein (CREB) has been identified in several studies as a downstream target of Ca^{2+}-mediated signaling events (Hahm *et al*. 2003; Mantelas *et al*. 2003).

Ca^{2+} regulates CREB-mediated signaling via activation of Ca^{2+}-dependent kinases or by Ca^{2+}-dependent phosphatases. The phosphorylation of CREB at a specific serine residue (Ser133) is the pivotal event regulating CREB's ability to modulate nuclear gene transcription. CREB activation requires phosphorylation by kinases including cAMP stimulated protein kinase A (PKA), PKC, ribosomal S6 kinase ($pp90^{RSK}$), CAMK, and mitogen-activated protein kinases (MAPK) (Ginty *et al*. 1994; de Groot *et al*. 1993; Brindle *et al*. 1995; Tan *et al*. 1996; Xing *et al*. 1998). Once phosphorylated, CREB forms a dimer via a conserved heptad repeat of leucine residues at the C-terminus then associates with CREB binding protein, which recruits and stabilizes RNA polymerase II, forming a transcription complex at the cAMP response element (CRE), an 8-bp motif 5′-TGACGTCA-3′ (Shaywitz and Greenberg 1999). Dephosphorylation of CREB by several phosphatases, including calcineurin, PP1, and PP2A, result in CREB

Received May 26, 2004; revised manuscript received August 5, 2004 accepted September 13, 2004.

Address correspondence and reprint requests to Dr Gary Fiskum, Department of Anesthesiology, 685 W. Baltimore Street, MSTF 5–34, Baltimore, Maryland 21201, USA. E-mail: gfisk001@umaryland.edu

Abbreviations used: CAMK, calmodulin kinase; COX, cytochrome *c* oxidase; CRE, cAMP response element; CREB, calcium/cAMP response element binding protein; CsA, cyclosporin A; Cyt *c*, cytochrome *c*; FK506, Tacrolimus; MAPK, mitogen-activated protein kinase; OA, okadaic acid; pCREB, phosphorylated calcium/cAMP response element binding protein; PKA, cAMP stimulated protein kinase A; PKC, protein kinase C; $pp90^{RSK}$, ribosomal S6 kinase.

returning to an inactive state (Choe *et al*. 2004; Zheng *et al*. 2004). Thus, the ratio of non-phosphorylated CREB to phosphorylated CREB (pCREB) becomes critical in maintaining a homeostatic cellular environment, not only physiologically, but also under pathological conditions including lack of neurotrophins or mitogens (Riccio *et al*. 1999), ischemia/reperfusion injury (Hu *et al*. 1999; Jin *et al*. 2001; Tanaka 2001) and other paradigms involving oxidative stress (Bedogni *et al*. 2003).

Most CREB studies, which included immunostaining of cells and immunoblotting of subcellular fractions, indicate that CREB is almost exclusively nuclear (Waeber and Habener 1991; Ginty *et al*. 1993). However, electron micrroscopy, gel shift and western blotting studies also identified the presence of CREB in rat brain mitochondria (Cammarota *et al*. 1999). While the functional significance of mitochondrial CREB is at this juncture unknown, preliminary evidence suggests that it is involved in regulation of mitochondrial gene expression (Ryu *et al.* Society for Neuroscience abstract, 2003). If transcription of one or more mitochondrial genes is regulated by CREB, mitochondrial CREB phosphorylation state would likely be regulated by Ca^{2+} and/or cAMP.

Intramitochondrial Ca^{2+} is known to regulate several mitochondrial metabolic enzymes, either directly or indirectly, via phosphorylation/dephosphorylation and responds to both physiological and pathological changes in cytosolic Ca^{2+} through Ca^{2+} influx and efflux pathways (for review see McCormack *et al*. 1990). This study tested the hypothesis that the phosphorylation state of mitochondrial CREB is regulated by extramitochondrial [Ca^{2+}] in the physiological range and that this signal pathway is transduced through the mitochondrial Ca^{2+} uniport uptake mechanism.

Materials and methods

All reagents were purchased from Sigma (St Louis, MO, USA) unless otherwise stated.

Mitochondrial isolation

Forebrains removed from adult male Sprague–Dawley rats were rapidly dissected then further processed to isolate mitochondria using the percoll isolation method described by Sims (1990). Briefly, following decapitation the forebrain was rapidly removed and placed in ice-cold mannitol-sucrose (MS) buffer pH 7.4 (225 mM mannitol, 75 mM sucrose, 5 mM Hepes, 1 mM EGTA). The brain was homogenized then centrifuged twice at 1317 *g* for 3 min. Following a further 10-min centrifugation at 21 074 *g,* the pellet was re-suspended in 15% percoll (Amersham Biosciences, Piscataway, NJ, USA) then layered on a discontinuous percoll gradient and spun at 29 718 *g* for 8 min. The mitochondrial fraction was re-suspended in MS buffer containing 1 mg/mL BSA and centrifuged at 16 599 *g* for 10 min, then again at 6668 *g* for 10 min. The mitochondrial pellet was re-suspended in MS buffer without bovine serum albumin (BSA) or EGTA. Protein concentrations were determined by the Biuret method.

Mitoplast preparation

Isolated rat brain mitochondria (approximately 50 mg protein/mL) were diluted 1 : 1 with 12 mg/mL digitonin (Spectrum Chemical, Gardena, CA, USA) in MS isolation buffer and incubated for 20 min at 4°. The digitonin-treated mitochondria were diluted 1 : 4 in KCl buffer pH 7.0 (125 mM KCl ultrapure (Merck, Whitehouse Station, NJ, USA), 20 mM Hepes, 2 mM K_2HPO_4, 0.01 mM EGTA, 5 mM malate, 5 mM glutamate, 1 mM $MgCl_2$, 3 mM ATP) and gently homogenized, then centrifuged at 18 522 *g* for 10 min at 4°. The supernatant was retained and the pellet re-suspended in KCl buffer then centrifuged at 18 522 *g* for 10 min. The pellet was re-suspended in KCl buffer and all fractions stored at −70° until utilized for western blot.

Western blot procedure

Isolated mitochondria were treated with 50 mM dithiothreitol (DTT) and NuPage 4 × LDS loading buffer (Invitrogen, Carlsbad, CA, USA) prior to heating at 70° for 10 min. The samples were rapidly centrifuged at 4° prior to separation by sodium dodecyl sulfate – polyacrylamide gel electrophresis (SDS–PAGE). Each lane was loaded with 25 μg of total protein, which was determined in separate studies to be in the linear range of the protein–immunoblot optical density relationship. Immunoblotting was performed as recommended by the manufacturers of the antibodies. Polyclonal rabbit anti-phospho-CREB (pCREB) and anti-CREB were purchased from Upstate Biotechnology (Lake Placid, NY, USA). Polyclonal rabbit anti-pCREB and anti-histone H3 were purchased from Cell Signaling Technology (Beverly, MA, USA). Cytochrome *c* oxidase subunit I (COX) monoclonal antibody was purchased from Molecular Probes (Eugene, OR, USA). Cytochrome *c* (Cyt *c*) monoclonal antibody was purchased from BD Biosciences (San Diego, CA, USA). Immunoreactivity was detected using the appropriate peroxidase-linked secondary antibody and enhanced chemiluminescence detection reagent purchased from Amersham Biosciences. Following detection of pCREB protein, membranes were stripped using Restore™ (Pierce, Rockford, IL, USA). The stripped membranes were re-probed with antibodies to COX, CREB, Cyt *c*, or histone H3. Optical densities of individual bands were quantified after subtraction of background levels of film exposure using the GelExpert software program (Nucleotech, San Carlos, CA, USA).

Enzyme-linked-immuno-sorbent assay (ELISA)

Mitochondrial samples previously assayed for immunoreactivity via western blot were also reassessed using an ELISA kit (BioSource International, Camarillo, CA, USA) that recognized pCREB phosphorylated at Ser133. pCREB levels were determined according to the manufacturer's protocol.

Calcium-uptake assay

Freshly isolated rat brain mitochondria (0.25 mg/mL protein) in the presence of the fluorescent dye Fura 6F potassium salt (250 nM) purchased from Molecular Probes, were incubated with buffer (pH 7.0) 125 mM KCl, 20 mM Hepes, 2 mM KH_2PO_4, 1.0 μM EGTA, 5 mM malate, 5 mM glutamate, and 1 mM $MgCl_2$. A further 3 mM $MgCl_2$, 3 mM ATP and 20–400 μM Ca^{2+} were added to the cuvette, then the calcium concentrations in the buffer surrounding the mitochondria were measured for 5–10 min on an FL-2500 fluorescence spectrophotometer (Hitachi, Japan). The excitation

wavelength for bound calcium was 340 nm and 380 nm for unbound calcium and the emission wavelength was 510 nm. Samples were then centrifuged at 18 522 *g* for 3 min and the pellet re-suspended in lysis buffer (pH 7.4) containing 0.5% non-idet p-40, 1% Triton X-100, 150 mM NaCl and 10 mM Tris. The aliquots were stored at −70° until western blotting or ELISA were performed.

Statistical analysis

Ca^{2+} uptake data are expressed as the mean ± SE and the statistical significance was determined by one-way ANOVA with the Tukey *post hoc* test. Statistical significance was assumed as $p < 0.05$. Results from tests on the effects of ATP and alamethicin are expressed as the mean ± SE and the statistical significance determined by Student *t*-test.

Results

Isolated rat brain mitochondria and mitoplasts possess phosphorylated CREB (pCREB) immunoreactivity

Isolated mitochondria from rat brain were analyzed by western blot using an antibody specific for CREB phosphorylated at Ser133 (pCREB). A strong band was revealed at 43 kDa with a less prominent band at 32 kDa in the mitochondrial extract. The band at 32 kDa likely represents cross reactivity to phospho-ATF1 (pATF1), as reported earlier (Huang *et al*. 2001). The brain homogenate at a protein level equivalent to that of isolated mitochondria exhibited a relatively weaker band at 43 kDa (Fig. 1a). The blots were then stripped and re-probed for the nuclear specific marker histone H3 to assess nuclear contamination of the mitochondrial separation. The brain homogenate extract had a very strong band at 17 kDa (Fig. 1a), whereas the mitochondrial extract had no detectable signal indicating a lack of nuclear contamination. Similar samples that were probed with histone H3 antibody then stripped and re-probed for pCREB yielded the same results (data not shown).

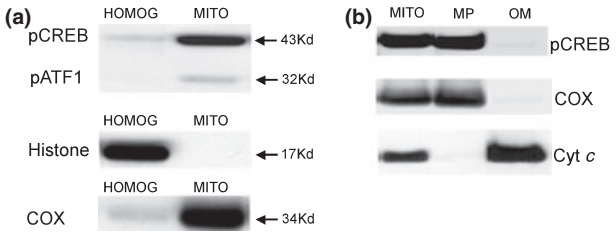

Fig. 1 pCREB immunoreactivity in rat forebrain homogenates, isolated mitochondria. (a) Brain homogenates and isolated non-synaptosomal brain mitochondria were treated with lysis buffer. Samples (25 μg protein) were applied to each lane of the electrophoresis gel. Immunoblots for pCREB (top), the nuclear marker histone H3 (middle), and the mitochondrial inner membrane marker cytochrome *c* oxidase subunit I (COX, bottom) were performed. (b) Isolated non-synaptosomal brain mitochondria, mitoplasts and outer membrane fractions (25 μg protein) were electrophoretically separated then blotted for pCREB (top), COX (middle) and the intermembrane marker cytochrome *c* (Cyt *c*, bottom).

Membranes were also stripped and re-probed with the mitochondrial marker COX revealing strong immunoreactivity for the mitochondrial extract and a relatively light band in the brain homogenate (Fig. 1a). These results suggest that pCREB immunoreactivity is present in rat brain mitochondria, in accordance with an earlier study (Cammarota *et al*. 1999), and that these mitochondrial extracts are not contaminated with nuclear components.

To further assess the localization of mitochondrial pCREB, isolated rat brain mitochondria were treated with the steroid glycoside digitonin to remove the outer membrane (OM), intermembrane proteins, and peripheral inner membrane proteins, e.g. cytochrome *c*, creating mitoplasts consisting of inner membrane and matrix proteins. Analysis by western blotting for pCREB revealed a strong band at 43 kDa in the mitoplasts (MP), with a barely detectable signal in the supernatant (OM) (Fig. 1b). The blots were then stripped and re-probed for COX, revealing a similar distribution (Fig. 1b). Conversely, the blots were stripped and re-probed for the intermembrane-localized cytochrome *c* (Cyt *c*) revealing a very strong band in the OM fraction with a barely detectable band in the MP (Fig. 1b). Taken together, these results suggest that pCREB is localized in the inner membrane or in the matrix.

Accumulation of Ca^{2+} in isolated mitochondria decreases pCREB levels

Ca^{2+} has been identified as a potent inducer of signal transduction pathways that have CREB as a downstream target. We therefore next determined if addition of exogenous Ca^{2+} to freshly isolated rat brain mitochondria would affect CREB/pCREB immunoreactivity. Isolated brain mitochondria were incubated for 5 min at 37° in a KCl-based medium containing respiratory substrates, ATP, phosphate and Mg^{2+} in the presence or absence of 50 μM EGTA and either 0.8 or 1.6 μmol Ca^{2+}/mg protein. These conditions support the mitochondrial uptake and retention of over 2 μmol Ca^{2+}/mg mitochondrial protein (Chinopoulos *et al*. 2003). The suspensions were then centrifuged and the mitochondrial pellets frozen and stored at −70° in lysis buffer. The mitochondrial lysates were later electrophoretically separated and immunoblotted with antibodies specific to pCREB (Fig. 2a, upper panel) then stripped and re-probed with an antibody that recognizes CREB regardless of phosphorylation state (total CREB, Fig. 2a, lower panel). Densitometric analysis of the pCREB to CREB ratio data indicates a 68% decrease in pCREB levels in isolated mitochondria exposed to 1.6 μmol Ca^{2+}/mg mitochondrial protein as compared with basal pCREB levels (no addition). Conversely, there was a 250% increase in pCREB levels following exposure to 50 μM EGTA (Fig. 2b). As there was no consistent difference in total CREB immunoreactivity between the treatment groups (Fig. 2a, lower panel), the effect of exposure to Ca^{2+} or EGTA on pCREB is not because of an effect on total CREB

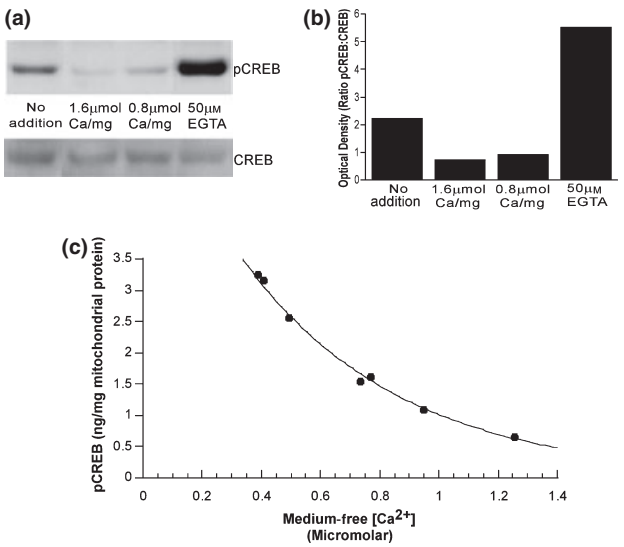

Fig. 2 pCREB and total CREB Immunoreactivity in brain mitochondria following incubation in the absence and presence of Ca^{2+}. (a) Representative immunoblots of mitochondrial lysates probed for pCREB (upper panel), then stripped and re-probed for total CREB (lower panel). (b) Optical density of bands from immunoblots (Fig. 2a) of mitochondrial lysates exposed to 50 μM EGTA or Ca^{2+} (0.8–1.6 μmol/mg mitochondrial protein). Data are expressed as the ratio of the pCREB : CREB optical densities and are representative of four separate experiments. (c) pCREB (ng/mg mitochondrial protein) as assessed by ELISA following exposure of isolated mitochondria to EGTA (1–101 μM). The medium free [Ca^{2+}] was determined from Fura 6F fluorescent measurements according to Grynkiewicz *et al.* (1985).

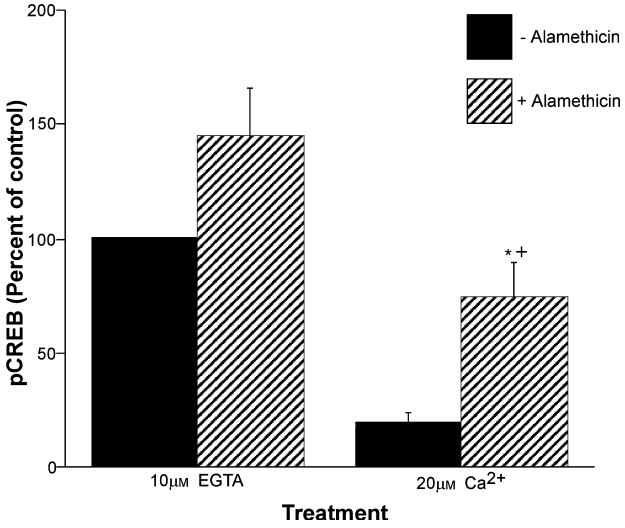

Fig. 3 Enrichment of pCREB by mitochondrial osmotic lysis. Mitochondria were incubated for 5 min in the presence of either EGTA (10 μM) or Ca^{2+} (20 μM) in the absence or presence of the pore-forming molecule alamethicin (80 μg/mL). Following centrifugation, mitochondrial pellets were analyzed for pCREB using ELISA. Data are expressed as the mean percentage of control values on each ELISA plate ± SE for $n = 3$–5 separate experiments. $^{+}$Significantly different ($p < 0.01$) from Ca^{2+} treatment alone; *significantly different ($p < 0.05$) from EGTA with alamethicin treatment.

protein levels. Subsequent measurements of pCREB utilized an enzyme-linked-immuno-sorbent assay (ELISA) specific for CREB phosphorylated at Ser133 as the results obtained with this convenient assay correlate well with those obtained using immunoblots (data not shown).

To further assess the effects of extramitochondrial [Ca^{2+}] at physiological, submicromolar concentrations, we exposed isolated rat brain mitochondria to medium containing concentrations of EGTA ranging from 1 to 101 μM. The initial medium free [Ca^{2+}] was measured using Fura 6F and calculated according to the method of Grynkiewicz *et al.* (1985). Analysis of the mitochondrial samples by ELISA indicates that mitochondrial pCREB is substantially reduced by increasing extramitochondrial Ca^{2+} in a physiological range of approximately 0.4–1.2 μM (Fig. 2c).

The effect of Ca^{2+} on pCREB phosphorylation state was also tested in the presence of the non-selective pore-forming molecule alamethicin (80 μg/mL) which causes osmotic swelling and equilibration of ions and small molecules across the mitochondrial inner membrane. Following incubation, the suspension was centrifuged and the mitochondrial pellet was used for ELISA measurements of pCREB. As in the absence of alamethicin, pCREB was significantly lower in the presence of Ca^{2+} compared with EGTA (Fig. 3). The additional finding that the ratio of pCREB to pellet protein was higher following alamethicin treatment is further evidence that pCREB is located on or within the mitochondrial inner membrane.

To investigate the potential dynamic regulation of Ca^{2+}-sensitive changes in the phosphorylation state of CREB, isolated respiring rat brain mitochondria were first exposed to EGTA (10 μM) and then incubated in the presence of excess Ca^{2+} (20 μM) to determine if CREB phosphorylation is reversible. As shown in Fig. 4, 5 min exposure to EGTA followed by 5 min exposure to Ca^{2+} resulted in a loss of CREB phosphorylation that was essentially as great as a 10 min exposure to Ca^{2+}.

Inhibition of the mitochondrial Ca^{2+} uniporter attenuates Ca^{2+}-dependent pCREB loss

Ca^{2+} and other divalent cations enter the mitochondrial matrix via a uniporter that can be blocked by RU360, a derivative of ruthenium red (Matlib *et al.* 1998). To assess the role of intramitochondrial Ca^{2+} in altering mitochondrial pCREB levels, isolated rat brain mitochondria were exposed to 500 nM RU360 in the absence or presence of 20 μM Ca^{2+}. RU360 inhibited the mitochondrial uptake of exogenous Ca^{2+} from the medium, as measured using the fluorimetric Ca^{2+} indicator Fura 6F (Fig. 5a). At the end of these

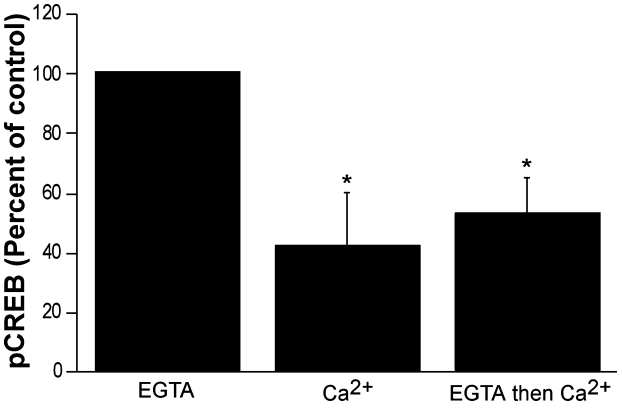

Fig. 4 Calcium-induced pCREB dephosphorylation following EGTA-induced phosphorylation. Mean pCREB levels as assessed by ELISA following exposure of isolated mitochondria to EGTA (10 μM) or Ca^{2+} (20 μM) alone, or addition of Ca^{2+} after 5 min of EGTA treatment. Data are expressed as a percentage of the control values (EGTA) on each ELISA plate. Each bar is the mean of four to five separate experiments; error bars are SEM. *Significantly different ($p < 0.05$) from control.

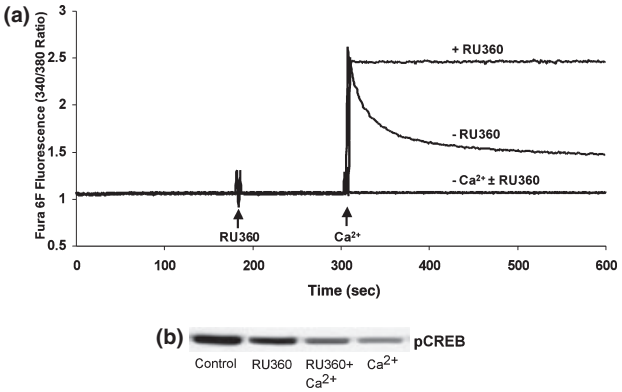

Fig. 5 Effect of mitochondrial calcium uptake inhibition on pCREB. (a) Fura 6F fluorescent recordings of the ambient free [Ca^{2+}] in the standard reaction medium containing isolated rat brain mitochondria (0.25 mg/mL), in the presence of the oxidizable substrates malate (5 mM) plus glutamate (5 mM) plus ATP (3 mM). The medium contained either EGTA (10 μM) or Ca^{2+} (20 μM) ± the mitochondrial Ca^{2+} uptake inhibitor RU360 (500 nM). (b) Typical immunoblot of pCREB in mitochondrial pellets obtained following centrifugation of suspensions as shown in (a), representative of three separate experiments.

measurements, the mitochondrial suspensions were centrifuged and the pellets used for immunoblot analysis of pCREB. The presence of RU360 partially inhibited the loss of pCREB immunoreactivity caused by exposure to Ca^{2+} (Fig. 5b). The inhibitory effect of RU360 on Ca^{2+}-induced dephosphorylation may be partially masked by the small decrease in pCREB levels caused by exposure to RU360 in the absence of Ca^{2+}.

Effect of exogenous ATP on mitochondrial pCREB

Mitochondrial CREB phosphorylation and its response to Ca^{2+} was measured in the absence and presence of ATP to further characterize the factors responsible for its regulation. Isolated rat brain mitochondria were exposed to either 10 or 1 μM EGTA or 20 μM Ca^{2+} in the presence or absence of 3 mM ATP. pCREB levels were approximately 70% lower ($p < 0.05$) in mitochondria exposed to EGTA in the absence of exogenous ATP compared with mitochondria exposed to EGTA in the presence of exogenous ATP (Table 1). Additionally, 20 μM Ca^{2+} without exogenous ATP decreased pCREB levels, although not significantly ($p = 0.07$) in mitochondria as compared with mitochondria exposed to Ca^{2+} in the presence of exogenous ATP (Table 1). Taken together, these results suggest that Ca^{2+}-sensitive decreases in mitochondrial pCREB levels may be as a result of activation of a Ca^{2+}-regulated phosphatase as such activity is not ATP dependent.

Effect of phosphatase inhibitors on Ca^{2+}-dependent loss of mitochondrial pCREB

To determine if the Ca^{2+}-sensitive reduction in mitochondrial pCREB immunoreactivity is because of Ca^{2+}-dependent phosphatase activity, experiments were performed in the presence of okadaic acid (OA, 10 nM), a broad spectrum phosphatase inhibitor, and Tacrolimus (FK506, 100 nM), an inhibitor of the Ca^{2+}-dependent phosphatase calcineurin. As expected, neither agent affected mitochondrial pCREB in the presence of EGTA (Fig. 6). These agents were, however, also ineffective at attenuating the Ca^{2+}-dependent loss of pCREB, as determined by ELISA (Fig. 6). Cyclosporin A (CsA, 1 μM), another inhibitor of calcineurin, was also not effective at reversing the Ca^{2+}-dependent loss of pCREB (data not shown).

Discussion

Our results confirm an earlier finding (Cammarota *et al.* 1999) that CREB and pCREB immunoreactivity is present in

Table 1 Mean pCREB values as assessed by ELISA of mitochondrial lysates in the presence or absence of ATP (3 mM) and EGTA (10 μM) or Ca^{2+} (20 μM)

	pCREB (ng/mg mitochondrial protein)	
	– ATP	+ ATP
10 μM EGTA	1.01 ± 0.32*	3.39 ± 0.90
No addition	0.77 ± 0.16	1.72 ± 0.42
20 μM Ca^{2+}	0.48 ± 0.08	0.83 ± 0.14

Data are expressed as mean ng pCREB/mg mitochondrial protein from four separate experiments ± SEM. *Significantly different ($p < 0.05$) from control (EGTA with ATP).

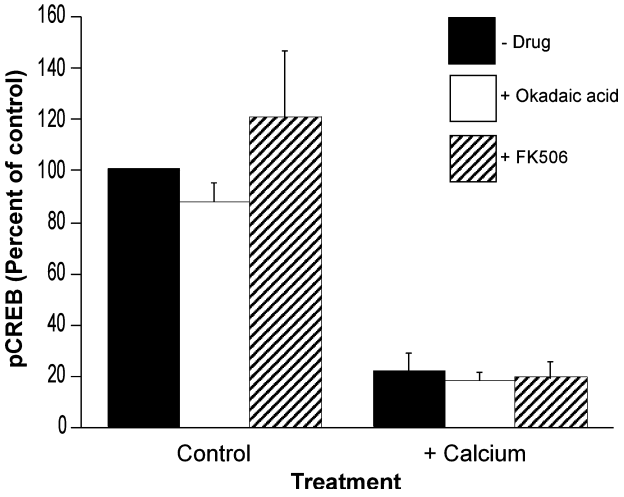

Fig. 6 Effect of phosphatase inhibitors on mitochondrial pCREB. Mitochondria were incubated for 5 min in the presence of either EGTA (10 μM) or Ca^{2+} (20 μM) in the absence or presence of okadaic acid (10 nM) or FK506 (100 nM). Following centrifugation, mitochondrial pellets were analyzed for pCREB using ELISA. Data are expressed as the mean percentage of control values on each ELISA plate ± SE for $n = 3$–12 separate experiments.

isolated mitochondria. Additionally, following digitonin permeabilization of mitochondria, we demonstrate that pCREB immunoreactivity is present in mitoplasts, but not outer membrane fractions that contain intermembrane-associated proteins (Fig. 1b), suggesting inner membrane or matrix localization of pCREB. Recent studies describe the mitochondrial localization of other proteins involved in transcriptional regulation, including NF-κB (Cogswell *et al*. 2003), estrogen receptor β (Yang *et al*. 2004) and Smad5 (Jullig and Stott 2003). These findings suggest that mitochondrial gene regulation may be controlled by a number of heretofore uncharacterized factors.

This study is the first to demonstrate that the phosphorylation state of mitochondrial CREB is sensitive to changes in extramitochondrial free [Ca^{2+}] in the physiological range. Blockade of the inner mitochondrial membrane uniporter by RU360 was shown in this study to attenuate, but not completely reverse, Ca^{2+}-sensitive loss of pCREB (Fig. 5b). Relatively small changes in intramitochondrial free Ca^{2+} levels would be sufficient to decrease pCREB levels based on our findings in this study (Fig. 2c). The incomplete inhibition of Ca^{2+}-dependent pCREB dephosphorylation could therefore be due to leakage of Ca^{2+} into the matrix.

The matrix localization of pCREB is further supported by the finding that pCREB is enriched in the mitochondrial pellet following the addition of alamethicin to the mitochondrial suspension (Fig. 3). Alamethicin releases mitochondrial intermembrane proteins e.g. cytochrome *c*, but many matrix proteins are retained following this treatment. The additional observation that sensitivity of pCREB dephosphorylation to Ca^{2+} is maintained in the presence of alamethicin indicates that the effect of Ca^{2+} is not because of its effects on mitochondrial bioenergetics or membrane permeability.

A partial CRE site has been demonstrated previously to be present in the regulatory D-loop of mitochondrial DNA (Ogita *et al*. 2002), indicating the potential for pCREB-induced mitochondrial gene transcription. Although at present a function for mitochondrial pCREB has not been elucidated, the possibility arises for mitochondrial pCREB to function as a transcription factor directly altering mitochondrial DNA or by cross-talk between the mitochondrion and the nucleus. Cross-talk between mitochondria and the nucleus as a result of cellular stress has been previously described (Biswas *et al*. 1999; Sawa 2001; Delsite *et al*. 2002). We estimate the mitochondrial pCREB contribution to total cellular pCREB is in the range of 15–20% based on relative levels of pCREB and COX immunoreactivity in the brain homogenates and isolated mitochondria (Fig. 1a). Mitochondrial pCREB therefore constitutes a significant fraction of total tissue pCREB in the rat brain.

It is well established that CREB plays a role in many diverse cellular activities, from cell growth and differentiation to apoptosis. In addition, neurodegenerative diseases, e.g. Alzheimer's and Huntington's diseases, and acute brain injury, have been associated with alterations in CREB-regulated gene expression. The finding that CREB is present in mitochondria, whose altered activities and gene expression are strongly implicated in these disorders, warrants further investigation into the role of mitochondrial CREB and its regulation by Ca^{2+} in both normal cell homeostasis and response to pathological stress.

Acknowledgements

This work was supported by National Institute of Environmental Health Sciences Grant ES07263 to RAS and NIH NS34152 and the US Army Medical Research and Material Command Neurotoxin Research Program Grant DAMD 17-99-1-9483 to GF.

References

Bedogni B., Pani G., Colavitti R., Riccio A., Borello S., Murphy M., Smith R., Eboli M. L. and Galeotti T. (2003) Redox regulation of cAMP-responsive element-binding protein and induction of manganese superoxide dismutase in nerve growth factor-dependent cell survival. *J. Biol. Chem.* **278**, 16 510–16 519.

Biswas G., Adebanjo O. A., Freedman B. D., Anandatheerthavarada H. K., Vijayasarathy C., Zaidi M., Kotlikoff M. and Avadhani N. G. (1999) Retrograde Ca^{2+} signaling in C2C12 skeletal myocytes in response to mitochondrial genetic and metabolic stress: a novel mode of inter-organelle crosstalk. *EMBO J.* **18**, 522–533.

Brindle P., Nakajima T. and Montminy M. (1995) Multiple protein kinase A-regulated events are required for transcriptional induction by cAMP. *Proc. Natl Acad. Sci. USA* **92**, 10 521–10 525.

Cammarota M., Paratcha G., Bevilaqua L., Levi de Stein M., Lopez M., Pellegrino de Iraldi A., Izquierdo I. and Medina J. H. (1999) Cyclic AMP-responsive element binding protein in brain mitochondria. *J. Neurochem.* **72**, 2272–2277.

Chinopoulos C., Starkov A. A. and Fiskum G. (2003) Cyclosporin A-insensitive permeability transition in brain mitochondria. *J. Biol. Chem.* **278**, 27 382–27 389.

Choe E. S., Parelkar N. K., Kim J. Y., Cho H. W., Kang H. S., Mao L. and Wang J. Q. (2004) The protein phosphatase 1/2A inhibitor okadaic acid increases CREB and Elk-1 phosphorylation and c-*fos* expression in the rat striatum *in vivo*. *J. Neurochem.* **89**, 383–390.

Cogswell P. C., Kashatus D. F., Keifer J. A., Guttridge D. C., Reuther J. Y., Bristow C., Roy S., Nicholson D. W. and Baldwin A. S. (2003) NF-κB and IκBα are found in the mitochondria. Evidence for regulation of mitochondrial gene expression by NF-κB. *J. Biol. Chem.* **278**, 2963–2968.

Delsite R., Kahhap S., Anbazhagan R., Gabrielson E. and Singh K. K. (2002) Nuclear genes involved in mitochondria-to-nucleus communication in breast cancer cells. *Mol. Cancer* **1**, 1–10.

Ginty D. D., Kornhauser J. M., Thompson M. A., Bading H., Mayo K. E., Takahashi J. S. and Greenberg M. E. (1993) Regulation of CREB phosphorylation in the suprachiasmatic nucleus by light and a circadian clock. *Science* **260**, 238–241.

Ginty D. D., Bonni A. and Greenberg M. E. (1994) Nerve growth factor activates a Ras-dependent protein kinase that stimulates c-fos transcription via phosphorylation of CREB. *Cell* **77**, 713–725.

de Groot R. P., den Hertog J., Vandenheede J. R., Goris J. and Sassone-Corsi P. (1993) Multiple and cooperative phosphorylation events regulate the CREM activator function. *EMBO J.* **12**, 3903–3911.

Grynkiewicz G., Poenie M. and Tsien R. Y. (1985) A new generation of Ca^{2+} indicators with greatly improved fluorescence properties. *J. Biol. Chem.* **260**, 3440–3450.

Hahm S. H., Chen Y., Vinson C. and Eiden L. E. (2003) A calcium-initiated signaling pathway propagated through calcineurin and cAMP response element binding protein activates proenkephalin gene transcription after depolarization. *Mol. Pharmacol.* **64**, 1503–1511.

Hu B. R., Fux C. M., Martone M. E., Zivin J. A. and Ellisman M. H. (1999) Persistent phosphorylation of cyclic AMP responsive element-binding protein and activating transcription factor-2 transcription factors following transient cerebral ischemia in rat brain. *Neuroscience* **89**, 437–452.

Huang H., Cheville J. C., Pan Y., Roche P. C., Schmidt L. J. and Tindall D. J. (2001) PTEN induces chemosensitivity in PTEN-mutated prostrate cancer cells by suppression of Bcl-2 expression. *J. Biol. Chem.* **276**, 38 830–38 836.

Jin K., Mao X., Simon R. and Greenberg D. (2001) Cyclic AMP response element binding protein (CREB) and CREB binding protein (CBP) in global ischemia. *J. Mol. Neurosci.* **16**, 49–56.

Jullig M. and Stott N. S. (2003) Mitochondrial localization of Smad5 in a human chondrogenic cell line. *Biochem. Biophys. Res. Comm.* **307**, 108–113.

Mantelas A., Stamatakis A., Kazanis I., Philippidis H. and Stylianopoulou F. (2003) Control of neuronal nitric oxide synthase and brain-derived neurotrophic factor levels by GABA-A receptors in the developing rat cortex. *Dev. Brain Res.* **145**, 185–195.

Matlib M. A., Zhou Z., Knight S. *et al.* (1998) Oxygen-bridged dinuclear ruthenium amine complex specifically inhibits Ca^{2+} uptake into mitochondria *in vitro and in situ* in single cardiac myocytes. *J. Biol. Chem.* **273**, 10 223–10 231.

McCormack J. G., Halestrap A. P. and Denton R. M. (1990) Role of calcium ions in regulation of mammalian intramitochondrial metabolism. *Physiol. Rev.* **70**, 391–425.

Ogita K., Okuda H., Kitano M., Fujinami Y., Ozaki K. and Yoneda Y. (2002) Localization of activator protein-1 complex with DNA binding activity in mitochondria of murine brain after *in vivo* treatment with kainite. *J. Neurosci.* **22**, 2561–2570.

Riccio A., Ahn S., Davenport C. M., Blendy J. A. and Ginty D. D. (1999) Mediation by a CREB family transcription factor of NGF-dependent survival of sympathetic neurons. *Science* **286**, 2358–2361.

Sawa A. (2001) Mechanisms for neuronal cell death and dysfunction in Huntington's disease: pathological cross-talk between the nucleus and the mitochondria? *J. Mol. Med.* **79**, 375–381.

Shaywitz A. J. and Greenberg M. E. (1999) CREB: a stimulus-induced transcription factor activated by a diverse array of extracellular signals. *Annu. Rev. Biochem.* **68**, 821–861.

Sims N. R. (1990) Rapid isolation of metabolically active mitochondria from rat brain and subregions using percoll density gradient centrifugation. *J. Neurochem.* **55**, 698–707.

Tan Y., Rouse J., Zhang A., Cariati S., Cohen P. and Combs M. J. (1996) FGF and stress regulate CREB and ATF-1 via a pathway involving p38 MAP kinase and MAPKAP kinase-2. *EMBO J.* **15**, 4629–4642.

Tanaka K. (2001) Alteration of second messengers during acute cerebral ischemia – adenylate cyclase, cyclic AMP-dependent protein kinase, and cyclic AMP response element binding protein. *Prog. Neurobiol.* **65**, 173–207.

Waeber G. and Habener J. F. (1991) Nuclear translocation and DNA recognition signals colocalized within the bZIP domain of cyclic adenosine 3′,5′-monophosphate response element-binding protein CREB. *Mol. Endocrinol.* **5**, 1431–1438.

Xing J., Kornhauser J. M., Xia Z., Thiele E. A. and Greenberg M. E. (1998) Nerve growth factor activates extracellular signal-regulated kinase and p38 mitogen-activated protein kinase pathways to stimulate CREB serine 133 phosphorylation. *Mol. Cell Biol.* **18**, 1946–1955.

Yang S., Liu R., Perez E. J. *et al.* (2004) Mitochondrial localization of estrogen receptor β. *Proc. Natl Acad. Sci. USA* **101**, 4130–4135.

Zheng Z., Wang Z. and Delbono O. (2004) Ca^{2+} calmodulin kinase and calcineurin mediate IGF-1-induced skeletal muscle dihydropyridine receptor α_{1S} transcription. *J. Membrane Biol.* **197**, 101–112.

Available online at www.sciencedirect.com
SCIENCE DIRECT®
Experimental Neurology 197 (2006) 235 – 243
Experimental Neurology
www.elsevier.com/locate/yexnr

Regular Article

Physiologic progesterone reduces mitochondrial dysfunction and hippocampal cell loss after traumatic brain injury in female rats

Courtney L. Robertson [a,b,*], April Puskar [c], Gloria E. Hoffman [c], Anne Z. Murphy [c], Manda Saraswati [a], Gary Fiskum [b]

[a] Department of Pediatrics, University of Maryland School of Medicine, Baltimore, MD 21201, USA
[b] Department of Anesthesiology, University of Maryland School of Medicine, Baltimore, MD 21201, USA
[c] Department of Anatomy and Neurobiology, University of Maryland School of Medicine, Baltimore, MD 21201, USA

Received 30 June 2005; revised 9 September 2005; accepted 24 September 2005
Available online 2 November 2005

Abstract

Growing literature suggests important sex-based differences in outcome following traumatic brain injury (TBI) in animals and humans. Progesterone has emerged as a key hormone involved in many potential neuroprotective pathways after acute brain injury and may be responsible for some of these differences. Many studies have utilized supraphysiologic levels of post-traumatic progesterone to reverse pathologic processes after TBI, but few studies have focused on the role of endogenous physiologic levels of progesterone in neuroprotection. We hypothesized that progesterone at physiologic serum levels would be neuroprotective in female rats after TBI and that progesterone would reverse early mitochondrial dysfunction seen in this model. Female, Sprague–Dawley rats were ovariectomized and implanted with silastic capsules containing either low or high physiologic range progesterone at 7 days prior to TBI. Control rats received ovariectomy with implants containing no hormone. Rats underwent controlled cortical impact to the left parietotemporal cortex and were evaluated for evidence of early mitochondrial dysfunction (1 h) and delayed hippocampal neuronal injury and cortical tissue loss (7 days) after injury. Progesterone in the low physiologic range reversed the early postinjury alterations seen in mitochondrial respiration and reduced hippocampal neuronal loss in both the CA1 and CA3 subfields. Progesterone in the high physiologic range had a more limited pattern of hippocampal neuronal preservation in the CA3 region only. Neither progesterone dose significantly reduced cortical tissue loss. These findings have implications in understanding the sex-based differences in outcome following acute brain injury.

Keywords: Brain mitochondria; Progesterone; Neuroprotection; Apoptosis; Hippocampus

Introduction

Growing evidence suggests important differences in outcomes between male and female subjects following severe acute brain injury. This is seen in many forms of acute brain injury in both animal and human studies (reviewed in Roof and Hall, 2000). One common form of acute brain injury, traumatic brain injury (TBI), affects approximately 1.5 million Americans each year (CDC). Although limited in number, epidemiologic studies in adult TBI looking at effects of gender describe differences between men and women. Some studies show improved neurologic outcome in women (Groswasser et al., 1998), while others suggest that females may have greater long-term deficits than males (Farace and Alves, 2000). More recent studies define important sex-based differences in response to excitotoxicity and oxidative stress after severe TBI, as measured by neurochemical alterations in the cerebrospinal fluid (Bayir et al., 2004; Wagner et al., 2004a,b, 2005).

The literature in animal models of TBI is broader and generally suggests neuroprotection in females. An initial study showed a marked reduction in cerebral edema after TBI in pseudopregnant female rats, compared to male and proestrous female rats (Roof et al., 1993a,b). These investigators

* Corresponding author. Department of Pediatrics, University of Maryland School of Medicine, 22 South Greene Street, #N5E13, Baltimore, MD 21201, USA. Fax: +1 410 328 0680.
E-mail address: croberts@peds.umaryland.edu (C.L. Robertson).

0014-4886/$ - see front matter © 2005 Elsevier Inc. All rights reserved.
doi:10.1016/j.expneurol.2005.09.014

hypothesized that circulating levels of endogenous progesterone played an important role in their findings. Other studies have demonstrated reduction in cortical contusion volume (Bramlett and Dietrich, 2001), alteration in the evolution of cytoskeletal protein degradation (Kupina et al., 2003), and improvement in motor (Wagner et al., 2004a,b) and cognitive (Roof et al., 1993a,b) outcomes after TBI in female versus male rats and mice. In addition, post-traumatic interventions, such as environmental enrichment (Wagner et al., 2002), and post-traumatic secondary insults, such as hyperthermia (Suzuki et al., 2004), have been shown to have sex-based differential response.

Although estrogen has been hypothesized to play a role in these sex differences (Wise et al., 2001), progesterone has recently emerged as a key hormone with many potential neuroprotective benefits after TBI (Roof and Hall, 2000) (Stein, 2001). Administration of progesterone, even post-injury, has been shown to reduce brain edema (Roof et al., 1996), secondary neuronal loss (Roof et al., 1994), and necrotic tissue loss (Shear et al., 2002). Progesterone, and its metabolite allopregnanolone, has also been associated with improved neurologic outcome (Roof et al., 1994; Djebaili et al., 2004, 2005; He et al., 2004a,b; Shear et al., 2002). Although the mechanisms of progesterone's neuroprotection are not fully understood, a series of studies by Stein et al. have shown that progesterone plays a role in reversing many of the pathologic post-traumatic pathways, such as reductions in lipid peroxidation (Roof et al., 1997) and inflammatory cytokines (He et al., 2004a,b) following injury.

Many of the proposed pathways of progesterone neuroprotection can have a significant influence on the function of brain mitochondria. These include progesterone's role in reducing oxidative injury (Roof et al., 1997), improving membrane stabilization (Roof and Hall, 2000), and reducing brain excitability (Hoffman et al., 2003; Smith, 1991, 1994; Smith et al., 1987). However, the effects of progesterone on mitochondrial dysfunction after TBI have not been directly evaluated. Therefore, one aim of this study was to evaluate the potential of progesterone in reversing the post-traumatic alterations in mitochondrial function. A second aim was to evaluate the neuroprotective properties of physiologic levels of serum progesterone that would be similar to those seen in normally cycling female rats. Many previous studies have administered progesterone over a series of days postinjury to male rats, resulting in high physiologic or supraphysiologic serum levels. Previous work in our laboratory in a kainite seizure model has shown that physiologic levels of progesterone were able to reduce seizure severity in ovariectomized female rats (Hoffman et al., 2003). However, there was an important dose–response relationship as only those rats treated in the low physiologic range had this reduction. Therefore, we hypothesized that low range physiologic progesterone would be neuroprotective in female rats after TBI and that progesterone would reverse early mitochondrial dysfunction seen in this model.

Methods

This study was approved by the University of Maryland Animal Care and Use Committee. All care and handling of rats were in compliance with the National Institute of Health guidelines. Adult female Sprague–Dawley rats (Zivic Miller Laboratories, Pittsburgh, PA; n = 67 rats total) weighing 200–225 g were used in all studies and were allowed free access to food and water before and after all surgical procedures.

Ovariectomy and hormone implant

Rats were anesthetized with 3% isoflurane and ovariectomized under sterile conditions. They were then subcutaneously implanted with blank silastic capsules (no hormone) or silastic capsules (length = 40 mm; OD = 0.125 mm; ID = 0.078 mm) containing crystalline progesterone (Sigma, St. Louis, MO). Two levels of physiological progesterone supplementation were studied by altering the number of progesterone capsules. The low level supplementation used 3 capsules, and the high level used 6 capsules. Previous work has demonstrated that the low level corresponds to a serum level of ~25 ng/ml, and the high level corresponds to ~50 ng/ml, which are both within the physiologic range (Hoffman et al., 2003).

Traumatic brain injury model

Anesthesia was induced in a Plexiglas chamber with 4% isoflurane (Easterling Veterinary Supply, West Columbia, SC). The head was then fixed in a stereotactic device (David Kopf, Tujunga, CA), and 2–2.5% isoflurane with 30% oxygen was administered via a nose-cone device for the duration of surgery. A rectal probe and heating blanket (Fine Science, Foster City, CA) were used to maintain rectal temperature at 37.0 ± 0.5°C. A midline scalp incision was made with exposure of the parietal bone. A left parietal craniotomy was performed using a high-speed dental drill (Henry Schein, Melville, NY). A brain temperature probe was placed in the contralateral temporalis muscle with temperature maintained at 37.0 ± 0.5°C. Rats were allowed a 30-min period of stable brain and rectal temperatures prior to TBI.

TBI was performed using the controlled cortical impact (CCI) device (Pittsburgh Precision Instruments, Pittsburgh, PA) as previously described (Dixon et al., 1991) with modification of settings. Briefly, injury was produced using a 6-mm metal impactor tip that is pneumatically driven in the vertical plane into the parietal cortex. CCI settings included a depth of penetration of 1.5 mm, a velocity of 5.5 ± 0.3 m/s, and a duration of deformation of 50 ms. Following injury, the bone flap was replaced, the craniotomy sealed with an acrylic mixture (Koldmount, Albany, NY), and the scalp incision was closed with interrupted sutures. At the completion of surgery, isoflurane was discontinued, and rats were awakened and returned to their cages. Sham rats (blank implanted) underwent identical surgeries, with the exclusion of the CCI.

Mitochondrial isolation

One hour after CCI, forebrains were quickly removed, separated into left and right hemispheres, and placed in ice-cold isolation buffer. Mitochondria (non-synaptosomal plus synaptosomal) were isolated as previously described (Starkov et al., 2004) using digitonin to disrupt synaptosomal membranes. Isolated mitochondria were kept on ice for the duration of the experimental protocols.

Mitochondrial studies were conducted on three groups: sham (blank implanted, $n = 8$), TBI vehicle (blank implanted, $n = 8$), and TBI-treated (low level progesterone implanted, $n = 8$). A separate cohort of uninjured rats was used to evaluate potential hormonal effects on mitochondrial respiration unrelated to injury. These rats underwent ovariectomy and implantation of either progesterone or vehicle ($n = 3$/group). Seven to ten days after ovariectomy and implant, forebrain mitochondria were isolated without separation of hemispheres and were analyzed.

Mitochondrial respiration

Mitochondrial oxygen consumption was measured using a Clark-type oxygen electrode (Hansatech Instruments/PP Systems, Amesbury, MA). Assays were conducted at 37°C at a pH of 7.0 in a KCl medium (125 mM KCl, 2 mM KH_2PO_4, and 20 mM Hepes–KOH). Mitochondria (0.5 mg/ml) were added to the chamber supplemented with 5 mM glutamate, 5 mM malate, 1 mM $MgCl_2$, and 1 μM EGTA in a total volume of 0.5 ml. State 3 respiration was initiated by the addition of 0.4 mM ADP, and State 4_o respiration was induced by the addition of the ATP synthetase inhibitor oligomycin (2.2 μg/ml). State 4 respiration measured in the presence of oligomycin (State 4_o) is not equivalent to the traditional State 4 respiration measured after all ADP has been converted to ATP. However, for our measurements, we wanted to eliminate the contribution of ATP cycling via hydrolysis by contaminating ATPases and resynthesis by mitochondrial ATP synthetase. Thus, the oligomycin-induced State 4_o rate of respiration reflects mitochondrial proton cycling limited by passive proton leakiness of the inner membrane. Mitochondrial respiratory energy coupling was evaluated by determining the respiratory control ratio (RCR), calculated as the ratio of the rate of ADP-stimulated State 3 respiration to the State 4_o rate in the presence of oligomycin.

Hippocampal cell counts

At 7 days after TBI, rats were anesthetized using an overdose of sodium pentobarbital (100 mg/kg, ip) and transcardially perfused with saline containing 2% sodium nitrite followed by fixation with acrolein (2.5%) in paraformaldehyde (4%) in a phosphate buffer (Hoffman et al., 2001). Four groups were analyzed for hippocampal cell counting: sham (blank implanted, $n = 7$), TBI vehicle (blank implanted, $n = 9$), TBI treated with low level progesterone ($n = 8$), and TBI treated with high level progesterone ($n = 7$). Brains were removed and placed in 25% sucrose solution until they sunk (2–4 days). This resulted in comparable amounts of shrinkage among all of the animals studied. Brains were sectioned coronally (30 μm) using a freezing microtome (Leica, Bannockburn, IL) and were placed into antifreeze cryoprotectant solution for storage at −20°C in a 1:6 series. For analysis of neuronal cell counts using NeuN labeling, a standard free-floating immunocytochemistry protocol was used as previously described (Hoffman et al., 2001). Briefly, sections were rinsed thoroughly to remove cryprotectant with potassium phosphate-buffered saline (KPBS), incubated with sodium borohydride, then rinsed again with KPBS. Sections were then incubated with the primary antibody, mouse monoclonal anti-NeuN (1:70,000, Chemicon, Temecula, CA), in KPBS with 0.4% Triton-X for 1 h at room temperature then for 24 h at 4°C. Sections were then rinsed with KPBS and incubated with the secondary antibody, biotinylated horse anti-mouse antibody (1:600) in KPBS with 0.4% Triton-X for 1 h. After rinsing again in KPBS, slices were prepared with the VectorStain Elite ABC kit. Following a series of rinses with KPBS and sodium acetate (0.175M), the slices were then placed into a Ni-DAB H_2O_2 chromogen solution (250 mg Ni sulfate, 2 mg DAB, and 8.3 μl 3% H_2O_2/10 ml 0.175 sodium acetate solution). Staining was terminated by transferring to the sodium acetate solution. Stained slices were then mounted on slides for quantification.

For quantification of hippocampal neuronal cells, analyses were performed with a computer-assisted image analysis system consisting of a Nikon Eclipse 800 photomicroscope, a Retiga EX digital camera (Biovision Technologies), and a Macintosh G4 computer with IP Spectrum software (Scientific Image Processing, Scanalytics, Fairfax, VA). Using 40× magnification, an equivalent slice through the hippocampus in the CA1 and CA3 subfields from both ipsilateral and contralateral hemispheres was analyzed. In order to provide consistency, the section selected for analysis was the section of hippocampus directly beneath the central area of cortical injury in each rat. In each analyzed subfield, the numbers of normally stained NeuN neurons were counted. Two 40× fields were analyzed per hippocampal subfield on both sides in every rat.

Normally, NeuN is localized in the nucleus. If present in the neuronal cytoplasm, the intensity of staining is less than in the nucleus. When neurons are injured, the nuclear NeuN becomes either fragmented or reduced, whereas cytoplasmic NeuN remains stable, thus altering the relative intensities of the nucleus to the cytoplasm. These changes are associated with the emergence of TUNEL reactivity (Hoffman et al., 2001) and with cresyl violet changes associated with acute ischemic neuronal death (Vereczki et al., in press). Therefore, for this study, neurons with more intense nuclear reactivity relative to the cytoplasm were counted as “normal”. Those that displayed either fragmentation of NeuN in the nucleus, or intensity of cytoplasmic NeuN that was greater than nuclear NeuN, were considered “abnormal” and were not counted. Data are expressed as the ratio of “normal” cells on the ipsilateral over contralateral side (as percent).

Cortical tissue loss analysis

Quantitative analysis of cortical tissue loss was performed on the same sections prepared as above with NeuN staining. To ensure that identical rostral caudal levels were obtained for each side (since shifts due to edema could skew the left–right symmetry), levels where the optic tract length matched on each side were selected. An image of the side of interest was captured with a 1× objective, and the total cell-rich area (cortical layers 2–5, in square μm) was determined, starting with the rhinal fissure up to the central sulcus. The area included was calculated by the software, and standard stereological calculation of volume (area × distance between sections) was performed.

In order to control for the contribution of any edema distortion of tissue size, a separate measurement was used. On the same section analyzed for cortical area, a rectangle whose length extended from the white matter underlying the cortex to the outer surface of the cortex, and from the center of the rhinal fissure to the beginning of the pyramidal cell layer of the somatosensory cortex, was drawn immediately superior to the rhinal fissure (Fig. 1). The area of this rectangle was calculated by the software, and this was compared between ipsilateral (injured) and contralateral sides, yielding an edema factor ratio, used in correcting the cortical tissue volume loss calculations.

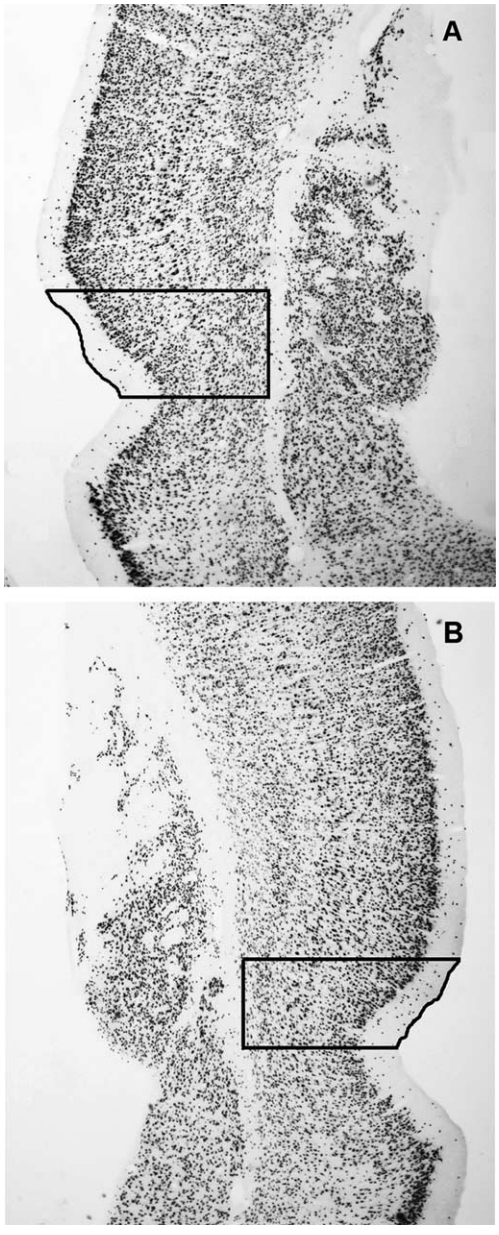

Fig. 1. Low-powered magnification of a photomicrograph from the ipsilateral (A) and contralateral (B) rhinal fissure region. The boxes represent the rectangular area used on each side for correction of distortion of tissue due to edema. The ratio of the area of this box (ipsilateral/contralateral) was used to correct cortical tissue volume loss calculations.

Statistics

Data are expressed as mean ± standard error of the mean (SEM). Data between groups were compared using one-way analysis of variance (ANOVA) with post-hoc individual two-way comparisons made using Fisher's LSD test. Non-parametric data across groups were compared using the Kruskal–Wallis test. Comparisons with a $P < 0.05$ were considered significant. Statistical analysis was performed using Sigma Stat (SPSS, Chicago, IL) and GB-Stat Software.

Results

Mitochondrial respiration

In normal uninjured rats, progesterone did not alter rates of mitochondrial respiration. There were no differences in State 3 and State 4_o respiratory rates or in the respiratory control ratio in the presence of the NAD-linked oxidizable substrates glutamate and malate. The respiratory control ratio in uninjured blank-implanted rats was 7.8 ± 1.1 and in progesterone-implanted rats was 7.3 ± 0.7 (P = NS between groups). There was also no difference in respiratory rates in the presence of the FAD-linked substrate succinate, with rotenone.

After TBI, mitochondria isolated from the left (ipsilateral) cortex in blank-implanted rats had a reduction in the respiratory control ratio (6.9 ± 0.7 vs. 9.5 ± 0.8 in sham rats, $P < 0.05$, Fig. 2A). Progesterone completely reversed this reduction, with respiratory control ratios similar to sham rats (10.0 ± 1.1, Fig. 2A). The TBI-induced reduction in respiratory control ratio was primarily a result of uncoupling, with comparable State 3 rates across groups (Fig. 2B) but a trend toward increased State 4 rates after TBI in blank-implanted rats (Fig. 2C).

Hippocampal neuronal cell injury

Representative examples of high-power photomicrographs from the CA1 subfield of ipsilateral hippocampus in blank-implanted versus progesterone-treated rats after TBI are seen in Fig. 3. This figure shows two main patterns of hippocampal neuronal cell injury in blank-implanted rats (Figs. 3A and B) compared to the relatively normal NeuN staining seen in progesterone-treated rats (Fig. 3C). The first type of hippo-

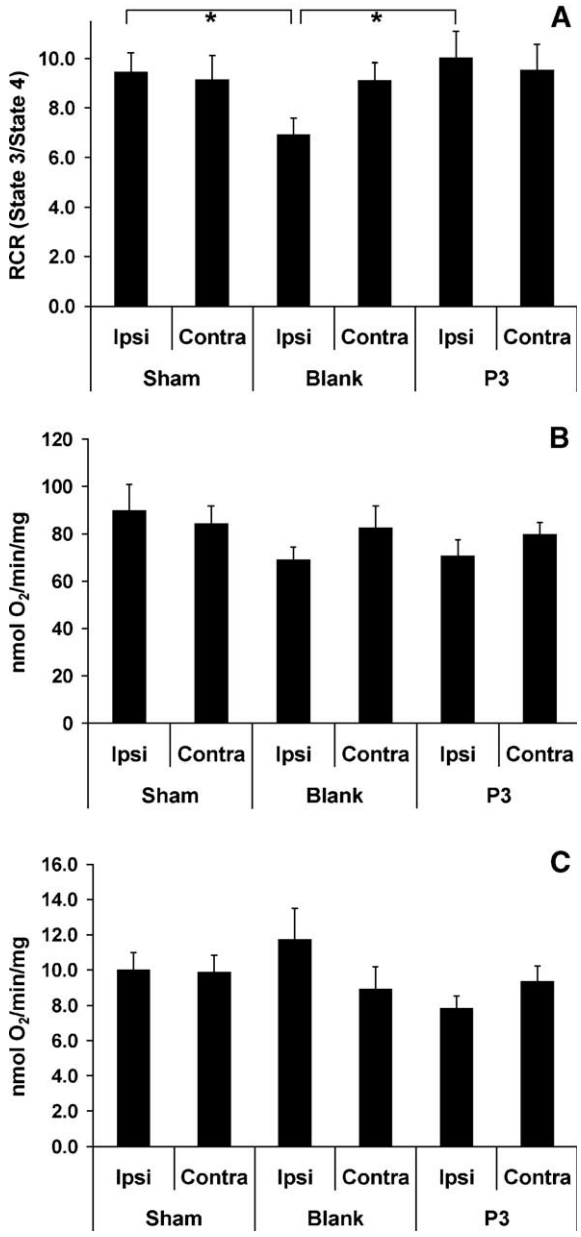

Fig. 2. Low range physiologic progesterone (P3) reversed the postinjury reduction in mitochondrial RCR. Isolated mitochondria (0.5 mg/ml) were incubated at 37°C with 5 mM glutamate and 5 mM malate in a KCl medium (125 mM KCl, 2 mM KH_2PO_4, and 20 mM Hepes–KOH; supplemented with 1 mM $MgCl_2$ and 1 μM EGTA). State 3 respiration was initiated by the addition of 0.4 mM ADP. State 4 respiration was induced by the addition of oligomycin (2.2 μg/ml). The respiratory control ratio (RCR) was determined as a ratio of State 3 to State 4 rates. The RCR was 6.9 ± 0.7 in blank-treated rats ipsilateral to injury, as compared to 9.5 ± 0.8 in sham and 10.0 ± 1.1 in progesterone-treated rats (A, $P < 0.05$ by ANOVA, $^*P < 0.05$ blank vs. sham and progesterone, P = NS sham vs. progesterone). State 3 was not significantly different across groups (B, P = NS by ANOVA). There was a trend toward a difference in State 4 rates when comparing ipsilateral samples across groups (C, $P = 0.10$ by Kruskal–Wallis). Data are expressed as mean ± SEM.

campal injury involved a generalized loss of neurons (Fig. 3A) and the presence of many abnormally stained neurons in those remaining (arrowheads in insert). The second type of pattern seen in some rats involved preservation of total neuronal numbers (Fig. 3B), but with an abundance of abnormally stained neurons (arrowheads in insert), representing injured neurons that would likely die in subsequent days. Progesterone-treated rats (Fig. 3C) had both preservation of total numbers of neurons and very few abnormally stained cells, with hippocampal NeuN labeling that was similar to contralateral and sham-operated rats (data not shown).

TBI resulted in significant neuronal cell injury in the ipsilateral hippocampus, with ~35% reduction in normal neurons in the CA1 subfield (Fig. 4A) and ~43% reduction in the CA3 subfield (Fig. 4B) of blank-implanted rats (n = 9) compared to the contralateral hemisphere. Low level progesterone (n = 8) almost completely protected against this cell injury in both subfields, with normal hippocampal cell counts

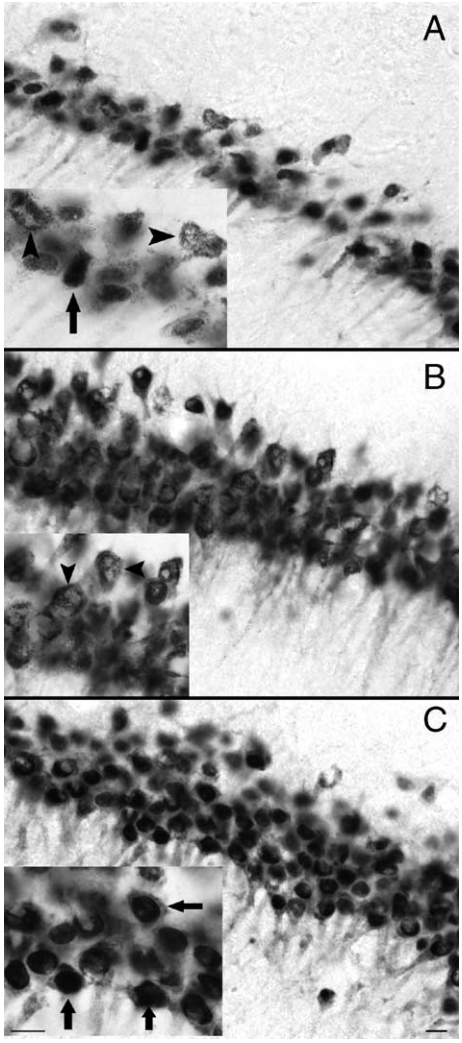

Fig. 3. Representative photomicrographs at high-powered magnification of the CA1 subfield of the hippocampus stained for NeuN from ipsilateral hemispheres in blank-treated (A, B) and low range progesterone-treated (C) at 7 days after TBI. In panel A, a blank-implanted rat shows a marked reduction in total hippocampal neurons seen with NeuN labeling, with many abnormally stained neurons (arrowheads in insert) and few normally stained neurons (arrow in insert) among remaining cells. In panel B, a blank-implanted rat shows a normal cell density but an abundance of abnormally stained neurons (arrowheads in insert). Panel C shows a progesterone-treated rat with preservation of normal cell numbers and a predominance of normal NeuN staining (arrows in insert).

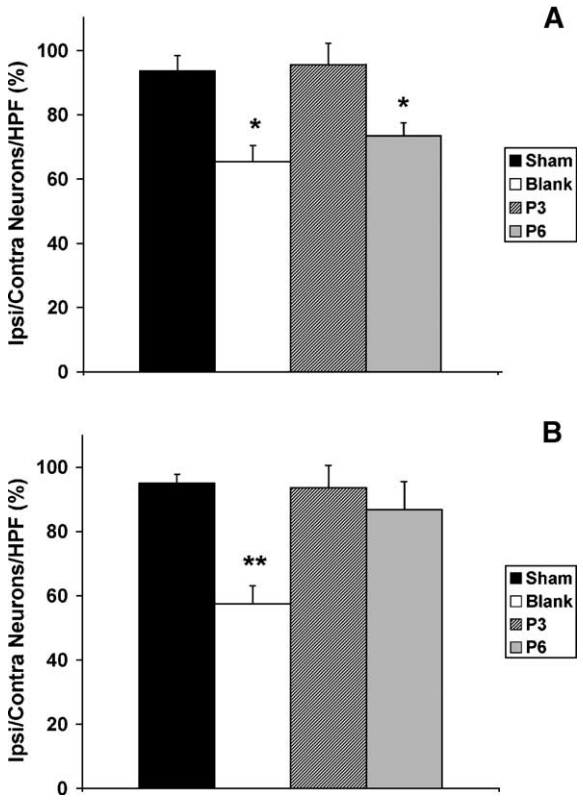

Fig. 4. Progesterone treatment preserved hippocampal neuronal cells at 7 days after TBI. Cell counts are expressed at the neurons per high-powered field (HPF) on the ipsilateral over contralateral (%) in the CA1 (A) and CA3 (B) subfields. Low range progesterone (P3) showed hippocampal preservation with cell counts similar to sham-operated control rats in both CA1 (A) and CA3 (B) subfields. High range progesterone (P6) preserved hippocampal neurons in the CA3 region, but not the CA1 region. Data are expressed as mean ± SEM. *P < 0.05 versus sham and P3, **P < 0.05 versus sham, P3, and P6.

in the ipsilateral hemisphere similar to contralateral and sham rats (Fig. 4). High level progesterone (n = 7) was protective in the CA3 region but failed to significantly reduce neuronal injury in the CA1 region (Fig. 4).

Cortical tissue loss

TBI resulted in an approximately 35–45% hemispheric volume loss on the side ipsilateral to injury. This was significantly greater than sham (n = 7) for all groups. Blank-implanted rats (n = 9) had a 37 ± 7% hemispheric volume loss at 7 days after injury. Low range progesterone-treated rats (n = 8) had a lower mean tissue loss at 31 ± 7%, and high range progesterone-treated rats (n = 7) had a higher mean tissue loss at 45 ± 10%. However, neither of these was significantly different from blank-implanted rats (Fig. 5).

Discussion

The results of this study demonstrate that progesterone in the low range of physiologic levels is neuroprotective in TBI in ovariectomized female rats. Progesterone in the high physiologic range had a more limited pattern of hippocampal neuronal preservation. We also demonstrated that progesterone reverses early postinjury alterations in mitochondrial respiration. To our knowledge, this is the first report to directly evaluate the neuroprotective effects of sex hormones on postinjury mitochondrial function.

There are several potential mechanisms to explain this early influence of progesterone on mitochondrial respiration. First, progesterone has antioxidant properties. Oxidative injury begins early, within minutes, after TBI, and mitochondria are important intracellular targets of reactive oxygen and nitrogen species (reviewed in Lewen et al., 2000). Specifically, lipid peroxidation could lead to loss of mitochondrial membrane integrity with resultant uncoupling of mitochondrial respiration. Progesterone treatment attenuated the induction of lipid peroxidation in hippocampal neurons exposed to $FeSO_4$ and amyloid β-peptide (Goodman et al., 1996), and progesterone reduced markers of lipid peroxidation in the brain following TBI in male rats (Roof et al., 1997). Second, progesterone may have a more direct structural effect on membrane phospholipids. A review by Roof et al. suggested that progesterone intercalates into membranes and directly protects them from free radical injury (Roof and Hall, 2000). One study of spinal cord neurodegeneration in Wobbler mice showed intense mitochondrial vacuolation with disruption of the outer and inner mitochondrial membranes that was reversed with progesterone (Gonzalez Deniselle et al., 2002). Lastly, it is possible that some of the progesterone-mediated effects on oxidative stress are indirect through other important pathologic pathways. For example, glutamate-mediated influx of calcium can activate intracellular free radical production, and progesterone has been shown to inhibit excitatory amino acid response (Smith, 1991; Smith et al., 1987). Progesterone inhibition of excitotoxic stimulation could also spare mitochondria from the respiratory uncoupling and other sequelae caused by pathologic mitochondrial Ca^{2+} accumulation (reviewed in Sullivan et al., 2005).

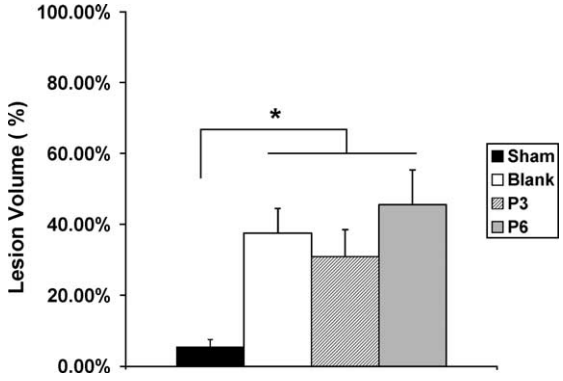

Fig. 5. Progesterone treatment did not alter lesion volume at 7 days after TBI. Lesion volume is expressed as percent contralateral (non-trauma hemispheric volume minus trauma hemispheric volume/non-trauma hemispheric volume), with trauma hemispheric volume corrected for edema as described in text. Cortical tissue loss on the side ipsilateral to injury was not different when comparing blank (open bar), low dose progesterone (P3, striped bar), and high dose progesterone (P6, gray bar, P = NS by ANOVA). All injury volumes were significantly greater than sham (*P < 0.01, blank/P3/P6 versus sham). Data are expressed as mean ± SEM.

Progesterone's ability to prevent secondary neuronal death in vulnerable subpopulations of neurons has been shown in several animal models of brain injury (Gonzalez-Vidal et al., 1998; Cervantes et al., 2002; Hoffman et al., 2003). In TBI models, progesterone and its metabolite allopregnanolone reduced secondary neuronal loss (Djebaili et al., 2004; He et al., 2004a,b; Roof et al., 1994). The ability of progesterone to preserve vulnerable neurons in any form of brain injury is strongly influenced by the dosing regimen used. In the present study, we used an ovariectomy approach to eliminate any potential confounding effects of endogenous estrogen as we evaluated the role of endogenous levels of progesterone at the time of TBI. We recognize that this also eliminates the significant estrogen induction of progesterone receptors shown in certain brain regions. However, progesterone activity can still be detected in the absence of estrogen (Le et al., 1997), and there are many important receptor-independent actions of progesterone.

We found that only low physiologic progesterone was able to protect both CA1 and CA3 hippocampal subfields. High physiologic progesterone preserved CA3 neurons, but the loss of normal CA1 cells was similar to blank-implanted rats (28% cell loss versus 36% in blank-treated rats). This dose–response relationship is similar to previous work in our laboratory, in which only rats with serum progesterone in the low physiologic range had a reduction in kainic-acid-induced seizure severity (Hoffman et al., 2003). The exact reason for the reduced protection at higher progesterone levels remains unclear. It may relate to differences in GABA innervation between CA1 and CA3 subfields of the hippocampus. It is also possible that the conversion of progesterone to allopregnanolone is altered at higher progesterone doses and may demonstrate biologic variability (George et al., 1994). Another possibility is that higher progesterone doses may lead to GABA receptor down-regulation or desensitization (Yu et al., 1996). Studies have shown alterations in $GABA_A$ receptor subunit expression and function with long-term progesterone exposure and withdrawal, which varied by brain region (summarized in Biggio et al., 2001; Follesa et al., 2004).

Other investigators have stressed the importance of dose in relationship to progesterone neuroprotection in animal models. One study of focal brain ischemia used ovariectomized female rats to evaluate the effects of acute and chronic progesterone treatment (Murphy et al., 2000). They showed no effect on overall cortical infarct volume with acute high range physiologic and supraphysiologic progesterone treatment approaches. Importantly, chronic progesterone exposure at high doses actually exacerbated infarct volume in the striatum. A series of studies by the laboratory of Stein et. al. have defined the optimal timing, dose, and duration of progesterone treatment after TBI in intact male rats (Goss et al., 2003; Roof et al., 1996; Shear et al., 2002). Although not directly comparable to the current study of ovariectomized female rats, these studies do highlight the importance of attention to dosing approach. One study suggested that the highest doses of progesterone (32 mg/kg) may have been detrimental to a subset of animals, while other doses (8 and 16 mg/kg) improved behavioral outcome (Goss et al., 2003). In order to improve our understanding of the potentially complex mechanisms of progesterone neuroprotection, close attention will need to be paid to the dosing approach, especially as comparisons are made between studies.

Despite preservation of hippocampal neurons, we were unable to demonstrate a protective effect of progesterone on cortical tissue loss at the site of injury. Although most studies in brain ischemia demonstrated reduced infarct volume with progesterone (Alkayed et al., 2000; Gibson and Murphy, 2004; Jiang et al., 1996; Kumon et al., 2000; Murphy et al., 2002), many studies in TBI have not been able to show significant reduction in cortical tissue loss with progesterone treatment (Djebaili et al., 2004; Goss et al., 2003; Roof et al., 1994). The exact reasons for this are not completely understood but may relate to timing of cell death after injury, with the necrotic cortical tissue loss occurring more rapidly than the hippocampal cell death (Conti et al., 1998; Hall et al., 2005; Yakovlev et al., 1997). Progesterone acts through both progesterone-receptor-dependent and receptor-independent mechanisms. The receptor-independent pathways may be important immediately after TBI, while the receptor-dependent pathways likely become important later, with alterations in nuclear gene expression. In addition, progesterone binding receptors have been identified at both the cellular membrane and the nucleus in the intact brain (Krebs et al., 2000). A study of spinal cord injury demonstrated that these two progesterone receptor types are very different in response to injury and exogenous hormone treatment (Labombarda et al., 2003).

There are several potential limitations of this study. First, we cannot propose a direct correlation between the early neuroprotective actions of progesterone on mitochondrial function and the preservation of hippocampal neurons. Due to technical feasibility, we are unable to obtain sufficient mitochondria for in vitro analysis from the unilateral hippocampus of one rat. The mitochondrial preparation in these studies is composed predominantly of cortical tissue, with ipsilateral hippocampal neurons only contributing a small fraction of mitochondria. Therefore, these two findings may have different mechanistic explanations. Second, as described above, we did not evaluate long-term neurologic outcome. Although significant hippocampal preservation has been correlated with improved memory and learning in various studies (Lee et al., 2004), we do not know if the degree of hippocampal preservation seen in the present study would translate into meaningful behavioral improvement, especially in the absence of significant cortical tissue preservation. Lastly, this study was designed to evaluate the effects of physiologic levels of progesterone during and following TBI. As a result, progesterone was present in the pre-injury period. In order to extend these findings for clinical relevance, we would need to evaluate similar levels of supplemental progesterone given postinjury.

In conclusion, our data show that low range physiologic progesterone is protective in TBI in female rats, with reversal of early mitochondrial dysfunction and a reduction in long-term hippocampal neuronal loss. We see moderate, but less substantial, protection with high range physiologic progester-

one. These findings have implications in understanding the sex-based differences in outcome following acute brain injury.

Acknowledgments

This work was supported by the U.S. Army Medical Research and Material Command Grant DAMD 17-99-1-9483 and NIH grant K08 NS42805.

References

Alkayed, N.J., Murphy, S.J., Traystman, R.J., Hurn, P.D., Miller, V.M., 2000. Neuroprotective effects of female gonadal steroids in reproductively senescent female rats. Stroke 31, 161–168.

Bayir, H., Marion, D.W., Puccio, A.M., Wisniewski, S.R., Janesko, K.L., Clark, R.S., Kochanek, P.M., 2004. Marked gender effect on lipid peroxidation after severe traumatic brain injury in adult patients. J. Neurotrauma 21, 1–8.

Biggio, G., Follesa, P., Sanna, E., Purdy, R.H., Concas, A., 2001. GABAA-receptor plasticity during long-term exposure to and withdrawal from progesterone. Int. Rev. Neurobiol. 46, 207–241.

Bramlett, H.M., Dietrich, W.D., 2001. Neuropathological protection after traumatic brain injury in intact female rats versus males or ovariectomized females. J. Neurotrauma 18, 891–900.

Cervantes, M., Gonzalez-Vidal, M.D., Ruelas, R., Escobar, A., Morali, G., 2002. Neuroprotective effects of progesterone on damage elicited by acute global cerebral ischemia in neurons of the caudate nucleus. Arch. Med. Res. 33, 6–14.

Conti, A.C., Raghupathi, R., Trojanowski, J.Q., McIntosh, T.K., 1998. Experimental brain injury induces regionally distinct apoptosis during the acute and delayed post-traumatic period. J. Neurosci. 18, 5663–5672 (8-1).

Dixon, C.E., Clifton, G.L., Lighthall, J.W., Yaghmai, A.A., Hayes, R.L., 1991. A controlled cortical impact model of traumatic brain injury in the rat. J. Neurosci. Methods 39, 253–262.

Djebaili, M., Hoffman, S.W., Stein, D.G., 2004. Allopregnanolone and progesterone decrease cell death and cognitive deficits after a contusion of the rat pre-frontal cortex. Neuroscience 123, 349–359.

Djebaili, M., Guo, Q., Pettus, E.H., Hoffman, S.W., Stein, D.G., 2005. The neurosteroids progesterone and allopregnanolone reduce cell death, gliosis, and functional deficits after traumatic brain injury in rats. J. Neurotrauma 22, 106–118.

Farace, E., Alves, W.M., 2000. Do women fare worse: a metaanalysis of gender differences in traumatic brain injury outcome. J. Neurosurg. 93, 539–545.

Follesa, P., Biggio, F., Caria, S., Gorini, G., Biggio, G., 2004. Modulation of GABA(A) receptor gene expression by allopregnanolone and ethanol. Eur. J. Pharmacol. 500, 413–425.

George, M.S., Guidotti, A., Rubinow, D., Pan, B., Mikalauskas, K., Post, R.M., 1994. CSF neuroactive steroids in affective disorders: pregnenolone, progesterone, and DBI. Biol. Psychiatry 35, 775–780 (5-15).

Gibson, C.L., Murphy, S.P., 2004. Progesterone enhances functional recovery after middle cerebral artery occlusion in male mice. J. Cereb. Blood Flow Metab. 24, 805–813.

Gonzalez Deniselle, M.C., Lopez Costa, J.J., Gonzalez, S.L., Labombarda, F., Garay, L., Guennoun, R., Schumacher, M., De Nicola, A.F., 2002. Basis of progesterone protection in spinal cord neurodegeneration. J. Steroid Biochem. Mol. Biol. 83, 199–209.

Gonzalez-Vidal, M.D., Cervera-Gaviria, M., Ruelas, R., Escobar, A., Morali, G., Cervantes, M., 1998. Progesterone: protective effects on the cat hippocampal neuronal damage due to acute global cerebral ischemia. Arch. Med. Res. 29, 117–124.

Goodman, Y., Bruce, A.J., Cheng, B., Mattson, M.P., 1996. Estrogens attenuate and corticosterone exacerbates excitotoxicity, oxidative injury, and amyloid beta-peptide toxicity in hippocampal neurons. J. Neurochem. 66, 1836–1844.

Goss, C.W., Hoffman, S.W., Stein, D.G., 2003. Behavioral effects and anatomic correlates after brain injury: a progesterone dose–response study. Pharmacol. Biochem. Behav. 76, 231–242.

Groswasser, Z., Cohen, M., Keren, O., 1998. Female TBI patients recover better than males. Brain Inj. 12, 805–808.

Hall, E.D., Sullivan, P.G., Gibson, T.R., Pavel, K.M., Thompson, B.M., Scheff, S.W., 2005. Spatial and temporal characteristics of neurodegeneration after controlled cortical impact in mice: more than a focal brain injury. J. Neurotrauma 22, 252–265.

He, J., Evans, C.O., Hoffman, S.W., Oyesiku, N.M., Stein, D.G., 2004a. Progesterone and allopregnanolone reduce inflammatory cytokines after traumatic brain injury. Exp. Neurol. 189, 404–412.

He, J., Hoffman, S.W., Stein, D.G., 2004b. Allopregnanolone, a progesterone metabolite, enhances behavioral recovery and decreases neuronal loss after traumatic brain injury. Restor. Neurol. Neurosci. 22, 19–31.

Hoffman, G.E., Le, W.W., Murphy, A.Z., Koski, C.L., 2001. Divergent effects of ovarian steroids on neuronal survival during experimental allergic encephalitis in Lewis rats. Exp. Neurol. 171, 272–284.

Hoffman, G.E., Moore, N., Fiskum, G., Murphy, A.Z., 2003. Ovarian steroid modulation of seizure severity and hippocampal cell death after kainic acid treatment. Exp. Neurol. 182, 124–134.

Jiang, N., Chopp, M., Stein, D., Feit, H., 1996. Progesterone is neuroprotective after transient middle cerebral artery occlusion in male rats. Brain Res. 735, 101–107 (9-30).

Krebs, C.J., Jarvis, E.D., Chan, J., Lydon, J.P., Ogawa, S., Pfaff, D.W., 2000. A membrane-associated progesterone-binding protein, 25-Dx, is regulated by progesterone in brain regions involved in female reproductive behaviors. Proc. Natl. Acad. Sci. U.S.A. 97, 12816–12821 (11-7).

Kumon, Y., Kim, S.C., Tompkins, P., Stevens, A., Sakaki, S., Loftus, C.M., 2000. Neuroprotective effect of postischemic administration of progesterone in spontaneously hypertensive rats with focal cerebral ischemia. J. Neurosurg. 92, 848–852.

Kupina, N.C., Detloff, M.R., Bobrowski, W.F., Snyder, B.J., Hall, E.D., 2003. Cytoskeletal protein degradation and neurodegeneration evolves differently in males and females following experimental head injury. Exp. Neurol. 180, 55–73.

Labombarda, F., Gonzalez, S.L., Deniselle, M.C., Vinson, G.P., Schumacher, M., De Nicola, A.F., Guennoun, R., 2003. Effects of injury and progesterone treatment on progesterone receptor and progesterone binding protein 25-Dx expression in the rat spinal cord. J. Neurochem. 87, 902–913.

Le, W.W., Attardi, B., Berghorn, K.A., Blaustein, J., Hoffman, G.E., 1997. Progesterone blockade of a luteinizing hormone surge blocks luteinizing hormone-releasing hormone Fos activation and activation of its preoptic area afferents. Brain Res. 778, 272–280 (12-19).

Lee, L.L., Galo, E., Lyeth, B.G., Muizelaar, J.P., Berman, R.F., 2004. Neuroprotection in the rat lateral fluid percussion model of traumatic brain injury by SNX-185, an N-type voltage-gated calcium channel blocker. Exp. Neurol. 190, 70–78.

Lewen, A., Matz, P., Chan, P.H., 2000. Free radical pathways in CNS injury. J. Neurotrauma 17, 871–890.

Murphy, S.J., Littleton-Kearney, M.T., Hurn, P.D., 2002. Progesterone administration during reperfusion, but not preischemia alone, reduces injury in ovariectomized rats. J. Cereb. Blood Flow Metab. 22, 1181–1188.

Murphy, S.J., Traystman, R.J., Hurn, P.D., Duckles, S.P., 2000. Progesterone exacerbates striatal stroke injury in progesterone-deficient female animals. Stroke 31, 1173–1178.

Roof, R.L., Hall, E.D., 2000. Gender differences in acute CNS trauma and stroke: neuroprotective effects of estrogen and progesterone. J. Neurotrauma 17, 367–388.

Roof, R.L., Duvdevani, R., Stein, D.G., 1993a. Gender influences outcome of brain injury: progesterone plays a protective role. Brain Res. 607, 333–336 (4-2).

Roof, R.L., Zhang, Q., Glasier, M.M., Stein, D.G., 1993b. Gender-specific impairment on Morris water maze task after entorhinal cortex lesion. Behav. Brain Res. 57, 47–51 (10-21).

Roof, R.L., Duvdevani, R., Braswell, L., Stein, D.G., 1994. Progesterone facilitates cognitive recovery and reduces secondary neuronal loss caused by cortical contusion injury in male rats. Exp. Neurol. 129, 64–69.

Roof, R.L., Duvdevani, R., Heyburn, J.W., Stein, D.G., 1996. Progesterone rapidly decreases brain edema: treatment delayed up to 24 hours is still effective. Exp. Neurol. 138, 246–251.

Roof, R.L., Hoffman, S.W., Stein, D.G., 1997. Progesterone protects against lipid peroxidation following traumatic brain injury in rats. Mol. Chem. Neuropathol. 31, 1–11.

Shear, D.A., Galani, R., Hoffman, S.W., Stein, D.G., 2002. Progesterone protects against necrotic damage and behavioral abnormalities caused by traumatic brain injury. Exp. Neurol. 178, 59–67.

Smith, S.S., 1991. Progesterone administration attenuates excitatory amino acid responses of cerebellar Purkinje cells. Neuroscience 42, 309–320.

Smith, S.S., 1994. Female sex steroid hormones: from receptors to networks to performance–actions on the sensorimotor system. Prog. Neurobiol. 44, 55–86.

Smith, S.S., Waterhouse, B.D., Chapin, J.K., Woodward, D.J., 1987. Progesterone alters GABA and glutamate responsiveness: a possible mechanism for its anxiolytic action. Brain Res. 400, 353–359 (1-6).

Starkov, A.A., Fiskum, G., Chinopoulos, C., Lorenzo, B.J., Browne, S.E., Patel, M.S., Beal, M.F., 2004. Mitochondrial alpha-ketoglutarate dehydrogenase complex generates reactive oxygen species. J. Neurosci. 24, 7779–7788 (9-8).

Stein, D.G., 2001. Brain damage, sex hormones and recovery: a new role for progesterone and estrogen? Trends Neurosci. 24, 386–391.

Sullivan, P.G., Rabchevsky, A.G., Waldmeier, P.C., Springer, J.E., 2005. Mitochondrial permeability transition in CNS trauma: cause or effect of neuronal cell death? J. Neurosci. Res. 79, 231–239 (1-1).

Suzuki, T., Bramlett, H.M., Ruenes, G., Dietrich, W.D., 2004. The effects of early post-traumatic hyperthermia in female and ovariectomized rats. J. Neurotrauma 21, 842–853.

Vereczki, V., Martin, E., Rosenthal, R.E., Hof, P.R., Hoffman, G.E., Fiskum, G., in press. Normoxic resuscitation after cardiac arrest protects against hippocampal oxidative stress, metabolic dysfunction, and neuronal death. J. Cereb. Blood Flow Metab.

Wagner, A.K., Kline, A.E., Sokoloski, J., Zafonte, R.D., Capulong, E., Dixon, C.E., 2002. Intervention with environmental enrichment after experimental brain trauma enhances cognitive recovery in male but not female rats. Neurosci. Lett. 334, 165–168 (12-16).

Wagner, A.K., Bayir, H., Ren, D., Puccio, A., Zafonte, R.D., Kochanek, P.M., 2004a. Relationships between cerebrospinal fluid markers of excitotoxicity, ischemia, and oxidative damage after severe TBI: the impact of gender, age, and hypothermia. J. Neurotrauma 21, 125–136.

Wagner, A.K., Willard, L.A., Kline, A.E., Wenger, M.K., Bolinger, B.D., Ren, D., Zafonte, R.D., Dixon, C.E., 2004b. Evaluation of estrous cycle stage and gender on behavioral outcome after experimental traumatic brain injury. Brain Res. 998, 113–121 (2-13).

Wagner, A.K., Fabio, A., Puccio, A.M., Hirschberg, R., Li, W., Zafonte, R.D., Marion, D.W., 2005. Gender associations with cerebrospinal fluid glutamate and lactate/pyruvate levels after severe traumatic brain injury. Crit. Care Med. 33, 407–413.

Wise, P.M., Dubal, D.B., Wilson, M.E., Rau, S.W., Bottner, M., 2001. Minireview: neuroprotective effects of estrogen—New insights into mechanisms of action. Endocrinology 142, 969–973.

Yakovlev, A.G., Knoblach, S.M., Fan, L., Fox, G.B., Goodnight, R., Faden, A.I., 1997. Activation of CPP32-like caspases contributes to neuronal apoptosis and neurological dysfunction after traumatic brain injury. J. Neurosci. 17, 7415–7424.

Yu, R., Follesa, P., Ticku, M.K., 1996. Down-regulation of the GABA receptor subunits mRNA levels in mammalian cultured cortical neurons following chronic neurosteroid treatment. Brain Res. Mol. Brain Res. 41, 163–168 (9-5).